



# **RAPID AND COST-EFFECTIVE TECHNOLOGIES TO DETECT THE PATHOGENS IN FOOD AND ENVIRONMENT**

EDITED BY: Xuejun Ma, Yi-Wei Tang, Xiyang Wu and Joseph Oliver Falkinham  
PUBLISHED IN: *Frontiers in Microbiology*



# frontiers

## Frontiers eBook Copyright Statement

The copyright in the text of individual articles in this eBook is the property of their respective authors or their respective institutions or funders. The copyright in graphics and images within each article may be subject to copyright of other parties. In both cases this is subject to a license granted to Frontiers.

The compilation of articles constituting this eBook is the property of Frontiers.

Each article within this eBook, and the eBook itself, are published under the most recent version of the Creative Commons CC-BY licence.

The version current at the date of publication of this eBook is CC-BY 4.0. If the CC-BY licence is updated, the licence granted by Frontiers is automatically updated to the new version.

When exercising any right under the CC-BY licence, Frontiers must be attributed as the original publisher of the article or eBook, as applicable.

Authors have the responsibility of ensuring that any graphics or other materials which are the property of others may be included in the CC-BY licence, but this should be checked before relying on the CC-BY licence to reproduce those materials. Any copyright notices relating to those materials must be complied with.

Copyright and source acknowledgement notices may not be removed and must be displayed in any copy, derivative work or partial copy which includes the elements in question.

All copyright, and all rights therein, are protected by national and international copyright laws. The above represents a summary only. For further information please read Frontiers' Conditions for Website Use and Copyright Statement, and the applicable CC-BY licence.

ISSN 1664-8714

ISBN 978-2-88976-564-5

DOI 10.3389/978-2-88976-564-5

## About Frontiers

Frontiers is more than just an open-access publisher of scholarly articles: it is a pioneering approach to the world of academia, radically improving the way scholarly research is managed. The grand vision of Frontiers is a world where all people have an equal opportunity to seek, share and generate knowledge. Frontiers provides immediate and permanent online open access to all its publications, but this alone is not enough to realize our grand goals.

## Frontiers Journal Series

The Frontiers Journal Series is a multi-tier and interdisciplinary set of open-access, online journals, promising a paradigm shift from the current review, selection and dissemination processes in academic publishing. All Frontiers journals are driven by researchers for researchers; therefore, they constitute a service to the scholarly community. At the same time, the Frontiers Journal Series operates on a revolutionary invention, the tiered publishing system, initially addressing specific communities of scholars, and gradually climbing up to broader public understanding, thus serving the interests of the lay society, too.

## Dedication to Quality

Each Frontiers article is a landmark of the highest quality, thanks to genuinely collaborative interactions between authors and review editors, who include some of the world's best academicians. Research must be certified by peers before entering a stream of knowledge that may eventually reach the public - and shape society; therefore, Frontiers only applies the most rigorous and unbiased reviews. Frontiers revolutionizes research publishing by freely delivering the most outstanding research, evaluated with no bias from both the academic and social point of view. By applying the most advanced information technologies, Frontiers is catapulting scholarly publishing into a new generation.

## What are Frontiers Research Topics?

Frontiers Research Topics are very popular trademarks of the Frontiers Journals Series: they are collections of at least ten articles, all centered on a particular subject. With their unique mix of varied contributions from Original Research to Review Articles, Frontiers Research Topics unify the most influential researchers, the latest key findings and historical advances in a hot research area! Find out more on how to host your own Frontiers Research Topic or contribute to one as an author by contacting the Frontiers Editorial Office: [frontiersin.org/about/contact](https://frontiersin.org/about/contact)



# RAPID AND COST-EFFECTIVE TECHNOLOGIES TO DETECT THE PATHOGENS IN FOOD AND ENVIRONMENT

Topic Editors:

**Xuejun Ma**, Chinese Center For Disease Control and Prevention, China

**Yi-Wei Tang**, Cepheid, United States

**Xiyang Wu**, Jinan University, China

**Joseph Oliver Falkinham**, Virginia Tech, United States

*Dr. Yi-Wei Tang is currently an employee of Danaher/Cepheid, a biotech company produces in vitro diagnostic devices. The other Topic Editors declare no competing interests with regard to the Research Topic project*

**Citation:** Ma, X., Tang, Y.-W., Wu, X., Falkinham, J. O., eds. (2022). Rapid and Cost-effective Technologies to Detect the Pathogens in Food and Environment. Lausanne: Frontiers Media SA. doi: 10.3389/978-2-88976-564-5

# Table of Contents

- 05 Editorial: Rapid and Cost-Effective Technologies to Detect the Pathogens in Food and Environment**  
Xuejun Ma, Yi-Wei Tang, Xiyang Wu and Joseph O. Falkinham
- 07 The *Aspergillus niger* Major Allergen (Asp n 3) DNA-Specific Sequence Is a Reliable Marker to Identify Early Fungal Contamination and Postharvest Damage in *Mangifera indica* Fruit**  
Jorge Martínez, Ander Nevado, Ester Suñén, Marta Gabriel, Ainara Vélez-del-Burgo, Patricia Sánchez and Idoia Postigo
- 17 Development of Moore Swab and Ultrafiltration Concentration and Detection Methods for *Salmonella Typhi* and *Salmonella Paratyphi A* in Wastewater and Application in Kolkata, India and Dhaka, Bangladesh**  
Pengbo Liu, Makoto Ibaraki, Renuka Kapoor, Nuhu Amin, Abhishek Das, Rana Miah, Asish K. Mukhopadhyay, Mahbubur Rahman, Shanta Dutta and Christine L. Moe
- 28 Development of a High-Efficiency Immunomagnetic Enrichment Method for Detection of Human Norovirus via PAMAM Dendrimer/SA-Biotin Mediated Cascade-Amplification**  
Junshan Gao, Le Zhang, Liang Xue, Weicheng Cai, Zhiwei Qin, Jiale Yang, Yanhui Liang, Linping Wang, Moutong Chen, Qinghua Ye, Ying Li, Juan Wang, Shi Wu, Qingping Wu and Jumei Zhang
- 36 Application of Engineered Bacteriophage T7 in the Detection of Bacteria in Food Matrices**  
Nicharee Wisuthiphaet, Xu Yang, Glenn M. Young and Nitin Nitin
- 48 Development and Application of a Novel Rapid and Throughput Method for Broad-Spectrum Anti-Foodborne Norovirus Antibody Testing**  
Yueting Zuo, Liang Xue, Junshan Gao, Yingyin Liao, Yueting Jiang, Ying Li, Yanhui Liang, Linping Wang, Weicheng Cai, Tong Cheng, Juan Wang, Moutong Chen, Jumei Zhang, Yu Ding and Qingping Wu
- 57 Development of a Loop-Mediated Isothermal Amplification Method for the Rapid Detection of *Phytophthora vexans***  
Tuhong Wang, Haojun Ji, Yongting Yu, Xiaojie Wang, Yi Cheng, Zhimin Li, Jia Chen, Litao Guo, Jianping Xu and Chunsheng Gao
- 68 Rapid and Sensitive Detection of *Salmonella* spp. Using CRISPR-Cas13a Combined With Recombinase Polymerase Amplification**  
Bailin An, Hongbin Zhang, Xuan Su, Yue Guo, Tao Wu, Yiyue Ge, Fengcai Zhu and Lunbiao Cui
- 76 Rapid and Sensitive Detection of *Vibrio vulnificus* Using CRISPR/Cas12a Combined With a Recombinase-Aided Amplification Assay**  
Xingxing Xiao, Ziqin Lin, Xianhui Huang, Jinfang Lu, Yan Zhou, Laibao Zheng and Yongliang Lou



- 86    *Genomic Epidemiology and Antimicrobial Susceptibility Profile of Enterotoxigenic Escherichia coli From Outpatients With Diarrhea in Shenzhen, China, 2015–2020***  
Chao Yang, Yinghui Li, Le Zuo, Min Jiang, Xianglilan Zhang, Li Xie, Miaomiao Luo, Yiyang She, Lei Wang, Yixiang Jiang, Shuang Wu, Rui Cai, Xiaolu Shi, Yujun Cui, Chengsong Wan and Qinghua Hu
- 99    *Diversification of Escherichia albertii H-Antigens and Development of H-Genotyping PCR***  
Koji Nakae, Tadasuke Ooka, Koichi Murakami, Yukiko Hara-Kudo, Naoko Imuta, Yasuhiro Gotoh, Yoshitoshi Ogura, Tetsuya Hayashi, Yasuhiro Okamoto and Junichiro Nishi
- 105    *Application of Lab-on-Chip for Detection of Microbial Nucleic Acid in Food and Environment***  
Liu Yang, Wei Yi, Fangfang Sun, Mengjiao Xu, Zhan Zeng, Xiaoyue Bi, Jianping Dong, Yao Xie and Minghui Li
- 122    *Genomic Characterization of Clinical Listeria monocytogenes Isolates in Beijing, China***  
Xiaoai Zhang, Yuzhu Liu, Penghang Zhang, Yanlin Niu, Qian Chen and Xiaochen Ma
- 134    *Advances in Metagenomics and Its Application in Environmental Microorganisms***  
Lu Zhang, FengXin Chen, Zhan Zeng, Mengjiao Xu, Fangfang Sun, Liu Yang, Xiaoyue Bi, Yanjie Lin, YuanJiao Gao, HongXiao Hao, Wei Yi, Minghui Li and Yao Xie



# Editorial: Rapid and Cost-Effective Technologies to Detect the Pathogens in Food and Environment

Xuejun Ma<sup>1</sup>, Yi-Wei Tang<sup>2</sup>, Xiyang Wu<sup>3</sup> and Joseph O. Falkinham<sup>4\*</sup>

<sup>1</sup> Chinese Center for Disease Control and Prevention, Beijing, China, <sup>2</sup> Cepheid, Sunnyvale, CA, United States, <sup>3</sup> Jinan University, Guangzhou, China, <sup>4</sup> Virginia Tech, Blacksburg, VA, United States

**Keywords:** microbial detection, plants, food, wastewater pathogens, DNA-based detection, immunomagnetic, CRISPR

## Editorial on the Research Topic

### OPEN ACCESS

#### Edited by:

Dario De Medici,  
National Institute of Health (ISS), Italy

#### Reviewed by:

Antonio Valero,  
University of Cordoba, Spain

#### \*Correspondence:

Joseph O. Falkinham  
jofiii@vt.edu

#### Specialty section:

This article was submitted to  
Food Microbiology,  
a section of the journal  
Frontiers in Microbiology

**Received:** 13 December 2021

**Accepted:** 25 February 2022

**Published:** 20 June 2022

#### Citation:

Ma X, Tang Y-W, Wu X and  
Falkinham JO (2022) Editorial: Rapid  
and Cost-Effective Technologies to  
Detect the Pathogens in Food and  
Environment.  
Front. Microbiol. 13:834774.  
doi: 10.3389/fmicb.2022.834774

## Rapid and Cost-Effective Technologies to Detect the Pathogens in Food and Environment

The value of this Research Topic lies in the breadth of microorganisms as subjects of interests, the applications of the technologies, and the different approaches. That breadth serves to guide anyone with interests in pathogen detection; all serve as instructive examples. The articles fall into two categories: (1) methods for detection of specific food-borne pathogens and (2) methods for detection of different food-borne pathogens, and (3) methods to overcome the challenges of different starting materials.

A wide variety of organisms are described, including: *Listeria* (Zhang X. et al.), *Aspergillus* (Martinez et al.), *Salmonella* (An et al.; Liu et al.), *Phytophthora* (Wang et al.), *Escherichia* (Nakae et al.; Yang et al.), *Vibrio* (Xiao et al.; Zhang X. et al.), and Norovirus (Zuo et al.). Each provides its own challenges to detection method development and therefore serve as guides to the challenges of detection in different starting materials. The breadth of methods for detection of foodborne pathogens is likewise quite wide. Metagenomics (Zhang L. et al.), CRISPR (Xiao et al.), Lab-on-Chip (Yang et al.), immunomagnetic enrichment (Gao et al.), bacteriophage-linked detection (Wisuthiphaet et al.), and other amplification methods (Zuo et al.; Wang et al.) are included to provide guidance in the choice of experimental approaches. Finally, the volume even has a contribution for detection of microbial DNA, applicable to a wide range of starting samples (e.g., water, wastewater, plants, and foods). We cannot forget that free DNA can be taken up and able to transform other microorganisms to express novel, unexpected traits.

A wide range of applications is described by this collection of papers from wastewater, to plants, fruits, and foods. Again, each application presents different challenges and those needing to develop protocols for pathogen detection can use this Research Topic's collection to guide their investigations.



All of the detection protocols are described in detail along with the challenges identified by the individual investigations. As all the detection methodologies described in the Research Topic are novel and cutting-edge, they deserve publication and dissemination. I worry, however, that the level of technology development and cost may take them out of the market for application amongst regions of the world that lack the technological or economic development to employ these methods. We are all challenged to develop low-cost, rapid methods for pathogen-detection that can be used throughout our world.

## AUTHOR CONTRIBUTIONS

All authors listed have made a substantial, direct, and intellectual contribution to the work and approved it for publication.

**Conflict of Interest:** Y-WT was employed by Cepheid.

The remaining authors declare that the research was conducted in the absence of any commercial or financial relationships that could be construed as a potential conflict of interest.

**Publisher's Note:** All claims expressed in this article are solely those of the authors and do not necessarily represent those of their affiliated organizations, or those of the publisher, the editors and the reviewers. Any product that may be evaluated in this article, or claim that may be made by its manufacturer, is not guaranteed or endorsed by the publisher.

*Copyright © 2022 Ma, Tang, Wu and Falkinham. This is an open-access article distributed under the terms of the Creative Commons Attribution License (CC BY). The use, distribution or reproduction in other forums is permitted, provided the original author(s) and the copyright owner(s) are credited and that the original publication in this journal is cited, in accordance with accepted academic practice. No use, distribution or reproduction is permitted which does not comply with these terms.*



# The *Aspergillus niger* Major Allergen (Asp n 3) DNA-Specific Sequence Is a Reliable Marker to Identify Early Fungal Contamination and Postharvest Damage in *Mangifera indica* Fruit

Jorge Martínez<sup>1</sup>, Ander Nevado<sup>1</sup>, Ester Suñén<sup>1</sup>, Marta Gabriel<sup>2</sup>, Ainara Vélez-del-Burgo<sup>1</sup>, Patricia Sánchez<sup>1</sup> and Idoia Postigo<sup>1\*</sup>

<sup>1</sup> Department of Immunology, Microbiology and Parasitology, Faculty of Pharmacy and Laboratory of Parasitology and Allergy, Lascaray Research Centre, University of the Basque Country, Vitoria-Gasteiz, Spain, <sup>2</sup> INEGI, Institute of Science and Innovation in Mechanical and Industrial Engineering, Porto, Portugal

## OPEN ACCESS

### Edited by:

Giovanna Suzzi,  
University of Teramo, Italy

### Reviewed by:

Magdalena Frac,  
Institute of Agrophysics (PAN), Poland  
Rosanna Tofalo,  
University of Teramo, Italy

### \*Correspondence:

Idoia Postigo  
idoia.postigo@ehu.eus

### Specialty section:

This article was submitted to  
Food Microbiology,  
a section of the journal  
Frontiers in Microbiology

**Received:** 02 February 2021

**Accepted:** 25 May 2021

**Published:** 28 June 2021

### Citation:

Martínez J, Nevado A, Suñén E, Gabriel M, Vélez-del-Burgo A, Sánchez P and Postigo I (2021) The *Aspergillus niger* Major Allergen (Asp n 3) DNA-Specific Sequence Is a Reliable Marker to Identify Early Fungal Contamination and Postharvest Damage in *Mangifera indica* Fruit. *Front. Microbiol.* 12:663323. doi: 10.3389/fmicb.2021.663323

The aim of this work was to study the value of the main allergen Asp n 3 of *Aspergillus niger* as a molecular marker of allergenicity and pathogenicity with the potential to be used in the identification of *A. niger* as a contaminant and cause of spoilage of *Mangifera indica*. Real-time polymerase chain reaction (RT-PCR) was used for the amplification of Asp n 3 gene. Two pairs of primers were designed: one for the amplification of the entire sequence and another one for the amplification of the most conserved region of this peroxisomal protein. The presence of *A. niger* was demonstrated by the early detection of the allergenic protein Asp n 3 coding gene, which could be considered a species-specific marker. The use of primers designed based on the conserved region of the Asp n 3 encoding gene allowed us to identify the presence of the closely related fungal species *Aspergillus fumigatus* by detecting Asp n 3 homologous protein, which can be cross-reactive. The use of conserved segments of the Asp n 3 gene or its entire sequence allows us to detect phylogenetically closely related species within the Aspergillaceae family or to identify species-specific contaminating fungi.

**Keywords:** food spoilage, *Aspergillus*, Asp n 3, DNA-marker, fungal food pathogen

## INTRODUCTION

Several species belonging to the fungal genus *Aspergillus* are well known as plant pathogens that may cause damage in plants as well as spoil postharvest fruit, vegetables, and cereals, resulting in serious agriculture and economic losses (Perrone et al., 2007; Samson et al., 2010; Mahfooz et al., 2017). Although the main substrate of black aspergilli (*Aspergillus* section Nigri) is soil, these fungi are among the most common fungi causing food spoilage and biodeterioration of other



materials. Several authors report that the *Aspergillus niger* species complex can be responsible for the postharvest decay of different fresh fruits and some vegetables (Gautam et al., 2011; Sharma, 2012). It has been demonstrated that *Aspergillus* spores are one of the most frequently identified fungal conidia in the atmosphere (Kasprzyk, 2008; Dijksterhuis, 2019). Its extensive ubiquity in nature probably justifies why this species is one of the most common contaminating fungal genera recorded in various agricultural commodities, such as fruit, nuts, beans, cereals, and vegetables (Samson et al., 2010). In particular, *A. niger* can produce rotting of numerous fruits and vegetables, causing a substantial economic loss. Onions, mangoes, grapes, or tomatoes are the most cited fruits to which *A. niger* can be the major cause of rot phenotype plant disease (Gautam et al., 2011). On the other hand, selected *A. niger* strains are also used in agriculture as promising beneficial microbes (Lubna et al., 2018; Pertile et al., 2021).

*Aspergillus niger* is described as a producer of a wide variety of toxic metabolites, including ochratoxins, a group of secondary metabolites that are classified as possible human carcinogens (Blumenthal, 2004; Tian et al., 2015). In addition to producing toxins, *Aspergillus* species are an important cause of allergy as a relevant source of allergen proteins that are involved in the development of allergic symptoms, particularly in atopic individuals (Simon-Nobbe et al., 2008; Gabriel et al., 2016b).

Among the several allergens described in this mold, the major *A. niger* allergen, Asp n 3, which is homologous to Asp f 3 of *Aspergillus fumigatus* (peroxisomal protein), has been demonstrated to be a clinically relevant component because 72% of the *Aspergillus* sensitized population shows reactive IgE specific to this allergen (Hemmann et al., 1997). This component is also a key marker to use in the differential diagnosis of some different types of aspergillosis (Cramer et al., 1998).

The fungal contamination of fruit with toxins or allergens can lead to a significant health risk to humans. Fruit colonization with these fungi might be used as a direct indicator of fruit or plant damage, food quality, and safety for human consumption (Battilani et al., 2008). Thus, to minimize the fungal diseases associated with both economic losses and health risk, it is essential to detect and identify pathogens at an early stage of the infection process (Amalaradjou and Venkitanarayanan, 2008). In fact, the early and accurate detection and identification of pathogens will allow the control of the spread of fungal infections as well as the implementation of disease management strategies.

The traditional identification of fungi by means of methodologies based on morphological characteristics has a low degree of sensitivity and requires considerable expertise. To address these shortcomings, in recent years, molecular methods such as polymerase chain reaction (PCR) have been considered suitable alternatives for the rapid and early diagnosis of fungal contamination (Gabriel et al., 2015, 2017).

With this in mind, the objective of this work was to study the value of the main allergen Asp n 3 of *A. niger* as a molecular marker of allergenicity and pathogenicity, with the potential to be used in the identification of *A. niger* as a contaminant and cause of spoilage of *Mangifera indica*. Its ability to identify closely related species of the genus *Aspergillus* was also analyzed. The

specific detection of Asp n 3 was evaluated in an experimental infection of *M. indica* fruit with *A. niger*, according to Gabriel et al. (2017), by a recently developed PCR method based on the Alt 1 coding gene for *Alternaria alternata*.

## MATERIALS AND METHODS

### Fungal Strains and Culture Conditions

The *A. niger* strain CECT 20156 Spanish Type Culture Collection (CECT, University of Valencia, Spain) and the *A. fumigatus* AF54 strain (Laboratory of Parasitology and Allergy, Lascaray Research Centre, University of the Basque Country, Vitoria-Gasteiz, Spain) were used in this study.

*Aspergillus niger* was grown on malt extract agar plates for 4 days at 25°C. The spores were collected in 0.2% agar and 0.05% Tween 80 solution. Then, the spore suspension was diluted 1:100, counted in a Neubauer chamber, and adjusted to a final concentration of  $1 \times 10^6$  spores/ml with sterile phosphate-buffered saline (PBS) and 0.05 Tween 80 (Gabriel et al., 2017).

### Fruit Inoculation and Incubation

Twenty fresh mangoes were sterilized by immersion in a solution of 1% (v/v) sodium hypochlorite for 1 h at room temperature. Later, they were rinsed out with sterile distilled water and dried out. Sixteen fruits were inoculated with 100  $\mu$ l of the spore suspension and four mangoes with 100  $\mu$ l of sterile distilled water as the negative control under sterile conditions. Inoculation was performed by the injection of the spore suspension at 3 mm deep under the fruit skin. Then, the mangoes were placed in polypropylene bags which were closed and incubated at 25°C for 2, 4, 8, and 14 days.

The infection areas in the fruit were measured daily. Contours of the infected zones were drawn into transparent adhesive tape, and the areas were measured by AutoCAD. The negative controls were also checked daily to discard any spontaneous fungal contamination growth.

### Sample Collection and Processing

Four samples from four different fruits corresponding to 2, 4, 8, and 14 days of incubation were analyzed. Samples of 2 cm<sup>2</sup>  $\times$  1 cm deep were obtained from the fruit area where the inoculation was performed. Half of the sample was frozen at  $-80^\circ\text{C}$  for further PCR analysis, and the other half was incubated in Czapek Dox agar medium at 25°C until visible growth. The negative controls were subjected to the same procedure (Gabriel et al., 2017). *A. niger* positive control and *A. fumigatus* specificity control for PCR were grown on Czapek Dox broth.

### RNA Extraction

The samples were ground in liquid nitrogen with a mortar and pestle. Previously, the material was treated with 70% ethanol, and RNases were removed by RNase Zap solution (Thermo Fisher Scientific, Waltham, MA, United States). Then, 4.5  $\mu$ l of 2-mercaptoethanol was added to 100 mg of the pulverized sample, and Qiagen RNeasy Plant Mini Kit (Qiagen, Hilden, Germany)

was used to extract the total RNA according to the instructions provided by the manufacturer (Gabriel et al., 2017).

## cDNA Synthesis, Primer Design, and PCR Amplification

The reverse transcription reactions were carried out with RevertAid First Strand cDNA Synthesis Kit (Fermentas, Sankt Leon-Rot, Germany). Two pairs of primers were manually designed by comparison of the complete sequence that encodes Asp n 3 with the consensus sequences of the related fungal species considered in the design (Figure 1). The GenBank accession numbers of fungal species used for the multiple alignment analysis by the ClustalW program are shown in Table 1.

The primers named Aspn3FL\_FW (ATCACCTCATG GCGCCGTGGG) and Aspn3FL\_RV (TGTTGTCGTA GCTTCGTAAGCGC) were designed to amplify the complete Asp n 3 gene of *A. niger*, including the non-conserved regions of the gene.

The primers named CRPEROX\_FW [CAAGAAGGT(C/T) (A/G)T(C/T)CTC(T/G)TCGCC] and CRPEROX\_RV (TGTT GTCGTAGCTTCGTAAGCGC) were designed on the basis of the highly conserved internal nucleotide region of the Asp n 3 gene sequence of *A. niger* and its homologs in the other *Aspergillus* species (Gabriel et al., 2017).

Polymerase chain reactions were carried out with a FastStart Taq DNA polymerase PCR kit (Roche, Mannheim, Germany), and a PCR-grade deoxynucleoside triphosphate set (Roche, Mannheim, Germany) was used, following the manufacturer's instructions. Separate PCRs were performed for each pair of primers. The RT-PCR mixture contained 38.6 µl of water, 5 µl of buffer 10× with 20 mM MgCl<sub>2</sub>, 2 µl of each primer, 1 µl of dNTP mix (10 mM), 0.4 µl of FastStart Taq DNA polymerase, and 1 µl of cDNA. The program set for the Aspn3\_FL primers started at 95°C for 4 min and then proceeded with 35 cycles consisting of the first 30 s at 95°C, 30 s at 62°C, and 75 s at 72°C. The program set for the CRPEROX primers started with natural denaturation at 95°C for 4 min followed by 35 amplification cycles consisting of 30 s at 95°C, 30 s at 53°C, and 45 s at 72°C. After that, there was a final extension phase at 72°C for 7 min in both cases. The RT-PCR detection limit was  $1 \times 10^4$  spores of *Aspergillus*.

Sequencing reactions were performed using the BigDye Terminator, v.3, sequencing kit (Applied Biosystems) according to the manufacturer's specifications, and the reactions were run in an ABI 3130XL sequencer (Servei de Genòmica, Universitat Autònoma de Barcelona). The amplicon sequence identity was confirmed with NCBI BLAST.

## Alignment of Homologs to Asp n 3 Gene Sequences and Phylogenetic Tree

A BLAST sequence alignment of the Asp n 3 gene with the genes encoding peroxisomal homologous proteins from all expressing species included in the database was carried out. A phylogenetic tree of the nearest neighborhood of representatives constructed based on the nucleotide sequences of Asp n 3 homologs (peroxisomal protein) was constructed using Molecular Evolutionary Genetics Analysis (Tamura et al., 2007).

## RESULTS

Inoculation with *A. niger* resulted in a depressed, circular, brown, soft area surrounding the point of insertion of the pathogen. That area grew, softening the tissues of the mango and cracking the skin. The fungus was able to form spores in the areas where the flesh of the fruit was exposed. No new point of infection was observed during the experiment.

At 2 days post-inoculation, the lesions provoked by *A. niger* were evident in 100% of the inoculated mangoes. These lesions grew until they covered large areas of the fruit surface (Figure 2). The injuries caused by *A. niger* inoculation grew exponentially, showing lesions 0.8, 3.4, and 6 cm in diameter after 4, 8, and 14 days of incubation, respectively (Figure 3).

The cultures of samples of infected fruit in mycological media were positive for *A. niger* after 3–4 days of incubation. The samples from fruit inoculated with sterile PBS did not show fungal growth.

The PCR amplicons of the 913-bp complete gene and the 171-bp amplified fragment corresponding to the conserved region of the gene are shown in Figure 4. In 100% of the samples of mangoes infected with *A. niger*, the complete gene and the conserved gene region were amplified. In the sample infected by *A. fumigatus*, only the conserved region of the Asp n 3 gene was amplified, but not the complete region. There was no amplification in the mangoes used as the negative control.

These results confirmed the specificity of the primers designed for the amplification of the Asp n 3 gene for detecting *A. niger* as well as the capability of detecting Asp n 3 cross-reactive proteins using the CRPEROX\_FW/CRPEROX\_RV primers. This technique allows detection of the presence of the allergen Asp n 3 and its homologs in infected mangoes from the early stages of infection (2 days after inoculation). It is known that the presence of inhibitory substances in food samples may often compromise DNA amplification and lead to the failure of PCR. To prevent false-negative results, positive controls using cDNA obtained from the mycelia of an *A. niger* reference strain (CECT 20156 Spanish Type Culture Collection University of Valencia, Spain) were also included. A sequence analysis of the amplicons allowed the confirmation of the identity of all DNA fragments as Asp n 3. No amplification products were detected in the PCRs using cDNA obtained from PBS-inoculated fruits (Figure 4, B1 and B2 lines).

The presence of *A. niger* was demonstrated by the early detection of the allergenic protein Asp n 3 coding gene, which could be considered a species-specific marker. The use of primers designed based on the conserved region of the Asp n 3 encoding gene allowed us to identify the presence of the closely related fungal species *A. fumigatus* by detecting Asp n 3 homologous protein, which can be cross-reactive. The detection of well-characterized fungal allergens could be considered a tool for identifying fruit rot by *Aspergillus* and to identify fruit contaminated by *Aspergillus* as an allergenic source.

A phylogenetic tree (based on the nearest-neighbor method) of representatives constructed based on the nucleotide sequences of Asp n 3 homologs (peroxisomal protein) is shown in Figure 5. The sequence alignment of the Asp n 3 homologs



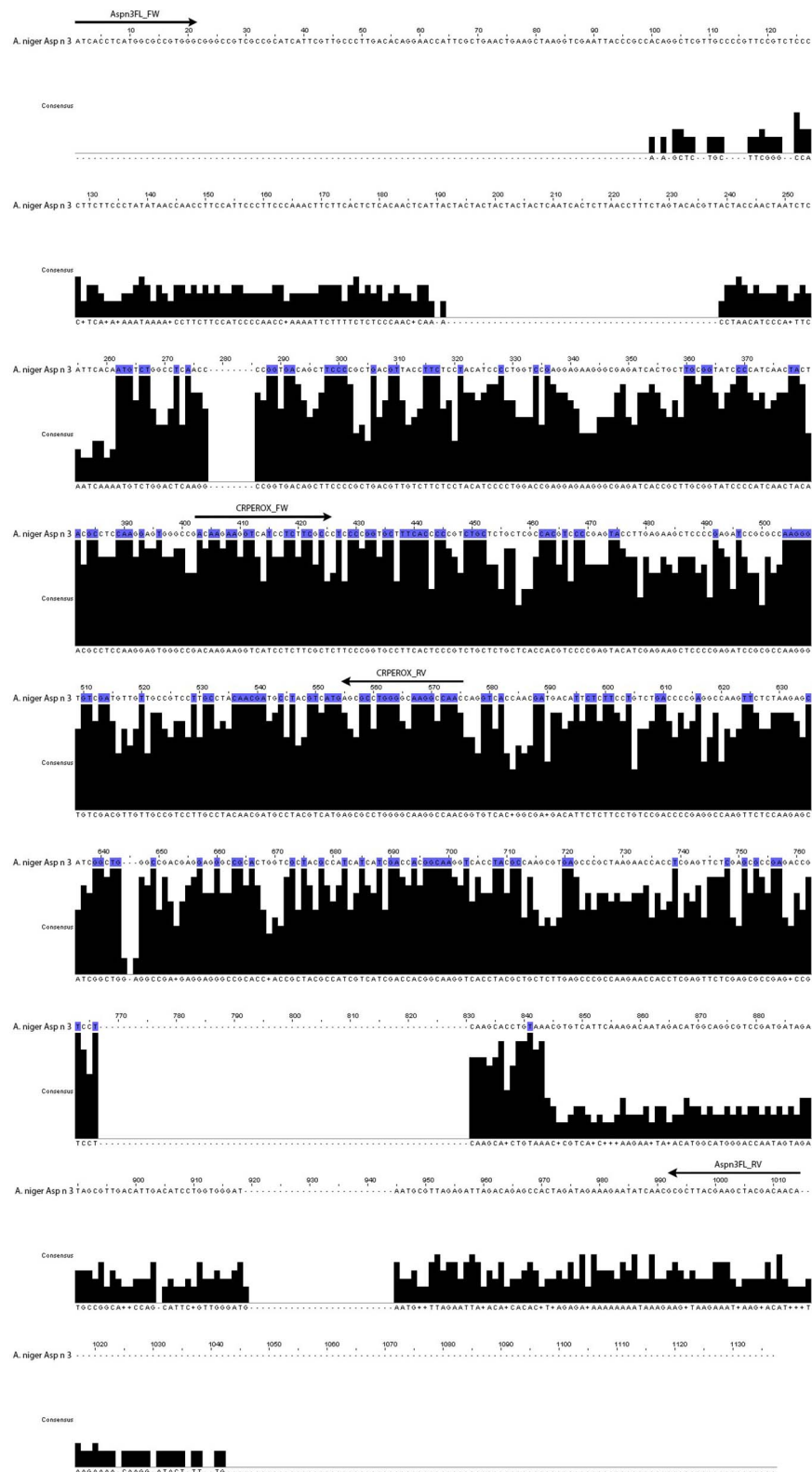


**FIGURE 1 |** Complete sequence of the gene that codifies for the allergen Asp n 3 compared to the consensus sequence of the fungal species considered in the design (*A. niger*, *A. fumigatus*, *A. terreus*, *A. clavatus*, *A. nidulans*, *A. flavus*, *A. oryzae*, *Penicillium citrium*, *P. chrysogenum*, *Trichophyton rubrum*, and *Neurospora crassa*). The arrows indicate the position of the two pairs of primers corresponding to complete cDNA gene and conserved region.

**TABLE 1** | GenBank accession numbers of the sequences used in multiple alignment analysis.

Species name	GenBank accession
<i>Aspergillus niger</i> CBS 513.88	XM 001395871.2
<i>Aspergillus terreus</i> NIH2624	XM 001209908.1
<i>Aspergillus fumigatus</i> ATCC 42202	U58050.1
<i>Aspergillus clavatus</i> NRRL 1	XM 001270302.1
<i>Aspergillus nidulans</i> FGSC A4	XM 676869.1
<i>Aspergillus flavus</i> NRRL3357	XM 002380885.1
<i>Aspergillus oryzae</i> RIB40	AB226160.1
<i>Penicillium chrysogenum</i> Wisconsin 54-1255	XM 002566221.1
<i>Penicillium citrium</i> 52-2	AF144753.1
<i>Trichophyton rubrum</i> CBS 118892	XM 003238084.1
<i>Neurospora crassa</i> OR74A	XM 959107.3

by BLAST, belonging to the different species considered to construct the phylogenetic tree, *A. niger*, *Aspergillus terreus*, *Neosartorya fischeri*, *A. fumigatus*, *Aspergillus clavatus*, and *Aspergillus nidulans*, showed more than 90% identity; *Aspergillus flavus* and *Aspergillus oryzae* revealed 86% identity; *Penicillium* species showed 81–84% identity; and *Talaromyces* and *Ramsonia* species showed 75–80% identity.

## DISCUSSION

Species from the genus *Aspergillus* are ubiquitous members of Ascomycotina, which are present in numerous and different habitats (Raper and Fennell, 1965; Christensen and Tuthill, 1986; Bennett, 2010).

*Aspergillus niger* is commonly isolated worldwide from soil, plant debris, air, and indoor environments, and it is considered a soil saprobe and a non-ligninolytic fungus able to produce numerous exoenzymes and organic acids involved in the decomposition cycle of organic matter. These features justify the capability of this fungus to cause the decay of fruits, vegetables, nuts, cereals, wood, or herbs. *A. niger* has also been described as a pathogen for humans and animals as an opportunistic parasite that causes allergic disorders or mycotoxin production (Gautam et al., 2011).

As a plant-pathogenic fungus, *A. niger* has been isolated from a variety of substrates, but its most prominent role is in the rotting or spoilage of numerous fruits, vegetables, and other food products, with relevant economic loss (Sharma, 2012).

The contamination of mango fruit by *A. niger* results in the qualitative deterioration of the product, showing a depressed, circular, brown, soft area surrounding the point where the pathogen starts the colonization (Palejwala et al., 1987; Al-Hindi et al., 2011).

The pathogenicity assay results obtained here showed that the mango fruit is very susceptible to contamination with *A. niger*, and the type of injuries caused by fungal colonization is compatible with that described by other authors (Kim et al., 2020; Shen et al., 2020). These results confirm the validity and applicability of this method for the study of the spoilage of mangoes by *A. niger*.

Because *A. niger* is a well-recognized producer of harmful toxins and significant allergenic proteins, exposure to *A. niger*-contaminated foodstuffs is likely to represent an inherent risk for human health (Simon-Nobbe et al., 2008; Gabriel et al., 2016a). This issue has been underestimated, and studies performed on it are very scarce (Simon-Nobbe et al., 2008; Gabriel et al., 2017). The precise and early detection of *A. niger* contamination would be a relevant added value to establish and prevent health risks and economic losses related to fungal colonization of foods such as fruits and vegetables.

The development of DNA technology has provided effective methods for microbial analysis. In recent decades, genetic studies have provided different nucleic acid markers for microbial identification. These markers are extensively used in PCR or chip-based detection. Based on 16S rDNA and internal transcribed spacer (ITS) sequencing, metagenomic approaches are now emerging technologies for analyzing the entire microbial community in a complex food and vegetable matrix (Shen et al., 2020). Recently, a multiplex RT-PCR has been developed, which is able to identify common *Aspergillus* sections quantitatively and detect the presence of azole-resistant strains, allowing the successful detection of early stage fungal colonies within a day of incubation (Kim et al., 2020).

In recent years, several fungal allergens (Alt a 1, Alt a 6, Asp f 1, Asp f 3, Asp n 1, Asp n 3, and others) have been presented as valuable molecular markers of allergenicity and pathogenicity (Matricardi et al., 2016). Accordingly, it is expected that the use of approaches targeting the Asp n 3 gene and/or protein to unequivocally identify and detect the pathogen *A. niger* will yield privileged and powerful information regarding the quality and biosecurity control of foodstuffs (Gabriel et al., 2016b, 2017).

Previously, our research group developed a PCR-based method targeting the gene coding for *A. alternata* major allergen Alt a 1 using species-specific primer sets, and these tools were used to successfully detect the infection of citrus fruit by *A. alternata* early (Gabriel et al., 2017). With this in mind and applying the same concept to the *A. niger* major allergen Asp n 3, further work was conducted to take advantage of the potential of this early detection method to reduce and control postharvest losses during the storage and transportation of fresh mango fruits.

The PCR based on specific Asp n 3 DNA expression gene sequences was able to detect the contamination of mango fruit from the first week of fungal colonization. The amplicons of the complete gene and the amplified fragment corresponding to the conserved region of the gene revealed positive results in 100% of the samples of mangoes infected with *A. niger*. As expected, there was a positive result in the *A. fumigatus* sample for the primers that amplify the conserved region, but not for the primers that amplify the complete Asp n 3 gene.

These results confirmed the specificity of the primers designed for the amplification of the Asp n 3 gene for detecting *A. niger* as well as the capability of detecting proteins susceptible to present cross-reactivity with Asp n 3 using the primers designed to amplify the conserved gene region. This technique allows the detection of the presence of the allergen Asp n 3 and its homologs in infected mangoes from the early stages of the infection (2 days after inoculation). These results are similar to those found by us



**FIGURE 2 |** Evolution of the injuries developed by *A. niger* in mango fruit: **(A)** 2 days post-infection (p.i.), **(B)** 4 days (p.i.), **(C)** 8 days (p.i.), and **(D)** 14 days (p.i.).

using the model of *A. alternata* infection in citrus fruit (Gabriel et al., 2017). These results shed light on ways to improve food and vegetable disease prevention, quality, and environmental control.

In the previous study, the gene encoding Alt a 1 defined a protein family associated only with the Pleosporaceae family of fungi (Chruszcz et al., 2012; Gabriel et al., 2017). In contrast, in this study, the peroxiredoxin Asp n 3 belongs to a large protein superfamily associated with numerous species from different kingdoms (Rhee, 2016; Harper et al., 2017). Thus, it could be expected that the specificity for the model studied in this work could be lower than that found previously for the Alt a 1 gene in the infection of citrus fruit with *A. alternata* (Sáenz-de-Santamaría et al., 2006; Gabriel et al., 2015, 2017).

Classically, the macro- and micromorphology of fungi have been the reference methodology for their identification (Visagie et al., 2014). Since the 1990s, DNA sequencing has become one of the most powerful tools for taxonomists because of creating new concepts for identifying the species and defining new tools to establish relationships among them, bringing the opportunity for sequence-based identification (Blaxter, 2003).

During the last decade, ITS rDNA was accepted as the official barcode for fungal identification. Since then, the ITS has been the most widely sequenced marker for fungi, and universal primers for this sequence are available (Schoch et al., 2012). After the introduction of ITS as the most relevant reference marker for taxonomy and phylogenetic relationship studies, in practice, several secondary markers have been analyzed for reliable species identification (Fitzpatrick et al., 2006; Houbraiken et al., 2012;

Samson et al., 2014; Visagie et al., 2014; Tsang et al., 2018). In *A. niger*, some genes, such as the collagen-like gene, beta-tubulin gene, and calmodulin gene, have been described as secondary markers (Bennett, 2010; Shen et al., 2020).

Peroxisomes make up a wide family of proteins associated with several biological functions, including fungal pathogenicity toward their host plants and animals (Chen et al., 2016; Rhee, 2016). The *Aspergillus* group 3 main allergens (Asp f 3, Asp fl 3, Asp n 3, Asp o 3, Asp t 3, Asp ni 3, and Neo fi 3) are peroxisomal proteins. Thus, it would be very interesting

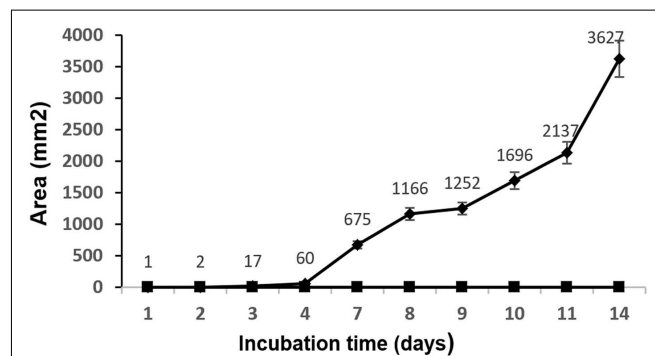


**FIGURE 3 |** Mean values (mm<sup>2</sup>) and standard deviation of the injured area by *A. niger* in mango fruit. ♦, samples infected with *A. niger* spores; ■, samples inoculated with sterile phosphate-buffered saline.

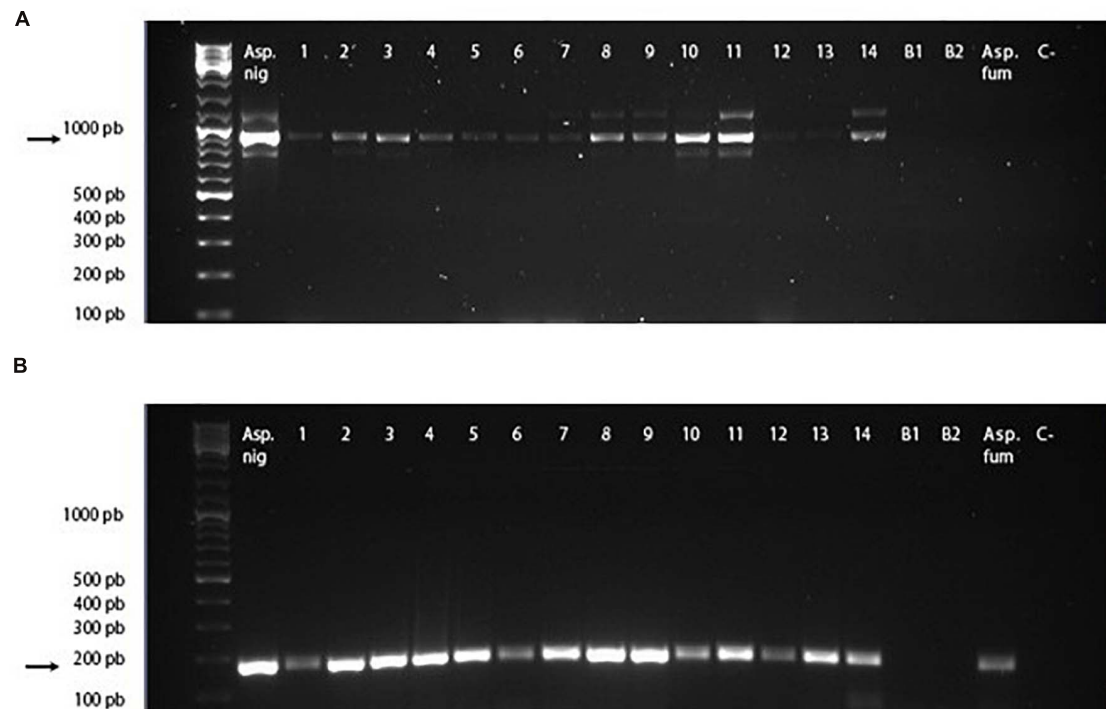


**FIGURE 4 |** cDNA PCR-amplified regions of Asp n gene. **(A)** Full cDNA gene amplicon using primers *Aspn3\_FW* and *Aspn3\_RV*. **(B)** Conserved cDNA gene region amplified using primers *CRPEROX\_FW* and *CRPEROX\_RV*. *Asp. Nig*, *Aspergillus niger* (positive control). Lines 1–14: samples of mangoes inoculated with spores of *A. niger*. B1 and B2: samples of mangoes inoculated with phosphate-buffered saline. *Asp. fum*, *Aspergillus fumigatus*. C- :PCR negative control.

to use the peroxiredoxin Asp n 3 as a secondary marker in the identification of the species of this genus and to study the phylogenetic relationships among species (Gautam et al., 2011; Heller and Tudzynski, 2011; Sharma, 2012).

The results presented in this work demonstrate that the Asp n 3 peroxiredoxin gene is an effective tool to identify *A. niger* and establish phylogenetic differences with other species from different taxa. The Asp n 3 peroxiredoxin gene was also demonstrated to be an effective tool to identify pathogenic *Aspergillus* of plant-based foods as well as to identify sources of fungal allergenic sources growing in plant foods.

Fungi from *Aspergillaceae* play diverse and significant roles in biotechnology and human, animal, and plant pathology. Several genomes from *Aspergillaceae* have been studied, including the two iconic genera *Aspergillus* and *Penicillium*. However, their analysis does not fully reflect the diversity of the family. Understanding the evolution of technologically and medically significant fungi through their intrinsic features requires a robust phylogeny (Steenwyk et al., 2019). Other authors suggest that the conflicting results in the fungal classification are likely associated with various processes, such as incomplete lineage sorting, hybridization, or introgression as well as with analytical issues associated with poor taxon sampling (Yilmaz et al., 2014).

DNA markers such as ITS regions or conserved genes such as calmodulin, tubulin, or RNA polymerase are used to conduct molecular phylogenetic studies on *Aspergillus* species. Despite

the fact that phylogenetic trees based on single genes are prone to errors, such analyses are robust and have contributed to improving taxonomic systems (Bennett, 2010).

The alignment of genes coding for peroxiredoxin proteins (homologous to Asp n 3) allowed the construction of an Asp n 3-based neighbor-joining phylogenetic tree of species expressing this family of proteins. A monophyletic clade containing species belonging to Eurotiales can be observed. In turn, this group is divided into two differentiate clades, each one containing species belonging to *Aspergillaceae* and *Trichomonaceae*.

In agreement with other authors, *Aspergillus* forms a monophyletic clade closely related to *Penicillium* (*Aspergillaceae*) (Samson et al., 2014). Within this clade, *A. niger*, *A. nomius*, *A. clavatus*, *N. fisheri*, and *A. fumigatus* form the closest *Aspergillus* species subgroup from the phylogenetic point of view. On the other branch, *A. nidulans*, *A. terreus*, *A. flavus*, *Aspergillus oryzae*, *Penicillium citrinum*, *Penicillium chrysogenum*, and *Penicillium digitatum* complete a second subgroup of species within the *Aspergillaceae* monophyletic clade closely related to *Penicillium*. Both subgroups matched *Aspergillaceae*.

*Penicillium* (*Talaromyces*) *marneffei*, *Talaromyces stipitatus*, and *Ramsonia emersonii* form a polyphyletic group matching *Trichomonaceae*, differentiating from the monophyletic clade containing *Aspergillus* and *Penicillium* species.

Some authors suggest the transference of *Penicillium* subgenus *Biverticillium* to *Talaromyces*, and others separate *Ramsonia* from the other genera of *Trichomonaceae* using a combination



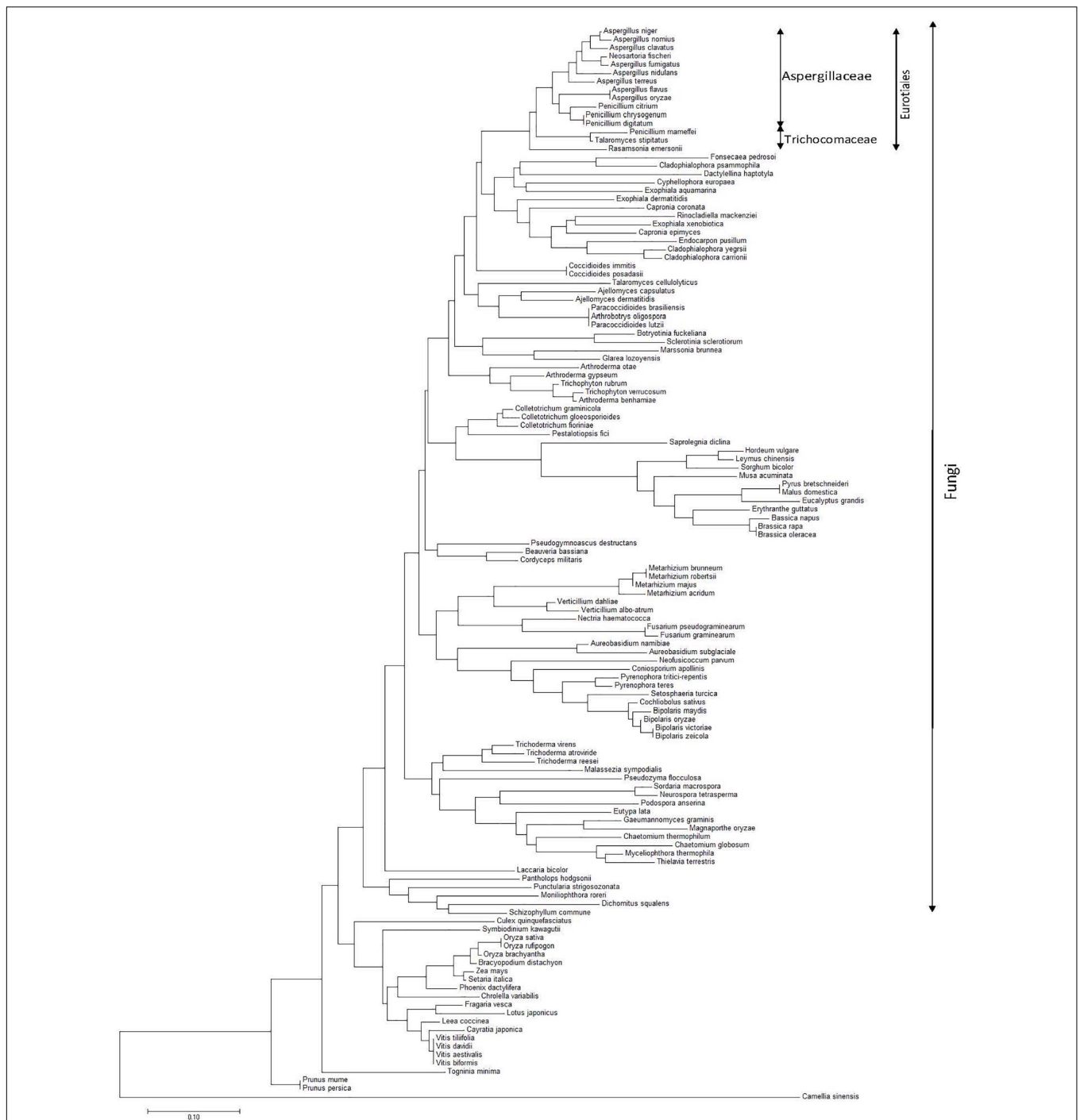


**FIGURE 5 |** Phylogenetic tree of the nearest neighborhood of representatives constructed on the basis of the nucleotide sequences of Asp n 3 homologs (peroxyredoxin proteins) encoding genes belonging to species from different kingdoms, with special accent on the fungi kingdom.

of phenotypic characters, extralite patterns, ITS, and partial calmodulin and b-tubulin sequences (Houbraken et al., 2012; Yilmaz et al., 2014).

The other monophyletic clade, including the species from *Fonsecaea pedrosoi* to *Cladophialophora carrionii*, is the nearest phylogenetic group to the clade that contains Eurotiales species.

This clade matches species belonging to Chaetothyriales. The results of this work suggest that Chaetothyriales is the closest related order to Eurotiales within the class Eurotiomycetes.

A phylogenetic analysis revealed a high level of divergence of Asp n 3 among filamentous fungi. The Asp n 3 peroxyredoxin DNA sequence is a marker able to identify *A. niger* species. The



use of a highly conserved internal nucleotide region makes it possible to detect, but not to identify, other *Aspergillus* species.

The alignment of peroxiredoxin nucleotides showed more than 86% identity among species from the *Aspergillus* genus, 81–84% identity when *Penicillium* species were included, and 76–80% identity when the alignment was extended to *Talaromyces* and *Ramsonia*, taking into account that all these genera belong to Eurotiales.

These results justify the detection of *Aspergillus* species, but not their identification, when only highly conserved regions are used. Species identification requires tools based on full gene sequences.

Previously, some authors demonstrated that cytochrome B coding genes or small heat shock protein coding genes were useful for the most accurate classification of fungi (Yokoyama et al., 2001; Wu et al., 2016). In our case, we demonstrate that the peroxiredoxin Asp n 3 can be used in the analysis of phylogeny, classification, and identification of aspergilli.

## CONCLUSION

The Asp n 3 DNA sequence is a reliable tool to detect and identify early fungal contamination by *Aspergillus* and postharvest damage in *M. indica* fruit. The use of conserved segments of the Asp n 3 gene or its entire sequence allows us to detect

phylogenetically closely related species within the Aspergilaceae family or to identify species-specific contaminating fungi.

## DATA AVAILABILITY STATEMENT

The original contributions presented in the study are included in the article/supplementary material, further inquiries can be directed to the corresponding author.

## AUTHOR CONTRIBUTIONS

JM, IP, and ES designed the experiments. AN and MG performed the experiments. AN, AV-d-B, and PS conducted bioinformatics for the amplicon sequencing results and phylogenetic studies. JM and IP wrote the manuscript. ES formatted the document. All the authors reviewed and revised the manuscript.

## FUNDING

This work was supported by the Government of the Basque Country, Department of Research and Education, Linguistic Policy and Culture in the Program: Grants for University Research Groups (project IT-1043-16).

## REFERENCES

- Al-Hindi, R. R., Al-Najada, A. R., and Mohamed, S. A. (2011). Isolation and identification of some fruit spoilage fungi: screening of plant cell wall degrading enzymes. *Afr. J. Microbiol. Res.* 5, 443–448. doi: 10.5897/AJMR10.896
- Amalaradjou, M. A. R., and Venkitanarayanan, K. (2008). "Chapter X: detection of *Penicillium*, *Aspergillus* and *Alternaria* species in fruits and vegetables," in *Mycotoxins in Fruits and Vegetables*, eds R. Barkai-Golan and N. Paster (Oxford: Academic Press, Elsevier), 225–247. doi: 10.1016/B978-0-12-374126-4.00010-3
- Battilani, P., Barbano, C., and Logrieco, A. (2008). "Chapter I: risk assessment and safety evaluation of mycotoxins in fruits," in *Mycotoxins in Fruits and Vegetables*, eds R. Barkai-Golan and N. Paster (Oxford: Academic Press, Elsevier), 1–26. doi: 10.1016/B978-0-12-374126-4.00001-2
- Bennett, J. W. (2010). "An overview of the genus *Aspergillus*," in *Aspergillus: Molecular Biology and Genomics*, ed. K. Gomi Machida (Portland, OR: Academic Press), 1–17.
- Blaxter, M. (2003). Counting angels with DNA. *Nature* 421, 1–3. doi: 10.1016/j.simyco.2014.09.001
- Blumenthal, C. Z. (2004). Production of toxic metabolites in *A. niger* and *T. reesei*: justification of mycotoxin testing in food grade enzyme preparations derived from the three fungi. *Regul. Toxicol. Pharmacol.* 39, 214–228. doi: 10.1016/j.yrtph.2003.09.002
- Chen, X. L., Wang, Z., and Liu, C. A. (2016). Roles of peroxisomes in the rice blast fungus. *BioMed. Res. Int.* 2016:9343417. doi: 10.1155/2016/9343417
- Christensen, M., and Tuthill, D. E. (1986). "Aspergillus: an overview," in *Advances in Penicillium and Aspergillus Systematics*. NATO ASI Series (Series A: Life Sciences), eds R. A. Samson and J. I. Pitt (Boston, MA: Springer), 102.
- Chruszcz, M., Chapman, M. D., Osinski, T., Solberg, R., Demas, M., Porebski, P. J., et al. (2012). *Alternaria alternata* allergen, Alt a 1-a unique,  $\beta$ -barrel protein dimer exclusively found in fungi. *J. Allergy Clin. Immunol.* 130, 241–247. doi: 10.1016/j.jaci.2012.03.047
- Cramer, C., Hemmann, S., Ismail, C., Menz, G., and Blaser, K. (1998). Disease-specific recombinant allergens for the diagnosis of allergic bronchopulmonary. *Int. Immunol.* 10, 1211–1216. doi: 10.1093/intimm/10.8.1211
- Dijksterhuis, J. (2019). Fungal spores: highly variable and stress-resistant vehicles for distribution and spoilage. *Food Microbiol.* 81, 2–11. doi: 10.1016/j.fm.2018.11.006
- Fitzpatrick, D. A., Logue, M. E., Stajich, J. E., and Butler, G. (2006). A fungal phylogeny based on 42 complete genomes derived from super tree and combined gene analysis. *BMC Evol. Biol.* 6, 99–113. doi: 10.1186/1471-2148-6-99
- Gabriel, M. F., Martínez, J., and Postigo, I. (2016a). "Chapter XIII: fungal allergens: recent trends and future prospects," in *Medical Mycology: Current Trends and Future Prospects*, eds M. Razzaghi-Abyaneh, M. Shams-Ghahfarokhi, and M. Rai (Boca Raton, FL: CRC Press), 315–333.
- Gabriel, M. F., Postigo, I., Gutiérrez, A., Suñén, E., Tomaz, C. T., and Martínez, J. (2015). Development of a PCR-based tool for detecting immunologically relevant Alt a 1 and Alt a 1 homologue coding sequences. *Med. Mycol.* 53, 636–642. doi: 10.1093/mmy/myv022
- Gabriel, M. F., Postigo, I., Tomaz, C. T., and Martínez, J. (2016b). *Alternaria alternata* allergens: markers of exposure, phylogeny and risk of fungi-induced respiratory allergy. *Environ. Int.* 89–90, 71–80. doi: 10.1016/j.envint.2016.01.003
- Gabriel, M. F., Uriel, N., Teifoori, F., Postigo, I., Suñén, E., and Martínez, J. (2017). The major *Alternaria alternata* allergen, Alt a 1: a reliable and specific marker of fungal contamination in citrus fruit. *Int. J. Food Microbiol.* 257, 26–30. doi: 10.1016/j.jifoodmicro.2017.06.006
- Gautam, A. K., Sharma, S., Avasthi, S., and Bhadauria, R. (2011). Diversity, pathogenicity and toxicology of *A. niger*: an important spoilage fungi. *Res. J. Microbiol.* 6, 270–280. doi: 10.3923/jm.2011.270.280
- Harper, A. F., Leuthaeuser, J. B., Babbitt, P. C., Morris, J. H., Ferrin, T. E., Poole, L. B., et al. (2017). An atlas of peroxiredoxins created using an active site profile-based approach to functionally relevant clustering of proteins. *PLoS Comput. Biol.* 13:e1005284. doi: 10.1371/journal.pcbi.1005284
- Heller, J., and Tudzynski, P. (2011). Reactive oxygen species in phytopathogenic fungi: signaling, development, and disease. *Annu. Rev. Phytopathol.* 49, 369–390. doi: 10.1146/annurev-phyto-072910-095355

- Hemmans, S., Blaser, K., and Cramer, R. (1997). Allergens of *Aspergillus fumigatus* and *Candida boidinii* share IgE-binding epitopes. *Am. J. Respir. Crit. Care Med.* 156, 1956–1962. doi: 10.1164/ajrccm.156.6.9702087
- Houbraken, J., Spierenburg, H., and Frisvad, J. C. (2012). *Rasamsonia*, a new genus comprising thermotolerant and thermophilic *Talaromyces* and *Geosmithia* species. *AvL* 101, 403–421. doi: 10.1007/s10482-011-9647-1
- Kasprzyk, I. (2008). Aeromycology main research fields of interest during the last 25 years. *Ann. Agric. Environ. Med.* 15, 1–7.
- Kim, W. B., Park, C., Cho, S. Y., Chun, H. S., and Lee, D. G. (2020). Development of multiplex real-time PCR for rapid identification and quantitative analysis of *Aspergillus* species. *PLoS One* 15:e0229561. doi: 10.1371/journal.pone.0229561
- Lubna, Asaf, S., Hamayun, M., Gul, H., Lee, I.-J., and Hussain, A. (2018). *Aspergillus niger* CSR3 regulates plant endogenous hormones and secondary metabolites by producing gibberellins and indoleacetic acid. *J. Plant Interact.* 1, 100–111. doi: 10.1080/17429145.2018.1436199
- Mahfooz, S., Singh, S. P., Mishra, N., and Mishra, A. (2017). A comparison of microsatellites in phytopathogenic *Aspergillus* species in order to develop markers for the assessment of genetic diversity among its isolates. *Front. Microbiol.* 8:1774. doi: 10.3389/fmicb.2017.01774
- Matricardi, P. M., Kleine-Tebbe, J., Hoffmann, H. J., Valenta, R., and Ollert, M. (2016). *Molecular Allergy user's Guide*. European Academy of Allergy and Clinical Immunology. Hoboken, NJ: John Wiley & Sons.
- Palejwala, V. A., Patki, C. K., Bhatt, S. V., and Modi, V. V. (1987). Post-harvest spoilage of mangoes by *Aspergillus niger*. *Int. J. Food Microbiol.* 5, 111–116. doi: 10.1016/0168-1605(87)90028-6
- Perrone, G., Susca, A., Cozzi, G., Ehrlich, K., Varga, J., Frisvad, J. C., et al. (2007). Biodiversity of *Aspergillus* species in some important agricultural products. *Stud. Mycol.* 59, 53–66. doi: 10.3114/sim.2007.59.07
- Pertile, G., Lamorski, K., Bieganski, A., Boguta, P., Brzezińska, M., Polakowski, C., et al. (2021). Immediate effects of the application of various fungal strains with urea fertiliser on microbiome structure and functions and their relationships with the physicochemical parameters of two different soil types. *Appl. Soil Ecol.* 163:103972. doi: 10.1016/j.apsoil.2021.103972
- Raper, K. B., and Fennell, D. I. (1965). *The Genus Aspergillus*. Baltimore, MD: Williams and Wilkins. doi: 10.1126/science.150.3697.736-a
- Rhee, S. G. (2016). Overview on peroxiredoxins. *Mol. Cells* 39, 1–5. doi: 10.14348/molcells.2016.2368
- Sáenz-de-Santamaría, M., Postigo, I., Gutiérrez-Rodríguez, A., Cardona, G., Guisantes, J. A., Asturias, A., et al. (2006). The major allergen of *Alternaria alternata* (Alt a 1) is expressed in other members of the Pleosporaceae family. *Mycoses* 49, 91–95. doi: 10.1111/j.1439-0507.2006.01195.x
- Samson, R. A., Houbraken, J., Thrane, U., Frisvad, J. C., and Andersen, B. (2010). *Food and Indoor Fungi*. CBS Laboratory Manual Series. Utrecht: CBS-KNAW Fungal Diversity Centre.
- Samson, R. A., Visagie, C. M., Houbraken, J., Hong, S. B., Hubka, V., Klaassen, C. H. W., et al. (2014). Phylogeny, identification and nomenclature of the genus *Aspergillus*. *Stud. Mycol.* 78, 141–173. doi: 10.1016/j.simyco.2014.07.004
- Schoch, C. L., Seifert, K. A., Huhndorf, S., Robert, V., Spouge, J. L., Levesque, C. A., et al. (2012). Nuclear ribosomal internal transcribed spacer (ITS) region as a universal DNA barcode marker for fungi. *Proc. Natl. Acad. Sci. U.S.A.* 109, 6241–6246. doi: 10.1073/pnas.1117018109
- Sharma, R. (2012). Pathogenicity of *Aspergillus niger* in plants. *CJM* 1, 47–45.
- Shen, Y., Nie, J., Kuang, L., Zhang, J., and Li, H. (2020). DNA sequencing, genomes and genetic markers of microbes on fruit and vegetables. *Microb. Biotech.* 14, 323–362. doi: 10.1111/1751-7915.13560
- Simon-Nobbe, B., Denk, U., Pöll, V., Rid, R., and Breitenbach, M. (2008). The Spectrum of Fungal Allergy. *Int. Arch. Allergy Immunol.* 145, 58–86. doi: 10.1159/000107578
- Steenwyk, J. L., Shen, X. X., Lind, A. L., Goldman, G. H., and Rokas, A. (2019). A robust phylogenomic time tree for biotechnologically and medically important fungi in the genera *Aspergillus* and *Penicillium*. *mBio* 10:e00925-19. doi: 10.1128/mBio.00925-19
- Tamura, K., Dudley, J., Nei, M., and Kumar, S. (2007). MEGA4: molecular evolutionary genetics analysis (MEGA) software version 4.0. *Mol. Biol. Evol.* 24, 1596–1599. doi: 10.1093/molbev/msm092
- Tian, J., Wang, Y., Zeng, H., Li, Z., Zhang, P., Tessema, A., et al. (2015). Efficacy and possible mechanisms of perillaldehyde in control of *Aspergillus niger* causing grape decay. *Int. J. Food Microbiol.* 202, 27–34. doi: 10.1016/j.ijfoodmicro.2015.02.022
- Tsang, C. C., Tang, J. Y. M., Lau, S. K. P., and Woo, P. C. Y. (2018). Taxonomy and evolution of *Aspergillus*, *Penicillium* and *Talaromyces* in the omics era. Past, present and future. *Comp. Struct. Biotech. J.* 16, 197–210. doi: 10.1016/j.csbj.2018.05.003
- Visagie, C. M., Houbraken, J., Frisvad, J. C., Hong, S. B., Klaassen, C. H. W., Perrone, G., et al. (2014). Identification and nomenclature of the genus *Penicillium*. *Stud. Mycol.* 78, 343–371.
- Wu, J., Wang, M., Zhou, L., and Yu, D. (2016). Small heat shock proteins, phylogeny in filamentous fungi and expression analyses in *Aspergillus nidulans*. *Gene* 575, 675–679. doi: 10.1016/j.gene.2015.09.044
- Yilmaz, N., Visagie, C. M., Houbraken, J., Frisvad, J. C., and Samson, R. A. (2014). Polyphasic taxonomy of the genus *Talaromyces*. *Stud. Mycol.* 78, 175–341. doi: 10.1016/j.simyco.2014.08.001
- Yokoyama, K., Wang, L., Miyaji, M., and Nishimura, K. (2001). Identification, classification and phylogeny of the *Aspergillus* section *Nigri* inferred from mitochondrial cytochrome b gene. *FEMS Microbiol. Lett.* 200, 241–246. doi: 10.1111/j.1574-6968.2001.tb10722.x

**Conflict of Interest:** The authors declare that the research was conducted in the absence of any commercial or financial relationships that could be construed as a potential conflict of interest.

Copyright © 2021 Martínez, Nevado, Suñén, Gabriel, Vélez-del-Burgo, Sánchez and Postigo. This is an open-access article distributed under the terms of the Creative Commons Attribution License (CC BY). The use, distribution or reproduction in other forums is permitted, provided the original author(s) and the copyright owner(s) are credited and that the original publication in this journal is cited, in accordance with accepted academic practice. No use, distribution or reproduction is permitted which does not comply with these terms.



# Development of Moore Swab and Ultrafiltration Concentration and Detection Methods for *Salmonella* Typhi and *Salmonella* Paratyphi A in Wastewater and Application in Kolkata, India and Dhaka, Bangladesh

## OPEN ACCESS

### Edited by:

Xiyang Wu,  
Jinan University, China

### Reviewed by:

Shabarinath Srikumar,  
United Arab Emirates University,  
United Arab Emirates  
Kien-Pong Yap,  
University of Malaya, Malaysia

### \*Correspondence:

Pengbo Liu  
pliu5@emory.edu

† These authors have contributed  
equally to this work and share senior  
authorship

### Specialty section:

This article was submitted to  
Food Microbiology,  
a section of the journal  
Frontiers in Microbiology

Received: 22 March 2021

Accepted: 23 June 2021

Published: 15 July 2021

### Citation:

Liu P, Ibaraki M, Kapoor R,  
Amin N, Das A, Miah R,  
Mukhopadhyay AK, Rahman M,  
Dutta S and Moe CL (2021)  
Development of Moore Swab  
and Ultrafiltration Concentration  
and Detection Methods  
for *Salmonella* Typhi and *Salmonella*  
*Paratyphi* A in Wastewater  
and Application in Kolkata, India  
and Dhaka, Bangladesh.  
Front. Microbiol. 12:684094.  
doi: 10.3389/fmicb.2021.684094

Pengbo Liu<sup>1\*†</sup>, Makoto Ibaraki<sup>1</sup>, Renuka Kapoor<sup>1</sup>, Nuhu Amin<sup>2</sup>, Abhishek Das<sup>3</sup>,  
Rana Miah<sup>2</sup>, Asish K. Mukhopadhyay<sup>3</sup>, Mahbubur Rahman<sup>2</sup>, Shanta Dutta<sup>3</sup> and  
Christine L. Moe<sup>1†</sup>

<sup>1</sup> Center for Global Safe Water, Sanitation, and Hygiene, Rollins School of Public Health, Emory University, Atlanta, GA, United States, <sup>2</sup> Environmental Interventions Unit, Infectious Disease Division, International Centre for Diarrhoeal Disease, Bangladesh (ICDDR,B), Dhaka, Bangladesh, <sup>3</sup> Indian Council of Medical Research (ICMR), National Institute of Cholera and Enteric Diseases (NICED), Kolkata, India

Enteric fever is a severe systemic infection caused by *Salmonella enterica* serovar Typhi (ST) and *Salmonella enterica* serovar Paratyphi A (SPA). Detection of ST and SPA in wastewater can be used as a surveillance strategy to determine burden of infection and identify priority areas for water, sanitation, and hygiene interventions and vaccination campaigns. However, sensitive and specific detection of ST and SPA in environmental samples has been challenging. In this study, we developed and validated two methods for concentrating and detecting ST/SPA from wastewater: the Moore swab trap method for qualitative results, and ultrafiltration (UF) for sensitive quantitative detection, coupled with qPCR. We then applied these methods for ST and SPA wastewater surveillance in Kolkata, India and Dhaka, Bangladesh, two enteric fever endemic areas. The qPCR assays had a limit of detection of 17 equivalent genome copies (EGC) for ST and 25 EGC for SPA with good reproducibility. In seeded trials, the Moore swab method had a limit of detection of approximately 0.05–0.005 cfu/mL for both ST and SPA. In 53 Moore swab samples collected from three Kolkata pumping stations between September 2019 and March 2020, ST was detected in 69.8% and SPA was detected in 20.8%. Analysis of sewage samples seeded with known amount of ST and SPA and concentrated via the UF method, followed by polyethylene glycol precipitation and qPCR detection demonstrated that UF can effectively recover approximately 8, 5, and 3 log<sub>10</sub> cfu of seeded ST and SPA in 5, 10, and 20 L of wastewater. Using the UF method in Dhaka, ST was detected in 26.7% (8/30) of 20 L drain samples with a range of 0.11–2.10 log<sub>10</sub> EGC per 100 mL and 100% (4/4) of 20 L canal samples with a range

of 1.02–2.02 log<sub>10</sub> EGC per 100 mL. These results indicate that the Moore swab and UF methods provide sensitive presence/absence and quantitative detection of ST/SPA in wastewater samples.

**Keywords:** *Salmonella Typhi*, *Salmonella Paratyphi A*, Moore swab, ultrafiltration, wastewater, surveillance

## INTRODUCTION

Typhoid and Paratyphoid fevers are leading causes of severe febrile disease in low-income countries with poor access to safe water, food, and sanitation (Dewan et al., 2013). The etiologic agents, *S. Typhi* (ST), and *S. Paratyphi A* (SPA), are human-specific pathogens transmitted through consumption of food and water contaminated by feces of an acutely or chronically infected person (Crump, 2019). Previous studies have shown that food and water contaminated with human feces are associated with typhoid and paratyphoid outbreaks (Usera et al., 1995; Kobayashi et al., 2016). In endemic urban settings, co-location of sewer pipes and poorly maintained water supply pipes facilitate cross-contamination and transmission of ST through the water system. Typhoid fever outbreaks (Egoz et al., 1988; Usera et al., 1995) have been associated with contaminated piped water and sewage-irrigated produce, emphasizing the importance of studying these pathways of disease transmission.

Detection of ST and SPA in drinking water, irrigation water, and environmental waters has usually been attempted in association with outbreak investigations (Murphy et al., 2017; Sikorski and Levine, 2020) and assessing risk of waterborne typhoid fever transmission in endemic settings (Andrews et al., 2020). Recently, we and other investigators have proposed detection of ST and SPA in wastewater from known catchment populations as a strategy to determine the burden of typhoid and paratyphoid fever in areas where clinic-based surveillance has limited sensitivity or is not feasible (Matrajt et al., 2020; Wang et al., 2020). However, environmental surveillance for typhoid and paratyphoid fever requires sensitive and specific methods to detect ST/SPA in wastewater, including samples where low pathogen concentrations are expected. It is usually necessary to concentrate ST/SPA in environmental samples in order to increase the sensitivity of detection. A wide range of methods have been used to concentrate bacterial pathogens from a variety of environmental waters (Matrajt et al., 2020). Among these methods, Moore swabs and ultrafiltration (UF) are two important and distinct concentration methods that have been shown to be effective in recovering ST from water and wastewater (Sears et al., 1984). The Moore swab was first introduced for *Salmonella* detection from sewage in 1948 in England during a paratyphoid epidemic (Sikorski and Levine, 2020). Subsequently, this method has been successfully used to isolate *Vibrio Cholerae* (Barrett et al., 1980), poliovirus (Tao et al., 2010) and *Burkholderia pseudomallei* (Vongphayloth et al., 2012) from sewage. In contrast to the Moore swab method that only shows the presence or absence of a target pathogen, UF is a quantitative method that can simultaneously concentrate multiple pathogens from large volumes of water or wastewater (Lindquist et al., 2007; Liu et al., 2012; McEgan et al., 2013), and we recently reported the application of this

method to detect *S. Typhi* in wastewater samples (Amin et al., 2020). The Moore swab method offers several advantages over UF, specifically, Moore swabs are inexpensive, simple to use, and do not require collecting and transporting large volume samples of water or wastewater. However, UF can provide quantitative results with greater sensitivity which are valuable for microbial risk assessment or estimating infection prevalence (Amin et al., 2020).

The ability to detect and quantify ST/SPA in the environment is critical for monitoring and controlling transmission particularly in urban settings in low- and middle-income countries. Historically, culture-based isolation and identification methods are considered the gold standard because infectious bacteria can be detected. However, culture of *S. Typhi* from environmental samples is challenging (Antillon et al., 2018). Alternatively, PCR and qPCR technologies have been widely used to rapidly detect and quantify ST/SPA due to higher sensitivity and specificity and short turnaround time. Limitations of molecular detection methods include the inability to distinguish between infectious and non-infectious ST/SPA cells, and the presence of PCR inhibitors in environmental matrices in samples that can potentially lead to an underestimation of the target nucleic acid or false negative results.

The overall goal of this study was to develop a qualitative and a quantitative method for ST and SPA detection in wastewater and apply these methods to detect ST and SPA in two typhoid fever endemic areas. The specific goals were to: (1) develop real-time qPCR methods with standard curves for detecting and quantifying ST and SPA DNA in sewage; (2) develop and validate Moore swab (qualitative) and UF concentration methods (quantitative); (3) apply the Moore swab method to detect ST/SPA in wastewater at three pumping stations in Kolkata, India; and (4) utilize the UF method to detect ST in drain and canal water samples in Dhaka, Bangladesh.

## MATERIALS AND METHODS

### Study Sites and Environmental Sample Collection

Wastewater collected from the WaterHub water reclamation facility on the Emory University campus between April 2019 and July 2020 were used for the Moore swab and UF methods development and validation studies in Atlanta. From April to October 2019, drain and canal water samples were collected in Mirpur, Dhaka, Bangladesh, a densely populated low-income area where residents live in compounds containing multiple families and the incidence of ST and SPA is high (Amin et al., 2020; Foster et al., 2021). Large volume (20 L) samples were collected and concentrated by UF as described below. In Kolkata, India,



Moore swabs were placed in three municipal sewage pumping stations between September 24, 2019 and March 19, 2020: (1) Palmer's Bridge station served Ward 55 with approximately 32,254 people; (2) Ambedkar station served Wards 66 and 108 with approximately 162,801 people; and (3) Topsia station served Wards 59 and 48 with approximately 90,698 people during the study period. The number of people served by the pumping stations was estimated by the 2011 census data of India (Office of the Registrar General & Census Commissioner MoHA, Government of India, 2011).

## ST and SPA Growth Conditions

ST (ATCC 19430) and SPA (ATCC 9150) cultures were prepared by overnight growth in LB (Luria-Bertani) broth at 37°C under shaking conditions to obtain a final concentration of 10<sup>8</sup> cells/mL, followed by 10-fold serial dilutions in 1 × PBS (0.01 M, pH 7.4). One milliliter aliquots of the diluted culture containing 10<sup>8</sup>–100 cells were used for seeding experiments.

## ST and SPA DNA Standard Development

ST and SPA DNA were extracted from the overnight fresh culture, and the DNA concentration was measured using NanoDrop<sup>TM</sup> spectrophotometer (Thermo Fisher Scientific, Waltham, MA United States). The concentrations and equivalent genome copies (EGC) of the ST and SPA DNA were determined from the concentration (ng/μL), the lengths of fragments, the Avogadro constant, and the average weight of double-stranded base pairs (Equation 1).

$$\text{Number of EGC} = \frac{X \text{ ng} \times 6.0221 \times 10^{23} \text{ molecules/mole}}{(N \times 660 \frac{\text{g}}{\text{mole}}) \times 1 \times 10^9} \quad (1)$$

Where: X = amount of amplicon (ng)

N = length of dsDNA amplicon (ST = 4,809,037 bp; SPA = 4,581,797 bp)

6.0221 × 10<sup>23</sup> = Avogadro constant

660 g/mole = average mass of 1 bp dsDNA

The known EGCs for each standard were serially diluted, and a standard curve was incorporated in each real-time PCR assay. Ten-fold serial dilution of the standards was used to estimate the numbers of genome copies of the target pathogens in samples.

## Ultrafiltration Method Validation

Large volume wastewater samples (5–20 L) were seeded with known amounts of ST and SPA (either 8, 5, or 3 log<sub>10</sub> CFU), and then each sample was concentrated by hollow fiber ultrafiltration (Figure 1). The entire amount of the seeded wastewater sample was circulated through Polynephron<sup>TM</sup> Synthetic Hollow-Fiber Dialyzer (NIPRO Medical United States, Bridgewater, United States) using a peristaltic pump to achieve approximately 100 mL of retentate (concentrated sample) which was collected in a 500 mL bottle. Ultrafilter elution was then performed using 500 mL of PBS with 0.01% Tween 80, 0.01% sodium polyphosphate and 0.001% Antifoam Y-30 emulsion. The elution solution was recirculated for 5 min, and the final eluate was merged into the concentrated sample. After elution, the ultrafilter was backwashed using 250 mL of PBS with 0.5%

Tween 80, 0.01% sodium polyphosphate and 0.001% Antifoam Y-30 emulsion. The backwash fraction was added to the previous mixture of the concentrate and the eluate.

## ST and SPA Concentration Using Polyethylene Glycol (PEG)

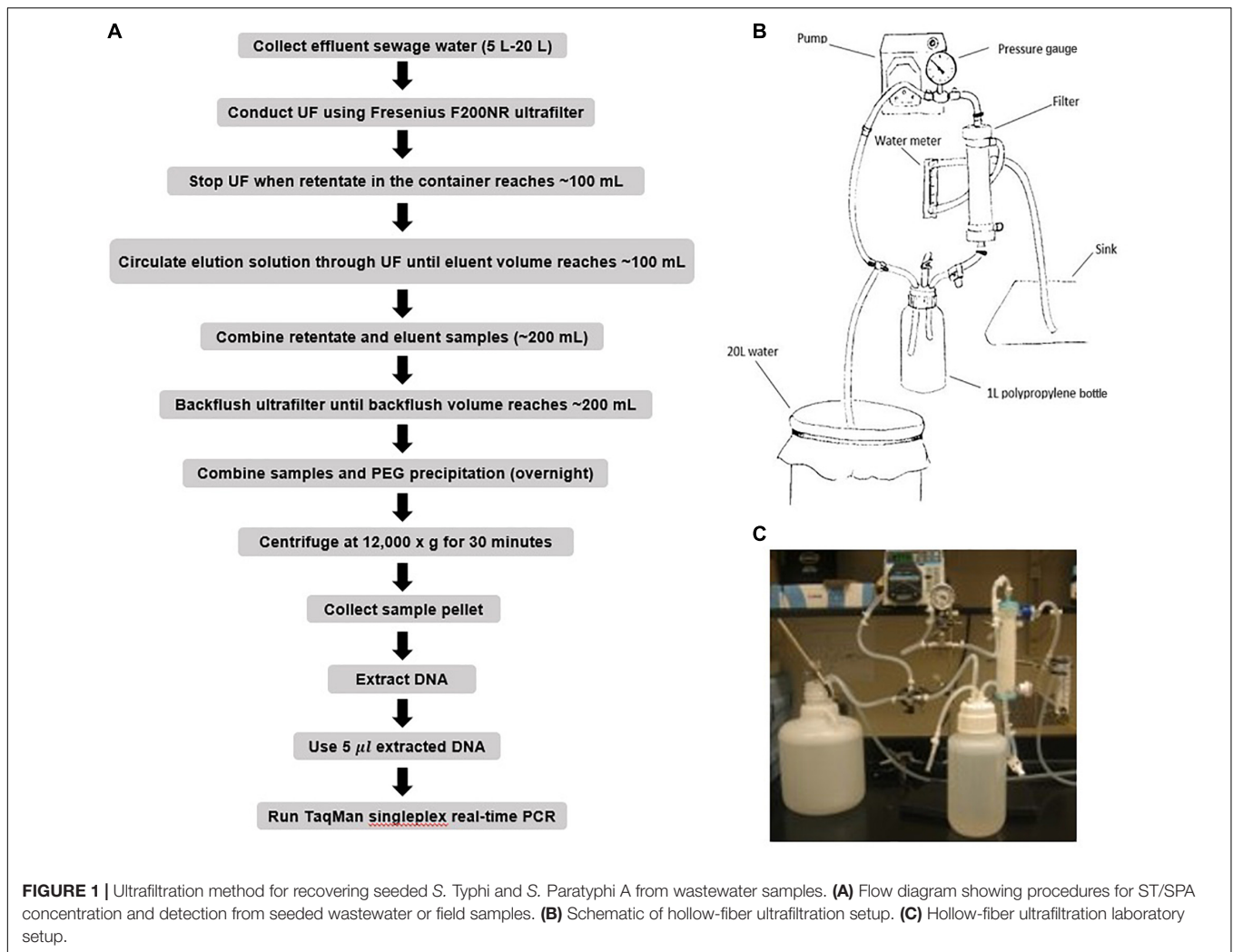
ST and SPA were precipitated from the merged retentate/eluate/backflush samples by adding 12% polyethylene glycol 8000 (Sigma, St. Louis, MO, United States), 0.9 mol sodium chloride, 1% bovine serum albumin (Sigma) and incubated and stirred overnight at 4°C. After centrifugation at 12,000 g for 60 min, the pellet was suspended in 1 mL of InhibitEX buffer provided by the QIAamp Fast DNA Stool Mini Kit (Qiagen, Valencia, CA, United States) prior to DNA extraction.

## Moore Swab Method Validation

Moore swabs (Figure 2B) were made by cutting pieces of cotton gauze to approximately 120 cm long × 15 cm wide and firmly tying the center with fishing line (W.C. Bradley/Zebco Holdings Inc., Tulsa OK). The swabs were sterilized before use by autoclaving. A Moore swab was placed in a plastic container filled with 2–20 L sewage collected from the Emory WaterHub, with the end of the fishing line attached to the outside of the container (Figure 2C). Sewage samples were seeded with either 50, 20, 10, 5, 0.05, or 0.005 cfu/mL of ST and SPA cells. The swab was submerged in the sewage to trap the ST and SPA cells while stirred continuously with an overhead spatula for 24 h as shown in Figure 2C. The swabs were then transferred to 450 mL of universal pre-enrichment broth (EPA, Standard Analytical Protocol for *Salmonella* Typhi in Drinking Water) and incubated at 37°C for 24 h with shaking. Then, a 20 mL volume of the pre-enrichment broth was filtered through a 0.45 μm filter and subjected to DNA extraction as described below after the addition of 1 mL of InhibitEX buffer (Figure 2A).

## ST/SPA DNA Extraction

For each sample or blank control, 1 mL of the final sample suspension, mixed with the InhibitEX buffer, was transferred into a 2 mL microcentrifuge tube. For membrane filtered samples and controls, microcentrifuge tubes with the filter and 1 mL of InhibitEX buffer were used. After 1 min of vortexing, the solution was centrifuged at maximum speed for 2–3 min, and the suspension was incubated at 95°C for 5 min, followed by full speed microcentrifugation for 15 s to pellet the sample particles. Subsequently, 600 μL of the supernatant was transferred into a 2 mL microcentrifuge tube containing 25 μL proteinase K, and then 600 μL of buffer AL was added. After vortexing for 15 s, the sample was incubated at 70°C for 10 min, and 600 μL of 100% ethanol was added to the lysate. A 600 μL volume of lysate was applied to a single QIAamp Mini column (Qiagen, Cat. # 51604, Hilden, Germany), and the column was centrifuged at full speed for 1 min. This procedure was repeated two additional times with the same column in order to use up all of the lysate. Finally, DNA was eluted from the column with 150 μL of the supplied elution



buffer. The extracted DNA samples were aliquoted and stored at  $-80^{\circ}\text{C}$  until analyzed by qPCR.

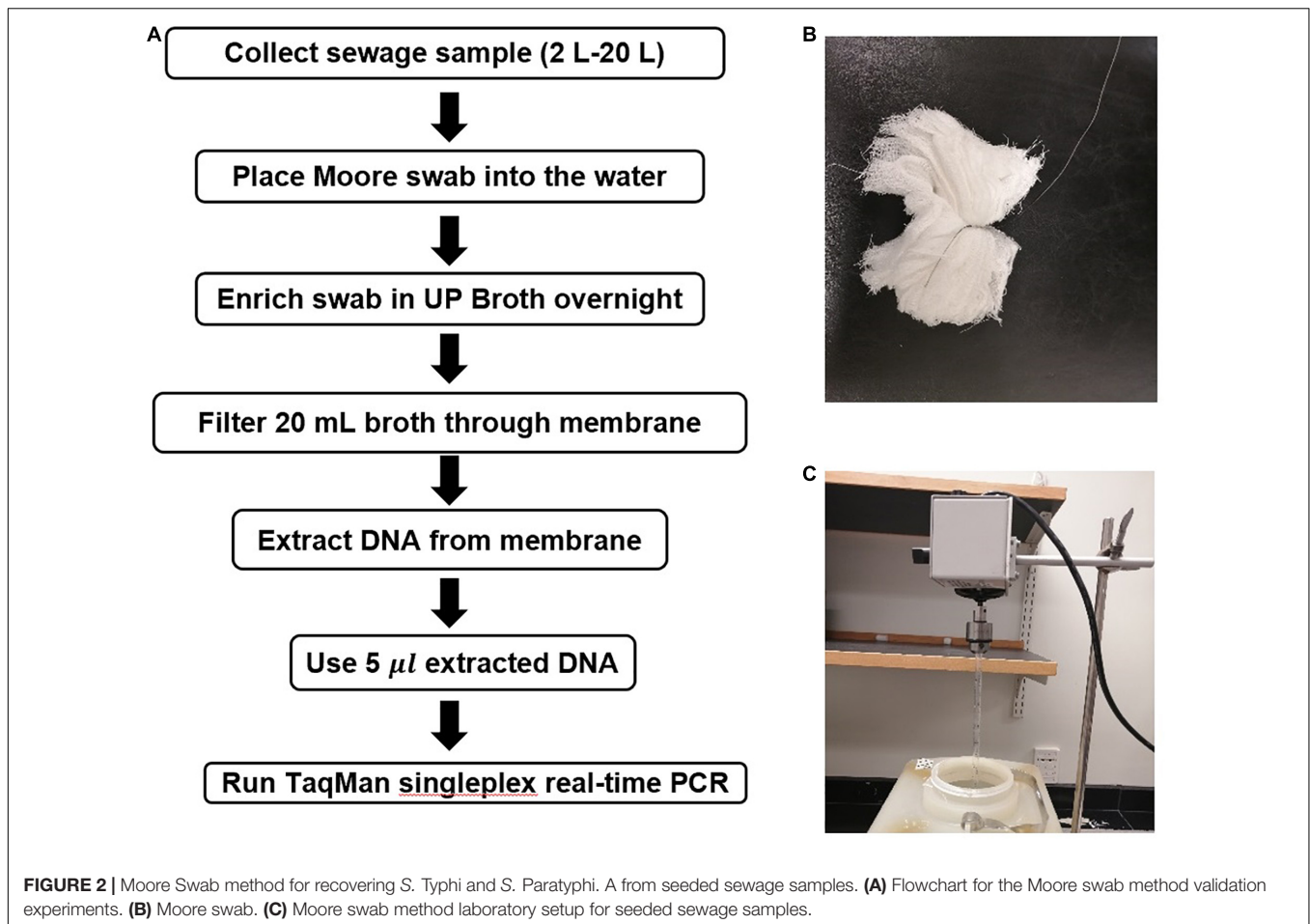
## TaqMan Singleplex Real–Time PCR for Detection of ST and SPA DNA

Quantitative singleplex real-time PCR assays for ST and SPA detection were performed using a Bio-Rad CFX96 thermal cycler (Bio-Rad Laboratories, Inc., Berkeley, CA). The SPA PCR primers and probe described by Karkey et al. (2016) were used for these laboratory assay evaluation experiments. For SPA detection in Moore swab samples in Kolkata, newly developed primers and probe targeting the intergenic region SSPAI (between SSPA1723a and SSPA1724) were used, and their sequences are as follows; SPA2RK\_F: 5'-ACCATCCGCAGGACAAATC-3'; SPA2RK\_R: 5'-GGGAGATTACTGATGGAGAGATTAC-3'; SPA2RK\_Probe: 5'-Cy5-AGAG TGCAAGT GGAGTGCCTCAAA-BHQ2-3'. For ST detection, two sets of primers/probe were used: (1) the primers/probe described by Karkey et al. (2016) for the samples concentrated by UF in Dhaka, and (2) a newly designed ST primers/probe set for the method validation work in Dr. Moe's

lab and the Moore swab samples in Kolkata. The newly designed ST primers/probe targeted the ST *stgA* gene (codes for putative fimbrial subunit protein) and the sequences are as follows: ST2RK\_F (forward): 5'-TATCGGCAACCCTGCTAATG-3'; ST2RK\_R (reverse) 5'-TATCCGCGCGG TTGTAAAT-3'; ST2RK\_Probe 5' FAM-CCATTACAG CATCTGGCGTAGCGA-BHQ1-3'. PCR reactions were performed in 25  $\mu\text{L}$  volumes consisting of 2  $\times$  Bio-Rad iQ power mix buffer (Bio-Rad, Hercules, CA) including 200  $\mu\text{M}$  dNTPs, 12 mM  $\text{Mg}^{2+}$ , 1 U iTaq DNA polymerase, 400 nM of each primer, 200 nM of each probe, and 5  $\mu\text{L}$  of template DNA or negative control. The amplification procedure consisted of a preliminary denaturation step at  $95^{\circ}\text{C}$  for 3 min and 45 cycles of  $95^{\circ}\text{C}$  for 30 s,  $60^{\circ}\text{C}$  for 30 s, and  $72^{\circ}\text{C}$  for 30 s. Fluorescence was collected at the annealing steps during the last cycles. To quantitatively detect equivalent genome copies of each pathogen in the samples, a 10-fold serial dilution of standards was added to each set of assay plates.

## Data Analysis

ST and SPA concentrations in each sample were estimated by interpolation of the mean Ct values from duplicate wells to



the standard curve, generated by 10-fold series diluted ST and SPA DNA standards, and the wastewater concentration factor. The quantification was expressed as  $\log_{10}$  EGC per 100 mL wastewater. Experiments evaluating the limit of detection of the Moore swab and UF concentration method were repeated three times for each volume and reported seeding level. Experiments for assessing ST and SPA recovery efficiencies were also repeated three times for each volume and seeding level. The number of equivalent genome copies in each test sample ( $N_{sample}$ ) was estimated based on the linear regression of  $\log_{10}(N_{sample})$  vs. Ct values using Equation 2. The amplification efficiency was estimated in each real-time PCR run using the slope  $m$  of the standard curve (Equation 3).

$$Ct_{observed} = m \times \log_{10}(N_{sample}) + b \quad (2)$$

$$E = 10^{(-\frac{1}{m})} - 1 \quad (3)$$

Where:  $m$  = slope

$N_{sample}$  = equivalent genome copies in sample

$b$  = intercept

$E$  = efficiency

## RESULTS

### Performance of ST and SPA qPCR Assays and DNA Standards

Two singleplex TaqMan real-time qPCR assays were evaluated for the detection of ST and SPA species using primers/probe previously described by Karkey et al. (2016). To evaluate the analytical sensitivity of the two qPCR assays, DNA from ST strain (ATCC 19430) and SPA strain (ATCC 9150), ranging from  $1.7 \times 10^4$  to 17 EGCs for ST, and  $2.5 \times 10^4$  to 25 EGC for SPA per reaction, were tested. Quantitative detection was achieved in the range of template DNA concentrations and the Ct values with  $R^2$  (coefficient of determination) between 0.98–1.00 for ST and 0.97–0.99 for SPA (Table 1 and Figure 3). The limit of detection was 17 EGC per reaction for ST and 25 EGC per reaction for SPA. The qPCR efficiency was between 76.3–127.9% for ST and 81.9–99.0% for SPA. The assay coefficient of variation (CV) was calculated by measuring the variation in the Ct values separately for the high ( $4-\log_{10}$ ) and low concentrations ( $1-\log_{10}$ ) in the range of standard concentrations in three replicate experiments on different days. The inter-assay CVs of the high and low ST concentrations from three replicate experiments ranged from 1.81 to 2.89%, respectively, whereas

**TABLE 1** | Performance of *S. Typhi* and *S. Paratyphi* qPCR assays<sup>†</sup> and DNA standards.

Pathogen	Strain	qPCR replicates	Efficiency (%)	R <sup>2</sup>	LOD* (EGC)	High concn. CV# (%)	Low concn. CV (%)
ST	ATCC 19430	3	76.3–127.9	0.98–1.00	17	1.81	2.89
SPA	ATCC 9150	3	81.9–99.0	0.97–0.99	25	1.59	2.08

<sup>†</sup>Using primers/probes described by Karkey et al. (2016).

\*Limit of detection.

#Coefficient of variation  $CV = \frac{\sigma}{\mu}$ ;  $\sigma$ : standard deviation;  $\mu$ : mean.

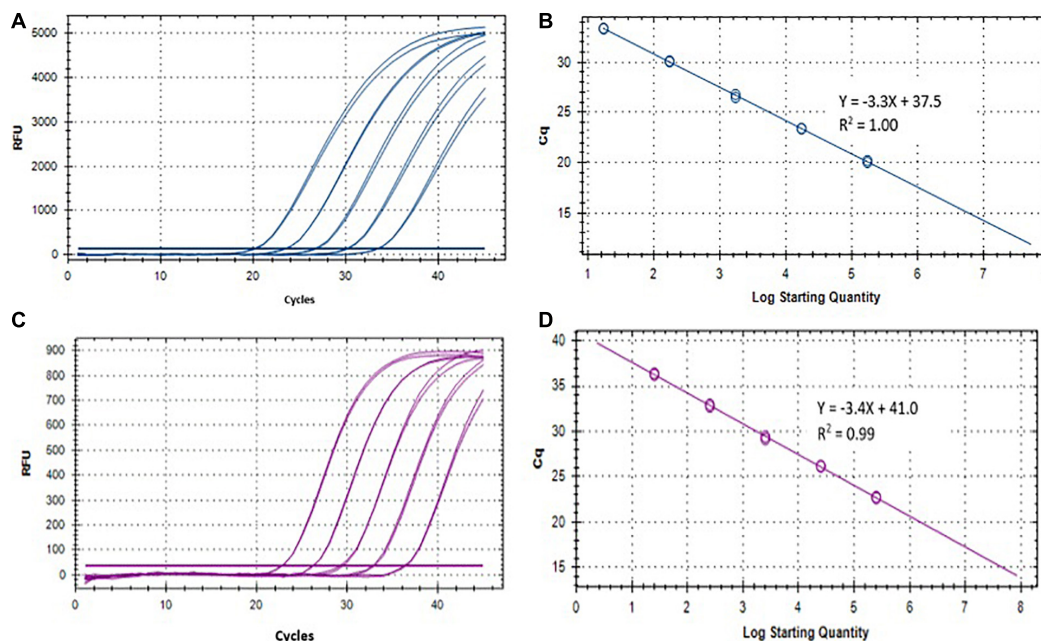


**FIGURE 3** | Performance of *S. Typhi* and *S. Paratyphi* A qPCR assays described by Karkey et al. (2016) and DNA standards. **(A)** Amplification of 10-fold serially diluted *S. Typhi* DNA standard. **(B)** Standard curve of *S. Typhi* DNA. **(C)** Amplification of 10-fold serially diluted *S. Paratyphi* A DNA standard. **(D)** Standard curve of *S. Paratyphi* A DNA.

the inter-assay CVs of the high and low SPA concentrations were 1.59 and 2.08%, respectively (Table 1). These results demonstrated that both ST and SPA qPCR assays were sensitive and reproducible.

### Limit of Detection of Moore Swabs for Recovering Seeded ST and SPA in Different Volumes of Sewage Samples

To determine the applicability and limit of detection of the Moore swab method and qPCR for the detection of ST and SPA in wastewater, samples of wastewater were collected from the Emory WaterHub and seeded with known concentrations (50, 20, 10, 5, 0.05, and 0.005 cfu/mL) of ST and SPA. When both ST and SPA were seeded at high concentrations (50, 20, 10, and 5 cfu/mL), all replicate experiments showed positive qPCR results. When the seeding level was reduced to 0.05 cfu/mL, ST was detected in all three replicate experiments, but SPA was only detected in two of the three replicate experiments. When the seeding level was further reduced to 0.005 cfu/mL, both

**TABLE 2** | Limit of detection of Moore swab method for recovering ST and SPA seeded into different volumes of sewage samples.

Sewage volume (L)	Seeding level (cfu/mL)	ST* positive swabs/total swabs	SPA# positive swabs/total swabs
2	50	3/3	3/3
5	20	3/3	3/3
10	10	3/3	3/3
20	5	3/3	3/3
20	0.05	3/3	2/3
20	0.005	3/3	3/3

\*Using the in-house designed primers/probe targeted the ST *stgA* gene.

#Using primers/probe described by Karkey et al. (2016).

SPA and ST were detected in all three replicate experiments (Table 2). Lower seeding concentrations of ST and SPA were not examined due to the high Ct values (38–40) that were observed at the 0.005 cfu/mL seeding level. These results indicate the limit of detection of both ST and SPA using the Moore swab method was approximately 0.05–0.005 cfu/mL.



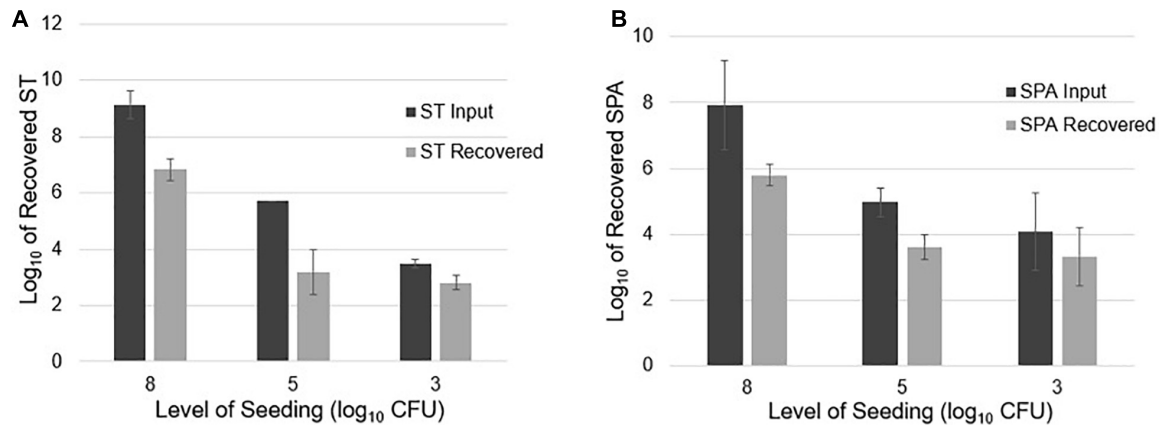


**FIGURE 4 |** ST and SPA mean recovery at different seeding levels (approximately 8, 5, and 3  $\log_{10}$  cfu) in 20 L of sewage using the ultrafiltration method in three replicate experiments. The experiments were validated using *Salmonella* strains from ATCC (ST: 19430; SPA:9150) tested by primers/probes described by Karkey et al. (2016). Error bars represent standard deviation in three replicate experiments. **(A)** Black bars represent the mean input of ST seeded into the 20 L sewage samples, and gray bars represent the mean recovered ST. **(B)** Black bars represent the mean amount of SPA seeded into the 20 L sewage samples, and gray bars represent the mean amount of SPA detected by qPCR.

## Quantification of ST and SPA Recovered From Seeded Sewage Samples Using UF

### Quantification of ST and SPA Recovered From Different Seeding Levels in 20 L Sewage Samples

Twenty-liter sewage samples seeded with known amounts of ST and SPA were concentrated by UF, followed by PEG precipitation and qPCR detection. After seeding an average of 9.13  $\log_{10}$  cfu ST in 20 L of sewage and concentrating the sample using UF, the ST qPCR assay detected a mean of 6.84  $\log_{10}$  EGC ST in three replicate experiments. When an average of 5.71  $\log_{10}$  cfu ST was seeded into 20 L samples in three experiments, 3.20  $\log_{10}$  EGC ST was recovered. Seeding 20 L wastewater samples with a mean total of 3.49  $\log_{10}$  cfu ST resulted in the recovery of an average 2.81  $\log_{10}$  EGC ST (**Figure 4A**). Similarly, seeding an average total of 7.94  $\log_{10}$  cfu SPA led to a mean total recovery of 5.80  $\log_{10}$  EGC SPA. When an average total of 5.0  $\log_{10}$  cfu SPA was seeded, an average total of 3.62  $\log_{10}$  EGC SPA was recovered. Seeding with a mean total of 4.07  $\log_{10}$  cfu SPA resulted a total of 3.32  $\log_{10}$  EGC SPA recovery (**Figure 4B**). These results indicate that UF followed by PEG concentration can effectively recover different concentrations of ST and SPA seeded in large volumes of sewage, but there is about a 2  $\log_{10}$  loss of the target bacteria during the concentration, DNA extraction, and qPCR process.

### Quantification of ST and SPA Recovered From Different Volume of Seeded Sewage

To examine if sample volume affects ST and SPA recovery using UF, an average total of 9.23, 8.54, and 9.13  $\log_{10}$  cfu ST were seeded into 5, 10, and 20 L sewage samples, respectively. Mean totals of 7.57, 6.13, and 6.84  $\log_{10}$  EGC ST were recovered (**Figure 5A**), respectively. Similarly, when an average total of 8.73, 8.74, and 7.94  $\log_{10}$  cfu SPA was seeded into 5, 10, and 20 L of sewage water, respectively, a mean total of 6.82, 5.97, and 5.70  $\log_{10}$  EGC SPA was recovered, respectively (**Figure 5B**). These

results indicate that sample volumes in the range of 5–20 liters did not affect the efficiency of ST and SPA recovery by UF.

## ST and SPA Detection in 20 L Environmental Water Samples Concentrated by UF in Dhaka, Bangladesh

In the study neighborhood in Dhaka, wastewater from toilets shared by multiple households discharges directly into open drains and canals adjacent to the streets. ST was detected in 26.7% (8/30) of drain samples and 100% (4/4) of canal samples that were concentrated by UF. Estimated concentrations of positive ST detected in drain samples ranged from 0.23 to 1.26  $\log_{10}$  EGC/100 mL with a mean of 0.82  $\log_{10}$  EGC/100 mL. In the canal samples, the estimated ST concentrations ranged from 0.71 to 2.14  $\log_{10}$  EGC/100 mL (mean 1.43  $\log_{10}$  EGC/100 mL) (**Table 3**). These results indicate that ultrafiltration is an effective quantitative method for ST detection in wastewater samples.

## ST and SPA Detection in Moore Swab Samples From Three Pumping Stations in Kolkata, India

Between September 24, 2019 and March 19, 2020, 14 Moore swabs were placed on a weekly basis at the Palmer Bridge pumping station, and ST was detected in 10 (71.4%) and SPA was detected in 4 (28.6%) of these swabs. Weekly Moore swabs were also placed in the Ambedkar Bridge pumping station and Topsia pumping station. ST and SPA were detected in 63.2% (12/19) and 31.6% (6/19) of the swabs at the Ambedkar Bridge pumping station, respectively. At the Topsia pumping station, ST and SPA were detected in 75.0% (15/20) and 5.0% (1/20) of the swabs, respectively (**Table 4**). These results suggest that ST and SPA infections are endemic in the city wards in Kolkata that are served

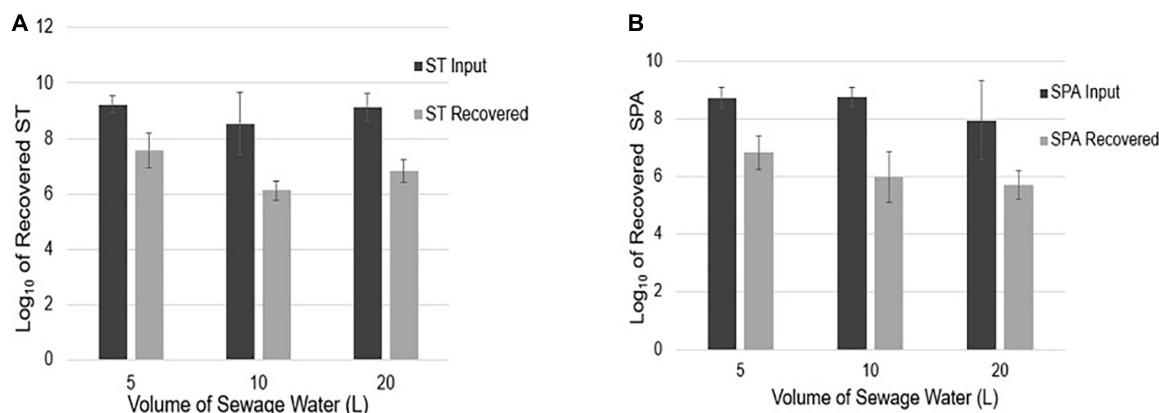


**FIGURE 5 |** ST and SPA mean recovery in different volumes (5, 10, and 20 L) of sewage samples using the ultrafiltration method in three replicate experiments. Error bars represent standard deviation. The experiments were validated using *Salmonella* strains from ATCC (ST: 19430; SPA:9150) tested by primers/probes described by Karkey et al. (2016). **(A)** Black bars represent the mean input ST seeded into 5, 10, and 20 L samples in three replicate experiments, and gray bars represent the mean recovered detected by qPCR. **(B)** Black bars represent the mean SPA seeded, and gray bars represent the mean recovered SPA detected by qPCR.

**TABLE 3 |** ST Detection using the primers/probe described by Karkey et al. (2016) in 20 L of environmental water samples concentrated by Ultrafiltration in Dhaka, Bangladesh, April to October 2019.

Sample type	No. samples	No. positive (%)	Mean*	95% CI <sup>#</sup> low	95% CI high
Drain	30	8 (26.7)	0.82	0.23	1.26
Canal	4	4 (100.0)	1.43	0.71	2.14
Total	34	12 (35.3)	1.02	0.81	1.23

\*log<sub>10</sub> EGC/100 ML.

<sup>#</sup> Confidence interval.

**TABLE 4 |** ST and SPA detection between September 2019 and March 2020 in Moore swab samples from three pumping stations in Kolkata, India.

Pumping station	No. swab	ST positive (%) <sup>*</sup>	SPA positive (%) <sup>#</sup>
Palmer Bridge	14	10 (71.4)	4 (28.6)
Ambedkar Bridge	19	12 (63.2)	6 (31.6)
Topsia Bridge	20	15 (75.0)	1 (5.0)
Total	53	37 (69.8)	11 (20.8)

<sup>\*\*</sup> Using the in-house designed primers/probes targeted the ST stgA gene.

by these pumping stations, and that the Moore swab method is an effective low-cost method for ST and SPA sewage surveillance.

## DISCUSSION

Environmental surveillance offers a low-cost, non-invasive, and sensitive strategy to characterize the burden of infection in specific populations for pathogens that may be challenging to diagnose through collection and analyses of clinical specimens—such as poliomyelitis, typhoid fever, and recently, COVID-19 (Manor et al., 1999; Hagedorn et al., 2020; Peccia et al., 2020; Hemalatha et al., 2021). The goal of this study was to develop and validate sensitive and specific methods for concentration

and PCR detection of ST and SPA in wastewater for typhoid environmental surveillance and also in other environmental samples that could serve as vehicles of ST and SPA transmission. We report here that UF followed by PEG precipitation allowed detection of 1,000 cells of ST and SPA seeded in 20 L (0.05 cells per ml) of sewage. Application of this method in a low-resource neighborhood in Dhaka, Bangladesh indicated that ST was present in 26.7% (8/30) of open drain samples and 100% (4/4) of canal samples. Moore swabs, followed by enrichment culture, could detect as few as 100 seeded ST and SPA cells in 20 L (0.005 cells per mL) of sewage in laboratory experiments. Application of this detection method at three sewage pumping stations in Kolkata, India indicated that 69.8% of Moore swab samples were positive for ST and 20.8% were positive for SPA. These results demonstrate that UF and Moore swabs are two sensitive and effective methods for concentrating and detecting ST and SPA in wastewater and other environmental water samples, and these methods can be used for typhoid environmental surveillance and risk assessment.

In typhoid-endemic areas of Nepal and Bangladesh, previous investigators have reported the detection of ST in grab samples of drinking water that were concentrated by membrane filtration, followed by DNA extraction from the filter and PCR analyses (Karkey et al., 2016; Saha et al., 2019). Moore swabs were instrumental in the detection of ST in sewage canals near Santiago, Chile that were used to irrigate vegetable crops typically eaten without cooking (Sikorski and Levine, 2020). These findings indicate risk of ST transmission via drinking water and raw produce, but these samples and methods do not provide quantitative information that could be used to estimate the burden of typhoid infection in the population. Quantitative detection of ST and SPA in wastewater samples collected from sites where the population catchment can be estimated allows modeling approaches to estimate prevalence of typhoid and paratyphoid infection in the catchment population (Wang et al., 2020). This goal requires careful selection of sample collection

sites and reliable methods to detect ST and SPA in samples that represent excreta from a defined population—typically wastewater samples. Ideally, methods to detect ST and SPA in wastewater for environmental surveillance are quantitative, sensitive, specific, low-cost, and feasible for laboratories in low-resource settings.

Currently, two types of samples have been used for ST and SPA wastewater surveillance: grab samples and trap samples using Moore swabs (Matrajt et al., 2020). Grab samples are typically concentrated through some type of filtration or centrifugation, sometimes allowed to incubate in an enrichment broth, and then analyzed by culture or PCR. Grab samples can be collected either in small volume or large volume, but microbial concentration from large volume samples can improve the sensitivity of detection. However, the volume of a grab sample that can be feasibly processed may be limited by the turbidity of the wastewater or environmental water that can clog filters used for sample concentration. Grab samples are usually analyzed without enrichment in order to obtain quantitative estimates of the pathogen concentration in the sample. In contrast, trap samples, such as Moore swabs, continuously filter and trap microbial pathogens in flowing water or wastewater and can be used successfully for turbid waters and wastewater. Moore swabs are often analyzed with primary enrichment, followed by PCR or culture methods, to increase the detection sensitivity. When an enrichment step is included in processing of grab samples or trap samples, the results only indicate the presence/absence of ST or SPA in the sample. One important difference between grab samples and trap samples is their ability to capture pathogen presence in wastewater in settings where there is large temporal variability. Results from grab samples reflect the presence/absence and concentration of a pathogen at a single point in time when the sample is collected. Moore swabs concentrate pathogens present in wastewater or environmental waters over a period of time (usually days), and therefore can be useful for sampling sites that represent smaller catchment populations where pathogen shedding may be infrequent and intermittent.

UF is an effective technique for concentrating multiple microbes simultaneously. Laboratory studies that seeded selected viruses, bacteria, and parasites into large-volume samples of tap water and reclaimed wastewater (100 L) reported mean recovery rates of five bacteria, protozoa, and viruses between 38 and 130% (Hill et al., 2007; Liu et al., 2012). Two UF techniques, hollow-fiber ultrafiltration (TFUF) using tangential-flow (Mull and Hill, 2012) and dead-end ultrafiltration (DEUF) (Smith and Hill, 2009), provide effective recovery of diverse microbes from different types of water and wastewater, and both methods have showed similar recovery efficiencies in previous studies (Smith and Hill, 2009; Mull and Hill, 2012). The main difference between the DEUF technique and TFUF configuration is that one of the ultrafilter ports is closed so that the water/wastewater sample must pass through the membrane. In contrast, the TFUF technique allows particles and other constituents larger than the membrane pore to be circulated and concentrated into a smaller volume. The DEUF technique is easier to perform than the TFUF because the water passes through the ultrafilter only once.

However, the DEUF approach is more likely to clog the ultrafilter than the TFUF configuration and therefore is more appropriate for samples with low turbidity (e.g., tap water or reclaimed water). In this study, we used the hollow-fiber TFUF technique to concentrate turbid samples (e.g., from open drains and canals). With this method, particles and microbes are maintained in the ultrafilter cartridge under pressure, and there is a low risk of the ultrafilter clogging (Mull and Hill, 2012). Although the UF method has been described previously (Hill et al., 2007; Liu et al., 2012), our recent deployment of this technique to process field samples in Dhaka, Bangladesh demonstrated the feasibility and value of this method to detect a range of pathogens, including *S. Typhi*, in high proportions of drain, canal, and flood water samples in a low-resource setting (Amin et al., 2020).

“Moore swabs” have been used for decades by public health professionals around the world to detect and isolate enteric pathogens from wastewater and environmental waters, and their use to recover typhoidal *Salmonella* bacteria has recently been reviewed by Sikorski and Levine (2020). Consisting of a strip of cotton gauze tied with string and suspended in flowing water, this sampling method acts as a trap that allows collection of pathogens over an extended period of time, especially when pathogen shedding is intermittent and in sites with smaller catchment populations. The Moore swab was first deployed by Brendan Moore in 1948 to trace *Salmonella* Paratyphi B from sewage in North Devon, England to determine the sources of contamination responsible for sporadic outbreaks of paratyphoid fever. Since the first application to detect typhoidal *Salmonella* in sewage, the Moore swab method has been utilized in several studies throughout the world to detect *Salmonella* Typhi in irrigation water, surface water, municipal sewers, and storm drains (Bowmer et al., 1959; Callaghan and Brodie, 1968; Conn et al., 1972; Sears et al., 1984). Given its effectiveness, simplicity, and affordability, we adapted this method for use in typhoid environmental surveillance of wastewater in Kolkata, India. We found that the Moore swab method has several advantages over UF in terms of greater sensitivity, simplicity, shorter processing time, less labor, and lower cost. However, the Moore swab method also has several limitations. First, this method only provides results on the presence or absence of ST and SPA in the sample and does not allow a quantitative assessment of ST or SPA concentration in the sample. Second, Moore swab sample collection requires two trips to place and later retrieve the swab, whereas grab samples only require a single collection trip. Third, deployment of Moore swabs for environmental surveillance has not been standardized in terms of sampling frequency, duration of immersion, and swab processing. This study addresses some of these information gaps by providing a standardized processing method for ST and SPA detection in wastewater with some benchmarks for limit of detection in wastewater matrices. We recognize that wastewater is a complex and highly variable matrix and that the limit of detection for this method will vary by setting.

The Moore swab method described in this study provides a low-cost, simple, and sensitive approach for presence/absence detection of ST and SPA in wastewater samples and is feasible to deploy in a wide range of low-resource settings. In addition, the UF method we have developed allows sensitive quantitative

detection of ST and SPA in large volume (20–80 L) samples of wastewater. Typhoid environmental surveillance strategies could start by deploying low-cost Moore swabs at a large number of sites in a screening stage to determine which locations provide the most valuable information. For sites where ST or SPA is detected in a Moore swab sample, follow-up large volume samples could be collected and processed by UF to obtain quantitative estimates of ST or SPA concentration which could be used to estimate infection prevalence in specific catchment populations. This type of two-stage approach for typhoid environmental surveillance would optimize use of human and financial resources and allow dynamic adaptive sampling site allocation that will more rapidly identify typhoid hotspots (Wang et al., 2020).

## DATA AVAILABILITY STATEMENT

The raw data supporting the conclusions of this article will be made available by the authors, without undue reservation.

## AUTHOR CONTRIBUTIONS

PL wrote the manuscript and contributed to design and concept of the study. MI performed all laboratory work at Emory and made draft the figures and tables. RK designed the in-house primers and probe. NA and MR led the sample collection in

Dhaka, Bangladesh. MR performed all laboratory work in Dhaka, Bangladesh. AM and SD led the sample collection in Kolkata, India. AD performed all laboratory work in Kolkata, India. CM contributed to conception and design of the study and revised the manuscript. All authors contributed to the article and approved the submitted version.

## FUNDING

This study was funded by The Bill and Melinda Gates Foundation (BMGF) grant OPP1150697. BMGF was the funding and management agency for this project. Funds are available for open access publication fees.

## ACKNOWLEDGMENTS

This study was funded by The Bill and Melinda Gates Foundation (BMGF) grant OPP1150697. We are in debt to Supriya Kumar and Megan Carey from the BMGF for their support and guidance. We are grateful to the environmental sample collection team from the National Institute of Cholera and Enteric Diseases (NICED), Kolkata, India and Infectious Disease Division, International Centre for Diarrhoeal Disease Research, Bangladesh (ICDDR,B) for their efforts to identify sewage sampling locations and their assistance with sample collection.

## REFERENCES

- Amin, N., Liu, P., Foster, T., Rahman, M., Miah, M. R., Ahmed, G. B., et al. (2020). Pathogen flows from on-site sanitation systems in low-income urban neighborhoods, Dhaka: a quantitative environmental assessment. *Int. J. Hyg. Environ. Health* 230:113619. doi: 10.1016/j.ijheh.2020.113619
- Andrews, J. R., Yu, A. T., Saha, S., Shakya, J., Aiemy, K., Horng, L., et al. (2020). Environmental surveillance as a tool for identifying high-risk settings for typhoid transmission. *Clin. Infect. Dis.* 71, S71–S78. doi: 10.1093/cid/ciaa513
- Antillon, M., Saad, N. J., Baker, S., Pollard, A. J., and Pitzer, V. E. (2018). The relationship between blood sample volume and diagnostic sensitivity of blood culture for typhoid and paratyphoid fever: a systematic review and meta-analysis. *J. Infect. Dis.* 218, S255–S267. doi: 10.1093/infdis/jiy471
- Barrett, T. J., Blake, P. A., Morris, G. K., Puh, N. D., Bradford, H. B., and Wells, J. G. (1980). Use of Moore swabs for isolating *Vibrio cholerae* from sewage. *J. Clin. Microbiol.* 11, 385–388. doi: 10.1128/jcm.11.4.385-388.1980
- Bowmer, E. J., Hudson, V. G., and Sunderland, W. F. (1959). Typhoid fever: where there's a carrier. *Can. Med. Assoc. J.* 80, 179–186.
- Callaghan, P., and Brodie, J. (1968). Laboratory investigation of sewer swabs following the Aberdeen typhoid outbreak of 1964. *J. Hyg.* 66, 489–497. doi: 10.1017/S0022172400028230
- Conn, N. K., Heymann, C. S., Jamieson, A., McWilliam, J. M., and Scott, T. G. (1972). Water-borne typhoid fever caused by an unusual Vi-phage type in Edinburgh. *J. Hyg.* 70, 245–253. doi: 10.1017/S0022172400022300
- Crump, J. A. (2019). Progress in typhoid fever epidemiology. *Clin. Infect. Dis.* 68, S4–S9. doi: 10.1093/cid/ciy846
- Dewan, A. M., Corner, R., Hashizume, M., and Onge, E. T. (2013). Typhoid fever and its association with environmental factors in the dhaka metropolitan area of Bangladesh: a spatial and time-series approach. *PLoS Negl. Trop. Dis.* 7:e1998. doi: 10.1371/journal.pntd.0001998
- Egoz, N., Shihab, S., Leitner, L., and Lucian, M. (1988). An outbreak of typhoid fever due to contamination of the municipal water supply in northern Israel. *Isr. J. Med. Sci.* 24, 640–643.
- Foster, T., Falletta, J., Amin, N., Rahman, M., Liu, P., Raj, S., et al. (2021). Modelling faecal pathogen flows and health risks in urban Bangladesh: implications for sanitation decision making. *Int. J. Hyg. Environ. Health* 233:113669. doi: 10.1016/j.ijheh.2020.113669
- Hagedorn, B. L., Gauld, J., Feasey, N., and Hu, H. (2020). Cost-effectiveness of using environmental surveillance to target the roll-out typhoid conjugate vaccine. *Vaccine* 38, 1661–1670. doi: 10.1016/j.vaccine.2019.12.061
- Hemalatha, M., Kiran, U., Kuncha, S. K., Kopperi, H., Gokulan, C. G., Mohan, S. V., et al. (2021). Surveillance of SARS-CoV-2 spread using wastewater-based epidemiology: comprehensive study. *Sci. Total Environ.* 768:144704. doi: 10.1016/j.scitotenv.2020.144704
- Hill, V. R., Kahler, A. M., Jothikumar, N., Johnson, T. B., Hahn, D., and Cromeans, T. L. (2007). Multistate evaluation of an ultrafiltration-based procedure for simultaneous recovery of enteric microbes in 100-liter tap water samples. *Appl. Environ. Microbiol.* 73, 4218–4225. doi: 10.1128/AEM.02713-06
- Karkey, A., Jombart, T., Walker, A. W., Thompson, C. N., Torres, A., Dongol, S., et al. (2016). The ecological dynamics of fecal contamination and *Salmonella typhi* and *Salmonella paratyphi* in municipal kathmandu drinking water. *PLoS Negl. Trop. Dis.* 10:e0004346. doi: 10.1371/journal.pntd.0004346
- Kobayashi, T., Kutsuna, S., Hayakawa, K., Kato, Y., Ohmagari, N., Uryu, H., et al. (2016). Case report: an outbreak of food-borne typhoid fever due to *Salmonella enterica* serotype typhi in Japan reported for the first time in 16 years. *Am. J. Trop. Med. Hyg.* 94, 289–291. doi: 10.4269/ajtmh.15-0484
- Lindquist, H. D., Harris, S., Lucas, S., Hartzel, M., Riner, D., Rochele, P., et al. (2007). Using ultrafiltration to concentrate and detect *Bacillus anthracis*, *Bacillus atrophaeus* subspecies *globigii*, and *Cryptosporidium parvum* in 100-liter water samples. *J. Microbiol. Methods* 70, 484–492. doi: 10.1016/j.mimet.2007.06.007
- Liu, P., Hill, V. R., Hahn, D., Johnson, T. B., Pan, Y., Jothikumar, N., et al. (2012). Hollow-fiber ultrafiltration for simultaneous recovery of viruses, bacteria and parasites from reclaimed water. *J. Microbiol. Methods* 88, 155–161. doi: 10.1016/j.mimet.2011.11.007



- Manor, Y., Handscher, R., Halmut, T., Neuman, M., Bobrov, A., Rudich, H., et al. (1999). Detection of poliovirus circulation by environmental surveillance in the absence of clinical cases in Israel and the palestinian authority. *J. Clin. Microbiol.* 37, 1670–1675. doi: 10.1128/JCM.37.6.1670-1675.1999
- Matrajt, G., Lillis, L., and Meschke, J. S. (2020). Review of methods suitable for environmental surveillance of *Salmonella* typhi and paratyphi. *Clin. Infect. Dis.* 71, S79–S83. doi: 10.1093/cid/ciaa487
- McEgan, R., Rodrigues, C. A., Sbodio, A., Suslow, T. V., Goodridge, L. D., and Danyluk, M. D. (2013). Detection of *Salmonella* spp. from large volumes of water by modified moore swabs and tangential flow filtration. *Lett. Appl. Microbiol.* 56, 88–94. doi: 10.1111/lam.12016
- Mull, B., and Hill, V. R. (2012). Recovery of diverse microbes in high turbidity surface water samples using dead-end ultrafiltration. *J. Microbiol. Methods* 91, 429–433. doi: 10.1016/j.mimet.2012.10.001
- Murphy, J. L., Kahler, A. M., Nansubuga, I., Nanyunja, E. M., Kaplan, B., Jothikumar, N., et al. (2017). Environmental survey of drinking water sources in Kampala, Uganda, during a typhoid fever outbreak. *Appl. Environ. Microbiol.* 83:e01706. doi: 10.1128/AEM.01706-17
- Office of the Registrar General & Census Commissioner MoHA, Government of India. (2011). *Census Data*. Available online at: <https://censusindia.gov.in/aboutus/personnel/perdirectory.aspx> (accessed February 14, 2021).
- Peccia, J., Zulli, A., Brackney, D. E., Grubaugh, N. D., Kaplan, E. H., Casanovas-Massana, A., et al. (2020). Measurement of SARS-CoV-2 RNA in wastewater tracks community infection dynamics. *Nat. Biotechnol.* 38, 1164–1167. doi: 10.1038/s41587-020-0684-z
- Saha, S., Tanmoy, A. M., Andrews, J. R., Sajib, M. S. I., Yu, A. T., Baker, S., et al. (2019). Evaluating PCR-Based detection of *Salmonella* typhi and paratyphi a in the environment as an enteric fever surveillance tool. *Am. J. Trop. Med. Hyg.* 100, 43–46. doi: 10.4269/ajtmh.18-0428
- Sears, S. D., Ferreccio, C., Levine, M. M., Cordano, A. M., Monreal, J., Black, R. E., et al. (1984). The use of Moore swabs for isolation of *Salmonella* typhi from irrigation water in Santiago, Chile. *J. Infect. Dis.* 149, 640–642. doi: 10.1093/infdis/149.4.640
- Sikorski, M. J., and Levine, M. M. (2020). Reviving the “Moore Swab”: a classic environmental surveillance tool involving filtration of flowing surface water and sewage water to recover typhoidal *Salmonella* bacteria. *Appl. Environ. Microbiol.* 86:e00060. doi: 10.1128/AEM.00060-20
- Smith, C. M., and Hill, V. R. (2009). Dead-end hollow-fiber ultrafiltration for recovery of diverse microbes from water. *Appl. Environ. Microbiol.* 75, 5284–5289. doi: 10.1128/AEM.00456-09
- Tao, Z., Wang, H., Xu, A., Zhang, Y., Song, L., Zhu, S., et al. (2010). Isolation of a recombinant type 3/type 2 poliovirus with a chimeric capsid VP1 from sewage in Shandong, China. *Virus Res.* 150, 56–60. doi: 10.1016/j.virusres.2010.02.014
- Usera, M. A., Echeita, A., Aladueno, A., Alvarez, J., Carreno, C., Orcau, A., et al. (1995). Investigation of an outbreak of water-borne typhoid fever in Catalonia in 1994. *Enferm. Infect. Microbiol. Clin.* 13, 450–454.
- Vongphayloth, K., Rattanavong, S., Moore, C. E., Phetsouvanh, R., Wuthiekanun, V., Sengdouangphachanh, A., et al. (2012). Burkholderia pseudomallei detection in surface water in southern Laos using Moore's swabs. *Am. J. Trop. Med. Hyg.* 86, 872–877. doi: 10.4269/ajtmh.2012.11-0739
- Wang, Y., Moe, C. L., Dutta, S., Wadhwa, A., Kanungo, S., Mairinger, W., et al. (2020). Designing a typhoid environmental surveillance study: a simulation model for optimum sampling site allocation. *Epidemics* 31:100391. doi: 10.1016/j.epidem.2020.100391

**Conflict of Interest:** The authors declare that the research was conducted in the absence of any commercial or financial relationships that could be construed as a potential conflict of interest.

Copyright © 2021 Liu, Ibaraki, Kapoor, Amin, Das, Miah, Mukhopadhyay, Rahman, Dutta and Moe. This is an open-access article distributed under the terms of the Creative Commons Attribution License (CC BY). The use, distribution or reproduction in other forums is permitted, provided the original author(s) and the copyright owner(s) are credited and that the original publication in this journal is cited, in accordance with accepted academic practice. No use, distribution or reproduction is permitted which does not comply with these terms.



# Development of a High-Efficiency Immunomagnetic Enrichment Method for Detection of Human Norovirus via PAMAM Dendrimer/SA-Biotin Mediated Cascade-Amplification

Junshan Gao<sup>1†</sup>, Le Zhang<sup>1†</sup>, Liang Xue<sup>1\*</sup>, Weicheng Cai<sup>1</sup>, Zhiwei Qin<sup>1</sup>, Jiale Yang<sup>1</sup>, Yanhui Liang<sup>1</sup>, Linping Wang<sup>1</sup>, Moutong Chen<sup>1</sup>, Qinghua Ye<sup>1</sup>, Ying Li<sup>1</sup>, Juan Wang<sup>1,2</sup>, Shi Wu<sup>1</sup>, Qingping Wu<sup>1</sup> and Jumei Zhang<sup>1\*</sup>

## OPEN ACCESS

### Edited by:

Joseph Oliver Falkinham,  
Virginia Tech, United States

### Reviewed by:

Matthew D. Moore,  
University of Massachusetts Amherst,  
United States  
Leena Maunula,  
University of Helsinki, Finland

### \*Correspondence:

Liang Xue  
scutphoenix@qq.com  
Jumei Zhang  
zhangjm926@126.com

<sup>†</sup> These authors have contributed  
equally to this work and share first  
authorship

### Specialty section:

This article was submitted to  
Food Microbiology,  
a section of the journal  
Frontiers in Microbiology

**Received:** 28 February 2021

**Accepted:** 29 June 2021

**Published:** 20 July 2021

### Citation:

Gao J, Zhang L, Xue L, Cai W,  
Qin Z, Yang J, Liang Y, Wang L,  
Chen M, Ye Q, Li Y, Wang J, Wu S,  
Wu Q and Zhang J (2021)  
Development of a High-Efficiency  
Immunomagnetic Enrichment Method  
for Detection of Human Norovirus via  
PAMAM Dendrimer/SA-Biotin  
Mediated Cascade-Amplification.  
Front. Microbiol. 12:673872.  
doi: 10.3389/fmicb.2021.673872

<sup>1</sup> Guangdong Provincial Key Laboratory of Microbial Safety and Health, State Key Laboratory of Applied Microbiology  
Southern China, Institute of Microbiology, Guangdong Academy of Sciences, Guangzhou, China, <sup>2</sup> College of Food Science,  
South China Agricultural University, Guangzhou, China

Human norovirus is a common cause of acute gastroenteritis worldwide, and oysters have been found to be the main carriers for its spread. The lack of efficient pre-treatment methods has been a major bottleneck limiting the detection of viruses in oysters. In this study, we established a novel immunomagnetic enrichment method using polyamidoamine (PAMAM) dendrimer/SA-biotin-mediated cascade amplification for reverse transcriptase quantitative real-time polymerase chain reaction (RT-qPCR) detection. We compared the capture efficiency of traditional immunomagnetic enrichment, biotin-amplified immunomagnetic enrichment, and PAMAM dendrimer/SA-biotin-mediated cascade-amplification immunomagnetic enrichment. The optimal capture efficiency of the novel method was  $44.26 \pm 1.45\%$ , which increased by 183.17% ( $P < 0.01$ ) and 18.09% ( $P < 0.05$ ) compared with the first two methods, respectively. Three methods were all applied in detecting norovirus in 44 retail oysters, the detection rate of the PAMAM dendrimer/SA-biotin-mediated method was 25.0%, which was higher than those of traditional IME (15.90%) and SA-biotin-amplified IME (18.80%) by 9.1 and 6.2%, respectively. In conclusion, the novel method can be applied for the rapid detection of norovirus in oysters, which can help reduce the cost and time of detection and improve detection rates.

**Keywords:** noroviruses, oysters, PAMAM-mediated, immunomagnetic enrichment, biotin amplification

## INTRODUCTION

Norovirus (NoV) is one of the main causes of acute gastroenteritis (Ahmed et al., 2014) and frequently appears in closed spaces in hospitals, schools, and cruise ships (Siebenga et al., 2009). The consumption of bivalve shellfish, such as oysters, is a common route of NoV infection (Woods et al., 2016; Le Mennec et al., 2017). Oysters are filter feeders, and NoV particles easily accumulate in their digestive tract (Le Guyader et al., 2012). As oysters are usually eaten raw, this increases the rate of NoV transmission (El Moqri et al., 2019).

Accurate diagnosis of NoV contamination in oysters is essential to control NoV outbreaks and to ensure that patients receive optimal treatment. Real time RT-PCR (RT-qPCR) is the “gold standard” for NoV diagnosis and detection (Vinjé, 2015). However, this method is often affected by low amounts of NoVs and by presence of inhibitors in the sample, such as polysaccharides, lipids, and proteins in oyster tissue. Therefore, it is necessary to establish an efficient NoV enrichment method to minimize the influence of the inhibitors. Traditional enrichment methods include direct treatment, proteinase K digestion and proteinase K digestion combined with polyethylene glycol precipitation (Lee and Lee, 1981; Wu et al., 2016). However, these methods are non-specific and cannot fully remove the interference of complex matrices.

Currently, immunomagnetic enrichment (IME) is widely used to separate and concentrate pathogens from food samples in a more effective way than traditional methods (Valdes et al., 2009; Xiong et al., 2014). Traditional IME combines magnetic beads with antibodies to enrich the target from a complex matrix (Yao et al., 2009), and covalent coupling is commonly used to immobilize antibodies on magnetic beads (Cao et al., 2012). Covalent coupling is simple and effective, but the system is easily affected by small changes in the pH and cross-linking time. The streptavidin (SA)-biotin mediated IME has gained widespread applications because of its high affinity and specificity. SA is a tetrameric protein composed of identical subunits. One streptavidin molecule can bind to four biotin molecules to achieve signal amplification (Yuan et al., 2000).

Polyamidoamine (PAMAM) is a dendritic polymer with a large number of functional groups available for surface modifications such as acetylation and glycosylation (Yellepeddi et al., 2009). PAMAM has good biocompatibility and no immunogenicity, it can be used as a coupling carrier for drugs and genes, and has good application prospects in the fields of biology and medicine. The molecular surface of PAMAM has a large number of positively charged amino groups, which can be combined with biotin to amplify the biotin signal. This makes a PAMAM-biotin monoclonal antibody (mAb) molecule capture more NoVs than SA-biotin mAb, increasing the capture efficiency (CE) of the enrichment process (Figure 1). In this study, cascade signal amplification was achieved by PAMAM as the coupling carrier for biotin. To the best of our knowledge, there are no reports on PAMAM as a carrier for cascade-amplification for NoV enrichment in oysters. We aimed to establish a sensitive and efficient PAMAM dendrimer/SA-biotin-mediated cascade-amplification IME (P-SA-BA-IME) method, which was combined with RT-qPCR to detect NoVs in oysters.

## MATERIALS AND METHODS

### NoV Stool Samples, Oyster Samples and Anti-NoV mAb

NoV-positive stool samples used in this study were collected from The Third Affiliated Hospital of Sun Yat-sen University in our previous works and stored at  $-80^{\circ}\text{C}$  in our laboratory

(Xue et al., 2013, 2016, 2019). In brief, the stools samples were diluted using diethyl pyrocarbonate (DEPC)-treated phosphate buffered saline (PBS) solution to 10–20% (m/v), and then centrifuged at  $7,000 \times g$  for 5 min. The supernatant was stored as the viral stock at  $-80^{\circ}\text{C}$ . The sample was identified as GII.4 by one-step RT-PCR and sequencing (Xue et al., 2013, 2016, 2019). Before use, the virus supernatant was taken out to extract total RNA, and the titer was determined by RT-qPCR as  $6.24 \times 10^5$  copies/ $\mu\text{L}$ . The appropriate titers used in this study were obtained by dilution with DEPC-treated PBS (Zhang et al., 2020). Oysters were obtained from Huangsha Aquatic Product Trading Market in Guangzhou. The anti-NoV mAb was prepared by immunizing P particles of GII.4 NoV in our previous experiment, it could react with GII.2, GII.3, GII.4, GII.6, GII.17 NoVs and be used in enzyme linked immunosorbent assay (ELISA) and colloidal gold immunochromatographic assay (Gao et al., 2021).

### Processing of the Oyster Samples

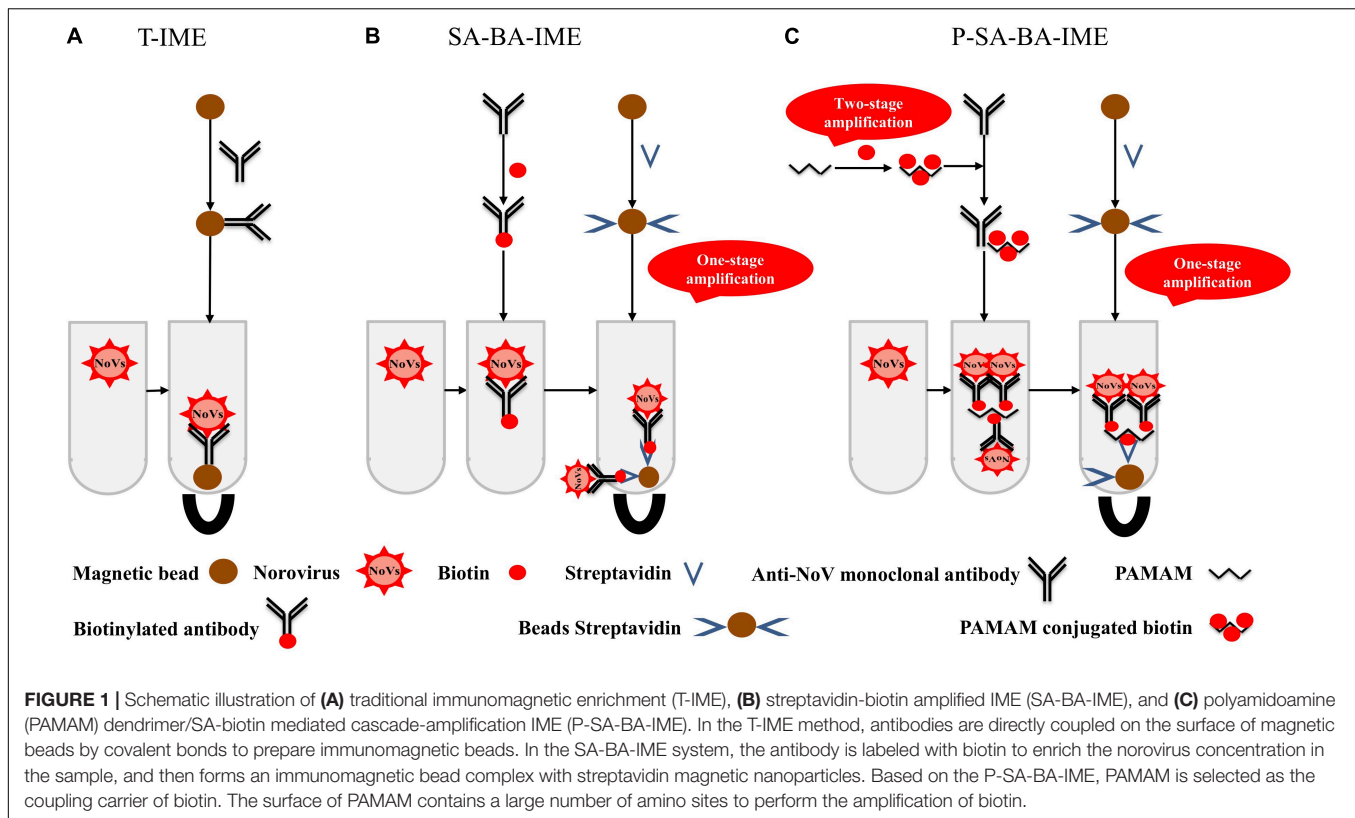
The oysters were dissected, and the digestive glands were removed and grounded to a homogenized state. One milliliter PBS and 1.5 g of oyster sample were mixed, centrifuged at  $3,000 \times g$  at  $4^{\circ}\text{C}$  for 10 min, and the supernatant was transferred to another clean tube for enrichment (When comparing the detection rates of the three methods, the supernatant of 4.5 g digestive glands was divided into three evenly). Oyster negative sample and oyster positive sample were used as a negative control and a positive control to avoid cross-contamination, they were tested by the P-SA-BA-IME method and a modified ISO/TS 15216-2:2013 standard method which was based on the protease K method with the increasing extraction buffer volume and PEG precipitation (Zhang et al., 2020).

### Preparation of the Traditional Immunomagnetic Beads (IMBs)

Nanomagnetic beads (750 nm) (Aorun Micronano New Material Technology Company, Shanghai, China) were washed with morpholine ethanesulfonic acid (Sigma Aldrich, St. Louis, MO, United States) three times at a volume ratio of 1:10 to ensure monodispersion, then 24  $\mu\text{L}$  1- (3-Dimethylaminopropyl)-3-ethylcarbodiimide hydrochloride (EDC-HCl) (200 mM) (Thermo Fisher Scientific Inc., Rockford, United States) and 240  $\mu\text{L}$  N-hydroxysulfosuccinimide (Sulfo-NHS) (200 mM) (Thermo Fisher Scientific Inc.) were added to 1 mg magnetic beads. The magnetic beads were mixed with 40  $\mu\text{g}$  monoclonal antibody for 30 min at  $37^{\circ}\text{C}$ , then 1 mL 1% (w/v) BSA (Sigma Aldrich, St. Louis, MO, United States) blocking buffer was added at  $37^{\circ}\text{C}$  for 2 h and stored at  $4^{\circ}\text{C}$ .

### Preparation of Biotinylated Monoclonal Antibody (Biotin-mAb)

The mAb was mixed with sulfo-NHS-LC-biotin (Thermo Fisher Scientific Inc.) at a volume ratio of 1:20 and placed on a dynabeads MX mixer (Thermo Fisher Scientific Inc.) at 15 rpm at room temperature for 30 min. The biotin-mAb was centrifuged in a 30 KDa ultrafiltration tube (Millipore, MWCo, 30000) (Millipore, Carrigtwohill, County Cork, Ireland) at  $6,000 \times g$  for



10 min to remove unbound biotin, and washed four times with PBS with 0.05% Tween 20 (PBST) (0.01 M, pH 7.4).

### Preparation of Biotin-PAMAM-mAb

PAMAM (Chenyuan Organic Silicon New Material Co., Ltd., Shandong, China) was dissolved in a pH 9.0 PBS solution for a final concentration of 10 mg/mL, then mixed 1.6 mg of sulfo-NHS-LC-biotin with 1 mL PAMAM on a rotary mixer for 2 h. The unbound sulfo-NHS-LC-biotin was removed using an ultrafiltration tube, and 2-iminosulfane hydrochloride (Traut's reagent) (Sigma Aldrich) at a final concentration of 1 mg/mL under nitrogen for 1 h to obtain biotin-PAMAM-SH. Sulfo-SMCC (Sigma Aldrich) and anti-NoV mAb were mixed at a ratio of 10:1 and incubated for 2 h at room temperature. The unbound sulfo-SMCC was removed using an ultrafiltration tube. SMCC-mAb and biotin-PAMAM-SH were mixed at a ratio of 10:1 and incubated overnight at room temperature, and then N-ethylmaleimide (Sigma Aldrich) was used to block unbound sulfhydryl groups.

### Pre-treatment Methods

Three NoV enrichment methods were compared: traditional IME (T-IME), SA-biotin-amplified IME (SA-BA-IME), and P-SA-BA-IME (Figure 1).

#### T-IME

Anti-NoV mAb-conjugated magnetic beads were added to 1 mL PBS containing  $1 \times 10^6$  copies of NoVs or the supernatant of

1.5 g oyster homogenate to enrich at room temperature. The IMBs were placed on a magnetic stand to remove the supernatant, resuspended and shaken with 1 mL 0.01 M PBST (pH 7.4) washing buffer, then placed on the magnetic stand to remove the supernatant for 3 times. Finally, the IMBs were resuspended in 140  $\mu$ L PBS buffer, and RNA was extracted and stored at  $-80^\circ\text{C}$ .

#### SA-BA-IME

One milliliter of PBS containing  $1 \times 10^6$  copies of NoVs or the supernatant of 1.5 g oyster homogenate with biotin-mAb was placed on the dynabeads MX mixer, then SA nanomagnetic beads (750 nm) (Aorun Micronano New Material Technology Company) were added and placed on the dynabeads MX mixer at 15 rpm at room temperature. The mixture was placed on a magnetic stand for magnetic separation and washed three times with 1 mL of PBST. The IMBs were resuspended in 140  $\mu$ L PBS, and RNA was extracted and stored at  $-80^\circ\text{C}$ .

#### P-SA-BA-IME

The procedure was the same as SA-BA-IME, with only biotin-mAb being replaced by biotin-PAMAM-mAb.

### RNA Extraction

Viral RNA was extracted from 140  $\mu$ L IMBs suspension after enriching the NoVs with a High Pure Viral RNA Mini Kit (Magen, Guangzhou, China) following the manufacturer's instructions. After repeated washing to remove impurities, 50  $\mu$ L of eluate was added to the column to elute the RNA.



## RT-qPCR Analysis

We quantitated enriched NoVs by RT-qPCR (Jothikumar et al., 2005) using a LightCycler® 96 System (Roche, Basel, Switzerland) using a RNA PrimeScript™ One-Step Quantitative RT-PCR System (TaKaRa, Dalian, China) and 2  $\mu$ L of the template was added in a total reaction volume of 20  $\mu$ L. The primers and probes for NoVs included QNIF2d (5' ATG TTC AGR TGG ATG AGR TTC TCW GA 3'), COG2R (5'-TCG ACG CCA TCT TCA TTC ACA 3'), and QNIFs (5' FAM-AGC ACG TGG GAG GGG ATC G-TAMRAC). Cycling times and temperatures were 42°C for 5 min and 95°C for 10 min, followed by 45 cycles of 95°C for 5 s and 60°C for 20 s. A standard virus titer curve was generated by extracting viral RNA from serially diluted ( $10^{-1}$ – $10^{-7}$ ) virus stock. RT-qPCR was performed, and the resulting cycle threshold (Ct) values were plotted against their respective dilutions. The highest measurable Ct was assigned the value of one RT-PCR unit, and a logarithmic trend line was plotted ( $R^2 = 0.999$ ). The copy numbers of positive and experimental samples were calculated using the standard curve equation. The samples showed a characteristic sigmoidal curve with a Ct-value < 43 were regarded as positive (> one viral genomic copy), the number of genome copies per gram of the oyster digestive gland tissue is less than 25 as negative.

## Calculation of Capture Efficiency

Capture efficiency (CE) was defined as the percentage of NoVs enriched by IMBs to the total number of NoVs. The CE (%) was calculated according to the following equation:  $CE (\%) = C_1/C_0 \times 100\%$ ,  $C_1$ : NoV genomic copy after enrichment, and  $C_0$ : NoV genomic copy before enrichment.

## Statistical Analysis

Statistical analyses were performed with Graphpad Prism 8.0.1. The CE of three methods were compared by using One-way ANOVA. Three independent experiments were conducted to determine assay consistency. The detection rate of three methods were compared through Chi-square test. For all analyses, significantly different was set as a  $P$ -value less than 0.05.

## RESULTS

### T-IME Optimization

The conditions to increase CE of the T-IME were optimized (Figure 2A and Supplementary Table 1). When the coupling time was 30, 60, and 90 min, the CE increased to  $12.68 \pm 1.00\%$ , and longer coupling times did not increase it any further. IMBs

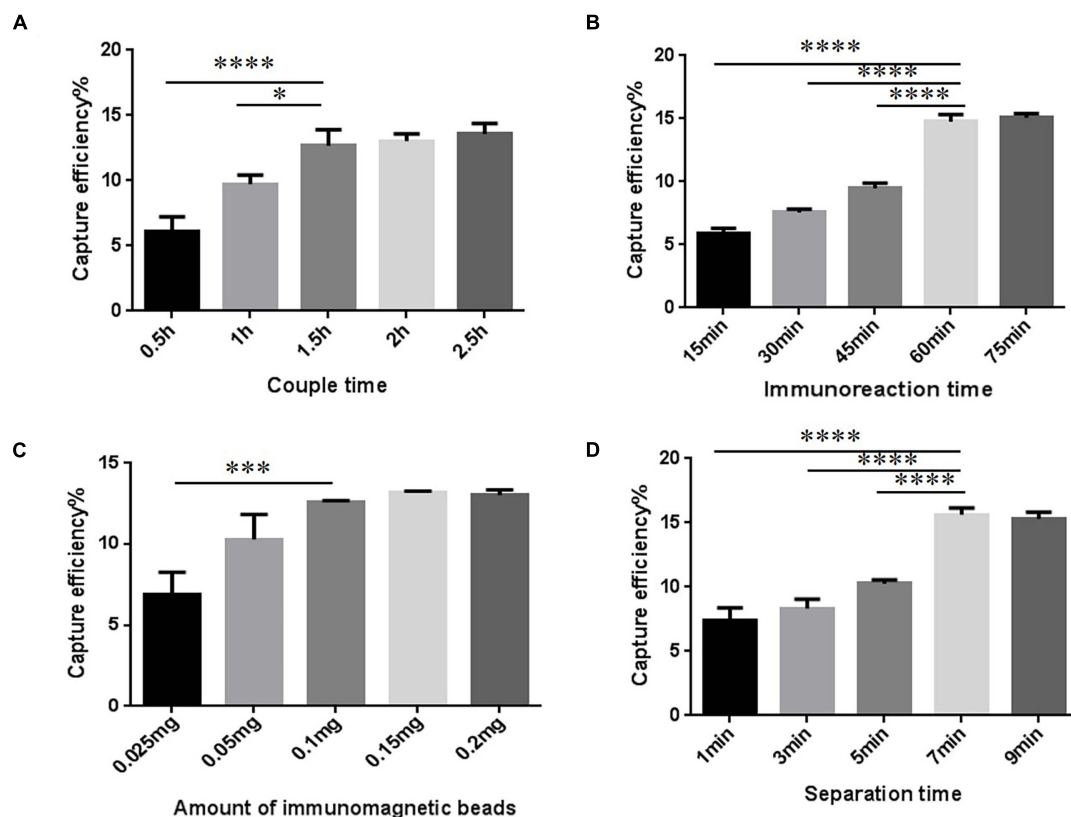


**FIGURE 2 |** Optimization of traditional immunomagnetic enrichment (T-IME) conditions. (A) Optimization of couple time. (B) Optimization of immunoreaction time. (C) Optimization of the amount of immunomagnetic beads. (D) Optimization of separation time. Optimization of the conditions of the T-IME method by setting a series of gradients. Capture efficiency (CE) under different conditions are calculated, and the best enrichment conditions are selected based on the principle of high CE, and time and cost saving. \* $P < 0.05$ , \*\*\* $P < 0.001$ , \*\*\*\* $P < 0.0001$ .

were incubated during five different times (15, 30, 45, 60, and 75 min). The optimal enrichment time was 60 min, resulting in a nearly constant CE in prolonged times (Figure 2B and Supplementary Table 2).

The amount of IMB was also optimized (Figure 2C and Supplementary Table 3). We tested different amounts of magnetic beads: 0.1, 0.15, and 0.2 mg. However, the CE was nearly stable at all quantities. Therefore, 0.1 mg of IMB was selected as the optimum amount of IMBs. The result of the separation time is shown in Figure 2D and Supplementary Table 4. When the magnetic separation time was 7 min, the CE increased to  $15.63 \pm 0.43\%$ , and longer separation times did not increase CE any further.

## SA-BA-IME Optimization

The amount of biotin mAb was optimized. When the amount of biotin-mAb was 40  $\mu\text{g}$ , CE was the highest. Application of more than 40  $\mu\text{g}$  biotin-mAb resulted in a sharp drop in CE (Figure 3A and Supplementary Table 5). To calculate the optimal immunoreaction time we used five different incubation times (5, 15, 25, 35, and 45 min). When the immunoreaction time reached 25 min, CE was stable (Figure 3B and Supplementary Table 6).

The results of the amount of SA magnetic beads are shown in Figure 3C and Supplementary Table 7. When the amount

of SA magnetic beads was 40–80  $\mu\text{g}$ , the CE increased from  $22.07 \pm 0.43\%$  to  $36.62 \pm 1.43\%$ , and then tended to stabilize with higher amounts. The incubation time was prolonged to 30 min, which was selected as the incubation time, as the CE of IME increased to  $37.48 \pm 0.20\%$  (Figure 3D and Supplementary Table 8).

## P-SA-BA-IME Optimization

P-SA-BA-IME conditions were the same as for SA-BA-IME optimization except that biotin-mAb was replaced with biotin-PAMAM-mAb. The results are presented in Figure 4. When we increased the amount of biotin-PAMAM-mAb from 40 to 50  $\mu\text{g}$ , the CE of NoVs dropped from  $40.34 \pm 2.04\%$  to  $17.18 \pm 0.57\%$ . Therefore, the optimal amount of biotin-PAMAM-mAb was 40  $\mu\text{g}$  (Figure 4A and Supplementary Table 9). The optimal immunoreaction time for CE was 15 min, after that there was no increasing effect (Figure 4B and Supplementary Table 10). The optimal amount of SA magnetic beads was 60  $\mu\text{g}$  (Figure 4C and Supplementary Table 11), and the best incubation time was 20 min (Figure 4D and Supplementary Table 12). Under these optimized conditions, the CE was  $44.26 \pm 1.45\%$ . Compared with the above T-IME ( $15.63 \pm 0.43\%$ ) and SA-BA-IME ( $37.48 \pm 0.20\%$ ), the CE of P-SA-BA-IME were increased by 183.17% ( $P < 0.01$ ) and 18.09% ( $P < 0.05$ ), respectively.

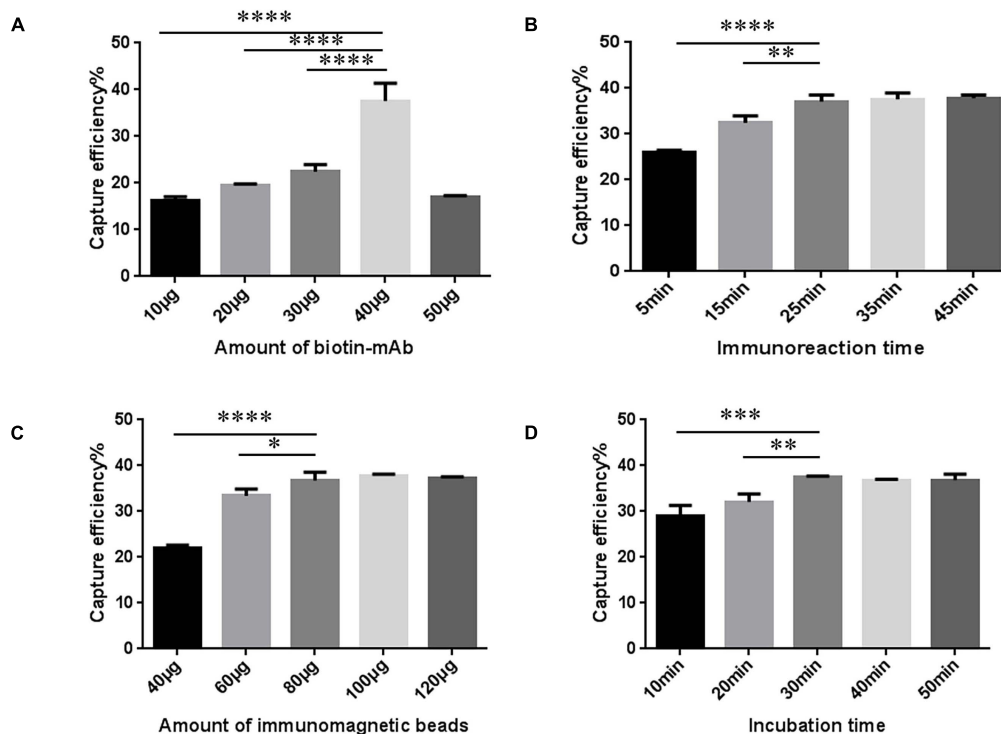


**FIGURE 3 |** Optimization of streptavidin-biotin amplified immunomagnetic enrichment (SA-BA-IME) conditions. **(A)** Amount of biotinylated monoclonal antibody (biotin-mAb) optimization. **(B)** Optimization of immunoreaction time of biotin-mAb with noroviruses. **(C)** Optimization of the amount of immunomagnetic beads. **(D)** Optimization of incubation time. Optimization of the amount of biotin-mAb, immunoreaction time, the amount of immunomagnetic beads, and incubation time that affect the capture efficiency (CE) of the SA-BA-IME. The best enrichment conditions are selected based on the principle of high CE, and time and cost saving. \* $P < 0.05$ , \*\* $P < 0.01$ , \*\*\* $P < 0.001$ , \*\*\*\* $P < 0.0001$ .

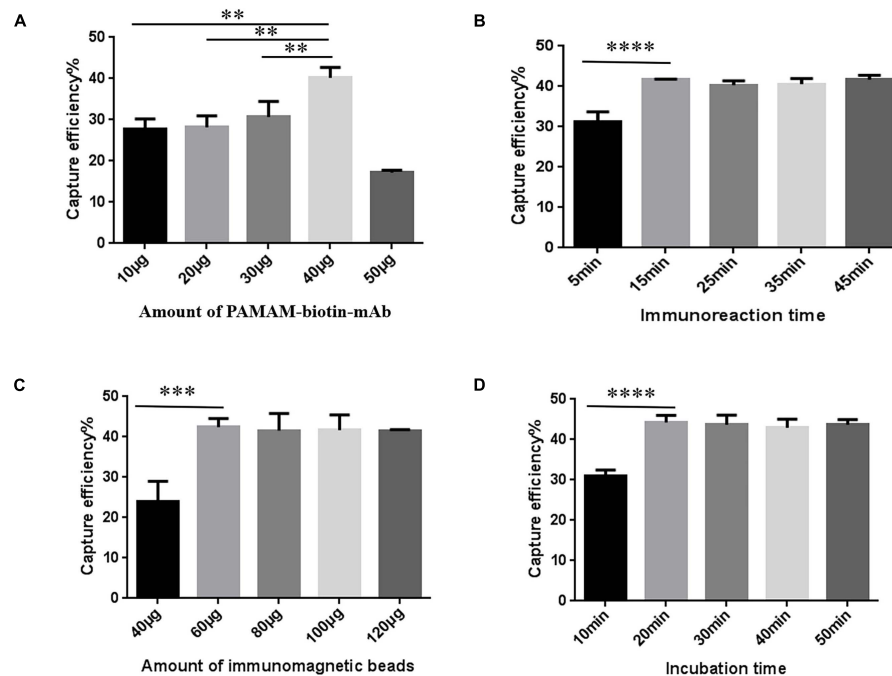


**FIGURE 4 |** Optimization of Polyamidoamine (PAMAM) dendrimer/SA-biotin mediated cascade-amplification IME (P-SA-BA-IME) conditions. **(A)** Amount of biotin-PAMAM- monoclonal antibody (mAb) optimization. **(B)** Optimization of immunoreaction time of biotin-PAMAM-mAb with noroviruses. **(C)** Optimization of the amount of immunomagnetic beads. **(D)** Optimization of incubation time. Optimization of the conditions of P-SA-BA-IME, the best condition according to the capture efficiency under different conditions is selected based on the principle of high capture efficiency, and time and cost saving. \*\* $P < 0.01$ , \*\*\* $P < 0.001$ , \*\*\*\* $P < 0.0001$ .

## Application of Novel Methods in NoVs Detection in Retail Oysters

The three methods were applied for NoV detection in retail oyster samples ( $n = 44$ ), and all NoV-positive results were shown in **Table 1**. The detection rate of P-SA-BA-IME was higher than that of the other two methods. The detection rate of T-IME was 15.90% (7/44), of SA-BA-IME was 18.80% (8/44), and of P-SA-BA-IME was 25% (11/44). There is no significant difference in the detection rates of the three methods ( $P > 0.05$ ). One sample tested positive by T-IME, but negative by SA-BA-IME and P-SA-BA-IME; One sample tested positive by SA-BA-IME, but negative by T-IME and P-SA-BA-IME.

## DISCUSSION

In recent years, NoV outbreaks have attracted increasing attention from public and researchers, and oysters are one of the main causes of the outbreaks (Cheng et al., 2005). Oysters are filter-feeding animals, and their digestive glands have substances similar to the NoVs receptor Human blood group antigens (HBGAs), which could help the virus be accumulated in the oysters (McLeod et al., 2009). Therefore, the digestive gland is used as the target tissue for the NoV detection in oysters in the ISO/TS 15216-2:2013 standard method.

IME pre-treatment methods have the advantage of being easy to use, not requiring complicated equipment, and achieving

effective removal of inhibitors and specific enrichment of pathogens in the samples. In this study, the T-IME, SA-BA-IME, and P-SA-BA-IME methods were established and compared. The T-IME enrichment method has limitations (Wang et al., 2011). It is based on the coupling of antibodies with magnetic beads

**TABLE 1 |** NoVs-positive oysters detected by three novel methods.

Oyster samples	T-IME (genome copies/g tissue)*	SA-BA-IME (genome copies/g tissue)*	P-SA-BA-IME (genome copies/g tissue)*
1902-3	—	$9.8 \times 10^1$	—
1905-3	—	$4.4 \times 10^1$	$8.0 \times 10^1$
1908-5	—	—	$9.8 \times 10^1$
1909-1	—	—	$3.5 \times 10^4$
1909-2	$6.7 \times 10^3$	$5.0 \times 10^3$	$1.1 \times 10^3$
1910-1	$1.2 \times 10^2$	—	—
1910-4	—	—	$9.1 \times 10^2$
1910-5	$3.8 \times 10^3$	$2.2 \times 10^3$	$5.5 \times 10^3$
1911-1	$4.8 \times 10^3$	$4.3 \times 10^3$	$9.4 \times 10^4$
1911-2	$1.1 \times 10^4$	—	$3.2 \times 10^3$
1911-3	—	$2.4 \times 10^2$	$3.3 \times 10^2$
1911-4	$3.8 \times 10^2$	$1.9 \times 10^2$	$1.5 \times 10^2$
1911-5	$1.2 \times 10^2$	$1.8 \times 10^2$	$1.3 \times 10^2$
Total number	$7.0 \times 10^0$	$8.0 \times 10^0$	$1.1 \times 10^1$

\*The numbers of NoV genome copies per gram of oyster digestive gland were left uncorrected.

directly through covalent bonds, however, the surface of the magnetic beads is rigid, and the connection stability is extremely poor, which may lead to changes in the spatial structure of the antibody and reduce its activity (Shan et al., 2014). Changes in the spatial direction of antibodies increase the steric hindrance between them, which will also reduce the CE (Jo et al., 2015). SA-BA-IME combines magnetic bead-coupled SA and biotinylated antibodies, which improves the stability during the reaction and indirectly increases the area where the antibody molecule binds to the target, so a higher CE can be obtained. P-SA-BA-IME consists of a two-stage amplification based on SA one-stage amplification.

IMS methods have been applied for detecting NoVs in different food samples (Park et al., 2008; Lee et al., 2013; Ha et al., 2014), the antibodies are the main factor affecting the broad spectrum of enrichment methods. Park et al. used polyclonal antibody coupled with magnetic beads (280  $\mu\text{m}$ ) combined with real-time RT-PCR to detect GI.1 and GII.4 NoV in artificially contaminated strawberries, the polyclonal antibody used in this method can react with more than 31 NoV genotypes (Park et al., 2008). The maximum recovery rate of this method was 30% lower than that of P-SA-BA-IME, but it had a good broad-spectrum combination. It should be noted that GI NoVs are also widely detected in foods such as shellfish. However, the diversity of human NoVs poses a challenge for the simultaneous capture of GI and GII NoVs. The development of high-titer and broad-spectrum antibodies is the key to the development of the NoV enrichment method with broader spectrum in the future.

As the particle size of the magnetic beads decreased, the number of magnetic beads that could be bound to the pathogen surface increased significantly. Yang et al. (2007) studied the CE of nanomagnetic beads and micromagnetic beads, and the results showed that the capture efficiency of nanomagnetic beads was 1–2 times higher than that of micromagnetic beads. The lower concentration of the targets in the solution, the stronger capture ability of the nanomagnetic beads. Therefore, nanomagnetic beads were selected for this study instead of micromagnetic beads to improve the CE.

In this study, PAMAM was used as the coupling carrier of biotin to achieve biotin amplification. However, when the amount of biotin-mAb was excessive, it competed to bind to SA magnetic beads, resulting in a decrease in CE. The anti-NoV mAb used in this study was prepared by using GII.4 NoV capsid P protein as immunogen with the titer  $>10^6$ , ELISA results showed that the anti-NoV mAb could react with GII.2, GII.3, GII.4, GII.6, GII.17 NoVs (Gao et al., 2021), which ensured the high efficiency of NoVs enrichment. The amount of biotin-mAb and the selection of anti-NoVs mAb are both the important factors affecting CE. And oysters purchased from the market were directly used for the evaluation of the three methods, the detection rate of the P-SA-BA-IME method was 25.0% which is higher than that of ISO/TS standard method for detection of retail oysters (20.71%, 16.9%) in China (Jiang et al., 2018; Zhang et al., 2021). However, we developed a modified ISO/TS 15216-2:2013 standard method which combined with the PEG precipitation concentration method to increase the detection rate to 34.21% (Zhang et al., 2020). In the next work, the sensitivity

of P-SA-BA-IME method can be further improved by changing the antibody or optimizing the conditions. Few samples were tested negative by P-SA-BA-IME but positive by T-IME and SA-BA-IME, which may have been caused by the low viral load. Besides, the genome copies numbers in some oyster detected by the new method were also not the highest, this may be due to insufficient mixing when the sample is divided into three equal parts resulting in uneven distribution, or the influence of impurities, IMBs and the NoVs in the suspension did not fully bind during the limited incubation time. A large number of samples may reflect the advantages of the P-SA-BA-IME method. The results showed that the CE of the T-IME was  $15.63 \pm 0.43\%$ , and the SA-BA-IME improved the CE to  $37.48 \pm 0.20\%$ . P-SA-BA-IME efficiently binds SA magnetic beads and PAMAM-conjugated biotin-mAb, with a CE of  $44.26 \pm 1.45\%$ .

In summary, we established a sensitive and efficient pre-treatment method for NoV detection in oysters. PAMAM-conjugated biotin-mAb combined with SA-biotin IMBs were used for the enrichment of NoVs in oysters for the first time, showing the utility of this method to increase the detection rate of NoVs in oysters. This is important for preventing NoV infection from shellfish.

## DATA AVAILABILITY STATEMENT

The original contributions presented in the study are included in the article/**Supplementary Material**, further inquiries can be directed to the corresponding author/s.

## AUTHOR CONTRIBUTIONS

JG, LX, and JZ designed the research. JG and LZ performed the experiments and wrote the manuscript. WC, ZQ, JY, YaL, and LW contributed to the reagents and materials. JG, LX, and WC analyzed the data. LX, JZ, and QW performed critical revisions of the manuscript. All authors contributed to the article and approved the submitted version.

## FUNDING

This study was supported by the National Key Research and Development Program of China (2018YFC1602500), the National Natural Science Foundation of China (31872912), the Natural Science Foundations of Guangdong Province for Distinguished Young Scholars (2019B151502065), the Key Research and Development Program of Guangdong Province (2019B020209001), and GDAS' Project of Science and Technology Development (2020GDASYL-20200104008).

## SUPPLEMENTARY MATERIAL

The Supplementary Material for this article can be found online at: <https://www.frontiersin.org/articles/10.3389/fmicb.2021.673872/full#supplementary-material>



## REFERENCES

- Ahmed, S. M., Hall, A. J., Robinson, A. E., Verhoeve, L., Premkumar, P., Parashar, U. D., et al. (2014). Global prevalence of norovirus in cases of gastroenteritis: a systematic review and meta-analysis. *Lancet Infect. Dis.* 14, 725–730. doi: 10.1016/s1473-3099(14)70767-4
- Cao, M., Li, Z. H., Wang, J. L., Ge, W. P., Yue, T. L., Li, R. H., et al. (2012). Food related applications of magnetic iron oxide nanoparticles: enzyme immobilization, protein purification, and food analysis. *Trends Food Sci. Tech.* 27, 47–56. doi: 10.1016/j.tifs.2012.04.003
- Cheng, P. K., Wong, D. K., Chung, T. W., and Lim, W. W. (2005). Norovirus contamination found in oysters worldwide. *J. Med. Virol.* 76, 593–597. doi: 10.1002/jmv.20402
- El Moqri, N., El Mellouli, F., Hassou, N., Benhafid, M., Abouchoaib, N., and Etahiri, S. (2019). Norovirus detection at oualidia lagoon, a moroccan shellfish harvesting area, by reverse transcription PCR analysis. *Food Environ. Virol.* 11, 268–273. doi: 10.1007/s12560-019-09386-0
- Gao, J. S., Xue, L., Cai, W. C., Liao, Y. Y., Zuo, Y. T., Zhang, J. M., et al. (2021). Preparation and application of GII norovirus broad-spectrum monoclonal antibody based on GII.4 norovirus P protein. *Chin. J. Virol.* doi: 10.13242/j.cnki.bingduxuebao.003923
- Ha, J. H., Choi, C., and Ha, S. D. (2014). Evaluation of immunomagnetic separation method for the recovery of hepatitis A virus and GII.1 and GII.4 norovirus strains seeded on oyster and mussel. *Food Environ. Virol.* 6, 290–296. doi: 10.1007/s12560-014-9156-2
- Jiang, S., Qiu, L., Wang, L., Jia, Z., Lv, Z., Wang, M., et al. (2018). Transcriptomic and quantitative proteomic analyses provide insights into the phagocytic killing of hemocytes in the oyster *Crassostrea gigas*. *Front. Immunol.* 9:1280. doi: 10.3389/fimmu.2018.01280
- Jo, S. M., Lee, J. J., Heu, W., and Kim, H. S. (2015). Nanotentacle-structured magnetic particles for efficient capture of circulating tumor cells. *Small* 11, 1975–1982. doi: 10.1002/smll.201402619
- Jothikumar, N., Lowther, J. A., Henshilwood, K., Lees, D. N., Hill, V. R., and Vinje, J. (2005). Rapid and sensitive detection of noroviruses by using TaqMan-based one-step reverse transcription-PCR assays and application to naturally contaminated shellfish samples. *Appl. Environ. Microbiol.* 71, 1870–1875. doi: 10.1128/aem.71.4.1870-1875.2005
- Le Guyader, F. S., Atmar, R. L., and Le Pendu, J. (2012). Transmission of viruses through shellfish: when specific ligands come into play. *Curr. Opin. Virol.* 2, 103–110. doi: 10.1016/j.coviro.2011.10.029
- Le Mennec, C., Parnaudeau, S., Rumebe, M., Le Saux, J. C., Piquet, J. C., and Le Guyader, S. F. (2017). Follow-up of norovirus contamination in an oyster production area linked to repeated outbreaks. *Food Environ. Virol.* 9, 54–61. doi: 10.1007/s12560-016-9260-6
- Lee, H. M., Kwon, J., Choi, J. S., Lee, K. H., Yang, S., Ko, S. M., et al. (2013). Rapid Detection of norovirus from fresh lettuce using immunomagnetic separation and a quantum dots assay. *J. Food Prot.* 76, 707–711. doi: 10.4315/0362-028x.jfp-12-343
- Lee, J. C., and Lee, L. L. Y. (1981). Preferential solvent interactions between proteins and polyethylene glycols. *J. Biol. Chem.* 256, 625–631. doi: 10.1016/s0021-9258(19)70019-2
- McLeod, C., Hay, B., Grant, C., Greening, G., and Day, D. (2009). Localization of norovirus and poliovirus in Pacific oysters. *J. Appl. Microbiol.* 106, 1220–1230. doi: 10.1111/j.1365-2672.2008.04091.x
- Park, Y., Cho, Y. H., Jee, Y., and Ko, G. (2008). Immunomagnetic separation combined with real-time reverse transcriptase PCR assays for detection of norovirus in contaminated food. *Appl. Environ. Microbiol.* 74, 4226–4230. doi: 10.1128/aem.00013-08
- Shan, S., Zhong, Z. Q., Lai, W. H., Xiong, Y. H., Cui, X., and Liu, D. F. (2014). Immunomagnetic nanobeads based on a streptavidin-biotin system for the highly efficient and specific separation of *Listeria monocytogenes*. *Food Control* 45, 138–142. doi: 10.1016/j.foodcont.2014.04.036
- Siebenga, J. J., Vennema, H., Zheng, D. P., Vinje, J., Lee, B. E., Pang, X. L., et al. (2009). Norovirus illness is a global problem: emergence and spread of norovirus GII.4 variants, 2001–2007. *J. Infect. Dis.* 200, 802–812. doi: 10.1086/605127
- Valdes, M. G., Gonzalez, A. C. V., Calzon, J. A. G., and Diaz-Garcia, M. E. (2009). Analytical nanotechnology for food analysis. *Microchimica Acta* 166, 1–19. doi: 10.1016/b978-0-12-820591-4.001-3
- Vinje, J. (2015). Advances in laboratory methods for detection and typing of norovirus. *J. Clin. Microbiol.* 53, 373–381. doi: 10.1128/jcm.01535-14
- Wang, H., Li, Y., Wang, A., and Slavik, M. (2011). Rapid, sensitive, and simultaneous detection of three foodborne pathogens using magnetic nanobead-based immunoseparation and quantum dot-based multiplex immunoassay. *J. Food Prot.* 74, 2039–2047. doi: 10.4315/0362-028x.jfp-11-144
- Woods, J. W., Calci, K. R., Marchant-Tambone, J. G., and Burkhardt, W. III (2016). Detection and molecular characterization of norovirus from oysters implicated in outbreaks in the US. *Food Microbiol.* 59, 76–84. doi: 10.1016/j.fm.2016.05.009
- Wu, Y. W., Chang, S., Nannapaneni, R., Coker, R., Haque, Z., and Mahmoud, B. S. M. (2016). The efficacy of X-ray doses on murine norovirus-1 (MNV-1) in pure culture, half-shell oyster, salmon sushi, and tuna salad. *Food Control* 64, 77–80. doi: 10.1016/j.foodcont.2015.12.018
- Xiong, Q. R., Cui, X., Saini, J. K., Liu, D. F., Shan, S., Jin, Y., et al. (2014). Development of an immunomagnetic separation method for efficient enrichment of *Escherichia coli* O157:H7. *Food Control* 37, 41–45. doi: 10.1016/j.foodcont.2013.08.033
- Xue, L., Cai, W., Gao, J., Zhang, L., Dong, R., Li, Y., et al. (2019). The resurgence of the norovirus GII.4 variant associated with sporadic gastroenteritis in the post-GII.17 period in South China, 2015 to 2017. *BMC Infect. Dis.* 19:696. doi: 10.1186/s12879-019-4331-6
- Xue, L., Dong, R., Wu, Q., Li, Y., Cai, W., Kou, X., et al. (2016). Molecular epidemiology of noroviruses associated with sporadic gastroenteritis in Guangzhou, China, 2013–2015. *Arch. Virol.* 161, 1377–1384. doi: 10.1007/s00705-016-2784-0
- Xue, L., Wu, Q., Dong, R., Kou, X., Li, Y., Zhang, J., et al. (2013). Genetic analysis of noroviruses associated with sporadic gastroenteritis during winter in Guangzhou, China. *Foodborne Pathog. Dis.* 10, 888–895. doi: 10.1089/fpd.2013.1521
- Yang, H., Qu, L., Wimbrow, A. N., Jiang, X., and Sun, Y. (2007). Rapid detection of *Listeria monocytogenes* by nanoparticle-based immunomagnetic separation and real-time PCR. *Int. J. Food Microbiol.* 118, 132–138. doi: 10.1016/j.ijfoodmicro.2007.06.019
- Yao, L., Wu, Q., Wang, D., Kou, X., and Zhang, J. (2009). Development of monoclonal antibody-coated immunomagnetic beads for separation and detection of norovirus (genogroup II) in faecal extract samples. *Lett. Appl. Microbiol.* 49, 173–178. doi: 10.1111/j.1472-765x.2009.02638.x
- Yellepeddi, V. K., Kumar, A., and Palakurthi, S. (2009). Surface modified poly(amido)amine dendrimers as diverse nanomolecules for biomedical applications. *Expert Opin. Drug Deliv.* 6, 835–850. doi: 10.1517/17425240903061251
- Yuan, C., Chen, A., Kolb, P., and Moy, V. T. (2000). Energy landscape of streptavidin-biotin complexes measured by atomic force microscopy. *Biochemistry* 39, 10219–10223. doi: 10.1021/bi992715o
- Zhang, H. N., Liu, D. L., Zhang, Z. L., Hewitt, J., Li, X. P., Hou, P. B., et al. (2021). Surveillance of human norovirus in oysters collected from production area in shandong province, china during 2017–2018. *Food Control* 121:107649. doi: 10.1016/j.foodcont.2020.107649
- Zhang, L., Xue, L., Gao, J. S., Cai, W. C., Jiang, Y. T., Zuo, Y. T., et al. (2020). Development of a high-efficient concentrated pretreatment method for noroviruses detection in independent oysters: an extension of the ISO/TS 15216-2:2013 standard method. *Food Control* 111:107032. doi: 10.1016/j.foodcont.2019.107032

**Conflict of Interest:** The authors declare that the research was conducted in the absence of any commercial or financial relationships that could be construed as a potential conflict of interest.

Copyright © 2021 Gao, Zhang, Xue, Cai, Qin, Yang, Liang, Wang, Chen, Ye, Li, Wang, Wu, Wu and Zhang. This is an open-access article distributed under the terms of the Creative Commons Attribution License (CC BY). The use, distribution or reproduction in other forums is permitted, provided the original author(s) and the copyright owner(s) are credited and that the original publication in this journal is cited, in accordance with accepted academic practice. No use, distribution or reproduction is permitted which does not comply with these terms.



# Application of Engineered Bacteriophage T7 in the Detection of Bacteria in Food Matrices

Nicharee Wisuthiphaet<sup>1</sup>, Xu Yang<sup>2</sup>, Glenn M. Young<sup>1</sup> and Nitin Nitin<sup>1,3\*</sup>

<sup>1</sup>Department of Food Science and Technology, University of California, Davis, Davis, CA, United States, <sup>2</sup>Department of Nutrition and Food Science, California State Polytechnic University Pomona, Pomona, CA, United States, <sup>3</sup>Department of Biological and Agricultural Engineering, University of California, Davis, Davis, CA, United States

## OPEN ACCESS

### Edited by:

Xiyang Wu,  
Jinan University, China

### Reviewed by:

Rolf Dieter Joerger,  
University of Delaware,  
United States  
Yi Wang,  
Auburn University, United States

### \*Correspondence:

Nitin Nitin  
nnitin@ucdavis.edu

### Specialty section:

This article was submitted to  
Food Microbiology,  
a section of the journal  
Frontiers in Microbiology

**Received:** 05 April 2021

**Accepted:** 12 July 2021

**Published:** 06 August 2021

### Citation:

Wisuthiphaet N, Yang X,  
Young GM and Nitin N (2021)  
Application of Engineered  
Bacteriophage T7 in the Detection of  
Bacteria in Food Matrices.  
Front. Microbiol. 12:691003.  
doi: 10.3389/fmicb.2021.691003

Detection of pathogens in a food matrix is challenging due to various constraints including complexity and the cost of sample preparation for microbial analysis from food samples, time period for the detection of pathogens, and high cost and specialized resources required for advanced molecular assays. To address some of these key challenges, this study illustrates a simple and rapid colorimetric detection of target bacteria in distinct food matrices, including fresh produce, without prior isolation of bacteria from a food matrix. This approach combines bacteriophage-induced expression of an exogenous enzyme, alkaline phosphatase, the specific colorimetric substrate that generates insoluble color products, and a simple filtration method to localize the generation of colored signal. Using this approach, this study demonstrates the specific detection of inoculated *Escherichia coli* in coconut water and baby spinach leaves. Without isolating bacteria from the selected food matrices and using a food sample size that is representative of industrial samples, the inoculated samples were added to the enrichment broth for a short period (5 h) and incubated with an engineered bacteriophage T7 with a *phoA* gene. The incubation period with the engineered bacteriophage was 30 min for liquid samples and 2 h for fresh produce samples. The samples were then filtered through a 0.2-micron polycarbonate membrane and incubated with a colorimetric substrate, i.e., nitro blue tetrazolium/5-bromo-4-chloro-3-indolyl phosphate (NBT/BCIP). This substrate forms a dark purple precipitate upon interactions with the released enzyme on a filter membrane. This approach successfully detected 10 CFU/ml of *E. coli* in coconut water and 10<sup>2</sup> CFU/g of *E. coli* on baby spinach leaves with 5 h of enrichment. Success of this approach illustrates potential for detecting target bacteria in food systems using a simple visual assay and/or quantitative colorimetric measurements.

**Keywords:** engineered bacteriophage, *Escherichia coli*, colorimetric detection, alkaline phosphatase, 5-bromo-4-chloro-3-indolyl phosphate

## INTRODUCTION

Globally, human illness due to foodborne pathogens is a major cause of morbidity and mortality. Even within the United States, which has advanced sanitation systems, an estimated 48 million people experience foodborne illness each year (Centers for Disease Control and Prevention, 2018). The leading cause of foodborne illnesses has been the contamination of food, such as fresh

produce, dairy and meat products with microbial pathogens, for example, among those pathogens of most concern are Shiga toxin-producing *Escherichia coli* (STEC), which are reported as a cause for an estimated 265,000 illnesses and 3,600 hospitalization annually in the United States (Scallan et al., 2011). Therefore, rapid and efficient detection of the microbial contaminants plays an important role in mitigating the risk of food borne outbreaks and improving sanitary controls in the food supply chain. Several approaches for pathogen detection have been deployed in the industry. However, rapid and sensitive detection of bacteria, especially in complex food matrices, continues to be a challenge.

In the food industry, multiple detection methods are used for the food safety assessment process. The conventional culture-dependent detection method is considered as the gold standard for bacterial detection; however, it is both time-consuming and labor-intensive. These limitations can be acute for food industries, such as the fresh produce industry, as products have limited shelf life (Cho and Ku, 2017). Therefore, more advanced rapid detection methods, including nucleic acid-based and immunological-based methods, are currently being employed in the food industry. Polymerase chain reaction (PCR) is a nucleic acid-based technique offering rapid and specific pathogen detection. This approach has high sensitivity enabling simultaneous amplification and quantification of specific nucleic acid sequences (Kralik and Ricchi, 2017). The most commonly used immunological-based method is enzyme-linked immunosorbent assay (ELISA) that can be automated to enable rapid detection of pathogens with reduced labor.

However, these advanced methods also have some drawbacks. PCR has suffered from complicated sample preparation, costly reagents, and technical support requirements. Using nucleic acid-based methods to detect pathogens in food samples can be challenging since foods are highly complex biomolecular matrices with diverse arrays of biomolecules such as proteins, carbohydrates, fats, oil, polyphenolics, and other small molecules. These compounds may act as inhibitors of the enzymatic reactions in PCR, resulting in false-negative results or limit sensitivity of the assay (Jaykus, 2003). The use of PCR in food is also limited by high sample volumes ( $\geq 25$  ml or g) compared to small amplification volumes (10–50  $\mu$ l) used for the PCR detection (Stevens and Jaykus, 2014). In the case of ELISA, reduced specificity due to the cross-reactivity of polyclonal antibodies with closely related antigens can be a limitation (Hornbeck, 2015). Therefore, constraints for the detection of foodborne pathogens by ELISA include a large number of background microflora present in food samples. Even though these microbes may not cause any health problems, they can interfere with the selective identification and isolation of target pathogenic bacteria, which are usually found in relatively low numbers. In order to improve the sensitivity of these detection methods, at least 4–5 h of enrichment is still required for both PCR and ELISA assays, which prolongs the overall turnaround time. Despite these enrichment steps, the detection sensitivity of typical RT-PCR assays using the isolation and detection of bacteria from food matrices ranges from  $10^2$  to  $10^4$  CFU/ml and for ELISA assays ranges from

$10^3$  to  $10^5$  CFU/ml (Sharma and Mutharasan, 2013). In addition, the standard PCR and ELISA methods provide limited specificity for differentiating live vs. dead microbes (De Boer and Beumer, 1999; Liu et al., 2017).

Considering the above challenges, there is still a significant unmet need for rapid, cost-effective, and easy-to-perform bacterial detection methods that can be applied to detect specific bacteria in the presence of complex food samples. Bacteriophages have become a valuable tool for developing bacterial detection assays due to their ability to recognize and infect specific strains of bacteria with the time of analysis ranging from 15 min to 8 h (Paczesny et al., 2020). For the detection of bacteria in complex food matrices, the common approach is to genetically engineer bacteriophages to express reporter genes upon infecting the target host bacteria. One of the most commonly used reporter genes is bacterial luciferase (*lux*) that generates a bioluminescence signal (Loessner et al., 1997; Kim et al., 2014), for example, the *E. coli* O157:H7-infecting bacteriophage  $\phi$ hV10 was genetically modified to express the *lux* operon and used for the detection of *E. coli* O157:H7. This approach was reported to detect 10 CFU/cm<sup>2</sup>, 13 CFU/ml, and 17 CFU/g of *E. coli* O157:H7 in romaine lettuce, apple juice, and ground beef, respectively, by detecting bioluminescence using a luminometer with 5-h pre-enrichment (Kim et al., 2017). Another commonly used reporter gene is *lacZ* encoding  $\beta$ -galactosidase. Using this approach, *E. coli* infected with T7 bacteriophage with the *lacZ* operon overexpresses  $\beta$ -galactosidase and allowed the detection of 10 CFU/ml of *E. coli* using a colorimetric substrate within 7 h and enabled the detection of  $10^2$  CFU/ml of *E. coli* in food samples (Chen et al., 2017a,b). The gene that encodes alkaline phosphatase (*phoA*) is another reporter gene that has been engineered into the bacteriophage T7 genome to induce the overexpression of alkaline phosphatase. Overexpression of alkaline phosphatase gene has been detected using both soluble colorimetric substrate, p-nitrophenyl phosphate (pNPP), which allows for the detection of  $10^4$  CFU/ml within 7.5 h and  $10^3$  CFU/ml of *E. coli* in 6 h using a chemiluminescent substrate (Alcaine et al., 2015). Enzyme-labeled fluorescence-97 (ELF-97), alkaline phosphatase substrate that gives insoluble fluorescent precipitated products, has been used to detect the engineered bacteriophage-induced alkaline phosphatase activity at the single-cell level using fluorescent imaging and image analysis. This approach was tested in beverage samples and was able to detect  $10^2$  CFU/ml of target bacteria within 6 h (Wisuthiphaet et al., 2019). Even though these methods have been proven to detect a low number of the specific bacteria in complex matrices, maintaining both rapidity and simplicity of the procedure can be challenging due to a range of issues related to sample preparation including bacteria isolation steps, instruments required for signal analysis, and distinguishing signal from high background noise in food samples.

The goal of this study was to develop a rapid bacteriophage-based colorimetric bacterial detection that is low-cost, easy-to-perform, and can be applied to detect bacteria in complex food samples without isolation of bacteria from food matrices.

Isolation of bacteria from food samples is a time, equipment, and labor-intensive process (Stevens and Jaykus, 2014). The approach evaluated in this study does not use any isolation of bacteria from food samples and thus reduces complexity of the assay. Furthermore, colorimetric detection approach was selected as it provides a simple read out for a visual analysis as well as quantitative measurement using a camera. For colorimetric detection, we evaluated insoluble substrates, nitro blue tetrazolium and 5-bromo-4-chloro-3-indolyl phosphate (NBT/BCIP) and commonly used soluble substrate, pNPP to detect the enzymatic activity. NBT/BCIP yields insoluble dark purple precipitate that is localized at the site of the reaction and can be visualized by the naked eye. After applying this substrate to the bacterial cells with overexpressed alkaline phosphatase, the precipitated product was accumulated inside the cells. After separation of bacterial cells from the combined culture medium and the food samples by filtration, the signal was concentrated and was enabled the detection of visible color change. The efficiency of bacterial detection using NBT/BCIP and engineered bacteriophage T7 was evaluated in coconut water and baby spinach leaves and compared with those of the commonly used soluble substrate, pNPP. Overall, the results of this study demonstrate the potential of visual detection of bacterial contaminants in food samples using engineered bacteriophages without extensive sample preparation steps.

## MATERIALS AND METHODS

### Bacteriophage and Bacterial Strain

Engineered bacteriophage used in this study, designated bacteriophage T7-ALP, was bacteriophage T7 that has been genetically modified to carry the gene for alkaline phosphatase production, *phoA*. The bacteriophage T7-ALP strain was kindly provided by Dr. Sam Nugen (Alcaine et al., 2015). *Escherichia coli* BL21 (ATCC BAA-1025) obtained from the American type culture collection was used as a host for the bacteriophage T7-ALP. Bacteria were stored in tryptic soy broth (TSB; Sigma-Aldridge, St. Louis, MO, United States) containing 15% (vol/vol) glycerol at  $-80^{\circ}\text{C}$ . For short-term storage, the glycerol stock was streaked onto tryptic soy agar (Sigma-Aldridge, St. Louis, MO, United States) plates. After incubation at  $37^{\circ}\text{C}$  for 24 h, the culture plates were stored at  $4^{\circ}\text{C}$ . Overnight culture of *E. coli* BL21 was prepared by inoculation a loop-full of culture on an agar plate in TSB, after 16 h of aerobic incubation at  $37^{\circ}\text{C}$ , bacteria with the concentration of  $10^9$  CFU/ml were obtained.

### Sample Preparation and Bacterial Inoculation

Overnight culture of *E. coli* BL 21 was centrifuged at  $16100 \times g$  for 1 min. The cell pellet was washed twice and re-suspended in sterile phosphate buffer saline (PBS; Fair Lawn, NJ, United States) at the population of  $10^9$  CFU/ml. The serial dilutions were performed using sterile PBS to obtain bacterial concentrations of  $10^3$  and  $10^2$  CFU/ml.

Sterile TSB was portioned to 10 ml in a 50-ml sterile centrifugal tube. Pasteurized coconut water (Vita coco 100% coconut water) purchased from local grocery store, and 5 ml was mixed with 5 ml of double concentrated TSB in a 50-ml sterile centrifugal tube. *Escherichia coli* BL21 with the final concentration of 10 CFU/ml was inoculated in 10 ml of the liquid media. The fresh produce sample was represented by baby spinach leaves. Store-bought baby spinach leaves were weighted 25 g in sterile sampling bag before inoculated with *E. coli* BL21 to achieve the final concentration of  $10^2$  CFU/g. The bags were tightly sealed and kept at  $4^{\circ}\text{C}$  for 24 h. Then 225 ml of TSB was added to 25 g inoculated spinach in the sampling bags.

### Enrichment and Bacteriophage Infection

The enrichment of all samples was carried out at  $37^{\circ}\text{C}$  with constant shaking at 200 rpm for 5 h. For spinach leaf samples, 10 ml of the TSB was collected in a 50-ml centrifugal tube. Genetically engineered bacteriophage T7-ALP was added into 10 ml of the enriched samples with a concentration of  $10^6$  PFU/ml. For liquid samples, the infection time was fixed at 30 min at  $37^{\circ}\text{C}$  with constant shaking at 200 rpm. For 25-g spinach leaf samples, the infection time was fixed at 2 h at  $37^{\circ}\text{C}$  with constant shaking at 200 RPM. Negative controls of each experiment were *E. coli* inoculated samples without bacteriophage infection and samples without bacteria inoculation with bacteriophage added.

### Colorimetric Assay of Alkaline Phosphatase Activity Using NBT/BCIP

After phage infection, 10 ml of TSB and coconut water samples, and 2 ml of spinach leaf samples were filtered through a 0.22-micron white polycarbonate membrane discs with a 19-mm diameter (Nucleopore Polycarbonate, Whatman) using a vacuum filtering system in order to capture infected bacterial cells harboring bacteriophage-induced alkaline phosphatase. After the filters were completely dry, 20  $\mu\text{l}$  of 1-Step™ NBT/BCIP substrate solution (Thermo Scientific, Rockford, IL, United States) was spotted on a petri dish. The filter was then transferred directly onto the NBT/BCIP drop with topside down. The visible color change due to the formation of black-purple precipitated product was observed and compared with those of negative controls and tryptic soy broth without bacteria and bacteriophage. The Hunter's color values ( $L^*$ ,  $a^*$ , and  $b^*$ ) of the filters were measured at five locations of each filter using the ColorFlex EZ Spectrophotometer (Hunter Lab, Reston, VA, United States). The delta E (dE) value was calculated using Equation 1.

$$\Delta E_{ab}^* = \sqrt{(L_2^* - L_1^*)^2 + (a_2^* - a_1^*)^2 + (b_2^* - b_1^*)^2} \quad (1)$$

### Colorimetric Assay of Alkaline Phosphatase Activity Using pNPP

After bacteriophage infection, 10 ml of all samples were centrifuged at  $4025 \times g$  for 10 min at room temperature.



The liquid media were discarded and the precipitated cells were re-suspended with 50  $\mu$ l of sterile PBS. Amplite™ Colorimetric Alkaline Phosphatase Assay Kit (AAT Bioquest, Sunnyvale, CA) was used to perform the assay. After adding the substrate, the absorbance at 400 nm was measured every 10 min for 4 h using a SpectraMax 340 spectrophotometric plate reader (Molecular Devices, Sunnyvale, CA, United States). The experiments were performed in parallel with the blank, which was TSB without *E. coli* and bacteriophage inoculation and negative control of *E. coli* without bacteriophage inoculation.

## Statistical Analysis

All experiments were repeated three times. Color value was measured at five random positions on the filter, and the mean and standard deviation values were calculated within the samples. The Tukey's HSD test were used to determine significant differences ( $\alpha = 0.05$ ) between mean values. All experimental data were analyzed using the R software.

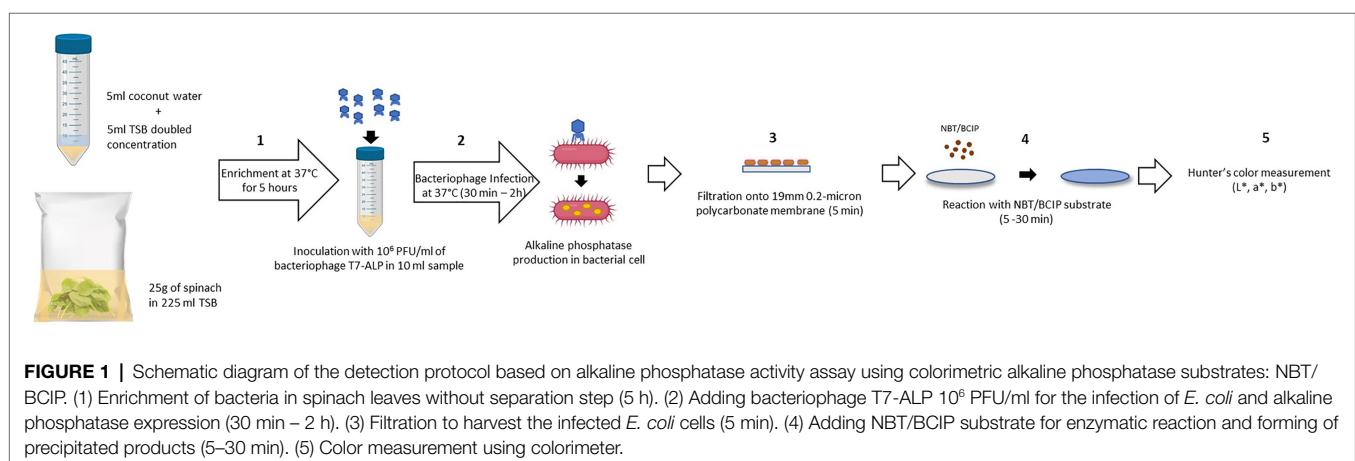
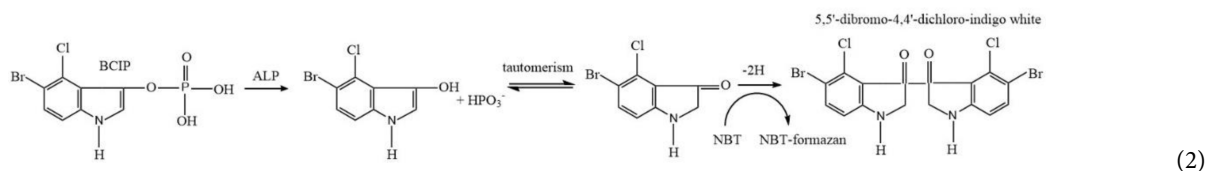
## RESULTS

### Colorimetric Detection of *E. coli* Using Engineered Bacteriophage T7-ALP and Alkaline Phosphatase Assay
















The schematic diagram (Figure 1) depicts the detection procedure developed in this study. One of the most challenging aspects in the detection of bacteria from a complex food system is the presence of food components and non-pathogenic microbes associated with the food. These elements can influence both the sensitivity and accuracy of the detection method. Developing a general protocol to separate and purify target cells from different food matrices is difficult as food matrices vary

significantly in composition and structure (Frederick et al., 2013). In order to overcome these constraints, the bacteriophage-based detection method developed in this study requires no complicated sample preparation and bacterial separation or concentration steps. The food samples, coconut water, and baby spinach leaves were simply mixed with the TSB before enrichment and used for the detection of bacteria using a simple colorimetric approach. The steps for sample preparation are illustrated in Figure 1. The steps include enrichment of bacteria (step 1), incubation with T7-ALP (step 2), filtration (step 3), and incubation with ALP substrate to form colorimetric precipitate (step 4). The details of these steps are described in the Material and Methods section. Among these steps, the incubation and infection time was a critical factor in this assay, as our goal was to overexpress and entrap the expressed enzyme inside the bacterial cells, thus the infection time should be long enough for the expression of the enzyme but not too long to have complete lysis of the bacterial cells and release of the enzyme. This approach helps to localize the colorimetric signal on a filter and increase sensitivity of the detection. According to a previous study, after 30 min of co-incubation with bacteriophage T7-ALP, *E. coli* BL21 cells were infected and alkaline phosphatase was produced while the majority of the cells were still intact (Wisuthiphaet et al., 2019). By filtration (Figure 1; step 3), bacterial cells with alkaline phosphatase were captured on the filter and the colorimetric signal was concentrated on the filter membrane for visual detection.

Alkaline phosphatase activity was analyzed with the chromogenic substrate 5-bromo-4-chloro-3-indolyl phosphate (BCIP) that forms a dark purple precipitated product (Figure 1; step 4). The color development was enhanced by nitro blue tetrazolium (NBT) yielding an insoluble black-purple precipitate as shown in the following reaction Equation 2 (Jékely and Arendt, 2007; Kundu, 2014).



**TABLE 1** | Filters with 5-h enriched 10 CFU/ml *Escherichia coli* BL21 and 30 min with and without infection with bacteriophage T7-ALP in TSB and bacteriophage T7-ALP in TSB after enzymatic reaction with NBT/BCIP for 5, 10, 20, and 30 min.

Reaction condition		Reaction time with substrate (min)				
<i>Escherichia coli</i> inoculation	T7 infection	0	5	10	20	30
+	+					
+	–					
–	+					

This enzymatic reaction took place on the filter. Therefore, the change in filter color to dark purple indicates the presence of the target bacteria. Color formation was observed visually as well as using a colorimeter (**Figure 1**; step 5). The detection method using a precipitated colorimetric substrate was compared to the soluble colorimetric alkaline phosphatase substrate, pNPP. In this method, infected cells with alkaline phosphatase were harvested by centrifugation before re-suspension in sterile PBS prior to the enzymatic reaction. Colorless pNPP was hydrolyzed to yellow p-nitro-phenol (pNP) in the presence of alkaline phosphatase and was quantified at 400 nm (Jackson et al., 2016).

### Detection of Bacteria Using Bacteriophage T7-ALP and Alkaline Phosphatase Substrate NBT/BCIP

For the proof-of-concept demonstration, the detection of bacteria was first investigated in TSB, which is the media for supporting bacterial growth and bacteriophage infection. **Table 1** shows the filters after adding NBT/BCIP substrate and incubating the filter at room temperature for 0, 5, 10, 20, and 30 min. For the samples with bacteriophage infection, after 10 min of incubation with the substrate, a visible dark purple color was observed and the color intensity increased with an increase in incubation time. In contrast, the negative control sample, i.e., filtered bacteria without bacteriophage infection showed no color change after 30 min of incubation with the substrate. The negative control of TSB with bacteriophage but without bacteria also showed no visible color change. In order to quantify the color change, the filters were also characterized using the Hunter's color scale measurements using a colorimeter.

In this measurement, the  $L^*$ ,  $a^*$ , and  $b^*$  color values were measured at random five locations of the filter and the  $dE$  values were calculated using the Equation 1. The  $dE$  value of the samples with T7-ALP infected bacteria and the negative control of bacteria without bacteriophage infection are shown in the **Figure 2**. After 5 min with the substrate, the  $dE$  value of the sample with T7-ALP infected bacteria is significantly higher than those of the controls and the  $dE$  value increases dramatically with an extended reaction time. On the other hand, the negative controls showed no significant change in the  $dE$  value after 20 min of incubation with the substrate.

The results indicate that, after 30 min of infection, the *E. coli* cells were still intact and the alkaline phosphatase induced by T7-ALP infection was produced inside the cells, which were captured on the filter after filtration. The results of the negative control sample, i.e., bacterial cells without T7-ALP infection, demonstrate a lack of significant endogenous alkaline phosphatase activity in the bacteria since this enzyme is usually produced by the bacteria only during phosphate starvation (Rani et al., 2012). When the bacteria are enriched in TSB, a nutrient rich environment for bacterial growth, endogenous bacterial alkaline phosphatase enzyme is not highly expressed in bacterial cells. Overall, these results demonstrate that using a combination of engineered bacteriophage T7-ALP and colorimetric substrate NBT/BCIP, *E. coli* cells can be specifically detected at the initial inoculation levels of 10 CFU/ml within 6 h using a simple visual analysis or quantitative color imaging.

In order to validate this method using complex food materials, the detection of target bacteria in coconut water and baby spinach leaves were evaluated. Coconut water was selected as

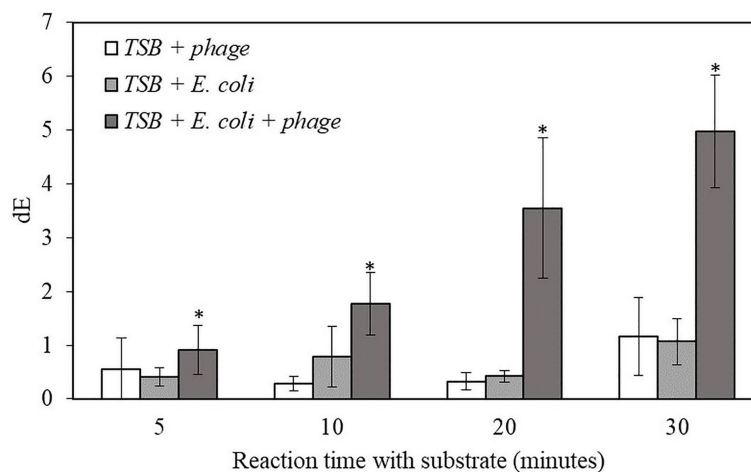


**FIGURE 2 |** The dE value of the filter with bacteriophage T7-ALP in TSB, 5-h enriched 10 CFU/mL *E. coli* BL21 and 30 min with and without infection with bacteriophage T7-ALP in TSB after enzymatic reaction with NBT/BCIP for 5, 10, 20, and 30 min. Treatments with "\*" are significantly different ( $p < 0.05$ ). Error bars indicate  $\pm$  standard deviation of means.

**TABLE 2 |** Filters with 5-h enriched 10 CFU/ml *E. coli* BL21 and 30 min with and without infection with bacteriophage T7-ALP in TSB-coconut water mixture and bacteriophage T7-ALP in TSB-coconut water mixture after enzymatic reaction with NBT/BCIP for 5, 10, 20, and 30 min.

Reaction condition		Reaction time with substrate (min)				
<i>Escherichia coli</i> inoculation	T7 infection	0	5	10	20	30
+	+					
+	-					
-	+					

it represents a beverage product with sugars, fatty acids, and amino acids (Prades et al., 2012). Before bacterial inoculation, coconut water was mixed with a double concentrated TSB in order to provide nutrients to support bacterial growth. The samples were then inoculated with *E. coli* BL21 10 CFU/ml and incubated at 37°C for enrichment for 5 h followed by infecting the enriched sample with the T7-ALP bacteriophage for 30 min and the detection of the alkaline phosphatase activity after filtration of the coconut water sample. As shown in Table 2, after adding NBT/BCIP substrate for 10 min, the color change to dark purple color was observed and the color intensity increased with extended reaction time while the

negative controls showed no color change after 30 min with the substrate.

The result indicates that this detection method can be applied to detect 10 CFU/ml of the target bacteria in coconut water samples within 6 h. The samples with infected *E. coli* gave significantly higher dE value compared to negative controls. The dE value increased with longer reaction time while there was no increase in dE value for the negative controls (Figure 3). The results for the detection of bacteria inoculated in coconut water were similar to those of the detection of bacteria inoculated in pure TSB (Figure 2.). However, the dE values of the bacteria inoculated in coconut water samples were lower than those

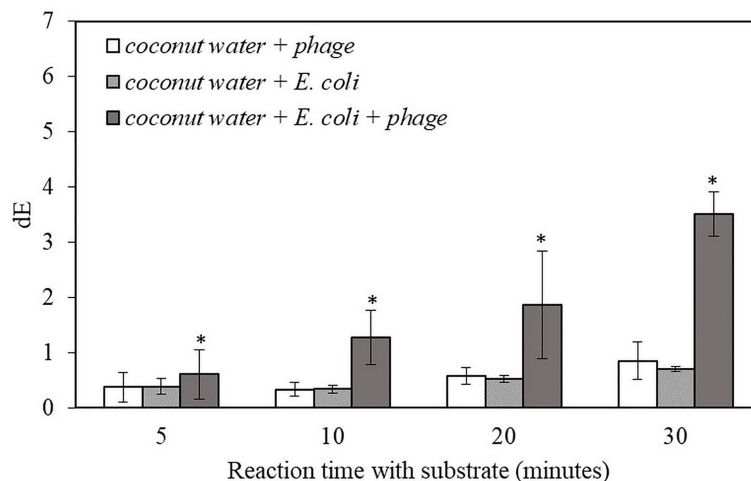


**FIGURE 3 |** The dE value of the filter with bacteriophage T7-ALP in TSB-coconut water mixture, 5-h enriched 10 CFU/ml *E. coli* BL21 and 30 min with and without infection with bacteriophage T7-ALP in TSB after enzymatic reaction with NBT/BCIP for 5, 10, 20, and 30 min. Treatments with "\*" are significantly different ( $p < 0.05$ ). Error bars indicate  $\pm$  standard deviation of means.

**TABLE 3 |** Filters with 5-h enriched 10 CFU/ml *E. coli* BL21 and 30 min with and without infection with bacteriophage T7-ALP in TSB-spinach and bacteriophage T7-ALP in TSB-spinach after enzymatic reaction with NBT/BCIP for 0 and 30 min.

Reaction condition		Reaction time with substrate (min)	
<i>Escherichia coli</i> inoculation	T7 infection	0	30
+	+		
	-		
	+		

of bacteria inoculated in TSB, indicating reduced alkaline phosphatase expression or activity in coconut water. Therefore, the composition of coconut water may have an influence on the signal from alkaline phosphatase enzymatic reaction and the formation of the precipitated colorimetric product.

Fresh produce is one of the food samples that is considered as challenging for bacterial detection since the plant samples contain solid particles, pigments, and diverse microflora. In order to validate this detection method, baby spinach was selected to

represent leafy greens. The sample size of baby spinach leaves was 25 g, which represent a more realistic sample size used in the industry. After inoculation with *E. coli* BL21, the sampling bags containing inoculated leaves were sealed and stored at 4°C for 24 h to simulated a scenario in the industry, where the harvested spinach leaves are stored at refrigerated temperature prior to washing and packaging. After 5 h of enrichment, spinach samples were then incubated with the bacteriophage T7-ALP for 2 h. The extended infection time was selected to reduce the influence of non-target microbes and the plant exudate from the spinach leaves. The release of plant exudate from the wound and cut of spinach leaves results in a green color that may interfere with the color change measurement induced by the overexpression of alkaline phosphatase and its colorimetric substrate. Moreover, an increase in the level of non-target bacteria may slow the growth of *E. coli* during enrichment and may physically obstruct the binding of bacteriophage and the target bacteria. Increase in infection time to 2 h allows an additional growth of *E. coli* during incubation with bacteriophages and increase the infection efficiency. Detection of *E. coli* in small scale of 1-gram spinach leaves was also conducted. With less interference from the plant exudate, the optimal coinoculation time was 30 min which the result is reported in the supplementary material.

After 2 h of infection with bacteriophage, 2 ml of enriched TSB was filtered through a 0.2-micron polycarbonate filter. Since the spinach samples contain solid plant particles and also native microflora from plant tissue that would clog the pores of the filter, the volume of sample subjected to filtration was limited to 2 ml. As shown in **Table 3**, the filters after filtration appeared slightly green due to the presence of released plant pigments. After 30 min of enzymatic reaction with the NBT/BCIP substrate, the filter appeared darker and the dE value of inoculated spinach samples with bacteriophage infection on a filter was significantly higher than the negative controls (**Figure 4**). The results demonstrate that this detection method



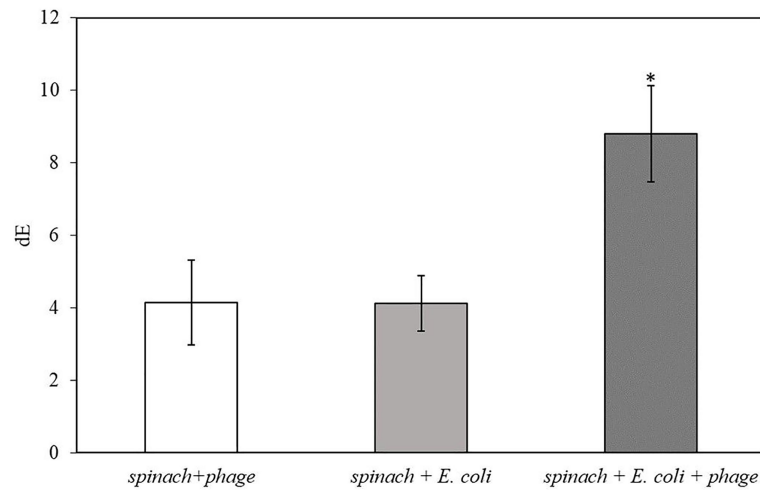


**FIGURE 4 |** The dE of the filter with 5 h-enriched 10 CFU/ml *E. coli* BL21 and 2 h infection with bacteriophage T7-ALP in 225 ml TSB with 25 g spinach leaves after enzymatic reaction with NBT/BCIP for 30 min. Treatments with "\*" are significantly different ( $p < 0.05$ ). Error bars indicate  $\pm$ standard deviation of means.

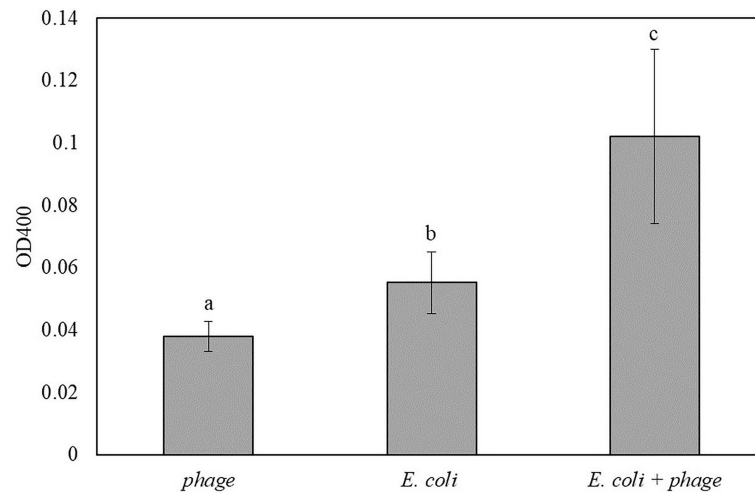


**FIGURE 5 |** The OD400 of 5 h-enriched 10 CFU/ml *E. coli* BL21 and 30 min infection with bacteriophage T7-ALP in TSB after enzymatic reaction with pNPP for 2 h. Treatments with different letters are significantly different ( $p < 0.05$ ) error bars indicate  $\pm$ standard deviation of means.

can be applied to detect bacteria using a realistic spinach sample size without isolating bacteria from the inoculated plant samples.

### Detection of Bacteria Using Bacteriophage T7-ALP and Alkaline Phosphatase Substrate pNPP

To detect the expression of alkaline phosphatase using colorimetric assays, often substrates, such as pNPP, that generate a soluble colorimetric signal are used. The advantage of the homogeneous assay is the ease of detection using a simple UV-Vis measurement. In this study, one of our objectives was to compare the sensitivity of colorimetric detection of target bacteria using both insoluble and soluble enzymatic substrates.

For this comparison, the experimental conditions for the enrichment and infection steps were maintained the same as in the case of when using the substrate that yields precipitated products, NBT/BCIP. The only difference was that after initial infection, the cells were harvested using a centrifuge and then the isolated cell pellet was re-suspended in PBS and incubated with the pNPP substrate as described in the Materials and Methods section. The absorbance of the resulting solution was measured at 400 nm using a UV-Vis spectrophotometer.

**Figure 5** shows the results for the detection of *E. coli* in TSB that was enriched for 5 h and infected with bacteriophage T7-ALP for 30 min. After 2 h of incubation with pNPP substrate, *E. coli* infected with bacteriophage had significantly higher absorbance compared to negative controls. For the soluble substrate assay, bacteria are incubated

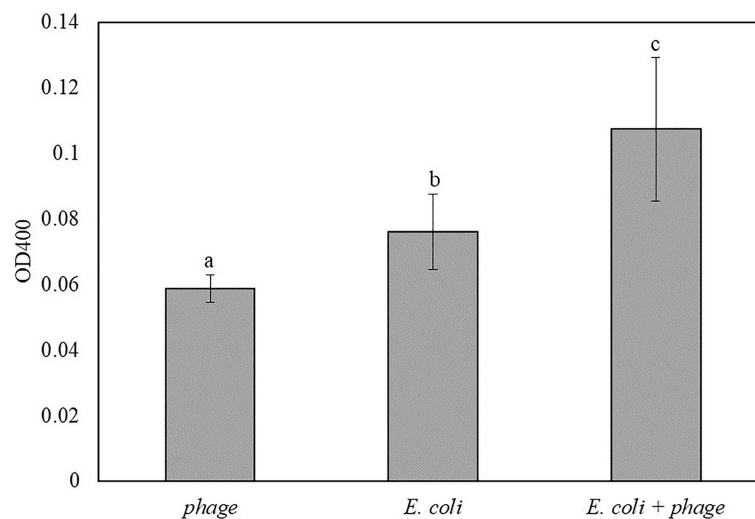


**FIGURE 6 |** The OD400 of 5 h-enriched 10 CFU/ml *E. coli* BL21 and 30 min infection with bacteriophage T7-ALP in coconut water-TSB after enzymatic reaction with pNPP for 2 h. Treatments with different letters are significantly different ( $p < 0.05$ ) error bars indicate  $\pm$ standard deviation of means.

in PBS for 2 h and this incubation of bacteria in a low nutrient environment can increase the endogenous expression of alkaline phosphatase compared to bacteria incubated with TSB. Increase in an endogenous expression of alkaline phosphatase can reduce the sensitivity of the detection using the soluble substrate.

Similar to the results in **Figure 5**, coconut water was used as a model liquid food system for the detection of *E. coli*. The mixture of 1:1 coconut water and double-concentrated TSB inoculated with 10 CFU/ml of *E. coli* was enriched for 5 h followed by 30 min of infection with bacteriophage T7-ALP. Then the bacterial cells were incubated with the soluble substrate for 2 h. The inoculated samples with bacteriophage infection had the highest OD400 followed by coconut water with *E. coli* without bacteriophage infection and coconut water and bacteriophage without *E. coli*, respectively (**Figure 6**). The trend was similar to those of bacteria in TSB alone.

This method using soluble substrate was not applicable for the detection of *E. coli* in 25 g of spinach samples and larger volume of media since enrichment steps results in the growth of other local microbes, and the centrifugation also harvested plant particles along with microbial cells, resulting in high turbidity after re-suspension, which interfered with the absorbance measurement.

## DISCUSSION

Detection of specific bacteria in food matrices is a challenging task. This challenge results because of low counts of target bacteria in food systems and also the interference due to the food matrix and other microbes. To address these challenges various processes have been designed to isolate, concentrate, and separate target bacteria from the food matrix using both physical and biochemical methods.

Physical methods, such as filtration and centrifugation, can improve the detection sensitivity but their drawback is that the solid food debris will also be concentrated along with bacteria (Benoit and Donahue, 2003) and can further limit detection sensitivity. Immunomagnetic separation has been used coupled with several bacterial detection methods in order to specifically separate target bacteria from food debris and other endogenous microbes. The significant challenge results due to the binding affinity and specificity of antibodies that can be reduced by food components due to the diversity of mechanisms (Van Aken and Lin, 2011). Moreover, an attachment of bacteria to food surface can significantly limit the overall capture efficiency using both physical and biochemical methods. In addition to these constraints, sample preparation for the detection of bacteria in food materials is often one of the key labor and resource intensive steps with a series of manual handling steps to prepare samples for enrichment and detection. These handling practices can lead to contaminations of the samples especially when multiple samples are being processed simultaneously (Benoit and Donahue, 2003). To overcome these limitations, the detection methods developed in this study require no sample preparation steps to isolate bacteria from diverse food matrices. Coconut water and baby spinach leaf samples, representing a liquid and a fresh produce model system inoculated with bacteria were added directly to the bacterial enrichment media that can enrich a diversity of bacteria, thus providing a general framework for the detection of bacteria. Furthermore, the time required for bacterial enrichment step was comparable or less than the average enrichment time used prior to other detection methods, such as RT-PCR and other nucleic acid or ELISA based methods (De Boer and Beumer, 1999), and was achieved in less than a single work shift in the industry. In addition, unlike PCR or other nucleic acid-based methods, the detection approach developed in this

study does not require isolation and purification of nucleic acids. Thus, overall, the simple workflow of the method described in the study significantly reduces the labor and resources typically required for the sample preparation and detection of bacteria. These simplifications combined with visual detection of bacteria using colorimetric analysis provide a simple yet effective approach to detect bacteria in food systems.

Colorimetric detection provides simple and low-cost operations since it does not require any advanced instruments, which allows portable and easy-to-use diagnostic. Prior studies have developed colorimetric assays for *E. coli* detection tested in culture media, drinking water, and liquid food matrices as summarized in **Table 4**.

To the best of our knowledge, most of these studies have focused on using soluble substrates whose chromatic products will be dissolved in the bulk solution. This limits the detection sensitivity compare to using substrates that yield localized enzymatic products inside the infected cells. Moreover, using soluble substrates requires the release of enzyme from cells to the aqueous phase, which may not be efficient as alkaline phosphatase have high molecular weight of 94 kDa. In our prior research, we have observed a significant retention of cellular content including DNA and cell membrane after bacteriophage lysis of cells (Yang et al., 2020). Thus, an extended time of incubation may result in more efficient release of enzymes from residual cellular content after lysis as well as multiple repeat cycles of phage infection and the expression of exogenous enzyme can increase the effective enzyme concentration.

In order to increase the sensitivity and simplicity of the detection, the substrate that forms colorimetric precipitated product after the enzymatic reaction, NBT/BCIP, were investigated in this study. This substrate has been used as the substrate for alkaline phosphatase in the *in-situ* hybridization for gene expression study (Jékely and Arendt, 2007; Trinh et al., 2007). The dark purple insoluble precipitated product is the result of the enzymatic reaction, and it can be visualized by the naked eye. The use of this substrate to detect bacterial alkaline phosphatase was supported by the study of Hinkley et al. (2018), which reported that BCIP substrate can be used to visualize bacterial colonies

infected by engineered bacteriophage with alkaline phosphatase. This method allows quantitative analysis of bacteria within 10 h of operation (Hinkley et al., 2018). For the detection method developed in this study, the samples after bacteriophage infection were filtered to capture bacterial cells with alkaline phosphatase. Since the product of NBT/BCIP is water insoluble and will localize inside bacterial cells, the release of enzyme was not required. The enzymatic product can be concentrated simultaneously with the bacterial cells by filtration, which can improve the detection sensitivity. The substrate can be applied directly to the filter and the color formation can be visualized within 10 min without any instruments or imaging system. As bacteriophage T7 is highly specific to *E. coli* infection; therefore, other bacteria present in the sample will not be infected thereby there is no overexpression of alkaline phosphatase, which eliminates the cause of false-positive result. Prior to this study, the T7-ALP has been tested against with food and agriculture related bacterial strains, including *Pseudomonas fluorescens* and *Listeria innocua*, and the results indicated no significant increase of alkaline phosphatase after bacteriophage T7-ALP infection (Wisuthiphaet et al., 2019).

Compared to the previous colorimetric bacteriophage-based detections, the detection approach developed in this study offers a rapid detection method that can be applied to detect target bacteria in beverage and fresh produce samples with more realistic sample size. The results indicated the successful detection of bacteria 10 CFU/ml and 10<sup>2</sup> CFU/g in coconut water and spinach leaves with 5-h enrichment. However, for the food samples containing solid particles and pigments like spinach, the filtration step could limit the detection efficiency. Due to the solid plant particles, the sample volume for filtration is limited, which affects the detection sensitivity. Moreover, the leaf pigments can interfere with the color readout. The higher sample volume results in the more food debris and local microbes, which leads to reduced filtration volume and detection sensitivity. Therefore, the reaction time was extended to 2 h to increase the alkaline phosphatase level to achieve the detection limit of 10<sup>2</sup> CFU/g of bacteria. The detection using pNPP substrate is not applicable since the centrifugation step did sediment all the debris and local microbes that might outgrow the

**TABLE 4 |** Summary of the previous studies on colorimetric bacteriophage-based detection of *E. coli*.

Sample matrices	Colorimetric detection approach	Detection limit	References
Drinking water	Chromogenic soluble substrate detection of $\beta$ -galactosidase released after phage-induced lysis of <i>Escherichia coli</i>	10 CFU/ml with 6 h of pre-enrichment	Chen et al., 2015
Culture medium	Detection of alkaline phosphatase overexpression induced by engineered bacteriophage T7 using pNPP	10 <sup>4</sup> CFU/ml within 7.5 h	Alcaine et al., 2015
Culture medium	Detection of $\beta$ -galactosidase induced by engineered T7 phage infection on <i>Escherichia coli</i>	10 CFU/ml within 7 h	Chen et al., 2017a
Drinking water, Skim milk, and Orange juice	Detection of $\beta$ -galactosidase induced by freeze-dried engineered T7 phage infection on <i>Escherichia coli</i>	10 <sup>2</sup> CFU/ml within 7 h	Chen et al., 2017b
Culture medium 100 ml	Detection of alkaline phosphatase overexpression induced by engineered bacteriophage T7 infection on <i>Escherichia coli</i>	<10 CFU/ml within 8 h	Singh et al., 2019

target bacteria causing high turbidity of the samples and prevent an accurate absorbance measurement.

Further refinement of the detection procedure is still needed in order to develop more efficient detection methods that can be applied to detect bacteria in complex food samples by focusing on eliminating the background noise from food particles and non-target microbes. Multistep filtration can be introduced to remove coarse suspended solids in the samples before harvesting the bacteriophage-infected bacteria. Selective media can be applied during the enrichment step to support the growth of the target bacteria and reduce the proportion of other non-target microbes. In addition, quantitative analysis of bacteria using this detection method can be further investigated as well as combining this detection approach with digital imaging and image processing also improve the detection specificity and sensitivity.

## CONCLUSION

This study demonstrates an isolation-free rapid bacterial detection strategy using engineered bacteriophage to induce alkaline phosphatase expression. The NBT/BCIP substrate of alkaline phosphatase allows the rapid colorimetric bacterial detection. The proposed method was validated to detect *E. coli* in complex food samples, coconut water, and baby spinach. The detection limit of 10 CFU/ml of bacteria in coconut water was achieved within 6 h of operation. For baby spinach leaves, 10<sup>2</sup> CFU/g of bacteria can be detected with an extended detection time of 8 h. Further study may be conducted in order to address some of the drawbacks including limitations of filtering large volume samples with food particulate matter and analyzing large number of samples.

## REFERENCES

- Alcaine, S. D., Pacitto, D., Sela, D. A., and Nugen, S. R. (2015). Phage & phosphatase: a novel phage-based probe for rapid, multi-platform detection of bacteria. *Analyst* 140, 7629–7636. doi: 10.1039/C5AN01181G
- Benoit, P. W., and Donahue, D. W. (2003). Methods for rapid separation and concentration of bacteria in food that bypass time-consuming cultural enrichment. *J. Food Prot.* 66, 1935–1948. doi: 10.4315/0362-028X-66.10.1935
- Centers for Disease Control and Prevention. (2018). Burden of foodborne illness: findings. Available at: <https://www.cdc.gov/foodborneburden/2011-foodborne-estimates.html> (Accessed September 10, 2020).
- Chen, J., Alcaine, S. D., Jiang, Z., Rotello, V. M., and Nugen, S. R. (2015). Detection of *Escherichia coli* in drinking water using T7 bacteriophage-conjugated magnetic. *Probe. Anal. Chem.* 87, 8977–8984. doi: 10.1021/acs.analchem.5b02175
- Chen, J., Alcaine, S. D., Jackson, A. A., Rotello, V. M., and Nugen, S. R. (2017a). Development of engineered bacteriophages for *Escherichia coli* detection and high-throughput antibiotic resistance determination. *ACS Sens.* 2, 484–489. doi: 10.1021/acssensors.7b00021
- Chen, J., Picard, R. A., Wang, D., and Nugen, S. R. (2017b). Lyophilized engineered phages for *Escherichia coli* detection in food matrices. *ACS Sens.* 2, 1573–1577. doi: 10.1021/acssensors.7b00561
- Cho, I. H., and Ku, S. (2017). Current technical approaches for the early detection of foodborne pathogens: challenges and opportunities. *Int. J. Mol. Sci.* 18:2078. doi: 10.3390/ijms18102078

## DATA AVAILABILITY STATEMENT

The original contributions presented in the study are included in the article/supplementary material, and further inquiries can be directed to the corresponding author.

## AUTHOR CONTRIBUTIONS

NW designed the study and performed the experiments, analyzed the data, and wrote the manuscript. XY designed the study and performed the experiments. NN and GY conceived, designed, and supervised the study. All authors contributed to the article and approved the submitted version.

## FUNDING

This study was supported by the USDA National Institute of Food and Agriculture (USDA-NIFA) grant no. 2015-68003-23411.

## ACKNOWLEDGMENTS

We want to thank Dr. Sam Nugen from Cornell University for providing the engineered bacteriophage T7-ALP.

## SUPPLEMENTARY MATERIAL

The Supplementary Material for this article can be found online at: <https://www.frontiersin.org/articles/10.3389/fmicb.2021.691003/full#supplementary-material>

- De Boer, E., and Beumer, R. R. (1999). Methodology for detection and typing of foodborne microorganisms. *Int. J. Food Microbiol.* 50, 119–130. doi: 10.1016/S0168-1605(99)00081-1
- Frederick, J. L., Walker, S. P., Newman, M., and Payne, F. (2013). Evaluation of chemical additives for the separation and recovery of bacteria from food matrices. *Biol. Eng. Trans.* 6, 105–115. doi: 10.13031/bet.6.10084
- Hinkley, T. C., Singh, S., Garing, S., Ny, A. M., Le, Nichols, K. P., Peters, J. E., et al. (2018). A phage-based assay for the rapid, quantitative, and single CFU visualization of *E. coli* (ECOR # 13) in drinking water. *Sci. Rep.* 8:14630. doi: 10.1038/s41598-018-33097-4
- Hornbeck, P. V. (2015). Enzyme-linked immunosorbent assays. *Curr. Protoc. Immunol.* 2015, 2.1.1–2.1.23. doi: 10.1002/0471142735.im0201s110
- Jackson, A. A., Hinkley, T. C., Talbert, J. N., Nugen, S. R., and Sela, D. A. (2016). Genetic optimization of a bacteriophage-delivered alkaline phosphatase reporter to detect *Escherichia coli*. *Analyst* 141, 5543–5548. doi: 10.1039/C6AN00479B
- Jaykus, L.-A. (2003). Challenges to developing real-time methods to detect pathogens in foods. *ASM News* 69, 341–347.
- Jékely, G., and Arendt, D. (2007). Cellular resolution expression profiling using confocal detection of NBT/BCIP precipitate by reflection microscopy. *BioTechniques* 42, 751–755. doi: 10.2144/000112462
- Kim, J., Kim, M., Kim, S., and Ryu, S. (2017). Sensitive detection of viable *Escherichia coli* O157:H7 from foods using a luciferase-reporter phage phiV10lux. *Int. J. Food Microbiol.* 254, 11–17. doi: 10.1016/j.jfoodmicro.2017.05.002
- Kim, S., Kim, M., and Ryu, S. (2014). Development of an engineered bioluminescent reporter phage for the sensitive detection of viable *Salmonella typhimurium*. *Anal. Chem.* 86, 5858–5864. doi: 10.1021/ac500645c



- Kralik, P., and Ricchi, M. (2017). A basic guide to real time PCR in microbial diagnostics: definitions, parameters, and everything. *Front. Microbiol.* 8:108. doi: 10.3389/fmicb.2017.00108
- Kundu, S. (2014). *BiomedRecent Advances in Immunoassays*, 130. doi: 10.13140/2.1.3444.5449.
- Liu, Y., Zhou, H., Hu, Z., Yu, G., Yang, D., and Zhao, J. (2017). Label and label-free based surface-494 enhanced Raman scattering for pathogen bacteria detection: A review. *Biosens. Bioelectron.* 94, 131–140. doi: 10.1016/j.bios.2017.02.032
- Loessner, M. J., Rudolf, M., Scherer, S., Loessner, M. J., Rudolf, M., and Scherer, S. (1997). Evaluation of luciferase reporter bacteriophage A511:: luxAB for detection of *Listeria monocytogenes* in contaminated foods. *Appl. Environ. Microbiol.* 63, 2961–2965. doi: 10.1128/aem.63.8.2961-2965.1997
- Paczynski, J., Richter, L., and Holyst, R. (2020). Recent progress in the detection of bacteria using bacteriophages: a review. *Viruses* 12:845. doi: 10.3390/v12080845
- Prades, A., Dornier, M., Diop, N., and Pain, J.-P. (2012). Coconut water uses, composition and properties: a review. *Fruits* 67, 87–107. doi: 10.1051/fruits/2012002
- Rani, K., Datt, S., and Rana, R. (2012). Brief review on alkaline phosphatases: an overview. *Int. J. Microbiol. Bioinforma.* 2, 1–4.
- Scallan, E., Hoekstra, R. M., Angulo, F. J., Tauxe, R. V., Widdowson, M. A., Roy, S. L., et al. (2011). Foodborne illness acquired in the United States—major pathogens. *Emerg. Infect. Dis.* 17, 7–15. doi: 10.3201/eid1701.P11101
- Sharma, H., and Mutharasan, R. (2013). Review of biosensors for foodborne pathogens and toxins. *Sensors Actuators B Chem.* 183, 535–549. doi: 10.1016/j.snb.2013.03.137
- Singh, S., Hinkley, T., Nugen, S. R., Talbert, J. N., and Talbert, J. N. (2019). Colorimetric detection of *Escherichia coli* using engineered bacteriophage and an affinity reporter system. *Anal. Bioanal. Chem.* 411, 7273–7279. doi: 10.1007/s00216-019-02095-4
- Stevens, K. A., and Jaykus, L. (2014). Bacterial separation and concentration from complex sample matrices: a review. *Crit. Rev. Microbiol.* 30, 7–24. doi: 10.1080/10408410490266410
- Trinh, L. A., McCutchen, M. D., Bonner-Fraser, M., Fraser, S. E., Bumm, L. A., and McCauley, D. W. (2007). Fluorescent in situ hybridization employing the conventional NBT/BCIP chromogenic stain. *BioTechniques* 42, 756–759. doi: 10.2144/000112476
- Van Aken, B., and Lin, L. S. (2011). Effect of the disinfection agents chlorine, UV irradiation, silver ions, and TiO<sub>2</sub> nanoparticles/near-UV on DNA molecules. *Water Sci. Technol.* 64, 1226–1232. doi: 10.2166/wst.2011.684
- Wisuthiphaet, N., Yang, X., Young, G. M., and Nitin, N. (2019). Rapid detection of *Escherichia coli* in beverages using genetically engineered bacteriophage T7. *AMB Express* 9:55. doi: 10.1186/s13568-019-0776-7
- Yang, X., Wisuthiphaet, N., Young, G. M., and Nitin, N. (2020). Rapid detection of *Escherichia coli* using bacteriophage-induced lysis and image analysis. *PLoS One* 15:e0233853. doi: 10.1371/journal.pone.0233853

**Conflict of Interest:** The authors declare that the research was conducted in the absence of any commercial or financial relationships that could be construed as a potential conflict of interest.

**Publisher's Note:** All claims expressed in this article are solely those of the authors and do not necessarily represent those of their affiliated organizations, or those of the publisher, the editors and the reviewers. Any product that may be evaluated in this article, or claim that may be made by its manufacturer, is not guaranteed or endorsed by the publisher.

Copyright © 2021 Wisuthiphaet, Yang, Young and Nitin. This is an open-access article distributed under the terms of the Creative Commons Attribution License (CC BY). The use, distribution or reproduction in other forums is permitted, provided the original author(s) and the copyright owner(s) are credited and that the original publication in this journal is cited, in accordance with accepted academic practice. No use, distribution or reproduction is permitted which does not comply with these terms.



# Development and Application of a Novel Rapid and Throughput Method for Broad-Spectrum Anti-Foodborne Norovirus Antibody Testing

Yueting Zuo<sup>1,2†</sup>, Liang Xue<sup>2†</sup>, Junshan Gao<sup>2</sup>, Yingyin Liao<sup>2</sup>, Yueting Jiang<sup>3</sup>, Ying Li<sup>2</sup>, Yanhui Liang<sup>2</sup>, Linping Wang<sup>2</sup>, Weicheng Cai<sup>2</sup>, Tong Cheng<sup>2</sup>, Juan Wang<sup>2</sup>, Moutong Chen<sup>2</sup>, Jumei Zhang<sup>2</sup>, Yu Ding<sup>2\*</sup> and Qingping Wu<sup>2\*</sup>

<sup>1</sup> School of Bioscience and Bioengineering, South China University of Technology, Guangzhou, China, <sup>2</sup> Guangdong Provincial Key Laboratory of Microbial Safety and Health, State Key Laboratory of Applied Microbiology Southern China, Institute of Microbiology, Guangdong Academy of Sciences, Guangzhou, China, <sup>3</sup> Department of Laboratory Medicine, First Affiliated Hospital of Guangzhou Medical University, Guangzhou, China

## OPEN ACCESS

### Edited by:

Xiyang Wu,  
Jinan University, China

### Reviewed by:

Hongtao Lei,  
South China Agricultural University,  
China  
Tony Mutukumira,  
Massey University, New Zealand

### \*Correspondence:

Qingping Wu  
wuqp203@163.com  
Yu Ding  
dingyu@jnu.edu.cn

<sup>†</sup>These authors share first authorship

### Specialty section:

This article was submitted to  
Food Microbiology,  
a section of the journal  
Frontiers in Microbiology

**Received:** 21 February 2021

**Accepted:** 13 August 2021

**Published:** 03 September 2021

### Citation:

Zuo Y, Xue L, Gao J, Liao Y, Jiang Y, Li Y, Liang Y, Wang L, Cai W, Cheng T, Wang J, Chen M, Zhang J, Ding Y and Wu Q (2021) Development and Application of a Novel Rapid and Throughput Method for Broad-Spectrum Anti-Foodborne Norovirus Antibody Testing. *Front. Microbiol.* 12:670488. doi: 10.3389/fmicb.2021.670488

Foodborne norovirus (NoV) is the leading cause of acute gastroenteritis worldwide. Candidate vaccines are being developed, however, no licensed vaccines are currently available for managing NoV infections. Screening for stimulated antibodies with broad-spectrum binding activities can be performed for the development of NoV polyvalent vaccines. In this study, we aimed to develop an indirect enzyme-linked immunosorbent assay (ELISA) for testing the broad spectrum of anti-NoV antibodies. Capsid P proteins from 28 representative NoV strains (GI.1–GI.9 and GII.1–GII.22 except GII.11, GII.18, and GII.19) were selected, prepared, and used as coating antigens on one microplate. Combined with incubation and the horseradish peroxidase chromogenic reaction, the entire process for testing the spectrum of unknown antibodies required 2 h for completion. The intra-assay and inter-assay coefficients of variation were less than 10%. The new method was successfully performed with monoclonal antibodies and polyclonal antibodies induced by multiple antigens. In conclusion, the indirect ELISA assay developed in this study had a good performance of reliability, convenience, and high-throughput screening for broad-spectrum antibodies.

**Keywords:** norovirus, capsid P protein, enzyme-linked immunosorbent assay, broad-spectrum antibodies, inter-assay/intra-assay variation

## INTRODUCTION

Foodborne Norovirus (NoV) is one of the leading causes of epidemic acute gastroenteritis (AGE) worldwide, accounting for one-fifth of all gastroenteritis cases globally (Lopman et al., 2016). Annually, NoV has been estimated to cause 677 million episodes of diarrheal disease (95% uncertainty interval [UI]: 468–1,153 million) and 213,515 deaths (95% UI: 171,783–266,561) for all ages and among all modes of transmission (Pires et al., 2015). NoV is extremely contagious, and transmission occurs directly from person to person via fecal-oral and vomit-oral routes, but can also be caused by food-borne, water-borne, or environmental factors (Verhoef et al., 2015). Vomitus and feces of infected patients contain a considerable number of virions, whereas as few

as 10 infectious particles are sufficient to cause AGE (Teunis et al., 2010). Additionally, NoV shedding after infection usually lasts for several weeks, and prolonged shedding post-infection can also contribute to spreading (Sukhrie et al., 2010). Thus, NoV remains a major threat to public health. Owing to the significant social and economic burden associated with the disease, adequate preventive measures against this virus should be formulated.

NoV strains can be classified into 10 genogroups (GI–GX) and at least 48 genotypes based on the diversity of the VP1 amino acid sequence; GI, GII, and GIV have been shown to cause infections in humans (Chhabra et al., 2019). Human histo-blood group antigens (HBGAs) can be used as receptor or co-receptor for NoV infection (Lindesmith et al., 2003; Rockx et al., 2005). The binding ability between NoVs and HBGAs is diverse, resulting in different infectivity. The global pandemic GII.4 NoV can infect almost all secretory individuals (Nordgren and Svensson, 2019); GI.1 VLP binds to A, AB, and O type, but not to B type saliva (Morozov et al., 2018); individuals with O type saliva are relatively susceptible to NoV, while with B type are not (Hutson et al., 2002); some strains do not bind any phenotype of HBGAs (Almand et al., 2017).

Several possible barriers hinder the development of effective NoV vaccines (Cortes-Penfield et al., 2017). First, circulating NoV exhibits genetic diversity and high variation, which may limit the durability of protection conferred by a vaccine that does not elicit broadly neutralizing antibodies. Second, the lack of sufficient cell lines for virus culture and successful animal models further hinders the development of antiviral drugs and vaccines. The following three types of NoV vaccines

have been developed: virus-like particles (VLPs) that resemble the organization and morphology of native virus, P particles that resemble the P domain of native virus, and recombinant adenoviruses (Esposito and Principi, 2020).

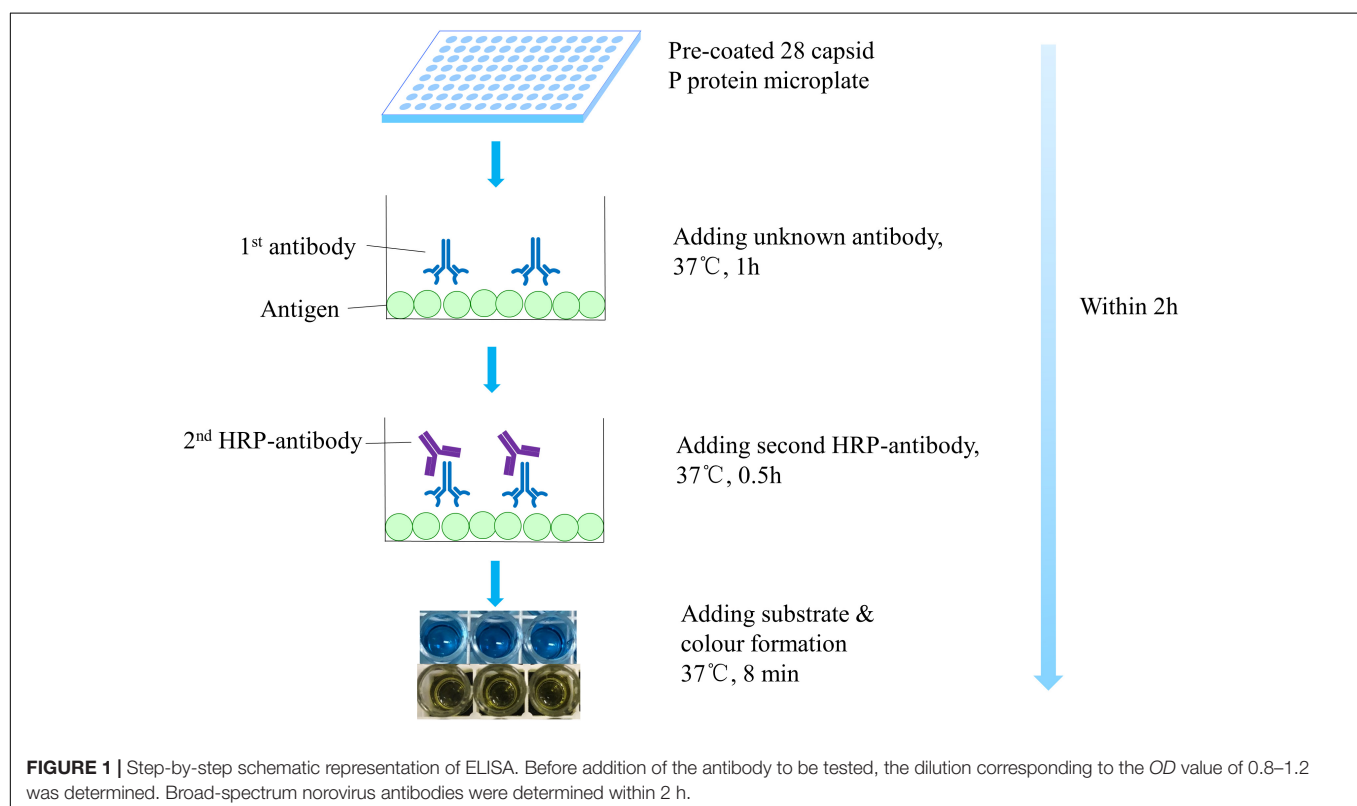
Enzyme-linked immunosorbent assay (ELISA) is a sensitive and specific analytical biochemistry assay utilized for the detection and quantitative or qualitative analysis of an analyte without the requirement for sophisticated or expensive equipment (Gan and Patel, 2013). Currently, ELISA is used as an ideal method for the detection of viruses and antibodies (Fan et al., 2013; Ledesma et al., 2017; Ding et al., 2019). However, few ELISA techniques demonstrate the ability to directly detect the broad-spectrum binding activities of antibodies against all NoV strains that infect humans. Therefore, it is necessary to develop an indirect ELISA technique for the detection of a wide range of antibodies.

In this study, we aimed to develop an ELISA technique for vaccine development via rapid, efficient, and accurate screening of a substantial number of broad-spectrum antibodies.

## MATERIALS AND METHODS

### Selection of Representative Strains

The antigen used in this experiment was capsid P protein for each representative strain of NoV stored in our laboratory. We selected nine GI strains (GI.1–GI.9) and nineteen GII strains (GII.1–GII.22) as representative NoV strains; GII.11, GII.18, and GII.19, which were detected in swine (Vinjé, 2015), were excluded. In our



previous study, GII.2, GII.3, GII.4, GII.6, GII.8, and GII.17 NoV were detected and preserved (Xue et al., 2015; Xue et al., 2016; Xue et al., 2019), which could be directly used for cloning. Others were synthesized.

## Pre-coated of Antigen

For preparation of microplates, 96-well plates were coated with 0.2  $\mu$ g of 28 NoV capsid P proteins after incubation at 4°C overnight (three well per P protein). After subjecting the wells to washing steps with phosphate-buffered saline containing Tween 20 (PBST) three times, the wells were blocked using 5% skim milk for 2 h at 37°C; then, the wells were washed three times using PBST, dried, and stored at 4°C until further use. A combination of glutathione S-transferase (GST)-tagged protein and commercial anti-GST antibodies was used as a quality control. The negative serum was used as a negative control.

## Enzyme Linked Immunosorbent Assay (ELISA)

The indirect ELISA method was used to detect the broad spectrum of antibodies (Figure 1). Briefly, the pre-coated microtiter plate was taken out. Serum samples were added at an appropriate dilution, which corresponded to the OD value in the range of 0.8–1.2, followed by incubation for 1 h at 37°C. Subsequently, secondary horseradish peroxidase-conjugated goat anti-mouse IgG antibodies (diluted 1: 3,000) were added and the plates were incubated for 30 min at 37°C. Tetramethylbenzidine was added as a peroxidase chromogenic substrate and reaction for 8 min at 37°C was performed. After terminating the substrate reaction with 2 M H<sub>2</sub>SO<sub>4</sub>, the optical density (OD) was measured at 450 nm. Positive signal is defined as a mean OD<sub>450</sub> > 0.2 after background subtraction (Uusi-Kerttula et al., 2014; Jin et al., 2016; Tamminen et al., 2019).

## PERFORMANCE ANALYSIS

### Intra-Assay Precision

Three replicates for each monoclonal antibody sample were analyzed using the same microplate. Precision was determined

by calculating the mean, standard deviation, and coefficient of variation (CV%).

### Inter-Assay Precision

For determination of inter-assay reproducibility, three replicates for each sample were analyzed in different microplates. Precision was determined by calculating the mean, standard deviation, and CV%.

**TABLE 1** | Selection of norovirus strains used as coating antigens.

Strain designation	GenBank accession no.
GI.1	NC_001959
GI.2	L07418
GI.3	KJ196292
GI.4	AB042808
GI.5	AB039774
GI.6	LC342057
GI.7	KU311161
GI.8	KJ196298
GI.9	KF586507
GII.1	HCU07611
GII.2	MK729086
GII.3	KY348697
GII.4	KT202793
GII.5	KJ196288
GII.6	JX989075
GII.7	KJ196295
GII.8	MK213549
GII.9	AY038599
GII.10	AF504671
GII.12	AB045603
GII.13	KJ196276
GII.14	KJ196278
GII.15	KJ196290
GII.16	AY772730
GII.17	KT970369
GII.20	EU424333
GII.21	KJ196284
GII.22	MG495082

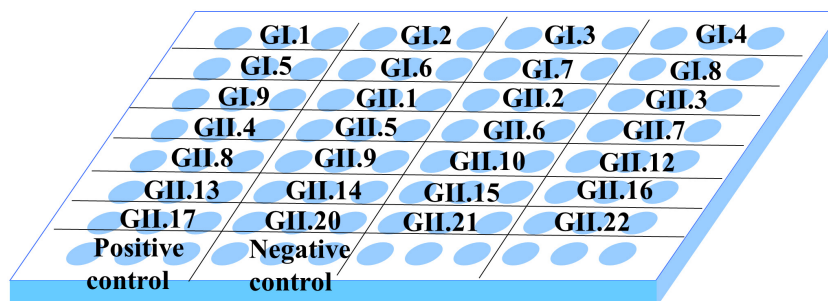


**FIGURE 2** | Distribution of antigen coating in 96-well microplate. In the plate, each well was coated with 0.2  $\mu$ g P protein, and each P protein was coated with three multiple wells. Wells coated with GST and coating buffer served as positive control and negative control, respectively.



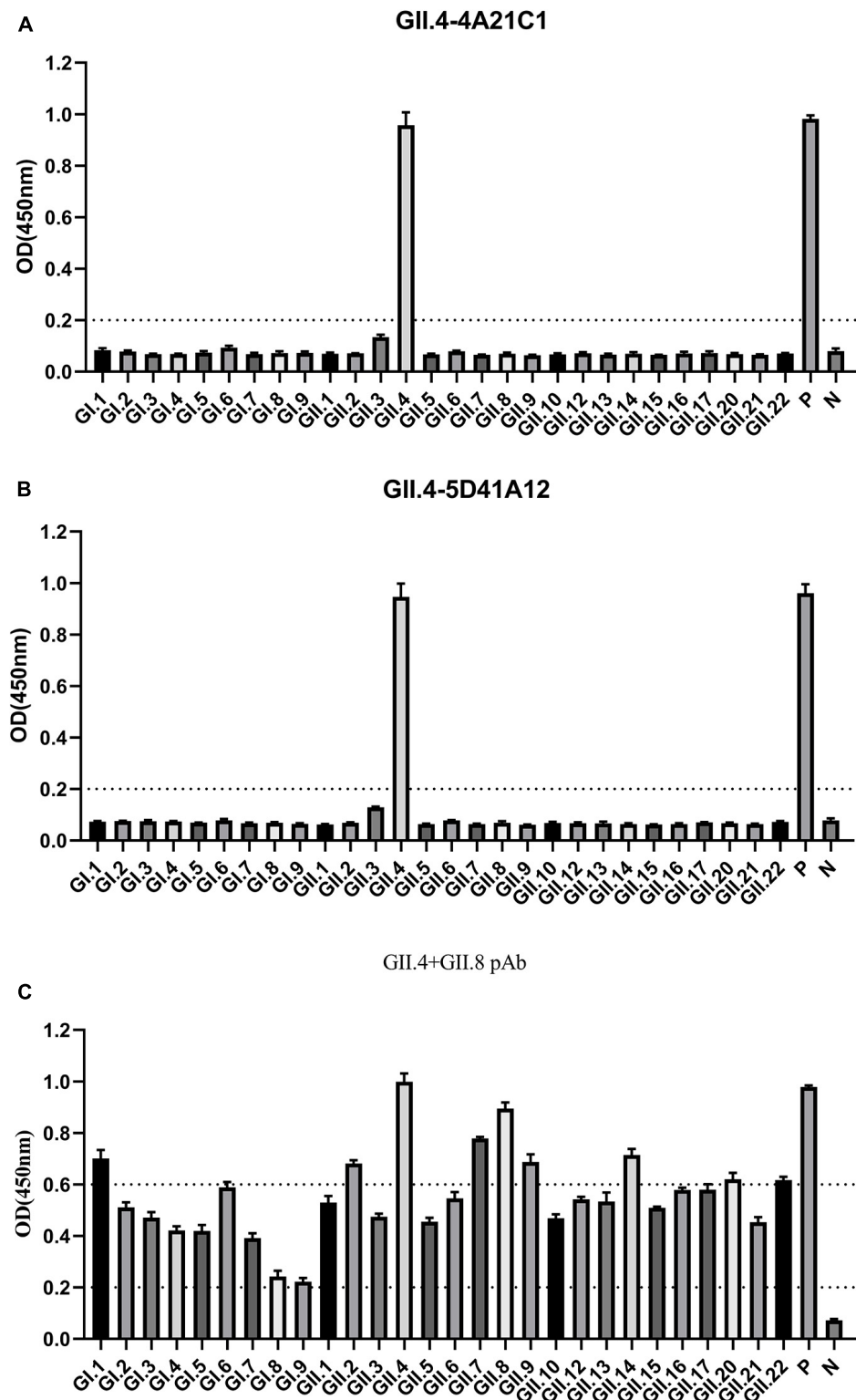


**FIGURE 3 |** Characterization the broad spectrum of antibodies. 9 GI and 19 GII P proteins were used as antigens with enzyme-linked immunosorbent assay (ELISA), reacting with GII.4-4A21C1 (A), GII.4-5D41A12 (B) mAbs, and GII.4 + GII.8 pAbs (C), and each protein was coated with three wells. The horizontal line at 0.2 illustrates the cut-off value for samples that are considered positive. 0.2–0.6 OD is considered a moderate binding. OD > 0.6 represents robust binding. P, positive control; N, negative control.

## Statistical Analysis

Statistical analyses were performed using Microsoft Excel 2016 and GraphPad Prism 8.0 software. Broad spectrum plot data are presented as mean  $\pm$  standard deviation.

## RESULTS

### Assembly of Microplates

To perform this experiment, we selected representative strains for capsid P proteins of all genotypes in GI (GI.1–GI.9) and GII (GII.1–GII.22), except for GII.18, GII.19, and GII.20 (Table 1 and Supplementary Figure 1). As shown in Figure 2, the microplate was coated with 28 capsid P proteins obtained from representative strains, and each P protein was coated in three wells.

### Broad-Spectrum Antibody Assay

To determine the effectiveness of the method, two GII.4 monoclonal antibodies (GII.4-4A21C1 and GII.4-5D41A12) and one bivalent (GII.4 + GII.8) polyclonal antibody were tested for broad-spectrum detection. When the OD was in the range of

0.8–1.2, the dilution of the above three antibodies were between 1:4000–1:16000, 1:4000–1:16000, and 1:500–1:1000, respectively (unpublished data). Accordingly, the two monoclonal antibodies dilution of 1:5000 and the polyclonal antibody dilution of 1:500 were used for broad-spectrum detection.

The GII.4-4A21C1 monoclonal antibodies only showed reaction with GII.4 P particles at a high OD value of 0.96 and did not exhibit reaction with the other 27 NoV P particles (Figure 3A), demonstrating that this monoclonal antibody had strong specificity. Similarly, GII.4-5D41A12 monoclonal antibodies had a binding signal of 0.95 (Figure 3B). The polyclonal antibodies (GII.4 + GII.8) showed the highest signal reaction with GII.4 and GII.8 P particles, followed by GI.1, GII.2, GII.7, GII.9, GII.14, GII.20, and GII.22, and moderate signals were observed for the remaining antibodies (Figure 3C). GST bound with GST monoclonal antibodies at OD values of 0.98, 0.96, and 0.98, indicating that the developed ELISA technique was reliable.

### Reproducibility of ELISA

Next, we evaluated intra-assay and inter-assay variabilities to test the reproducibility of the method. The monoclonal

**TABLE 2 |** Intra- and inter-assay coefficients of variation (%) for the broad-spectrum detection of GII.4-4A21C1 monoclonal antibodies by ELISA.

Antigen designation	Intra-assay Precision CV/%			Inter-assay Precision CV/%
	1	2	3	–
GI.1	1.80	8.02	9.01	3.52
GI.2	3.87	4.02	5.76	1.83
GI.3	9.45	3.22	2.94	5.37
GI.4	2.12	0.83	2.22	1.65
GI.5	3.81	4.68	7.88	1.98
GI.6	1.67	5.08	7.53	1.43
GI.7	2.50	1.85	7.22	1.08
GI.8	5.65	2.66	8.41	1.52
GI.9	2.55	3.77	6.42	5.26
GII.1	2.59	3.13	5.80	4.07
GII.2	2.31	3.87	0.81	0.22
GII.3	6.32	4.49	7.12	1.27
GII.4	3.36	4.82	5.24	9.08
GII.5	4.63	3.28	3.72	3.18
GII.6	0.63	0.65	2.62	1.85
GII.7	8.62	3.13	2.34	1.54
GII.8	1.86	6.25	6.78	1.59
GII.9	8.09	0.97	2.71	1.39
GII.10	1.75	6.81	5.59	1.54
GII.12	2.35	8.70	5.28	2.99
GII.13	3.20	4.92	4.58	0.26
GII.14	1.64	3.70	9.23	1.08
GII.15	0.00	8.84	0.88	5.09
GII.16	4.01	3.23	8.80	3.13
GII.17	0.82	3.28	9.62	0.24
GII.20	2.55	2.30	5.88	1.24
GII.21	1.61	2.40	1.52	1.33
GII.22	3.81	3.44	3.28	7.69

antibodies GII.4-4A21C1 and GII.4-5D41A12 and the polyclonal antibodies GII.4 + GII.8 were analyzed three times in each microplate. Intra-assay CVs were observed to be in the ranges of 0.63–9.62% (Table 2), 0–9.99% (Table 3), and 0.55–9.88% (Table 4), respectively. After repeating the experiments in three batches of plates prepared for 3 days, the inter-assay CVs were found to be in the ranges of 0.22–9.08% (Table 2), 0.3–9.76% (Table 3), and 0.21–9.99% (Table 4). These results indicated that the developed ELISA technique showed good reproducibility.

## DISCUSSION

Owing to the high frequencies of NoV outbreaks (Hall et al., 2011; Verhoef et al., 2013; Grytdal et al., 2016) and severe acute gastroenteritis (Atmar and Mullen, 2013; Cardemil et al., 2017), high risk of infection transmission (Sukhrie et al., 2010; Teunis et al., 2010; Verhoef et al., 2015), and enormous socioeconomic burden after infection (Pires et al., 2015), the development of NoV vaccines is critical for improving public health. However, the characteristics of NoV

genetic diversity and high variation have markedly hindered vaccine development.

At present, NoV vaccines rely on VLP and P particles prepared by bioengineering technology as subunit vaccines. The morphology and antigenicity of recombinant NoV VLP are similar to natural virus particles (Estes et al., 2000). Preclinical studies have shown that VLP is immunogenic when administered by intranasal, oral or parenteral routes, which can induce serum and mucosal immune responses, and co-administration with mucosal adjuvants induces stronger immune responses (Estes et al., 2000). Three surface loops per P domain are potential sites for foreign antigen presentation, which could enhance the antigenicity and immunogenicity of antigens (Tan et al., 2011). Su et al. (2015) have shown that immune P particles induced antiserum in both mice (1:245,600) and rabbits (1:145,700), and also induced neutralizing antibodies to block the binding of NoV variants and receptors. The results prove the immunogenicity of P particles. Therefore, both NoV VLP and P particles are suitable choices for vaccine preparation.

Several NoV vaccines using a variety of different technologies have been developed, including three in clinical trials. The first is the bivalent intramuscular GI/GII.4 vaccine developed

**TABLE 3 |** Intra- and inter-assay coefficients of variation for the broad-spectrum detection of GII.4-5D41A12 monoclonal antibodies by ELISA.

Antigen designation	Intra-assay Precision CV/%			Inter-assay Precision CV/%
	1	2	3	–
GI.1	5.41	6.14	2.83	2.59
GI.2	1.81	2.41	1.32	8.92
GI.3	1.61	1.63	5.53	9.76
GI.4	2.71	4.27	2.34	8.71
GI.5	9.88	4.41	0.83	2.87
GI.6	4.20	0.00	6.40	4.07
GI.7	4.68	3.68	3.08	5.57
GI.8	0.00	6.83	3.63	8.63
GI.9	2.26	2.71	3.89	2.98
GII.1	0.00	1.82	2.79	1.23
GII.2	2.08	7.23	2.51	6.57
GII.3	8.52	3.76	1.95	8.95
GII.4	6.80	5.54	5.38	3.81
GII.5	3.12	1.68	1.79	3.26
GII.6	3.72	6.59	1.28	9.47
GII.7	4.27	2.36	1.79	2.28
GII.8	8.52	2.94	9.05	3.38
GII.9	0.98	1.76	1.64	5.77
GII.10	0.88	2.37	6.09	5.61
GII.12	1.67	2.11	5.62	3.61
GII.13	5.23	5.91	9.99	1.77
GII.14	8.65	4.13	5.95	0.30
GII.15	0.00	0.91	1.61	1.54
GII.16	2.44	2.30	5.00	2.85
GII.17	4.20	4.26	2.17	1.64
GII.20	2.22	2.31	3.74	5.82
GII.21	3.59	1.49	2.37	2.36
GII.22	4.68	0.83	5.01	2.52

**TABLE 4 |** Intra- and inter-assay coefficients of variation for the broad-spectrum detection of GI.4 + GI.8 polyclonal antibodies by ELISA.

GI.4 + II.8 Antigen designation	Intra-assay Precision CV/%			Inter-assay Precision CV/%
	1	2	3	–
GI.1	3.44	2.81	3.88	9.21
GI.2	5.49	3.50	4.21	0.94
GI.3	2.50	2.94	6.57	9.99
GI.4	3.26	4.40	2.81	1.27
GI.5	2.68	2.40	2.60	3.63
GI.6	6.46	4.00	5.03	4.48
GI.7	3.72	4.73	0.97	8.74
GI.8	3.77	1.27	1.24	9.16
GI.9	3.43	0.92	1.71	3.56
GII.1	4.67	1.43	3.76	4.39
GII.2	3.29	3.22	2.27	3.31
GII.3	4.35	4.22	3.07	1.88
GII.4	3.35	1.48	1.68	2.43
GII.5	4.03	6.63	5.23	3.83
GII.6	4.35	0.95	0.62	9.79
GII.7	4.59	1.88	3.77	2.50
GII.8	1.75	2.09	3.40	4.95
GII.9	4.46	0.55	5.55	2.25
GII.10	3.20	2.84	3.00	1.12
GII.12	0.82	1.10	1.01	2.25
GII.13	4.42	3.09	2.85	9.25
GII.14	3.65	1.58	2.52	2.73
GII.15	8.80	8.86	4.57	7.19
GII.16	2.43	3.79	4.28	2.12
GII.17	0.75	4.23	3.17	1.79
GII.20	1.76	0.81	4.09	1.89
GII.21	1.47	1.71	4.89	0.21
GII.22	2.03	0.49	6.46	3.27

by Takeda Pharmaceutical Company Limited (Treanor et al., 2014). The second, developed by Vaxart, Inc., is based on a G I.1 NoV sequence (Kim et al., 2018). The third is the NoV tetravalent vaccine developed by Institut Pasteur of Shanghai Chinese Academy of Sciences and Chongqing Zhifei Biological Products Co., Ltd. (XINHUANET, 2019). Therefore, analysis of cross-protection among different strains is a significant step for the development of a successful NoV vaccine.

The immune cross-protection between different genotypes is complicated. Studies have shown GI.1 can induce blockade antibodies against other GI strains (Lindesmith et al., 2015); GII.4 antiserum and GII.17 antiserum have limited cross-reactivity or no cross-protection; Malm et al. (2015) demonstrated there is no cross-cluster protection between GI and GII, but the research of Czako et al. (2015) showed GI.1 infection will cause an increase of GII.4 antiserum. In short, the development of effective vaccines must contain both GI and GII viruses.

In addition to vaccine development, detection technology is also an important part of NoV prevention and control. The immunoassay methods mainly include enzyme linked immunosorbent assay (ELISA) and immunochromatographic (ICG). In this study, capsid P proteins of 28 representative

NoV strains were used as coating antigens for the development of an indirect ELISA to detect their binding ability with antibodies. The broad spectrum of NoV antisera could be quickly detected using this method. Furthermore, one genotype or a combination of genotypes with broad-spectrum detection could be screened for the design of multivalent vaccines. Owing to the genetic diversity of NoV and 5%–10% cross-reactivity observed among genotypes (lower cross-reactivity among genogroups), the development of a broad-spectrum multivalent vaccine platform is necessary to protect against as many NoV-prevalent strains as possible (LoBue et al., 2006).

In summary, in this study, we developed an indirect ELISA with the potential to serve as a rapid, reliable, and high-throughput method for screening broad-spectrum antibodies to expedite the development of NoV vaccines.

## DATA AVAILABILITY STATEMENT

The original contributions presented in the study are included in the article/**Supplementary Material**, further inquiries can be directed to the corresponding authors.



## AUTHOR CONTRIBUTIONS

YZ and LX designed the experiments and wrote the manuscript. YJ and WC contributed reagents, materials, and analysis tools. JG, YyL, and YhL performed the experiments. YLi, TC, and LW analyzed the data. MC and JW revised the manuscript. YD, JZ, and QW provided project funding. All authors have read and agreed to the published version of the manuscript.

## FUNDING

This study was supported by the National Natural Science Foundation of China (31872912 and 31701717),

the Natural Science Foundations of Guangdong Province for Distinguished Young Scholars (2019B151502065), the Key Research and Development Program of Guangdong Province (2019B020209001), and GDAS'Project of Science and Technology Development (2020GDASYL-20200104008).

## SUPPLEMENTARY MATERIAL

The Supplementary Material for this article can be found online at: <https://www.frontiersin.org/articles/10.3389/fmicb.2021.670488/full#supplementary-material>

## REFERENCES

- Almand, E. A., Moore, M. D., and Jaykus, L.-A. (2017). Norovirus binding to ligands beyond histo-blood group antigens. *Front. Microbiol.* 8:2549. doi: 10.3389/fmicb.2017.02549
- Atmar, J., and Mullen, E. (2013). Norovirus in immunocompromised patients. *Oncol. Nurs. Forum* 40, 434–436. doi: 10.1188/13.ONF.434-436
- Cardemil, C. V., Parashar, U. D., and Hall, A. J. (2017). Norovirus infection in older adults: epidemiology, risk factors, and opportunities for prevention and control. *Infect. Dis. Clin. North Am.* 31, 839–870. doi: 10.1016/j.idc.2017.07.012
- Chhabra, P., De Graaf, M., Parra, G. I., Chan, M. C., Green, K., Martella, V., et al. (2019). Updated classification of norovirus genogroups and genotypes. *J. Gen. Virol.* 100, 1393–1406. doi: 10.1099/jgv.0.001318
- Cortes-Penfield, N. W., Ramani, S., Estes, M. K., and Atmar, R. L. (2017). Prospects and challenges in the development of a norovirus vaccine. *Clin. Ther.* 39, 1537–1549. doi: 10.1016/j.clinthera.2017.07.002
- Czakó, R., Atmar, R. L., Opekun, A. R., Gilger, M. A., Graham, D. Y., and Estes, M. K. (2015). Experimental human infection with Norwalk virus elicits a surrogate neutralizing antibody response with cross-genogroup activity. *Clin. Vaccine Immunol.* 22, 221–228. doi: 10.1128/CVI.00516-14
- Ding, H., Zhou, Y., and Wang, H. (2019). Development of an indirect ELISA for detecting humoral immunodominant proteins of *Mycoplasma hyopneumoniae* which can discriminate between inactivated bacterin-induced hyperimmune sera and convalescent sera. *BMC Vet. Res.* 15:327. doi: 10.1186/s12917-019-2077-4
- Esposito, S., and Principi, N. (2020). Norovirus vaccine: priorities for future research and development. *Front. Immunol.* 11:1383. doi: 10.3389/fimmu.2020.01383
- Estes, M. K., Ball, J. M., Guerrero, R. A., Opekun, A. R., Gilger, M. A., Pacheco, S. S., et al. (2000). Norwalk virus vaccines: challenges and progress. *J. Infect. Dis.* 181, S367–S373. doi: 10.1086/315579
- Fan, J. H., Zuo, Y. Z., Yang, Z., and Pei, L. H. (2013). The development of an indirect ELISA for the detection of antibodies to goose parvovirus in blood serum. *Lett. Appl. Microbiol.* 57, 26–32. doi: 10.1111/lam.12070
- Gan, S. D., and Patel, K. R. (2013). Enzyme immunoassay and enzyme-linked immunosorbent assay. *J. Invest. Dermatol.* 133:e12. doi: 10.1038/jid.2013.287
- Grytdal, S. P., Debess, E., Lee, L. E., Blythe, D., Ryan, P., Biggs, C., et al. (2016). Incidence of norovirus and other viral pathogens that cause acute gastroenteritis (AGE) among Kaiser Permanente member populations in the United States, 2012–2013. *PLoS One* 11:e0148395. doi: 10.1371/journal.pone.0148395
- Hall, A. J., Rosenthal, M., Gregoricus, N., Greene, S. A., Ferguson, J., Henao, O. L., et al. (2011). Incidence of acute gastroenteritis and role of norovirus, Georgia, USA, 2004–2005. *Emerg. Infect. Dis.* 17, 1381–1388. doi: 10.3201/eid1708.101533
- Hutson, A. M., Atmar, R. L., Graham, D. Y., and Estes, M. K. (2002). Norwalk virus infection and disease is associated with ABO histo-blood group type. *J. Infect. Dis.* 185, 1335–1337. doi: 10.1086/339883
- Jin, M., Zhou, Y. K., Xie, H. P., Fu, J. G., He, Y. Q., Zhang, S., et al. (2016). Characterization of the new GII.17 norovirus variant that emerged recently as the predominant strain in China. *J. Gen. Virol.* 97, 2620–2632. doi: 10.1099/jgv.2016.000000
- Kim, L., Liebowitz, D., Lin, K., Kasperek, K., Pasetti, M. F., Garg, S. J., et al. (2018). Safety and immunogenicity of an oral tablet norovirus vaccine, a phase I randomized, placebo-controlled trial. *JCI Insight* 3:e121077. doi: 10.1172/jci.insight.121077
- Ledesma, D., Berriatua, E., Thomas, M. C., Bernal, L. J., Ortuño, M., Benitez, C., et al. (2017). Performance of Leishmania PFR1 recombinant antigen in serological diagnosis of asymptomatic canine leishmaniasis by ELISA. *BMC Vet. Res.* 13:304. doi: 10.1186/s12917-017-1224-z
- Lindesmith, L. C., Beltramello, M., Swanstrom, J., Jones, T. A., Corti, D., Lanzavecchia, A., et al. (2015). Serum immunoglobulin a cross-strain blockade of human noroviruses. *Open Forum Infect. Dis.* 2:ofv084. doi: 10.1093/ofid/ofv084
- Lindesmith, L., Moe, C. S., Ruvoen, N., Jiang, X., Lindblad, L., Stewart, P., et al. (2003). Human susceptibility and resistance to Norwalk virus infection. *Nat. Med.* 9, 548–553. doi: 10.1038/nm860
- LoBue, A. D., Lindesmith, L., Yount, B., Harrington, P. R., Thompson, J. M., Johnston, R. E., et al. (2006). Multivalent norovirus vaccines induce strong mucosal and systemic blocking antibodies against multiple strains. *Vaccine* 24, 5220–5234. doi: 10.1016/j.vaccine.2006.03.080
- Lopman, B. A., Steele, D., Kirkwood, C. D., and Parashar, U. D. (2016). The vast and varied global burden of norovirus: prospects for prevention and control. *PLoS Med.* 13:e1001999. doi: 10.1371/journal.pmed.1001999
- Malm, M., Tamminen, K., Lappalainen, S., Uusi-Kerttula, H., Vesikari, T., and Blazevic, V. (2015). Genotype considerations for virus-like particle-based bivalent norovirus vaccine composition. *Clin. Vaccine Immunol.* 22, 656–663. doi: 10.1128/CVI.00015-15
- Morozov, V., Hanisch, F. G., Wegner, K. M., and Schrotten, H. (2018). Pandemic GII.4 Sydney and epidemic GII.17 Kawasaki308 noroviruses display distinct specificities for histo-blood group antigens leading to different transmission vector dynamics in Pacific oysters. *Front. Microbiol.* 9:2826. doi: 10.3389/fmicb.2018.02826
- Nordgren, J., and Svensson, L. (2019). Genetic susceptibility to human norovirus infection: an update. *Viruses* 11:226. doi: 10.3390/v11030226
- Pires, S. M., Fischer-Walker, C. L., Lanata, C. F., Devleeschauwer, B., Hall, A. J., Kirk, M. D., et al. (2015). Aetiology-specific estimates of the global and regional incidence and mortality of diarrhoeal diseases commonly transmitted through food. *PLoS One* 10:e0142927. doi: 10.1371/journal.pone.0142927
- Rock, B. H. G., Vennema, H., Hoebe, C. J. P. A., Duizer, E., and Koopmans, M. P. G. (2005). Association of histo-blood group antigens and susceptibility to norovirus infections. *J. Infect. Dis.* 191, 749–754. doi: 10.1086/427779
- Su, W., Gao, J., Zang, Y., Wu, H., Wang, L., Hu, H., et al. (2015). Production, characterization and immunogenicity of P particles derived from norovirus GII.4 genotype 2004 variant. *Acta Virol.* 59, 33–39. doi: 10.4149/av\_2015\_01\_33
- Sukhrie, F. H. A., Siebenga, J. J., Beersma, M. F. C., and Koopmans, M. (2010). Chronic shedders as reservoir for nosocomial transmission of norovirus. *J. Clin. Microbiol.* 48, 4303–4305. doi: 10.1128/JCM.01308-10

- Tamminen, K., Malm, M., Vesikari, T., and Blazevic, V. (2019). Immunological cross-reactivity of an ancestral and the most recent pandemic norovirus GII.4 variant. *Viruses* 11:91. doi: 10.3390/v11020091
- Tan, M., Huang, P., Xia, M., Fang, P.-A., Zhong, W., Mcneal, M., et al. (2011). Norovirus P particle, a novel platform for vaccine development and antibody production. *J. Virol.* 85, 753–764. doi: 10.1128/JVI.01835-10
- Teunis, P. F., Moe, C. L., Liu, P., Miller, S. E., Lindesmith, L., Baric, R. S., et al. (2010). Norwalk virus: how infectious is it? *J. Med. Virol.* 80, 1468–1476. doi: 10.1002/jmv.21237
- Treanor, J. J., Atmar, R. L., Frey, S. E., Gormley, R., Chen, W. H., Ferreira, J., et al. (2014). A novel intramuscular bivalent norovirus virus-like particle vaccine candidate—reactogenicity, safety, and immunogenicity in a phase 1 trial in healthy adults. *J. Infect. Dis.* 210, 1763–1771. doi: 10.1093/infdis/jiu337
- Uusi-Kerttula, H., Tamminen, K., Malm, M., Vesikari, T., and Blazevic, V. (2014). Comparison of human saliva and synthetic histo-blood group antigens usage as ligands in norovirus-like particle binding and blocking assays. *Microbes Infect.* 16, 472–480. doi: 10.1016/j.micinf.2014.02.010
- Verhoef, L., Hewitt, J., Barclay, L., Ahmed, S. M., Lake, R., Hall, A. J., et al. (2015). Norovirus genotype profiles associated with foodborne transmission, 1999–2012. *Emerg. Infect. Dis.* 21, 592–599. doi: 10.3201/eid2104.141073
- Verhoef, L., Koopmans, M., Van Pelt, W., Duizer, E., Haagsma, J., Werber, D., et al. (2013). The estimated disease burden of norovirus in The Netherlands. *Epidemiol. Infect.* 141, 496–506. doi: 10.1017/S0950268812000799
- Vinje, J. (2015). Advances in laboratory methods for detection and typing of norovirus. *J. Clin. Microbiol.* 53, 373–381. doi: 10.1128/jcm.01535-14
- XINHUANET (2019). Available online at: [http://www.xinhuanet.com/201906/04/c\\_1124582589.htm](http://www.xinhuanet.com/201906/04/c_1124582589.htm) (accessed June 4, 2019).
- Xue, L., Cai, W., Gao, J., Zhang, L., Wu, H., Pang, R., et al. (2019). Genome characterization and temporal evolution analysis of a non-epidemic norovirus variant GII.8. *Infect. Genet. Evol.* 70, 15–23. doi: 10.1016/j.meegid.2019.02.010
- Xue, L., Dong, R., Wu, Q., Li, Y., Cai, W., Kou, X., et al. (2016). Molecular epidemiology of noroviruses associated with sporadic gastroenteritis in Guangzhou, China, 2013–2015. *Arch. Virol.* 161, 1377–1384. doi: 10.1007/s00705-016-2784-0
- Xue, L., Wu, Q., Kou, X., Cai, W., Zhang, J., and Guo, W. (2015). Genome characterization of a GII.6 norovirus strain identified in China. *Infect. Genet. Evol.* 31, 110–117. doi: 10.1016/j.meegid.2015.01.027

**Conflict of Interest:** The authors declare that the research was conducted in the absence of any commercial or financial relationships that could be construed as a potential conflict of interest.

The handling editor declared a shared affiliation, with one of the author YD at the time of the review.

**Publisher's Note:** All claims expressed in this article are solely those of the authors and do not necessarily represent those of their affiliated organizations, or those of the publisher, the editors and the reviewers. Any product that may be evaluated in this article, or claim that may be made by its manufacturer, is not guaranteed or endorsed by the publisher.

Copyright © 2021 Zuo, Xue, Gao, Liao, Jiang, Li, Liang, Wang, Cai, Cheng, Wang, Chen, Zhang, Ding and Wu. This is an open-access article distributed under the terms of the Creative Commons Attribution License (CC BY). The use, distribution or reproduction in other forums is permitted, provided the original author(s) and the copyright owner(s) are credited and that the original publication in this journal is cited, in accordance with accepted academic practice. No use, distribution or reproduction is permitted which does not comply with these terms.



# Development of a Loop-Mediated Isothermal Amplification Method for the Rapid Detection of *Phytophthora vexans*

Tuhong Wang<sup>1†</sup>, Haojun Ji<sup>1,2†</sup>, Yongting Yu<sup>1†</sup>, Xiaojie Wang<sup>2</sup>, Yi Cheng<sup>1</sup>, Zhimin Li<sup>1</sup>, Jia Chen<sup>1</sup>, Litao Guo<sup>1</sup>, Jianping Xu<sup>1,3\*</sup> and Chunsheng Gao<sup>1\*</sup>

<sup>1</sup> Institute of Bast Fiber Crops and Center of Southern Economic Crops, Chinese Academy of Agricultural Sciences, Changsha, China, <sup>2</sup> State Key Laboratory of Crop Stress Biology for Arid Areas, College of Life Sciences, Northwest A&F University, Yangling, China, <sup>3</sup> Department of Biology, McMaster University, Hamilton, ON, Canada

## OPEN ACCESS

### Edited by:

Xiyang Wu,  
Jinan University, China

### Reviewed by:

Antonella Amicucci,  
University of Urbino Carlo Bo, Italy  
Shiro Fukuta,  
Aichi Prefectural Institute of Hygiene,  
Japan

### \*Correspondence:

Chunsheng Gao  
gaochunsheng@caas.cn  
Jianping Xu  
jpxu@mcmaster.ca

<sup>†</sup>These authors share first authorship

<sup>‡</sup>Deceased

### Specialty section:

This article was submitted to  
Food Microbiology,  
a section of the journal  
Frontiers in Microbiology

Received: 04 June 2021

Accepted: 06 August 2021

Published: 06 September 2021

### Citation:

Wang T, Ji H, Yu Y, Wang X,  
Cheng Y, Li Z, Chen J, Guo L, Xu J  
and Gao C (2021) Development of a  
Loop-Mediated Isothermal  
Amplification Method for the Rapid  
Detection of *Phytophthora vexans*.  
Front. Microbiol. 12:720485.  
doi: 10.3389/fmicb.2021.720485

Brown root rot caused by *Phytophthora vexans* is a new destructive root disease on many plants such as Gingko, Citrus, kiwifruit, and ramie. The establishment of loop-mediated isothermal amplification (LAMP) technology for detecting *P. vexans* can help monitor and control brown root rot quickly, efficiently, and accurately. LAMP technology is known for its simplicity, sensitivity, and speed; and it does not require any specialized equipment – a water bath or a thermoblock is sufficient for isothermal amplifications. LAMP products can be visualized by using hydroxy naphthol blue (HNB) dye or agarose gel electrophoresis. In this study, by searching and comparing the internal transcribed spacer (ITS) sequences of *P. vexans* and the related species in oomycete genera *Pythium*, *Phytophthora*, and *Phytophthora*, we designed specific primers targeting the ITS gene region of *P. vexans*. Using HNB dye, we established a LAMP technique for rapid detection of *P. vexans* by visible color change. In addition, we optimized the protocol to enhance both sensitivity and specificity for *P. vexans* detection. Under the optimized condition, our protocol based on LAMP technology could detect as low as 24 copies of the *P. vexans* genomic DNA, which is ~100 times more sensitive than conventional PCR. This method can successfully detect *P. vexans* using cell suspensions from *P. vexans* – infected ramie root tissues.

**Keywords:** *Phytophthora vexans*, loop mediated isothermal amplification, internal transcribed spacer (ITS) sequence, hydroxynaphthol blue (HNB), diagnosis

## INTRODUCTION

Oomycetes belong to the Kingdom Stramenopila (Baldauf et al., 2000; Yoon et al., 2002), which includes diverse microorganisms living in marine, freshwater, and terrestrial environments (Sparrow, 1960; Karling, 1981). *Phytophthora* is a genus in the family Pythiaceae of oomycete. At present, there are over 20 species in this genus, with most of them showing strong association with the freshwater environment (Tkaczyk, 2020) and being saprophytes. However, a few *Phytophthora* species have been observed to cause diseases in plants, such as *Phytophthora litorale* infecting the Old-World sycamore *Platanus orientalis* (Derviş et al., 2020); *Phytophthora helicoides* causing citrus fruit and root rot (Chen X. R. et al., 2016);

and *Phytophthora vexans* (de Bary) (Lévesque et al., 2008; Bala et al., 2010) causing root rot in many economically important plants (Adhikari et al., 2013; de Cock et al., 2015).

*Phytophthora vexans*, formerly known as *Pythium vexans*, is found in many parts of the world. In recent years, diseases caused by *P. vexans* have been frequently reported. In Africa, the species was identified to infect citrus trees and grapevine (Spies et al., 2009; Benfradj et al., 2017; Langenhoven et al., 2018). In the United States, *P. vexans* was reported to cause root and crown rot of woody ornamentals (flowering cherry, Ginkgo, and red maple) (Panth et al., 2020; Baysal-Gurel et al., 2021). In China, *P. vexans* has been reported to cause diseases on ramie, tobacco, rubber trees, and dendrobium (Zeng et al., 2005; Tao et al., 2011; Bian et al., 2015; Chen B. et al., 2016; Yu et al., 2016). In addition, *P. vexans* can cause patch canker, damping-off, and crown rot, stem rot, and root rot in many economically important fruit trees, such as durian, kiwifruit, apple, and avocado in Vietnam, Turkey, Morocco, and Mexico, respectively (Polat et al., 2017; Hernández et al., 2019; Jabiri et al., 2020; Thao et al., 2020). The increasing reports of diseases caused by *P. vexans* suggest that this pathogen has the potential to cause large-scale disease outbreaks across multiple plants in the future.

Pathogen detection is a fundamental part of disease control. At present, the identification method of *P. vexans* mainly relies on visible disease symptoms and microbial cultures. However, due to (i) difficulties in isolation and cultivation of *Phytophthora* spp. and *Pythium* spp., (ii) similarities in hyphal and spore morphologies among related *Phytophthora* species (Schroeder et al., 2006), and (iii) similarities in disease symptoms caused by *P. vexans* and many other disease agents belonging to genera *Phytophthora* and *Pythium*, and even plant fungal pathogens, it's been difficult to identify *P. vexans* based on disease symptom and culture characteristics as the causal agent of diseases (Li et al., 2018). Indeed, traditional identification methods require a wealth of knowledge and experience, is time-consuming and laborious, and lacks accuracy, all of which contribute to making them difficult to apply for the analysis and identification of large samples (Wang et al., 2020). In recent years, with the rapid development of molecular biological technology, a variety of detection technologies based on polymerase chain reaction (PCR) and real-time fluorescent quantitative PCR have been developed. These methods have become the main means for rapid, accurate and specific identification of pathogens, avoiding the shortcomings of uncertainty in traditional morphology-based identifications (Schroeder et al., 2013). However, most current molecular detection technologies require professional instruments, reagents, and strict environmental conditions in a lab setting. The instruments and reagents are often expensive, the operation requirements are high, the process is complex, and the detection time is still long. These shortcomings make most of these methods not suitable in the field or in resource-limited laboratories.

Loop-mediated isothermal amplification (LAMP) is a molecular detection technology with limited technical and instrumental requirements. It uses four to six specific primers to amplify the target DNA in a short time under constant temperature by using *Bst* DNA polymerase (Notomi et al., 2000).

The reaction products can be detected using multiple methods, of which gel electrophoresis is the most accurate and generates typical ladder-like banding patterns. The amplified products can also be detected visually by adding different dyes, including SYBR green, hydroxynaphthol blue (HNB), or calcein, which can be seen with the naked eye (Mori et al., 2001; Goto et al., 2009). The advantages of LAMP include being simple, having easy detection of products, and low cost, as well as being suitable for rapid detection of pathogens in both lab and field conditions (Parida et al., 2010). So far, LAMP technology has been widely used in the rapid detection of oomycete, fungi, bacteria, viruses, nematodes, including many plant and animal pathogens (Liu et al., 2010; Fukuta et al., 2013a,b; Feng L. et al., 2015; Wei et al., 2016; Zeng et al., 2018). However, a LAMP rapid detection method for *P. vexans* has not been reported.

The objective of this study is to develop a LAMP assay for the detection of *P. vexans*. Here, we selected the internal transcribed spacer (ITS) regions of the nuclear ribosomal RNA gene cluster as the detection target sequence. We designed and evaluated the specificity of the primers, optimized the LAMP protocol, and determined the sensitivity of this method. Using this protocol, we successfully identified *P. vexans* in laboratory-infected ramie samples. Our method should facilitate the rapid diagnosis of *P. vexans* in agricultural and forestry environments.

## MATERIALS AND METHODS

### Isolates Used in the LAMP Assay

Although *Phytophthora* is a relatively newly defined genus different from the *Pythium* and *Phytophthora* genera, organisms in all three genera have similar micromorphology and growth patterns. Therefore, in this study, 20 representative isolates of *Phytophthora*, *Pythium*, and *Phytophthora*, as well as of selected *Fusarium* species that are also common causes of brown root rot in plants (Table 1) were selected for this study. The 20 isolates representing 19 brown root rot species were collected from different provinces in China and were maintained at the Institute of Bast Fiber Crops, Chinese Academy of Agricultural Sciences (Changsha, China). All isolates were grown on potato dextrose agar (PDA) medium at 25°C for 3–5 days before extracting DNA. Mycelia were harvested, collected, and stored at –20°C. Mycelial DNA was extracted by a Rapid Extraction Kit for Fungi Genomic DNA (Aidlab, Beijing, China) following the user's manual. Conventional PCR amplification was carried out with the specific primers of *P. vexans* (PvF1/PvR1) (Spies et al., 2011b). The ITS region (ITS1, 5.8S, and ITS2) of all 20 isolates was amplified and sequenced using primers V9G (5'-TTACGTCCCTGCCCTTTGTA-3') and LS266 (5'-GCATTCCCAACAACCTCGACTC-3') (van den Ende and de Hoog, 1999).

### Designing and Screening of LAMP Primers

In this study, the ITS sequence was selected as the target gene for LAMP assay. To identify the portions of ITS sequence that are unique to *P. vexans*, we performed multiple sequence alignment



**TABLE 1** | Isolates used to test the specificity of the loop-mediated isothermal amplification (LAMP) method and the assay results.

Species	Clade <sup>a</sup>	Clade <sup>b</sup>	Origin	Locality	LAMP detection <sup>c</sup>
<i>Phytophthora vexans</i> HF1	K	Phytophthora	<i>Boehmeria nivea</i>	Hunan	+
<i>Phytophthora vexans</i>	K	Phytophthora	<i>Nicotiana tabacum</i>	Shandong	+
<i>Pythium spinosum</i>	F	F	<i>Boehmeria nivea</i>	Hunan	—
<i>Pythium irregulare</i>	F	F	<i>B. nivea</i>	Henan	—
<i>Pythium sylvaticum</i>	F	F	<i>B. nivea</i>	Henan	—
<i>Phytophthora helicoides</i>	K	Phytophthora	<i>B. nivea</i>	Hunan	—
<i>Pythium ultimum</i>	I	I	<i>B. nivea</i>	Shandong	—
<i>Pythium myriotylum</i>	B1	B	<i>B. nivea</i>	Shandong	—
<i>Phytophthora litorale</i> (FL242)	K	Phytophthora	<i>B. nivea</i>	Henan	—
<i>Pythium oligandrum</i>	D	D	<i>Nicotiana tabacum</i>	Henan	—
<i>Pythium heterothallicum</i>	I	I	<i>N. tabacum</i>	Hunan	—
<i>Pythium carolinianum</i>		E	<i>N. tabacum</i>	Henan	—
<i>Pythium guiyangense</i>			<i>N. tabacum</i>	Guizhou	—
<i>Pythium aphanidermatum</i>	A	A	<i>N. tabacum</i>	Henan	—
<i>Pythium recalcitrans</i>	F	F	<i>N. tabacum</i>	Hunan	—
<i>Fusarium oxysporum</i>			<i>Dioscorea batatas</i>	Hunan	—
<i>Fusarium graminearum</i>			<i>D. batatas</i>	Hunan	—
<i>Fusarium solani</i>			<i>D. batatas</i>	Hunan	—
<i>Fusarium verticillioides</i>			<i>Lilium brownii</i>	Hunan	—
<i>Phytophthora capsici</i>		Clade 2	<i>Capsicum frutescent</i>	Hunan	—

<sup>a</sup>Phylogenetic clades of *Pythium* species from Lévesque and de Cock (2004).

<sup>b</sup>de Cock et al. (2015).

<sup>c</sup>LAMP specificity detection using primer set Pv8.

“+” and “—” indicate positive and negative results, respectively.

including sequences of tested isolates as well as sequences of type strains of *P. vexans* (GenBank accession number: HQ643400.2), *P. irregulare* (AY598702.2), *Pythium ultimum* (AY598657.2), *Pythium spinosum* (AY598701.2), *Pythium aphanidermatum* (AY598622.2), *Pythium myriotylum* (AY598678.2), *P. litorale* (NNIBRFG9359), *Pythium sylvaticum* (AY598645), *P. helicoides* (AB108026), *Pythium recalcitrans* (KJ716861), *Pythium oligandrum* (AY598618), *Pythium heterothallicum* (AY598654), *Pythium carolinianum* (HQ643484.1), *Pythium guiyangense* (AY987037), and *Phytophthora capsici* (FN257939) that were retrieved from the NCBI databases. The program ClustalW2<sup>1</sup> (Larkin et al., 2007) was used to perform multiple sequence alignment to find the regions within ITS which were specific for *P. vexans*. Based on the aligned sequences, a set of primers was designed. The LAMP primers were designed using PrimerExplore V5,<sup>2</sup> all the parameters were set by default, and primers were synthesized by TSINGKE Biotechnology Co. Ltd. Nine primers sets were tested (Supplementary Table 1), however, the best primers (Pv8 primers set) were screened by specificity and sensitivity test. In addition, a phylogenetic tree was constructed with the maximum likelihood method implemented in MEGA 7.0 (Kumar et al., 2016). A Poisson correction was used for multiple substitution models and a pairwise deletion was used for handling missing data. Statistical support for individual branches of the phylogenetic tree showing taxa relationships was assessed with 1,000 bootstrap replicates.

<sup>1</sup><http://www.ebi.ac.uk/Tools/msa/clustalw2/>

<sup>2</sup><http://primerexplorer.jp/>

## LAMP Reaction Condition and Optimization

The LAMP reaction was carried out in a total volume of 25  $\mu$ L containing 1.6  $\mu$ M of each FIP and BIP primer, 0.2  $\mu$ M of each F3 and B3 primer, 20 mM Tris-HCl (pH 8.8), 10 mM KCl, 0.1% Tween20, 0.8 M betaine (Shanghai Yuanye Bio-Technology, Shanghai, China), 8 mM MgSO<sub>4</sub>, 10 mM (NH<sub>4</sub>)<sub>2</sub>SO<sub>4</sub>, 1.4 mM dNTPs, and 8U *Bst* DNA polymerase large fragment (New England Biolabs Japan, Tokyo, Japan), 180  $\mu$ M HNB (Macklin, Shanghai, China), and 2  $\mu$ L template DNA (Feng W. et al., 2015). The mixture was incubated at 64°C for 60 min to perform the LAMP reaction. The genomic DNA template of *P. vexans* was diluted in a 10-fold series after concentration determination, so that the DNA concentration gradient was 100 ng/ $\mu$ L, 10 ng/ $\mu$ L, 1 ng/ $\mu$ L, 100 pg/ $\mu$ L, 10 pg/ $\mu$ L, 1 pg/ $\mu$ L, 100 fg/ $\mu$ L, 10 fg/ $\mu$ L, and 1 fg/ $\mu$ L. Among them, 1 pg DNA contained 23.4 copies of the *P. vexans* genome.

Based on the above LAMP reaction system, the reaction time and temperature, the concentration of MgSO<sub>4</sub>, betaine, dNTPs were optimized using a gradient of values. Specifically, the reaction temperatures were set at 60, 62, 64, 66, and 68°C; the reaction times were set at 10, 20, 30, 40, 50, 60, 70, and 80 min; the concentrations of betaine were 0, 0.2, 0.4, 0.6, 0.8, 1.0, and 1.2 M; of MgSO<sub>4</sub> were 0.2, 4, 6, 8, and 10 mM; and of dNTP were 0, 0.2, 0.4, 0.6, 0.8, 1.0, 1.2, 1.4, and 1.6 mM. In all optimizations, a negative control was set up with sterilized distilled water instead of DNA template. The LAMP products were visualized by adding HNB before amplification. Samples that turned blue were considered positive, while samples that remained violet

were negative. In addition, the LAMP products were detected through electrophoresis in 1.5% agarose gel by staining with GelRed (TSINGKE Biological Technology, Beijing, China), and positive reactions resulted in a ladder-like banding pattern. The reaction was performed with three biological repeats.

### Detection of *P. vexans* From Extracted Genomic DNA From Pure Culture

Using the selected primers, the genomic DNA of 20 strains were used as templates, and sterilized distilled water instead of DNA template was used as negative control. The optimized LAMP reaction system was used for amplification. After the reaction, a color change in the products was assessed with the naked eyes of at least two independent investigators.

### Detection of *P. vexans* in Infected Plants

To evaluate the application of the developed LAMP protocol as a tool for the diagnosis of *P. vexans* in infected plants, ramie cultivar “Zhongzhu No. 1” roots were inoculated as described below. Two-week-old seedlings (approximately 20–30 cm tall) were prepared via the cutting propagation method (Yu et al., 2015). To inoculate ramie plants, mycelial disks (8 mm in

diameter) obtained from 3-day-old culture of each of the 20 isolates of *Phytophthora* spp., *Pythium* spp., and *Phytophthora* spp. on PDA were placed upside-down on the roots. Plants inoculated with agar disks without mycelia were used as controls. Both the inoculated and control plants were grown in the greenhouse at  $26 \pm 1^\circ\text{C}$  with a 12 h photoperiod. After 10 days, tissues surrounding the infected region was harvested for DNA extraction by a Rapid Extraction Kit for Fungi Genomic DNA (Aidlab, Beijing, China). These DNA samples were evaluated using the developed LAMP technique.

## RESULTS

### Selection of Primers in LAMP Detection System

In total, two *P. vexans* isolates, two isolates of two other *Phytophthora* species, 11 isolates of 11 *Pythium* species, one *P. capsici* isolate, and four isolates of four *Fusarium* species obtained from different provinces in China (Table 1) were used to test the specificity of the LAMP primers and reaction conditions. All tested strains were first analyzed with the above-mentioned *P. vexans* diagnostic primers PvF1 and PvR1, a reported specific

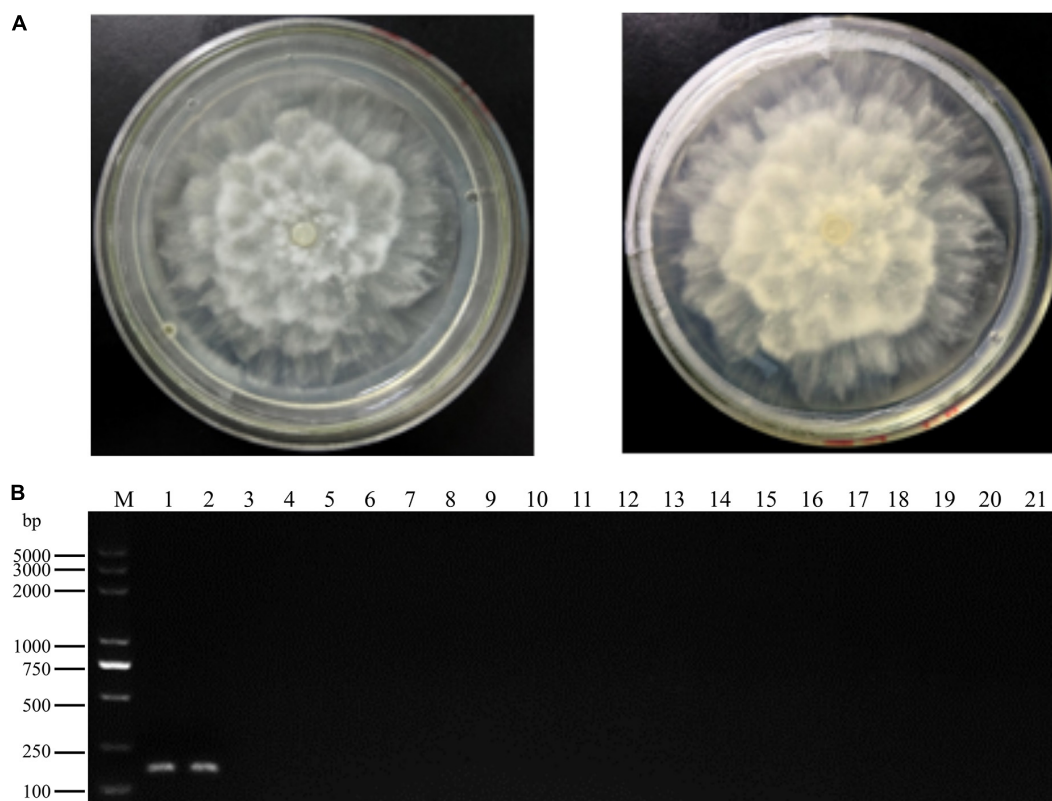


**FIGURE 1 |** Colony morphology and specific polymerase chain reaction (PCR) primer detection of *Phytophthora vexans*. **(A)** Colony morphology of *P. vexans*. **(B)** Confirmation of primer specificity for *P. vexans*, lanes 1 and 2 are strains of *P. vexans*; lanes 3–20 correspond to the following species *Pythium spinosum*, *Pythium irregulare*, *Pythium sylvaticum*, *Phytophthora helicoides*, *Pythium ultimum*, *Pythium myriotylum*, *Phytophthora litorale*, *Pythium oligandrum*, *Pythium heterothallicum*, *Pythium carolinianum*, *Pythium guiyangense*, *Pythium aphanidermatum*, *Pythium recalcitrans*, *Fusarium oxysporum*, *Fusarium graminearum*, *Fusarium solani*, *Fusarium verticillioides*, and *Phytophthora capsici*, respectively; lane 21 is a negative control.



primer of *P. vexans*. The results showed that lanes 1 and 2 are strains of *P. vexans*, and the other tested strains were not *P. vexans* (Figure 1). For all 20 isolates, their species identities were confirmed based on their ITS sequences. Based on the ITS sequences of type strains of these species, we constructed a phylogeny among the tested species (Supplementary Figure 1).

The phylogenetic relationships among these strains and species are overall consistent with what has been described previously for these organisms. Specifically, the fungal genus *Fusarium* is distinct from the oomycetes. Among the three oomycete genera, the genus *Phytophthora* was diverged first, followed by *Phytophthium* and *Pythium* (Supplementary Figure 1).

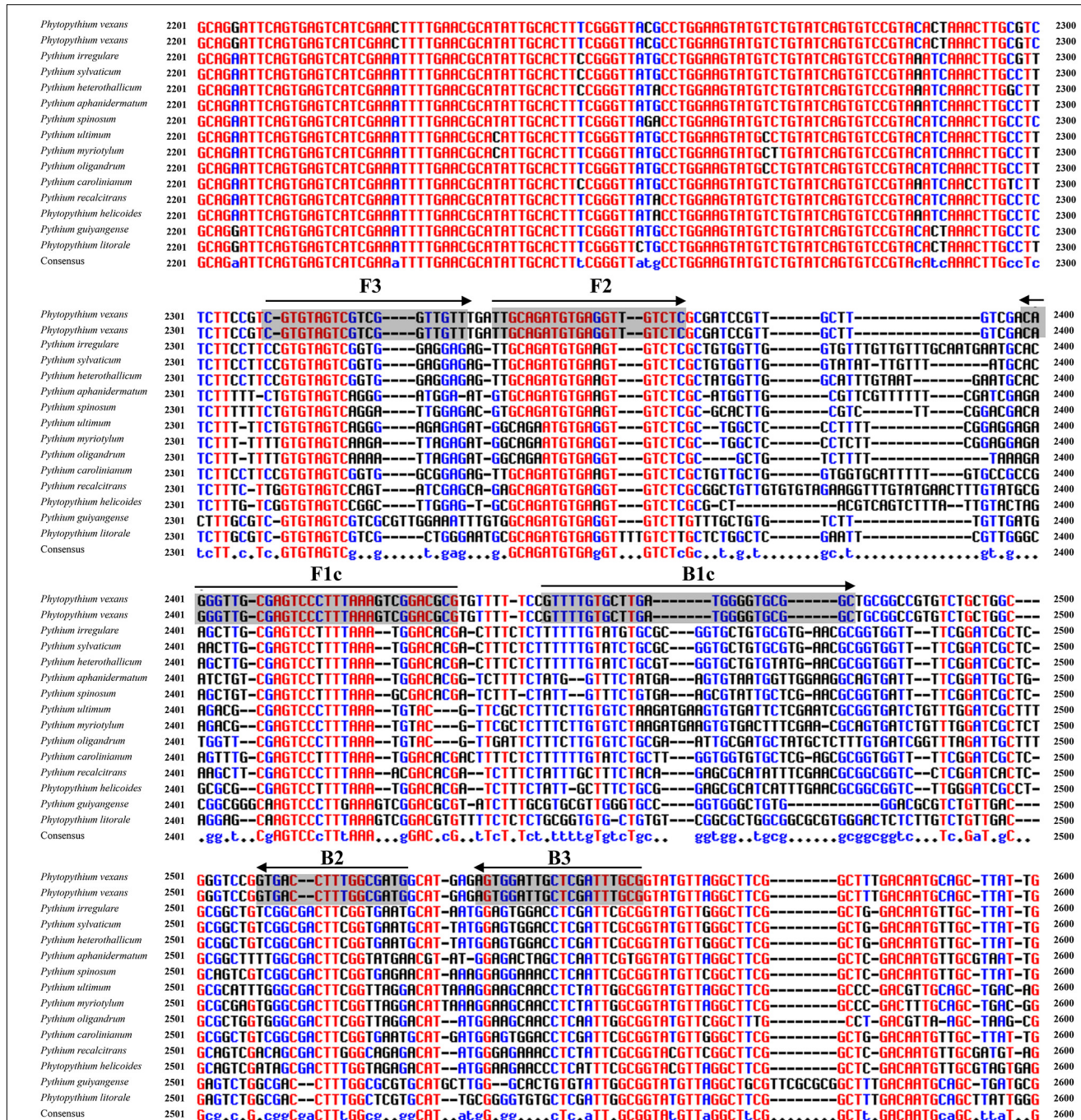


**FIGURE 2 |** Nucleotide sequence alignment of internal transcribed spacer (ITS) sequences from *P. vexans* and closely related isolates. Partial sequences of ITS and the location of the Pv8 set consists of four loop-mediated isothermal amplification (LAMP) core primers [Pv8F3, Pv8B3, Pv8FIP (F1c-F2), and Pv8BIP (B1c-B2)] are shown. Arrows indicate the 5' to 3' direction of primer extension during amplification.



**FIGURE 3 |** Specificity of LAMP detection of *P. vexans*. **(A)** Detection of LAMP products by 2% agarose gel electrophoresis. **(B)** Detection of LAMP products detected by HNB, 1 and 2, *P. vexans*; 3–20 indicate *P. spinosum*, *P. irregulare*, *P. sylvaticum*, *P. helicoides*, *P. ultimum*, *P. myriotylum*, *P. litoreale*, *P. oligandrum*, *P. heterothallicum*, *P. carolinianum*, *P. guiyangense*, *P. aphanidermatum*, *P. recalcitrans*, *F. oxysporum*, *F. graminearum*, *F. solani*, *F. verticillioides*, and *P. capsici*, respectively.

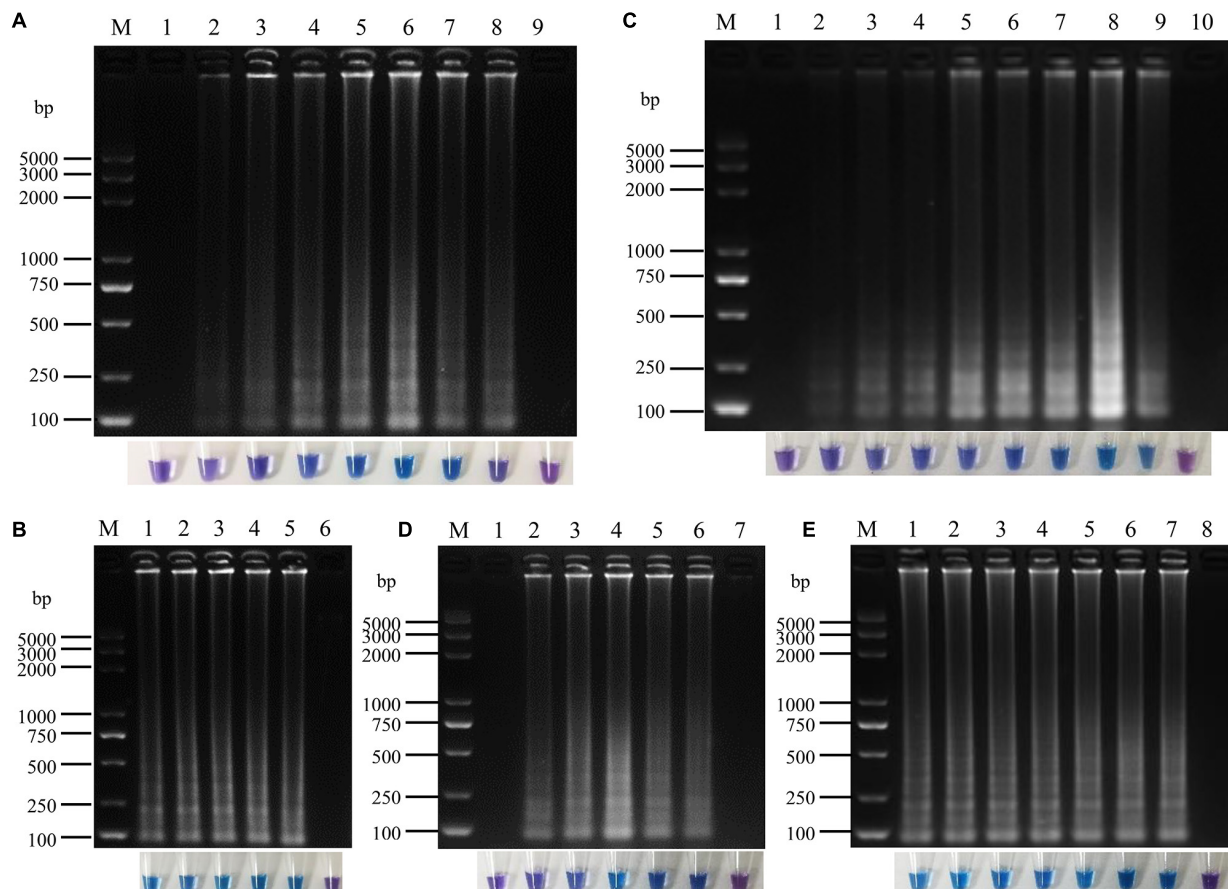


**FIGURE 4 |** Optimization of loop-mediated isothermal amplification (LAMP) reaction system for *P. vexans*. **(A)** The reaction time of lanes 1–8 were 10, 20, 30, 40, 50, 60, 70, and 80 min, lane 9 was negative control. **(B)** The reaction temperature of lanes 1–5 were 60, 62, 64, 66, and 68°C, lane 6 was negative control. **(C)** Lanes 1–9 corresponded to 0, 0.2, 0.4, 0.6, 0.8, 1.0, 1.2, 1.4, and 1.6 mM dNTPs, respectively, and lane 10 was negative control. **(D)** Lanes 1–6 indicated that the concentrations of  $MgSO_4$  were 0, 2, 4, 6, 8, and 10 mM, respectively, lane 7 was negative control. **(E)** Lanes 1–7 indicated that the concentrations of betaine were 0, 0.2, 0.4, 0.6, 0.8, 1.0, and 1.2 M, lane 8 was negative control. In all optimizations, a negative control was set up that contained pure sterilized distilled water without any template DNA.



To identify *P. vexans*-specific LAMP primers at the ITS region, multiple sequence alignment of ITS sequences between *P. vexans* and other 18 isolates was carried out. The variable regions of ITS between *P. vexans* and other isolates were found (Figure 2). Based on the sequence variability patterns, nine primer sets were designed using the online tool PrimerExplore V5 (Supplementary Table 1). Then, according to the LAMP amplification system and procedure, reactions were set up for all the 20 isolates. The specificity and sensitivity of various primer combinations were compared. Finally, among these nine sets of primer combinations, the Pv8 set consists of four core primers Pv8F3 (5'-CGTGTAGTCGTCGGTTGTT-3'), Pv8B3 (5'-CGCAAATCGAGCAATCCACT-3'), Pv8FIP (5'-CGCGTCCGACTTTAAAGGGACTTGCAGATGTGAGGTTG TCTC-3'), and Pv8BIP (5'-GTTTTGTGCTTGATGGGGTG CGGCCATCGCCAAAGGTCAC-3') performed the best and was the most consistent for detecting *P. vexans* (Figure 2). Using the Pv8 primer combinations, positive amplifications were obtained only with the two *P. vexans* isolates in Table 1 while no amplification product (Figure 3A) nor color change (Figure 3B) was observed for the remaining 18 isolates.

## Optimization of LAMP Reaction System for *P. vexans*

A 25  $\mu$ L LAMP reaction system was established with *P. vexans* DNA as template for optimizing the reaction temperature and time, and the concentrations of dNTPs, MgSO<sub>4</sub> and betaine in the system. The evaluated reaction temperatures were set at 60, 62, 64, 66, and 68°C; the reaction times were set at 10, 20, 30, 40, 50, 60, 70, and 80 min; the concentrations of betaine were 0, 0.2, 0.4, 0.6, 0.8, 1.0, and 1.2 M; of MgSO<sub>4</sub> were 0, 2, 4, 6, 8, and 10 mM; and of dNTP were 0, 0.2, 0.4, 0.6, 0.8, 1.0, 1.2, 1.4, and 1.6 mM. In each series of amplifications, we included a negative control where pure sterilized distilled water without any DNA template was used. The results showed that under the recommended LAMP condition, the amplification products could be detected between reaction time 20–80 min. However, the brightest amplification products and the amplification efficiency was reached at a reaction time of 60 min (Figure 4A). Thus, we chose 60 min as the reaction time to observe the LAMP amplified products, and with coloration intensity from HNB staining and/or DNA band brightness through agarose gel electrophoresis as indicators of amplification efficiency in each reaction. Among the tested temperature range 60–68°C, we found little difference among the five temperature treatments in both color change and in the amounts of amplified products as shown on the electrophoretic gel. The temperature experiments indicated that the LAMP reaction condition was robust in the 60–68°C temperature range; therefore, for the following experiments, we chose the optimum temperature of *Bst* DNA polymerase, i.e., at 64°C (Figure 4B). Among the concentrations of dNTP from 0.2 to 1.6 mM, the amplification products could all be detected, but the highest amplification product was observed at the dNTP concentration of 1.4 mM (Figure 4C). Similar to the limited effect of dNTP concentration change, the change of concentration had relatively little effect on amplification efficiency, but the highest

amplification efficiency was observed at the concentration of 6.0 mM MgSO<sub>4</sub> (Figure 4D). In contrast to MgSO<sub>4</sub>, where no MgSO<sub>4</sub> resulted in no amplification product, betaine was found to be not essential in our LAMP protocol. However, because betaine has the effect of stabilizing enzyme activity and promoting melting (Rees et al., 1993; Notomi et al., 2000), to improve the stability of the reaction system, especially for field applications, 0.8 M betaine where the color change was the most obvious was added to the system (Figure 4E). In conclusion, the optimal LAMP reaction system was determined as follows: 1.6  $\mu$ M FIP/BIP, 0.2  $\mu$ M F3/B3, and 8U *Bst* DNA polymerase, 1 $\times$  isothermal amplification buffer [20 mM Tris-HCL (pH 8.8), 10 mM (NH<sub>4</sub>)<sub>2</sub>SO<sub>4</sub>, 50 mM KCl, 0.1% Tween20], 6 mM MgSO<sub>4</sub>, 1.4 mM dNTPs, 0.8 M betaine, 180  $\mu$ M HNB, 2  $\mu$ L DNA template in a total volume of 25  $\mu$ L with the final volume adjusted with sterilized distilled water, with the reaction temperature of 64°C for 60 min.

## Comparison of the Sensitivity of LAMP and Conventional PCR Assays

To determine the sensitivity of primer set Pv8, ten-fold serial dilutions of *P. vexans* genomic DNA were tested. The DNA template concentrations ranged from 10 ng/ $\mu$ L to 1 fg/ $\mu$ L. The detection limit of the conventional PCR assay using the specific primers Pv8F3 and Pv8R3 was 100 pg/ $\mu$ L DNA (~2,350 copy of the *P. vexans* genome) (Figure 5A). In comparison, as indicated by a color change and DNA amplification of the reaction products, the lowest limit of *P. vexans* detection was 1 pg/ $\mu$ L DNA (~24 copy of the *P. vexans* genome) for the LAMP assay (Figures 5B,C). This indicates that the LAMP assay has a wider dynamic range, with a sensitivity at least 100 times greater than that of conventional PCR for the detection of *P. vexans*.

## Successful Detection in *P. vexans* Infected Plants

All 15 *Phytophthora* and *Pythium* isolates were inoculated onto the “Zhongzhu No. 1” cultivar of ramie plants. After 10 days at 25°C, the fibrous roots of all inoculated plants turned red-brown surrounding the inoculation site. However, no symptom was observed on the roots of negative control plants (Supplementary Figure 2). Genomic DNA was extracted from the infected region and subjected to the LAMP reaction. The results of electrophoresis showed that, except for *P. vexans*, no DNA bands were produced in the DNA system of ramie roots infected by other 13 tested pathogens (Figure 6A). The results were confirmed based on color change as shown in Figure 6B. Both assay systems indicate that LAMP amplification reaction using primer set Pv8 can accurately detect *P. vexans* in ramie roots.

## DISCUSSION

*Phytophthora vexans* is the most well-known plant-pathogenic species of the genus *Phytophthora*. This pathogen can attack roots, stems, and crown of a wide range of plants worldwide (Spies et al., 2011a; Panth et al., 2020). For example, brown root rot of ramie caused by *P. vexans* has become an increasingly

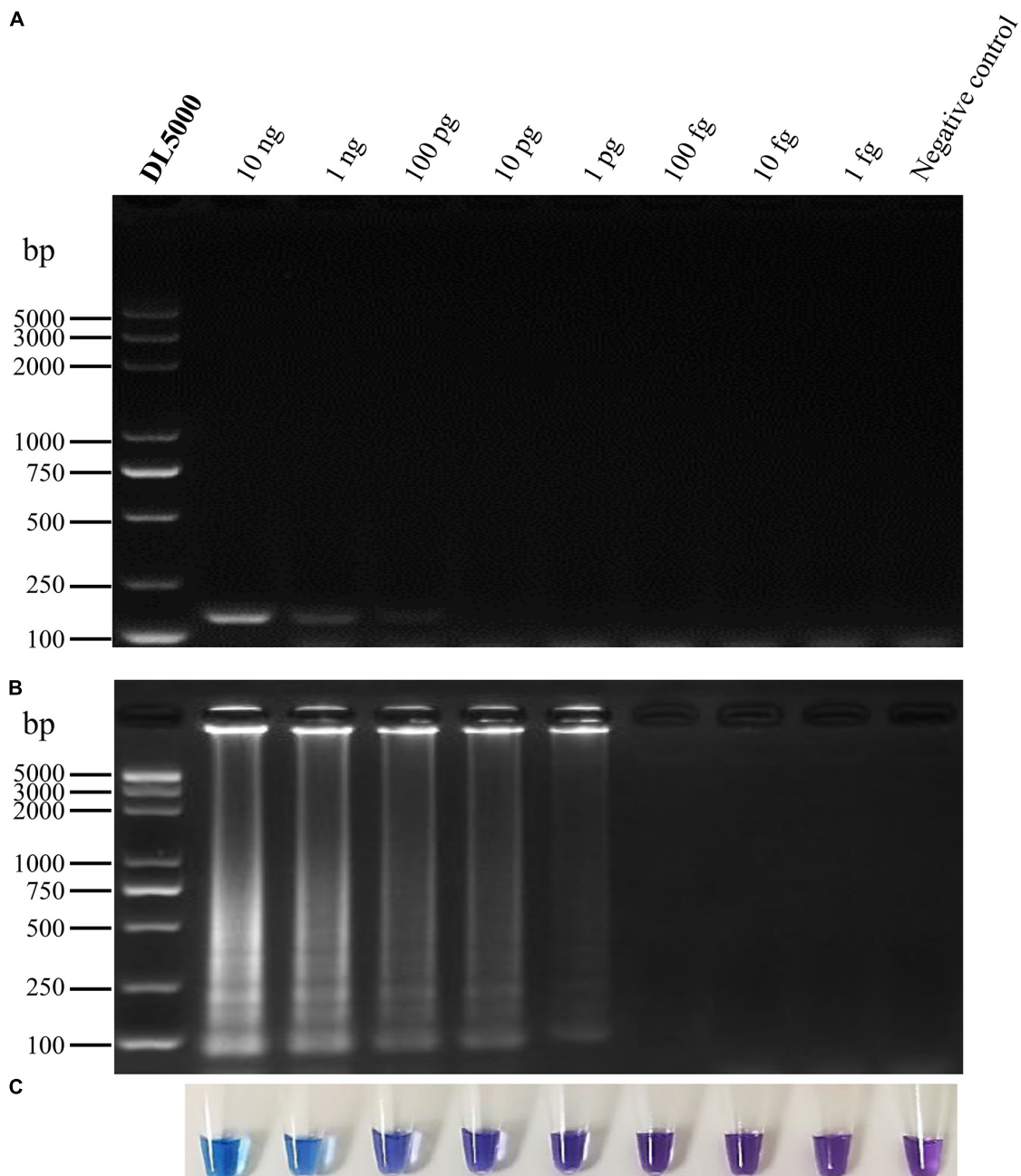


**FIGURE 5 |** Sensitivity of conventional PCR and the LAMP assays for detecting *P. vexans*. **(A)** Detection of conventional PCR products by agarose gel electrophoresis. **(B)** Detection of LAMP products by agarose gel electrophoresis. **(C)** Detection of LAMP products using HNB as a visual indicator.

important disease endangering ramie production in China, resulting in >40% yield loss in some ramie plantations (Zhu et al., 2014; Yu et al., 2016). Therefore, a rapid and accurate detection of *P. vexans* is especially important for its identification and disease management. In this study, a rapid, sensitive, and accurate LAMP detection method for *P. vexans* based on color observation was established by using ITS gene sequence as the detection target. This technique was successfully used to detect *P. vexans* in infected ramie root tissues. It should be directly used

in field conditions for the rapid diagnosis of ramie brown root rot caused by *P. vexans*.

A key factor influencing the LAMP method is target selection. Due to the divergence of ITS sequences among many closely-related species and its high copy number in each genome, ITS is often used as the detection target gene in oomycete. For example, ITS has been used as target gene for sequence-based identification of *P. aphanidermatum* (Fukuta et al., 2013a,b), *P. helicoides* (= *P. helicoides*) (Takahashi et al., 2014),

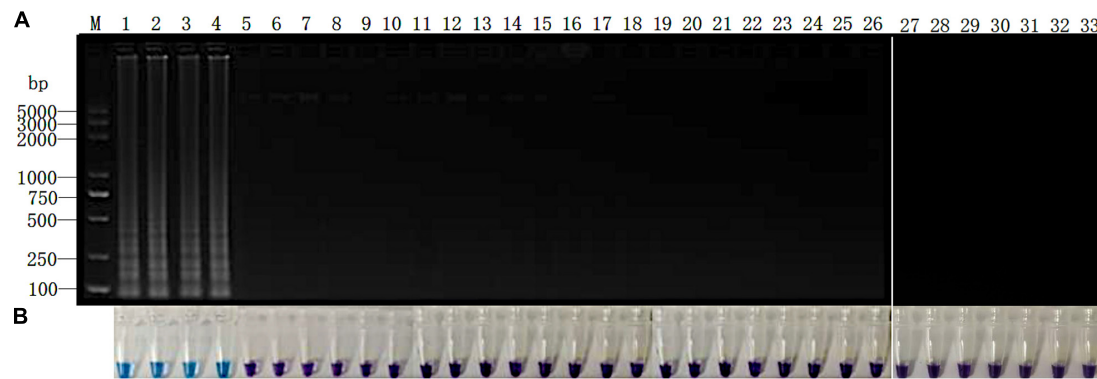


**FIGURE 6 |** Detection of *P. vexans* in infected ramie roots. **(A)** Detection of LAMP products by 2% agarose gel electrophoresis. **(B)** Detection of LAMP products detected by HNB. Lanes 1–4, *P. vexans*; lanes 5 and 6, *P. spinosum*; lanes 7 and 8, *P. irregulare*; lanes 9 and 10, *P. sylvaticum*; lanes 11 and 12, *P. helicoides*; lanes 13 and 14, *P. ultimum*; lanes 15 and 16, *P. myriotylum*; lanes 17 and 18, *P. litorale*; lanes 19 and 20, *P. oligandrum*; lanes 21 and 22, *P. heterothallicum*; lanes 23 and 24, *P. carolinianum*; lanes 25 and 26, *P. guiyangense*; lanes 27 and 28, *P. aphanidermatum*; lanes 29 and 30, *P. recalcitrans*; lanes 31 and 32, CK. Lane 33, negative control.

*P. myriotylum* (Fukuta et al., 2014), *Pythium irregulare* (Feng W. et al., 2015), and *Phytophthora infestans* (Ristaino et al., 2019). In our study, ITS sequence was successfully used in LAMP detection of *P. vexans*. However, in other pathogen groups such as *P. ultimum* and related *Pythium* species (Shen et al., 2017), *Phytophthora alni* and *Phytophthora cambivora* (Brasier et al., 2004), the ITS sequences of closely related sister species are often too similar to allow effective discrimination. In the *Phytophthium* genus, *Phytophthium chamaeophyon*, and *P. helicoides* also have highly similar ITS sequences that can't be used to design LAMP primers for detection (de Cock et al., 2015). In the case of similar ITS sequences among closely related species, researchers have recently developed other genes for LAMP-based species-specific detection. For example, a target gene encoding a spore wall protein was developed to detect *P. ultimum* (Shen et al., 2017); while a target gene encoding trypsin protease was used to detect *P. aphanidermatum* (Li et al., 2018).

Another key factor of molecular detection technology is sensitivity. The higher the sensitivity is, the more favorable it is to detect target pathogens from samples. It is generally believed that compared with conventional and real-time PCR assays, the LAMP assay is simple, rapid, specific, and sensitive. However, previous studies also suggest that the LAMP assay has the same sensitivity than the PCR assay (Fukuta et al., 2013a,b; Ishiguro et al., 2013; Feng W. et al., 2015). Due to differences in target gene copy number among species and strains in their genomes and to differences in their genome sizes, the detection limit among species and strains could be different. For example, previous studies have shown the detection limits of LAMP ranging from 100 fg/ $\mu$ L to 1 pg/ $\mu$ L, while the detection limits of conventional PCR ranging from 100 fg/ $\mu$ L to 100 pg/ $\mu$ L (Takahashi et al., 2014; Shen et al., 2017; Ristaino et al., 2019). In this study, the LAMP assay was about 100 times more sensitive than conventional PCR, even though the primers of LAMP assay and conventional PCR primers were all designed according to ITS sequence. Specifically, the sensitivity evaluation showed that the detection limit of LAMP was 1 pg/ $\mu$ L ( $\sim$ 24 copies of *P. vexans* genome), while

that of conventional PCR was 100 pg/ $\mu$ L ( $\sim$ 2,350 copies of *P. vexans* genome).

Our analyses showed that our LAMP protocol could become a new reliable method for the diagnosis of *P. vexans* infection. However, the method has only been tested on pure DNA and laboratory-infected plant tissues. Direct field applicability has not been conducted and additional optimization may be needed in agricultural and forestry field application. In addition, our analyses used fresh cultures and recently infected plant tissues, the applicability of our LAMP technology to old samples and shipped materials from distant locations needs further testing. Regardless, the technology described here represents a promising approach for rapid, specific, and sensitive identification of *P. vexans* using DNA from pure cultures and from plant tissues infected with this pathogen.

In conclusion, we developed a visual LAMP assay for the diagnosis of *P. vexans*. This LAMP method has high specificity, sensitivity, and accuracy, and can identify *P. vexans* in infected plants. This method should facilitate the early and accurate diagnosis of *P. vexans* in the field so that timely plant protection measures can be initiated.

## DATA AVAILABILITY STATEMENT

The datasets presented in this study can be found in online repositories. Representative isolates can be obtained from the corresponding author CG upon request.

## AUTHOR CONTRIBUTIONS

YY and CG designed and supervised the research. TW and HJ performed the research, analyzed the data, and prepared the draft manuscript. XW, YC, ZL, JC, LG, CG, and JX contributed to the literature search, reviewing, and finalizing the manuscript. All authors have read and approved the final manuscript.

## FUNDING

This work was financially supported by the Agricultural Science and Technology Innovation Program of the Chinese Academy of Agricultural Sciences (CAAS-ASTIP-2015-IBFC).

## ACKNOWLEDGMENTS

We sincerely thank all the researchers who provided the test strains.

## REFERENCES

- Adhikari, B. N., Hamilton, J. P., Zerillo, M. M., Tisserat, N., Lévesque, C. A., and Buell, C. R. (2013). Comparative genomics reveals insight into virulence strategies of plant pathogenic oomycetes. *PLoS One* 8:e75072. doi: 10.1371/journal.pone.0075072
- Bala, K., Robideau, G. P., Lévesque, C. A., De Cock, A. W. A. M., Abad, Z. G., Lodhi, A. M., et al. (2010). *Phytophthora* gen. nov. and *Phytophthora sindhum* sp. nov. *Persoonia* 24, 36–137.
- Baldauf, S. L., Roger, A. J., Wenk-Siefert, I., and Doolittle, W. F. (2000). A kingdom-level phylogeny of eukaryotes based on combined protein data. *Science* 290, 972–977. doi: 10.1126/science.290.5493.972
- Baysal-Gurel, F., Liyanapathirana, P., Panth, M., Avin, F. A., and Simmons, T. (2021). First report of *Phytophthora vexans* causing root and crown rot on flowering cherry in Tennessee. *Plant Dis.* 105:232. doi: 10.1094/PDIS-06-20-1166-PDN
- Benfradj, N., Migliorini, D., Luchi, N., Santini, A., and Boughalleb-M'Hamdi, N. (2017). Occurrence of *Pythium* and *Phytophthora* species isolated from citrus trees infected with gummosis disease in Tunisia. *Arch. Phytopathol. Plant Protect.* 50, 286–302. doi: 10.1080/03235408.2017.1305479
- Bian, C., Wang, W., Zhao, S., and Kang, Y. (2015). Molecular identification and pathogenicity of *Pythium vexans* isolated from tobacco (In Chinese). *J. Agric.* 5, 32–36.
- Brasier, C. M., Kirk, S. A., Delcan, J., Cooke, D. E. L., Jung, T., and Veld, W. A. M. I. (2004). *Phytophthora alni* sp. nov. and its variants: designation of emerging heteroploid hybrid pathogens spreading on *Alnus* trees. *Mycol. Res.* 108, 1172–1184. doi: 10.1017/S0953756204001005
- Chen, B., Chen, J., Mu, B., Zeng, M., Yu, J., Zhao, J., et al. (2016). Advances in medicinal health protection studies of *Boehmeria Jacq.* Spp. (In Chinese). *Plant Fiber Sci. China* 38, 237–241. doi: 10.3969/j.issn.1671-3532.2016.05.008
- Chen, X. R., Liu, B. B., Xing, Y. P., Cheng, B. P., Liu, M. L., Tong, Y. H., et al. (2016). Identification and characterization of *Phytophthora helicoides* causing stem rot of shatangju mandarin seedlings in china. *Eur. J. Plant Pathol.* 146, 715–727. doi: 10.1007/s10658-016-0952-4
- de Cock, A. W., Lodhi, A. M., Rintoul, T. L., Bala, K., Robideau, G. P., Abad, Z. G., et al. (2015). *Phytophthora*: molecular phylogeny and systematics. *Persoonia* 34, 25–39. doi: 10.3767/003158515X685382
- Derviş, S., Türkölmez, Ş., Çiftçi, O., Özer, G., Ulubaş Serçe, Ç., and Dikilitas, M. (2020). *Phytophthora litorale*: A novel killer pathogen of plane (*Platanus orientalis*) causing canker stain and root and collar rot. *Plant Dis.* 104, 2642–2648. doi: 10.1094/PDIS-01-20-0141-RE
- Feng, L., Ni, X., Wu, X., Lun, C., Wu, C., and Luan, J. (2015). Loop-mediated isothermal amplification (LAMP) for detection of *Pantoea stewartii* subsp. *stewartii* (In Chinese). *J. Plant Protect.* 42, 347–352. doi: 10.13802/j.cnki.zwbhxb.2015.03.010
- Feng, W., Ishiguro, Y., Hotta, K., Watanabe, H., Suga, H., and Kageyama, K. (2015). Simple detection of *Pythium irregulare* using loop-mediated isothermal amplification assay. *FEMS Microbiol. Lett.* 362:fnv174. doi: 10.1093/fems/lnv174
- Fukuta, S., Takahashi, R., Kuroyanagi, S., Ishiguro, Y., Miyake, N., Nagai, H., et al. (2014). Development of loop-mediated isothermal amplification assay for the

## SUPPLEMENTARY MATERIAL

The Supplementary Material for this article can be found online at: <https://www.frontiersin.org/articles/10.3389/fmicb.2021.720485/full#supplementary-material>

**Supplementary Figure 1** | Maximum likelihood tree showing phylogenetic relationships among the 19 tested species. The tree was constructed based on ITS sequence of oomycetes listed in **Table 1**. Statistical support for the branches was assessed by bootstrap with 1,000 replicates. Bootstrap values above 50 are shown near the branch node.

**Supplementary Figure 2** | Symptoms of ramie roots after infected with *Phytophthora* and *Pythium* spp.

- detection of *Pythium myriotylum*. *Lett. Appl. Microbiol.* 59, 49–57. doi: 10.1111/lam.12244
- Fukuta, S., Takahashi, R., Kuroyanagi, S., Miyake, N., Nagai, H., Suzuki, H., et al. (2013a). Detection of *Pythium aphanidermatum* in tomato using loop-mediated isothermal amplification (LAMP) with species-specific primers. *Eur. J. Plant Pathol.* 136, 689–701. doi: 10.1007/s10658-013-0198-3
- Fukuta, S., Tamura, M., Maejima, H., Takahashi, R., Kuwayama, S., Tsuji, T., et al. (2013b). Differential detection of wheat yellow Mosaic virus, Japanese soil-borne wheat mosaic virus and Chinese wheat mosaic virus by reverse transcription loop-mediated isothermal amplification reaction. *J. Virol. Methods* 1089, 348–354. doi: 10.1016/j.jviromet.2013.03.005
- Goto, M., Honda, E., Ogura, A., Nomoto, A., and Hanaki, K. (2009). Colorimetric detection of loop-mediated isothermal amplification reaction by using hydroxy naphthol blue. *Biotechniques* 46, 167–172. doi: 10.2144/000113072
- Hernández, P. A., Chávez, E. C., Ortiz, J. D., Beache, M. B., Vargas, L. T., and Fuentes, Y. O. (2019). First report of *Phytophthora vexans* causing the “Avocado sadness” in Michoacan, Mexico. *Phyton Int. J. Exp. Bot.* 88, 11–13. doi: 10.32604/phyton.2019.04608
- Ishiguro, Y., Asano, T., Otsubo, K., Suga, H., and Kageyama, K. (2013). Simultaneous detection by multiplex PCR of the high-temperature-growing *Pythium* species: *P. aphanidermatum*, *P. helicoides* and *P. myriotylum*. *J. Gen. Plant Pathol.* 79, 350–358. doi: 10.1007/s10327-013-0466-2
- Jabiri, S., Lahlali, R., Bahra, C., Amraoui, M. B., Tahiri, A., and Amiri, S. (2020). First report of *Phytophthora vexans* associated with dieback disease of apple trees in Morocco. *J. Plant Pathol.* 102, 1319–1319. doi: 10.1007/s42161-020-00606-2
- Karling, J. S. (1981). *Predominantly Holocarpic and Eucarpic Simple Biflagellate Phycomycetes*, 2nd Edn. Germany: J. Cramer.
- Kumar, S., Stecher, G., and Tamura, K. (2016). MEGA7: molecular evolutionary genetics analysis version 7.0 for bigger datasets. *Mol. Biol. Evol.* 33, 1870–1874. doi: 10.1093/molbev/msw054
- Langenhoven, S., Halleen, F., Spies, C., Stempien, E., and Mostert, L. (2018). Detection and quantification of black foot and crown and root rot pathogens in grapevine nursery soils in the Western Cape of South Africa. *Phytopathol. Mediterr.* 57, 519–537. doi: 10.14601/Phytopathol\_Mediterr-23921
- Larkin, M. A., Blackshields, G., Brown, N. P., Chenna, R., McGettigan, P. A., McWilliam, H., et al. (2007). Clustal W and Clustal X version 2.0. *Bioinformatics* 23, 2947–2948. doi: 10.1093/bioinformatics/btm404
- Lévesque, C. A., and de Cock, A. W. (2004). Molecular phylogeny and taxonomy of the genus *Pythium*. *Mycol. Res.* 108, 1363–1383. doi: 10.1017/s0953756204001431
- Lévesque, C. A., Robideau, G. P., Desaulniers, N., Bala, K., Chen, W., and Tambong, J. T. (2008). “Molecular phylogeny, barcoding and ecology of *Pythium* species. (Abstr.),” in *3rd International Workshop on Phytophthora/Pythium and related genera*, Turin.
- Li, Q., Shen, D., Yu, J., Zhao, Y., Zhu, Y., and Dou, D. (2018). Rapid detection of *Pythium aphanidermatum* by loop-mediated isothermal amplification (In Chinese). *J. Nanjing Agric. Univ.* 41, 79–87. doi: 10.7685/jnau.2017.03.025



- Liu, J., Huang, C., Wu, Z., Zhang, X., and Wang, Y. (2010). Detection of *Tomato aspermy virus* infecting chrysanthemums by LAMP (In Chinese). *Sci. Agric. Sin.* 43, 1288–1294. doi: 10.4028/www.scientific.net/AMM.37-38.1549
- Mori, Y., Nagamine, K., Tomita, N., and Notomi, T. (2001). Detection of loop-mediated isothermal amplification reaction by turbidity derived from magnesium pyrophosphate formation. *Biochem. Biophys. Res. Commun.* 289, 150–154. doi: 10.1006/bbrc.2001.5921
- Notomi, T., Okayama, H., Masubuchi, H., Yonekawa, T., Watanabe, K., Amino, N., et al. (2000). Loop-mediated isothermal amplification of DNA. *Nucleic Acids Res.* 28:e63. doi: 10.1097/RLU.0b013e3181f49ac7
- Panth, M., Baysal-Gurel, F., Avin, F. A., and Simmons, T. (2020). Identification and chemical and biological management of *Phytophthora vexans*, the causal agent of *Phytophthora* root and crown rot of woody ornamentals. *Plant Dis.* 105, 1091–1100. doi: 10.1094/PDIS-05-20-0987-RE
- Parida, M., Sannarangaiah, S., Dash, P. K., Rao, P. V. L., and Morita, K. (2010). Loop mediated isothermal amplification (LAMP): a new generation of innovative gene amplification technique; perspectives in clinical diagnosis of infectious diseases. *Rev. Med. Virol.* 18, 407–421. doi: 10.1002/rmv.593
- Polat, Z., Awan, Q. N., Hussain, M., and Akgül, D. S. (2017). First report of *Phytophthora vexans* causing root and collar rot of kiwifruit in Turkey. *Plant Dis.* 101:1058. doi: 10.1094/PDIS-11-16-1554-PDN
- Rees, W. A., Yager, T. D., Korte, J., and von Hippel, P. H. (1993). Betaine can eliminate the base pair composition dependence of DNA melting. *Biochemistry* 32, 137–144. doi: 10.1021/bi00052a019
- Ristaino, J. B., Saville, A. C., Paul, R., Cooper, D. C., and Wei, Q. (2019). Detection of *Phytophthora infestans* by LAMP, real-time LAMP and droplet digital PCR. *Plant Dis.* 104, 1–9.
- Schroeder, K. L., Martin, F. N., de Cock, A. W. A. M., Lévesque, C. A., and Paulitz, T. C. (2013). Molecular detection and quantification of *Pythium* species: evolving taxonomy, new tools, and challenges. *Plant Dis.* 97, 4–20. doi: 10.1094/PDIS-03-12-0243-FE
- Schroeder, K. L., Okubara, P. A., Tambong, J. T., Lévesque, C. A., and Paulitz, T. C. (2006). Identification and quantification of pathogenic *Pythium* spp. from soils in eastern Washington using real-time polymerase chain reaction. *Phytopathology* 96, 637–647. doi: 10.1094/PHYTO-96-0637
- Shen, D., Li, Q., Yu, J., Zhao, Y., Zhu, Y., Xu, H., et al. (2017). Development of a loop-mediated isothermal amplification method for the rapid detection of *Pythium ultimum*. *Australas. Plant Pathol.* 46, 571–576. doi: 10.1007/s13313-017-0517-9
- Sparrow, F. K. (1960). *Aquatic Phycomycetes*. Ann Arbor, MI: University of Michigan Press.
- Spies, C. F. J., Mazzola, M., Botha, W. J., Koopman, T. A., Meitz, J., Paarwater, H., et al. (2009). “Characterisation of the *Pythium vexans* species complex from fruit crops in South Africa,” in *46th SASPP Congress*. Gordon’s Bay: SASPP council.
- Spies, C. F. J., Mazzola, M., Botha, W. J., Van der Rijst, M., Mostert, L., and McLeod, A. (2011a). Oogonial biometry and phylogenetic analyses of the *Pythium vexans* species group from woody agricultural hosts in South Africa reveal distinct groups within this taxon. *Fungal Biol.* 115, 157–168. doi: 10.1016/j.funbio.2010.11.005
- Spies, C. F. J., Mazzola, M., and McLeod, A. (2011b). Characterisation and detection of *Pythium* and *Phytophthora* species associated with grapevines in South Africa. *Eur. J. Plant Pathol.* 131, 103–119. doi: 10.1007/s10658-011-9791-5
- Takahashi, R., Fukuta, S., Kuroyanagi, S., Miyake, N., Nagai, H., Kageyama, K., et al. (2014). Development and application of a loop-mediated isothermal amplification assay for rapid detection of *Pythium helicoides*. *FEMS Microbiol. Lett.* 355, 28–35. doi: 10.1111/1574-6968.12453
- Tao, Y., Zeng, F., Ho, H., Wei, J., Wu, Y., Yang, L., et al. (2011). *Pythium vexans* causing stem rot of Dendrobium in Yunnan Province, China. *J. Phytopathol.* 159, 255–259. doi: 10.1111/j.1439-0434.2010.01756.x
- Thao, L., Hien, L., Liem, N., Thanh, H., Khanh, T., Binh, V., et al. (2020). First report of *Phytophthora vexans* causing root rot disease on durian in Vietnam. *New Dis. Rep.* 41:2. doi: 10.5197/j.2044-0588.2020.041.002
- Tkaczyk, M. (2020). *Phytophthora*: origin, differences and meaning in modern plant pathology. *Folia For. Pol. Ser. A For.* 62, 227–232. doi: 10.2478/ffp-2020-0022
- van den Ende, A. H. G., and de Hoog, G. S. (1999). Variability and molecular diagnostics of the neurotropic species *Cladophialophora bantiana*. *Stud. Mycol.* 43, 151–162.
- Wang, T., Gao, C., Cheng, Y., Li, Z., Chen, J., Guo, L., et al. (2020). Molecular diagnostics and detection of oomycetes on fiber crops. *Plants (Basel)* 2020:769. doi: 10.3390/plants9060769
- Wei, H., Wang, X., Li, H., Sun, W., and Gu, J. (2016). Loop-mediated isothermal amplification assay for rapid diagnosis of *Meloidogyne mali* (In Chinese). *J. Plant Protect.* 43, 260–266. doi: 10.13802/j.cnki.zwbhxb.2016.02.012
- Yoon, H. S., Hackett, J. D., and Bhattacharya, D. (2002). A single origin of the peridinin- and fucoxanthin-containing plastids in dinoflagellates through tertiary endosymbiosis. *Proc. Natl. Acad. Sci. U. S. A.* 99, 11724–11729. doi: 10.1073/pnas.172234799
- Yu, Y., Chen, J., Gao, C. S., Zeng, L. B., Li, Z. M., Zhu, T. T., et al. (2016). First report of brown root rot caused by *Pythium vexans* on ramie in Hunan, China. *Can. J. Plant Pathol.* 38, 405–410. doi: 10.1080/07060661.2016.1230150
- Yu, Y., Zeng, L., Yan, Z., Liu, T., Sun, K., Zhu, T., et al. (2015). Identification of ramie genes in response to *Pratylenchus coffeae* infection challenge by digital gene expression analysis. *Int. J. Mol. Sci.* 16, 21989–22007. doi: 10.3390/ijms160921989
- Zeng, D., Rong, Z., Yuan, Y., Wang, X., and Zheng, X. (2018). Rapid diagnosis of rice bakanae disease caused by *Fusarium verticillioides* using a loop-mediated isothermal amplification assay (In Chinese). *J. Nanjing Agric. Univ.* 41, 286–292. doi: 10.7685/jnau.201705023
- Zeng, H. C., Ho, H. H., and Zheng, F. C. (2005). *Pythium vexans* causing patch canker of rubber trees on Hainan Island, China. *Mycopathologia* 159, 601–606. doi: 10.1007/s11046-005-5258-6
- Zhu, R., Yang, F., Zhou, B., Li, Y., Lin, N., Yang, Y., et al. (2014). Origin, distribution of *Boehmeria nivea* and its history of cultivation and utilization in China (In Chinese). *Chin. Agric. Sci. Bull.* 30, 258–266.

**Conflict of Interest:** The authors declare that the research was conducted in the absence of any commercial or financial relationships that could be construed as a potential conflict of interest.

**Publisher’s Note:** All claims expressed in this article are solely those of the authors and do not necessarily represent those of their affiliated organizations, or those of the publisher, the editors and the reviewers. Any product that may be evaluated in this article, or claim that may be made by its manufacturer, is not guaranteed or endorsed by the publisher.

Copyright © 2021 Wang, Ji, Yu, Wang, Cheng, Li, Chen, Guo, Xu and Gao. This is an open-access article distributed under the terms of the Creative Commons Attribution License (CC BY). The use, distribution or reproduction in other forums is permitted, provided the original author(s) and the copyright owner(s) are credited and that the original publication in this journal is cited, in accordance with accepted academic practice. No use, distribution or reproduction is permitted which does not comply with these terms.





# Rapid and Sensitive Detection of *Salmonella* spp. Using CRISPR-Cas13a Combined With Recombinase Polymerase Amplification

Bailin An<sup>1,2†</sup>, Hongbin Zhang<sup>3†</sup>, Xuan Su<sup>2</sup>, Yue Guo<sup>4</sup>, Tao Wu<sup>1</sup>, Yiyue Ge<sup>1</sup>, Fengcai Zhu<sup>1</sup> and Lunbiao Cui<sup>1,4\*</sup>

<sup>1</sup> National Health Commission (NHC) Key Laboratory of Enteric Pathogenic Microbiology, Jiangsu Provincial Center for Disease Control and Prevention, Nanjing, China, <sup>2</sup> College of Pharmacy, Nankai University, Tianjin, China, <sup>3</sup> Jiangyin City Center for Disease Control and Prevention, Wuxi, China, <sup>4</sup> School of Public Health, Nanjing Medical University, Nanjing, China

## OPEN ACCESS

### Edited by:

Xuejun Ma,  
Chinese Center for Disease Control  
and Prevention, China

### Reviewed by:

Jesús Navas,  
University of Cantabria, Spain  
Zhiyang Li,  
Nanjing Drum Tower Hospital, China

### \*Correspondence:

Lunbiao Cui  
lbrcui@jscdc.cn

<sup>†</sup> These authors have contributed  
equally to this work

### Specialty section:

This article was submitted to  
Food Microbiology,  
a section of the journal  
Frontiers in Microbiology

Received: 29 June 2021

Accepted: 14 September 2021

Published: 18 October 2021

### Citation:

An B, Zhang H, Su X, Guo Y,  
Wu T, Ge Y, Zhu F and Cui L (2021)  
Rapid and Sensitive Detection of  
*Salmonella* spp. Using  
CRISPR-Cas13a Combined With  
Recombinase Polymerase  
Amplification.  
Front. Microbiol. 12:732426.  
doi: 10.3389/fmicb.2021.732426

*Salmonella* spp. is one of the most common foodborne disease-causing pathogens that can cause severe diseases in very low infectious doses. Rapid and sensitive detecting *Salmonella* spp. is advantageous to the control of its spread. In this study, a conserved short fragment of the *Salmonella invA* gene was selected and used to design primers and specific crRNA (CRISPR RNA) for establishing a one-tube and two-step reaction system for *Salmonella* spp. detection, by combining recombinase polymerase amplification (RPA) with CRISPR-Cas13a (Clustered Regularly Interspaced Short Palindromic Repeats associated protein 13a) cleavage. The established one-tube RPA-Cas13a method can complete the detection within 20 min and the two-step RPA-Cas13a method detection time within 45 min. The designed primers were highly specific to *Salmonella* spp. and had no cross-reaction with the other nine diarrheal bacteria. The one-tube RPA-Cas13a could detect the *Salmonella* genome with the limit of  $10^2$  copies, which was the same as real-time polymerase chain reaction (PCR), but less sensitive than two-step RPA-Cas13a ( $10^0$  copies). The detection results of one-tube or two-step RPA-Cas13a and real-time PCR were highly consistent in clinical samples. One-tube RPA-Cas13a developed in this study provides a simple, rapid, and specific detection method for *Salmonella* spp. While two-step assay was more sensitive and suitable for samples at low abundance.

**Keywords:** *Salmonella*, foodborne disease, RPA, CRISPR-Cas13a, molecular detection

## INTRODUCTION

*Salmonella*, a gram-negative bacillus, is the most common diarrheal pathogenic bacteria and infects millions of people across the world every year, with the most common clinical manifestations being acute gastroenteritis, encephalitis, pericarditis, sepsis, and even death (Hugas and Beloeil, 2014; Ferrari et al., 2019). According to statistics by the World Health Organization, the number of outbreaks of different food-borne intestinal diseases since 2010 has reached 582 million, with nearly 350,000 deaths, including 52,000 *Salmonella* cases (World Health Organization [WHO], 2016)].

In the United States, the Centers for Disease Control and Prevention (CDC) estimated food was one of the main sources of *Salmonella* infection; *Salmonella* caused approximately 1.35 million infections, 26,500 hospitalizations, and 420 deaths every year (CDC, 2020). In the European Union, European Centre for Disease Prevention and Control reported 91,857 *Salmonella* infection cases in humans, and *Salmonella* caused 30.7% of all food-borne outbreaks during 2018 (European Food Safety Authority, & European Centre for Disease Prevention and Control, 2020). In China, the previous study has estimated the incidence of non-typhoid salmonellosis at 626.6 cases per 100,000 people (Yue et al., 2020). Timely screening of *Salmonella* is the key to prevent and control diarrheal disease outbreaks. To date, the detection methods for *Salmonella*, including traditional biochemical culture, immune testing, and molecular biological approaches, are represented by polymerase chain reaction (PCR)/real-time PCR. These methods are time-consuming, or poor in specificity or of low sensitivity, and sometimes require expensive instruments for laboratory setup. Especially, many diarrheal pathogenic bacteria, including *Salmonella*, can cause severe infectious diseases at low infectious doses. More sensitive and specific *Salmonella* detection methods are urgently needed.

Over the past year, researchers have applied the latest recombinase polymerase amplification (RPA)/recombinase aided amplification (RAA) techniques to achieve amplification for *Salmonella*. However, the detection of amplification products by agarose gel electrophoresis showed poor sensitivity, and fluorescent probes for visual detection were expensive. A typical detection of pathogenic *Salmonella* was reported by Zhang et al. (2017) using the real-time fluorescence RAA detection system, but the detection limit was  $10^3$  copies/ $\mu$ L, equivalent to  $\sim 5$  fg plasmid DNA. An optical biosensor reported by Zheng et al. (2020) could detect  $1.8 \times 10^1$  copies/ $\mu$ L but was not useful in POCT (point-of-care testing).

The CRISPR-Cas (Clustered Regularly Interspaced Short Palindromic Repeats-CRISPR associated protein) system is a sophisticated adaptive immune system, and the different CRISPR-Cas nucleases display specific cleavage activity when target-specific crRNA recognizes the DNA target (Bhaya et al., 2011; Jackson et al., 2014; Kirchner and Schneider, 2015). In recent years, researchers have found that the cleavage activity of CRISPR-Cas nucleases could be used not only as a programmable tool for gene editing but also for *in vitro* nucleic acid detection (Arslan et al., 2014; Zhou et al., 2020). In this study, we established a one-tube and a two-step reaction system for *Salmonella* spp. detection by combining RPA with CRISPR-Cas13a cleavage, which provided a sensitive and convenient molecular detection method for the early diagnosis of diarrheal diseases of *Salmonella* infection.

## MATERIALS AND METHODS

### Cas13a Protein Expression and Purification

Cas13a was purified as referred to in previous studies (East-Seletsky et al., 2016, 2017; Su et al., 2020). Briefly, the Cas13a

gene in plasmid pC019-LwCas13a from *Leptotrichia wadei* (Addgene, United States) was subcloned into the psmarti vector (*xhoI* restriction site), and the correct plasmid was transformed into BL21(DE3) (General Biosystem, China). The expression of the target protein was induced at different temperatures (15 and 37°C) and different concentrations of IPTG (0.2 and 1.0 mM) (Amresco, United States). The Cas13a protein was purified by Ni-NTA (Smart-Lifesciences, China) using the  $6 \times$  His Tag antibody and horseradish peroxidase conjugate (Invitrogen, United States). After the addition of SUMO Protease (General Biosystem, China) to remove the fusion SUMO label, and the purified target protein was dialyzed into protein buffer [50 mM Tris, pH 7.5, 600 mM NaCl, 5% (vol/vol) glycerol, and 2 mM DTT].

### Strains, Clinical Samples, and Nucleic Acid Extraction

*Salmonella* and other diarrheal pathogenic bacteria (*Staphylococcus aureus*, *Listeria monocytogenes*, *Enterococcus faecalis*, *Shigella flexneri*, *Vibrio parahaemolyticus*, *Escherichia coli* O157, *Yersinia enterocolitica*, *Campylobacter jejuni*, *Vibrio vulnificus*) were provided by Jiangsu Provincial Center for Disease Control and Prevention. A total of 84 clinical stool samples that were selected for clinical validation of the method were collected from different hospitals in Jiangsu Province in 2019. The nucleic acid was extracted by EX-DNA Bacterial Genomic Extraction Kit (Tianlong, China) on a fully automatic nucleic acid extractor (Tianlong, China).

### Preparation of Primers, Probes, and crRNA

*Salmonella*-specific *invA* gene was retrieved from GenBank, and the conservative sequence region was selected to design RPA amplification primers using Primer 5 software, and Primer-BLAST software was used to verify the specificity of the primer sequence. The designed primers, probes, and oligonucleotides were synthesized by Sangon Biotech (Shanghai, China). The oligonucleotides containing T7 promoter, repeat, and spacer sequences were annealed with a T7 primer. Then, the crRNA was synthesized by incubating at 42°C for 2 h with T7 RNA polymerase (TaKaRa, China). The synthesized crRNA was digested with DNase I (TaKaRa, China) at 37°C for 1 h followed by purification with RNA rapid concentration and purification kit (Sangon Biotech, China) according to the manufacturer's protocol. The concentration of crRNA was quantified using Qubit 2.0 (Invitrogen, United States). All nucleic acid sequences used in this study are shown in Table 1.

### Collateral Cutting Capacity of CRISPR-Cas13a

The amplicon of the RPA reaction was used as the template for transcription *in vitro* with T7 RNA polymerase, and the transcription product was purified to obtain the *Salmonella* target RNA. Then, the target RNAs were diluted gradiently ( $10^0$ – $10^5$  pM). The synthesized oligonucleotide *Salmonella*-RPA-R was

**TABLE 1** | RPA primers, crRNA, and RNA reporter probe sequences.

Name	Sequences(5'-3')
<i>Salmonella</i> RPA-F	TGTTGTCTCTCTATTGTCACCGTGGTCCAG
<i>Salmonella</i> RPA-R	TAATACGACTCACTATAGGGTAC CGGGCATACCATCCAGAGAAATCGGGCCGC
<i>Salmonella</i> crRNA	GACACGTTCTGAACCTTTGGTAA TAACGGTTTTAGTCCCTTCGTTTTGGGGTA GTCTAAATCCCTAT AGTGAGTCGTATTA
RNA probe	FAM-TtUrUrUrUrC-BHQ1

used as a non-target control (500 ng/μL). Verification of CRISPR-Cas13a cutting activity was completed as follows: 5 × reaction buffer 5 μL (final concentration 20 mM HEPES, 60 mM NaCl, 6 mM MgCl<sub>2</sub>, pH 6.8), 25 mM NTP mix 1 μL (ATP, GTP, CTP, UTP, Bio Lab, China), Recombinant RNase Inhibitor (TaKaRa, China) 0.5 μL, 1.2 μM crRNA 0.6 μL, 10 μM RNA-probe 0.5 μL, 1 μM Cas13a 1 μL, or 10<sup>3</sup> pM target RNA or non-target control 2 μL, adding RNase-free ddH<sub>2</sub>O to 25 μL. The reaction was conducted at 39°C for 30 min, and RNase A was used as the positive control.

## Two-Step RPA-Cas13a

In the two-step RPA-Cas13a assay, basic RPA reactions were first conducted according to the instructions of the TwistAmp Basic Kit (Twist Dx, Cambridge, United Kingdom). Each RPA reaction was carried out in a 50 μL reaction volume containing Primer Free Rehydration buffer 29.5 μL, 0.24–0.96 μM forward and reverse primers each 0.5 μL, target DNA template 2 μL, and RNase-free ddH<sub>2</sub>O 15 μL. The reaction mixes were vortexed and spun briefly, and then 280 mM magnesium acetate (MgOAc) 2.5 μL was added and mixed well to start a reaction in fluorescence detector F1620 (Qitian, China) at 37, 39, and 41°C for 20 min. Then, a 25 μL CRISPR-Cas13a reaction system was performed with 5 × reaction buffer 5 μL, 25 mM NTP mix 1 μL, Recombinant RNase Inhibitor 0.5 μL, 1.2 μM *Salmonella*-crRNA 0.6 μL, 10 μM RNA-probe 0.5 μL, T7 RNA Polymerase 0.3 μL, 1 μM Cas13a 1 μL, and added RNase-free ddH<sub>2</sub>O to 23 μL, and RPA products 2 μL. The fluorescent signals were collected at 39°C for 30 min in fluorescence detector F1620.

## One-Tube RPA-Cas13a

The one-tube RPA-Cas13a assay combined RPA with CRISPR-Cas13a in a one-tube reaction system. Briefly, the 50 μL one-tube reaction system consisted of Primer Free Rehydration buffer 29.5 μL, 25 mM NTP mix 4 μL, Recombinant RNase Inhibitor 4 μL, T7 RNA Polymerase 1 μL, 0.24–0.96 μM primers each 0.5 μL, 1.2 μM crRNA 1 μL, 10 μM RNA-probe 1 μL, 1 μM Cas13a 2 μL, target DNA template 2 μL, and RNase-free ddH<sub>2</sub>O 1 μL. The reaction mixes were vortexed and spun briefly, and then 280 mM MgOAc 2.5 μL was added to the tube cap and was centrifuged into the reaction solution. Fluorescent signals were collected at 37, 39, and 41°C for 2 h in fluorescence detector F1620.

## Sensitivity and Specificity of One-Tube and Two-Step RPA-Cas13a

To evaluate the minimum detection limit, serial dsDNA standards were prepared as follows: using the extracted nucleic acid of *Salmonella* as a template, a 50 μL LA Taq PCR (TaKaRa, China) containing LA Taq 0.5 μL, 2.5 μM dNTP 4 μL, 10 × buffer 5 μL, 10 μM forward/reverse primer each 1 μL, and RNase-free ddH<sub>2</sub>O 37.5 μL was performed. The PCR amplification product was purified by High Pure PCR Product Purification Kit (Roche, CH). The dsDNA quantification was performed in a Qubit digital fluorimeter using the Qubit dsDNA BR Assay (Invitrogen, Waltham, United States). The dsDNA copy number was then determined using the following formula:  $\{[6.02 \times 10^{14} \times \text{dsDNA concentration (ng/μL)} \times 10^{-9}]\} / [\text{DNA in length} \times 660]$ . The gradiently diluted dsDNA standards (10<sup>7</sup>–10<sup>1</sup> copies/μL) were detected by the one-tube and two-step RPA-Cas13a. We also chose real-time PCR (Hein et al., 2006) (TaKaRa, China) as the reference test. The specificity of the one-tube and two-step RPA-Cas13a was tested by using nucleic acid extracted from diarrheal pathogenic bacteria strains: *Salmonella*, *S. aureus*, *L. monocytogenes*, *E. faecalis*, *S. flexneri*, *V. parahemolyticus*, *E. coli* O157, *Y. enterocolitica*, *C. jejuni*, and *V. vulnificus*.

## Real-Time Polymerase Chain Reaction

Real-time PCR was performed on the LightCycler 2.0 instrument in which premix Ex Taq<sup>TM</sup> (Takara, China) was used (Hein et al., 2006). The reaction was performed as follows: 95°C for 30 s, followed by 40 cycles of 95°C for 5 s and then 60°C for 20 s.

## Consistency Comparison Using Real-Time Polymerase Chain Reaction

Genomic DNAs from 84 clinical stool samples were selected for a clinical comparison experiment. All samples were tested with the two-step, one-tube RPA-Cas13a, and real-time PCR assay (Hein et al., 2006). The consistency of the three methods above was compared using SPSS 24.0 software. κ-tests were used for consistency analysis.

## RESULTS

### Collateral Cutting Capacity of CRISPR-Cas13a

A significant fluorescent signal in the reactions of the positive control within was verified with RNase A. Compared with the detection of Cas13a for target RNA and non-target RNA control, the results showed that Cas13a could achieve specific detection for target RNA of *Salmonella* in the presence of its corresponding crRNA. Furthermore, there was no detection signal generated for Cas12a compared to Cas13a. The detection signal of CRISPR-Cas13a for 10<sup>3</sup> pM was almost identical to that of the positive control (Figure 1). The results of different dilutions for RNA standards showed that the minimum test limit was 10 pM (Figure 2).

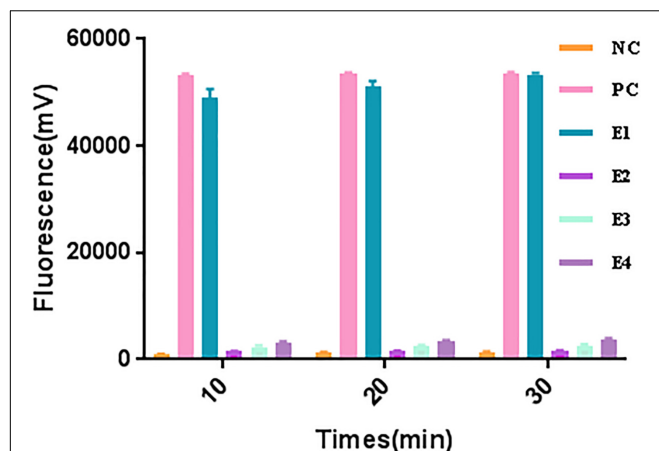


**FIGURE 1 |** The collateral cutting activity of CRISPR-Cas13a. NC, negative control (RNase-free ddH<sub>2</sub>O); PC, positive control (RNase A); E1, Cas13a with 10<sup>3</sup> pM target RNA; E2, Cas13a with 10<sup>3</sup> pM non-target control; E3, Cas13a with 10<sup>3</sup> pM target RNA; E4, Cas13a with non-crRNA.

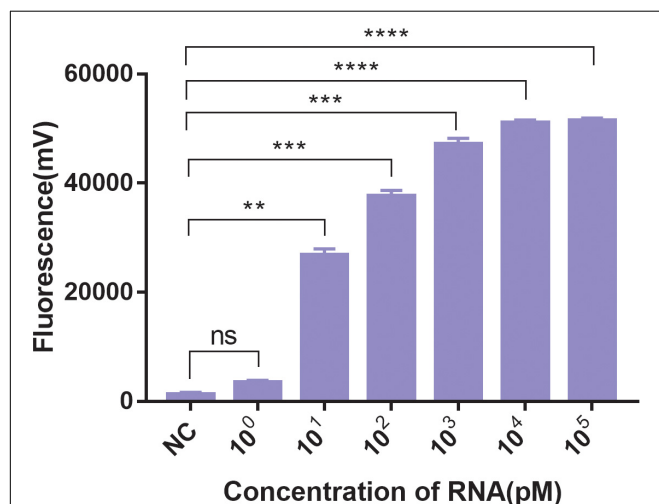


**FIGURE 2 |** The sensitivity of CRISPR-Cas13a. 10<sup>0</sup>–10<sup>5</sup> pM were the concentrations of RNA standards. NC, negative control (RNase-free ddH<sub>2</sub>O). Unpaired two-tailed *t*-test was used to analyze the difference from NC. \*\**p* < 0.01; \*\*\**p* < 0.001; \*\*\*\**p* < 0.0001. ns, not significant.

## Optimization of Two-Step RPA-Cas13a Detection System

We first tested the best RPA amplification temperature using 0.48  $\mu$ M primer concentration. The results showed the highest fluorescent signals were obtained at 39°C in all three Cas13a detecting time points (Figure 3A). Therefore, 39°C was selected as the best RPA amplification temperature. Then, the best primer concentrations were explored at 39°C. The optimal primer concentration of 0.48  $\mu$ M was found (Figure 3B). Therefore, we chose 0.48  $\mu$ M and 39°C as the best RPA primer concentration and amplification temperature.

## Optimization of One-Tube RPA-Cas13a Detection System

We first tested the different temperature (37, 39, 41°C) in a one-tube RPA-Cas13a detection system and found that 39°C had the highest fluorescent signals. The detection signal grew stronger from 10 to 90 min and reached its peak at 90 min, whereas the negative control had no visible detection signal (Figure 4A). We then explored the optimal primer concentration under 39°C and found the highest fluorescent signals were obtained at 0.48  $\mu$ M primer concentrations. Therefore, the optimized conditions of one-tube RPA-Cas13a were 39°C with 0.48  $\mu$ M primer concentration (Figure 4B).

## Sensitivity and Specificity of One-Tube and Two-Step RPA-Cas13a

As shown in Figure 5A, the limit of detection of one-tube RPA-Cas13a for *Salmonella* was 10<sup>2</sup> copies/ $\mu$ L, which showed the same sensitivity to real-time PCR (10<sup>2</sup> copies/ $\mu$ L, Figure 6) and slightly lower than that of two-step RPA-Cas13a (10<sup>0</sup> copies/ $\mu$ L, Figure 5B). The whole detection time of one-tube RPA-Cas13a for 10<sup>2</sup> copies/ $\mu$ L was only 20 min (Figure 5A), which was shorter than those for two-step RPA-Cas13a (RPA: 20 min, transfer time: 5 min, and CRISPR-Cas13a: 20 min, Figure 5B) and real-time PCR (60 min or much longer, Figure 6). For specificity assessment, whether one-tube RPA-Cas13a at 60 min (Figure 7A) or two-step RPA-Cas13a at 30 min (Figure 7B), only the *Salmonella* showed detection signals among the 10 common diarrheal bacteria, and no cross-reactions were found.

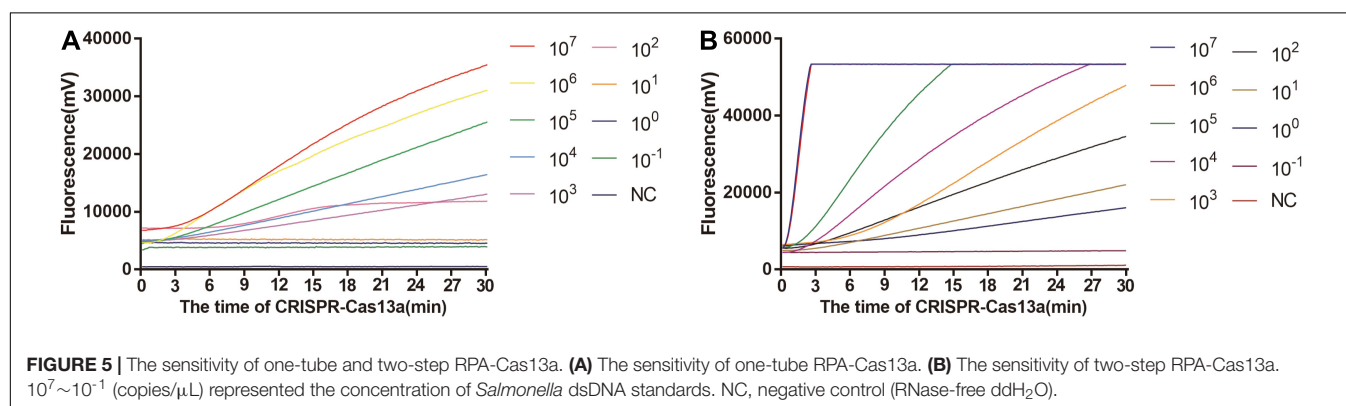
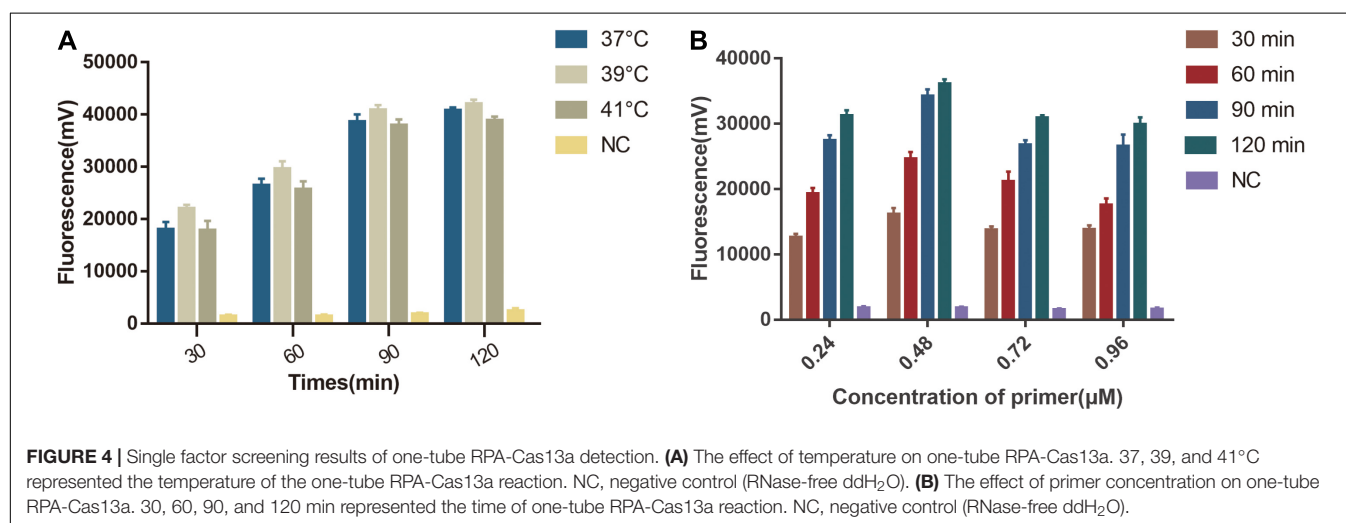
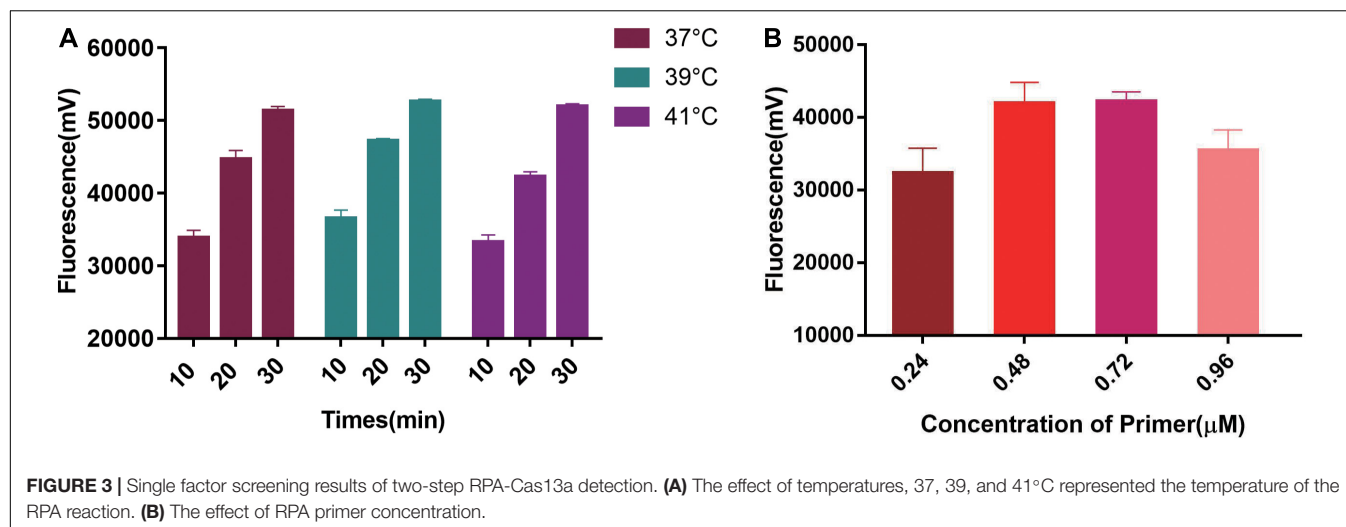
## Consistency Comparison Using Real-Time Polymerase Chain Reaction

For evaluating the applicability of developed one-tube and two-step RPA-Cas13a for *Salmonella* in clinical stool samples, a total of 84 clinical stool samples from different hospitals were selected and tested by real-time PCR, two-step RPA-Cas13a, and one-tube RPA-Cas13a. Sixteen samples were detected positive for *Salmonella* by real-time PCR. Besides those 16 samples, three additional samples were judged as positive by two-step RPA-Cas13a in which one was also detected positive by one-tube RPA-Cas13a. However, the signal intensity was significantly lower than that of the other 16 positive samples but significantly higher than that of the negative control sample. At the same time, those three samples were also identified by Sanger sequencing technology and determined to be positive for *Salmonella*. The two-step RPA-Cas13a detection results are in good consistency with real-time PCR ( $\kappa$  = 0.892), the one-tube RPA-Cas13a detection results are also in good consistency with real-time PCR ( $\kappa$  = 0.962), and the statistical results are shown in Table 2.

## DISCUSSION

Currently, the isothermal amplification of nucleic acid technology has been used for the rapid pathogen detection of infectious diseases because of its high specificity, efficiency, and simplicity and plays an increasingly important role in





promoting field detection and control of pathogen diseases. But the isothermal amplification of nucleic acid technology has its disadvantages, such as the LAMP (loop-mediated isothermal amplification) having an intricate primer design and non-specific reactions. Compared with other isothermal amplification technologies, RPA/RAA can be performed near

ambient temperature (37–42°C) and has higher amplification efficiencies in recent years. The RPA process relies on three core enzymes, the recombinant enzymes uvsX and uvsY, SSB gp32 (Single-stranded DNA-binding protein), and Bsu DNA polymerase helping target regions of the template that can exponentially amplify within 20 min (Ahmed et al., 2015;



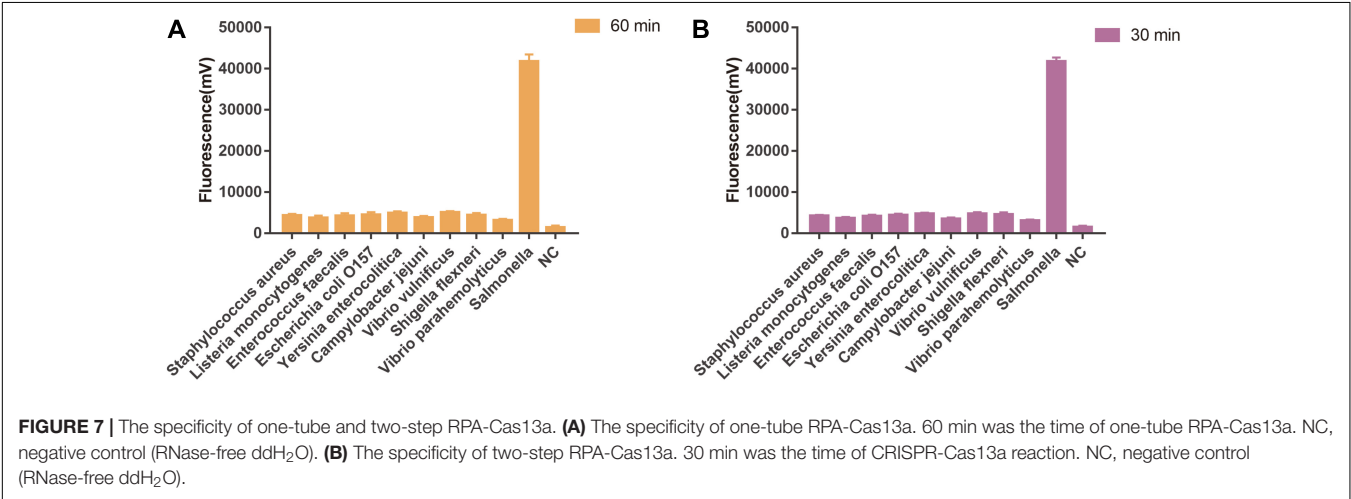
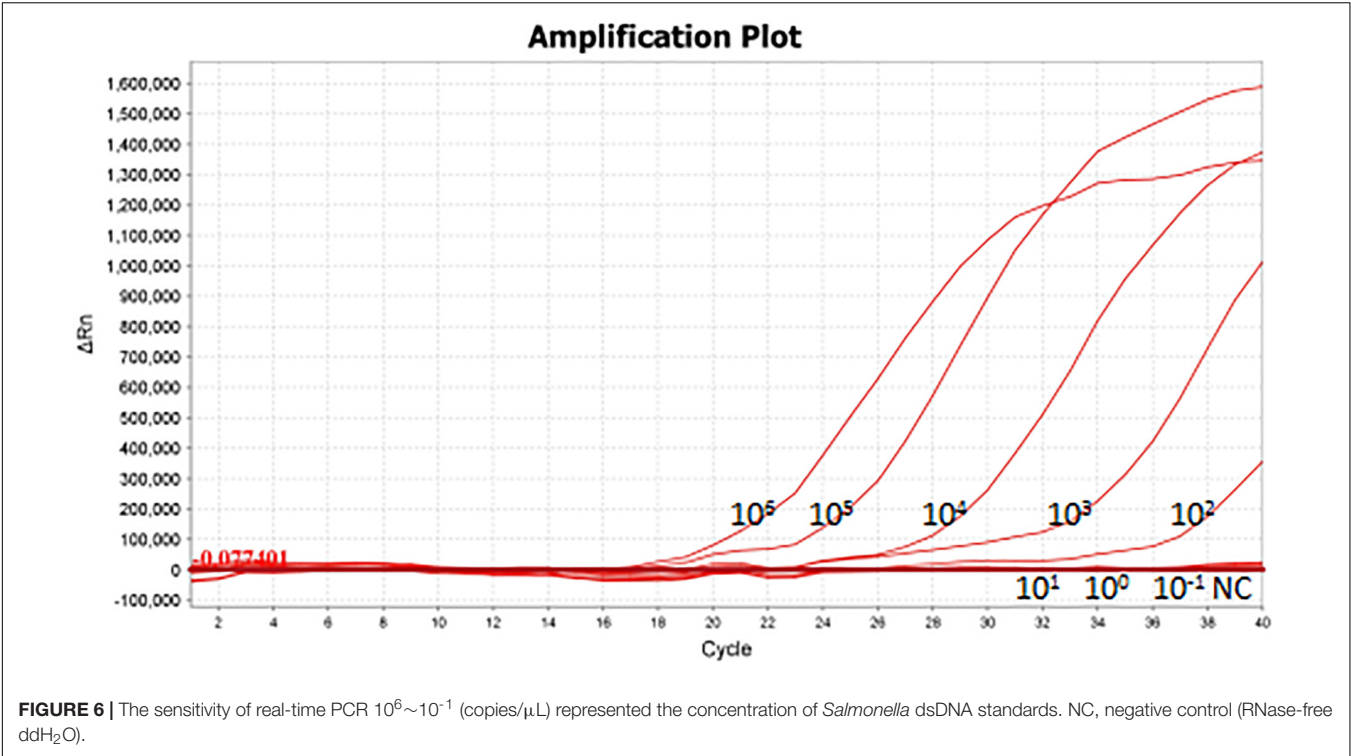


TABLE 2 | Clinical samples consistency comparison using three detection methods.

		Real-time PCR result		Total	Sensitivity (%) (95% CI)	Specificity (%) (95% CI)	$\kappa$
		+	–				
One-tube RPA-Cas13a	+	16	1	17	100	98.50	0.962
	–	0	67	67			
	Total	16	68	84			
Two-step RPA-Cas13a	+	16	3	19	100	95.60	0.892
	–	0	65	65			
	Total	16	68	84			

+, Positive; –, negative; CI, confidence interval. Data determined by SPSS 24.0 software. One-tube RPA-Cas13a–positive result, 17; one-tube RPA-Cas13a–negative result, 67; two-tube RPA-Cas13a–positive result, 19; two-tube RPA-Cas13a–negative result, 65; real-time PCR–positive result, 16; real-time PCR–negative result, 68.

Ma et al., 2019). Most importantly, the RPA/RAA has a fairly simple primer design. Commonly, the detection platforms most used for post-RPA detection are fluorescence RPA/RAA, gel electrophoresis, or LFD (lateral flow dipstick), but these methods require an expensive design for the probe, low sensitivity, or lack of specificity. It is necessary to establish a more sensitive and specific detection method that can be combined with RPA.

In recent years, studies have found that the collateral cutting activity of CRISPR-Cas13a is activated by a specific crRNA that targets a specific single-stranded RNA sequence, and collateral cutting activity can then cleave nearby non-specific RNAs (Knott et al., 2017; Zuo et al., 2017). Based on this principle, non-specific RNA reporting probes can add to the reaction system to achieve specific detection of target molecules (Abudayyeh et al., 2016; Gootenberg et al., 2017). The feature of collateral cutting activity has been used in the field of nucleic acid detection (Shen et al., 2020), among which the most representative is the SHERLOCK (Specific High-sensitivity Enzymatic Reporter UnLOCKing) by combining RPA with CRISPR-Cas13a (Myhrvold et al., 2018). This method provides a new direction for developing nucleic acid detection technology for pathogenic microbes, with the advantages of simplicity, rapidity, sensitivity, and specificity. The current detection based on SHERLOCK is mainly a two-step method. The one-tube method has been reported, but its sensitivity is insufficient.

The T7 promoter sequence is introduced into the RPA amplification primer, and the RPA amplification products are transcribed into a large amount of RNA by T7 RNA polymerase, which improves the sensitivity of detecting *Salmonella* targets. The results showed that two-step RPA-Cas13a is more sensitive than real-time PCR. Its detection limit for *Salmonella* can reach  $10^0$  copies/ $\mu$ L. One-tube RPA-Cas13a could achieve the same detection sensitivity as real-time PCR with  $10^2$  copies/ $\mu$ L. In addition, the crRNA design of CRISPR-Cas13a is relatively simple, requiring only 24 bases. The target-specific crRNA would further increase the detection specificity. The specificity results showed that there is no cross-reaction between the RPA-Cas13a of *Salmonella* and the other nine diarrheal pathogenic bacteria. Compared with the fluorescence probes used in RPA/RAA assay, the CRISPR non-specific detection probe is pretty easy to design in the present study and cost saving. In addition, both RPA and CRISPR detection can be conducted on a simple constant temperature equipment, which greatly reduces the requirements for equipment and personnel. The one-tube RPA-Cas13a detection process can detect *Salmonella* within 20 min, while two-step RPA-Cas13a costs 45 min, which was shorter compared with LAMP and real-time PCR method. The influence of clinical samples on RPA-Cas13a detection performance was verified: the *Salmonella* detection rate of the two-step or one-tube RPA-Cas13a detection method was highly consistent as that of real-time PCR and could even detect clinical stool samples at low infectious doses, whereas three samples with low doses cannot be detected by real-time PCR. Of the three low infectious dose samples, one can detect by one-step assay, and three can detect by two-step assay. Although the two-step RPA-Cas13a assay is more

sensitive, it is also more easily contaminated. Some intervention measures, such as using oily non-interfering substances to seal the liquid surface, the use of specific reagent tubes, and so on, can be used to reduce or avoid the contamination, which would help this assay to be used in routine clinical trials. We recommend one-tube RPA-Cas13a assay as the rapid POCT method for *Salmonella* in rural hospitals with resource-poor settings, whereas two-step RPA-Cas13a for low abundance detection.

## CONCLUSION

In this study, a novel molecular diagnostic method based on CRISPR-Cas13a combined with RPA was successfully demonstrated for rapid, sensitive, and specific detection of *Salmonella* and provides a new approach for the rapid screening of clinical samples in hospitals.

## DATA AVAILABILITY STATEMENT

The raw data supporting the conclusions of this article will be made available by the authors, without undue reservation.

## ETHICS STATEMENT

The studies involving human participants were reviewed and approved by the Jiangsu Provincial Center for Disease Control and Prevention. The ethics committee waived the requirement of written informed consent for participation.

## AUTHOR CONTRIBUTIONS

BA: methodology establishment, data sorting, and analysis, visualization, writing—original draft. HZ: methodology establishment, data sorting, writing—review and editing, and software. XS: methodology establishment, data sorting, and analysis. YuG and TW: methodology establishment. YiG: funding acquisition and writing—review and editing. FZ: project administration and supervision. LC: conceptualization, funding acquisition, project administration, validation, and writing—review and editing. All authors contributed to the article and approved the submitted version.

## FUNDING

The study was supported in part by the Key Research and Development Project of Jiangsu Province (BE2019761), the Natural Science Foundation of Jiangsu Province (BK20211373), the Jiangsu Provincial Key Medical Discipline of Epidemiology (ZDXKA2016008), and “333” Projects of Jiangsu Province (BRA2017552).

## REFERENCES

- Abudayyeh, O. O., Gootenberg, J. S., Konermann, S., Joung, J., Slaymaker, I. M., Cox, D., et al. (2016). C2c2 is a single-component programmable RNA-guided RNA-targeting CRISPR effector. *Science* 353:aaf5573. doi: 10.1126/science.aaf5573
- Ahmed, A., Pranav, P., Oumar, F., Sasikanya, T., Doris, H., Ponpan, M., et al. (2015). Recombinase polymerase amplification assay for rapid diagnostics of dengue infection. *PLoS One* 10:e0129682. doi: 10.1371/journal.pone.0129682
- Arslan, Z., Hermanns, V., Wurm, R., Wagner, R., and Pul, U. (2014). Detection and characterization of spacer integration intermediates in type I-E CRISPR-Cas system. *Nucleic Acids Res.* 42, 7884–7893. doi: 10.1093/nar/gku510
- Bhaya, D., Davison, M., and Barrangou, R. (2011). CRISPR-Cas systems in bacteria and archaea: versatile small RNAs for adaptive defense and regulation. *Annu. Rev. Genet.* 45, 273–297. doi: 10.1146/annurev-genet-110410-132430
- CDC (2020). *Centers for Disease Control and Prevention Salmonella*. Available online at: <https://www.cdc.gov/Salmonella/index.html> [Accessed Nov 3, 2020].
- East-Seletsky, A., O'Connell, M. R., Burstein, D., Knott, G. J., and Doudna, J. A. (2017). RNA targeting by functionally orthogonal type VI-A CRISPR-Cas enzymes. *Mol. Cell* 66, 373–383.e3.
- East-Seletsky, A., O'Connell, M. R., Knight, S. C., Burstein, D., Cate, J., Tjian, R., et al. (2016). Two distinct RNase activities of CRISPR-C2c2 enable guide-RNA processing and RNA detection. *Nature* 538, 270–273. doi: 10.1038/nature19802
- European Food Safety Authority, & European Centre for Disease Prevention and Control (2020). The European Union Summary Report on Antimicrobial Resistance in zoonotic and indicator bacteria from humans, animals and food in 2017/2018. *EFSA J.* 18:e06007. doi: 10.2903/j.efsa.2020.6007
- Ferrari, R. G., Rosario, D., Neto, A. C., Borges, S., and Junior, C. (2019). Worldwide epidemiology of salmonella serovars in animal-based foods: a meta-analysis. *Appl. Environ. Microbiol.* 85:e591. doi: 10.1128/AEM.00591-19
- Gootenberg, J. S., Abudayyeh, O. O., Lee, J. W., Essletzbichler, P., Dy, A. J., Joung, J., et al. (2017). Nucleic acid detection with CRISPR-Cas13a/C2c2. *Science* 356, 438–442. doi: 10.1126/science.aam9321
- Hein, I., Flekna, G., Krassnig, M., and Wagner, M. (2006). Real-time PCR for the detection of *Salmonella* spp. in food: an alternative approach to a conventional PCR system suggested by the FOOD-PCR project. *J. Microbiol. Methods* 66, 538–547. doi: 10.1016/j.mimet.2006.02.008
- Hugas, M., and Beloeil, P. (2014). Controlling *Salmonella* along the food chain in the European Union – progress over the last ten years. *Euro Surveill.* 19:20804. doi: 10.2807/1560-7917.es2014.19.19.20804
- Jackson, R. N., Wiedenheft, B., Oost, J., and Westra, E. R. (2014). Unravelling the structural and mechanistic basis of CRISPR-Cas systems. *Nat. Rev. Microbiol.* 12, 479–492. doi: 10.1038/nrmicro3279
- Kirchner, M., and Schneider, S. (2015). CRISPR-Cas: from the bacterial adaptive immune system to a versatile tool for genome engineering. *Angew. Chem. Int. Edn.* 54, 13508–13514. doi: 10.1002/anie.201504741
- Knott, G. J., East-Seletsky, A., Cofsky, J. C., Holton, J. M., Charles, E., O'Connell, M. R., et al. (2017). Guide-bound structures of an RNA-targeting A-cleaving CRISPR-Cas13a enzyme. *Nat. Struct. Mol. Biol.* 24, 825–833. doi: 10.1038/nsmb.3466
- Ma, L., Zeng, F., Huang, B., Zhu, Y., and Guo, P. (2019). Point-of-care diagnostic assay for rapid detection of porcine deltacoronavirus using the recombinase polymerase amplification method. *Transbound. Emerg. Dis.* 66, 1324–1331. doi: 10.1111/tbed.13155
- Myhrvold, C., Freije, C. A., Gootenberg, J. S., Abudayyeh, O. O., Metsky, H. C., Durbin, A. F., et al. (2018). Field-deployable viral diagnostics using CRISPR-Cas13. *Science* 360, 444–448. doi: 10.1126/science.aas8836
- Shen, J., Zhou, X., Shan, Y., Yue, H., Huang, R., Hu, J., et al. (2020). Sensitive detection of a bacterial pathogen using allosteric probe-initiated catalysis and CRISPR-Cas13a amplification reaction. *Nat. Commun.* 11:267. doi: 10.1038/s41467-019-14135-9
- Su, X., Ge, Y., Zhang, Q., Lin, Z., Ehsan, M., Xiao, X., et al. (2020). Rapid detection of *Staphylococcus aureus* by CRISPR-Cas13a combined with recombinase aided amplification(RAA). *J. Pathog. Biol.* 159, 11–16. doi: 10.13350/j.cjpb.200302
- World Health Organization [WHO] (2016). *WHO Estimates of the Global Burden of Foodborne Diseases: Foodborne Disease Burden Epidemiology Reference Group 2007–2015*. Available online at: [https://apps.who.int/bitstream/10665/199350/1/9789241565165\\_eng.pdf](https://apps.who.int/bitstream/10665/199350/1/9789241565165_eng.pdf) [Accessed March 1, 2016].
- Yue, M., Song, H., and Bai, L. (2020). Call for special issue papers: food safety in china: current practices and future needs. *Foodborne Pathog. Dis.* 17:529. doi: 10.1089/fpd.2020.29013.cfp5
- Zhang, X., Guo, L., Ma, R., Cong, L., Wu, Z., Wei, Y., et al. (2017). Rapid detection of *Salmonella* with recombinase aided amplification. *J. Microbiol. Methods* 139, 202–204. doi: 10.1016/j.mimet.2017.06.011
- Zheng, L., Cai, G., Qi, W., Wang, S., and Lin, J. (2020). Optical biosensor for rapid detection of *salmonella typhimurium* based on porous gold@platinum nanocatalysts and a 3D fluidic chip. *ACS Sens.* 5, 65–72. doi: 10.1021/acssensors.9b01472
- Zhou, J., Yin, L., Dong, Y., Peng, L., Liu, G., Man, S., et al. (2020). CRISPR-Cas13a based bacterial detection platform: sensing pathogen *Staphylococcus aureus* in food samples. *Anal. Chim. Acta* 1127, 225–233. doi: 10.1016/j.aca.2020.06.041
- Zuo, X., Fan, C., and Chen, H. Y. (2017). Biosensing: CRISPR-powered diagnostics. *Nat. Biomed. Eng.* 1:0091. doi: 10.1038/s41551-017-0091

**Conflict of Interest:** The authors declare that the research was conducted in the absence of any commercial or financial relationships that could be construed as a potential conflict of interest.

**Publisher's Note:** All claims expressed in this article are solely those of the authors and do not necessarily represent those of their affiliated organizations, or those of the publisher, the editors and the reviewers. Any product that may be evaluated in this article, or claim that may be made by its manufacturer, is not guaranteed or endorsed by the publisher.

Copyright © 2021 An, Zhang, Su, Guo, Wu, Ge, Zhu and Cui. This is an open-access article distributed under the terms of the Creative Commons Attribution License (CC BY). The use, distribution or reproduction in other forums is permitted, provided the original author(s) and the copyright owner(s) are credited and that the original publication in this journal is cited, in accordance with accepted academic practice. No use, distribution or reproduction is permitted which does not comply with these terms.



# Rapid and Sensitive Detection of *Vibrio vulnificus* Using CRISPR/Cas12a Combined With a Recombinase-Aided Amplification Assay

Xingxing Xiao<sup>†</sup>, Ziqin Lin<sup>†</sup>, Xianhui Huang, Jinfang Lu, Yan Zhou, Laibao Zheng\* and Yongliang Lou\*

## OPEN ACCESS

### Edited by:

Xuejun Ma,  
Chinese Center For Disease Control  
and Prevention, China

### Reviewed by:

Puey Ounjai,  
Mahidol University, Thailand  
Aly Farag El Sheikh,  
Jiangxi Agricultural University, China

### \*Correspondence:

Laibao Zheng  
zhenglaibao@wmu.edu.cn  
Yongliang Lou  
lyl@wmu.edu.cn

<sup>†</sup> These authors have contributed  
equally to this work

### Specialty section:

This article was submitted to  
Food Microbiology,  
a section of the journal  
Frontiers in Microbiology

**Received:** 30 August 2021

**Accepted:** 04 October 2021

**Published:** 21 October 2021

### Citation:

Xiao X, Lin Z, Huang X, Lu J,  
Zhou Y, Zheng L and Lou Y (2021)  
Rapid and Sensitive Detection  
of *Vibrio vulnificus* Using  
CRISPR/Cas12a Combined With  
a Recombinase-Aided Amplification  
Assay. *Front. Microbiol.* 12:767315.  
doi: 10.3389/fmicb.2021.767315

Wenzhou Key Laboratory of Sanitary Microbiology, Key Laboratory of Laboratory Medicine, Ministry of Education, School of Laboratory Medicine and Life Science, Wenzhou Medical University, Wenzhou, China

*Vibrio vulnificus* is an important zoonotic and aquatic pathogen and can cause vibriosis in humans and aquatic animals (especially farmed fish and shrimp species). Rapid and sensitive detection methods for *V. vulnificus* are still required to diagnose human vibriosis early and reduce aquaculture losses. Herein, we developed a rapid and sensitive diagnostic method comprising a recombinase-aided amplification (RAA) assay and the CRISPR/Cas12a system (named RAA-CRISPR/Cas12a) to detect *V. vulnificus*. The RAA-CRISPR/Cas12a method allows rapid and sensitive detection of *V. vulnificus* in 40 min without a sophisticated instrument, and the limit of detection is two copies of *V. vulnificus* genomic DNA per reaction. Meanwhile, the method shows satisfactory specificity toward non-target bacteria and high accuracy in the spiked blood, stool, and shrimp samples. Therefore, our proposed rapid and sensitive *V. vulnificus* detection method, RAA-CRISPR/Cas12a, has great potential for early diagnosis of human vibriosis and on-site *V. vulnificus* detection in aquaculture and food safety control.

**Keywords:** *Vibrio vulnificus*, recombinase-aided amplification assay, CRISPR/Cas12a, early diagnosis, on-site detection

## INTRODUCTION

*Vibrio vulnificus*, a zoonotic and aquatic pathogen found worldwide, causes vibriosis in aquatic animals and humans (Oliver, 2015; Baker-Austin and Oliver, 2018), which can bring heavy economic losses to aquaculture and seriously affect the personal safety of fishermen and consumers, respectively. The fatality rate of human vibriosis caused by foodborne *V. vulnificus* infection is as high as 50%, while it is about 25% if caused by wound infection (Jones and Oliver, 2009). Clinical studies have found that timely treatment after the onset of vibriosis will significantly reduce the mortality of patients, from 100% after 72 h to 33% after 24 h (Klontz, 1988; Heng et al., 2017).



However, the key to timely treatment is to detect *V. vulnificus* rapidly and sensitively. Furthermore, to detect *V. vulnificus* in outdoors and resource-poor areas, rapid method without a sophisticated instrument is favored by inspectors (Choi et al., 2017). Therefore, it is important to develop a rapid, sensitive, and unsophisticated method for detection of *V. vulnificus* to better control its spread and permit the early diagnosis of human vibriosis.

The traditional methods for detection of *V. vulnificus* are laborious, time-consuming, and even false positive (O'Hara et al., 2003; Hartnell et al., 2019), which is obviously not suitable for early diagnosis and on-site detection; thus, they are gradually being replaced by simpler and faster nucleic acid amplification technology (NAT) comprising thermocycler-dependent NAT and thermocycler-independent (isothermal) NAT (Asiello and Baeumner, 2011; El Sheikha et al., 2018). In thermocycler-dependent NAT, quantitative PCR (qPCR) assay has been widely used in *V. vulnificus* detection (Campbell and Wright, 2003; Panicker and Bej, 2005). However, qPCR depends on an expensive real-time PCR instrument and well-trained operators, limiting its usage in on-site detection and resource-poor areas. With the development of NAT, isothermal NAT (iNAT)—which does not require sophisticated equipment, is time-saving, and can be carried out under constant temperature conditions—has emerged, such as recombinase-aided amplification (RAA) (Piepenburg et al., 2006; Qi et al., 2019), loop-mediated isothermal amplification (Han and Ge, 2010) and strand displacement amplification (Lu et al., 2017). Based on the advantages mentioned above, iNAT is a very promising method for on-site detection and early diagnosis, especially RAA, which can even be completed within 10 min using body heat (Wang et al., 2017b). Frustratingly, RAA also has some flaws, such as the lower sensitivity compared with qPCR (Moore and Jaykus, 2017; Gallardo et al., 2019) and the relatively complex terminal test involving purification and gel electrophoresis (Daher et al., 2015; Mayboroda et al., 2018).

Recently, a new detection platform based on clustered regularly interspaced short palindromic repeats (CRISPR) and CRISPR-related protein (Cas) called the CRISPR/Cas system has strongly promoted the development of nucleic acid detection technology (Gootenberg et al., 2017; Chen et al., 2018; Li et al., 2018). This platform relies on the collateral cleavage capability of CRISPR RNA (crRNA)-guided Cas12a or Cas13 to ssDNA or ssRNA reporter after recognizing the target nucleic acid (DNA for Cas12a and RNA for Cas13), can satisfy simplicity, speed, and specificity at the same time, and is considered a very promising technology in pathogen detection. Because of the advantages of the CRISPR/Cas system and the DNA-targeting property of Cas12a, CRISPR/Cas12a system shows great potential for the early diagnosis and on-site detection of bacteria and viruses. However, the detection sensitivity of CRISPR/Cas12a alone is very low (Chen et al., 2018; Li et al., 2018). A seminal study by the Doudna lab (Chen et al., 2018) created the DETECTR method, which consists of a recombinase polymerase amplification (RPA) assay and the CRISPR/Cas12a system, and the sensitivity of DETECTR can be as low as the attomolar level. This method not only inherits the advantages of RPA and

the CRISPR/Cas12a system, but also avoids the shortcomings of RPA and the CRISPR/Cas12a system. At present, the DETECTR method has been used to detect a variety of pathogens, such as SARS-CoV-2 (Broughton et al., 2020; Wang et al., 2020), *Vibrio parahaemolyticus* (Zhang et al., 2020) and *Pseudomonas aeruginosa* (Mukama et al., 2020).

In this study, we employed an RAA assay and the CRISPR/Cas12a system to develop a *V. vulnificus* detection method (Figure 1), RAA-CRISPR/Cas12a, targeting the *vvhA* gene. The whole process using this method takes 40 min; the limit of detection is 2 copies/reaction, which is comparable with qPCR; the readout can be evaluated by the naked eye using a UV torch; the fluorescence signal can only be detected in all samples spiked with *V. vulnificus*. The rapid and sensitive characteristics of this method make it a promising candidate for early diagnosis of human vibriosis and on-site *V. vulnificus* detection.

## MATERIALS AND METHODS

### Bacterial Strains

A total of 10 bacterial strains (five reference strains and five isolation strains) employed in this study were stored in our lab. The five reference strains were *V. vulnificus* (ATCC 27562), *V. harveyi* (ATCC 14126), *V. alginolyticus* (ATCC 17749), *Staphylococcus aureus* (ATCC 25923), and *Bacillus cereus* (ATCC 14579). The five isolation strains were *V. vulnificus*, *V. parahaemolyticus*, *Salmonella typhimurium*, *Edwardsiella piscicida*, and *Aeromonas hydrophila*, which were isolated from eel, clinical sample, clinical sample, carp, and crucian, respectively. All strains were verified by PCR assays targeting the specific segment of 16S rRNA gene.

### Genomic DNA Extraction

Two DNA extraction methods, NaOH-based and Kit-based, were employed to extract bacterial genomic DNA. The NaOH-based method was used to crudely extract the genomic DNA of *V. vulnificus*. Briefly, 50  $\mu$ L of *V. vulnificus* suspension was added to 200  $\mu$ L of 0.5 M NaOH solution and incubated at room temperature for 3 min. After being diluted 20-fold with nuclease-free water (Qiagen, Germany), 2  $\mu$ L of cell lysate was used as template for the RAA assay. A MiniBEST Bacterial Genomic DNA Extraction Kit (TaKaRa, China) was also used to extract bacterial genomic DNA according to the user manual.

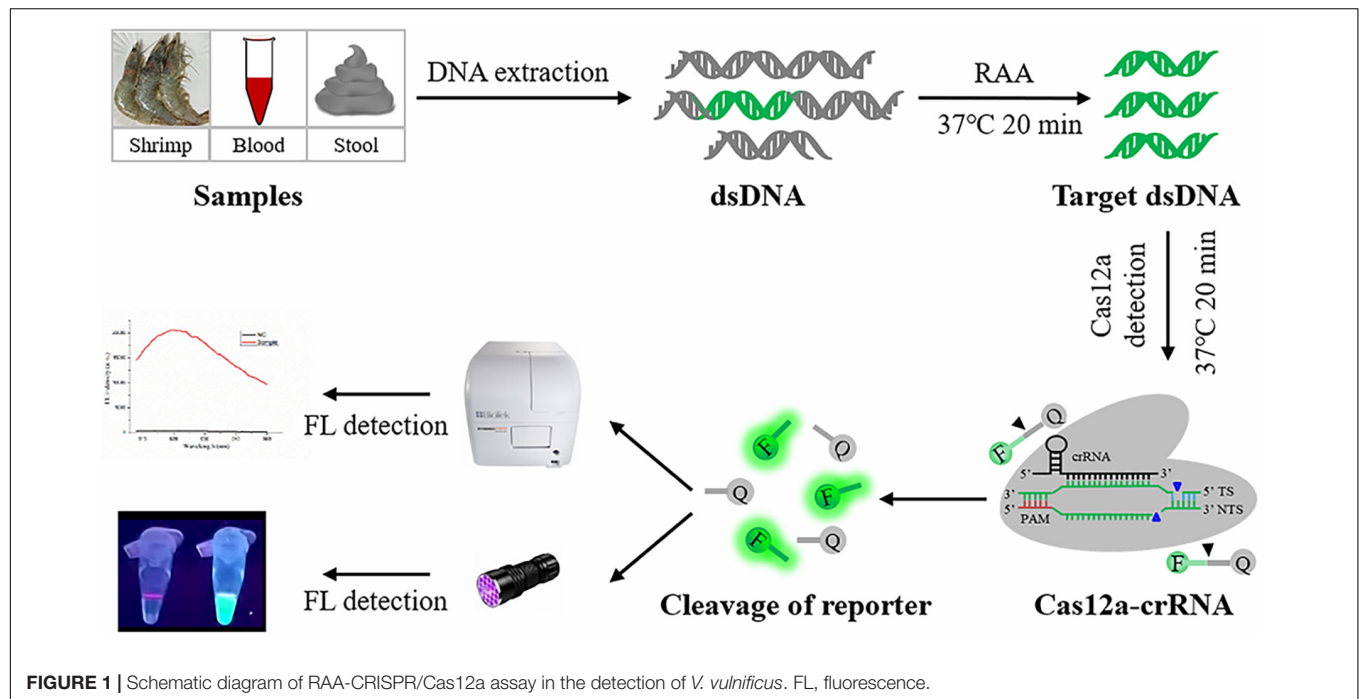
### Nucleic Acid Preparation

The *vvhA* gene fragment of *V. vulnificus* (ATCC 27562) obtained by PCR using primer F (5'-CTCTGTTTACCCTTTCTCTTTTAGC-3') and primer R (5'-GAGTTTGACTTGTGTGAATGTGGGT-3') was cloned into the pMD19-T vector and then sequenced by Tsingke (Tsingke Biotechnology, China).

Five published *vvhA* sequences (accession number: M34670.1, KC821520.1, FJ222405.1, AB124802.1, and AB124803.1) were downloaded from GenBank and aligned with the obtained *vvhA* gene sequence using the Clustal Omega<sup>1</sup>. Nine pairs of RAA

<sup>1</sup><https://www.ebi.ac.uk/Tools/msa/clustalo/>





primers targeting the conserved region of the *vvhA* sequence were designed according to the Assay Design Manual of the TwistAmp™ DNA Amplification Kits<sup>2</sup> and were listed in **Supplementary Table 1**.

As for crRNA design, two factors must be considered: one is that the crRNA sequence lacks overlap with the RAA primers, and the other is that the crRNA sequence targets the conserved region of the RAA amplicon. The ssDNA-FQ reporter modified with fluorophore 6-FAM and quencher BHQ1 (5′-/6-FAM/TTATT/BHQ1/-3′) was used to be *trans*-cleaved by Cas12a and then indicate the presence or absence of the target gene (Chen et al., 2018; Li et al., 2018). crRNA and ssDNA-FQ were synthesized by Sangon Biotech (Shanghai, China), and they were then dissolved in the desired concentration (200 nM for crRNA and 500 nM for ssDNA-FQ) with 1 × NEB buffer 2.1 (NEB ENGLAND BioLabs Inc., United States), aliquoted into 10 μL per tube, and stored at −80°C.

The genomic DNA of *V. vulnificus* (ATCC 27562) extracted by Kit was diluted with 1 × NEB buffer 2.1, and different concentrations ( $1 \times 10^0$  to  $1 \times 10^8$  copies/μL) of *V. vulnificus* genomic DNA were obtained and stored at −80°C with 6 μL of an aliquot of each gradient.

## RAA-CRISPR/Cas12a Assay

The RAA assay was conducted with an RAA Nucleic Acid Amplification Kit (Jiangsu Qitian Gene Biological Co., China) according to the user manual. Briefly, 25 μL of buffer V, 2 μL of forward primer (10 μM), 2 μL of reverse primer (10 μM), 2 μL of DNA template, 16.5 μL of purified water, and 2.5 μL of magnesium acetate were mixed in tube and then incubated

at 37°C for 40 min. The RAA products were analyzed with 2% agarose gel or with the CRISPR/Cas12a system.

A Cas12a-mediated collateral cleavage assay was conducted similarly to the methods used by Chen et al. (2018) and Li et al. (2018). Briefly, 10 μL of 200 nM Cas12a (NEB ENGLAND BioLabs Inc., United States) diluted with 1 × NEB buffer 2.1 was preincubated with 10 μL of 200 nM crRNA for 20 min at 37°C. After this, 10 μL of 500 nM ssDNA-FQ and 2 μL of RAA products were mixed with 20 μL of Cas12a-crRNA complex, and the 32 μL mixture was immediately incubated at 37°C for 35 min. Upon incubation, the readout could be observed using a UV device, such as a UV torch, or detected using a multifunctional microplate reader ( $\lambda_{ex}$ : 485 nm and  $\lambda_{em}$ : 520 nm). In this study, the RAA reaction time and Cas12a cleavage time were optimized.

## qPCR Assay

A qPCR assay used as a standard method to detect *V. vulnificus* (Campbell and Wright, 2003; Panicker and Bej, 2005) was performed with *vvhA*-F (5′-TGTTTATGGTGAGAACGGTGACA-3′) and *vvhA*-R (5′-TTCTTTATCTAGGCCCCAACTTG-3′) using a CFX96 real-time PCR detection (Bio-Rad, United States) system. The qPCR reaction mixtures contained 10 μL of SYBR® Premix Ex Taq™ II (TaKaRa, China), 0.8 μL of each primer (5 μM), 2 μL of DNA template, and 6.4 μL of nuclease-free water. The reaction condition was: 95°C for 30 s, and 39 cycles of 95°C for 5 s and 60°C for 30 s.

## Detection of Shrimp Samples Using RAA-CRISPR/Cas12a Assay

Eleven fresh shrimps purchased from a local supermarket were proved to be free of *V. vulnificus* by qPCR. Eight of

<sup>2</sup><https://www.twistdx.co.uk>

them were spiked with *V. vulnificus* by a researcher according to the methods used by Zhang et al. (2020) and Wang et al. (2017a). Briefly, the fresh shrimps were de-headed and sterilized with 75% ethanol for 2 min. The obtained shrimp samples were incubated in *V. vulnificus* suspensions ( $1.1 \times 10^4$  CFU/mL) for 30 min at 23°C and then transferred onto a clean workbench for bacterial attachment. After 30 min of attachment, 11 shrimps were numbered by this researcher. The RAA-CRISPR/Cas12a assay was then conducted by the other researcher, who did not know the real situation of these shrimps. A Q-tip was used to sample the shrimp by wiping it, and it was then placed into 200  $\mu$ L of nuclease-free water to obtain *V. vulnificus* suspension. The NaOH-based method mentioned above was performed to extract *V. vulnificus* genomic DNA, and the Kit-based extraction method was used as a comparative test. 2  $\mu$ L of genomic DNA extracted by these two methods was used as template for the RAA-CRISPR/Cas12a assay.

## Detection of Human Blood and Stool Samples Using RAA-CRISPR/Cas12a Assay

Blood and stool samples were collected from three healthy volunteers, and 100  $\mu$ L of blood or 200 mg of stool was added into the tube containing  $1.1 \times 10^3$  CFU of *V. vulnificus*. Then, these blood and stool samples were used to extract genomic DNA using the MiniBEST Universal Genomic DNA Extraction Kit Ver.5.0 (TaKaRa, China) and the TIANamp Stool DNA Kit (TIANGEN, China), respectively. 2  $\mu$ L of genomic DNA extracted from spiked blood and stool samples were then used as templates for RAA-CRISPR/Cas12a assay, while 2  $\mu$ L of blood or stool DNA was used as a negative control.

## RESULTS

### Screening an Optimal Primer Set for RAA Assay

To obtain the optimal primers, nine primer sets were designed (Supplementary Table 1), and the RAA assay was performed with *V. vulnificus* genomic DNA and each primer set. The primers were then screened according to the gel electrophoresis of RAA products. As shown in Figure 2A, the predicted bands of each RAA product were visible; however, the intensity of two bands amplified with the No. 1 primer set (F1: 5'-TTCAACGCCACACGAGACTGGTGTAATGCGG-3' and R1: 5'-CCAATGTAAGTGCGGCGTTTGCCCAACTCTGG-3') and the No. 7 primer set (F7: 5'-TTATGGTGAGACGGTGACAAAACGGTTGCGGG-3' and R7: 5'-CCTTCCCAATACCATTCTGTGCTAAGTTCGC-3') were significantly stronger than the other seven bands, indicating the high amplification efficiency of the No. 1 and No. 7 primer sets. Therefore, these two primer sets were selected as candidates for subsequent RAA assay, and their amplicons were used to design crRNA.

### Screening an Optimal crRNA for RAA-CRISPR/Cas12a Assay

According to the two factors mentioned in Materials and Methods, only four crRNAs (CR1 and CR2 targeting the No. 1 amplicon; CR3 and CR4 targeting the No. 7 amplicon) were designed (Figure 2B). Because the efficiency of each crRNA and crRNAmix (crRNA mixture) in triggering the *trans*-cleavage capability of Cas12a may be different (Creutzburg et al., 2020; Wang et al., 2020), the RAA-CRISPR/Cas12a assay was performed using *V. vulnificus* genomic DNA as template and F1/R1 or F7/R7 as primer set to test the capacity of CR1, CR2, CR1 + 2, CR3, CR4, and CR3 + 4 and then screen an optimal crRNA. As shown in Figure 2C, all four crRNAs and the two crRNAmixes could trigger fluorescence signal generation; however, the fluorescence signals triggered by crRNAmixes were stronger than those triggered by single crRNA. Furthermore, CR3 + 4 triggered a stronger fluorescence signal than CR1 + 2. Therefore, CR3 + 4 and its corresponding primer set, F7/R7, were chosen as the optimal crRNA and primer set, and would be used in the subsequent RAA-CRISPR/Cas12a assay.

### Optimizing RAA Reaction Time and Cas12a Cleavage Time

To shorten the assay time with minimal difference in reaction efficacy, we optimized the RAA reaction time and Cas12a cleavage time using the RAA-CRISPR/Cas12a assay with the same template concentration of *V. vulnificus* genomic DNA ( $1 \times 10^4$  copies/ $\mu$ L). As for optimization of RAA reaction time, 0, 5, 10, 15, 20, 25, 30, 35, and 40 min were tested. The results showed that fluorescence intensity reached a plateau after 20 min (Figure 3A), indicating that 20 min was the optimal time for RAA reaction. As for optimization of Cas12a cleavage time, 0, 5, 10, 15, 20, 25, 30, 35, 40, and 45 min were tested. The results shown in Figure 3B indicated that 20 min was the optimal time for Cas12a cleavage. Therefore, the reaction time for the RAA-CRISPR/Cas12a assay we developed to detect *V. vulnificus* was 40 min, consisting of 20 min for the RAA reaction and 20 min for Cas12a cleavage.

### Sensitivity of RAA-CRISPR/Cas12a Assay in the Detection of *Vibrio vulnificus*

To evaluate the sensitivity of the RAA-CRISPR/Cas12a assay in detecting *V. vulnificus*, 2  $\mu$ L of different concentrations ( $1 \times 10^0$  to  $1 \times 10^6$  copies/ $\mu$ L) of *V. vulnificus* genomic DNA and nuclease-free H<sub>2</sub>O were used as RAA templates, and 2  $\mu$ L of RAA product was then detected with a Cas12a-mediated cleavage assay. As shown in Figure 4A, all samples except H<sub>2</sub>O could generate fluorescence signals detected by a multifunctional microplate reader or a UV device, indicating that the limit of detection (LOD) of this method in *V. vulnificus* detection reached 2 copies/reaction.

To compare the sensitivity of RAA-CRISPR/Cas12a with RAA, qPCR, or CRISPR-Cas12a in the detection of *V. vulnificus*, we also assessed the sensitivity of the RAA, qPCR, and

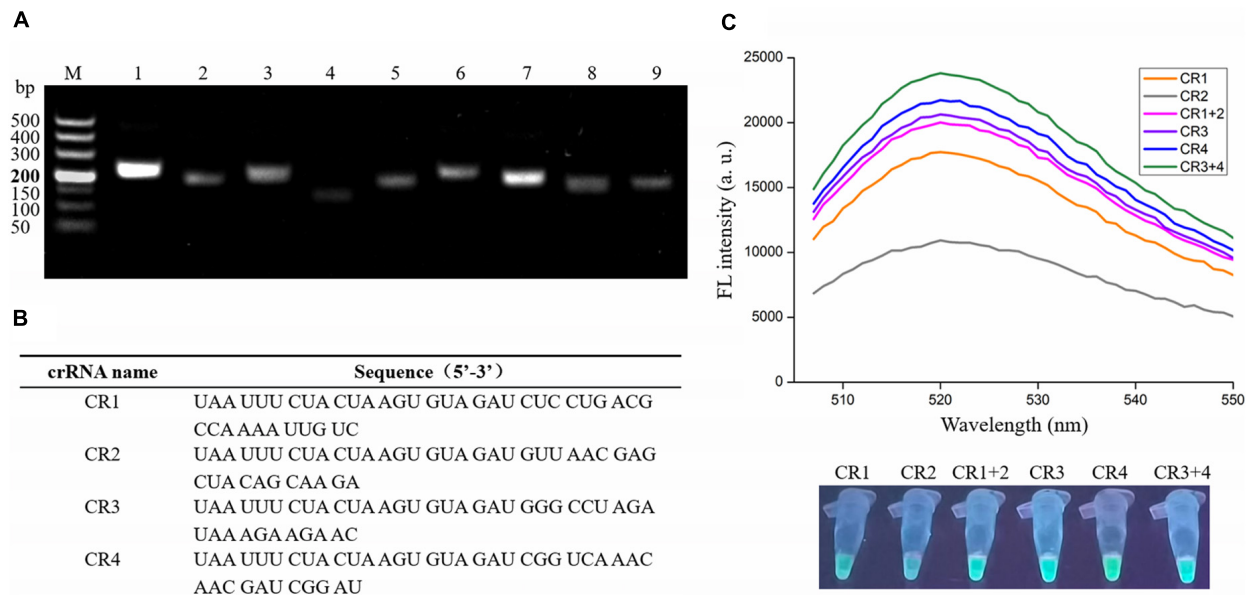


**FIGURE 2 |** Screening optimal RAA primers and crRNA for the RAA-CRISPR/Cas12a assay. **(A)** Gel electrophoresis analysis of RAA products amplified with different primer set. M, 500 DNA marker; lanes 1–9, RAA products amplified by primer set 1, 2, 3, 4, 5, 6, 7, 8, and 9, respectively. **(B)** crRNA sequences designed in this study. **(C)** Analysis of fluorescence signals triggered by the different crRNA using a multifunctional microplate reader (upper) or a UV torch (below). Data is one representative of three experiments.

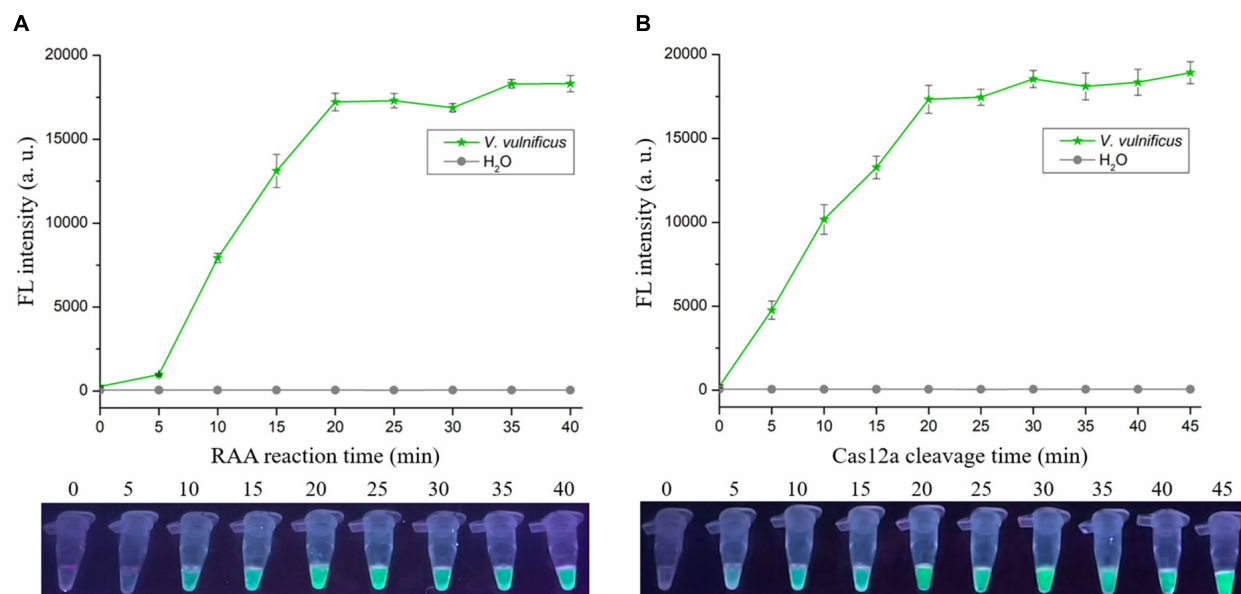


**FIGURE 3 |** Optimizing the RAA reaction time and Cas12a cleavage time. The RAA-CRISPR/Cas12a assay was performed using  $1 \times 10^4$  copies/ $\mu$ L of *V. vulnificus* genomic DNA as the template, F7/R7 as the primer set, and CR3 + 4 as the crRNA to optimize the RAA reaction time **(A)** and Cas12a cleavage time **(B)**, and the fluorescence signal was analyzed using a multifunctional microplate reader (upper) or a UV torch (below).

CRISPR-Cas12a assay. As for the sensitivity of the RAA assay that was performed under the same condition as the RAA-CRISPR/Cas12a assay, the result of gel electrophoresis employed to analyze the RAA products showed that the LOD of the RAA assay was  $1 \times 10^3$  copies/ $\mu$ L (**Figure 4B**), which was lower than

the sensitivity of RAA-CRISPR/Cas12a. The LOD of qPCR assay was 2 copies/reaction (**Figure 4C**), consistent with the sensitivity of RAA-CRISPR/Cas12a assay. As for the CRISPR-Cas12a assay, we did not detect a fluorescence signal from all samples, even though the sample concentration was  $1 \times 10^8$  copies/ $\mu$ L (data not

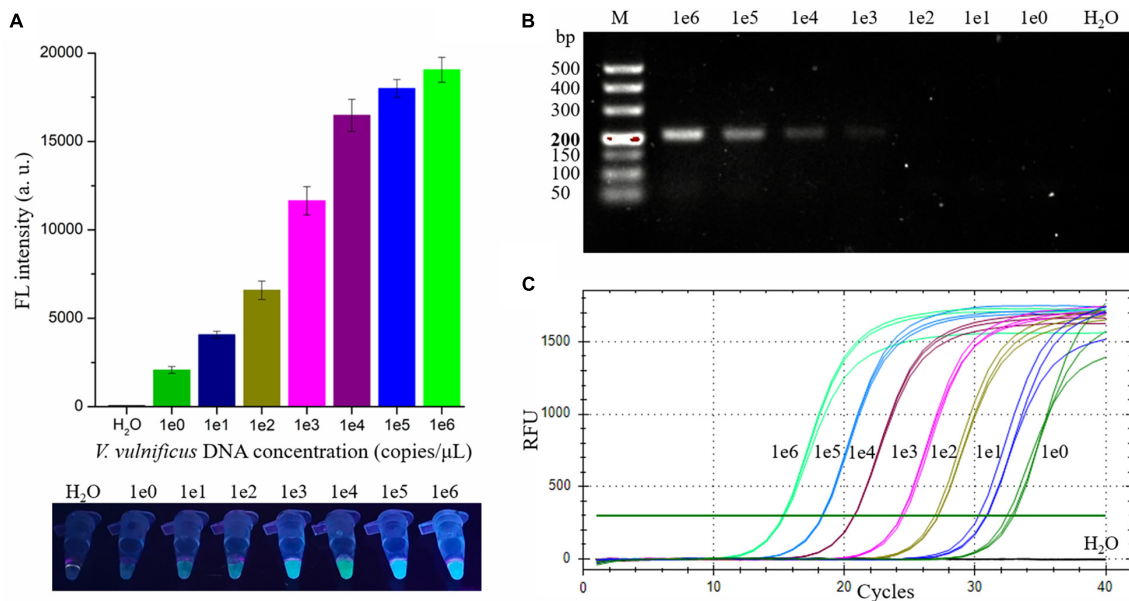


**FIGURE 4 |** Evaluating the sensitivity of the RAA-CRISPR/Cas12a, RAA, and qPCR assay in *V. vulnificus* detection. 2  $\mu$ L of nuclease-free water and  $1 \times 10^0$  to  $1 \times 10^6$  copies/ $\mu$ L of *V. vulnificus* genomic DNA were used as templates in these assays. **(A)** The sensitivity of the RAA-CRISPR/Cas12a assay. The results were detected using a multifunctional microplate reader (upper) or a UV torch (below). **(B)** The sensitivity of the RAA assay. RAA reaction time was 20 min, consistent with the RAA-CRISPR/Cas12a assay. The results were analyzed using gel electrophoresis. **(C)** The sensitivity of the qPCR assay. qPCR was conducted with the CFX96 real-time PCR detection systems, and the amplification curves of each sample were shown in this figure. Data is one representative of three experiments.

shown), which was consistent with the reports that the detection sensitivity of CRISPR-Cas12a alone was very low (Chen et al., 2018; Li et al., 2018).

Taken together, the sensitivity of the RAA-CRISPR/Cas12a assay we established was two copies of *V. vulnificus* genomic DNA per reaction, which is comparable with qPCR but significantly higher than that of RAA and CRISPR-Cas12a.

### Specificity of RAA-CRISPR/Cas12a Assay in Detecting *Vibrio vulnificus*

The genomic DNA extracted from two *V. vulnificus* strains and eight other strains of foodborne pathogenic bacteria were used to assess the specificity of the RAA-CRISPR/Cas12a assay in *V. vulnificus* detection. The results showed that the fluorescence signal could be detected in those two *V. vulnificus* strains using this method, but not in the strains of *Bacillus cereus*, *Edwardsiella piscicida*, *Staphylococcus aureus*, *Salmonella typhimurium*, *Aeromonas hydrophila*, *V. harveyi*, *V. alginolyticus*, and *V. parahaemolyticus* (Figure 5), indicating no cross-reactions of the RAA-CRISPR/Cas12a assay in the detection of *V. vulnificus*. Therefore, the method we established displayed a high specificity for *V. vulnificus* detection.

### Detection of *Vibrio vulnificus* in Spiked Samples With RAA-CRISPR/Cas12a Assay

Finally, we evaluated the performance of the RAA-CRISPR/Cas12a assay in the detection of shrimp samples, drawing on eight *V. vulnificus*-spiked samples and three

*V. vulnificus*-free samples. This experiment was conducted by two researchers: one was responsible for preparation of the  $1.1 \times 10^4$  CFU/mL *V. vulnificus*-spiked samples and numbered

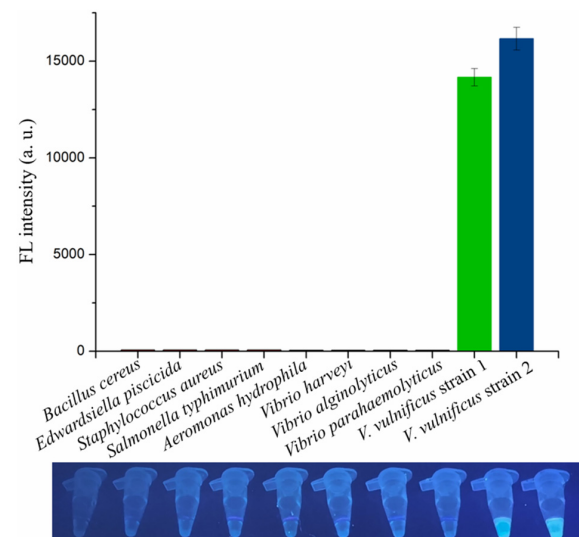


**FIGURE 5 |** Evaluating the specificity of RAA-CRISPR/Cas12a assay in *V. vulnificus* detection. Ten bacterial strains were used to evaluate the specificity of RAA-CRISPR/Cas12a assay, and the fluorescence sigils were analyzed using a multifunctional microplate reader (upper) or a UV torch (below). *V. vulnificus* strain 1 was isolated from eel, and strain 2 was isolated from human.



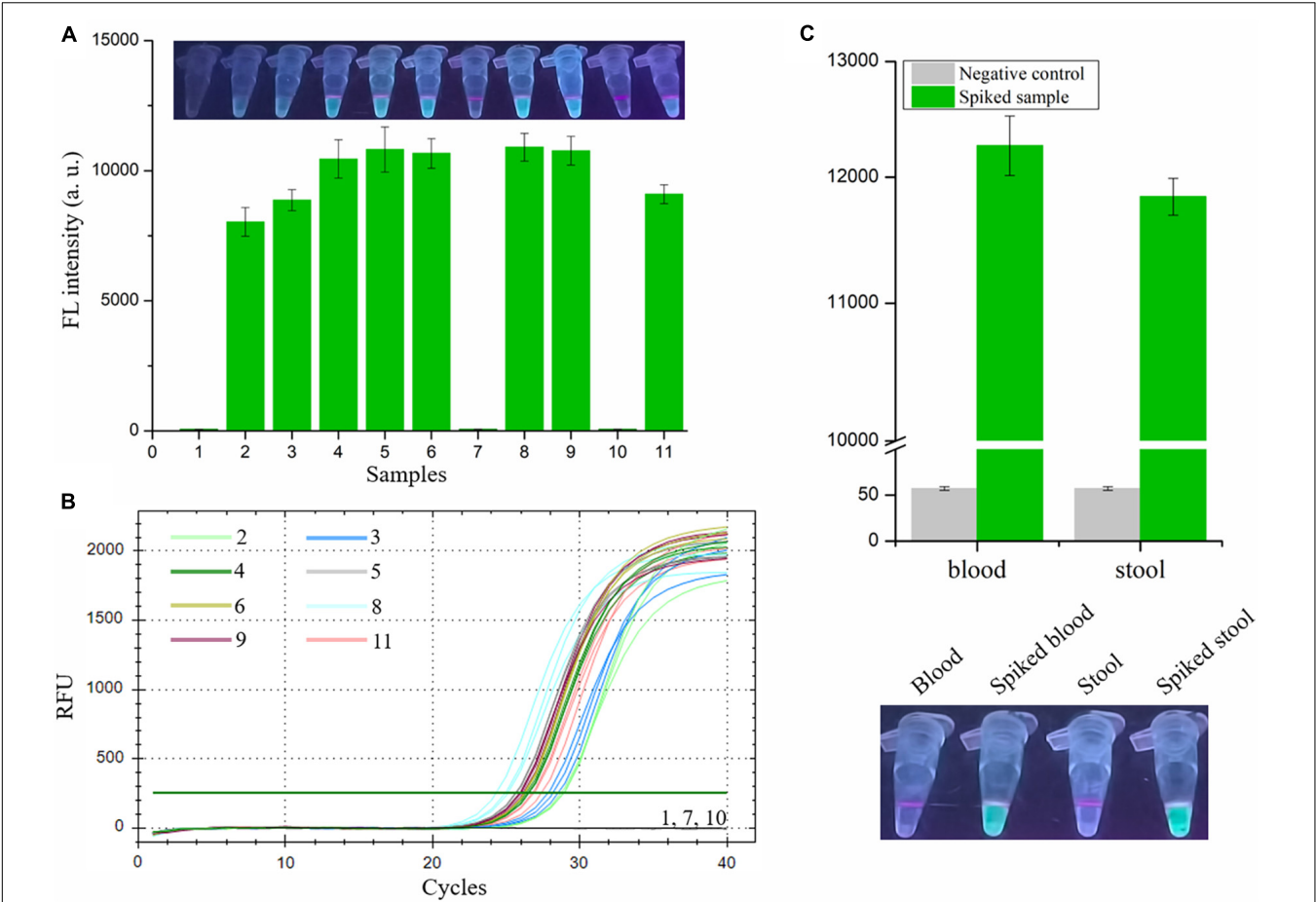


**FIGURE 6 |** Analysis the feasibility of RAA-CRISPR/Cas12a assay in the detection of *V. vulnificus* in spiked samples. The genomic DNA was extracted from 11 shrimps, eight of which were spiked with  $1.1 \times 10^4$  CFU/mL of *V. vulnificus*, using the NaOH-based DNA extraction method. **(A)** The RAA-CRISPR/Cas12a assay was performed to detect *V. vulnificus* in those 11 DNA samples using a multifunctional microplate reader (below) or a UV torch (upper). **(B)** The qPCR assay was performed as a standard method to detect *V. vulnificus* in those 11 DNA samples. The amplification curves of each sample were shown. Data is one representative of three experiments. **(C)** Human blood and stool samples were employed to evaluate the feasibility of RAA-CRISPR/Cas12a assay in diagnosis of human vibriosis. 100  $\mu$ L of blood or 200 mg of stool was added into the tube containing  $1.1 \times 10^3$  CFU of *V. vulnificus*, and then these samples were used to extract genomic DNA. 2  $\mu$ L of genomic DNA extracted from spiked samples were used as templates for RAA-CRISPR/Cas12a assays, while 2  $\mu$ L of blood DNA or stool DNA was used as a negative control. Fluorescence signals were analyzed using a multifunctional microplate reader (upper) or a UV torch (below). Data is one representative of three experiments.

**TABLE 1 |** Comparison of different methods for detection of *Vibrio vulnificus*.

Method	Equipment required	Speed	Sensitivity	Specificity	References
Culture	Incubator	Days	Variable	Case-specific	O'Hara et al., 2003; Hartnell et al., 2019
qPCR	Real-time PCR instrument	Hours	High	High	Campbell and Wright, 2003; Panicker and Bej, 2005
iNAT <sup>#</sup>	Real-time PCR instrument	Minutes	High	High	Han and Ge, 2010; Yang et al., 2020
	LFD* or electrophoresis apparatus	Minutes, hours	Medium	High	Surasilp et al., 2011; Yang et al., 2021
RAA-CRISPR/Cas12a	UV torch	Minutes	High	High	This study

<sup>#</sup>Isothermal nucleic acid amplification technology.  
<sup>\*</sup>Lateral flow dipstick.

the 11 shrimps, while the other one with no idea about the situation of shrimps extracted the genomic DNA from shrimps using the NaOH-based and Kit-based methods and then carried out the RAA-CRISPR/Cas12a assay. As shown in **Figure 6A**, the fluorescence signal could only be detected in eight spiked samples using the RAA-CRISPR/Cas12a assay, which was exactly matched with the results of the qPCR assay (**Figure 6B**), indicating the high accuracy of this method in *V. vulnificus* detection. Moreover, the RAA-CRISPR/Cas12a assay was also performed using the DNA template extracted through the

Kit-based method, which still only detected all the spiked samples (**Supplementary Figure 1**).

To investigate whether our proposed RAA-CRISPR/Cas12a method has potential to diagnose human vibriosis using human blood or stool samples, the blood and stool samples spiked with  $1.1 \times 10^3$  CFU of *V. vulnificus* were prepared and used to extract genomic DNA. 2  $\mu$ L of genomic DNA extracted from blood or stool samples were used as templates. As shown in **Figure 6C**, apart from the negative controls, the fluorescence signal could be detected in all spiked samples. These results indicated that the RAA-CRISPR/Cas12a assay could resist the influence of human genomic DNA and gut flora DNA, further implying the great feasibility of this assay in the detection of human samples.

Taken together, these results showed that the presented RAA-CRISPR/Cas12a assay could be used to detect *V. vulnificus* in the samples collected from seafood and human beings.

## DISCUSSION

*Vibrio vulnificus* is a mesophilic and zoonotic bacterium (Oliver, 2015; Baker-Austin and Oliver, 2018). With global warming, the populations of *V. vulnificus* are larger, and cases of vibriosis are increasing (Baker-Austin et al., 2013, 2018), seriously threatening aquaculture, food safety, and human health. A more rapid and sensitive detection method is good for reducing the harm caused by *V. vulnificus* infection. Currently, the reported methods for *V. vulnificus* detection are based on NAT and can be divided into two main types: qPCR-based method (Campbell and Wright, 2003; Panicker and Bej, 2005) and iNAT-based method (**Table 1**), which mainly depends on a real-time PCR instrument or lateral flow dipstick (Han and Ge, 2010; Surasilp et al., 2011; Yang et al., 2020, 2021). However, the qPCR-based and iNAT-based pathogen detection methods depending on the real-time PCR instrument are not convenient for use in on-site detection and resource-poor areas, while the iNAT-based pathogen detection methods depending on the lateral flow dipstick or gel electrophoresis analysis show lower sensitivity than qPCR (Panicker and Bej, 2005; Surasilp et al., 2011; Wang et al., 2017b; Gallardo et al., 2019). To circumvent these defects, we developed an RAA-CRISPR/Cas12a assay to detect *V. vulnificus* (**Figure 1**), which does not require a sophisticated instrument, only takes 40 min from adding DNA templates to obtaining the results (**Figure 3**), and can detect *V. vulnificus* genomic DNA in as low as 2 copies/reaction (**Figure 4A**).

The target gene of the presented method is *vvhA*, which encodes an important toxin hemolysin in *V. vulnificus* pathogenicity (Kreger and Lockwood, 1981; Lee et al., 2004). Because of the species specificity and high conservation of *vvhA* gene (Wright et al., 1985; Morris et al., 1987; Hill et al., 1991), detection of the *vvhA* gene has been used as a standard method to identify *V. vulnificus* (Hill et al., 1991; Campbell and Wright, 2003). Because of the diversity of *vvhA* gene (Senoh et al., 2005), six *vvhA* sequences were aligned, and the conserved region was then used to design the RAA primers and crRNA sequences. The specificity tests showed that only two

*V. vulnificus* strains (a clinical isolate and an eel isolate) could be detected using the RAA-CRISPR/Cas12a method (**Figure 5**), indicating that the primers and crRNA sequences we designed were valid. Moreover, we also evaluated the feasibility of this method in the detection of spiked samples. As for detection of *V. vulnificus* in shrimps (**Figure 6A**), the results showed that the RAA-CRISPR/Cas12a assay could detect all the spiked samples, indicating the great potential of this assay for on-site *V. vulnificus* detection.

Apart from detection of *V. vulnificus* in spiked shrimp samples using the RAA-CRISPR/Cas12a method, we also investigated the feasibility of this method in diagnosis of human vibriosis. As we all known, primary septicemia and gastroenteritis are two major clinical syndromes of *V. vulnificus* infections (Chuang et al., 1992; Shapiro et al., 1998). Therefore, human blood and stool samples were used to conduct this experiment (**Figure 6C**). The results demonstrated that our proposed RAA-CRISPR/Cas12a method showed high accuracy in the detection of human samples, indicating the great potential of this method for the early diagnosis of human vibriosis.

In conclusion, our presented method, the RAA-CRISPR/Cas12a assay, simultaneously satisfies speed, specificity, sensitivity, and unsophisticated to detect *V. vulnificus*, and shows great potential for on-site *V. vulnificus* detection in aquaculture and food safety and for the early diagnosis of human vibriosis, especially in resource-poor areas.

## DATA AVAILABILITY STATEMENT

The original contributions presented in the study are included in the article/**Supplementary Material**, further inquiries can be directed to the corresponding author/s.

## AUTHOR CONTRIBUTIONS

XX, LZ, and YL designed the study. XX and ZL wrote the manuscript. ZL and XH performed the experiments and analyzed the data. JL and YZ reviewed the manuscript. All authors contributed to the article and approved the submitted version.

## FUNDING

This work was supported by the Science and Technology Bureau of Wenzhou (Grant Number Y20210109), the National Natural Science Foundation of China (Grant Number 82002117), and the Key Discipline of Zhejiang Province in Medical Technology (First Class, Category A).

## SUPPLEMENTARY MATERIAL

The Supplementary Material for this article can be found online at: <https://www.frontiersin.org/articles/10.3389/fmicb.2021.767315/full#supplementary-material>

## REFERENCES

- Asiello, P. J., and Baumann, A. J. (2011). Miniaturized isothermal nucleic acid amplification, a review. *Lab Chip* 11, 1420–1430. doi: 10.1039/c0lc00666a
- Baker-Austin, C., and Oliver, J. D. (2018). *Vibrio vulnificus*: new insights into a deadly opportunistic pathogen. *Environ. Microbiol.* 20, 423–430. doi: 10.1111/1462-2920.13955
- Baker-Austin, C., Oliver, J. D., Alam, M., Ali, A., Waldor, M. K., Qadri, F., et al. (2018). *Vibrio* spp. infections. *Nat. Rev. Dis. Primers* 4:8. doi: 10.1038/s41572-018-0005-8
- Baker-Austin, C., Trinanes, J. A., Taylor, N. G., Hartnell, R., Siitonen, A., and Martinez-Urtaza, J. (2013). Emerging *Vibrio* risk at high latitudes in response to ocean warming. *Nat. Clim. Change* 3, 73–77. doi: 10.1038/NCLIMATE1628
- Broughton, J. P., Deng, X., Yu, G., Fasching, C. L., and Chiu, C. Y. (2020). CRISPR–Cas12-based detection of SARS-CoV-2. *Nat. Biotechnol.* 38, 870–874. doi: 10.1038/s41587-020-0513-4
- Campbell, M. S., and Wright, A. C. (2003). Real-time PCR analysis of *Vibrio vulnificus* from oysters. *Appl. Environ. Microb.* 69, 7137–7144. doi: 10.1128/AEM.69.12.7137-7144.2003
- Chuang, Y. C., Yuan, C. Y., Liu, C. Y., Lan, C. K., and Huang, A. H. (1992). *Vibrio vulnificus* infection in Taiwan: report of 28 cases and review of clinical manifestations and treatment. *Clin. Infect. Dis.* 15, 271–276. doi: 10.1093/clinids/15.2.271
- Chen, J. S., Ma, E., Harrington, L. B., Costa, M., Tian, X., Palefsky, J. M., et al. (2018). CRISPR-Cas12a target binding unleashes indiscriminate single-stranded DNase activity. *Science* 360:ear6245. doi: 10.1126/science.ear6245
- Choi, J., Seong, T. W., Jeun, M., and Lee, K. H. (2017). Field-Effect Biosensors for On-Site Detection: Recent Advances and Promising Targets. *Adv. Healthc. Mater.* 6:20 doi: 10.1002/adhm.201700796
- Creutzburg, S. C. A., Wu, W. Y., Mohanraj, P., Swartjes, T., Alkan, F., Gorodkin, J., et al. (2020). Good guide, bad guide: spacer sequence-dependent cleavage efficiency of Cas12a. *Nucleic Acids Res.* 48, 3228–3243. doi: 10.1093/nar/gkz1240
- Daher, R. K., Stewart, G., Boissinot, M., Boudreau, D. K., and Bergeron, M. G. (2015). Influence of sequence mismatches on the specificity of recombinase polymerase amplification technology. *Mol. Cell. Probe* 29, 116–121. doi: 10.1016/j.mcp.2014.11.005
- El Sheikh, A. F., Levin, R., and Xu, J. P. (2018). *Molecular Techniques in Food Biology: Safety, Biotechnology, Authenticity and Traceability*. Chichester: John Wiley & Sons Ltd.
- Gallardo, C., Fernandez-Pinero, J., and Arias, M. (2019). African swine fever (ASF) diagnosis, an essential tool in the epidemiological investigation. *Virus Res.* 271:197676. doi: 10.1016/j.virusres.2019.197676
- Gootenberg, J. S., Abudayyeh, O. O., Lee, J. W., Essletzbichler, P., Dy, A. J., Joung, J., et al. (2017). Nucleic acid detection with CRISPR-Cas13a/C2c2. *Science* 356, 438–442. doi: 10.1126/science.aam9321
- Han, F., and Ge, B. (2010). Quantitative detection of *Vibrio vulnificus* in raw oysters by real-time loop-mediated isothermal amplification. *Int. J. Food Microbiol.* 142, 60–66. doi: 10.1016/j.ijfoodmicro.2010.05.029
- Hartnell, R. E., Stockley, L., Keay, W., Rose, J. P., Hervio-Heath, D., Van den Berg, H., et al. (2019). A pan-European ring trial to validate an International Standard for detection of *Vibrio cholerae*, *Vibrio parahaemolyticus* and *Vibrio vulnificus* in seafoods. *Int. J. Food Microbiol.* 288, 58–65. doi: 10.1016/j.ijfoodmicro.2018.02.008
- Hill, W. E., Keasler, S. P., Trucksess, M. W., Feng, P., Kaysner, C. A., and Lampel, K. A. (1991). Polymerase chain reaction identification of *Vibrio vulnificus* in artificially contaminated oysters. *Appl. Environ. Microb.* 57, 707–711. doi: 10.1128/aem.57.3.707-711.1991
- Jones, M. K., and Oliver, J. D. (2009). *Vibrio vulnificus*: disease and pathogenesis. *Infect. Immun.* 77, 1723–1733. doi: 10.1128/IAI.01046-08
- Klontz, K. (1988). Syndromes of *Vibrio vulnificus* infections: clinical and epidemiologic features in Florida cases, 1981–1987. *Ann. Int. Med.* 109, 318–323. doi: 10.7326/0003-4819-109-4-318
- Kreger, A., and Lockwood, D. (1981). Detection of extracellular toxin(s) produced by *Vibrio vulnificus*. *Infect. Immun.* 33, 583–590. doi: 10.1128/iai.33.2.583-590.1981
- Lee, S. E., Ryu, P. Y., Kim, S. Y., Kim, Y. R., Koh, J. T., Kim, O. J., et al. (2004). Production of *Vibrio vulnificus* hemolysin in vivo and its pathogenic significance. *Biochem. Biophys. Res. Commun.* 324, 86–91. doi: 10.1016/j.bbrc.2004.09.020
- Li, S. Y., Cheng, Q. X., Wang, J. M., Li, X. Y., Zhang, Z. L., Gao, S., et al. (2018). CRISPR-Cas12a-assisted nucleic acid detection. *Cell Discov.* 4:20. doi: 10.1038/s41421-018-0028-z
- Lu, W., Yuan, Q., Yang, Z., and Yao, B. (2017). Self-primed isothermal amplification for genomic DNA detection of human papillomavirus. *Biosens. Bioelectron.* 90, 258–263. doi: 10.1016/j.bios.2016.10.024
- Mayboroda, O., Katakis, I., and O'Sullivan, C. K. (2018). Multiplexed isothermal nucleic acid amplification. *Anal. Biochem.* 545, 20–30. doi: 10.1016/j.ab.2018.01.005
- Moore, M. D., and Jaykus, L. A. (2017). Development of a Recombinase Polymerase Amplification Assay for Detection of Epidemic Human Noroviruses. *Sci. Rep.* 7:40244. doi: 10.1038/srep40244
- Morris, J. G. Jr., Wright, A. C., Roberts, D. M., Wood, P. K., Simpson, L. M., and Oliver, J. D. (1987). Identification of environmental *Vibrio vulnificus* isolates with a DNA probe for the cytotoxin-hemolysin gene. *Appl. Environ. Microb.* 53, 193–195. doi: 10.1128/aem.53.1.193-195.1987
- Mukama, O., Wu, J., Li, Z., Liang, Q., and Zeng, L. (2020). An ultrasensitive and specific point-of-care CRISPR/Cas12 based lateral flow biosensor for the rapid detection of nucleic acids. *Biosens. Bioelectron.* 159:112143. doi: 10.1016/j.bios.2020.112143
- O'Hara, C. M., Sowers, E. G., Bopp, C. A., Duda, S. B., and Strockbine, N. A. (2003). Accuracy of six commercially available systems for identification of members of the family vibrionaceae. *J. Clin. Microbiol.* 41, 5654–5659. doi: 10.1128/JCM.41.12.5654-5659.2003
- Oliver, J. D. (2015). The Biology of *Vibrio vulnificus*. *Microbiol. Spectr.* 3:3. doi: 10.1128/microbiolspec.VE-0001-2014
- Panicker, G., and Bej, A. K. (2005). Real-Time PCR Detection of *Vibrio vulnificus* in Oysters: Comparison of Oligonucleotide Primers and Probes Targeting *vvhA*. *Appl. Environ. Microb.* 71, 5702–5709. doi: 10.1128/AEM.71.10.5702-5709.2005
- Piepenburg, O., Williams, C. H., Stemple, D. L., and Armes, N. A. (2006). DNA detection using recombination proteins. *PLoS Biol.* 4:e204. doi: 10.1371/journal.pbio.0040204
- Qi, J., Li, X., Zhang, Y., Shen, X., Song, G., Pan, J., et al. (2019). Development of a duplex reverse transcription recombinase-aided amplification assay for respiratory syncytial virus incorporating an internal control. *Arch. Virol.* 164, 1843–1850. doi: 10.1007/s00705-019-04230-z
- Senoh, M., Miyoshi, S., Okamoto, K., Fouz, B., Amaro, C., and Shinoda, S. (2005). The cytotoxin-hemolysin genes of human and eel pathogenic *Vibrio vulnificus* strains: comparison of nucleotide sequences and application to the genetic grouping. *Microbiol. Immunol.* 49, 513–519. doi: 10.1111/j.1348-0421.2005.tb03756.x
- Shapiro, R. L., Altekruze, S., Hutwagner, L., Bishop, R., Hammond, R., Wilson, S., et al. (1998). The role of Gulf Coast oysters harvested in warmer months in *Vibrio vulnificus* infections in the United States, 1988–1996. *J. Infect. Dis.* 178, 752–759. doi: 10.1086/515367
- Heng, S. P., Letchumanan, V., Deng, C. Y., Ab, Mutalib NS, Khan, T. M., Chuah, L. H., et al. (2017). *Vibrio vulnificus*: An Environmental and Clinical Burden. *Front. Microbiol.* 8:997. doi: 10.3389/fmicb.2017.00997
- Surasit, P., Longyant, S., Rukpratanporn, S., Sridulyakul, P., Sithigorngul, P., and Chaivisuthangkura, P. (2011). Rapid and sensitive detection of *Vibrio vulnificus* by loop-mediated isothermal amplification combined with lateral flow dipstick targeted to *rpoS* gene. *Mol. Cell. Probe* 25, 158–163. doi: 10.1016/j.mcp.2011.04.001
- Wang, R., Zhang, F., Wang, L., Qian, W., Qian, C., Wu, J., et al. (2017b). Instant, Visual, and Instrument-Free Method for On-Site Screening of GTS 40-3-2 Soybean Based on Body-Heat Triggered Recombinase Polymerase Amplification. *Anal. Chem.* 89, 4413–4418. doi: 10.1021/acs.analchem.7b00964
- Wang, R., Xiao, X., Chen, Y., Wu, J., Qian, W., Wang, L., et al. (2017a). A loop-mediated, isothermal amplification-based method for visual detection of *Vibrio parahaemolyticus* within only 1 h, from shrimp sampling to results. *Anal. Methods* 9, 1695–1701. doi: 10.1039/C7AY00165G
- Wang, X., Zhong, M., Liu, Y., Ma, P., and Liu, M. (2020). Rapid and sensitive detection of COVID-19 using CRISPR/Cas12a-based detection with naked eye readout, CRISPR/Cas12a-NER. *Sci. Bull.* 65, 1436–1439. doi: 10.1016/j.scib.2020.04.041

- Wright, A. C., Morris, J. G. Jr., Maneval, D. R. Jr., Richardson, K., and Kaper, J. B. (1985). Cloning of the cytotoxin-hemolysin gene of *Vibrio vulnificus*. *Infect. Immun.* 50, 922–924. doi: 10.1128/iai.50.3.922-924.1985
- Yang, X., Zhang, X., Wang, Y., Shen, H., Jiang, G., Dong, J., et al. (2020). A Real-Time Recombinase Polymerase Amplification Method for Rapid Detection of *Vibrio vulnificus* in Seafood. *Front. Microbiol.* 11:586981. doi: 10.3389/fmicb.2020.586981
- Yang, X., Zhao, P., Dong, Y., Chen, S., Shen, H., Jiang, G., et al. (2021). An isothermal recombinase polymerase amplification and lateral flow strip combined method for rapid on-site detection of *Vibrio vulnificus* in raw seafood. *Food Microbiol.* 98:103664. doi: 10.1016/j.fm.2020.103664
- Zhang, M., Liu, C., Shi, Y., Wu, J., and Chen, H. (2020). Selective endpoint visualized detection of *Vibrio parahaemolyticus* with CRISPR/Cas12a assisted PCR using thermal cycler for on-site application. *Talanta* 214:120818. doi: 10.1016/j.talanta.2020.120818

**Conflict of Interest:** The authors declare that the research was conducted in the absence of any commercial or financial relationships that could be construed as a potential conflict of interest.

**Publisher's Note:** All claims expressed in this article are solely those of the authors and do not necessarily represent those of their affiliated organizations, or those of the publisher, the editors and the reviewers. Any product that may be evaluated in this article, or claim that may be made by its manufacturer, is not guaranteed or endorsed by the publisher.

Copyright © 2021 Xiao, Lin, Huang, Lu, Zhou, Zheng and Lou. This is an open-access article distributed under the terms of the Creative Commons Attribution License (CC BY). The use, distribution or reproduction in other forums is permitted, provided the original author(s) and the copyright owner(s) are credited and that the original publication in this journal is cited, in accordance with accepted academic practice. No use, distribution or reproduction is permitted which does not comply with these terms.





## OPEN ACCESS

## Edited by:

Xuejun Ma,  
Chinese Center for Disease Control  
and Prevention, China

## Reviewed by:

Enrique Joffré,  
Karolinska Institutet (KI), Sweden  
Shaofu Qiu,  
Chinese PLA Center for Disease  
Control and Prevention, China

## \*Correspondence:

Yujun Cui  
cuiyujun.new@gmail.com  
Chengsong Wan  
gzwcs@smu.edu.cn  
Qinghua Hu  
huqinghua03@163.com

† These authors have contributed  
equally to this work and share first  
authorship

## Specialty section:

This article was submitted to  
Food Microbiology,  
a section of the journal  
Frontiers in Microbiology

Received: 28 June 2021

Accepted: 08 October 2021

Published: 28 October 2021

## Citation:

Yang C, Li Y, Zuo L, Jiang M,  
Zhang X, Xie L, Luo M, She Y,  
Wang L, Jiang Y, Wu S, Cai R, Shi X,  
Cui Y, Wan C and Hu Q (2021)  
Genomic Epidemiology  
and Antimicrobial Susceptibility Profile  
of Enterotoxigenic *Escherichia coli*  
From Outpatients With Diarrhea  
in Shenzhen, China, 2015–2020.  
Front. Microbiol. 12:732068.  
doi: 10.3389/fmicb.2021.732068

# Genomic Epidemiology and Antimicrobial Susceptibility Profile of Enterotoxigenic *Escherichia coli* From Outpatients With Diarrhea in Shenzhen, China, 2015–2020

Chao Yang<sup>1,2,3†</sup>, Yinghui Li<sup>1†</sup>, Le Zuo<sup>1†</sup>, Min Jiang<sup>1</sup>, Xianglilan Zhang<sup>3</sup>, Li Xie<sup>4</sup>, Miaomiao Luo<sup>5</sup>, Yiyang She<sup>5</sup>, Lei Wang<sup>1</sup>, Yixiang Jiang<sup>1</sup>, Shuang Wu<sup>1</sup>, Rui Cai<sup>1</sup>, Xiaolu Shi<sup>1</sup>, Yujun Cui<sup>3\*</sup>, Chengsong Wan<sup>2\*</sup> and Qinghua Hu<sup>1\*</sup>

<sup>1</sup> Shenzhen Center for Disease Control and Prevention, Shenzhen, China, <sup>2</sup> Department of Microbiology, School of Public Health, Southern Medical University, Guangzhou, China, <sup>3</sup> State Key Laboratory of Pathogen and Biosecurity, Beijing Institute of Microbiology and Epidemiology, Beijing, China, <sup>4</sup> School of Public Health, University of South China, Hengyang, China, <sup>5</sup> School of Public Health, Shanxi Medical University, Taiyuan, China

Enterotoxigenic *Escherichia coli* (ETEC) is the leading cause of severe diarrhea in children and the most common cause of diarrhea in travelers. However, most ETEC infections in Shenzhen, China were from indigenous adults. In this study, we characterized 106 ETEC isolates from indigenous outpatients with diarrhea (77% were adults aged >20 years) in Shenzhen between 2015 and 2020 by whole-genome sequencing and antimicrobial susceptibility testing. Shenzhen ETEC isolates showed a remarkable high diversity, which belonged to four *E. coli* phylogroups (A: 71%, B1: 13%, E: 10%, and D: 6%) and 15 ETEC lineages, with L11 (25%, O159:H34/O159:H43, ST218/ST3153), novel L2/4 (21%, O6:H16, ST48), and L4 (15%, O25:H16, ST1491) being major lineages. Heat-stable toxin (ST) was most prevalent (76%, ST<sub>h</sub>: 60% ST<sub>p</sub>: 16%), followed by heat-labile toxin (LT, 17%) and ST + LT (7%). One or multiple colonization factors (CFs) were identified in 68 (64%) isolates, with the common CFs being CS21 (48%) and CS6 (34%). Antimicrobial resistance mutation/gene profiles of genomes were concordant with the phenotype testing results of 52 representative isolates, which revealed high resistance rate to nalidixic acid (71%), ampicillin (69%), and ampicillin/sulbactam (46%), and demonstrated that the novel L2/4 was a multidrug-resistant lineage. This study provides novel insight into the genomic epidemiology and antimicrobial susceptibility profile of ETEC infections in indigenous adults for the first time, which further improves our understanding on ETEC epidemiology and has implications for the development of vaccine and future surveillance and prevention of ETEC infections.

**Keywords:** enterotoxigenic *Escherichia coli* (ETEC), molecular epidemiology, whole genome sequencing (WGS), virulence factor, antimicrobial resistance (AMR), pathogenicity, public health surveillance

## INTRODUCTION

Enterotoxigenic *Escherichia coli* (ETEC) is the leading cause of severe diarrhea particularly among young children aged less than five in developing countries, and is also the most common cause of diarrhea in travelers to ETEC-endemic areas, accounting for more than 200 million diarrheal cases and 50,000 deaths annually (Khalil et al., 2018; Fleckenstein and Kuhlmann, 2019). ETEC is defined by production of heat-stable toxin (ST) and/or heat-labile toxin (LT), and ST includes two subtypes, human ST (STh) and porcine ST (STp). STh is the most prevalent enterotoxin associated with human diarrhea, while STp is originally isolated from a porcine source and more prevalent in isolates from animals (So et al., 1976, 1978). There is a remarkable genetic diversity of ST and LT, and multiple variants have been identified (Joffré et al., 2015, 2016). In addition to enterotoxins, most ETEC isolates express one or more plasmid-encoded colonization factors (CF), which are fimbrial or afimbrial surface structures that enable adherence to intestinal epithelium. At least 27 known or putative CFs have been identified to date, including a novel CF, CS30 identified by genomic analysis, and the most prevalent CFs are colonization factor antigen I (CFA/I) and *coli* surface antigens 1–6 (CS1–CS6) (Gaastra and Svennerholm, 1996; Nada et al., 2011; von Mentzer et al., 2017; Vidal et al., 2019). Besides the classic virulence factors of enterotoxins and CFs, multiple non-classic virulence factors have been identified in recent years, including a cytoplasmic protein (LeoA), three adhesins (Tia, TibA, and EtpA), an extracytoplasmic protein (CexE), a hemolysin (ClyA), two mucinases (EatA and YghJ), three iron acquisition systems (Irp1, Irp2, and FyuA), and an enteroaggregative heat-stable toxin 1 (EAST1) (Turner et al., 2006; Pilonieta et al., 2007; Del Canto et al., 2011; Gonzales et al., 2013; Luo et al., 2014; Sjöling et al., 2015).

Enterotoxigenic *Escherichia coli* is genetically highly diverse, and more than 100 serotypes have been identified in clinical isolates (Wolf, 1997; Isidean et al., 2011). Multi-locus sequence type (MLST)-based studies showed that ETEC isolates can be found across five *E. coli* phylogroups including A, B1, B2, D, and E, with A and B1 being more prevalent (Turner et al., 2006; Sahl et al., 2011). Whole genome sequencing (WGS) of a large collection of representative global ETEC isolates further identified 21 robust lineages (L1–L21) characterized by distinct enterotoxin and CF profiles, which belonged to phylogroups A (12 lineages), B1 (7 lineages), C (1 lineage), and E (1 lineage) (von Mentzer et al., 2014; Denamur et al., 2021). Despite the diversity, a clear association between lineage and enterotoxin, CF, serotype, and plasmid content was identified. For example, close related lineages L1 and L2 encoded CS1 + CS3 and CS2 + CS3 (with/without CS21), respectively, but shared common enterotoxin profiles (STh + LT) and O antigen (O6) (von Mentzer et al., 2014). In addition, WGS has been used to characterize the epidemiology of ETEC infections in Bangladesh and Chile, and identified remarkable diversity of local circulating phylogroups and lineages. However, the dominant pathogenic phylogroups were distinct, with more Bangladeshi isolates belonging to phylogroup B1 while most Chilean isolates were from phylogroup A (Sahl et al., 2017; Rasko et al., 2019).

With the widespread use of antimicrobial agents, antimicrobial resistance (AMR) has emerged in ETEC isolates from both children and travelers with diarrhea (Qadri et al., 2005). AMR to commonly used agents such as nalidixic acid (NAL), ampicillin (AMP), tetracycline (TET), and sulfonamides has been frequently detected in ETEC isolates in Peru (Rivera et al., 2010), Bangladesh (Begum et al., 2016), South Korea (Oh et al., 2014), and China (Li et al., 2017), and the emergence of extended-spectrum  $\beta$ -lactamase (ESBL)-producing ETEC poses a new challenge to clinical treatment and public health (Margulieux et al., 2018; Guiral et al., 2019). Moreover, high-level and multidrug-resistant (MDR) had developed in ETEC isolates, which might be related to heavy clinical use of antimicrobial agents (Begum et al., 2016; Li et al., 2017). Due to the increased AMR in many areas over time, azithromycin and fluoroquinolones have been used as the first-line drugs for ETEC infections (Xiang et al., 2020). However, azithromycin-resistant ETEC also emerged in multiple countries (Abraham et al., 2014; Begum et al., 2016; Xiang et al., 2020), and is highly prevalent in Shanghai, China (Xiang et al., 2020), highlighting the necessity of ongoing surveillance of AMR, especially to first-line drugs.

While ETEC mainly causes diarrhea among children and travelers, most ETEC infections in Shenzhen, a populous developed city in southern China, were from indigenous adults, and the genomic epidemiology of Shenzhen ETEC isolates remains unclear. In this study, we sequenced the whole genomes of 106 ETEC isolates from indigenous outpatients with diarrhea in Shenzhen between 2015 and 2020, and compared them to a global collection of representative *E. coli* and ETEC genomes (von Mentzer et al., 2014; Horesh et al., 2021), to characterize the genomic diversity and virulence factors of ETEC in Shenzhen. Moreover, we integrated WGS-based *in silico* AMR mutation/gene detection and antimicrobial susceptibility testing to characterize the AMR profiles of Shenzhen ETEC isolates.

## MATERIALS AND METHODS

### Strain Collection

ETEC strains were isolated from stool samples of outpatients with diarrhea in 16 sentinel hospitals in Shenzhen, China during routine foodborne disease surveillance between 2015 and 2020 as previously described (Li et al., 2017). Stool samples were enriched or inoculated on selective medium to isolate common foodborne pathogens, including *Salmonella*, *Shigella*, *Vibrio cholerae*, *Vibrio parahaemolyticus*, *Staphylococcus aureus*, *E. coli* O157:H7, ETEC, enteropathogenic *E. coli*, enteroinvasive *E. coli*, enterohemorrhagic *E. coli*, *Bacillus cereus*, group A *Streptococcus*, and *Listeria monocytogenes*. For ETEC, stool samples were further inoculated on CHROMagar ECC plates and incubated at 37°C overnight. Then, three colonies were randomly selected and inoculated on triple sugar iron agar for incubation and identification by screening ST and LT genes using a modified molecular beacon-based multiplex real-time PCR assay (Chen Q. et al., 2014). ETEC isolates were defined by either ST or LT gene was positive, and a total of 106 ETEC isolates were included in this study.

## Whole Genome Sequencing and Genome Dataset

Genomic DNA was extracted using the QIAamp DNA Mini Kit (QIAGEN, Hilden, Germany) according to manufacturer's instructions. Pair-end libraries with a mean insert size of 350 bp were prepared for sequencing using Illumina NovaSeq 6000 platforms. The average read length is 150 bp, and ~1.2 Gb clean data were generated for each isolate on average. Short-read sequencing data of Shenzhen isolates have been deposited in the NCBI Sequence Read Archive under the BioProject PRJNA739477, and the accession numbers were listed in **Supplementary Table 1**.

A total of 177 genomes were analyzed in this study, including 106 newly sequenced genomes of Shenzhen isolates and 71 publicly available representative genomes. These representative genomes were from the largest 50 *E. coli* lineages (Horesh et al., 2021) and 21 global ETEC lineages (von Mentzer et al., 2014), representing the phylogenetic diversity of *E. coli* and ETEC.

## Genome Assembly, Annotation, and Pan-Genome Analysis

We performed *de novo* assembling of genomes using SPAdes v3.14.1 (Bankevich et al., 2012) and obtained the assembled genomes of 106 ETEC isolates. The average number of contigs and size of assemblies were 123 (61–244, >500 bp) and 5.0 Mb (4.7–5.2), with an average of 102-fold (88–128) depth for each genome.

The assembled genomes were annotated using Prokka (Seemann, 2014) with default settings, and the gene annotation results (GFF3 files) were used in Panaroo (Tonkin-Hill et al., 2020) to identify the pan-genome and generate the matrix of accessory gene presence/absence. Genes presented in ≥99% isolates were defined as core genes, and the other genes were defined as accessory genes. EggNOG-mapper (Huerta-Cepas et al., 2019) was used to annotate the Clusters of Orthologous Groups (COGs) classifications of accessory genes.

## Serotyping and Multi-Locus Sequence Typing

*In silico* serotyping was performed using ECTyper<sup>1</sup> based on assembled genomes. MLST sequence type (MLST-ST) was obtained by scanning the sequences of seven house-keeping genes (*adh*, *fumC*, *gyrB*, *icd*, *mdh*, *purA*, and *recA*) against PubMLST typing schemes using mlst.<sup>2</sup>

## Virulence Factors and Plasmid Detection and Typing

The presence or absence of classic virulence genes (enterotoxins and CFs) and non-classic virulence genes were identified using ABRicate<sup>3</sup> and BLASTN by scanning against the ETEC virulence database<sup>4</sup> and a custom non-classic virulence genes database. We

analyzed a total of 11 non-classic virulence genes, including *leoA* (accession number: AF170971), *tia* (U20318), *tibA* (AF109215), *etpA* (AY920525, position: 2718–8021), *cexE* (LR883053, position: 25424–25792), *clyA* (AY576657, position: 241–1152), *eataA* (AY163491), *yghJ* (DQ866820, position: 322–622), *irp2* (NC\_003143, position: 2156049–2162156), *fyuA* (NC\_003143.1, position: 2140840–2142861), and *astA* (AB042005). A gene was considered present if the overall coverage and identity were larger than 80%.

The ST and LT nucleotide sequences of Shenzhen isolates were extracted from assembled genomes using BLASTN and were aligned against the sequences of previously reported ST and LT variants<sup>5</sup> (Joffré et al., 2015, 2016; von Mentzer et al., 2021) using MAFFT v7.480 (Katoh and Standley, 2013). Multiple sequence alignments were used to construct the maximum likelihood phylogenetic trees, and the ST and LT variants of Shenzhen isolates were determined based on the phylogenetic trees (**Supplementary Figure 1**).

PlasmidFinder v2.1 (Carattoli et al., 2014) was used to detect and determine the incompatibility groups of plasmids based on assembled genomes with default settings.

## Single-Nucleotide Polymorphism Calling and Phylogenetic Analyses

Core-genome (regions present in >99% strains) single-nucleotide polymorphisms (SNPs) were identified using Snippy v4.6.0 pipeline,<sup>6</sup> with *E. coli* K12 (accession number: NC\_000913) as the reference genome. Briefly, for each isolate, clean sequencing reads were mapped to reference genome using BWA-mem (Li and Durbin, 2009), and SNPs were called using SAMtools (Li et al., 2009) and FreeBayes (Garrison and Marth, 2012). Repetitive regions of the reference genome were identified using Tandem Repeats Finder (TRF) (Benson, 1999) and by self-aligning using BLASTN as previously described (Yang et al., 2019). SNPs located in repetitive regions were removed prior to phylogenetic analysis. The maximum likelihood trees based on non-repetitive core-genome SNPs and alignments of ST and LT nucleotide sequences were constructed using IQ-TREE v2.0.3 (Minh et al., 2020) with auto-detected best-fitting substitution model, respectively.

## Antimicrobial Resistance Mutation/Gene Detection and Phenotype Testing

ResFinder 4.1 (Bortolaia et al., 2020) was used to detect the AMR related mutations and genes based on clean sequencing reads with default settings. Based on the lineage classification and AMR mutation/gene distribution, we selected 52 representative isolates for AMR phenotype testing. The susceptibilities of the representative isolates were determined using disc diffusion assay against 17 antimicrobial agents, including NAL, AMP, TET, ampicillin/sulbactam (AMS), cefotaxime (CTX), trimethoprim/sulfamethoxazole (SXT), azithromycin (AZI), streptomycin (STR), ciprofloxacin (CIP),

<sup>1</sup>[https://github.com/phac-nml/ecoli\\_serotyping](https://github.com/phac-nml/ecoli_serotyping)

<sup>2</sup><https://github.com/tseemann/mlst>

<sup>3</sup><https://github.com/tseemann/abricate>

<sup>4</sup>[https://github.com/avonm/ETEC\\_vir\\_db/](https://github.com/avonm/ETEC_vir_db/)

<sup>5</sup>[https://github.com/avonm/ETEC\\_toxin\\_variants\\_db](https://github.com/avonm/ETEC_toxin_variants_db)

<sup>6</sup><https://github.com/tseemann/snippy>



ceftazidime (CAZ), amikacin (AMK), chloramphenicol (CHL), colistin (CT), ceftazidime/avibactam (CZA), ertapenem (ETP), meropenem (MEM), and tigecycline (TGC). Breakpoints for sensitive, intermediate, and resistant were defined by the Clinical and Laboratory Standards Institute (CLSI) document M100-S26, and *E. coli* ATCC25922 was used as the control. ESBL-producing isolates were identified by assessing susceptibility phenotype to CTX, CAZ, and CZA.

## RESULTS

### Demographic and Clinical Symptom Characteristics

A total of 106 ETEC isolates from indigenous outpatients with diarrhea collected during routine foodborne disease surveillance between 2015 and 2020 were included in this study (Supplementary Table 1). These outpatients had a median age of 27 years (interquartile range: 21–36), of which only seven (7%) was children aged <5 years and 82 (77%) were adults aged >20 years. There were more males (51%, 54/106) than females (49%, 52/106), and the clinical symptoms included diarrhea (95%, 100/106), abdominal pain (29%, 31/106), vomiting (8%, 9/106), and fever (8%, 9/106).

### *Escherichia coli* Phylogroup and Enterotoxigenic *Escherichia coli* Lineage

To investigate the *E. coli* phylogroup and ETEC lineage classification of Shenzhen isolates, we compared the 106 Shenzhen isolates to 71 representative isolates from the largest 50 *E. coli* lineages (Horeish et al., 2021) and 21 global ETEC lineages (von Mentzer et al., 2014), and constructed a maximum-likelihood (ML) tree of 177 isolates based on 267,822 SNPs in the core-genome (Figure 1). Shenzhen isolates showed a remarkably high diversity, which can be attributed to four *E. coli* phylogroups and 15 ETEC lineages (Table 1 and Figure 1). The majority of Shenzhen isolates belonged to phylogroup A (71%, 75/106), and the remaining were assigned into phylogroup B1 (13%, 14/106), D (6%, 6/106), and E (10%, 11/106). Phylogroup A can be further divided into eight ETEC lineages, and lineage L11 (25%, 26/106), a novel lineage L2/4 (between L2 and L4, 21%, 22/106, Figure 1), and L4 (15%, 16/106) were major circulating lineages. Phylogroup B1 can be divided into five lineages (L5, L8, and L17–L19) each with few isolates ( $n \leq 3$ ), and D and E each contained one lineage, a novel lineage L-N1 ( $n = 6$ ) and L7 ( $n = 11$ ), respectively (Figure 1).

Phylogroup A has always been dominant during the 6-year sampling period, while the fractions of other phylogroups were variable. At the end of sampling in 2020, only two phylogroups A and B1 persisted (Figure 2A). The fractions of different ETEC lineages were also variable. Lineage L11 was dominant before 2016; since 2017, multiple lineages coexisted and no obvious dominant lineage was identified (Figure 2B).

### Serotype and Sequence Type

To compare with traditional subtyping results, we performed *in silico* serotyping and MLST-ST based on assembled genome sequences. There was a close association of ETEC lineage with serotype and MLST-ST, with isolates within a lineage belonging to 1–2 serotypes or STs (Table 1). The most prevalent serotype was O6:H16 (26%, 28/106), followed by O159:H34 (21%, 22/106) and O25:H16 (15%, 16/106). The most prevalent MLST-ST was ST48 (21%, 22/106), followed by ST218 (19%, 20/106) and ST1491 (15%, 16/106). The serotype and MLST-ST of three major lineages were O159:H34/O159:H43 and ST218/ST3153 for L11, O6:H16 and ST48 for L2/4, and O25:H16 and ST1491 for L4 (Table 1).

### Virulence Factors

Heat-stable toxin (ST)-positive ETEC has been most prevalent (76%, 81/106) in Shenzhen throughout the sampling period (Figure 2C), followed by LT-positive ETEC (17%, 18/106). ST and LT-positive ETEC was only detected in seven isolates (7%) in three of the 6-year sampling period. Among ST-positive ETEC, STh-positive isolates (60%, 64/106) was more prevalent than STp-positive ones (16%, 17/106) throughout the sampling period (Figure 2C). More specifically, the most prevalent ST variant was STa3/4 (57%, 60/106), followed by STa5 (15%, 16/106) and STa7 (8%, 9/106); the most prevalent LT variant was LT17 (15%, 16/106). Two novel variants of STp and LT, designated as STa8 and LT29, were identified in one isolate, respectively (Table 1, Supplementary Table 1, and Supplementary Figure 1).

One to three known CFs were identified in 68 (64%) Shenzhen isolates. The most prevalent CF was CS21 (48%, 51/106, with or without other CFs), followed by CS6 (34%, 36/106) throughout the sampling period (Figure 2D). Except CS21 and CS6, the fraction of other CFs was low and they were only detected in 3 years. The most prevalent combination was CS6 + CS21 (18%, 19/106).

In addition to enterotoxins and CFs, 10 of 11 detected non-classic virulence genes were identified in Shenzhen isolates with different frequencies (2–100%, Table 1 and Supplementary Table 1). The hemolysin gene *clyA* (100%, 106/106) and mucinase gene *yghJ* (97%, 103/106) were most prevalent in Shenzhen isolates, followed by enteroaggregative heat-stable toxin gene *astA* (75%, 79/106), adhesion gene *etpA* (63%, 67/106), and another mucinase gene *eatA* (30%, 32/106). The other five non-classic virulence genes were detected with low frequencies (2–8%). Co-presence of classic and non-classic virulence genes was identified. The *etpA* (94%, 60/64) and *astA* (91%, 58/64) genes were mostly detected along with STh, and *eatA* (89%, 16/18) gene was mostly detected along with LT.

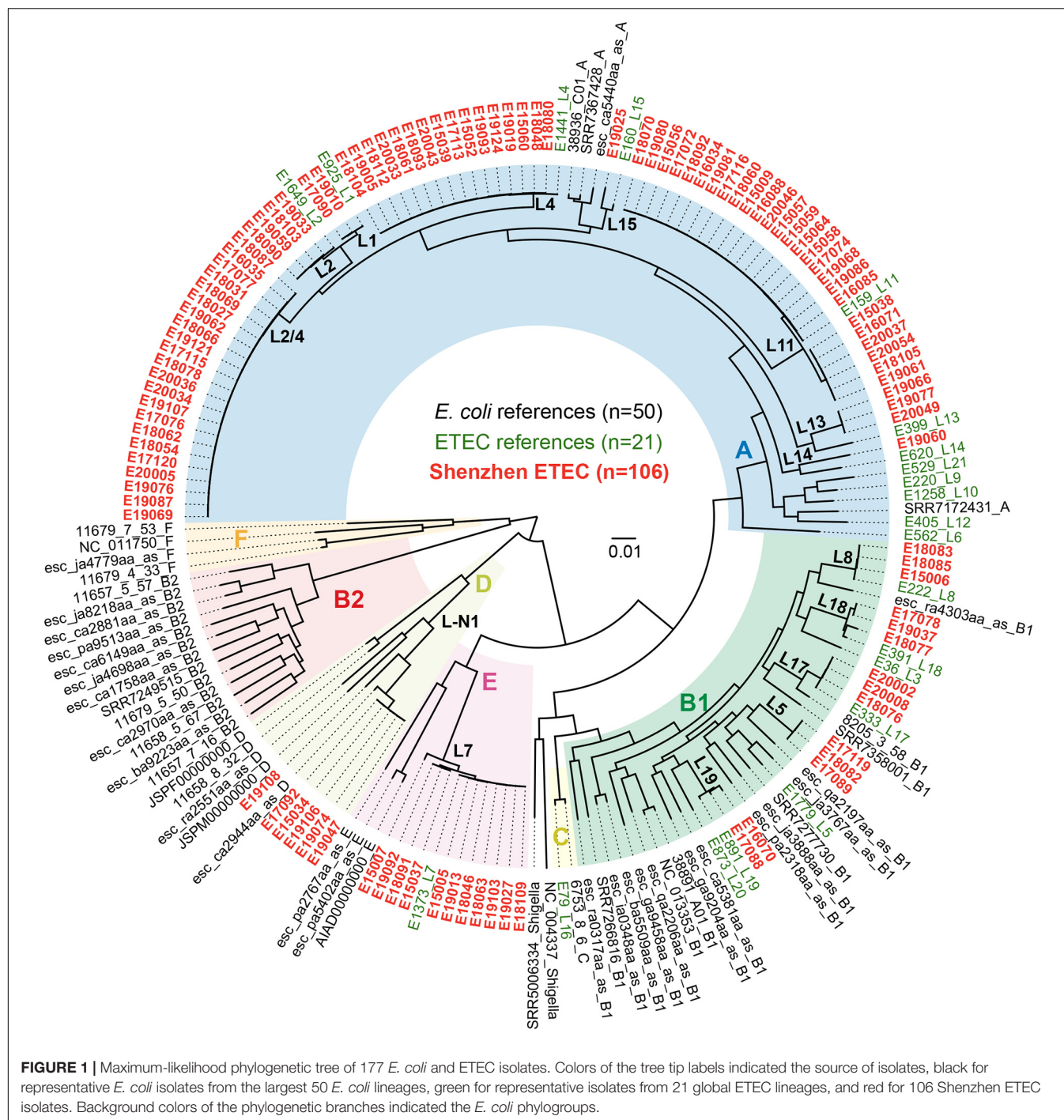
The distribution of classic and non-classic virulence genes in different lineages was shown in Table 1 and Supplementary Table 1. Twelve (80%) of 15 lineages were ST-positive (53%, 8/15) or contained ST-positive isolates (27%, 4/15), and STh-positive lineages (40%, 6/15) or lineages containing STh-positive isolates (20%, 3/15) were more prevalent than STp-positive lineages (13%, 2/15) or lineages containing STp-positive isolates (13%, 2/15). CFs were detected in 11 lineages (73%), and the most prevalent CFs, CS21, and CS6 were detected in seven (47%) and



**TABLE 1** | Classification, enterotoxin, and colonization factor distribution of 106 ETEC isolates in Shenzhen, 2015–2020.

<i>E. coli</i> phylogroup	ETEC lineage	No. of isolates	Serotype <sup>1</sup>	Sequence type (ST) <sup>1</sup>	Enterotoxin variant	Colonization factor	Non-classic virulence genes	Plasmid incompatibility groups
A ( <i>n</i> = 75)	L1	2	O6:H16	ST6955	STh (STa3/4) + LT (LT20)	CS1 + CS3 + CS21	<i>tia</i> , <i>etpA</i> , <i>cexE</i> , <i>clyA</i> , <i>eatA</i> , <i>yghJ</i> , <i>astA</i>	FII, FIB, I1 ( <i>n</i> = 1); FII, FIB, I1, B/O/K/Z ( <i>n</i> = 1)
	L2	4	O6:H16	ST4	STh (STa3/4) + LT (LT20)	CS2 + CS3 + CS21	<i>etpA</i> , <i>clyA</i> , <i>eatA</i> , <i>yghJ</i> , <i>astA</i>	FII, FIB ( <i>n</i> = 2); FII, FIB, I2 ( <i>n</i> = 3)
	L2/4	22	O6:H16	ST48	STh (STa3/4, <i>n</i> = 21); STp (STa1, <i>n</i> = 1)	CS21 ( <i>n</i> = 21)	<i>etpA</i> , <i>clyA</i> , <i>yghJ</i> , <i>astA</i> ( <i>n</i> = 21); <i>etpA</i> , <i>clyA</i> , <i>eatA</i> , <i>yghJ</i> , <i>astA</i> ( <i>n</i> = 1)	FII, FIB, I1 ( <i>n</i> = 18); FII, FIB ( <i>n</i> = 1); FII, FIB, I1, B/O/K/Z ( <i>n</i> = 1); FII, I1, N ( <i>n</i> = 1)
	L4	16	O25:H16	ST1491	LT (LT17)	CS6 + CS21	<i>clyA</i> , <i>eatA</i> , <i>yghJ</i>	FII, FIB ( <i>n</i> = 4); FII, FIB, B/O/K/Z ( <i>n</i> = 6); FII, FIB, B/O/K/Z, Y ( <i>n</i> = 1); FII, FIB, I1 ( <i>n</i> = 1)
	L11	26	O159:H34 ( <i>n</i> = 20); O159:H43 ( <i>n</i> = 6)	ST218 ( <i>n</i> = 20), ST3153 ( <i>n</i> = 6)	STh (STa3/4)		<i>etpA</i> , <i>clyA</i> , <i>yghJ</i> , <i>astA</i>	FII ( <i>n</i> = 13); FII, B/O/K/Z ( <i>n</i> = 7); FII, I1 ( <i>n</i> = 6)
	L13	3	O-:H10	ST226	STh (STa3/4)		<i>etpA</i> , <i>clyA</i> , <i>yghJ</i> , <i>astA</i>	FII, I1
	L14	1	O25:H42	ST1201	STh (STa2)	CS4 + CS6	<i>clyA</i> , <i>eatA</i> , <i>yghJ</i> , <i>astA</i>	FII, FIB, B/O/K/Z
	L15	1	O107/117:H27	ST10	STh (STa7)	CS21	<i>etpA</i> , <i>clyA</i> , <i>eatA</i> , <i>yghJ</i>	FII, FIB
	L5	3	O159:H20	ST2040	STh (STa3/4)		<i>etpA</i> , <i>clyA</i> , <i>yghJ</i> , <i>astA</i>	FII, B/O/K/Z
	L8	3	O148:H28	ST94	STh (STa7)	CS6 + CS21	<i>clyA</i> , <i>astA</i>	FII, FIB
B1 ( <i>n</i> = 14)	L17	3	O27:H7	ST316	STp (STa5)	CS6	<i>clyA</i> , <i>yghJ</i>	FII, FIB
	L18	3	O159:H34 ( <i>n</i> = 2); O23:H16 ( <i>n</i> = 1)	ST1490 ( <i>n</i> = 2), ST- ( <i>n</i> = 1)	STp ( <i>n</i> = 2, STa5), LT ( <i>n</i> = 1, LT29)	CS6 + CS23 ( <i>n</i> = 2)	<i>clyA</i> , <i>eatA</i> , <i>yghJ</i> , <i>astA</i>	FII, FIB
	L19	2	O29:H12 ( <i>n</i> = 1); O153:H12 ( <i>n</i> = 1)	ST155	STh ( <i>n</i> = 1, STa3/4), LT ( <i>n</i> = 1, LT15)		<i>etpA</i> , <i>clyA</i> , <i>yghJ</i> , <i>astA</i> ( <i>n</i> = 1); <i>clyA</i> , <i>yghJ</i> ( <i>n</i> = 1)	FII ( <i>n</i> = 1); FII, FIB ( <i>n</i> = 1)
	L-N1	6	O15:H18 ( <i>n</i> = 5); O-/H18 ( <i>n</i> = 1)	ST69 ( <i>n</i> = 5), ST1380 ( <i>n</i> = 1)	STh ( <i>n</i> = 5, STa7), STp + LT (STa8 + LT4, <i>n</i> = 1)	CS21 ( <i>n</i> = 4)	<i>etpA</i> , <i>clyA</i> , <i>eatA</i> , <i>yghJ</i> , <i>irp2</i> , <i>fyuA</i> ( <i>n</i> = 5); <i>clyA</i> , <i>yghJ</i> , <i>astA</i> ( <i>n</i> = 1)	FII, FIB ( <i>n</i> = 4); FII ( <i>n</i> = 1); FII, FIB, B/O/K/Z, FIA ( <i>n</i> = 1)
D ( <i>n</i> = 6)								
E ( <i>n</i> = 11)	L7	11	O169:H41 ( <i>n</i> = 10); O167:H41 ( <i>n</i> = 1)	ST182 ( <i>n</i> = 10), ST3930 ( <i>n</i> = 1)	STp (STa5)	CS6	<i>leoA</i> , <i>tia</i> , <i>clyA</i> , <i>yghJ</i> , <i>astA</i> ( <i>n</i> = 7); <i>clyA</i> , <i>yghJ</i> , <i>astA</i> ( <i>n</i> = 4)	FII, FIB

<sup>1</sup> Untypeable serotype O and MLST sequence type was denoted by O- and ST-, respectively.



six (40%) lineages, respectively. Except two prevalent non-classic virulence genes *clyA* and *yghJ*, *astA*, *etpA*, and *eatA* genes were detected in 12 (80%), 9 (60%), and 8 (53%) lineages, respectively.

In addition to the association between lineage and serotype and MLST-ST, the association of lineage with enterotoxin and CF was also identified. Most isolates within a lineage shared identical virulence gene (classic and non-classic) profiles, except for five lineages (L2/4, L7, L18, L19, and L-N1) in which two or three types of virulence gene combinations were detected. In

contrast, the virulence gene profiles of different lineages were largely distinct (Table 1 and Supplementary Table 1).

### Plasmid Incompatibility Groups

*In silico* plasmid typing analysis identified replicons belonging to eight incompatibility (Inc) groups in all the 106 Shenzhen isolates, with one to four Inc groups present in each isolate (Table 1 and Supplementary Table 1). The replicon IncFII was most prevalent and can be detected in all Shenzhen isolates,

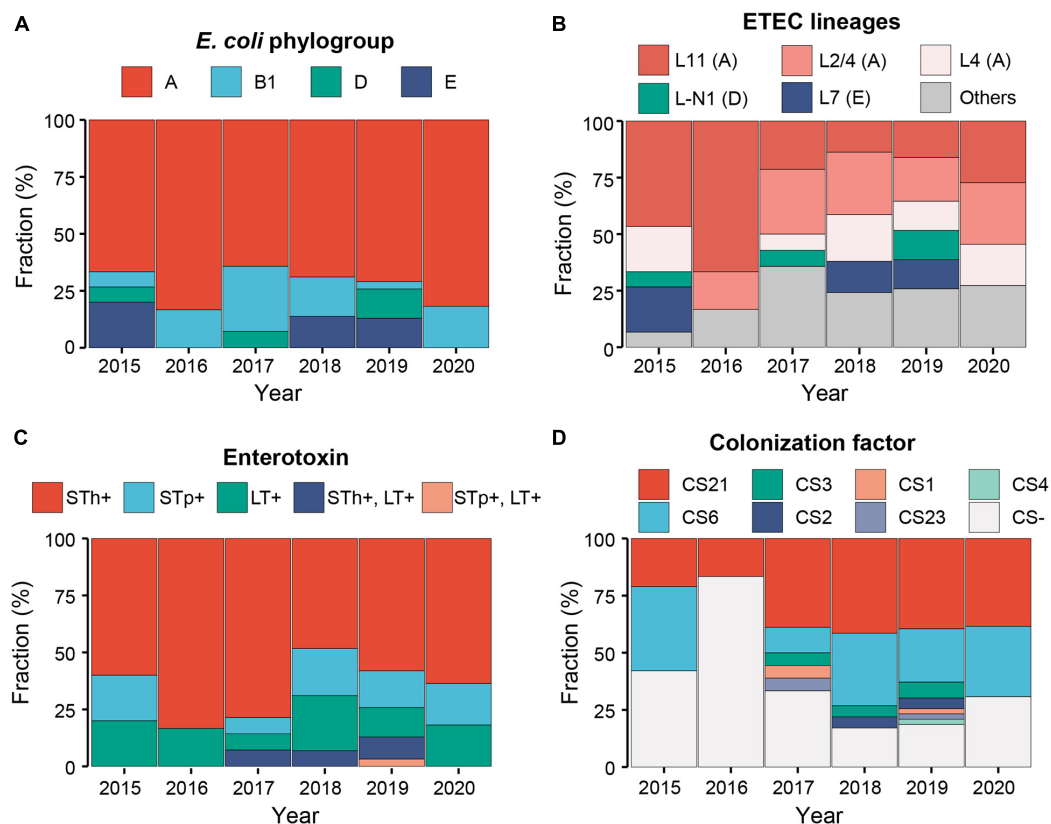


**FIGURE 2 |** Temporal dynamics of the *E. coli* phylogroups (A), ETEC lineages (B), enterotoxins (C), and colonization factors (D) of Shenzhen isolates during the 6-year sampling period. Colors indicated different classifications as shown in the legends above.

followed by IncFIB (67%, 71/106), IncI1 (31%, 33/106), and IncB/O/K/Z (20%, 21/106); the other replicons (IncFIA, IncI2, LncN, and LncY) were only detected in one isolate, respectively. There was an association between the replication IncFIB and virulence gene CS21, and 72% (51/71) IncFII-positive isolates also encode CS21. Only one type of replicon profile was identified in eight lineages, and the other seven lineages each contained two to four types of replicon profiles (Table 1 and Supplementary Table 1).

## Pan-Genome Analysis

We performed pan-genome analysis of 127 ETEC genomes of Shenzhen isolates ( $n = 106$ ) and globally representative isolates ( $n = 21$ ) to identify genes unique to or significantly associated with Shenzhen isolates. A total of 11,813 pan-genes were identified in these 127 genomes, including 3,307 core-genes (present in  $\geq 99\%$  isolates) and 8,506 accessory genes. There were no genes unique to Shenzhen or non-Shenzhen isolates; however, we identified significant differences ( $p < 0.01$ , Fisher's exact tests) in the frequencies of 589 accessory genes between Shenzhen and non-Shenzhen isolates (Supplementary Table 2). There were 178 accessory genes significantly enriched in Shenzhen isolates, of which two were known virulence genes STh and *etpA*, and the other genes encoded hypothetical proteins with unknown functions (46%) or were associated

with replication and repair (COG category L; 37%) and cell wall/membrane/envelop biogenesis (COG category M; 19%). For example, STh was present in 66% Shenzhen isolates and 29% non-Shenzhen isolates, respectively; the gene *group\_4545* encoding a hypothetical protein was present in 91% Shenzhen isolates but in only 19% non-Shenzhen isolates. In addition, there were 411 accessory genes significantly enriched in non-Shenzhen isolates including the virulence gene LT (Supplementary Table 2).

We further attempted to identify genes unique to two novel lineages L2/4 and L-N1. A total of 25 L2/4 lineage unique genes were identified (Supplementary Table 3), of which 76% encoded hypothetical proteins and 20% were associated with replication and repair (COG category L). There were 105 genes unique to L-N1 lineage (Supplementary Table 3), of which 72% encoded hypothetical proteins, 10% were associated with cell motility (COG category N) and intracellular trafficking and secretion (COG category U), and 5% were associated with transcription (COG category K). None of these L2/4 and L-N1 lineage unique genes were known ETEC virulence genes.

## Antimicrobial Susceptibility

To characterize the AMR profiles of Shenzhen isolates, we firstly scanned the genomes to identify AMR related mutations and genes. A total of 21 AMR mutations/genes were detected (Figure 3), which were involved in resistance to

five classes of antimicrobial agents, including fluoroquinolone (two mutations and two genes), beta-lactam (seven genes), tetracycline (two genes), macrolide (one gene), and folate pathway antagonist (seven genes).

Fluoroquinolone resistance mutations/genes were most prevalent, which were detected in 99 (93%) isolates. For example, DNA gyrase gene *gyrA* p.S83L mutation and quinolone resistance gene *qnrS1* were detected in 63 (59%) and 37 (35%) isolates, respectively. Beta-lactam resistance genes ranked second and were detected in 63 (59%) isolates, of which *bla<sub>TEM-1B</sub>* and *bla<sub>CTX-M-15</sub>* were more prevalent and were detected in 40 (38%) and 18 (17%) isolates, respectively. Tetracycline resistance genes were detected in 34 (32%) isolates, of which *tet(A)* and *tet(B)* were detected in 24 (23%) and 11 (10%) isolates, respectively. A macrolide resistance gene *mph(A)* was detected in 29 (27%) isolates. Notably, this gene has been reported to mediate azithromycin resistance, which is usually less frequent in ETEC (Xiang et al., 2020). Folate pathway antagonist resistance genes, including *sul1*, *sul2*, *dfrA1*, *dfrA8*, *dfrA14*, *dfrA15*, and *dfrA17* were detected in 22 (21%) isolates, and each gene appeared in 3–13 isolates.

Unlike the close association of lineage with serotype, MLST-ST and virulence factors, there was no obvious association between lineages and most AMR mutations/genes, with multiple AMR mutations/genes combinations being identified in isolates of a lineage (Figure 3). Notably, most isolates of two major lineages L11 and L2/4 had *gyrA* p.S83L mutations, and all the L2/4 lineage isolates also carried *bla<sub>TEM-1B</sub>* and *mph(A)* genes.

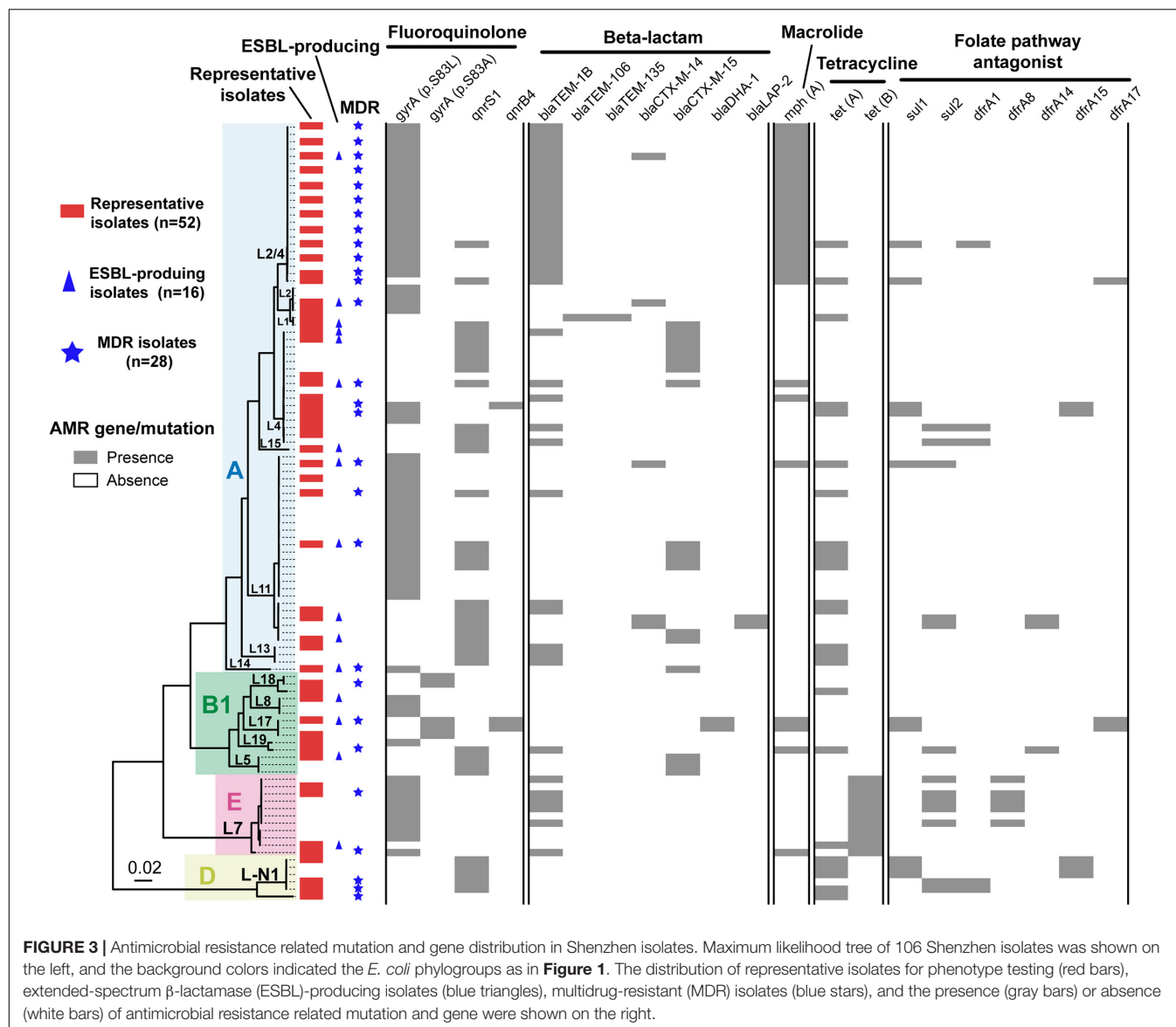
We further selected 52 isolates representing all the lineages and AMR mutations/genes combinations for AMR phenotype testing against 17 antimicrobial agents (Table 2 and Figure 3). AMR mutations/genes distributions were generally concordant with phenotype testing results. The resistance to a quinolone agent, NAL was highest (71%, 37/52) in Shenzhen isolates, and 78% (29/37) of them carried *gyrA* (p.S83L or p.S83A) mutations. However, only two (4%) isolates were resistant to another quinolone agent ciprofloxacin. The resistance to beta-lactam agents, including AMP (69%, 36/52), AMS (46%, 24/52), and CTX (31%, 16/52) was also prevalent. Sixteen (31%) representative isolates were identified as ESBL-producing, of which 81% (13/16) encode at least one type of  $\beta$ -lactamase associated gene, with *bla<sub>CTX-M-15</sub>* (50%, 8/16) and *bla<sub>CTX-M-14</sub>* (25%, 4/16) being most common. In addition, the resistance to other three classes of antimicrobial agents were detected, including AZI (38%, 20/52, macrolide class), TET (37%, 19/52, tetracycline class), and SXT (29%, 15/52, folate pathway antagonist class). There was a close association between azithromycin resistance and the presence of *mph(A)* gene, with 18 of 20 azithromycin-resistant isolates encoding *mph(A)*. No resistance to seven antimicrobial agents was detected, including AMK, CHL, CT, CZA, ETP, MEM, and TGC. All (12/12) the tested representative L2/4 lineage isolates were resistant to at least three classes of agents, i.e., multidrug-resistant (MDR); 16 (40%) of 40 representative isolates of non-L2/4 lineages were MDR (Table 2 and Figure 3).

## DISCUSSION

Despite the high prevalence in children and travelers, ETEC also lead to substantial infections in adults in endemic areas (Lamberti et al., 2014). Moreover, it is intriguing that most ETEC infections in Shenzhen (Li et al., 2017), as well as several other developed cities and province in China (Chen Y. et al., 2014; Qu et al., 2014; Pan et al., 2015), such as Beijing and Shanghai, were from indigenous adults. However, there is currently a lack of understanding on the epidemiology of ETEC infections in indigenous adults. Compared to traditional molecular subtyping methods, WGS not only provides the ultimate resolution on reconstruction the relationships between isolates, but also can be used for secondary in-depth virulence factors and AMR genes analysis, which has been one of the most powerful methods to characterize the epidemiology of pathogens (Didelot et al., 2012; Allard et al., 2016; Ronholm et al., 2016). We reconstructed the WGS-based population structure of Shenzhen isolates in the context of global ETEC and *E. coli* lineages, and linked the genomic diversity to traditional subtyping results based on serotyping and MLST-ST. In addition, we characterized the virulence factors, AMR mutation/gene and phenotype profiles of Shenzhen isolates. To our knowledge, this is the first study on the genomic epidemiology and AMR profile of ETEC infections in indigenous adults.

Shenzhen ETEC isolates showed a remarkable diversity, which can be attributed to four *E. coli* phylogroups, with the majority falling into phylogroup A (71%). The phylogroup distribution is different from that of global (von Mentzer et al., 2014) and Bangladeshi (Sahl et al., 2017) isolates [high fraction (>40%) of B1 isolates], and is similar to that of Chilean isolates (phylogroup A: 81%) (Rasko et al., 2019). More specifically, three major lineages, L11 (25%), L2/4 (21%), and L4 (15%), persisted in Shenzhen throughout the 6-year sampling period, together accounting for 60% cases. L11 can be detected in children aged <5 years and adult travelers from multiple countries, but at a low fraction (4%) in the global dataset (von Mentzer et al., 2014). If taken serotype and MLST-ST into consideration, L11 (O159:H34, ST218) isolates was only identified in local diarrheal cases of Korea (Chung et al., 2019) and China (Chen Y. et al., 2014; Pan et al., 2015; Li et al., 2017), and the virulence factor profiles (STh+, without known CS) of isolates from two countries were identical, indicating the possibility of recent transmission. L2/4 was a previously undefined lineage, which located between L2 and L4 in the phylogenetic tree. However, it had a different virulence factor profile (STh: 21/22, STp: 1/22, CS21: 22/22) from L2 (global dataset: STh + LT, CS2 + CS3  $\pm$  CS21) or L4 (global dataset: STh/LT, CS6  $\pm$  CS21/CS6 + CS8/CS21). The serotype and MLST-ST of L2/4 was O6:H16 and ST48, respectively, and ETEC isolates with this subtyping combination were previously identified from pigs in Denmark (García et al., 2020) and from human cases in China (Chen Y. et al., 2014; Li et al., 2017). However, no CF was reported in Danish isolates whereas all Shenzhen isolates carried CS21. L4 lineage was also detected at low fraction (6%) in the global dataset (von Mentzer et al., 2014), and the subtyping combination of Shenzhen isolates, i.e., L4 (O25:H16, ST1491), was only identified in isolates from few travelers returning to the





UK (Boxall et al., 2020) and from local diarrheal cases of China (Chen Y. et al., 2014; Pan et al., 2015; Li et al., 2017). Taken together, these results revealed that the major circulating ETEC lineages in Shenzhen, as well as in several other developed regions of China were distinctive, which are not the commonly detected global or endemic lineages.

In addition to subtyping, the virulence factor profile of Shenzhen and other Chinese ETEC isolates was also distinctive. ST-positive ETEC has been dominant (76%) in Shenzhen throughout the sampling period and 80% circulating lineages were ST-positive (53%) or contained ST-positive isolates (27%), whereas the fractions of LT-positive and ST + LT-positive isolates and lineages were lower. CS21 was the most prevalent CF (48%) in Shenzhen isolates, followed by CS6 (34%). Similar virulence factor profile was also observed in ETEC isolates from diarrheal cases in Shanghai, China (ST: 74%, CS21: 63%,

CS6: 41%) (Pan et al., 2015). In contrast, a systematic review showed that globally, ST-positive, LT-positive, and ST + LT-positive ETEC accounted for 50, 25, and 27% non-travel human infections, respectively, and the most prevalent CFs were CFA/I, followed by CS21 and CS6 (Isidean et al., 2011). There was a considerable variability of virulence factor profiles across regions and populations. High ST-prevalence was only observed among travelers in East Asia/Pacific (75%) and non-travelers in Europe/Central Asia (77%), however, the most prevalent CF in East Asia/Pacific was CFA/I and CS21 was rarely detected (CF-prevalence in Europe/Central Asia is unavailable) (Isidean et al., 2011). Interestingly, CS21 was most prevalent CFs in ETEC-endemic regions including Latin America/Caribbean and the Middle East/North Africa, and among global travelers with a frequency of ~22% (Isidean et al., 2011). Notably, the most commonly detected CF globally, CFA/I, was not identified in

**TABLE 2** | Antimicrobial resistance of 52 representative Shenzhen ETEC isolates.

Antimicrobial agent <sup>1</sup>	Antimicrobial resistance rate (%)						Total (n = 52)
	L11 (n = 7)	L2/4 (n = 12)	L4 (n = 10)	L7 (n = 4)	L-N1 (n = 4)	Other <sup>2</sup> (n = 15)	
NAL	71	92	60	75	50	67	71
AMP	86	100	40	75	25	67	69
AMS	29	100	20	25	0	47	46
AZI	14	100	20	25	0	27	38
TET	43	50	20	100	100	27	37
CTX	57	25	30	25	0	47	31
SXT	14	50	30	25	75	33	29
STR	43	25	0	25	50	20	19
CIP	0	0	10	0	0	7	4
CAZ	0	0	0	0	0	7	2
ESBL	57	8	30	25	0	47	31
MDR	43	100	30	50	75	33	54

<sup>1</sup>Only 10 of 17 antimicrobial agents with at least one resistant isolate were shown. <sup>2</sup>Lineages with <3 isolates together were defined as others. NAL, nalidixic acid; AMP, ampicillin; TET, tetracycline; AMS, ampicillin/sulbactam; CTX, cefotaxime; SXT, trimethoprim/sulfamethoxazole; AZI, azithromycin; STR, streptomycin; CIP, ciprofloxacin; CAZ, ceftazidime. ESBL, extended-spectrum  $\beta$ -lactamase; MDR, multidrug-resistant, defined as resistant to  $\geq 3$  classes of antimicrobial agents.

Shenzhen isolates. Moreover, a recent Global Enteric Multicenter Study (GEMS) report (Vidal et al., 2019) showed that the prevalence of ST, LT, and ST + LT among ETEC isolates from children aged <5 years with moderate-to-severe diarrhea in Africa and Asia were 36, 32, and 32%, respectively; the prevalence from the matched controls were 21, 47, and 33%, respectively. The most commonly detected CFs were CFA/IV (CS6 alone or with CS4 or CS5), CS5 + CS6, and CFA/I. Among all the sampling sites of this study, ST-positive ETEC isolates were not dominant (<50%), and CS21 was rarely detected (<2%). More specifically, the most prevalent ST variants in Shenzhen isolates were STa3/4 and STa5, which were consistent with that in global isolates (Joffré et al., 2016). However, the most prevalent LT variant in Shenzhen isolates was LT17. By contrast, the most prevalent LT variant in global isolates was LT1 (41%), while LT17 was rarely detected (2.1%) (Joffré et al., 2015).

The unique ETEC epidemiology in Shenzhen and China, i.e., most infections were from indigenous adults, might be related to several reasons. First, the pathogenicity of China ETEC isolates may be higher in adults than in children, given the distinctive lineage and virulence factor profiles. This hypothesis was supported by the observation in Guatemala (Torres et al., 2015), where ST-positive ETEC infections were significantly more prevalent in adult travelers compared to indigenous children, suggesting higher pathogenicity of ST-positive ETEC in adults, whereas most Chinese ETEC isolates were ST-positive. Moreover, a recent study showed that a ST enterotoxin variant STa5 was associated with ETEC infections in adults, suggesting that specific type of ETEC may have higher pathogenicity in adults (Joffré et al., 2016). However, the prevalence of STa5 variant in Shenzhen isolates was only 15%, indicating the existence of other known/unknown virulence genes associated with ETEC infections in adults. We identified multiple accessory genes significantly enriched in Shenzhen isolates by pan-genome analysis including the known virulence genes ST<sub>h</sub> and *etpA*, which provides candidate targets for further

studies. Second, different characterization between children and adult populations, such as eating habits and immunity, may also be associated with the unique ETEC epidemiology. For example, a study showed that dietary calcium can improve human resistance to ETEC infection (Bovee-Oudenhoven et al., 2003), while children usually tend to consume more calcium than the adult population. Besides, it has been reported that breastfeeding may protect infants against severe ETEC infection (Clemens et al., 1997). Furthermore, eating out is a major risk factor of foodborne disease (Liu et al., 2018), and the frequency in the adult population is usually higher than that in children. In addition, the immunity provided by previous ETEC infection or vaccine may decrease over age, leading to more ETEC infections in adults.

Characterizing the antibiotic susceptibility profile of ETEC would be helpful to guide the clinical treatment. In this study, we investigated the AMR mutation/genes and phenotype of Shenzhen ETEC isolates by integrating WGS-based analysis and antimicrobial susceptibility testing. AMR mutation/gene profile was generally concordant with the phenotype testing results of 52 representative isolates, which revealed high resistance rate to NAL (71%), AMP (69%), and AMS (46%). In recent years, high resistance of ETEC to these commonly used agents was also reported in multiple other countries including Peru (Rivera et al., 2010), Bangladesh (Begum et al., 2016), South Korea (Oh et al., 2014), and in other cities of China (Chen Y. et al., 2014; Pan et al., 2015). Due to the increased AMR, new antimicrobial agents such as azithromycin have been used as the first-line agent for ETEC infection treatment. Azithromycin is a broad-spectrum macrolide antimicrobial agent against several bacterial species, and is very effective for *Enterobacteriaceae* infection treatment (Gomes et al., 2019). However, azithromycin-resistant ETEC isolates from diarrheal patients have recently been reported in several countries at a moderate frequency (10–30%) (Begum et al., 2016; Guiral et al., 2019), and in Shanghai, China at a very high frequency (87%) (Xiang et al., 2020). Macrolides inactivation mediated by macrolide-resistant phosphotransferase *mph(A)*

gene was the most common mechanism for the azithromycin resistance (Gomes et al., 2019; Xiang et al., 2020). We found that 38% representative Shenzhen ETEC isolates were resistant to azithromycin, and most of these isolates carried *mph(A)* gene. Moreover, we showed that the prevalence of ESBL-producing ETEC isolates from outpatients was 31% in Shenzhen, China, which is similar to that of diarrheal patients in Nepal post-2013 (30%) (Margulieux et al., 2018) and travel cases to Southeast Asia/India (43%) (Guiral et al., 2019). In addition, nearly all the isolates of a major circulating lineage L2/4 carried *gyrA* p.S83L mutation, *bla<sub>TEM-1B</sub>* and *mph(A)* genes, and AMR phenotype testing showed that all the representative L2/4 isolates were resistant to AMP, AMS, and AZI and most (11/12) of them were resistant to NAL, suggesting that L2/4 was a MDR lineage. The identification of azithromycin-resistant, ESBL-producing ETEC and a major MDR lineage L2/4 in Shenzhen highlighted the importance of ongoing AMR surveillance.

In summary, during routine foodborne disease surveillance, we found that the epidemiology of ETEC infections in Shenzhen, China is distinctive, with most infections occurring in indigenous adults. By integrating WGS and antimicrobial susceptibility testing, we characterized the temporal dynamics of population structure and virulence factors, and the AMR mutation/gene and phenotype profile of Shenzhen ETEC isolates in 6 years. Shenzhen ETEC isolates showed a remarkable high diversity, which belonged to four *E. coli* phylogroups and 15 ETEC lineages, and the major virulence factors were enterotoxin ST and CF CS21 and CS6. Intriguingly, the major circulating lineages in Shenzhen and their virulence factor profiles were distinctive, which are different from the commonly detected global or endemic ETEC lineages. Furthermore, we showed that AMR mutation/gene profiles of genomes were concordant with the phenotype testing results, and revealed that Shenzhen isolates had high resistance rates to several commonly used antimicrobial agents and identified a MDR lineage. To our knowledge, our study provides novel insight into the genomic epidemiology and antimicrobial susceptibility profile of ETEC infections in indigenous adults for the first time, which will not only enhance our comprehensive understanding on ETEC epidemiology, but also have implications for the

development of vaccine and future surveillance and prevention of ETEC infections.

## DATA AVAILABILITY STATEMENT

The datasets presented in this study can be found in online repositories. The names of the repository/repositories and accession number(s) can be found in the article/Supplementary Material.

## AUTHOR CONTRIBUTIONS

CY, YC, CW, and QH conceived and designed the study. CY, YL, LZ, MJ, LX, ML, YS, LW, YJ, SW, RC, and XS performed the experiments and data analysis. CY and LZ wrote the original draft. CY, XZ, YL, MJ, YC, CW, and QH reviewed and revised the manuscript. All authors have read and agreed to the published version of the manuscript.

## FUNDING

This research was supported by the National Key Research and Development Program of China (No. 2018YFC1603902), Sanming Project of Medicine in Shenzhen (No. SZSM201811071) and China Postdoctoral Science Foundation (No. 2020M672836), Natural Science Foundation of Guangdong Province (No. 2018B030311063), Institute Fund of Chinese Academy of Medical Sciences (No. 2020-PT330-006), Shenzhen Key Medical Discipline Construction Fund (No. SZXK064), and China National Science and Technology Major Projects Foundation (No. 2017ZX10303406).

## SUPPLEMENTARY MATERIAL

The Supplementary Material for this article can be found online at: <https://www.frontiersin.org/articles/10.3389/fmicb.2021.732068/full#supplementary-material>

## REFERENCES

- Abraham, S., Trott, D. J., Jordan, D., Gordon, D. M., Groves, M. D., Fairbrother, J. M., et al. (2014). Phylogenetic and molecular insights into the evolution of multidrug-resistant porcine enterotoxigenic *Escherichia coli* in Australia. *Int. J. Antimicrob. Agents* 44, 105–111. doi: 10.1016/j.ijantimicag.2014.04.011
- Allard, M. W., Strain, E., Melka, D., Bunning, K., Musser, S. M., Brown, E. W., et al. (2016). Practical value of food pathogen traceability through building a whole-genome sequencing network and database. *J. Clin. Microbiol.* 54, 1975–1983. doi: 10.1128/JCM.00081-16
- Bankevich, A., Nurk, S., Antipov, D., Gurevich, A. A., Dvorkin, M., Kulikov, A. S., et al. (2012). SPAdes: a new genome assembly algorithm and its applications to single-cell sequencing. *J. Comput. Biol.* 19, 455–477. doi: 10.1089/cmb.2012.0021
- Begum, Y. A., Talukder, K. A., Azmi, I. J., Shahnaiz, M., Sheikh, A., Sharmin, S., et al. (2016). Resistance pattern and molecular characterization of enterotoxigenic *Escherichia coli* (ETEC) strains isolated in Bangladesh. *PLoS One* 11:e0157415. doi: 10.1371/journal.pone.0157415
- Benson, G. (1999). Tandem repeats finder: a program to analyze DNA sequences. *Nucleic Acids Res.* 27, 573–580. doi: 10.1093/nar/27.2.573
- Bortolaia, V., Kaas, R. S., Ruppe, E., Roberts, M. C., Schwarz, S., Cattoir, V., et al. (2020). ResFinder 4.0 for predictions of phenotypes from genotypes. *J. Antimicrob. Chemother.* 75, 3491–3500. doi: 10.1093/jac/dkaa345
- Bovee-Oudenhoven, I. M., Lettink-Wissink, M. L., Van Doesburg, W., Witteman, B. J., and Van Der Meer, R. (2003). Diarrhea caused by enterotoxigenic *Escherichia coli* infection of humans is inhibited by dietary calcium. *Gastroenterology* 125, 469–476. doi: 10.1016/S0016-5085(03)00884-9
- Boxall, M. D., Day, M. R., Greig, D. R., and Jenkins, C. (2020). Antimicrobial resistance profiles of diarrhoeagenic *Escherichia coli* isolated from travellers returning to the UK, 2015–2017. *J. Med. Microbiol.* 69, 932–943. doi: 10.1099/JMM.0.001214

- Carattoli, A., Zankari, E., García-Fernández, A., Larsen, M. V., Lund, O., Villa, L., et al. (2014). In Silico detection and typing of plasmids using plasmidfinder and plasmid multilocus sequence typing. *Antimicrob. Agents Chemother.* 58, 3895–3903. doi: 10.1128/AAC.02412-14
- Chen, Q., Shi, X., Li, Y., Jiang, Y., Lin, Y., Qiu, Y., et al. (2014). Rapid genetic typing of diarrheagenic *Escherichia coli* using a two-tube modified molecular beacon based multiplex real-time PCR assay and its clinical application. *Ann. Clin. Microbiol. Antimicrob.* 13, 1–9.
- Chen, Y., Chen, X., Zheng, S., Yu, F., Kong, H., Yang, Q., et al. (2014). Serotypes, genotypes and antimicrobial resistance patterns of human diarrhoeagenic *Escherichia coli* isolates circulating in southeastern China. *Clin. Microbiol. Infect.* 20, 52–58. doi: 10.1111/1469-0691.12188
- Chung, S. Y., Kwon, T., Bak, Y. S., Park, J. J., Kim, C. H., Cho, S. H., et al. (2019). Comparative genomic analysis of enterotoxigenic *Escherichia coli* O159 strains isolated from diarrheal patients in Korea. *Gut Pathog.* 11, 1–10. doi: 10.1186/s13099-019-0289-6
- Clemens, J. D., Rao, M. R., Chakraborty, J., Yunus, M., Ali, M., Kay, B., et al. (1997). Breastfeeding and the risk of life-threatening enterotoxigenic *Escherichia coli* diarrhea in Bangladeshi infants and children. *Pediatrics* 100:e2.
- Del Canto, F., Valenzuela, P., Cantero, L., Bronstein, J., Blanco, J. E., Blanco, J., et al. (2011). Distribution of classical and nonclassical virulence genes in enterotoxigenic *Escherichia coli* isolates from Chilean children and tRNA gene screening for putative insertion sites for genomic islands. *J. Clin. Microbiol.* 49, 3198–3203. doi: 10.1128/JCM.02473-10
- Denamur, E., Clermont, O., Bonacorsi, S., and Gordon, D. (2021). The population genetics of pathogenic *Escherichia coli*. *Nat. Rev. Microbiol.* 19, 37–54. doi: 10.1038/s41579-020-0416-x
- Didelot, X., Bowden, R., Wilson, D. J., Peto, T. E. A., and Crook, D. W. (2012). Transforming clinical microbiology with bacterial genome sequencing. *Nat. Rev. Genet.* 13, 601–612. doi: 10.1038/nrg3226
- Fleckenstein, J. M., and Kuhlmann, F. M. (2019). Enterotoxigenic *Escherichia coli* Infections. *Curr. Infect. Dis. Rep.* 21:9. doi: 10.1007/s11908-019-0665-x
- Gaaster, W., and Svennerholm, A.-M. (1996). Colonization factors of human enterotoxigenic *Escherichia coli* (ETEC). *Trends Microbiol.* 4, 444–452.
- García, V., Gambino, M., Pedersen, K., Haugegaard, S., Olsen, J. E., and Herrero-Fresno, A. (2020). F4- and F18-Positive Enterotoxigenic *Escherichia coli* Isolates from Diarrhea of Postweaning Pigs: genomic Characterization. *Appl. Environ. Microbiol.* 86, 1–18. doi: 10.1128/AEM.01913-20
- Garrison, E., and Marth, G. (2012). Haplotype-based variant detection from short-read sequencing. *arXiv [Preprint]*. arXiv:1207.3907.
- Gomes, C., Ruiz-Roldán, L., Mateu, J., Ochoa, T. J., and Ruiz, J. (2019). Azithromycin resistance levels and mechanisms in *Escherichia coli*. *Sci. Rep.* 9:6089. doi: 10.1038/s41598-019-42423-3
- Gonzales, L., Sanchez, S., Zambrana, S., Iñiguez, V., Wiklund, G., Svennerholm, A. M., et al. (2013). Molecular characterization of enterotoxigenic *Escherichia coli* isolates recovered from children with diarrhea during a 4-year period (2007 to 2010) in Bolivia. *J. Clin. Microbiol.* 51, 1219–1225. doi: 10.1128/JCM.02971-12
- Guiral, E., Quiles, M. G., Muñoz, L., Moreno-Morales, J., Alejo-Cancho, I., Salvador, P., et al. (2019). Emergence of Resistance to Quinolones and -Lactam Antibiotics in Enterotoxigenic and Enterotoxigenic *Escherichia coli* Causing Traveler's Diarrhea. *Antimicrob. Agents Chemother.* 63, 1–9. doi: 10.1128/AAC.01745-18
- Horesh, G., Blackwell, G. A., Tonkin-Hill, G., Corander, J., Heinz, E., and Thomson, N. R. (2021). A comprehensive and high-quality collection of *Escherichia coli* genomes and their genes. *Microb. Genomics* 7:000499. doi: 10.1099/mgen.0.000499
- Huerta-Cepas, J., Szklarczyk, D., Heller, D., Hernández-Plaza, A., Forslund, S. K., Cook, H., et al. (2019). EggNOG 5.0: a hierarchical, functionally and phylogenetically annotated orthology resource based on 5090 organisms and 2502 viruses. *Nucleic Acids Res.* 47, D309–D314. doi: 10.1093/nar/gky1085
- Isidean, S. D., Riddle, M. S., Savarino, S. J., and Porter, C. K. (2011). A systematic review of ETEC epidemiology focusing on colonization factor and toxin expression. *Vaccine* 29, 6167–6178. doi: 10.1016/j.vaccine.2011.06.084
- Joffré, E., von Mentzer, A., Abd El Ghany, M., Oezguen, N., Savidge, T., Dougan, G., et al. (2015). Allele variants of enterotoxigenic *Escherichia coli* heat-labile toxin are globally transmitted and associated with colonization factors. *J. Bacteriol.* 197, 392–403. doi: 10.1128/JB.02050-14
- Joffré, E., von Mentzer, A., Svennerholm, A. M., and Sjöling, Å (2016). Identification of new heat-stable (STa) enterotoxin allele variants produced by human enterotoxigenic *Escherichia coli* (ETEC). *Int. J. Med. Microbiol.* 306, 586–594. doi: 10.1016/j.ijmm.2016.05.016
- Katoh, K., and Standley, D. M. (2013). MAFFT multiple sequence alignment software version 7: improvements in performance and usability. *Mol. Biol. Evol.* 30, 772–780. doi: 10.1093/molbev/mst010
- Khalil, I. A., Troeger, C., Blacker, B. F., Rao, P. C., Brown, A., Atherly, D. E., et al. (2018). Morbidity and mortality due to shigella and enterotoxigenic *Escherichia coli* diarrhoea: the Global Burden of Disease Study 1990–2016. *Lancet Infect. Dis.* 18, 1229–1240. doi: 10.1016/S1473-3099(18)30475-4
- Lamberti, L. M., Bourgeois, A. L., Fischer Walker, C. L., Black, R. E., and Sack, D. (2014). Estimating Diarrheal Illness and Deaths Attributable to *Shigellae* and Enterotoxigenic *Escherichia coli* among Older Children, Adolescents, and Adults in South Asia and Africa. *PLoS Negl. Trop. Dis.* 8:e2705. doi: 10.1371/journal.pntd.0002705
- Li, H., and Durbin, R. (2009). Fast and accurate short read alignment with Burrows-Wheeler transform. *Bioinformatics* 25, 1754–1760. doi: 10.1093/bioinformatics/btp324
- Li, H., Handsaker, B., Wysoker, A., Fennell, T., Ruan, J., Homer, N., et al. (2009). The Sequence Alignment/Map format and SAMtools. *Bioinformatics* 25, 2078–2079. doi: 10.1093/bioinformatics/btp352
- Li, Y., Luo, Q., Shi, X., Lin, Y., Qiu, Y., Lv, D., et al. (2017). Phenotypic and genotypic characterization of clinical enterotoxigenic *Escherichia coli* isolates from Shenzhen, China. *Foodborne Pathog. Dis.* 14, 333–340. doi: 10.1089/fpd.2016.2233
- Liu, J., Bai, L., Li, W., Han, H., Fu, P., Ma, X., et al. (2018). Trends of foodborne diseases in China: lessons from laboratory-based surveillance since 2011. *Front. Med.* 12:48–57. doi: 10.1007/s11684-017-0608-6
- Luo, Q., Kumar, P., Vickers, T. J., Sheikh, A., Lewis, W. G., Rasko, D. A., et al. (2014). Enterotoxigenic *Escherichia coli* secretes a highly conserved mucin-degrading metalloprotease to effectively engage intestinal epithelial cells. *Infect. Immun.* 82, 509–521. doi: 10.1128/IAI.01106-13
- Margulieux, K. R., Srijan, A., Ruekit, S., Nobthai, P., Poramathikul, K., Pandey, P., et al. (2018). Extended-spectrum  $\beta$ -lactamase prevalence and virulence factor characterization of enterotoxigenic *Escherichia coli* responsible for acute diarrhea in Nepal from 2001 to 2016. *Antimicrob. Resist. Infect. Control* 7, 1–7. doi: 10.1186/s13756-018-0377-2
- Minh, B. Q., Schmidt, H. A., Chernomor, O., Schrempf, D., Woodhams, M. D., Von Haeseler, A., et al. (2020). IQ-TREE 2: new Models and Efficient Methods for Phylogenetic Inference in the Genomic Era. *Mol. Biol. Evol.* 37, 1530–1534. doi: 10.1093/molbev/msaa015
- Nada, R. A., Shaheen, H. I., Khalil, S. B., Mansour, A., El-Sayed, N., Touni, I., et al. (2011). Discovery and phylogenetic analysis of novel members of class B enterotoxigenic *Escherichia coli* adhesive fimbriae. *J. Clin. Microbiol.* 49, 1403–1410.
- Oh, K.-H., Kim, D. W., Jung, S.-M., and Cho, S.-H. (2014). Molecular Characterization of Enterotoxigenic *Escherichia coli* Strains Isolated from Diarrheal Patients in Korea during 2003–2011. *PLoS One* 9:e96896. doi: 10.1371/journal.pone.0096896
- Pan, H., Zhang, J., Kuang, D., Yang, X., Ju, W., Huang, Z., et al. (2015). Molecular analysis and antimicrobial susceptibility of enterotoxigenic *Escherichia coli* from diarrheal patients. *Diagn. Microbiol. Infect. Dis.* 81, 126–131. doi: 10.1016/j.diagmicrobio.2014.10.008
- Pilonieta, M. C., Boder, M. D., and Munson, G. P. (2007). CfaD-Dependent Expression of a Novel Extracytoplasmic Protein from Enterotoxigenic *Escherichia coli*. *J. Bacteriol.* 189, 5060–5067. doi: 10.1128/JB.00131-07
- Qadri, F., Svennerholm, A.-M., Faruque, A. S. G., and Sack, R. B. (2005). Enterotoxigenic *Escherichia coli* in Developing Countries: epidemiology, Microbiology, Clinical Features, Treatment, and Prevention. *Clin. Microbiol. Rev.* 18, 465–483. doi: 10.1128/CMR.18.3.465-483.2005
- Qu, M., Zhang, X., Qian, H., Lyu, B., Huang, Y., Yan, H., et al. (2014). Study on the genotype and epidemic characteristics of diarrheagenic *Escherichia coli* isolated from diarrheal patients in Beijing. *Zhonghua Liu Xing Bing Xue Za Zhi* 35, 1123–1126.
- Rasko, D. A., Del Canto, F., Luo, Q., Fleckenstein, J. M., Vidal, R., and Hazen, T. H. (2019). Comparative genomic analysis and molecular examination of the diversity of enterotoxigenic *Escherichia coli* isolates



- from Chile. *PLoS Negl. Trop. Dis.* 13:e0007828. doi: 10.1371/journal.pntd.0007828
- Rivera, F. P., Ochoa, T. J., Maves, R. C., Bernal, M., Medina, A. M., Meza, R., et al. (2010). Genotypic and Phenotypic Characterization of Enterotoxigenic *Escherichia coli* Strains Isolated from Peruvian Children. *J. Clin. Microbiol.* 48, 3198–3203. doi: 10.1128/JCM.00644-10
- Ronholm, J., Nasheri, N., Petronella, N., and Pagotto, F. (2016). Navigating microbiological food safety in the era of whole-genome sequencing. *Clin. Microbiol. Rev.* 29, 837–857. doi: 10.1128/CMR.00056-16
- Sahl, J. W., Sistrunk, J. R., Baby, N. I., Begum, Y., Luo, Q., Sheikh, A., et al. (2017). Insights into enterotoxigenic *Escherichia coli* diversity in Bangladesh utilizing genomic epidemiology. *Sci. Rep.* 7:3402. doi: 10.1038/s41598-017-03631-x
- Sahl, J. W., Steinsland, H., Redman, J. C., Angiuli, S. V., Nataro, J. P., Sommerfelt, H., et al. (2011). A comparative genomic analysis of diverse clonal types of enterotoxigenic *Escherichia coli* reveals pathovar-specific conservation. *Infect. Immun.* 79, 950–960. doi: 10.1128/IAI.00932-10
- Seemann, T. (2014). Prokka: rapid prokaryotic genome annotation. *Bioinformatics* 30, 2068–2069. doi: 10.1093/bioinformatics/btu153
- Sjöling, Å., von Mentzer, A., and Svennerholm, A. M. (2015). Implications of enterotoxigenic *Escherichia coli* genomics for vaccine development. *Expert Rev. Vaccines* 14, 551–560. doi: 10.1586/14760584.2015.996553
- So, M., Boyer, H. W., Betlach, M., and Falkow, S. (1976). Molecular cloning of an *Escherichia coli* plasmid determinant than encodes for the production of heat-stable enterotoxin. *J. Bacteriol.* 128, 463–472.
- So, M., Dallas, W. S., and Falkow, S. (1978). Characterization of an *Escherichia coli* plasmid encoding for synthesis of heat-labile toxin: molecular cloning of the toxin determinant. *Infect. Immun.* 21, 405–411.
- Tonkin-Hill, G., MacAlasdair, N., Ruis, C., Weimann, A., Horesh, G., Lees, J. A., et al. (2020). Producing polished prokaryotic pangenomes with the Panaroo pipeline. *Genome Biol.* 21:180. doi: 10.1186/s13059-020-02090-4
- Torres, O. R., González, W., Lemus, O., Pratdesaba, R. A., Matute, J. A., Wiklund, G., et al. (2015). Toxins and virulence factors of enterotoxigenic *Escherichia coli* associated with strains isolated from indigenous children and international visitors to a rural community in Guatemala. *Epidemiol. Infect.* 143, 1662–1671. doi: 10.1017/S0950268814002295
- Turner, S. M., Chaudhuri, R. R., Jiang, Z. D., DuPont, H., Gyles, C., Penn, C. W., et al. (2006). Phylogenetic comparisons reveal multiple acquisitions of the toxin genes by enterotoxigenic *Escherichia coli* strains of different evolutionary lineages. *J. Clin. Microbiol.* 44, 4528–4536. doi: 10.1128/JCM.01474-06
- Vidal, R. M., Muhsen, K., Tennant, S. M., Svennerholm, A.-M., Sow, S. O., Sur, D., et al. (2019). Colonization factors among enterotoxigenic *Escherichia coli* isolates from children with moderate-to-severe diarrhea and from matched controls in the Global Enteric Multicenter Study (GEMS). *PLoS Negl. Trop. Dis.* 13:e0007037. doi: 10.1371/journal.pntd.0007037
- von Mentzer, A., Blackwell, G. A., Pickard, D., Boinett, C. J., Joffré, E., Page, A. J., et al. (2021). Long-read-sequenced reference genomes of the seven major lineages of enterotoxigenic *Escherichia coli* (ETEC) circulating in modern time. *Sci. Rep.* 11:9256. doi: 10.1038/s41598-021-88316-2
- von Mentzer, A., Connor, T. R., Wieler, L. H., Semmler, T., Iguchi, A., Thomson, N. R., et al. (2014). Identification of enterotoxigenic *Escherichia coli* (ETEC) clades with long-term global distribution. *Nat. Genet.* 46, 1321–1326. doi: 10.1038/ng.3145
- von Mentzer, A., Tobias, J., Wiklund, G., Nordqvist, S., Aslett, M., Dougan, G., et al. (2017). Identification and characterization of the novel colonization factor CS30 based on whole genome sequencing in enterotoxigenic *Escherichia coli* (ETEC). *Sci. Rep.* 7:12514. doi: 10.1038/s41598-017-12743-3
- Wolf, M. K. (1997). Occurrence, distribution, and associations of O and H serogroups, colonization factor antigens, and toxins of enterotoxigenic *Escherichia coli*. *Clin. Microbiol. Rev.* 10, 569–584.
- Xiang, Y., Wu, F., Chai, Y., Xu, X., Yang, L., Tian, S., et al. (2020). A new plasmid carrying mphA causes prevalence of azithromycin resistance in enterotoxigenic *Escherichia coli* serogroup O6. *BMC Microbiol.* 20:247. doi: 10.1186/s12866-020-01927-z
- Yang, C., Pei, X., Wu, Y., Yan, L., Yan, Y., Song, Y., et al. (2019). Recent mixing of *Vibrio parahaemolyticus* populations. *ISME J.* 13, 2578–2588. doi: 10.1038/s41396-019-0461-5

**Conflict of Interest:** The authors declare that the research was conducted in the absence of any commercial or financial relationships that could be construed as a potential conflict of interest.

**Publisher's Note:** All claims expressed in this article are solely those of the authors and do not necessarily represent those of their affiliated organizations, or those of the publisher, the editors and the reviewers. Any product that may be evaluated in this article, or claim that may be made by its manufacturer, is not guaranteed or endorsed by the publisher.

Copyright © 2021 Yang, Li, Zuo, Jiang, Zhang, Xie, Luo, She, Wang, Jiang, Wu, Cai, Shi, Cui, Wan and Hu. This is an open-access article distributed under the terms of the Creative Commons Attribution License (CC BY). The use, distribution or reproduction in other forums is permitted, provided the original author(s) and the copyright owner(s) are credited and that the original publication in this journal is cited, in accordance with accepted academic practice. No use, distribution or reproduction is permitted which does not comply with these terms.



# Diversification of *Escherichia albertii* H-Antigens and Development of H-Genotyping PCR

Koji Nakae<sup>1</sup>, Tadasuke Ooka<sup>2\*</sup>, Koichi Murakami<sup>3</sup>, Yukiko Hara-Kudo<sup>4</sup>, Naoko Imuta<sup>2</sup>, Yasuhiro Gotoh<sup>5</sup>, Yoshitoshi Ogura<sup>5,6</sup>, Tetsuya Hayashi<sup>5</sup>, Yasuhiro Okamoto<sup>1</sup> and Junichiro Nishi<sup>2</sup>

<sup>1</sup> Department of Pediatrics, Kagoshima University Hospital, Kagoshima, Japan, <sup>2</sup> Department of Microbiology, Kagoshima University Graduate School of Medical and Dental Sciences, Kagoshima, Japan, <sup>3</sup> Center for Emergency Preparedness and Response, National Institute of Infectious Diseases, Tokyo, Japan, <sup>4</sup> National Institute of Health Sciences, Kawasaki, Japan, <sup>5</sup> Department of Bacteriology, Faculty of Medical Sciences, Kyushu University, Fukuoka, Japan, <sup>6</sup> Department of Infectious Medicine, Division of Microbiology, Kurume University School of Medicine, Kurume, Japan

## OPEN ACCESS

### Edited by:

Xiyang Wu,  
Jinan University, China

### Reviewed by:

Marianne De Paepe,  
Institut National de Recherche pour  
l'Agriculture, l'Alimentation et  
l'Environnement (INRAE), France  
Masahiro Eguchi,  
National Institute of Animal Health,  
National Agriculture and Food  
Research Organization, Japan

### \*Correspondence:

Tadasuke Ooka  
taohoka1@m.kufm.kagoshima-u.ac.jp

### Specialty section:

This article was submitted to  
Food Microbiology,  
a section of the journal  
Frontiers in Microbiology

Received: 08 July 2021

Accepted: 07 October 2021

Published: 01 November 2021

### Citation:

Nakae K, Ooka T, Murakami K,  
Hara-Kudo Y, Imuta N, Gotoh Y,  
Ogura Y, Hayashi T, Okamoto Y and  
Nishi J (2021) Diversification  
of *Escherichia albertii* H-Antigens  
and Development of H-Genotyping  
PCR. *Front. Microbiol.* 12:737979.  
doi: 10.3389/fmicb.2021.737979

*Escherichia albertii* is a recently recognized human enteropathogen that is closely related to *Escherichia coli*. As *E. albertii* sometimes causes outbreaks of gastroenteritis, rapid strain typing systems, such as the O- and H-serotyping systems widely used for *E. coli*, will be useful for outbreak investigation and surveillance. Although an O-genotyping system has recently been developed, the diversity of *E. albertii* H-antigens (flagellins) encoded by *fliC* genes remains to be systematically investigated, and no H-serotyping or genotyping system is currently available. Here, we analyzed the *fliC* genes of 243 genome-sequenced *E. albertii* strains and identified 73 sequence types, which were grouped into four clearly distinguishable types designated *E. albertii* H-genotypes 1–4 (EAHg1–EAHg4). Although there was a clear sign of intraspecies transfer of *fliC* genes in *E. albertii*, none of the four *E. albertii* H-genotypes (EAHGs) were closely related to any of the 53 known *E. coli* H-antigens, indicating the absence or rare occurrence of interspecies transfer of *fliC* genes between the two species. Although the analysis of more *E. albertii* strains will be required to confirm the low level of variation in their *fliC* genes, this finding suggests that *E. albertii* may exist in limited natural hosts or environments and/or that the flagella of *E. albertii* may function in a limited stage(s) in their life cycle. Based on the *fliC* sequences of the four EAHGs, we developed a multiplex PCR-based H-genotyping system for *E. albertii* (EAH-genotyping PCR), which will be useful for epidemiological studies of *E. albertii* infections.

**Keywords:** *Escherichia albertii*, flagellin, *fliC*, H-antigen, genotyping

## INTRODUCTION

*Escherichia albertii* is a recently recognized human enteropathogen and an avian pathogen (Albert et al., 1992; Huys et al., 2003; Oaks et al., 2010; Ooka et al., 2012). *E. albertii* is often misidentified as enteropathogenic *Escherichia coli* (EPEC) or enterohemorrhagic *E. coli* (EHEC) due to similar phenotypic and genetic characteristics, including similar biochemical properties and possession of a locus of enterocyte effacement (LEE) encoding a type III secretion system (Ooka et al., 2012; Gomes et al., 2020). In addition, as multiple outbreaks of *E. albertii* have recently been reported (Konno et al., 2012; Ooka et al., 2013; Masuda et al., 2020), rapid strain typing systems, such as

the PCR-based O- and H-genotyping systems widely used for *E. coli* (Iguchi et al., 2015; Banjo et al., 2018), should be useful for *E. albertii* outbreak investigation and surveillance. In *E. albertii*, although only a genotyping system based on the variation in O-antigen biosynthesis genes has been developed thus far (Ooka et al., 2019), rapid, and low-cost effective H-genotyping system are useful to increase the discrimination power and to assist epidemiological studies in combination with O-genotyping system.

H-antigens (flagellins) are used for the serotyping of strains in many Gram-negative bacteria (Orskov and Orskov, 1992). In *E. coli*, flagellin is encoded by the *fliC* gene in the *fliY-T* region on the chromosome or its homologs, such as *fliK*, *fliA*, and *fimA* (Ratiner, 1998; Wang et al., 2003; Tominaga, 2004; Feng et al., 2008; Ratiner et al., 2010), and a total of 53 H-antigens have been identified thus far. The flagellar filament is composed of a single protein, flagellin. Flagellin is composed of four major domains: the N- and C-terminal domains (D0 and D1, respectively) form the inner and outer tubules of the flagellum, respectively, and internal D2 and D3 domains are exposed on the surface of the flagellar filament. The D0 and D1 domains are highly conserved among bacterial species, whereas the D2 and D3 domains are highly variable even between strains belonging to the same species (Samatey et al., 2001). In *E. albertii*, the gene cluster associated with flagellar biosynthesis and its regulation, including the *fliY-T* region, is conserved in most strains (Ooka et al., 2015). Although the flagellum is not produced under routine culture conditions, it has recently been revealed that its production is induced under conditions of low temperature and nutrient limitation (Ikeda et al., 2020; Murakami et al., 2020). However, the sequence variation of the *fliC* gene has not yet been examined. To clarify this issue, we systematically analyzed the *fliC* genes of 243 *E. albertii* strains sequenced thus far and compared them with the sequences of 53 known *E. coli* H-antigens. In addition, we attempted to develop a multiplex PCR-based H-genotyping system for *E. albertii* strains based on the sequence diversity of their *fliC* genes.

## MATERIALS AND METHODS

### *Escherichia albertii* Genome Sequences and Strains Analyzed in This Study

In this study, we analyzed the 243 *E. albertii* genome sequences used in our previous study (Ooka et al., 2019). Detailed information of the strains is shown in **Supplementary Table 1**. The strain information for the 92 *E. albertii* strains used for the evaluation of EAH-genotyping PCR is provided in **Supplementary Table 2**.

### Identification of *fliC* Genes

In previously sequenced *E. albertii* genomes, the *fliC* gene has been found to be located between *fliA* and *fliD* (Ooka et al., 2015). In the first-step analysis, as it is known that *fliC* sequences are highly diverse in *E. coli* (Ratiner et al., 2010), the *fliC*-containing regions of the 243 *E. albertii* genomes were identified by blastn search using the *fliA* and *fliD* sequences of *E. albertii* strain

CB9786 as queries, with an *E*-value threshold of 0.01. The *fliC* gene of each strain was then manually annotated with *in silico* Molecular Cloning Genomics Edition software version 7.29L (IMC-GE; In Silico Biology, Japan). For the strains not identified the *fliC* gene in the first-step analysis, we performed the second-step analysis by blastn search using the *fliC* sequences identified in the first step analysis or the primer sequences designed for EAH-genotyping PCR, which was described below, as queries, with an *E*-value threshold of 0.01.

### Sequence Comparison and Phylogenetic Analysis

Multiple alignment of nucleotide sequences of the *fliC* gene of *E. albertii* strains and amino acid sequences of the flagellin of *E. albertii* and *Salmonella* Typhimurium strain SJW1103 was prepared using GENETYX (version 15.0.1). After identical sequences showing no SNPs were deduplicated, the nucleotide sequence alignment of *E. albertii* *fliC* genes with those of 53 known *E. coli* H-serotypes (H1–H56, but missing H13, H22, and H50; **Supplementary Table 3**) was performed using the ClustalW program in MEGA (version 7.0.26) with the default parameters (Kumar et al., 2016).

The phylogenetic analysis of *fliC* genes was performed with MEGA using the obtained multiple alignment. A phylogenetic tree was reconstructed by the neighbor-joining (NJ) method with the *p*-distance model. Bootstrap analysis with 1000 replicates was performed to assess the significance of internal branching. The core-gene SNP-based maximum-likelihood (ML) phylogenetic tree of the 243 *E. albertii* strains was constructed previously (Ooka et al., 2019) using RAXML v8 (Stamatakis, 2014) and displayed and annotated using iTOL v4<sup>1</sup> (Letunic and Bork, 2016).

### Development of a Multiplex PCR-Based *Escherichia albertii* H-Genotyping System

Based on the variation in the sequences of the *E. albertii* *fliC* genes, we designed four pairs of PCR primers to specifically detect each of the four *E. albertii* H-genotypes (EAHgs) (**Table 1**). As a positive control for PCR and a genetic marker of

<sup>1</sup><https://itol.embl.de>

**TABLE 1** | Primer information for EAH-genotyping PCR.

Primer name	Sequence (5'–3')	Product size (bp)	Reference strain	Note
EAHg_F (common)	CAGGTTGGCGCGAATGA TGG	–	–	–
EAHg1_R	GCATCTAGTTTAACTGACTG	167	EC05-81	EAHg1
EAHg2_R	GGTTGCAGAAGTAACGGTAG	309	NIAH_Bird 25	EAHg2
EAHg3_R	GGCTGACCAGTTTGTTCGCG	404	NIAH_Bird 3	EAHg3
EAHg4_R	GTACCATTTGTACCAGCAAG	515	NIAH_Bird 5	EAHg4
E_a1_1_NF	CAGTCGATGGTTTCACCTGA	731	–	<i>E. albertii</i> -specific
E_a1_1_NR	ACACCGTGGCGAAATGGCA			

*E. albertii*, one primer pair targeting an *E. albertii*-specific region (*E\_al\_1\_NF/NR* primers) (Ooka et al., 2019) was also included in the primer set. Template DNA for PCR was prepared by the alkaline boiling method. KOD -Multi&Epi- DNA polymerase (TOYOBO, Osaka, Japan) was used for PCR. Each reaction mixture (25  $\mu$ l) contained 1  $\mu$ l of template DNA, each primer at 1  $\mu$ M, and 0.5 U of polymerase. PCR was performed with 25 cycles of 94°C for 2 min for initial denaturation, followed by 10 s at 98°C, 30 s at 60°C, and 60 s at 68°C. The PCR products were analyzed by agarose electrophoresis using 2% agarose S (Nippon Gene, Tokyo, Japan).

## RESULTS

### Identification and Sequence Comparison of *fliC* Genes in *Escherichia albertii* Genomes

Among the 243 *E. albertii* genomes examined by the first and second step analysis, intact and partial sequence of the *fliC* genes were identified in 231 and 9 genomes and no sequences were detected in the remaining 3 genomes (Supplementary Table 1). Through the clustering analysis of the 231 of intact *fliC* gene sequences, we identified a total of 73 sequence types with one or more SNPs (Supplementary Table 1), among which 42 were singletons, and 31 were composed of sequences from multiple genomes (named clusters C1–C31).

### Phylogenetic Analysis of *Escherichia albertii fliC* Genes With Those of *Escherichia coli* as References

The phylogenetic analysis of the 73 *fliC* sequences identified in *E. albertii* with 53 *fliC* sequences of known *E. coli* H-serotypes as references revealed that the *fliC* genes of *E. albertii* formed a monophyletic branch, separate from those of *E. coli* (Figure 1A). To obtain more detailed information on the sequence variation in *E. albertii fliC* genes, we performed a phylogenetic analysis of only the *E. albertii fliC* genes (Figure 1B). This analysis revealed that the *E. albertii fliC* genes can be divided into four distinct groups, in which the nucleotide sequence identities between the groups were less than 90%, and those within each group were over 97%. We defined these four groups as the genotypes of *E. albertii fliC* genes and named them *E. albertii* H-genotypes 1–4 (EAHg1–EAHg4). In addition, by the primer screening analysis for the nine strains with partial sequences of the *fliC* gene, all nine strains could be genotyped into either of the four EAHGs. Together with the results of *in silico* analysis of 231 genome-sequenced strains, the most dominant type among the 243 *E. albertii* genomes was EAHg4 (109 strains; 44.9%), followed by EAHg1 (59 strains; 24.3%), EAHg3 (50 strains; 20.6%), EAHg2 (22 strains; 9.0%), and no *fliC* gene (3 strains; 1.2%) (Table 2).

Amino acid sequence comparison of the representative *fliC*-encoded flagellin of the four genotypes and *Salmonella* Typhimurium strain SJW1103 revealed that while the sequences of the D0 and D1 domains were highly conserved, those of the D2 and D3 domains were variable (Supplementary Figure 1).

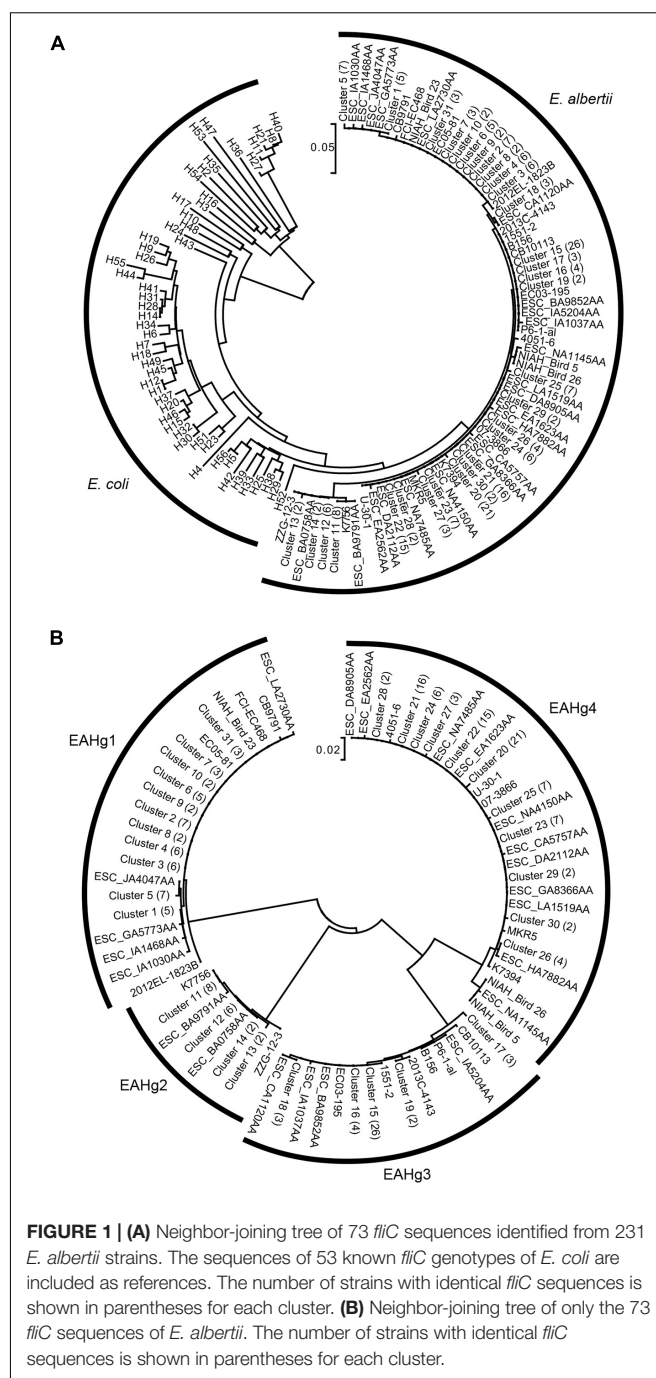


**FIGURE 1 | (A)** Neighbor-joining tree of 73 *fliC* sequences identified from 231 *E. albertii* strains. The sequences of 53 known *fliC* genotypes of *E. coli* are included as references. The number of strains with identical *fliC* sequences is shown in parentheses for each cluster. **(B)** Neighbor-joining tree of only the 73 *fliC* sequences of *E. albertii*. The number of strains with identical *fliC* sequences is shown in parentheses for each cluster.

### Development and Evaluation of the Multiplex H-Genotyping PCR System for *Escherichia albertii*

We designed a multiplex PCR primer set (Table 1) based on the sequence variation in the *fliC* genes of the four EAHGs. A forward universal primer was designed based on the highly conserved sequences of all four EAHGs, and reverse primers were designed based on the variable regions of each EAHg (Supplementary Figure 2), so that the amplicons generated with the combinations of the universal forward primer and the reverse primers exhibited



**TABLE 2** | Summary of *in silico*- and PCR-based EAH genotyping.

EAH-genotype	Number of strains (%)	
	<i>In silico</i> *	PCR
EAHg1	59 [1] (24.3%)	24 (26.1%)
EAHg2	22 [0] (9.0%)	16 (17.4%)
EAHg3	50 [2] (20.6%)	13 (14.1%)
EAHg4	109 [6] (44.9%)	39 (42.4%)
Not identified	3 (1.2%)	0 (0%)
Total	243	92

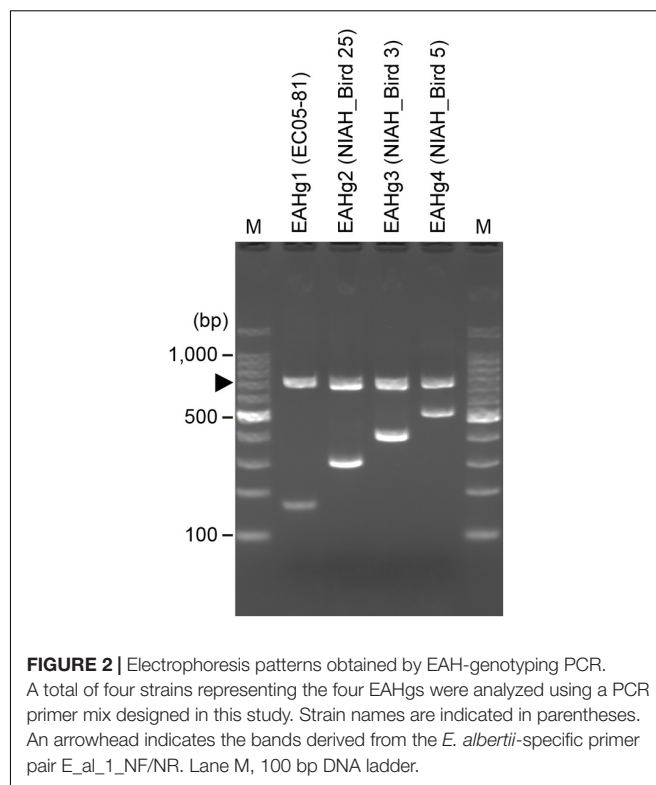
\*The number of strains genotyped by primer screening were shown in brackets.

a ladder pattern that ranged from 167 to 515 bp. One *E. albertii*-specific primer pair (E\_al\_1\_NF/E\_al\_1\_NR) (Ooka et al., 2015) was included in the primer set as a marker to detect *E. albertii* and as a positive control for PCR. The examination of the primer set in four strains representing each of the four EAHGs confirmed that the primer set yielded PCR products of the expected sizes for each genotype (**Figure 2**). To validate the PCR-based genotyping system, we performed the comparison of *in silico* and PCR-based genotyping on the same dataset of genomes. In this analysis, only 42 strains were used because the remaining 201 strains are not available in our laboratories. As shown in **Supplementary Figure 3**, all of the 42 strains exhibited the same results between *in silico* and the PCR-based genotyping. In addition, we applied the mixed DNA samples containing four strains with different EAH-genotypes as a template for the system to evaluate the specificity and obtained the primer set yielded PCR products of the expected sizes for four genotypes (**Supplementary Figure 4**).

To further evaluate the performance of the system, we determined the H-genotypes of 92 *E. albertii* strains using this system. These strains were isolated from diarrheal patients and birds in various regions of Japan. In this analysis, we were able to genotype all strains (**Supplementary Table 2**). Similar to the results of *in silico* analysis of the 240 genome-sequenced strains, EAHg4 (48 strains; 43.6%) was found to be predominant, followed by EAHg1 (29 strains; 26.4%), EAHg2 (18 strains; 16.4%), and EAHg3 (15 strains; 13.6%) (**Table 2**). These results suggest that our system is useful for the H-genotyping of *E. albertii* and that the four genotypes cover the most of the diversity of H-genotypes in the *E. albertii* lineage.

### Distribution of the 4 *Escherichia albertii* H-Genotypes and the 40 *Escherichia albertii* O-Genotypes in Genome-Sequenced *Escherichia albertii* Strains

Finally, we investigated the relationship between the phylogeny of the genome-sequenced strains used in this study and the distribution of the four EAHGs and the 40 *Escherichia albertii* O-genotypes (EAOgs), identified in our previous study (Ooka et al., 2019), in these strains by mapping H- and O-genotype information in a core-gene sequence-based ML phylogenetic tree of the strains (**Figure 3**). This analysis revealed that although very closely related strains shared the same H-genotype,

**FIGURE 2** | Electrophoresis patterns obtained by EAH-genotyping PCR.

A total of four strains representing the four EAHGs were analyzed using a PCR primer mix designed in this study. Strain names are indicated in parentheses. An arrowhead indicates the bands derived from the *E. albertii*-specific primer pair E\_al\_1\_NF/NR. Lane M, 100 bp DNA ladder.

each EAHg appeared in multiple sublineages in both clades 1 and 2, suggesting relatively frequent within-species transfer of *fliC* genes in *E. albertii*. In addition, there is no correlation between the combination of the H- and O-genotypes and their phylogenetic relationship.

## DISCUSSION

In this study, we analyzed the sequence variation of *fliC* genes among 231 genome-sequenced *E. albertii* strains and identified 73 sequence types, which were grouped into four clearly distinguishable genotypes (EAHg1–EAHg4). The four genotypes showed >97% sequence identity within each group and <90% identity between groups. As seen in *E. coli fliC* genes (Samatey et al., 2001), the sequences encoding domains D0 and D1 (corresponding to the N- and C-terminal regions of flagellin, respectively) were highly conserved, but those of domains D2 and D3 (forming the surface exposed region) were variable between H-genotypes (**Supplementary Figure 1**). In our previous analysis (Ooka et al., 2015), we revealed that flagellar biosynthesis-related genes other than *fliC* show high conservation of nucleotide sequences (>90% identity). Therefore, it appears that the *fliC* gene is under a certain amount of immunological selection in its hosts or environmental selection. However, it was notable that only four H-genotypes were identified in *E. albertii*, in sharp contrast to the situation in *E. coli*, in which as many as 53 H-genotypes have been identified. Although the analysis of more *E. albertii* strains will be required to confirm the low level of variation in their *fliC* genes, this finding may suggest the possibility that this species is living in limited natural hosts or

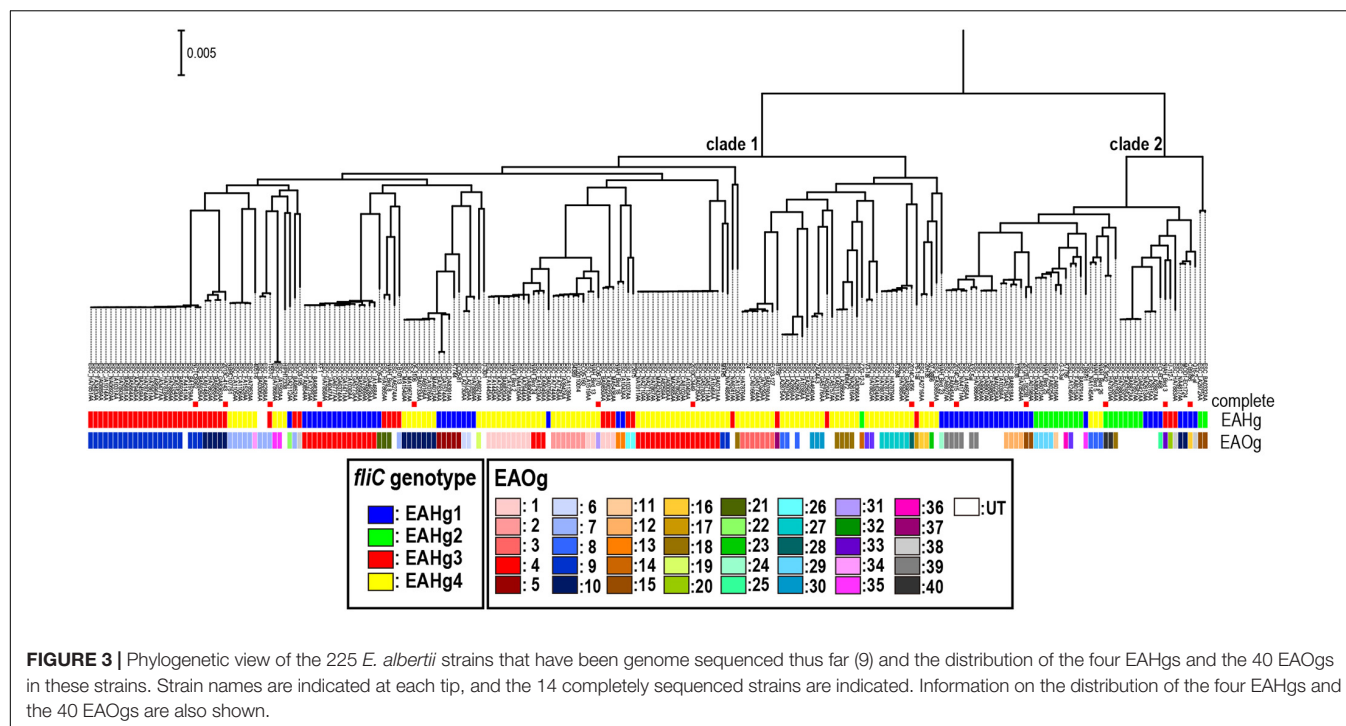


**FIGURE 3 |** Phylogenetic view of the 225 *E. albertii* strains that have been genome sequenced thus far (9) and the distribution of the four EAHgs and the 40 EAOgs in these strains. Strain names are indicated at each tip, and the 14 completely sequenced strains are indicated. Information on the distribution of the four EAHgs and the 40 EAOgs are also shown.

environments and/or that their flagella are required in a limited stage in their life cycle. This possibility may receive some support from the recent finding that flagella are produced only at lower temperatures and under nutrient-limited conditions (Ikeda et al., 2020; Murakami et al., 2020). It is also noteworthy that although a low level of sequence variation was observed for *E. albertii* *fliC* genes, we detected a sign of relatively frequent within-species transfer of this gene in *E. albertii* (Figure 3). However, none of the four H-genotypes identified in this study were closely related to any of the 53 H-genotypes of *E. coli*, suggesting the absence or very rare occurrence of interspecies transfer of *fliC* between *E. albertii* and *E. coli*. This is in marked contrast to the situation for O-antigen biosynthesis loci, which show clear signs of interspecies transfer between the two species (Ooka et al., 2019). Although the mechanism(s) generating such a difference is currently unknown, there may be some restriction of the flagellin sequence of *E. albertii*.

Although only four H-genotypes were identified in *E. albertii*, the multiplex PCR system that we constructed to identify H-genotypes in *E. albertii* will be a useful tool for epidemiological studies of *E. albertii* infections, particularly if used in combination with the O-genotyping system that we previously constructed (Ooka et al., 2019). In addition, the H-genotyping system will be useful for further analyzing the diversity of *fliC* genes in *E. albertii* or searching for additional genotypes.

## DATA AVAILABILITY STATEMENT

The original contributions presented in the study are included in the article/Supplementary Material,

further inquiries can be directed to the corresponding author.

## AUTHOR CONTRIBUTIONS

KN and TO designed the study and wrote the manuscript. KM and YH-K provided the samples. KN, TO, YG, NI, and YoO analyzed the data. TO, YaO, TH, and JN were responsible for supervision and management of the study. All authors contributed to the article and approved the submitted version.

## FUNDING

This work was supported by the Japan Society for the Promotion of Science KAKENHI (Grant Numbers 25460539, 16K08781, and 20K07498 to TO, and 20310116 and 221S0002 to TH), and a Health Labour Sciences Research Grant (H30-Shokuhin-Ippan-001 to YH-K).

## ACKNOWLEDGMENTS

The authors thank F. Funakura, S. Yamada, and T. Oku for providing technical assistance.

## SUPPLEMENTARY MATERIAL

The Supplementary Material for this article can be found online at: <https://www.frontiersin.org/articles/10.3389/fmicb.2021.737979/full#supplementary-material>

## REFERENCES

- Albert, M. J., Faruque, S. M., Ansaruzzaman, M., Islam, M. M., Haider, K., Alam, K., et al. (1992). Sharing of virulence-associated properties at the phenotypic and genetic levels between enteropathogenic *Escherichia coli* and *Hafnia alvei*. *J. Med. Microbiol.* 37, 310–314. doi: 10.1099/00222615-37-5-310
- Banjo, M., Iguchi, A., Seto, K., Kikuchi, T., Harada, T., Scheutz, F., et al. (2018). *Escherichia coli* H-Genotyping PCR: a Complete and Practical Platform for Molecular H Typing. *J. Clin. Microbiol.* 56, e00190–18. doi: 10.1128/JCM.00190-18
- Feng, L., Liu, B., Liu, Y., Ratiner, Y. A., Hu, B., Li, D., et al. (2008). A genomic islet mediates flagellar phase variation in *Escherichia coli* strains carrying the flagellin-specifying locus *flk*. *J. Bacteriol.* 190, 4470–4477. doi: 10.1128/JB.01937-07
- Gomes, T. A. T., Ooka, T., Hernandez, R. T., Yamamoto, D., and Hayashi, T. (2020). *Escherichia albertii* Pathogenesis. *EcoSal Plus* 9, 1–18. doi: 10.1128/ecosalplus.ESP-0015-2019
- Huys, G., Cnockaert, M., Janda, J. M., and Swings, J. (2003). *Escherichia albertii* sp. nov., a diarrhoeagenic species isolated from stool specimens of Bangladeshi children. *Int. J. Syst. Evol. Microbiol.* 53, 807–810. doi: 10.1099/ijss.0.02475-0
- Iguchi, A., Iyoda, S., Seto, K., Morita-Ishihara, T., Scheutz, F., Ohnishi, M., et al. (2015). *Escherichia coli* O-Genotyping PCR: a Comprehensive and Practical Platform for Molecular O Serogrouping. *J. Clin. Microbiol.* 53, 2427–2432. doi: 10.1128/JCM.00321-15
- Ikeda, T., Shinagawa, T., Ito, T., Ohno, Y., Kubo, A., Nishi, J., et al. (2020). Hypoosmotic stress induces flagellar biosynthesis and swimming motility in *Escherichia albertii*. *Commun. Biol.* 3:87. doi: 10.1038/s42003-020-0816-5
- Konno, T., Tatsuyanagi, J., Takahashi, S., Kumagai, Y., Wada, E., Chiba, M., et al. (2012). Isolation and identification of *Escherichia albertii* from a patient in an outbreak of gastroenteritis. *Jpn. J. Infect. Dis.* 65, 203–207. doi: 10.7883/yoken.65.203
- Kumar, S., Stecher, G., and Tamura, K. (2016). MEGA7: molecular Evolutionary Genetics Analysis Version 7.0 for Bigger Datasets. *Mol. Biol. Evol.* 33, 1870–1874. doi: 10.1093/molbev/msw054
- Letunic, I., and Bork, P. (2016). Interactive tree of life (iTOL) v3: an online tool for the display and annotation of phylogenetic and other trees. *Nucleic Acids Res.* 44, W242–W245. doi: 10.1093/nar/gkw290
- Masuda, K., Ooka, T., Akita, H., Hiratsuka, T., Takao, S., Fukada, M., et al. (2020). Epidemiological Aspects of *Escherichia albertii* Outbreaks in Japan and Genetic Characteristics of the Causative Pathogen. *Foodborne Pathog. Dis.* 17, 144–150. doi: 10.1089/fpd.2019.2654
- Murakami, K., Kimura, S., Nagafuchi, O., Sekizuka, T., Onozuka, D., Mizukoshi, F., et al. (2020). Flagellum expression and swimming activity by the zoonotic pathogen *Escherichia albertii*. *Environ. Microbiol. Rep.* 12, 92–96. doi: 10.1111/1758-2229.12818
- Oaks, J. L., Besser, T. E., Walk, S. T., Gordon, D. M., Beckmen, K. B., Burek, K. A., et al. (2010). *Escherichia albertii* in wild and domestic birds. *Emerg. Infect. Dis.* 16, 638–646. doi: 10.3201/eid1604.090695
- Ooka, T., Ogura, Y., Katsura, K., Seto, K., Kobayashi, H., Kawano, K., et al. (2015). Defining the Genome Features of *Escherichia albertii*, an Emerging Enteropathogen Closely Related to *Escherichia coli*. *Genome Biol. Evol.* 7, 3170–3179. doi: 10.1093/gbe/evv211
- Ooka, T., Seto, K., Kawano, K., Kobayashi, H., Etoh, Y., Ichihara, S., et al. (2012). Clinical significance of *Escherichia albertii*. *Emerg. Infect. Dis.* 18, 488–492. doi: 10.3201/eid1803.111401
- Ooka, T., Seto, K., Ogura, Y., Nakamura, K., Iguchi, A., Gotoh, Y., et al. (2019). O-antigen biosynthesis gene clusters of *Escherichia albertii*: their diversity and similarity to *Escherichia coli* gene clusters and the development of an O-genotyping method. *Microb. Genom.* 5:e000314. doi: 10.1099/mgen.0.000314
- Ooka, T., Tokuoka, E., Furukawa, M., Nagamura, T., Ogura, Y., Arisawa, K., et al. (2013). Human gastroenteritis outbreak associated with *Escherichia albertii*, Japan. *Emerg. Infect. Dis.* 19, 144–146. doi: 10.3201/eid1901.120646
- Orskov, F., and Orskov, I. (1992). *Escherichia coli* serotyping and disease in man and animals. *Can. J. Microbiol.* 38, 699–704.
- Ratiner, Y. A. (1998). New flagellin-specifying genes in some *Escherichia coli* strains. *J. Bacteriol.* 180, 979–984. doi: 10.1128/JB.180.4.979-984.1998
- Ratiner, Y. A., Sihvonen, L. M., Liu, Y., Wang, L., and Siitonen, A. (2010). Alteration of flagellar phenotype of *Escherichia coli* strain P12b, the standard type strain for flagellar antigen H17, possessing a new non-*flhC* flagellin gene *flnA*, and possible loss of original flagellar phenotype and genotype in the course of subculturing through semisolid media. *Arch. Microbiol.* 192, 267–278. doi: 10.1007/s00203-010-0556-x
- Samatey, F. A., Imada, K., Nagashima, S., Vonderviszt, F., Kumasaka, T., Yamamoto, M., et al. (2001). Structure of the bacterial flagellar protofilament and implications for a switch for supercoiling. *Nature* 410, 331–337. doi: 10.1038/35066504
- Stamatakis, A. (2014). RAxML version 8: a tool for phylogenetic analysis and post-analysis of large phylogenies. *Bioinformatics* 30, 1312–1313. doi: 10.1093/bioinformatics/btu033
- Tominaga, A. (2004). Characterization of six flagellin genes in the H3, H53 and H54 standard strains of *Escherichia coli*. *Genes Genet. Syst.* 79, 1–8. doi: 10.1266/ggs.79.1
- Wang, L., Rothenmund, D., Curd, H., and Reeves, P. R. (2003). Species-wide variation in the *Escherichia coli* flagellin (H-antigen) gene. *J. Bacteriol.* 185, 2936–2943. doi: 10.1128/jb.185.9.2936-2943.2003

**Conflict of Interest:** The authors declare that the research was conducted in the absence of any commercial or financial relationships that could be construed as a potential conflict of interest.

**Publisher's Note:** All claims expressed in this article are solely those of the authors and do not necessarily represent those of their affiliated organizations, or those of the publisher, the editors and the reviewers. Any product that may be evaluated in this article, or claim that may be made by its manufacturer, is not guaranteed or endorsed by the publisher.

Copyright © 2021 Nakae, Ooka, Murakami, Hara-Kudo, Imuta, Gotoh, Ogura, Hayashi, Okamoto and Nishi. This is an open-access article distributed under the terms of the Creative Commons Attribution License (CC BY). The use, distribution or reproduction in other forums is permitted, provided the original author(s) and the copyright owner(s) are credited and that the original publication in this journal is cited, in accordance with accepted academic practice. No use, distribution or reproduction is permitted which does not comply with these terms.



# Application of Lab-on-Chip for Detection of Microbial Nucleic Acid in Food and Environment

Liu Yang<sup>1†</sup>, Wei Yi<sup>2†</sup>, Fangfang Sun<sup>1†</sup>, Mengjiao Xu<sup>1</sup>, Zhan Zeng<sup>3</sup>, Xiaoyue Bi<sup>1</sup>, Jianping Dong<sup>4\*</sup>, Yao Xie<sup>1,3\*\*</sup> and Minghui Li<sup>1,3\*†</sup>

## OPEN ACCESS

### Edited by:

Xuejun Ma,  
Chinese Center for Disease Control  
and Prevention, China

### Reviewed by:

Changchun Liu,  
University of Connecticut Health  
Center, United States  
Thomas S. Hammack,  
United States Food and Drug  
Administration, United States

### \*Correspondence:

Yao Xie  
xieyao00120184@sina.com  
Jianping Dong  
13611351665@163.com  
Minghui Li  
wuhm2000@sina.com

<sup>†</sup>These authors have contributed  
equally to this work

### \*ORCID:

Minhui Li  
orcid.org/0000-0003-3233-5473  
Yao Xie  
orcid.org/0000-0003-4108-7037

### Specialty section:

This article was submitted to  
Food Microbiology,  
a section of the journal  
Frontiers in Microbiology

**Received:** 27 August 2021

**Accepted:** 08 October 2021

**Published:** 04 November 2021

### Citation:

Yang L, Yi W, Sun F, Xu M,  
Zeng Z, Bi X, Dong J, Xie Y and Li M  
(2021) Application of Lab-on-Chip for  
Detection of Microbial Nucleic Acid in  
Food and Environment.  
Front. Microbiol. 12:765375.  
doi: 10.3389/fmicb.2021.765375

<sup>1</sup> Department of Hepatology Division 2, Beijing Ditan Hospital, Capital Medical University, Beijing, China, <sup>2</sup> Department of Gynecology and Obstetrics, Beijing Ditan Hospital, Capital Medical University, Beijing, China, <sup>3</sup> Department of Hepatology Division 2, Peking University Ditan Teaching Hospital, Beijing, China, <sup>4</sup> Department of Infectious Diseases, Haidian Hospital, Beijing Haidian Section of Peking University Third Hospital, Beijing, China

Various diseases caused by food-borne or environmental pathogenic microorganisms have been a persistent threat to public health and global economies. It is necessary to regularly detect microorganisms in food and environment to prevent infection of pathogenic microorganisms. However, most traditional detection methods are expensive, time-consuming, and unfeasible in practice in the absence of sophisticated instruments and trained operators. Point-of-care testing (POCT) can be used to detect microorganisms rapidly on site and greatly improve the efficiency of microbial detection. Lab-on-chip (LOC) is an emerging POCT technology with great potential by integrating most of the experimental steps carried out in the laboratory into a single monolithic device. This review will primarily focus on principles and techniques of LOC for detection of microbial nucleic acid in food and environment, including sample preparation, nucleic acid amplification and sample detection.

**Keywords:** food, environment, microorganism enrichment, LOC, isothermal amplification, biosensor

## INTRODUCTION

Pathogenic microorganisms refer to any microorganism capable of injuring its host by competing with it for metabolic resources, destroying its cells or tissues, or secreting toxins. The injurious microorganisms include viruses, bacteria, parasites, fungi, chlamydia, mycoplasma, etc. They can reside in food and the environment (e.g., water, soil, and air) and transmit disease, posing a serious threat to human health (Table 1). About 420,000 deaths and 600 million foodborne illnesses caused by 31 species of food-borne pathogenic microorganisms were reported in 2010. The burden of foodborne disease is rather high in low-income areas such as Africa, South-east Asia and the Eastern Mediterranean (Havelaar et al., 2015). Therefore, more convenient, rapid and economical microbial detection methods are needed to strengthen the detection of pathogenic microorganisms in food and environment, so as to achieve the purpose of prevention, timely diagnosis and isolation.

Cell culturing and identification of the pathogen type by microscopy or other biochemical tests is the most common method of detecting pathogenic microorganisms, but it takes several days. In addition, some bacteria such as *Staphylococcus aureus* and *E. coli* can enter a viable but non-culturable state under severe harsh survival pressure. In this case, these bacteria remain to be harmful because of their virulence and pathogenicity (Chen et al., 2020; Liao et al., 2021).



Thus, scientists have designed nucleic acid-based or immunological detection methods such as DNA probe, polymerase chain reaction (PCR), reverse transcription polymerase chain reaction (RT-PCR), lateral flow dipstick (LFD), enzyme linked immunosorbent assay (ELISA) and enzyme linked fluorescent assay (ELFA), etc. Unfortunately, most of them are expensive and unaffordable in low-income areas. What's more, these technologies usually rely on sophisticated instruments and trained operators, which prevents them from on-site testing of food and environmental pathogenic microorganisms.

Point-of-care testing (POCT) is carried out in the field of sampling. It can quickly obtain results by using portable analytical instruments, while no professional laboratorians are needed. The development of POCT equipment that can be applied to low-income developing countries should follow the "ASSURED" principles as proposed by the World Health Organization, namely "(1) affordable, (2) sensitive, (3) specific, (4) user-friendly, (5) rapid and robust, (6) equipment-free and (7) deliverable to end-users" (Chen et al., 2019). Currently a research hotspot in the field of POCT is microfluidic technology, which allows precise control of micro-scale fluids in micro-nano scale space. Microfluidic technology offers unique advantages such as faster response, smaller volume of sample and reagent, greater sensitivity, shorter diffusion distances, and smaller system sizes. Lab-on-chip (LOC) uses microfluidic technology to integrate all steps from sample preparation to sample testing into a micro device. Here, we reviewed the recent advances in the application of LOC in food and environmental microbial detection. Since nucleic acid detection techniques have made great progress recently, this paper focuses on application of LOC for the nucleic acid detection of food and environmental microorganisms.

## OVERVIEW OF LAB-ON-CHIP

Lab-on-chip, also known as a micro total analysis system, uses microfluidic technology to integrate sample input, dilution, reaction and separation within a single monolithic device. The micro total analytical system was first proposed by A. Maz, N. Gaber and H.M. Idmer in 1990. Based on flow injection analysis, chromatography and electrophoresis, the micro total analytical system can achieve faster and more efficient chromatographic separation, faster electrophoresis separation speed, shorter transmission time, and remarkably reduce the consumption of carrier, reagent or mobile phase (A. Manz et al., 1990). Since then, LOC has attracted attention of researchers in biology, medicine, chemistry, electronics, materials science and many other fields. The preparation materials were developed from silicon and quartz glass to high polymer such as thiolene polymer, polystyrene, polycarbonate, polydimethylsiloxane (PDMS), polymethylmethacrylate (PMMA), cellulose acetate paper (Mauk et al., 2015; Hansen et al., 2018; Xiong et al., 2019; Hasan et al., 2020; Yin et al., 2020). The chip was prepared with ultraviolet lithography, soft lithography (Hansen et al., 2018), and 3D printing technology (Kim et al., 2018). New materials and fabrication processes make

it possible to produce large numbers of identical chips within a short time.

Most of the existing LOC equipment for microbial detection in food and the environment are based on immunological principles, as immunological-based methods are simple to operate. In contrast, nucleic acid testing often requires elaborate sample handling to release, separate, and concentrate nucleic acid, and is not commonly used in LOC equipment. But sensitivity and specificity of nucleic acid testing is superior to immune assays. By *in vitro* amplification, nucleic acid-based tests can achieve a higher specificity and sensitivity (1,000 times or more) than immunoassay (Mauk et al., 2015).

As shown in **Figure 1**, the main steps of nucleic acid detection of microorganisms in the food environment include pathogen capture, cell lysis, nucleic acid extraction and purification, nucleic acid amplification and nucleic acid detection. Each step can be accurately controlled by micro-pump, micro-valve, and micro-column on the chip (Romao et al., 2017).

## SAMPLE PREPARATION IN LOC FOR NUCLEIC ACID DETECTION OF FOOD AND ENVIRONMENTAL MICROORGANISMS

Generally the content of target microorganisms and nucleic acids in the matrix of food environmental samples is too few to be used directly for nucleic acid amplification. Moreover, the efficiency of nucleic acid amplification reaction is affected by many disadvantages in the complex sample matrix, such as plasmin and calcium ion in milk, myoglobin in muscle, humic acid in soil, particulate matter in indoor air, etc. (Hedman and Rådström, 2013). Therefore, a reliable sample preparation method, namely pathogen capture, is required to isolate the target microorganisms from the complex sample matrix before nucleic acid amplification. After being isolated from a complex sample matrix, the target microorganism can be used for nucleic acid amplification after elution, cell lysis, nucleic acid extraction and purification. Currently, methods of pathogen capture commonly used in LOC devices include microsphere, filter or membrane, dielectrophoresis (DEP), magnetophoresis, acoustophoresis, etc, which are highlighted below.

### Microspheres, Filters or Membranes

The target microbes in samples can be attracted by specific antibodies in the microspheres, and then detected quickly by immunofluorescence and other technologies (Chen and Park, 2018). Zhao et al. (2021) developed a highly sensitive fluorescent immunosensor to detect *E. coli* O157:H7 in milk. In this system, the target cells are captured by the microspheres marked with carbon dots (CDs). CDs has excellent optical properties, so the microspheres have strong fluorescence intensity, good stability and uniformity, and great potential as a fast and sensitive tool for detecting pathogens in milk and other foods. Cai et al. (2019) modified magnetic

**TABLE 1 |** Common pathogenic microorganisms in food, environment, related diseases, and main source.

Pathogen	Disease	Main source	References
<i>Norovirus</i>	Acute gastroenteritis.	Bivalve shellfish, vegetables, drinking water, surface water, sewage, recycled water, <i>etc.</i>	Kittigul et al., 2019; Miura et al., 2019; Sarmiento et al., 2020
<i>Salmonella</i>	Salmonellosis, such as septicaemia, typhoid fever, acute gastroenteritis, <i>etc.</i>	Animal-derived foods such as pork, lamb, beef and poultry and poultry products such as laying hens, turkeys, eggs, drinking water, ocean, surface water, low temperature, organic manure improved clay, <i>etc.</i>	Arce et al., 2018; Phan-Thien et al., 2020; Mejia et al., 2021
<i>Campylobacter</i>	Acute self-limited enteritis, autoimmune diseases such as Miller Fisher syndrome, reactive arthritis, <i>etc.</i> Bacteremia and Guillain-Barre syndrome can occur in people with low immunity.	Poultry, especially broiler chickens, surface water, drinking water, <i>etc.</i>	Kaakoush et al., 2015; Ferrari et al., 2019; Sinulingga et al., 2020
<i>Escherichia coli</i>	Diarrhea, especially infants and childhood diarrhea in developing countries.	Dairy and meat products, surface waters, tap and well water, bottled drinking water, forest and pasture soils, <i>etc.</i>	Dusek et al., 2018; Abri et al., 2019; Topalcengiz and Danyluk, 2019; Vasconcellos et al., 2019
<i>Vibrio cholerae</i>	Choler, acute gastroenteritis, wound infection, otitis media, sepsis.	Fishes, shrimps, shellfish, crustaceans and other aquatic animals, coastal waters, reservoir, estuary, lake water, <i>etc.</i>	Fu et al., 2020; Daboul et al., 2020; Mavian et al., 2020
<i>Shigellai</i>	Bacillary dysentery.	Fresh vegetables, fresh fruit, meat, drinking water, surface water, municipal wastewater, <i>etc.</i>	Shahin et al., 2019; Vadde et al., 2019; Gebrewahd et al., 2020
<i>Hepatitis A virus</i>	Acute hepatitis A.	Bivalve shellfish, vegetables, fruit, <i>etc.</i>	Lowther et al., 2019
<i>Staphylococcus aureus</i>	Food poisoning.	Dairy products, meat, <i>etc.</i>	Velasco et al., 2018; Dai et al., 2019
<i>Rotavirus</i>	Diarrhea, especially in children below five years old worldwide.	Drinking water, surface water, sewage, recycled water and contaminated food, <i>etc.</i>	Miura et al., 2019; Tarek et al., 2019; Ahmed et al., 2020
<i>Clostridium tetani</i>	Tetanus.	Neutral or alkaline soils, with temperatures >20°C and humidity reaching at least 15%.	Popoff, 2020
<i>Bacillus anthracis</i>	Anthrax.	Clayey soils rich in organic matter and Ca <sup>2+</sup> , with pH above 6.0 and temperatures above 15.5°C.	Salgado et al., 2020
<i>Clostridium perfringens</i>	Gas gangrene, food poisoning.	Soil contaminated with feces, acid soils with pH values between 4.5 and 6.5.	Voidarou et al., 2011
<i>Yersinia pestis</i>	Plague.	Arid, highly saline soils.	Barbieri et al., 2020
<i>Leptospira</i>	Leptospirosis.	Warm, moist soils. There is a significant positive relationship between presence of <i>Leptospira</i> and concentration of iron, manganese and copper in soil.	Lall et al., 2018; Cucchi et al., 2019
<i>Soil-transmitted helminths</i>	Diarrhea, malnutrition, anemia, stunted growth, and impaired intellectual development.	Warm moist soil contaminated with feces.	Moser et al., 2019
<i>Mycobacterium tuberculosis</i>	Tuberculosis, such as pulmonary TB, TB meningitis, and TB lymph nodes.	Bioaerosol and droplets containing <i>Mycobacterium tuberculosis</i> exhaled by patients with active tuberculosis.	Patterson et al., 2020
<i>Measles virus</i>	Measles.	Bio aerosol and droplets containing measles virus, produced when an infected person coughs.	Zemouri et al., 2020
<i>Legionella</i>	Legionnaires' disease.	Aerosols containing <i>Legionella</i> bacteria from cooling tower or other air-conditioning systems.	Crook et al., 2020
<i>Varicella-zoster virus</i>	Varicella, zoster.	Aerosol containing varicella-zoster virus from blistering skin lesions.	Lachiewicz and Srinivas, 2019
H1N1 virus	Bird flu.	Biological aerosols and droplets containing influenza A viruses produced when an infected person coughs, speaks, and sneezes.	Prost et al., 2019
COVID-19	Novel coronavirus pneumonia.	Respiratory droplets and air pollution particles (>1 µm)	Nazarenko, 2020
Non-tuberculous mycobacteria	Opportunistic lung infection.	It is ubiquitous and abundant in soil, but most of it is abundant in cold, damp, acidic soil, and the abundance is positively correlated with the content of iron in soil.	Walsh et al., 2019; Glickman et al., 2020
<i>Sporothrix</i>	Sporotrichosis.	Its distribution is related to a variety of plants, flowers, sawdust, reed leaves, corn stalks, leaves and sawdust, <i>etc.</i> , and can survive in soil at temperatures from 6.6 to 28.84°C and 37.5% to 99.06% relative humidity.	Ramirez-Soto et al., 2018
<i>Aspergillus fumigatus</i>	It can lead to invasive lung disease in immunocompromised patients.	Can live in a wide range of pH and moisture conditions in the soil, heat resistant but not thermophilic, continuous temperature of 60°C will cause significant growth slowdown.	Wang D. et al., 2018; Stewart et al., 2020

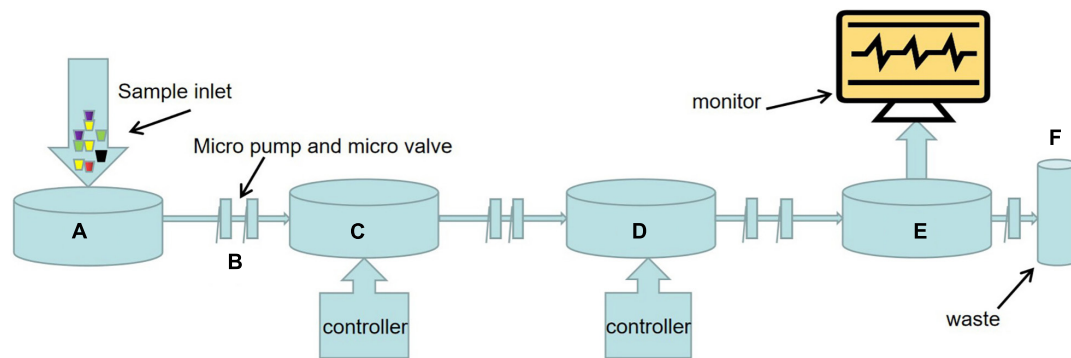


**FIGURE 1 |** Schematic diagram of LOC process for nucleic acid detection of food and environmental microorganisms. **(A)** Sample injection. **(B)** There are a large number of micro-pumps and micro-valves on the chip to precisely control the flow direction and flow rate of microfluids. **(C)** Sample preparation including pathogen capture, cell lysis, nucleic acid extraction and purification, etc. The methods of pathogen capture mainly include microsphere, filter or membrane, dielectrophoresis, magnetophoresis, acoustophoresis, etc. This part often needs external electric field, magnetic field, ultrasonic, and its strength is controlled by the controller. **(D)** Nucleic acid amplification. In addition to traditional PCR, various emerging isothermal nucleic acid amplification techniques have been applied to LOC equipment. The substrate used for nucleic acid amplification is packed into a micro chamber in advance, and the temperature of the reaction process is controlled by a temperature controller. **(E)** Sample detection devices, primarily sensors. Such as fluorescence sensors, surface plasma resonance (SPR) sensors, surface enhanced Raman scattering (SERS) sensors, electrochemical biosensors. **(F)** Results are visually displayed on the display.

nanoparticles with anti-*Salmonella* monoclonal antibodies for the enrichment of *Salmonella* Typhimurium from samples. Then they were conjugated with anti-*Salmonella* polyclonal antibody and catalase modified polystyrene microspheres to form magnetic nanoparticle-bacteria-polystyrene-catalase sandwiches. Catalase from the complex passes through a micromixer to catalyze the decomposition of hydrogen peroxide to produce oxygen. The oxygen increases the pressure in the microchannel and pushes the indicative red dye solution to move along the channel. The movement distance of the red dye can be visually seen using calibration scales and is related to the number of *Salmonella* typhimurium. In the LOC equipment based on nucleic acid detection, various methods such as magnetophoresis and acoustophoresis are needed to separate the bacteria-microspheres complex from the microspheres without bacteria. After washing and cell lysis, DNA/RNA is obtained for nucleic acid amplification (Kant et al., 2018). Kubo et al. (2020) designed a LOC device to detect *Salmonella* in egg yolks using magnetic beads modified with anti-*Salmonella* antibodies. After thermal lysis, the target genes were amplified by PCR, and then detected by fluorescence probe.

Filters or membranes can also be used for pathogen enrichment. Kim and Oh (2019) inoculated *E. coli* O157:H7 on beef, then filtered the beef homogenate at a concentration of  $10^2$  CFU/mL with 0.45  $\mu\text{m}$  cellulose fiber membrane. DNA in concentrated *E. coli* was amplified and analyzed by loop-mediated isothermal amplification (LAMP). The results showed that the sensitivity of sample testing of the filtered samples was 100 times higher than that of the unfiltered samples, for the homogenate at a concentration of  $10^2$  CFU/mL, while the total reaction time from sample preparation to confirmation of *E. coli* was within 3 h. Vibbert et al. (2015) used hollow fiber membranes with a diameter of 0.28 mm to microfilter the chicken homogenate after endopeptidase treatment, which

could increase the microbial concentration to the detectable level within a few of hours.

## Dielectrophoresis

Dielectrophoresis is a method of separating suspended particles by producing a polarizing force in a non-uniform electric field. The particles in DEP are uncharged but must be polarizable (Zhang et al., 2019). Large amounts of electrical charges can be generated at the surface of the polarizable particles exposed to a non-uniform electric field. These charges form dipoles (a pair of charges with opposite signs that are very close together) arranged in parallel with the applied magnetic field. Each half of the dipole in a non-uniform electric field is subjected to an unequal force, so the net force on the particle is not zero, which then pushes the particle toward or away from a region of strong electric field. Cells are typically polarizable particles. The net force depends on the dielectric constant, size and shape of the particle, and the dielectric constant of the medium, so it can selectively target the particle according to its phenotype (Khoshmanesh et al., 2011). Abdullah et al. (2019) used positive dielectrophoresis (pDEP) based focusing electrodes and biosensors to detect *Salmonella* in concentrations as low as 10 pieces/mL from chicken products in less than 1 h. Cai et al. (2018) designed a kind of microfluidic device based on pDEP, which integrated H-type filter desalination and pDEP, and could directly enrich *E. coli* from physiological samples with high conductivity and viscosity such as milk. In the main channel of the H-type filter, the electrolyte is continuously diffused into the deionized water, while the bacteria remain in the sample. After desalination, the sample is pumped into the DEP chamber, where the bacterial cells are captured through the pDEP. Jasim et al. (2019) designed a microfluid-based impedance biosensor that could rapidly detect three *Salmonella* serogroups simultaneously. It consists of three microchannels, and in which *Salmonella* cells are focused on the centerline and guided to the sensing area by pDEP to obtain highly concentrated samples.

## Magnetophoresis

Magnetophoresis is a technology that uses a flexible and controllable magnetic field to manipulate the motion of magnetic beads in a microchannel (Cao et al., 2014). The magnetic beads can be separated according to their different size and magnetic content, which leads to different direction of magnetic beads deviating from laminar flow (Pamme and Manz, 2004). Magnetophoresis can be used to separate various bacterial microbead complexes from microbeads without bacteria. Ngamsom et al. (2016a) used two different commercial magnetic beads (Dynabeads® *Salmonella* resistant magnetic beads and Hyglos-Streptavidin magnetic beads) to multiple separate *Salmonella* typhimurium and *E. coli* in food preconcentration. The mixed cultures of the bacterial microbead complexes are introduced into the separation chamber with the buffer, and the two types of microbeads are isolated because of different magnetic forces under the influence of the array magnets. Malec et al. (2018) designed a microfluidic device based on magnetophoresis and obtained reliable parameters for predicting *E. coli* concentration. In this system, *E. coli* is captured by streptavidin coated magnetic particles (MPs) to form magnetically labeled bacteria (MLBs). The MLBs are suspended in the liquid of the microchannel and are accelerated toward the exit by means of a magnetic field gradient. The magnetic field gradient is generated by the integrated microconductor and controlled by the microcontroller. As a reference, the reference MPs was added to the same liquid in parallel microchannel, and the velocities of MLBs and reference MPs were compared in real time using a digital camera mounted on an optical microscope combined with particle track tracking software.

## Acoustophoresis

Acoustophoresis can be used to separate particles with different acoustic physical properties without labeling, that is, antibody staining or other labeling is not needed. Acoustophoresis uses ultrasonic waves in microchannels to control the migration of suspended particles of different size, compressibility, and density. The denser or less compressible particles move more rapidly toward the pressure node in the center of the channel than the less dense or more compressible particles. Therefore, acoustophoresis can selectively direct suspended particles with different acoustic physical properties to different microchannel outlets (Olm et al., 2021). The recovery of *Salmonella* typhimurium from chicken and beef samples by acoustophoresis has achieved high recovery rates (60–90%) (Ngamsom et al., 2016b). GN6 aptamer is a type of aptamer that binds specifically to gram-negative bacteria, so when mixed with a complex sample matrix, it can selectively capture gram-negative bacteria and leave gram-positive bacteria behind. Lee S. et al. (2019) mixed microspheres coated with GN6 aptamers with samples and injected them into microchannels. As the mixture enters the acoustic standing wave field, the microspheres bound to gram-negative bacteria migrate along the buffer center and exit the system through the outlet center. Gram-positive bacteria remained in the original buffer flow along the side wall and were removed through the side wall. Using ultrasound to manipulate particles in microfluidics channels is a

promising research direction. Aghakhani et al. (2021) reported an acoustophoresis system based on flexural wave, which can capture micron-sized particles or cells on the soft wall. The acoustophoresis system is expected to play an important role in enhancing immunoassays and particle sensors.

## NUCLEIC ACID AMPLIFICATION IN LOC FOR NUCLEIC ACID DETECTION OF FOOD AND ENVIRONMENTAL MICROORGANISMS

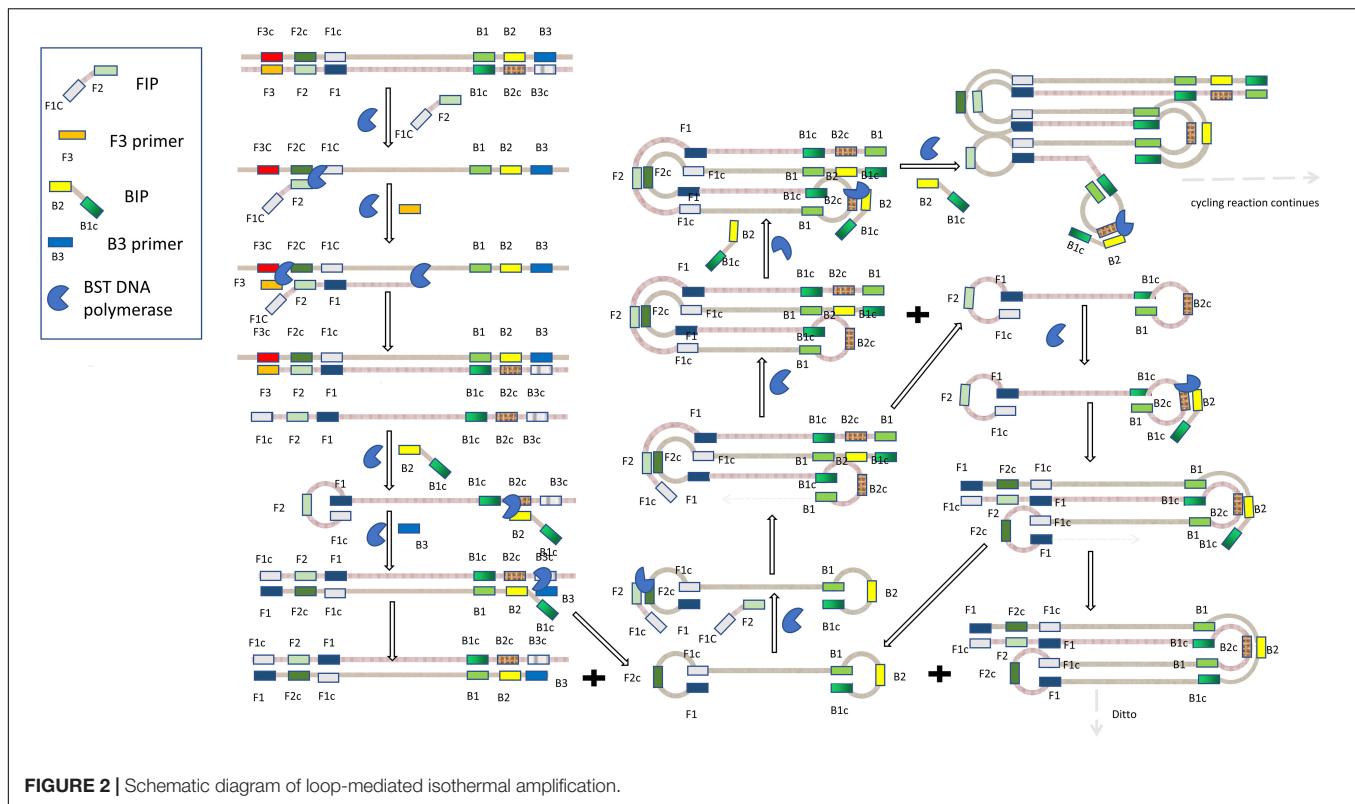
### Polymerase Chain Reaction

Polymerase chain reaction (PCR) is a molecular biology technique to greatly increase the amount of nucleic acid *in vitro* (Saiki et al., 1988). After the completion of nucleic acid amplification, methods such as gel electrophoresis are needed to quantify the DNA. Real-time quantitative PCR is a technique for real-time amplification of target DNA and quantification of products in a system, but it's not absolutely quantitative (Singh and Roy-Chowdhuri, 2016). Digital PCR is a kind of absolute quantitative method. It mainly disperses the diluted nucleic acid solution into microreactors or droplets of the chip, and the number of nucleic acid templates in each reactor or droplet is  $\leq 1$ . After the PCR cycle, only the reactor with a template of the nucleic acid molecule will give a fluorescence signal (Catarsi, 2019). Reverse transcription polymerase chain reaction (RT-PCR) is used to detect RNA. In RT-PCR, RNA is firstly transcribed into complementary DNA (cDNA), which can then be amplified by PCR (Elfman and Li, 2020). Microfluidic digital PCR has been successfully used to detect norovirus and hepatitis A in soft berries, water samples and lettuce, and hepatitis E virus in naturally contaminated pig liver products (Coudray-Meunier et al., 2015; Martin-Latil et al., 2016; Fraisse et al., 2017). A shunt PCR method was reported by Salman et al. (2020). In this microfluidic device, the PCR reaction chamber can be heated or cooled in a short period of time by a thin layer of fluid and a large static heating system with high thermal inertia elements and stabilized at a preset reaction temperature. The reaction chamber is not fixed, but is cycled between the reaction temperatures required for the denaturation, annealing and extension stages. Fluorescent dyes were embedded in the PCR products, and the whole PCR process was monitored in real time by the fluorescence detection lock-on photodetector.

### Isothermal Nucleic Acid Amplification

Polymerase chain reaction-based nucleic acid amplification is complex and requires expensive instruments, which does not meet the goals of LOC development. Isothermal nucleic acid amplification is an ideal alternative to PCR given that it is performed at constant temperatures and can be used for nucleic acid amplification without programmable thermal cyclers. In recent years, isothermal nucleic acid amplification technology has been developed rapidly, and the most mature ones include loop-mediated isothermal amplification (LAMP), recombinase polymerase amplification





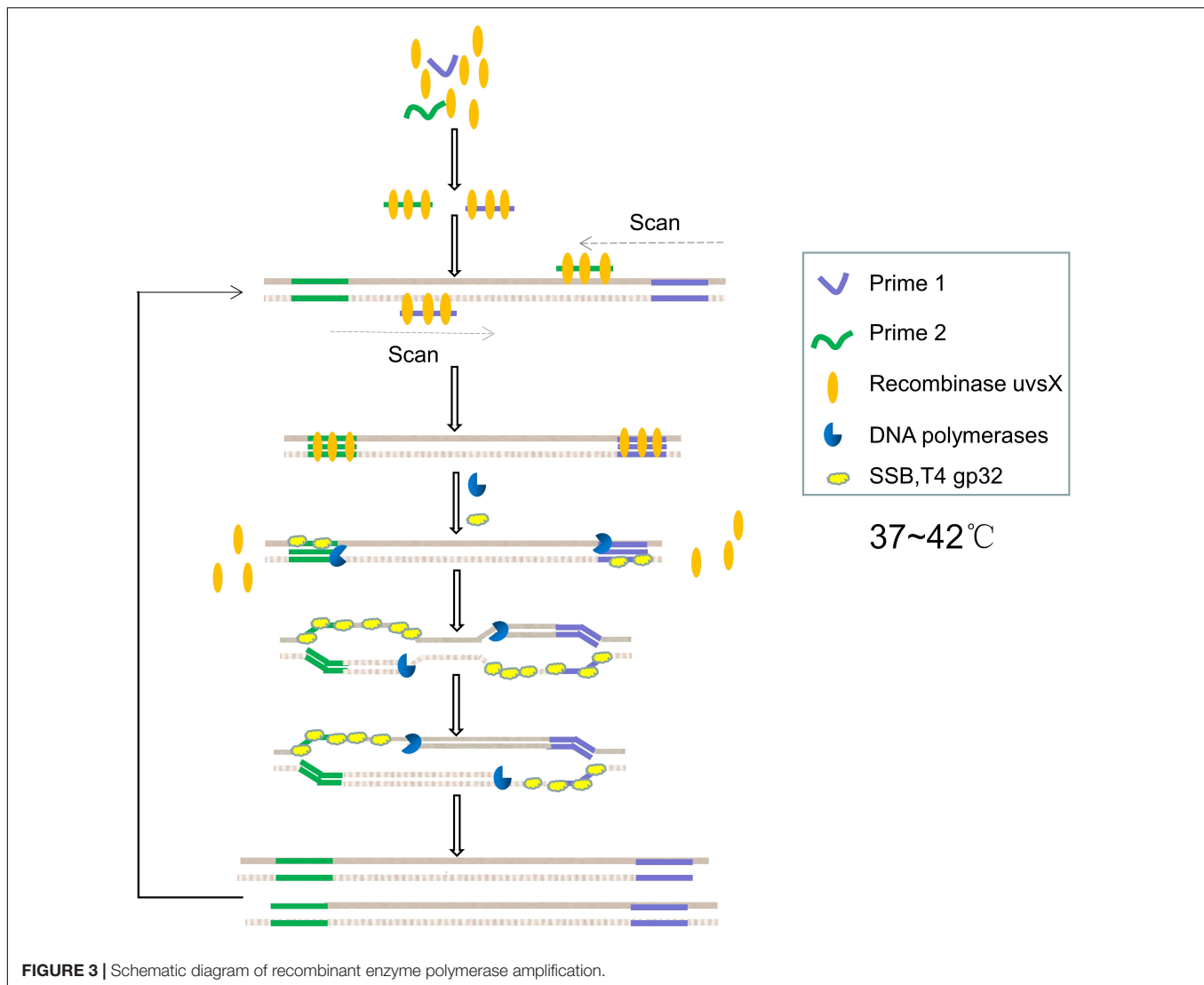
(RPA), helicase-dependent amplification (HDA), rolling circle amplification (RCA), nucleic acid sequence-based amplification (NASBA), cross priming amplification (CPA) (Woźniakowski et al., 2018), strand swat amplification (SDA) (Walker et al., 1994) and recombinant enzyme assisted amplification assay (RAA) (Shen et al., 2019).

### Loop-Mediated Isothermal Amplification

Loop-mediated isothermal amplification, which was first proposed by Notomi et al. (2000), has the advantages of high specificity, sensitivity, speediness and simplicity (Guan and Ma, 2014). As shown in **Figure 2**, it requires a BST DNA polymerase with strand displacement activity and four primers specifically designed to identify six different regions of the target DNA, and the reaction takes place at 60–65°C. The four primers include forward internal primer (FIP), F3 primer, reverse internal primer (BIP), B3 primer. As is shown in **Figure 2**, FIP consists of F2 and F1c region, which are complementary to F2c and F1 regions in the two strands of DNA, respectively. The primer of this structure is the basis of the formation of stem-loops in the subsequent amplification process. The F3 primer, also known as forward outer primer, is complementary to the F3c region. Similarly, BIP consists of B2 and B1c region, and B3 primer, also known as backward outer primer, is complementary to B3c region. At first, the F2 region of FIP hybridizes with the F2c region of DNA to initiate complementary strand synthesis with the action of BST DNA polymerase. The F3c region is exposed at this moment. However, since F3 primer is shorter than FIP and has a lower concentration in the system, F3 primer will hybridize with F3c

region for a period of time after FIP mediates amplification with the action of BST DNA polymerase and releases complementary chain connected to FIP. The end of the released complementary chain includes F1 and F1c regions, thus forming a loop, while the other end serves as a template for BIP-initiated DNA synthesis and subsequent B3 prime-initiated strand replacement. The first stage eventually produces dumbbell-shaped DNA, which serves as the starting material for the second stage of the LAMP reaction. The LAMP reaction then continues in this manner, eventually producing a mixture of stem-loop DNA with different stem lengths and cauliflower shaped structures with multiple loops (Notomi et al., 2000; Li et al., 2016).

Zhou et al. (2021) developed a microfluidic chip integrating real-time fluorescence and LAMP technology, which could simultaneously detect 10 pathogenic microorganisms. They used a universal genomic DNA extraction kit in advance to extract total DNA from the sample and then added it to the system for sample testing. The average detection time was less than 30 min. The limits of detection of bacterial genomic DNA was  $10^0$ – $10^{-1}$  pg/μL, and the limits of detection of recombinant plasmid DNA was  $10^{-4}$ – $10^{-5}$  pg/μL. Compared to the conventional microbial detection method, its specificity and sensitivity were 85.53% and 93.52%, respectively. Trinh and Lee (2018) designed a LAMP-based plastic microdevice for the detection of *E. coli* O157:H7, *Staphylococcus aureus*, *Salmonella*, and others in milk samples. Jiang et al. (2016) developed a LAMP-based microfluidic chip for rapid capture, enrichment and detection of airborne *Staphylococcus aureus*. The entire analysis process took about 4 h and 40 min, and the detection limit was as low as about 27



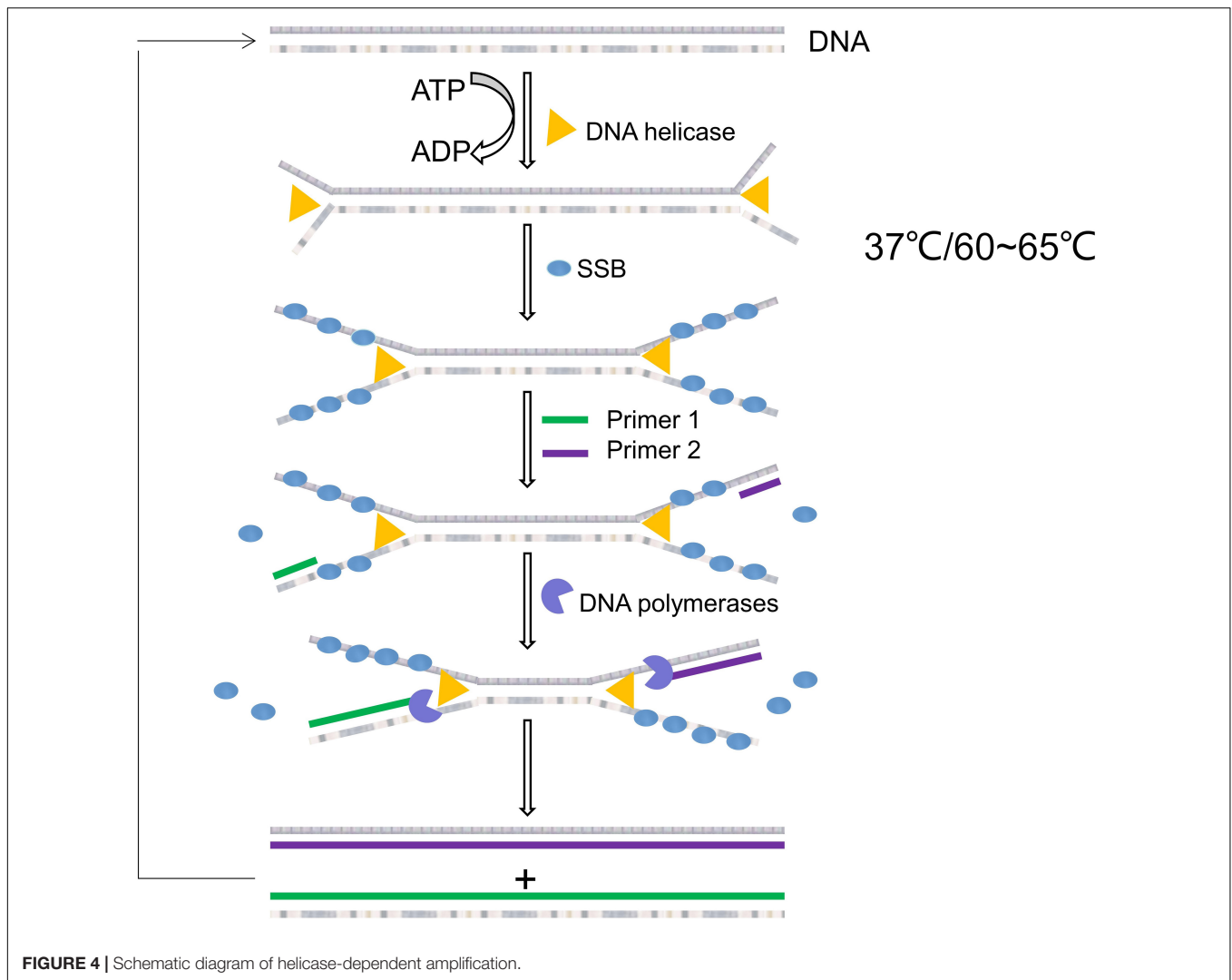
cells. LAMP has also been used in LOC applications for *Vibrio parahaemolyticus* in aquatic products, *Aspergillus fumigata* in clinical and environmental isolates, and *Salmonella* in food (Pang et al., 2017; Wang et al., 2020; Yu L. S. et al., 2020).

### Recombinant Enzyme Polymerase Amplification

Recombinant enzyme polymerase amplification was first proposed by Piepenburg et al. (2006). The whole reaction system consists of bacteriophage recombinase uvsX and cofactor uvsY, primers, single-stranded DNA-binding protein (SSB) T4 GP32, DNA polymerase, deoxynucleotide triphosphate (dNTP) and buffer, etc. RPA is usually performed under isothermal conditions between 37°C and 42°C, which is suitable for on-site pathogenic diagnosis in field lack of instruments and for preventing heat-induced DNA mutations. The reaction time is usually 15–40 min, which is shorter than most PCR reactions (Yang et al., 2018; Lee J. et al., 2019).

The principle of PRA is shown in **Figure 3**. Firstly, the recombinase forms a complex with the primers, which scans the

DNA sequence and inserts the primers into homologous locus through the strand displacement activity of the recombinant enzyme. Meanwhile, SSB stabilizes the replaced single-stranded DNA. The recombinase then disintegrates, making it easy for DNA polymerase with strand displacement activity to enter the 3'-end of the primers to prolong the primers. Exponential amplification is achieved by repeating the process over and over again (Lobato and O'Sullivan, 2018). Lee et al. (2021) introduced a high-performance nanogap impedimetric sensor that uses RPA to amplify nucleic acids in real time. The nanogap impedimetric sensor was immersed in the RPA reaction solution to detect *E. coli* O157:H7. The amplification of the target DNA was evaluated by impedance spectroscopy changes per minute during the RPA process. Yin et al. (2020) presented an integrated multiplex digital RPA (ImdRPA) microfluidic chip that successfully detected *E. coli* O157:H7, *Salmonella* enteritis and *Listeria monocytogenes* in milk within 45 min. Ahn et al. (2018) developed an RPA method based on a paper chip device, which is made by simply stacking functional paper and drying the RPA reagent and fluorescent



probe in the reaction zone of a poly (ether sulfone) membrane. *E. coli*, *Staphylococcus aureus* and *Salmonella typhimurium* can be detected simultaneously based on fluorescent signal of paper chip, and the detection limit was  $10^2$  CFU/mL.

### Helicase-Dependent Amplification

Helicase-dependent amplification was first proposed in 2004 by Vincent et al. (2004). The whole reaction system is composed of helicase, SSB, DNA polymerase, two primers, dNTP, and buffer. The helicase and the polymerase must work jointly to prevent the polymerase from being replaced by the helicase. Pairs of helicases/polymerases that work together in natural systems must therefore be used. Vincent et al. initially used *E. coli* UvrD helicase/DNA polymerase I Klenow fragment, which can be performed at 37°C. If thermophilic helicase/polymerase is used for HDA, the reaction can be carried out at 60~65°C, which is called thermophilic helicase dependent HDA (tHDA) (Xu et al., 2018).

The principle of HDA is shown in **Figure 4**. In the reaction system, the helicase uses energy of adenosine triphosphate

hydrolysis to break the hydrogen bonds between the complementary bases of double-stranded DNA, thus untying the double-stranded DNA. Therefore, the dNTPs mixture must be rich in dATP as a cofactor of the helicase. If *E. coli* UvrD helicase is used, the methyl directed mismatch repair protein (MUTL protein) should be added to the reaction system. This collaboration between UvrD helicase and MutL protein is associated with the repair of DNA mismatches in *E. coli*. After the double chain is unchained, the SSB binds to the unchained single chain to prevent recombination of the complementary chains. After stabilizing the DNA, the two primers bind to the target sequence, and DNA polymerase extends the primers using dNTP to produce a double-stranded amplification product (Barreda-García et al., 2018). Chen et al. (2015) extracted genomic DNA from lysed bacteria using silica coated magnetic nanoparticles and amplified it using tHDA to detect *Staphylococcus aureus* in dairy and meat products. The detection limit of the system was  $5 \times 10^0$  CFU/mL for milk powder samples and  $5 \times 10^1$  CFU/mL for pork samples within less than 2 h. HDA has also been used to detect *Enterobacter*

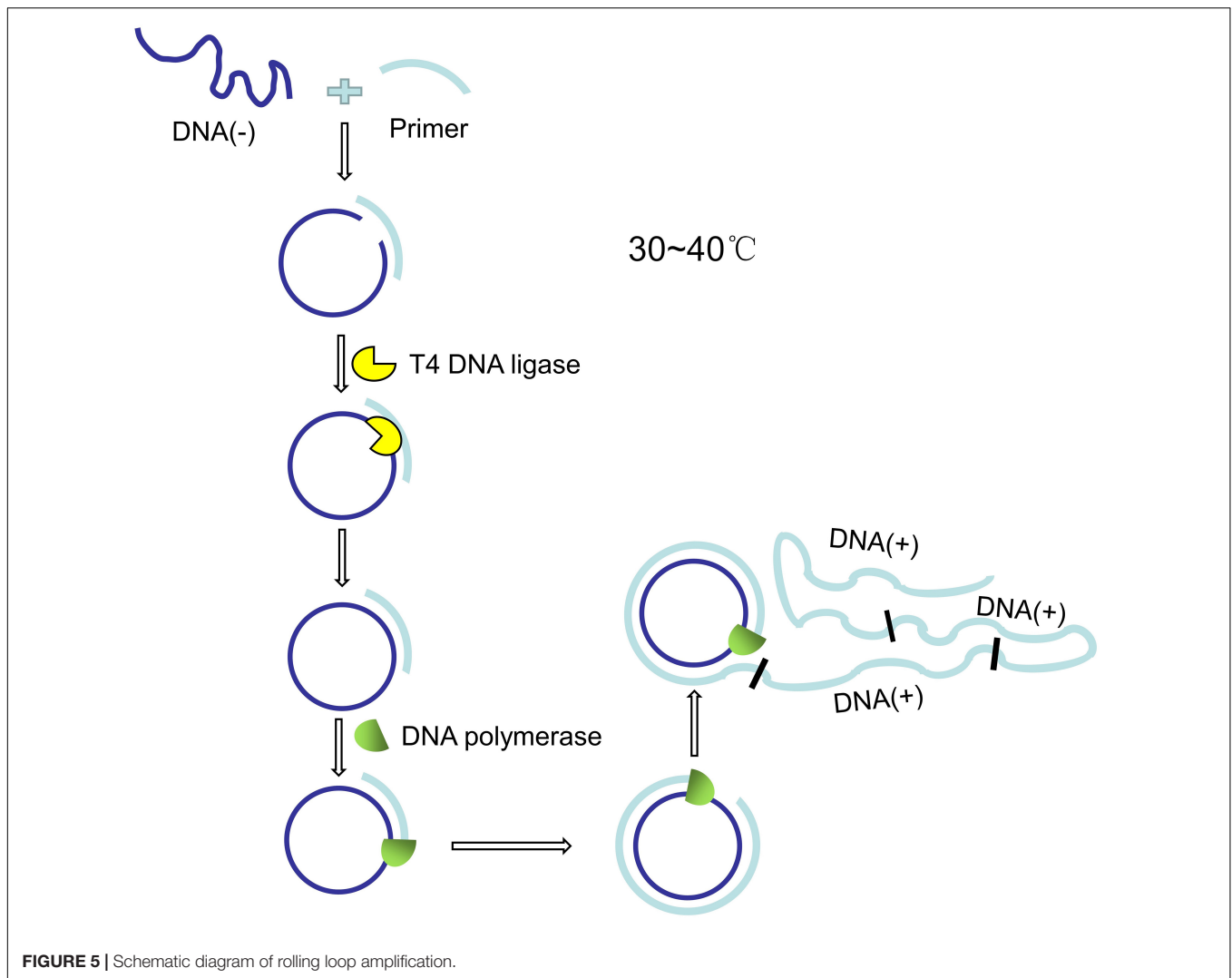


**FIGURE 5** | Schematic diagram of rolling loop amplification.

sakazakii in infant formula with high sensitivity (94%) and specificity (100%) (Xu et al., 2018).

### Rolling Loop Amplification

The concept of RCA was first presented in the 1990s (Liu et al., 1996), using circular DNA/RNA templates and special DNA or RNA polymerases to amplify short DNA or RNA primers into long single-stranded DNA or RNA. A typical DNA amplification reaction system consists of primers P, T4 ligase, bacteriophage  $\phi$ 29 DNA polymerase, dNTP and buffer, and the reaction usually takes place at 30~40°C. The principle of RCA is shown in **Figure 5**.

The circular DNA/RNA template is generated by hybridizing primer P with long chain T. Primer P is designed to have a larger and a shorter overlap with T, and the long chain T can be converted into circular molecules by T4 ligase. The RCA reaction for DNA amplification is performed with bacteriophage  $\phi$ 29 DNA polymerase, which has special chain displacement properties. The polymerase begins to synthesize the complementary chain at primer P. After a round of

polymerization, it displaces the newly synthesized strand and continues to polymerize, which eventually leads to the formation of a single long strand with a repeating sequence of T (Beyer et al., 2005). Minero et al. (2019) designed a microfluidic device that uses magnetic microspheres to capture the target microorganism and amplify nucleic acids with RCA, which is expected to be used in the detection of microorganisms in food and environment. Jiang et al. (2020) proposed a novel dual-RCA microfluidic platform for the detection of *E. coli* O157:H7, which could significantly improve the detection signal by about 250 times. RCA was used twice in this process. The first RCA was used for *in situ* amplification of aptamers conjugated to the surface of microchannels. The aptamers are used to capture *E. coli* O157:H7, and its nucleic acid sequence will be amplified several times by RCA. The target cells captured by RCA amplified microchannels were 3 times more than those without RCA amplified microchannels. The second RCA reaction was aimed to amplify the detection signal of *E. coli* O157:H7. The product was a long extended repetitive *E. coli* O157:H7 DNA sequence complementary to the signal probe. The microfluidic platform



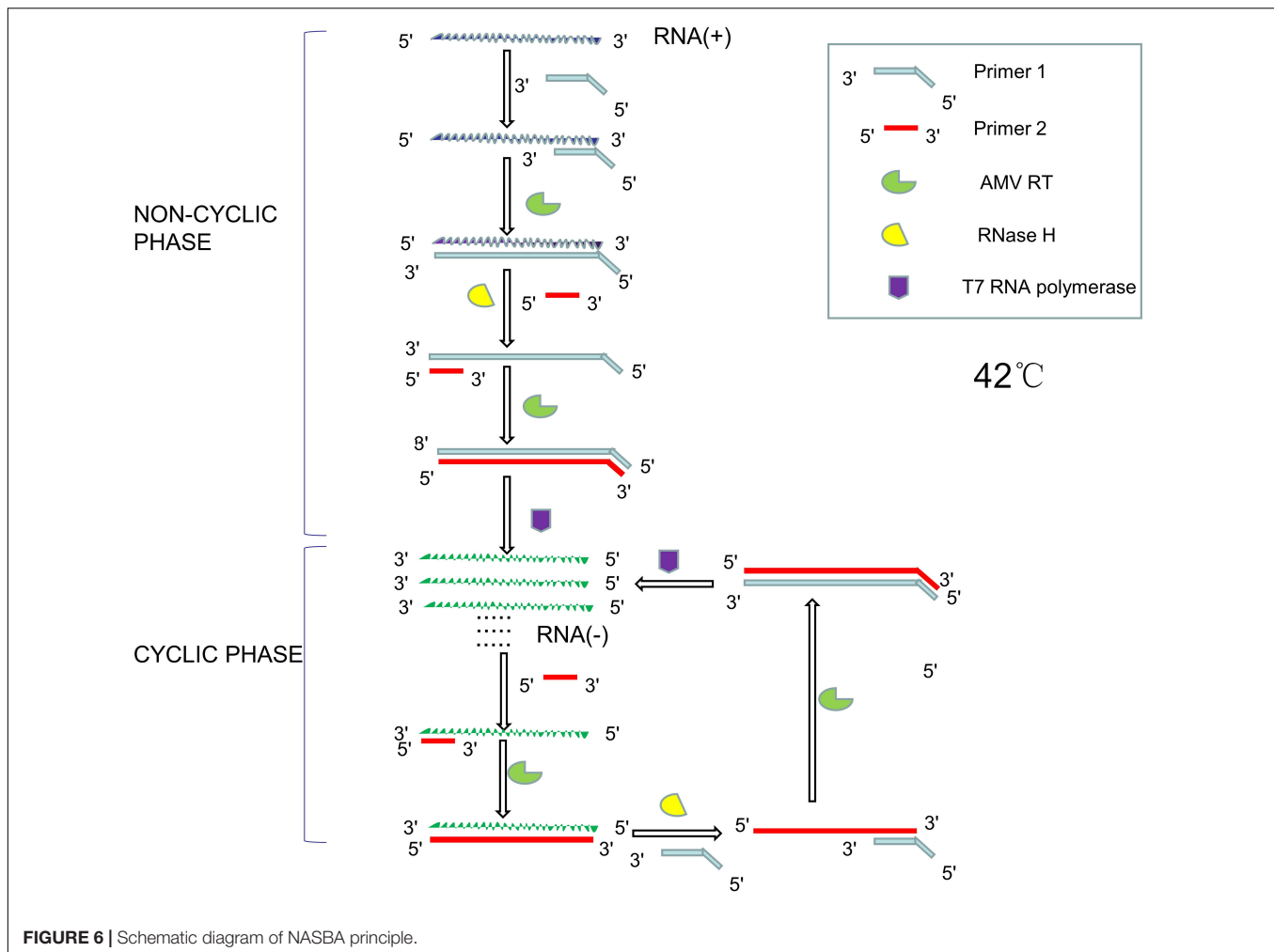


**FIGURE 6 |** Schematic diagram of NASBA principle.

can be used in a variety of food matrices, including orange juice and milk, with a detection limit of 80 cells/mL.

### Nucleic Acid Sequence-Dependent Amplification

Nucleic acid sequence-dependent amplification is a technique for isothermal RNA amplification firstly proposed by Compton (1991). The entire reaction system consist of Avian Myeloblastosis Virus Reverse Transcriptase (AMV RT), bacteriophage T7 RNA polymerase, ribonuclease H, two primers (the 5' end of primer 1 contains a T7 promoter sequence recognized by bacteriophage T7 RNA polymerase), dNTP, nucleotide triphosphates (NTP), and buffer. AMV RT can synthesize DNA using either DNA or RNA as templates. Bacteriophage T7 RNA polymerase is a DNA-dependent 5'→3' RNA polymerase that highly specifically recognizes the T7 promoter sequence. RNase H specifically hydrolyzes RNA in the DNA-RNA heterozygote. The reaction usually takes place at around 42°C (Huang et al., 2019). Its principle is shown in **Figure 6**.

The reaction consists of two parts, namely non-cyclic phase and cyclic phase. In the non-cyclic phase, the forward primer (primer 1) hybridizes with the single-stranded RNA to synthesize

complementary DNA strands with the action of AMV RT, and then RNase H hydrolyze the RNA strand. The reverse primer (primer 2) hybridizes with the remaining DNA single strand, and the DNA is synthesized to form double stranded DNA with the help of the AMV RT. The T7 RNA polymerase then recognizes the promoter sequence of the DNA and transcribes it into single stranded RNA. In the cyclic phase, single-stranded RNA binds to reverse primers to synthesize single-stranded DNA under the action of AMV RT. The RNA strand in DNA-RNA heterozygote strand will be hydrolyzed by RNase H, and the remaining DNA is hybridized with forward primers to synthesize the DNA sequence with the T7 promoter sequence with the help of AMV RT. T7 RNA polymerase can then use DNA as a template to produce large amounts of single-stranded RNA (Wang J. et al., 2018). Aufdembrink et al. (2020) used a set of fluorescent aptamers as NASBA labels to significantly improve sensitivity of the assay, which can be used for nucleic acid detection of microorganisms in food and environment by using a fluorescent microplate reader and 3D-printed microfluidic platform. NASBA-based LOC devices have been successfully used to detect *E. coli* and Rotavirus in water and *Salmonella* in pork, beef and milk (Zhao et al., 2012; Zhai et al., 2019; Pilevar et al., 2021).

## SAMPLE DETECTION IN LOC FOR NUCLEIC ACID DETECTION OF FOOD AND ENVIRONMENTAL MICROORGANISMS

Besides pathogen capture, cell lysis, nucleic acid extraction, and nucleic acid amplification, LOC equipment also need a variety of sample testing methods to detect microorganisms qualitatively or quantitatively. Biosensor is a device that measures biological or chemical reactions by producing a signal proportional to the concentration of an analyte. Molecules that specifically recognize the analyte are called biological receptors. The signal generation resulting from the interaction between the biological receptors and the analyte is called biometrics, and mainly in the form of light, heat, pH, charge or mass changes. Most transducers produce optical, electrical, or other measurable signals. These energy signals are then processed and monitored by electronic equipment (Bhalla et al., 2016). Several common sensors such as fluorescence sensor, SPR sensor, SERS sensor and electrochemical biosensor are briefly introduced as below.

### Fluorescence Detection

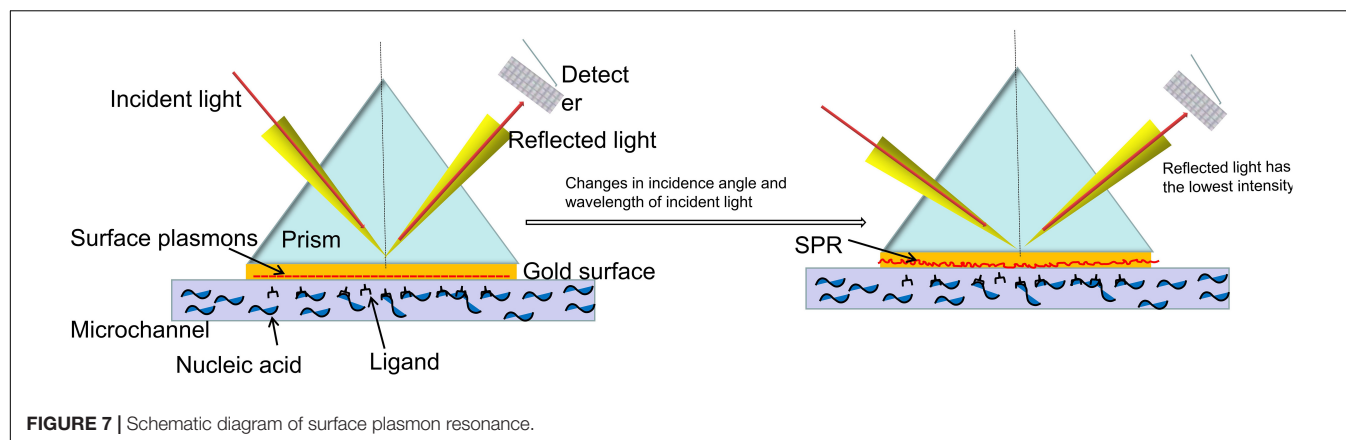
Fluorescent probes are often used to detect nucleic acids in real-time PCR (Ahn et al., 2018; Aufdembrink et al., 2020; Salman et al., 2020; Zhou et al., 2021). Some nucleic acids have a very weak internal fluorescence that is hardly detected. Fluorescent probes are small fluorescent molecules which can enhance the fluorescence intensity after binding with nucleic acid. Fluorescence signal was then detected by fluorescence microscope and fluorescence biosensor. Fluorescent probes include organic fluorescent dyes, metal complexes, metal particles, nanoparticles, etc. (Kricka and Fortina, 2009). For example, 4', 6-diamidino-2-phenylindole (DAPI) is a DNA-specific probe that forms fluorescent complexes by attaching to A-T-rich DNA sequences (Kapuscinski, 1995). Wei et al. (2020) designed and synthesized a small-molecule fluorescent probe based on adenine-coumarin derivative. The probe showed significant fluorescence enhancement to nucleic acid at 495 nm (DNA) and 487 nm (RNA), and the fluorescence intensity showed a good linear relationship with the concentration of nucleic acid. Peptide nucleic acids (PNAs) are synthetic DNA analogs that can be used as probes to strongly hybridize with DNA (Park et al., 2019). Klimkowski et al. (2019) synthesized a series of thiazole orange (TO) functionalized oligonucleotides for nucleic acid detection. They found that 2'-OME RNA probes with TO at uracil 5 or ribose 2' were extremely effective, showing up to 44-fold fluorescence enhancement to DNA and RNA.

Nucleic acid detection based on CRISPR/Cas system also utilizes fluorescence detection methods. The CRISPR/Cas system is an adaptive immune system which is widely present in bacteria and archaea. It includes three stages: adaptation, expression, and interference. In the adaptation phase, bacteria or archaea carrying one or more CRISPR loci can integrate short DNA fragments homologous to foreign virus or plasmid sequences into host chromosomes. In the expression stage, pre-CrRNA, a primary transcript of the CRISPR gene sequence,

is produced and processed into crRNA. crRNA matches the target sequence of the virus or plasmid. In the interference stage, crRNA guides Cas protein to the target sequence of virus or plasmid to form the effector complex, and uses Cas protein to cut the target sequence (Makarova et al., 2011). Nucleic acid detection based on CRISPR/Cas system mainly utilizes Cas9, Cas12, and Cas13. Cas9 has two domains, HNH domain and RuvC\_like domain, which cleave complementary and non-complementary strands of target DNA, respectively. Zhang et al. (2017) mutated these two domains of Cas9 and obtained nuclease-deactivated Cas9 (dCas9). The luciferase was divided into two parts (Nfluc or Cfluc) and fused with two dCas9 proteins, respectively. Using two types of single guide RNA (sgRNA) complementary to the upstream and downstream segments of the target DNA sequence, two dCas9 were guided to the upstream and downstream segments of the target DNA, and the distance between the two parts of luciferase was shortened. Its catalytic activity was restored to emit light to achieve the detection effect. Different from Cas9, Cas12 and Cas13 have additional accessory cutting activity. When Cas protein forms an efficacious complex with sgRNA and target sequence, its accessory cutting activity is activated to indiscriminately cut the surrounding non-target nucleic acid that has been labeled by fluorescence, thus releasing signals for detection (Abudayyeh et al., 2016). Gootenberg et al. (2017) designed a platform called SHERLOC that utilizes this accessory cutting activity of CRISPR/Cas13a to detect Zika virus and Dengue virus. Chen et al. (2018) designed a platform called DETECTR that utilizes this accessory cutting activity of CRISPR/Cas12a to detect human papillomavirus. However, the CRISPR-based nucleic acid detection methods mentioned above still rely on traditional PCR or isothermal amplification technology to amplify target molecules. For example, SHERLOCK and DETECTR both use RPA to amplify target nucleic acids. Nucleic acid detection technology based on CRISPR/Cas system is rarely used in LOC of nucleic acid detection of food and environmental microorganisms, though it has great research prospects.

### Surface Plasmon Resonance

The principle of Surface plasmon resonance (SPR) is shown in **Figure 7**. SPR is an optical phenomenon. The evanescent wave, which occurs when light is completely reflected at the glass interface, can trigger free electrons on the metal surface to produce plasmon. Under certain circumstances, the surface plasma and the evanescent wave will resonate if their frequency and wave number of are equal. Then the incident light is absorbed and the reflected light energy drops sharply, so a resonance peak will appear on the reflected spectrum when the reflected intensity reaches the lowest value. The resonance angle or resonance wavelength varies with the surface medium of metal film. Therefore, SPR spectrum can reflect changes of the surface of the metal film. The resonance angle or resonance wavelength will be changed by combining the biological receptors with the analyte (Fathi et al., 2019). Huang et al. (2020) designed a portable multi-angle scan SPR sensor that uses a motor to rotate and drive the belt to control the angle of the motor's incident and reflected light for real-time monitoring. The nucleic acid hybridization



experiment on gold film chip can obtain the sample information by observing the reflection spectrum.

## Surface-Enhanced Raman Scattering

Raman spectra is a kind of scattering spectrum, which can obtain molecular structure information by analyzing the scattering spectrum caused by different incident light frequencies. After the analyte is fixed on the metal surface through interaction with biological receptors, its molecular structure can be identified by Raman spectra. It is found that the intensity of Raman spectra can be greatly improved when the sample is adsorbed on nano-metal particles or metal pieces with rough surface, which is called surface enhanced Raman scattering (SERS) (Butler et al., 2016; Barbosa et al., 2021). Yu H. et al. (2020) developed a new SERS-based sensor, which uses gold nanoflowers (AuNFs) to improve the intensity of Raman spectra. The sensor enables sensitive and quantitative analysis of biomolecules. It can distinguish different bacteria with a sensitivity as low as a single bacteria, suggesting a great application prospect. Zhou et al. (2020) designed an SERS-based biosensor for the detection of *E. coli* O157:H7 from food. Aptamer (APT-1) and signaling molecule Rhodamine B (RhB) were bound to gold nanorods (GNRs) to form a gold

nanobone (NBs). Apt-1 and RhB were embedded in NBs, and the combination showed good recognition, excellent stability and significant enhancement of Raman signal strength in the detection of *E. coli* O157:H7.

## Electrochemical Biosensors

Biological reactions often cause consumption or production of electrons or ions, and the reaction between the receptors and the targets is no exception. The electrical properties of the solution, such as potential and current, may thus change. The transducer can be used to transform the biological signal into a detectable electrical signal proportional to the target concentration (Ferapontova, 2018; Wu et al., 2019). Conductance/impedance, amperometric/voltammetric, and potentiometric methods are the most commonly used electrochemical biosensing methods that can be integrated into microfluidic devices (Kant et al., 2018). Park et al. (2018a) designed a membrane based integrated chip to detect *Staphylococcus aureus* and *E. coli* in food. The system can simultaneously perform nucleic acid amplification and electrochemical detection, and accurately analyze the target pathogen genes by square wave voltammetry (SWV) in 25 s. But before these samples can be used in the developed sensor,

**TABLE 2 |** Five typical Lab-on-chip (LOC) devices for detection of microbial nucleic acid in food and environment.

Pathogen	Sample	Nucleic acid extraction method	Nucleic acid amplification method	Sample test method	Detection limit	Detection time	References
<i>Salmonella</i>	Pork	Immunomagnetic beads	LAMP	Real-time fluorescence detection.	50 cells per test.	40 min	Sun et al., 2015
<i>E. coli</i> O157: H7, <i>Listeria monocytogenes</i> and <i>Salmonella</i>	MILK	Magnetic bead	RPA	Real-time fluorescence detection.	10 cells for each kind of pathogen.	15 min	Yin et al., 2020
<i>Staphylococcus aureus</i>	Milk powder and pork	Silica-coated magnetic nanoparticles	HDA	Fluorescence detection	$5 \times 10$ (1) CFU/mL for milk powder samples and $5 \times 10$ (1) CFU/mL for pork samples.	2 h	Chen et al., 2015
<i>Staphylococcus aureus</i>	Air	Don't require.	LAMP	Fluorescence detection	27 cells per test.	4 h and 40 min	Jiang et al., 2016
<i>E. coli</i> O157: H7	Orange juice and milk.	Poly-aptamers modified microchannels	RCA	Fluorescence detection	80 cells/mL	—	Jiang et al., 2020

DNA must be extracted and purified, which can take a long time. Liébana et al. (2016) proposed an electrochemical magnetogenosensing approach for the detection of *Salmonella*, *Listeria*, and *E. coli*. This method used a set of specific primers for each pathogen, followed by electrochemical magnetogenosensing on silica magnetic particles. Park et al. (2018b) produced highly ordered nanocolumnar electrodes by means of soft lithography and metal evaporation. It had wide electrochemical and mechanical properties and wide reaction space, which could be used for sensitive analysis. The gold and silver electrodes prepared on the nanocolumn array shows strong and stable electrochemical performance and can detect amplified genes from foodborne *E. coli* pathogens.

## SUMMARY AND PROSPECT

Microfluidic technology integrates sample preparation, nucleic acid amplification, and sample detection on a chip. The technology of nucleic acid amplification and sample detection has been well developed, and a variety of emerging experimental technologies have been timely designed and implemented on chip. However, the development of sample preparation technology is relatively slow, and most LOC equipment still needs sample pretreatment in advance, which is inconsistent with the concept of micro total analysis system and LOC. As mentioned above, the microfluidic chip integrated with real-time fluorescence loop-mediated isothermal amplification technology developed by Zhou et al. (2021) has good sensitivity and specificity, but preprocessing of samples is required to enrich target DNA. The integrated chip designed by Park et al. (2018a) for the detection of *Staphylococcus aureus* and *E. coli* in food integrates nucleic acid amplification and electrochemical detection, but also requires advance DNA extraction and purification. This makes them unable to meet the requirements of POCT. In fact, most LOC equipment used for food and environmental microbiological detection have not yet been integrated with sample processing equipment. Although several techniques have been developed for sample preparation in LOC, including microsphere, filter or membrane, dielectrophoresis, magnetophoresis, acoustophoresis, an equipment that can directly test the obtained samples without sample processing is the ideal LOC. For example, Sun et al. (2015) reported on an 8-chamber LOC system that integrates microsphere-based sample preparation, LAMP, and real-time fluorescence detection for rapid quantitative detection of *Salmonella* in food samples. The entire diagnostic procedure is performed in a single chamber, and up to eight samples can be processed simultaneously. Yin et al. (2020) successfully detected *E. coli* O157:H7, *Listeria monocytogenes* and *Salmonella enteritidis* in milk within 45 min by integrating magnetic bead enrichment target nucleic acid and

multiple digital RPA (ImdRPA) into microfluidic chip. Chen et al. (2015) used magnetic nanoparticles to extract genomic DNA from lytic bacteria and used HDA amplification to detect *Staphylococcus aureus* in dairy and meat products. The detection limit was  $5 \times 10^0$  CFU/mL for milk powder samples and  $5 \times 10^1$  CFU/mL for pork samples in less than 2 h. The detection time would be greatly reduced if the sample preparation can be integrated into the LOC device (Table 2).

Another challenge for LOC development is interaction between biomolecules and wall of the microfluidic channel. The extremely high surface-to-volume ratio of microchannels may lead to a high incidence of non-specific adsorption and surface effects, that may limit or inhibit amplification reactions. Proper surface treatments, such as polymer coatings with polyethylene glycol (PEG) and linear polyacrylamide (LPA), or sealing with bovine serum albumin, are required to mitigate these effects (Asiello and Baeumner, 2011).

At present, microfluidics and LOC technologies are booming. With the help of scientists in biology, medicine, chemistry, electronics, materials and other fields, we believe that LOC for nucleic acid detection of food and environmental microorganisms will finally meet the “ASSURED” principles as proposed by WHO, and play an important role in the real-time detection of pathogenic microorganisms in food and environment.

## AUTHOR CONTRIBUTIONS

YX and ML contributed to study concept and design. LY, WY, FS, MX, ZZ, XB, and JD collected and sorted out literatures. LY, YX, and ML drew pictures. LY, WY, and FS wrote the first draft. YX and ML edited the English version. JD, YX, and ML approved the submitted version after modification. All authors contributed to the article and approved the submitted version.

## FUNDING

This work was supported by Beijing Hospitals Authority Clinical Medicine Development of Special Funding Support (Nos. XMLX 201706 and XMLX 202127), Special Public Health Project for Health Development in Capital (2021-1G-4061), The Digestive Medical Coordinated Development Center of Beijing Hospitals Authority (Nos. XXZ0302 and XXT28), National Science and Technology Major Project of China (Nos. 2017ZX10201201-001-006 and 2017ZX10201201-002-006, and 2018ZX10715-005-003-005), Beijing Municipal Science & Technology Commission (No. Z151100004015122), Project supported by Beijing Science and Technology Commission (No. D161100002716002).

## REFERENCES

- Abdullah, A., Dastider, S. G., Jasim, I., Shen, Z., Yuksek, N., Zhang, S., et al. (2019). Microfluidic based impedance biosensor for pathogens detection in food products. *Electrophoresis* 40, 508–520. doi: 10.1002/elps.201800405
- Abri, R., Javadi, A., Asghari, R., Razavilar, V., Salehi, T. Z., Safaeeyan, F., et al. (2019). Surveillance for enterotoxigenic & enteropathogenic *Escherichia coli* isolates from animal source foods in Northwest Iran. *Indian J. Med. Res.* 150, 87–91. doi: 10.4103/ijmr.IJMR\_2019\_17



- Abudayyeh, O. O., Gootenberg, J. S., Konermann, S., Joung, J., Slaymaker, I. M., Cox, D. B., et al. (2016). C2c2 is a single-component programmable RNA-guided RNA-targeting CRISPR effector. *Science* 353:aaf5573. doi: 10.1126/science.aaf5573
- Aghakhani, A., Cetin, H., Erkok, P., Tombak, G. I., and Sitti, M. (2021). Flexural wave-based soft attractor walls for trapping microparticles and cells. *Lab Chip* 21, 582–596. doi: 10.1039/d0lc00865f
- Ahmed, J., Wong, L. P., Chua, Y. P., Channa, N., Mahar, R. B., Yasmin, A., et al. (2020). Quantitative microbial risk assessment of drinking water quality to predict the risk of waterborne diseases in primary-school children. *Int. J. Environ. Res. Public Health* 17:2774. doi: 10.3390/ijerph17082774
- Ahn, H., Batule, B. S., Seok, Y., and Kim, M. G. (2018). Single-Step recombinase polymerase amplification assay based on a paper chip for simultaneous detection of multiple foodborne pathogens. *Anal. Chem.* 90, 10211–10216. doi: 10.1021/acs.analchem.8b01309
- Arce, C., Cahya-Mawarda, P., Arroyo-Manzanares, N., Garrido, J. J., and Arce, L. (2018). CE method for analyzing *Salmonella typhimurium* in water samples. *J. Sep. Sci.* 41, 534–539. doi: 10.1002/jssc.201700705
- Asiello, P. J., and Baumann, A. J. (2011). Miniaturized isothermal nucleic acid amplification, a review. *Lab Chip* 11, 1420–1430. doi: 10.1039/c0lc00666a
- Aufdembrink, L. M., Khan, P., Gaut, N. J., Adamala, K. P., and Engelhart, A. E. (2020). Highly specific, multiplexed isothermal pathogen detection with fluorescent aptamer readout. *RNA* 26, 1283–1290. doi: 10.1261/rna.075192.120
- Barbieri, R., Texier, G., Keller, C., and Drancourt, M. (2020). Soil salinity and aridity specify plague foci in the United States of America. *Sci. Rep.* 10:6186. doi: 10.1038/s41598-020-63211-4
- Barbosa, I. B., Barbosa-Dekker, A. M., Dekker, R., Bezerra, A. G. Jr., de Santana, H., and Orsato, A. (2021). Polysaccharide-based substrate for surface-enhanced Raman spectroscopy. *Spectrochim. Acta A Mol. Biomol. Spectrosc.* 249:119255. doi: 10.1016/j.saa.2020.119255
- Barreda-García, S., Miranda-Castro, R., de-Los-Santos-Álvarez, N., Miranda-Ordieres, A. J., and Lobo-Castañón, M. J. (2018). Helicase-dependent isothermal amplification: a novel tool in the development of molecular-based analytical systems for rapid pathogen detection. *Anal. Bioanal. Chem.* 410, 679–693. doi: 10.1007/s00216-017-0620-3
- Beyer, S., Nickels, P., and Simmel, F. C. (2005). Periodic DNA nanotemplates synthesized by rolling circle amplification. *Nano Lett.* 5, 719–722. doi: 10.1021/nl050155a
- Bhalla, N., Jolly, P., Formisano, N., and Estrela, P. (2016). Introduction to biosensors. *Essays Biochem.* 60, 1–8. doi: 10.1042/EBC20150001
- Butler, H. J., Ashton, L., Bird, B., Cinque, G., Curtis, K., Dorney, J., et al. (2016). Using Raman spectroscopy to characterize biological materials. *Nat. Protoc.* 11, 664–687. doi: 10.1038/nprot.2016.036
- Cai, D., Yi, Q., Shen, C., Lan, Y., Urban, G., and Du, W. (2018). Direct enrichment of pathogens from physiological samples of high conductivity and viscosity using H-filter and positive dielectrophoresis. *Biomicrofluidics* 12:014109. doi: 10.1063/1.5016413
- Cai, G., Zheng, L., Liao, M., Li, Y., Wang, M., Liu, N., et al. (2019). A microfluidic immunosensor for visual detection of foodborne bacteria using immunomagnetic separation, enzymatic catalysis and distance indication. *Mikrochim. Acta* 186:757. doi: 10.1007/s00604-019-3883-x
- Cao, Q., Han, X., and Li, L. (2014). Configurations and control of magnetic fields for manipulating magnetic particles in microfluidic applications: magnet systems and manipulation mechanisms. *Lab Chip* 14, 2762–2777. doi: 10.1039/c4lc00367e
- Catarsi, P. (2019). Digital PCR – methods and protocols. *Eur. J. Histochem.* 63:3074. doi: 10.4081/ejh.2019.3074
- Chen, H., Liu, K., Li, Z., and Wang, P. (2019). Point of care testing for infectious diseases. *Clin. Chim. Acta* 493, 138–147. doi: 10.1016/j.cca.2019.03.008
- Chen, J. S., Ma, E., Harrington, L. B., Da Costa, M., Tian, X., Palefsky, J. M., et al. (2018). CRISPR-Cas12a target binding unleashes indiscriminate single-stranded DNase activity. *Science* 360, 436–439. doi: 10.1126/science.aar6245
- Chen, J., and Park, B. (2018). Effect of immunomagnetic bead size on recovery of foodborne pathogenic bacteria. *Int. J. Food Microbiol.* 267, 1–8. doi: 10.1016/j.jfoodmicro.2017.11.022
- Chen, S., Zeng, J., Wang, Y., Ye, C., Zhu, S., Feng, L., et al. (2020). Modelling the effect of chlorination/chloramination on induction of viable but non-culturable (VBNC) *Escherichia coli*. *Environ. Technol.* 41, 3443–3455. doi: 10.1080/09593330.2019.1611939
- Chen, X., Wu, X., Gan, M., Xu, F., He, L., Yang, D., et al. (2015). Rapid detection of *Staphylococcus aureus* in dairy and meat foods by combination of capture with silica-coated magnetic nanoparticles and thermophilic helicase-dependent isothermal amplification. *J. Dairy Sci.* 98, 1563–1570. doi: 10.3168/jds.2014-8828
- Compton, J. (1991). Nucleic acid sequence-based amplification. *Nature* 350, 91–92. doi: 10.1038/350091a0
- Coudray-Meunier, C., Fraisse, A., Martin-Latil, S., Guillier, L., Delannoy, S., Fach, P., et al. (2015). A comparative study of digital RT-PCR and RT-qPCR for quantification of Hepatitis A virus and Norovirus in lettuce and water samples. *Int. J. Food Microbiol.* 201, 17–26. doi: 10.1016/j.jfoodmicro.2015.02.006
- Crook, B., Willerton, L., Smith, D., Wilson, L., Poran, V., Helps, J., et al. (2020). Legionella risk in evaporative cooling systems and underlying causes of associated breaches in health and safety compliance. *Int. J. Hyg. Environ. Health* 224:113425. doi: 10.1016/j.ijheh.2019.113425
- Cucchi, K., Liu, R., Collender, P. A., Cheng, Q., Li, C., Hoover, C. M., et al. (2019). Hydroclimatic drivers of highly seasonal leptospirosis incidence suggest prominent soil reservoir of pathogenic *Leptospira* spp. in rural western China. *PLoS Negl. Trop. Dis.* 13:e0007968. doi: 10.1371/journal.pntd.0007968
- Daboul, J., Weghorst, L., DeAngelis, C., Plecha, S. C., Saul-McBeth, J., and Matson, J. S. (2020). Characterization of *Vibrio cholerae* isolates from freshwater sources in northwest Ohio. *PLoS One* 15:e0238438. doi: 10.1371/journal.pone.0238438
- Dai, J., Wu, S., Huang, J., Wu, Q., Zhang, F., Zhang, J., et al. (2019). Prevalence and characterization of *Staphylococcus aureus* isolated from pasteurized milk in China. *Front. Microbiol.* 10:641. doi: 10.3389/fmicb.2019.00641
- Dusek, N., Hewitt, A. J., Schmidt, K. N., and Bergholz, P. W. (2018). Landscape-Scale factors affecting the prevalence of *Escherichia coli* in surface soil include land cover type, edge interactions, and soil pH. *Appl. Environ. Microbiol.* 84:e02714-17. doi: 10.1128/AEM.02714-17
- Elfman, J., and Li, H. (2020). Detection and measurement of chimeric RNAs by RT-PCR. *Methods Mol. Biol.* 2079, 83–94. doi: 10.1007/978-1-4939-9904-0\_6
- Fathi, F., Rashidi, M. R., and Omid, Y. (2019). Ultra-sensitive detection by metal nanoparticles-mediated enhanced SPR biosensors. *Talanta* 192, 118–127. doi: 10.1016/j.talanta.2018.09.023
- Ferapontova, E. E. (2018). DNA electrochemistry and electrochemical sensors for nucleic acids. *Annu. Rev. Anal. Chem. (Palo Alto Calif)* 11, 197–218. doi: 10.1146/annurev-anchem-061417-125811
- Ferrari, S., Frosth, S., Svensson, L., Fernström, L. L., Skarin, H., and Hansson, I. (2019). Detection of *Campylobacter* spp. in water by dead-end ultrafiltration and application at farm level. *J. Appl. Microbiol.* 127, 1270–1279. doi: 10.1111/jam.14379
- Fraisse, A., Coudray-Meunier, C., Martin-Latil, S., Hennechart-Collette, C., Delannoy, S., Fach, P., et al. (2017). Digital RT-PCR method for hepatitis A virus and norovirus quantification in soft berries. *Int. J. Food Microbiol.* 243, 36–45. doi: 10.1016/j.jfoodmicro.2016.11.022
- Fu, H., Yu, P., Liang, W., Kan, B., Peng, X., and Chen, L. (2020). Virulence, resistance, and genomic fingerprint traits of *Vibrio cholerae* isolated from 12 species of aquatic products in Shanghai, China. *Microb. Drug Resist.* 26, 1526–1539. doi: 10.1089/mdr.2020.0269
- Gebrewahd, A., Adhanom, G., Gebremichael, G., Kahsay, T., Berhe, B., Asfaw, Z., et al. (2020). Bacteriological quality and associated risk factors of drinking water in Eastern zone, Tigray, Ethiopia, 2019. *Trop. Dis. Travel Med. Vaccines* 6:15. doi: 10.1186/s40794-020-00116-0
- Glickman, C. M., Viridi, R., Hasan, N. A., Epperson, L. E., Brown, L., Dawrs, S. N., et al. (2020). Assessment of soil features on the growth of environmental nontuberculous mycobacterial isolates from Hawai'i. *Appl. Environ. Microbiol.* 86:e00121-20. doi: 10.1128/AEM.00121-20
- Gootenberg, J. S., Abudayyeh, O. O., Lee, J. W., Essletzbichler, P., Dy, A. J., Joung, J., et al. (2017). Nucleic acid detection with CRISPR-Cas13a/C2c2. *Science* 356, 438–442. doi: 10.1126/science.aam9321
- Guan, L., and Ma, X. J. (2014). [Advance in loop-mediated isothermal amplification technique and its applications in point-of-care testing platforms]. *Bing Du Xue Bao* 30, 470–475.

- Hansen, F. A., Sticker, D., Kutter, J. P., Petersen, N. J., and Pedersen-Bjergaard, S. (2018). Nanoliter-Scale electromembrane extraction and enrichment in a microfluidic chip. *Anal. Chem.* 90, 9322–9329. doi: 10.1021/acs.analchem.8b01936
- Hasan, M. N., Fraiwan, A., An, R., Alapan, Y., Ung, R., Akkus, A., et al. (2020). Paper-based microchip electrophoresis for point-of-care hemoglobin testing. *Analyst* 145, 2525–2542. doi: 10.1039/c9an02250c
- Havelaar, A. H., Kirk, M. D., Torgerson, P. R., Gibb, H. J., Hald, T., Lake, R. J., et al. (2015). World health organization global estimates and regional comparisons of the burden of foodborne disease in 2010. *PLoS Med.* 12:e1001923. doi: 10.1371/journal.pmed.1001923
- Hedman, J., and Rådström, P. (2013). Overcoming inhibition in real-time diagnostic PCR. *Methods Mol. Biol.* 943, 17–48. doi: 10.1007/978-1-60327-353-4\_2
- Hida, K., Papafragkou, E., and Kulka, M. (2018). Testing for human norovirus and recovery of process control in outbreak-associated produce items. *J. Food Prot.* 81, 105–114. doi: 10.4315/0362-028X.JFP-17-134
- Huang, C., Huang, P. T., Yao, J. Y., Li, Z. W., Weng, L. B., and Guo, X. G. (2019). Pooled analysis of nuclear acid sequence-based amplification for rapid diagnosis of *Mycoplasma pneumoniae* infection. *J. Clin. Lab. Anal.* 33:e22879. doi: 10.1002/jcla.22879
- Huang, Y., Zhang, L., Zhang, H., Li, Y., Liu, L., Chen, Y., et al. (2020). Development of a portable SPR sensor for nucleic acid detection. *Micromachines (Basel)* 11:526. doi: 10.3390/mi11050526
- Jasim, I., Shen, Z., Mlaji, Z., Yuksek, N. S., Abdullah, A., Liu, J., et al. (2019). An impedance biosensor for simultaneous detection of low concentration of *Salmonella* serogroups in poultry and fresh produce samples. *Biosens. Bioelectron.* 126, 292–300. doi: 10.1016/j.bios.2018.10.065
- Jiang, X., Liu, Y., Liu, Q., Jing, W., Qin, K., and Sui, G. (2016). Rapid capture and analysis of airborne *Staphylococcus aureus* in the hospital using a microfluidic chip. *Micromachines (Basel)* 7:169. doi: 10.3390/mi7090169
- Jiang, Y., Qiu, Z., Le, T., Zou, S., and Cao, X. (2020). Developing a dual-RCA microfluidic platform for sensitive *E. coli* O157:H7 whole-cell detections. *Anal. Chim. Acta* 1127, 79–88. doi: 10.1016/j.aca.2020.06.046
- Kaakoush, N. O., Castaño-Rodríguez, N., Mitchell, H. M., and Man, S. M. (2015). Global epidemiology of campylobacter infection. *Clin. Microbiol. Rev.* 28, 687–720. doi: 10.1128/CMR.00006-15
- Kant, K., Shahbazi, M. A., Dave, V. P., Ngo, T. A., Chidambara, V. A., Than, L. Q., et al. (2018). Microfluidic devices for sample preparation and rapid detection of foodborne pathogens. *Biotechnol. Adv.* 36, 1003–1024. doi: 10.1016/j.biotechadv.2018.03.002
- Kapuscinski, J. (1995). DAPI: a DNA-specific fluorescent probe. *Biotech. Histochem.* 70, 220–233. doi: 10.3109/10520299509108199
- Khoshmanesh, K., Nahavandi, S., Baratchi, S., Mitchell, A., and Kalantar-zadeh, K. (2011). Dielectrophoretic platforms for bio-microfluidic systems. *Biosens. Bioelectron.* 26, 1800–1814. doi: 10.1016/j.bios.2010.09.022
- Kim, J. H., and Oh, S. W. (2019). Development of a filtration-based LAMP-LFA method as sensitive and rapid detection of *E. coli* O157:H7. *J. Food Sci. Technol.* 56, 2576–2583. doi: 10.1007/s13197-019-03740-7
- Kim, K., Kim, H., Kim, S., and Jeon, J. S. (2018). MineLoC: a rapid production of lab-on-a-chip biosensors using 3D printer and the sandbox game, minecraft. *Sensors (Basel)* 18:1896. doi: 10.3390/s18061896
- Kittigul, L., Ruppom, K., Che-Arsae, M., Pombubpa, K., Thongprachum, A., Hayakawa, S., et al. (2019). Occurrence of noroviruses in recycled water and sewage sludge: emergence of recombinant norovirus strains. *J. Appl. Microbiol.* 126, 1290–1301. doi: 10.1111/jam.14201
- Klimkowski, P., De Ornellas, S., Singleton, D., El-Sagheer, A. H., and Brown, T. (2019). Design of thiazole orange oligonucleotide probes for detection of DNA and RNA by fluorescence and duplex melting. *Org. Biomol. Chem.* 17, 5943–5950. doi: 10.1039/c9ob00885c
- Kricka, L. J., and Fortina, P. (2009). Analytical ancestry: “firsts” in fluorescent labeling of nucleosides, nucleotides, and nucleic acids. *Clin. Chem.* 55, 670–683. doi: 10.1373/clinchem.2008.116152
- Kubo, I., Kajiya, M., Aramaki, N., and Furutani, S. (2020). Detection of *Salmonella Enterica* in Egg Yolk by PCR on a microfluidic disc device using immunomagnetic beads. *Sensors (Basel)* 20:1060. doi: 10.3390/s20041060
- Lachiewicz, A. M., and Srinivas, M. L. (2019). Varicella-zoster virus post-exposure management and prophylaxis: a review. *Prev. Med. Rep.* 16:101016. doi: 10.1016/j.pmedr.2019.101016
- Lall, C., Vinod Kumar, K., Raj, R. V., Vedhagiri, K., Sunish, I. P., and Vijayachari, P. (2018). Correlation between physicochemical properties of soil and presence of *Leptospira*. *Ecohealth* 15, 670–675. doi: 10.1007/s10393-018-1346-1
- Lee, H., Yi, S. Y., Kwon, J. S., Choi, J. M., Lee, D. S., Lee, S. H., et al. (2021). Rapid and highly sensitive pathogen detection by real-time DNA monitoring using a nanogap impedimetric sensor with recombinase polymerase amplification. *Biosens. Bioelectron.* 179:113042. doi: 10.1016/j.bios.2021.113042
- Lee, J., Heo, S., and Bang, D. (2019). Applying a linear amplification strategy to recombinase polymerase amplification for uniform DNA library amplification. *ACS Omega* 4, 19953–19958. doi: 10.1021/acsomega.9b02886
- Lee, S., Kim, B. W., Shin, H. S., Go, A., Lee, M. H., Lee, D. K., et al. (2019). Aptamer affinity-bead mediated capture and displacement of gram-negative bacteria using acoustophoresis. *Micromachines (Basel)* 10:770. doi: 10.3390/mi10110770
- Li, J. J., Xiong, C., Liu, Y., Liang, J. S., and Zhou, X. W. (2016). Loop-Mediated isothermal amplification (LAMP): emergence as an alternative technology for herbal medicine identification. *Front. Plant Sci.* 7:1956. doi: 10.3389/fpls.2016.01956
- Liao, X., Hu, W., Liu, D., and Ding, T. (2021). Stress resistance and pathogenicity of nonthermal-plasma-induced viable-but-nonculturable *Staphylococcus aureus* through energy suppression, oxidative stress defense, and immune-escape mechanisms. *Appl. Environ. Microbiol.* 87:e02380-20. doi: 10.1128/AEM.02380-20
- Liébana, S., Brandão, D., Cortés, P., Campoy, S., Alegret, S., and Pividori, M. I. (2016). Electrochemical genosensing of *Salmonella*, *Listeria* and *Escherichia coli* on silica magnetic particles. *Anal. Chim. Acta* 904, 1–9. doi: 10.1016/j.aca.2015.09.044
- Liu, D., Daubendiek, S. L., Zillman, M. A., Ryan, K., and Kool, E. T. (1996). Rolling circle DNA synthesis: small circular oligonucleotides as efficient templates for DNA polymerases. *J. Am. Chem. Soc.* 118, 1587–1594. doi: 10.1021/ja952786k
- Lobato, I. M., and O’Sullivan, C. K. (2018). Recombinase polymerase amplification: basics, applications and recent advances. *Trends Analyt. Chem.* 98, 19–35. doi: 10.1016/j.trac.2017.10.015
- Lowther, J. A., Bosch, A., Butot, S., Ollivier, J., Mäde, D., Rutjes, S. A., et al. (2019). Validation of EN ISO method 15216 - Part 1 – Quantification of hepatitis A virus and norovirus in food matrices. *Int. J. Food Microbiol.* 288, 82–90. doi: 10.1016/j.jiffoodmicro.2017.11.014
- Makarova, K. S., Haft, D. H., Barrangou, R., Brouns, S. J., Charpentier, E., Horvath, P., et al. (2011). Evolution and classification of the CRISPR-Cas systems. *Nat. Rev. Microbiol.* 9, 467–477. doi: 10.1038/nrmicro2577
- Malec, A., Kokkinis, G., Haiden, C., and Giouroudi, I. (2018). Biosensing system for concentration quantification of magnetically labeled *E. coli* in water samples. *Sensors (Basel)* 18:2250. doi: 10.3390/s18072250
- Manz, A., Graber, N., and Widmer, H. M. (1990). Miniaturized total chemical analysis systems: a novel concept for chemical sensing. *Sens. Actuators B Chem.* 1, 244–248. doi: 10.1016/0925-4005(90)80209-1
- Martin-Latil, S., Hennechart-Collette, C., Delannoy, S., Guillier, L., Fach, P., and Perelle, S. (2016). Quantification of hepatitis E virus in naturally-contaminated pig liver products. *Front. Microbiol.* 7:1183. doi: 10.3389/fmicb.2016.01183
- Mauk, M. G., Liu, C., Sadik, M., and Bau, H. H. (2015). Microfluidic devices for nucleic acid (NA) isolation, isothermal NA amplification, and real-time detection. *Methods Mol. Biol.* 1256, 15–40. doi: 10.1007/978-1-4939-2172-0\_2
- Mavian, C., Paisie, T. K., Alam, M. T., Browne, C., Beau De Rochars, V. M., Nembrini, S., et al. (2020). Toxigenic *Vibrio cholerae* evolution and establishment of reservoirs in aquatic ecosystems. *Proc. Natl. Acad. Sci. U.S.A.* 117, 7897–7904. doi: 10.1073/pnas.1918763117
- Mejia, L., Vela, G., and Zapata, S. (2021). High occurrence of multiresistant *Salmonella* Infantis in retail meat in Ecuador. *Foodborne Pathog. Dis.* 18, 41–48. doi: 10.1089/fpd.2020.2808
- Minero, G., Cangiano, V., Garbarino, F., Fock, J., and Hansen, M. F. (2019). Integration of microbead DNA handling with optomagnetic detection in rolling circle amplification assays. *Mikrochim. Acta* 186:528. doi: 10.1007/s00604-019-3636-x
- Miura, T., Gima, A., and Akiba, M. (2019). Detection of norovirus and rotavirus present in suspended and dissolved forms in drinking water sources. *Food Environ. Virol.* 11, 9–19. doi: 10.1007/s12560-018-9361-5

- Moser, W., Schindler, C., and Keiser, J. (2019). Drug combinations against soil-transmitted helminth infections. *Adv. Parasitol.* 103, 91–115. doi: 10.1016/bs.apar.2018.08.002
- Nazarenko, Y. (2020). Air filtration and SARS-CoV-2. *Epidemiol. Health* 42:e2020049. doi: 10.4178/epih.e2020049
- Ngamsom, B., Esfahani, M. M., Phurimsak, C., Lopez-Martinez, M. J., Raymond, J. C., Broyer, P., et al. (2016a). Multiplex sorting of foodborne pathogens by on-chip free-flow magnetophoresis. *Anal. Chim. Acta* 918, 69–76. doi: 10.1016/j.aca.2016.03.014
- Ngamsom, B., Lopez-Martinez, M. J., Raymond, J. C., Broyer, P., Patel, P., and Pamme, N. (2016b). On-chip acoustophoretic isolation of microflora including *S. typhimurium* from raw chicken, beef and blood samples. *J. Microbiol. Methods* 123, 79–86. doi: 10.1016/j.mimet.2016.01.016
- Notomi, T., Okayama, H., Masubuchi, H., Yonekawa, T., Watanabe, K., Amino, N., et al. (2000). Loop-mediated isothermal amplification of DNA. *Nucleic Acids Res.* 28:E63. doi: 10.1093/nar/28.12.e63
- Olm, F., Lim, H. C., Schallmoser, K., Strunk, D., Laurell, T., and Scheduling, S. (2021). Acoustophoresis enables the label-free separation of functionally different subsets of cultured bone marrow stromal cells. *Cytometry A* 99, 476–487. doi: 10.1002/cyto.a.24171
- Pamme, N., and Manz, A. (2004). On-chip free-flow magnetophoresis: continuous flow separation of magnetic particles and agglomerates. *Anal. Chem.* 76, 7250–7256. doi: 10.1021/ac049183o
- Pang, B., Ding, X., Wang, G., Zhao, C., Xu, Y., Fu, K., et al. (2017). Rapid and quantitative detection of vibrio parahaemolyticus by the mixed-dye-based loop-mediated isothermal amplification assay on a self-priming compartmentalization microfluidic chip. *J. Agric. Food Chem.* 65, 11312–11319. doi: 10.1021/acs.jafc.7b03655
- Park, J. Y., Kim, S. H., Lee, K. K., Kim, Y. H., Moon, B. Y., So, B., et al. (2019). Differential detection of porcine reproductive and respiratory syndrome virus genotypes by a fluorescence melting curve analysis using peptide nucleic acid probe-mediated one-step real-time RT-PCR. *J. Virol. Methods* 267, 29–34. doi: 10.1016/j.jviromet.2019.02.008
- Park, Y. M., Lim, S. Y., Shin, S. J., Kim, C. H., Jeong, S. W., Shin, S. Y., et al. (2018a). A film-based integrated chip for gene amplification and electrochemical detection of pathogens causing foodborne illnesses. *Anal. Chim. Acta* 1027, 57–66. doi: 10.1016/j.aca.2018.03.061
- Park, Y. M., Lim, S. Y., Jeong, S. W., Song, Y., Bae, N. H., Hong, S. B., et al. (2018b). Flexible nanopillar-based electrochemical sensors for genetic detection of foodborne pathogens. *Nano Conver.* 5:15. doi: 10.1186/s40580-018-0147-0
- Patterson, B., Dinkels, R., Gessner, S., Morrow, C., Kamariza, M., Bertozzi, C. R., et al. (2020). Sensitivity optimisation of tuberculosis bioaerosol sampling. *PLoS One* 15:e0238193. doi: 10.1371/journal.pone.0238193
- Phan-Thien, K., Metaferia, M. H., Bell, T. L., Bradbury, M. I., Sassi, H. P., van Ogtrop, F. F., et al. (2020). Effect of soil type and temperature on survival of *Salmonella enterica* in poultry manure-amended soils. *Lett. Appl. Microbiol.* 71, 210–217. doi: 10.1111/lam.13302
- Piepenburg, O., Williams, C. H., Stemple, D. L., and Armes, N. A. (2006). DNA detection using recombination proteins. *PLoS Biol.* 4:e204. doi: 10.1371/journal.pbio.0040204
- Pilevar, M., Kim, K. T., and Lee, W. H. (2021). Recent advances in biosensors for detecting viruses in water and wastewater. *J. Hazard. Mater.* 410:124656. doi: 10.1016/j.jhazmat.2020.124656
- Popoff, M. R. (2020). Tetanus in animals. *J. Vet. Diagn. Invest.* 32, 184–191. doi: 10.1177/1040638720906814
- Prost, K., Kloeze, H., Mukhi, S., Bozek, K., Poljak, Z., and Mubareka, S. (2019). Bioaerosol and surface sampling for the surveillance of influenza A virus in swine. *Transbound. Emerg. Dis.* 66, 1210–1217. doi: 10.1111/tbed.13139
- Ramirez-Soto, M. C., Aguilar-Ancori, E. G., Tirado-Sánchez, A., and Bonifaz, A. (2018). Ecological determinants of sporotrichosis etiological agents. *J. Fungi (Basel)* 4:95. doi: 10.3390/jof4030095
- Romao, V. C., Martins, S., Germano, J., Cardoso, F. A., Cardoso, S., and Freitas, P. P. (2017). Lab-on-Chip devices: gaining ground losing size. *ACS Nano* 11, 10659–10664. doi: 10.1021/acsnano.7b06703
- Saiki, R. K., Gelfand, D. H., Stoffel, S., Scharf, S. J., Higuchi, R., Horn, G. T., et al. (1988). Primer-directed enzymatic amplification of DNA with a thermostable DNA polymerase. *Science* 239, 487–491. doi: 10.1126/science.2448875
- Salgado, J. R., Rabinovitch, L., Gomes, M., Allil, R., Werneck, M. M., Rodrigues, R. B., et al. (2020). Detection of *Bacillus anthracis* and *Bacillus anthracis*-like spores in soil from state of Rio de Janeiro, Brazil. *Mem. Inst. Oswaldo Cruz* 115:e200370. doi: 10.1590/0074-02760200370
- Salman, A., Carney, H., Bateson, S., and Ali, Z. (2020). Shunting microfluidic PCR device for rapid bacterial detection. *Talanta* 207:120303. doi: 10.1016/j.talanta.2019.120303
- Sarmiento, S. K., Guerra, C. R., Malta, F. C., Coutinho, R., Miagostovich, M. P., and Fumian, T. M. (2020). Human norovirus detection in bivalve shellfish in Brazil and evaluation of viral infectivity using PMA treatment. *Mar. Pollut. Bull.* 157:111315. doi: 10.1016/j.marpolbul.2020.111315
- Shahin, K., Bouzari, M., Wang, R., and Yazdi, M. (2019). Prevalence and molecular characterization of multidrug-resistant *Shigella* species of food origins and their inactivation by specific lytic bacteriophages. *Int. J. Food Microbiol.* 305:108252. doi: 10.1016/j.ijfoodmicro.2019.108252
- Shen, X. X., Qiu, F. Z., Shen, L. P., Yan, T. F., Zhao, M. C., Qi, J. J., et al. (2019). A rapid and sensitive recombinase aided amplification assay to detect hepatitis B virus without DNA extraction. *BMC Infect. Dis.* 19:229. doi: 10.1186/s12879-019-3814-9
- Singh, C., and Roy-Chowdhuri, S. (2016). Quantitative real-time PCR: recent advances. *Methods Mol. Biol.* 1392, 161–176. doi: 10.1007/978-1-4939-3360-0\_15
- Sinulingga, T. S., Aziz, S. A., Bitrus, A. A., Zunita, Z., and Abu, J. (2020). Occurrence of *Campylobacter* species from broiler chickens and chicken meat in Malaysia. *Trop. Anim. Health Prod.* 52, 151–157. doi: 10.1007/s11250-019-01995-y
- Stewart, J., Fava, V. M., Kerkaert, J. D., Subramanian, A. S., Gravelat, F. N., Lehoux, M., et al. (2020). Reducing *Aspergillus fumigatus* virulence through targeted dysregulation of the conidiation pathway. *mBio* 11:e03202-19. doi: 10.1128/mBio.03202-19
- Sun, Y., Quyen, T. L., Hung, T. Q., Chin, W. H., Wolff, A., and Bang, D. D. (2015). A lab-on-a-chip system with integrated sample preparation and loop-mediated isothermal amplification for rapid and quantitative detection of *Salmonella* spp. in food samples. *Lab Chip* 15, 1898–1904. doi: 10.1039/c4lc01459f
- Tarek, F., Hassou, N., Bencheikroun, M. N., Boughribil, S., Hafid, J., and Ennaji, M. M. (2019). Impact of rotavirus and hepatitis A virus by worldwide climatic changes during the period between 2000 and 2013. *Bioinformation* 15, 194–200. doi: 10.6026/97320630015194
- Topalcengiz, Z., and Danyluk, M. D. (2019). Fate of generic and Shiga toxin-producing *Escherichia coli* (STEC) in Central Florida surface waters and evaluation of EPA Worst Case water as standard medium. *Food Res. Int.* 120, 322–329. doi: 10.1016/j.foodres.2019.02.045
- Trinh, T., and Lee, N. Y. (2018). A rapid and eco-friendly isothermal amplification microdevice for multiplex detection of foodborne pathogens. *Lab Chip* 18, 2369–2377. doi: 10.1039/c8lc00424b
- Vadde, K. K., McCarthy, A. J., Rong, R., and Sekar, R. (2019). Quantification of microbial source tracking and pathogenic bacterial markers in water and sediments of tiaoxi river (Taihu Watershed). *Front. Microbiol.* 10:699. doi: 10.3389/fmicb.2019.00699
- Vasconcellos, L., Medeiros, V. M., Rosas, C. O., Forsythe, S. J., Romão, C., and Brandão, M. (2019). Occurrence of total coliforms, *Escherichia coli* and *Cronobacter* species in commercially available 20 l bottled drinking water sold in Rio de Janeiro State, Brazil. *Lett. Appl. Microbiol.* 69, 431–437. doi: 10.1111/lam.13235
- Velasco, V., Vergara, J. L., Bonilla, A. M., Muñoz, J., Mallea, A., Vallejos, D., et al. (2018). Prevalence and characterization of *Staphylococcus aureus* strains in the pork chain supply in Chile. *Foodborne Pathog. Dis.* 15, 262–268. doi: 10.1089/fpd.2017.2381
- Vibbert, H. B., Ku, S., Li, X., Liu, X., Ximenes, E., Kreke, T., et al. (2015). Accelerating sample preparation through enzyme-assisted microfiltration of *Salmonella* in chicken extract. *Biotechnol. Prog.* 31, 1551–1562. doi: 10.1002/btpr.2167
- Vincent, M., Xu, Y., and Kong, H. (2004). Helicase-dependent isothermal DNA amplification. *EMBO Rep.* 5, 795–800. doi: 10.1038/sj.embor.7400200
- Voidarou, C., Bezirtzoglou, E., Alexopoulos, A., Plessas, S., Stefanis, C., Papadopoulos, I., et al. (2011). Occurrence of *Clostridium perfringens* from different cultivated soils. *Anaerobe* 17, 320–324. doi: 10.1016/j.anaerobe.2011.05.004



- Walker, G. T., Nadeau, J. G., Spears, P. A., Schram, J. L., Nycz, C. M., and Shank, D. D. (1994). Multiplex strand displacement amplification (SDA) and detection of DNA sequences from *Mycobacterium tuberculosis* and other mycobacteria. *Nucleic Acids Res.* 22, 2670–2677. doi: 10.1093/nar/22.13.2670
- Walsh, C. M., Gebert, M. J., Delgado-Baquerizo, M., Maestre, F. T., and Fierer, N. (2019). A global survey of mycobacterial diversity in soil. *Appl. Environ. Microbiol.* 85:e01180–19. doi: 10.1128/AEM.01180-19
- Wang, D., Zhang, L., Zou, H., and Wang, L. (2018). Secretome profiling reveals temperature-dependent growth of *Aspergillus fumigatus*. *Sci. China Life Sci.* 61, 578–592. doi: 10.1007/s11427-017-9168-4
- Wang, J., Kreutz, J. E., Thompson, A. M., Qin, Y., Sheen, A. M., Wang, J., et al. (2018). SD-chip enabled quantitative detection of HIV RNA using digital nucleic acid sequence-based amplification (dNASBA). *Lab Chip* 18, 3501–3506. doi: 10.1039/c8lc00956b
- Wang, S., Liu, N., Zheng, L., Cai, G., and Lin, J. (2020). A lab-on-chip device for the sample-in-result-out detection of viable *Salmonella* using loop-mediated isothermal amplification and real-time turbidity monitoring. *Lab Chip* 20, 2296–2305. doi: 10.1039/d0lc00290a
- Wei, Y. F., Wang, Y., Wei, X. R., Sun, R., Xu, Y. J., and Ge, J. F. (2020). Adenine-based small molecule fluorescent probe for imaging mitochondrial nucleic acid. *Spectrochim. Acta A Mol. Biomol. Spectrosc.* 229:117865. doi: 10.1016/j.saa.2019.117865
- Woźniakowski, G., Frączyk, M., and Mazur, N. (2018). Comparison of loop-mediated isothermal amplification (LAMP) and cross-priming amplification (CPA) for detection of African swine fever virus. *Pol. J. Vet. Sci.* 21, 827–830. doi: 10.24425/pjvs.2018.125597
- Wu, Q., Zhang, Y., Yang, Q., Yuan, N., and Zhang, W. (2019). Review of electrochemical DNA biosensors for detecting food borne pathogens. *Sensors (Basel)* 19:4916. doi: 10.3390/s19224916
- Xiong, R., Chai, W., and Huang, Y. (2019). Laser printing-enabled direct creation of cellular heterogeneity in lab-on-a-chip devices. *Lab Chip* 19, 1644–1656. doi: 10.1039/c9lc00117d
- Xu, D., Ming, X., Gan, M., Wu, X., Dong, Y., Wang, D., et al. (2018). Rapid detection of *Cronobacter* spp. in powdered infant formula by thermophilic helicase-dependent isothermal amplification combined with silica-coated magnetic particles separation. *J. Immunol. Methods* 462, 54–58. doi: 10.1016/j.jim.2018.08.008
- Yang, H. L., Wei, S., Gooneratne, R., Mutukumira, A. N., Ma, X. J., Tang, S. Z., et al. (2018). Development of a recombinase polymerase amplification assay for *Vibrio parahaemolyticus* detection with an internal amplification control. *Can. J. Microbiol.* 64, 223–230. doi: 10.1139/cjm-2017-0504
- Yin, J., Zou, Z., Hu, Z., Zhang, S., Zhang, F., Wang, B., et al. (2020). A "sample-in-multiplex-digital-answer-out" chip for fast detection of pathogens. *Lab Chip* 20, 979–986. doi: 10.1039/c9lc01143a
- Yu, H., Xiao, M., Lai, W., Alam, M. F., Zhang, W., Pei, H., et al. (2020). A self-calibrating surface-enhanced Raman scattering-active system for bacterial phenotype detection. *Anal. Chem.* 92, 4491–4497. doi: 10.1021/acs.analchem.9b05614
- Yu, L. S., Rodriguez-Manzano, J., Moser, N., Moniri, A., Malpartida-Cardenas, K., Miscourides, N., et al. (2020). Rapid detection of azole-resistant *Aspergillus fumigatus* in clinical and environmental isolates by use of a lab-on-a-chip diagnostic system. *J. Clin. Microbiol.* 58:e00843–20. doi: 10.1128/JCM.00843-20
- Zemouri, C., Awad, S. F., Volgenant, C., Crielaard, W., Laheij, A., and de Soet, J. J. (2020). Modeling of the transmission of Coronaviruses, measles virus, Influenza virus, *Mycobacterium tuberculosis*, and *Legionella pneumophila* in dental clinics. *J. Dent. Res.* 99, 1192–1198. doi: 10.1177/0022034520940288
- Zhai, L., Liu, H., Chen, Q., Lu, Z., Zhang, C., Lv, F., et al. (2019). Development of a real-time nucleic acid sequence-based amplification assay for the rapid detection of *Salmonella* spp. from food. *Braz. J. Microbiol.* 50, 255–261. doi: 10.1007/s42770-018-0002-9
- Zhang, H., Chang, H., and Neuzil, P. (2019). DEP-on-a-Chip: dielectrophoresis applied to microfluidic platforms. *Micromachines (Basel)* 10:423. doi: 10.3390/mi10060423
- Zhang, Y., Qian, L., Wei, W., Wang, Y., Wang, B., Lin, P., et al. (2017). Paired design of dCas9 as a systematic platform for the detection of featured nucleic acid sequences in pathogenic strains. *ACS Synth. Biol.* 6, 211–216. doi: 10.1021/acssynbio.6b00215
- Zhao, X., Dong, T., Yang, Z., Pires, N., and Høivik, N. (2012). Compatible immuno-NASBA LOC device for quantitative detection of waterborne pathogens: design and validation. *Lab Chip* 12, 602–612. doi: 10.1039/c1lc20836e
- Zhao, Y., Li, Y., Zhang, P., Yan, Z., Zhou, Y., Du, Y., et al. (2021). Cell-based fluorescent microsphere incorporated with carbon dots as a sensitive immunosensor for the rapid detection of *Escherichia coli* O157 in milk. *Biosens. Bioelectron.* 179:113057. doi: 10.1016/j.bios.2021.113057
- Zhou, Q. J., Lu, J. F., Su, X. R., Jin, J. L., Li, S. Y., Zhou, Y., et al. (2021). Simultaneous detection of multiple bacterial and viral aquatic pathogens using a fluorogenic loop-mediated isothermal amplification-based dual-sample microfluidic chip. *J. Fish Dis.* 44, 401–413. doi: 10.1111/jfd.13325
- Zhou, S., Lu, C., Li, Y., Xue, L., Zhao, C., Tian, G., et al. (2020). Gold nanobones enhanced ultrasensitive surface-enhanced Raman scattering Aptasensor for detecting *Escherichia coli* O157:H7. *ACS Sens.* 5, 588–596. doi: 10.1021/acssensors.9b02600

**Conflict of Interest:** The authors declare that the research was conducted in the absence of any commercial or financial relationships that could be construed as a potential conflict of interest.

**Publisher's Note:** All claims expressed in this article are solely those of the authors and do not necessarily represent those of their affiliated organizations, or those of the publisher, the editors and the reviewers. Any product that may be evaluated in this article, or claim that may be made by its manufacturer, is not guaranteed or endorsed by the publisher.

Copyright © 2021 Yang, Yi, Sun, Xu, Zeng, Bi, Dong, Xie and Li. This is an open-access article distributed under the terms of the Creative Commons Attribution License (CC BY). The use, distribution or reproduction in other forums is permitted, provided the original author(s) and the copyright owner(s) are credited and that the original publication in this journal is cited, in accordance with accepted academic practice. No use, distribution or reproduction is permitted which does not comply with these terms.





# Genomic Characterization of Clinical *Listeria monocytogenes* Isolates in Beijing, China

Xiaoai Zhang<sup>1,2</sup>, Yuzhu Liu<sup>1,2</sup>, Penghang Zhang<sup>1,2</sup>, Yanlin Niu<sup>1,2</sup>, Qian Chen<sup>1,2\*</sup> and Xiaochen Ma<sup>1,2\*</sup>

<sup>1</sup> Institute for Nutrition and Food Hygiene, Beijing Center for Disease Prevention and Control (CDC), Beijing, China, <sup>2</sup> Beijing Research Centre for Preventive Medicine, Beijing, China

## OPEN ACCESS

### Edited by:

Yi-Wei Tang,  
Cepheid, United States

### Reviewed by:

Ben Pascoe,  
University of Bath, United Kingdom  
Laurel S. Burall,  
United States Food and Drug  
Administration, United States

### \*Correspondence:

Qian Chen  
cchenqian@263.net  
Xiaochen Ma  
xiaoch-ma@126.com

### Specialty section:

This article was submitted to  
Food Microbiology,  
a section of the journal  
Frontiers in Microbiology

Received: 31 July 2021

Accepted: 22 November 2021

Published: 10 December 2021

### Citation:

Zhang X, Liu Y, Zhang P, Niu Y,  
Chen Q and Ma X (2021) Genomic  
Characterization of Clinical *Listeria*  
*monocytogenes* Isolates in Beijing,  
China. *Front. Microbiol.* 12:751003.  
doi: 10.3389/fmicb.2021.751003

*Listeria monocytogenes* is a foodborne human pathogen that affects public health worldwide. Whole-genome sequencing (WGS) can classify *L. monocytogenes* isolates and identify virulence islands and resistance genes potentially influencing infectivity. Herein, WGS was used to assess 151 *L. monocytogenes* isolates from 120 cases of clinical infection in Beijing, China, between 2014 and 2018. Most isolates were either serogroup 1/2a,3a or serogroup 1/2b,3b,7, with 25 multilocus sequence typing (MLST) types (STs) represented, of which ST8, ST87, and ST5 were the most common. Core-genome MLST (cgMLST) grouped the 151 isolates into 116 cgMLST types. The discriminatory power of cgMLST was greater than other subtypes, revealing that isolates from the same patient were highly related (only differing at one allele). Eighty-six isolates formed 30 complexes with  $\leq 7$  cgMLST alleles between neighboring isolates, suggesting possible outbreaks. Compared with isolates in the United States, ST8, ST121, ST619, ST87, and ST155 isolates were grouped into unified clades. All 151 isolates were positive for common virulence-associated loci, and 26 lineage I isolates harbored the pathogenicity island 3 (LIPI-3) locus, while 42 lineage I isolates harbored the complete LIPI-4 locus. Eleven ST619 isolates had both LIPI-3 and LIPI-4. Among the 151 isolates, 13 were resistant to at least one antibiotic, and no multidrug-resistant isolates were identified. Resistance phenotypes correlated with genotypes, apart from two meropenem resistance isolates. The findings provided insight into the nature of *L. monocytogenes* strains currently causing clinical disease in Beijing, and WGS analysis indicated possible outbreaks.

**Keywords:** genomic characterization, *Listeria monocytogenes*, clinical isolates, virulence islands, resistance genes

## INTRODUCTION

*Listeria monocytogenes* ubiquitous in the environment and is a major foodborne pathogen affecting public health (de Noordhout et al., 2014). It causes listeriosis, a severe infection characterized by sepsis, meningitis, pregnancy loss, and can even be fatal to immuno-compromised or older patients. Listeriosis accounts for a disproportionate share of the foodborne disease burden, with

high hospitalization and fatality rates (Scallan et al., 2011; de Noordhout et al., 2014), ranging from 15 to 30%, the highest among all foodborne infectious diseases (Barton Behravesh et al., 2011; Scallan et al., 2011; Hernandez-Milian and Payeras-Cifre, 2014). As a special pilot project of the National Foodborne Disease Surveillance Plan, human listeriosis surveillance has been implemented in 2013, and the fatality rate of listeriosis was 26.1% in China during 2013–2017 (Li et al., 2019).

*L. monocytogenes* causes sporadic cases or protracted outbreaks, and even multi-country outbreaks, and often the specific source may not be known (Halbedel et al., 2018). A subtyping method with high resolution, reproducibility, and exchangeability is required for international surveillance and investigation. Different methods are used to subtype *L. monocytogenes*. Pulsed-field gel electrophoresis (PFGE), the typing golden standard, has been used internationally, but lacks comparability between different networks and sufficient discriminatory power, and does not reflect the evolutionary relationships among strains (Gerner-Smidt et al., 2006). The other standardized genotyping method, multilocus sequence typing (MLST) based on seven genes, is an internationally comparable subtyping method, but lacks the discriminatory power required for epidemiological surveillance (Ragon et al., 2008; Chenal-Francisque et al., 2011; Haase et al., 2014). Whole-genome sequencing (WGS), a powerful epidemiological typing tool, can differentiate isolates that are indistinguishable by other typing methods (Harris et al., 2010; Mutreja et al., 2011; Maury et al., 2016; Moura et al., 2016). Thus, WGS has been widely applied for investigating outbreaks and contamination of food production plants (Schmid et al., 2014; Stasiewicz et al., 2015; Bergholz et al., 2016; Kwong et al., 2016). WGS can also help to predict pathogenic loci in virulent or hypervirulent strains. Furthermore, WGS can reveal population structure and infer evolutionary relationships among strains from a wide range of geographic, temporal and epidemiological origins (Moura et al., 2016).

*L. monocytogenes* encodes internalins and genomic islands (Listeria pathogenicity islands, LIPIs), that play important roles in pathogen virulence. Internalins help *L. monocytogenes* invade host cells (Gaillard et al., 1991). Some *L. monocytogenes* strains isolated from environment and food sources produce a truncated form of the InlA protein, and virulence is reduced (Jacquet et al., 2004; Nightingale et al., 2008). LIPI-1, the main pathogenicity island, is well conserved across strains independent of lineage (Gouin et al., 1994). LIPI-3, encoding a second haemolysin known as listeriolysin S (LLS), is strongly associated with lineage I strains (Cotter et al., 2008). LIPI-4, which includes a cellobiose family phosphotransferase system, is strongly associated with certain lineage I strains that are associated with invasion of the central nervous system (Maury et al., 2016).

In this study, we used WGS to assess the genomic diversity of *L. monocytogenes* in Beijing, China, to compare methods (PFGE, MLST, cgMLST, and wgSNP) for determining relatedness of the isolates. We also aim to characterize the distribution of virulence determinants of *L. monocytogenes*, to detect the absence/presence

of antimicrobial resistance-encoding genes and their relationship with antimicrobial resistance profiles.

## MATERIALS AND METHODS

### Bacterial Isolates

Human listeriosis surveillance in Beijing, as a special pilot project of the National Foodborne Disease Surveillance Plan has been implemented since 2013. In this surveillance, all the suspected clinical cases of listeriosis were included in the survey. Samples were collected and used to isolate *L. monocytogenes*. We defined invasive listeriosis as isolation of *L. monocytogenes* strains from a normally sterile site or from products of conception (Li et al., 2018). A total of 129 human patients who had a severe illness with serious suspicion of *L. monocytogenes* infection were supervised between 2014 and 2018. Among the 129 human patients, 151 isolates were isolated from 120 human patients, while the isolates in other 9 cases were lost. All *L. monocytogenes* isolates identified by clinical microbiology laboratories were sent to the Beijing CDC lab. All isolates were firstly identified using a VITEK 2-compact System (bioMérieux, Lyons, France) or matrix-assisted laser desorption/ionization time of flight (MALDI-TOF) mass spectrometry (Bruker, Leipzig, Germany).

Furthermore, the genome sequences, which were downloaded from Genbank, of 368 human *L. monocytogenes* strains from the United States were used for comparing with that of our isolates (Moura et al., 2016). The 368 strains were isolated between 2009 and 2014. The information of these strains were shown in **Supplementary Table 1**.

### Serotyping, Multilocus Sequence Typing and Pulsed-Field Gel Electrophoresis Analyses

*L. monocytogenes* isolates were serotyped by multiplex PCR assay (Doughith et al., 2004). MLST analysis was performed by sequencing seven housekeeping genes. Alleles and sequences types (STs) were determined by comparison with allelic profiles for *L. monocytogenes* in the MLST database.<sup>1</sup> For PFGE analysis, the *AscI* restriction enzyme was used according to the PulseNet International protocol (Almeida et al., 2017).

### Antimicrobial Susceptibility Testing

Antimicrobial susceptibility testing of *L. monocytogenes* isolates was performed using the broth dilution method. We measured the minimum inhibitory concentrations (MICs) of ampicillin (AMP), penicillin (PEN), tetracycline (TET), meropenem (MRP), trimethoprim-sulfamethoxazole (SXT), erythromycin (ERY), vancomycin (VAN), and ciprofloxacin (CIP) (Xingbai, Shanghai, China). The MICs of AMP, PEN, SXT, and MRP were interpreted using the Clinical and Laboratory Standard Institute (CLSI) International Guidelines, and the MIC of ERY was interpreted according to European Committee on Antimicrobial Susceptibility Testing (EUCAST) International

<sup>1</sup><http://bigsdb.pasteur.fr/listeria/listeria.html>

Guidelines. Resistance criteria have not been reported for TET, VAN or CIP for *L. monocytogenes*, hence, the MICs of these three antimicrobials were interpreted using those recommended for *Staphylococcus* spp. ATCC29213, which was used as the reference strain.

## Whole-Genome Sequencing

Isolates of *L. monocytogenes* were routinely grown in brain heart infusion broth overnight at 37°C. DNA was extracted using a DNeasy UltraClean Microbial Kit (Qiagen, Germany). Sequencing was performed using an Illumina Novaseq apparatus (Illumina Inc., San Diego, CA, United States) and constructing two paired-end (PE) libraries with average insertion lengths of 350 and 2,000 bp, respectively. Raw data were processed in four steps, including removing reads with 5 bp of ambiguous bases, removing reads with 20 bp of low quality ( $\leq Q20$ ) bases, removing adapter contamination, and removing duplicated reads. Finally, 100 × libraries were obtained with clean PE read data.

## Phylogenetic Analysis

The WGS raw data were imported into BioNumerics software (version 7.6 Applied Maths, Kortrijk, Belgium), then uploaded to the National Molecular Tracing Network for Foodborne Diseases Surveillance (TraNet) calculation engine at aliyun for *de novo* assembly, core genome MLST (cgMLST), and whole-genome single-nucleotide polymorphism (wgSNP) analyses using default settings (Li et al., 2021). The cgMLST scheme included 1748 loci for *L. monocytogenes* in BioNumerics. The wgSNP analysis was further carried out on the 86 isolates with cgMLST  $\leq 7$  different alleles. F2365, EGDe and ICDC\_LM188 were chosen as reference genomes for 4b,4d,4e, 1/2a,3a, and 1/2b,3b,7 serogroup strains, respectively. SNPs were filtered using the BioNumerics strict SNP filtering template. CgMLST and wgSNP spanning tree were created in BioNumerics using categorical differences and the unweighted-pair group method with arithmetic mean.

## Virulence and Resistance Gene Profiles

For virulence identification, the 151 isolates were analyzed using the virulence factor database (VFDB)<sup>2</sup> on August 15th, 2021. The analysis was performed with a minimum 75% identity and 60% coverage.

For resistance gene identification, the 151 isolates were analyzed using ResFinder 3.0 (Center for Genomic Epidemiology). Genes involved in pathogenicity islands, internalins, adherence, invasion, stress, intracellular growth, immunomodulator, peptidase function, immune evasion and bile resistance were investigated. The analysis was performed with a minimum 90% identity and 60% coverage.

## Nucleotide Sequence Accession Number

These assembled genomes were uploaded to NCBI under the Bioproject ID PRJNA759341, accession SAMN21163725-SAMN21163875.

## RESULTS

### Origins of Isolates

One hundred and fifty-one isolates were isolated from 120 cases between 2014 and 2018 in Beijing, China. The origins of the cases are summarized in Table 1. Sixty-three cases were pregnancy-associated infections, in which all mothers were cured; 32 neonates survived, and 28 fetuses died in the womb or after birth. No data were available for three

**TABLE 1** | Characteristics of 120 isolates isolated from 120 cases in Beijing, China, between 2014 and 2018.

Characteristics	Pregnancy-associated, no (%)	Non-pregnancy-associated, no (%)	Total, no.(%)
<b>Total</b>	63 (52.5)	57 (47.5)	120 (100.0)
<b>Age</b>			
Newborns and fetus	12 (19.0)	0	12 (10.0)
≤ 20	0	13 (22.8)	13 (10.8)
21~40	50 (79.4)	13 (22.8)	63 (52.5)
> 40	1 (1.6)	31 (54.4)	32 (26.7)
<b>Gender</b>			
Female	63 (100.0)	26 (45.6)	89 (74.2)
Male	0	31 (54.4)	31 (25.8)
<b>Specimen type</b>			
Blood	38 (60.3)	41 (71.9)	79 (65.8)
CSF*	2 (3.2)	11 (19.3)	13 (10.8)
Placenta	18 (28.6)	0	18 (15.0)
Other	5 (7.9)	5 (8.8)	10 (8.3)
<b>Outcome</b>			
Survival	32 (50.8)	36 (63.2)	68 (56.7)
Death or fetal loss	28 (44.4)	6 (10.5)	34 (28.3)
Unknown	3 (4.8)	15 (26.3)	18 (15.0)
<b>Serotype</b>			
1/2a,3a	21 (33.3)	36 (63.2)	57 (47.5)
1/2b,3b,7	35 (55.6)	14 (24.6)	49 (40.8)
4b,4d,4e	7 (11.1)	7 (12.3)	14 (11.7)
<b>ST<sup>#</sup></b>			
ST8	8 (12.7)	14 (24.6)	22 (18.3)
ST87	13 (20.6)	7 (12.3)	20 (16.7)
ST5	11 (17.5)	1 (1.8)	12 (10.0)
ST619	5 (7.9)	4 (7.0)	9 (7.5)
ST155	0	8 (14.0)	8 (6.67)
ST121	4 (6.3)	4 (7.0)	8 (6.67)
Others	22 (34.9)	19 (33.3)	41 (34.2)
<b>Pulsotypes</b>			
GX6A16.BJ0012	10 (15.9)	1 (1.8)	11 (9.2)
GX6A16.BJ0003	7 (11.1)	9 (15.8)	16 (13.3)
GX6A16.BJ0044	4 (6.3)	1 (1.8)	5 (4.2)
GX6A16.BJ0132	4 (6.3)	0	4 (3.3)
GX6A16.BJ0176	0	4 (7.0)	4 (3.3)
GX6A16.BJ0013	2 (3.2)	2 (3.5)	4 (3.3)

\*CSF, cerebrospinal fluid; #ST, multilocus sequence typing (MLST) types.

<sup>2</sup><http://www.mgc.ac.cn/VFs/main.htm>

fetuses. Most of the 57 non-pregnancy-associated patients were older people, or patients with various underlying diseases such as cancer and autoimmune disease. The median age of patients with non-pregnancy-associated infections was 46 years old, 18 patients were > 60 years old and 10 patients were < 6 years old. Thirty-one non-pregnancy-associated patients were males and 26 were females. Among the 57 non-pregnancy-associated patients, 35 patients were cured, 7 patients died and 15 patients were lost during follow-up. Blood (65.8%) was the largest sample source. The sample source for 13 cases was cerebrospinal fluid (10.8%) and for 18 pregnancy-associated cases it was placenta (15.0%). Ten samples were from other sources, including neonate pharyngeal smear and external ear canal, infant cord blood, cervical smear, amniotic fluid, ascites, pleural effusion, cystic fluid, bone marrow and subcutaneous drainage.

### Distribution of Serotypes, Multilocus Sequence Typing and Pulsed-Field Gel Electrophoresis Types

More than one isolate were isolated from different samples at different times (2 cases) or different locations (17 cases) in each of the 19 cases. Among the 19 cases, 11 were mother-infant cases. Isolates from the same cases had the same serogroup, antimicrobial susceptibilities, PFGE types (PTs), and STs. Therefore, only one isolate from each patient was used for these analyses. Almost half of the strains belonged to serogroup 1/2a,3a ( $n = 57$ , 47.5%), followed by serogroup 1/2b,3b,7 ( $n = 49$ , 40.8%) and serogroup 4b,4d,4e ( $n = 14$ , 11.7%). Serogroup distribution differed between pregnancy-associated cases and non-pregnancy-associated cases (Figure 1A). Serogroup 1/2a,3a was more common in non-pregnancy-associated cases, and serogroup 1/2b,3b,7 was more common in pregnancy-associated cases. One hundred and twenty isolates belonged to 25 STs, with one new ST designated (Figure 1B). ST8 (22 isolates, 18.3%), ST87 (20 isolates, 16.7%) and ST5 (12 isolates, 10.0%) were the most frequent STs, followed by ST619 (9 isolates, 7.5%), ST155 (8 isolates, 6.7%), ST121 (8 isolates, 6.7%), ST1 (7 isolates, 5.8%) and ST2 (7 isolates, 5.8%). The other 17 STs contained between one and three isolates. The distribution of STs differed between pregnancy-associated cases and non-pregnancy-associated cases. All ST155 strains were isolated from non-pregnancy-associated patients, whereas 11 of the 12 ST5 isolates were linked to pregnancy-associated infection. One hundred and twenty isolates belonged to 59 PTs, and GX6A16.BJ0003 (16 isolates, 13.3%) was the most frequent PT, followed by GX6A16.BJ0012 (11 isolates, 9.2%), GX6A16.BJ0044 (5 isolates, 4.2%), GX6A16.BJ0132 (4 isolates, 3.3%), GX6A16.BJ0176 (4 isolates, 3.3%) and GX6A16.BJ0013 (4 isolates, 3.3%). The distribution of PTs differed between pregnancy-associated cases and non-pregnancy-associated cases (Table 1). Most GX6A16.BJ0012 isolates (CC87) were from pregnancy-associated cases. All GX6A16.BJ0132 isolates (CC5) were from pregnancy-associated cases, while all GX6A16.BJ0176 isolates (CC87, CC2) were from non-pregnancy-associated cases.

### Cluster Detection Using Core Genome MLST

All 151 isolates were divided into 116 cgMLST types (CTs; Figure 2). Twenty-four CTs contained more than one isolate. Of 17 CTs among these 24 CTs, each CT contained strains isolated from the same patient, with 13 pregnancy-associated cases and 4 non-pregnancy-associated cases, albeit from different sample sources or different sample times. The same CT contained up to five isolates belonging to a single patient. Not all isolates from the same patient had the same CTs. Isolates from the same patient for three cases had a single allele difference in cgMLST. Eighty-six isolates formed 30 complexes with  $\leq 7$  different alleles between a pair of neighboring isolates (Supplementary Figure 1). The 30 complexes contained between 2 and 13 isolates, between 1 and 8 cases, and between 1 and 4 PTs, but isolates in the same complex had the same STs (Table 2). Isolates in 16 complexes were from two or more cases, indicating possible outbreaks. Among them, seven complexes had no different alleles (C1, C3, C6, C7, C9, C12, C24). In C1, these two strains were isolated from separate patients in the same hospital, but more than 7 months apart. In C6 and C7, the two strains were isolated from different years. WgSNP analysis carried on the 86 isolates yielded similar results to cgMLST (Supplementary Figure 2). Using wgSNP  $\leq 12$  as a cutoff, eight complexes were detected with more than one case (Table 2).

### Typing Resolution of Different Typing Methods

All 151 isolates were grouped into 2 lineages, 3 serogroups, 25STs, 59PTs and 116 CTs. The discriminatory power of cgMLST is apparently superior to the other four types. For example, 62.1% (18) PTs with  $\geq 2$  isolates (29 PTs) could be further differentiated by cgMLST. Isolates in five PTs with the same CTs were from different patients, and isolates in six PTs with the same CTs were from the same patients. By contrast, only one CT with  $\geq 2$  isolates could be further discriminated by PFGE, and there was only one pattern difference between these two isolates.

### Comparison With Isolates in the United States

Compared with genomes of 368 human isolates from the United States downloaded from Genbank (Moura et al., 2016), the cgMLST results showed that some of our isolates were dominant in several clusters (Figure 3). Almost all isolates of ST8, ST121, ST619, ST87, and ST155 in our study were clustered with no or few isolates from the United States. Also, there were some Chinese isolates located with the same cluster with isolates from the United States. However, no complexes with  $\leq 7$  cgMLST alleles were found between isolates of China and the United States.

### *Listeria* Pathogenicity Islands

The virulence and stress resistance gene results revealed important differences between lineage I and lineage II (Figure 4). As expected, the major pathogenicity island LIPI-1 was highly



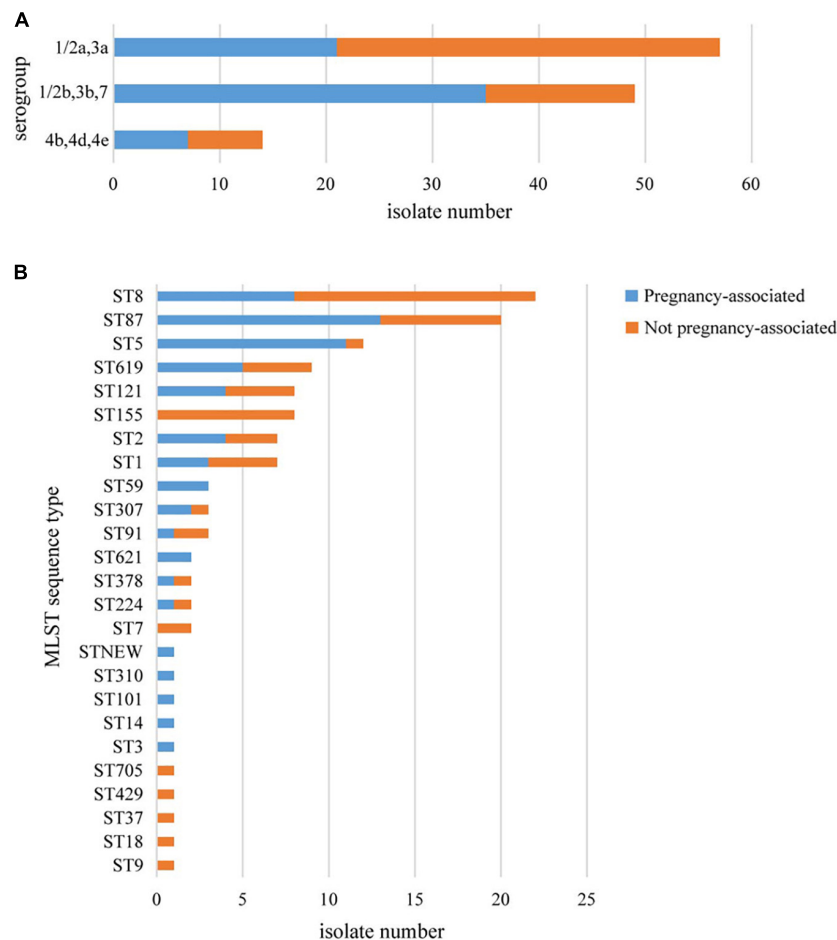


**FIGURE 1 |** Basic epidemiological characteristics of 120 *L. monocytogenes* isolates isolated from 120 cases in this study. The distribution of isolates is shown according to their molecular serogroup **(A)** and their MLST sequence type **(B)**.

conserved except in one isolate (h92). LIPI-3 was present in some lineage I isolates (16 1/2b,3b,7 isolates and 10 4b,4d,4e isolates) but no lineage II isolates. LIPI-3 was present in all clonal complex (CC) 224, CC3, ST619 and CC1 isolates. Forty-two isolates (41 serogroup 1/2b,3b,7 and 1 serogroup 4b,4d,4e) had a complete LIPI-4 recently described and one isolate (h92, serogroup 1/2a,3a) had an incomplete LIPI-4 with no *x7012* gene. Among these isolates, 13 were from 12 non-pregnancy-associated cases, and the other 29 isolates were from 19 pregnancy-associated cases. The presence of LIPI-4 was confirmed in all CC87, all ST619, and one CC2 isolates. Eleven ST619 isolates were confirmed to have both LIPI-3 and LIPI-4. Isolate h92 (1/2a,3a, CC121) had no LIPI-1 but an incomplete LIPI-4 lacking the *x7012* gene.

All isolates encoded full-length *inlA* except one isolate (182). *inlC*, *J* and *K* were present in all isolates, while *InternalinB* was found in all but one isolate. *inlF* was present in almost all isolates except 11 1/2a,3a isolates (8 CC121, 2 CC11, 1 CC14). Genes involved in adherence (*ami*, *fbpA*, *lap*, *lapB*) were present in all isolates. Three of the genes involved in invasion (*cwhA*, *lpeA*, *gtcA*) were present in all isolates, while *aut* was detected in all

isolates with the exception of 4b,4d,4e isolates, and *vip* was found in some of the 1/2a,3a isolates.

## Antimicrobial Resistance and Antibiotic Genes

All 151 isolates were found to be susceptible to CIP, VAN, PEN and AMP. Resistance to the other four antibiotics was as follows: TET (11 isolates, 7.28%), ERY (4 isolates, 2.65%), MRP (2 isolates, 1.32%) and SXT (1 isolates, 0.66%). Thirteen isolates (8.6%) were resistant to at least one antibiotic. Four isolates were found to be resistant to two antibiotics. No isolate was defined as multidrug-resistant (MDR). Antibiotic resistance genes were identified in 11 of the 13 isolates (**Figure 5**). Resistance phenotypes correlated with genotypes, with the exception of MRP resistance, since two isolates were resistant to MRP, but no genes known to encode resistance to MRP were detected. Some resistance genes were identified, including *tetM* (encoding resistance to TET), *drfG* (encoding resistance to SXT), *msrD* and *mefA* (encoding resistance to ERY). As shown in **Figure 5**, all resistant isolates belonged to serogroup 1/2a,3a and 1/2b,3b,7, CC155 and CC87.

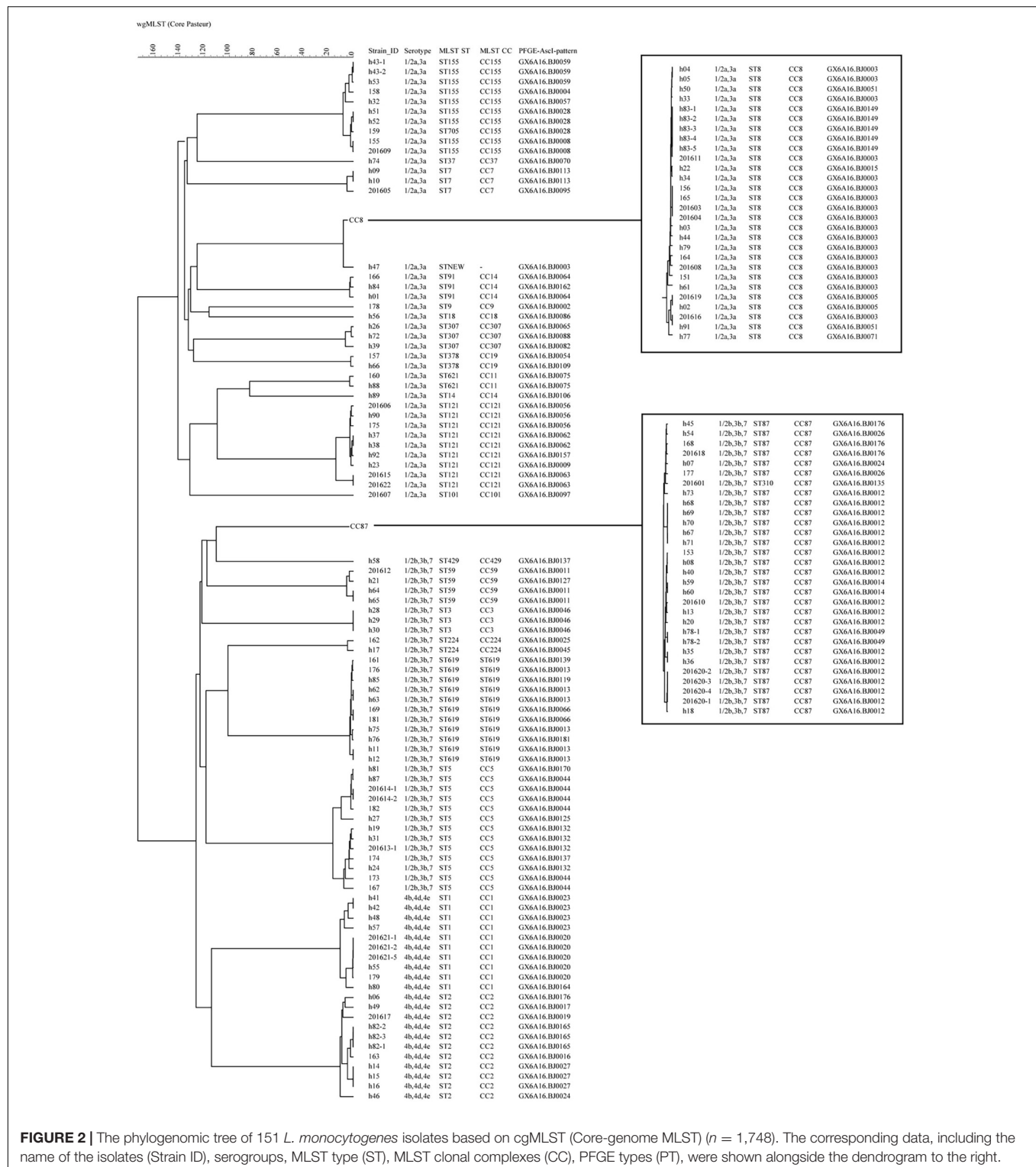


**FIGURE 2 |** The phylogenomic tree of 151 *L. monocytogenes* isolates based on cgMLST (Core-genome MLST) ( $n = 1,748$ ). The corresponding data, including the name of the isolates (Strain ID), serogroups, MLST type (ST), MLST clonal complexes (CC), PFGE types (PT), were shown alongside the dendrogram to the right.

## DISCUSSION

In this study, analysis of 5 years of data (2014–2018) on clinical *L. monocytogenes* isolates in Beijing, China, showed that pregnancy-associated cases and non-pregnancy-associated cases

accounted for half each. Listeriosis is an important disease that needs attention and continuous surveillance. Some listeriosis and deaths might go undiagnosed and unreported (Anand et al., 2016; Kylat et al., 2016; Fan et al., 2019). Serogroups 1/2a,3a and 1/2b,3b,7 were the dominant serogroups in our study, consistent

**TABLE 2** | Relatedness of isolates as determined by cgMLST ( $\leq 7$  different alleles).

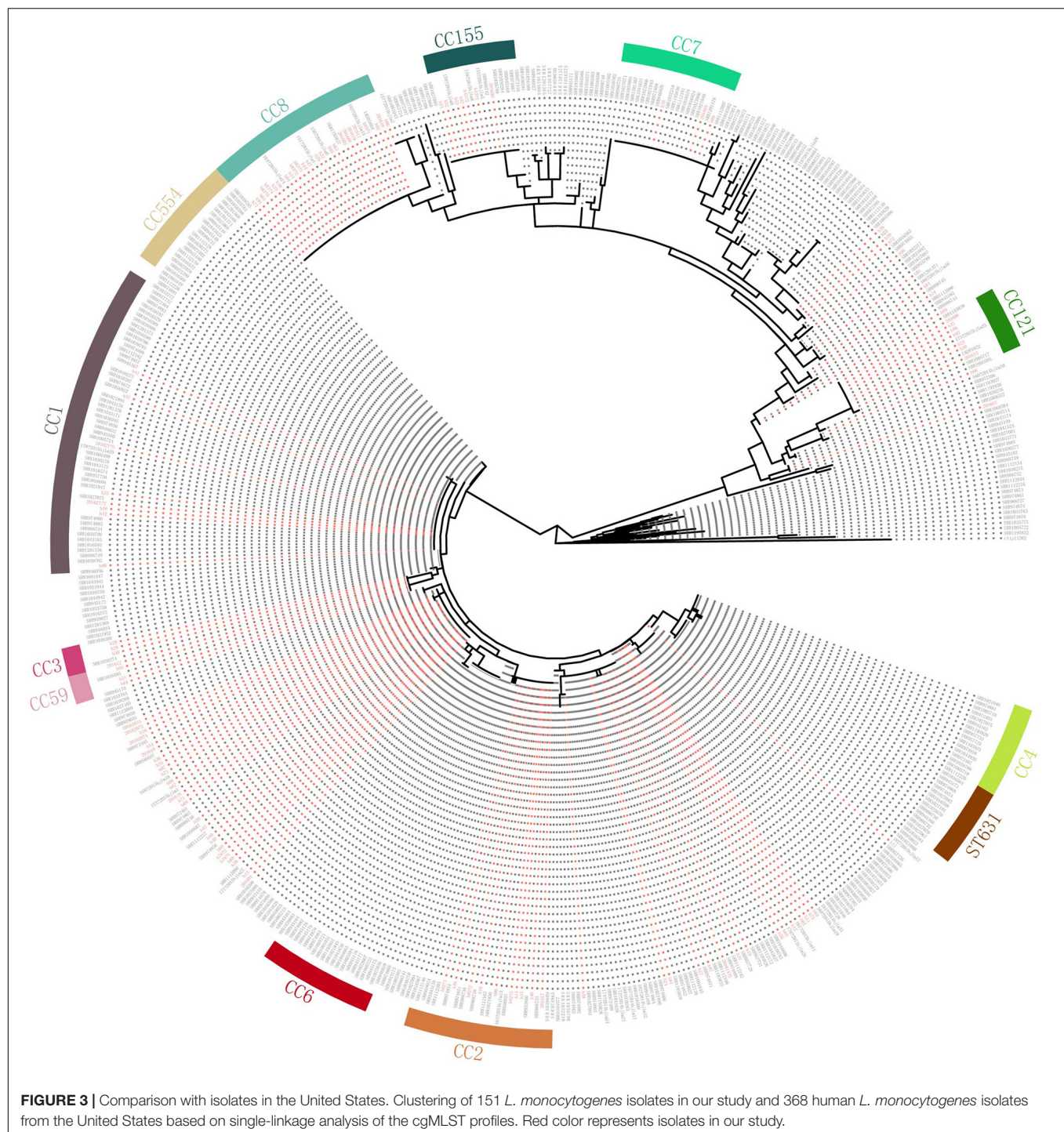
Complexes	Possible outbreaks	Isolates	Number of cases	Maximum number of cgMLST alleles	Maximum number of SNPs	ST	Serogroup
C1	O1	201615, 201622	2	0	0	121	1/2a,3a
C2		h37, h38	1	0	0	121	1/2a,3a
C3	O2	h51, h52	2	0	0	155	1/2a,3a
C4	O3	155, 201609	2	2	4	155	1/2a,3a
C5		h43-1, h43-2	1	0	0	155	1/2a,3a
C6	O4	h02, 201619	2	0	0	8	1/2a,3a
C7	O5	h91, 201616	2	0	1	8	1/2a,3a
C8	O6	h05, h04, h50, h03, h33, h22, h34, h83-1, h83-2, h83-3, h83-4, h83-5, 201611	8	7	34	8	1/2a,3a
C9	O7	201603, 201604, 156, 165	3	0	3	8	1/2a,3a
C10		h09, h10	1	1	2	7	1/2a,3a
C11	O8	h08, h40, 153	3	3	6	87	1/2b,3b,7
C12	O9	h59, h60	2	0		87	1/2b,3b,7
C13	O10	h13, 201610	2	7	15	87	1/2b,3b,7
C14		h78-1, h78-2	1	0	0	87	1/2b,3b,7
C15		h35, h36	1	0	0	87	1/2b,3b,7
C16	O11	201620-1, 201620-2, 201620-3, 201620-4, h18	2	5	7	87	1/2b,3b,7
C17		h67, h68, h69, h70, h71	1	1	1	87	1/2b,3b,7
C18		h64, h65	1	0	0	59	1/2b,3b,7
C19		h28, h29, h30	1	0	0	3	1/2b,3b,7
C20	O12	161, 176	2	5	18	619	1/2b,3b,7
C21		h62, h63	1	0		619	1/2b,3b,7
C22	O13	h75, h76	2	7	9	619	1/2b,3b,7
C23		h11, h12	1	0	0	619	1/2b,3b,7
C24	O14	169, 181	2	0	0	619	1/2b,3b,7
C25	O15	h81, h87	2	3	4	5	1/2b,3b,7
C26		201614-1, 201614-2	1	0	0	5	1/2b,3b,7
C27	O16	201621-1, 201621-2, 201621-5, h55, 179	3	4	6	1	4b,4d,4e
C28		h41, h42	1	0		1	4b,4d,4e
C29		h82-1, h82-2, h82-3	1	1	1	2	4b,4d,4e
C30		h14, h15, h16	1	0	0	2	4b,4d,4e

with food source strains in China, but different from clinical source strains from other countries (Mammina et al., 2009; Centers for Disease Control and Prevention, 2014; Chen et al., 2015; Maury et al., 2016; Wu et al., 2016; Jennison et al., 2017). In many countries such as the United States, Australia, France and Italy, serotype 4b is the most commonly identified serotype of clinical *L. monocytogenes* (Mammina et al., 2009; Centers for Disease Control and Prevention, 2014; Jennison et al., 2017). The distribution of STs in clinical *L. monocytogenes* strains in Beijing, China differs from those in other countries (Maury et al., 2016; Bergholz et al., 2018; Halbedel et al., 2018). The three most common STs were ST8, ST87 and ST5. While ST8 is distributed globally and ST5 caused several outbreaks in the United States in recent years (Lomonaco et al., 2013; Centers for Disease Control and Prevention, 2015; Jackson et al., 2015), ST87 is seldom linked to human infection in other countries. Approximately 7.5% of STs were ST619 (9 isolates), which has been seldom reported in other countries. The possible reasons for these differences in

serogroups and STs are that some clonal groups may not be disseminated widely because of their own characteristics, also there are different types of circulating food, production links, processing techniques and eating habits among regions, resulting in relatively unique clonal groups in different regions. However, some STs prevalent worldwide such as ST1, ST2, ST9, ST121 and ST155 were also identified in this study.

We present a collection of genome-sequenced *L. monocytogenes* isolates from listeriosis patients in Beijing, China, over 5 years. Typing resolution increased from serogroups (3) to MLST (25 STs) to PFGE (59 PTs) to cgMLST (116 CTs), which is consistent with other studies (Kwong et al., 2016; Moura et al., 2016; Halbedel et al., 2018). In our study, most PTs with  $\geq 2$  isolates could be further differentiated by cgMLST. Only two isolates with the same CTs were further discriminated by PFGE, with one pattern difference. Genomic variation outside the core genome or variations in intergenic region may account for this variability in isolates with identical CTs. In





our study, a maximum of one cgMLST locus and two wgSNP loci were found in isolates from the same case isolated in different sample sources or at different sample times that were expected to be highly related. Each of seven CTs included two or three cases, indicating that isolates in the same CTs are likely to be phylogenetically linked. However, following further retrospective investigation, no epidemiological links between the cases in the same CTs could be determined. Previous research

(Moura et al., 2016) showed that most isolates sampled during investigations of single outbreaks had seven or fewer allelic mismatches, and isolates with no documented epidemiological links typically differed by more than 10 mismatches. In our study, we used  $\text{cgMLST} \leq 7$  as a cutoff for the classification of closely linked isolates, and 16 complexes were identified. When  $\text{wgSNP} \leq 12$  was used as a cutoff, eight complexes were found. These results imply that strains in the same complex should



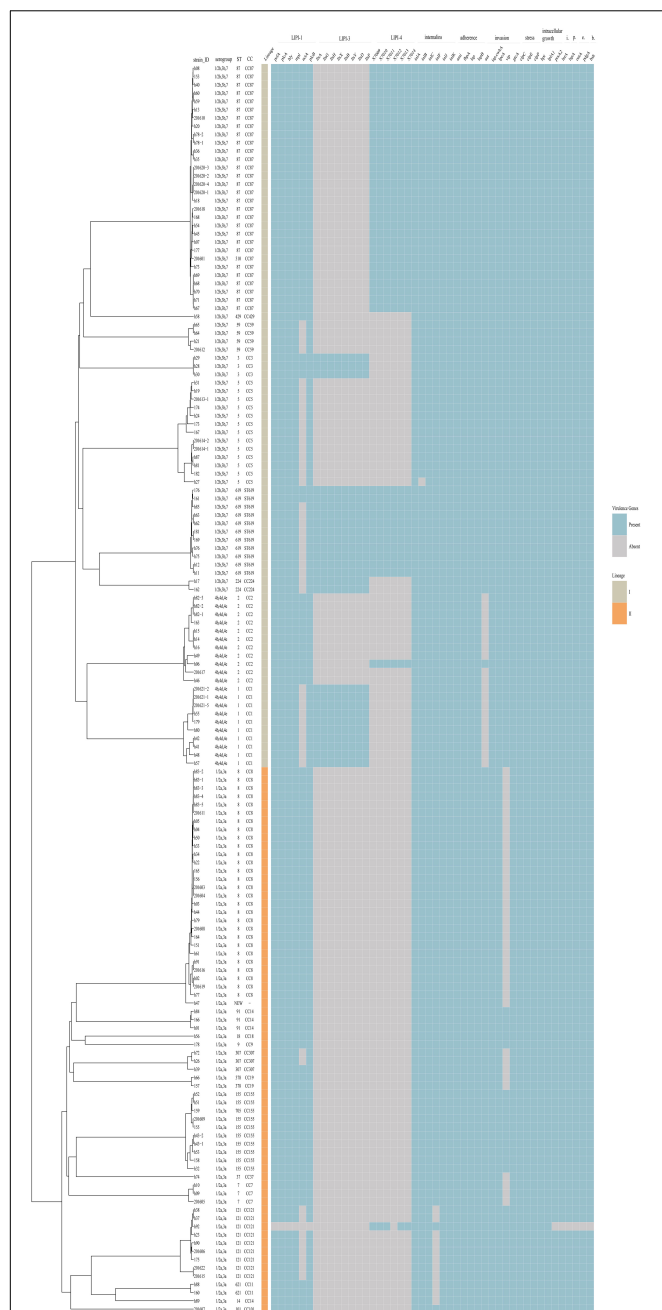


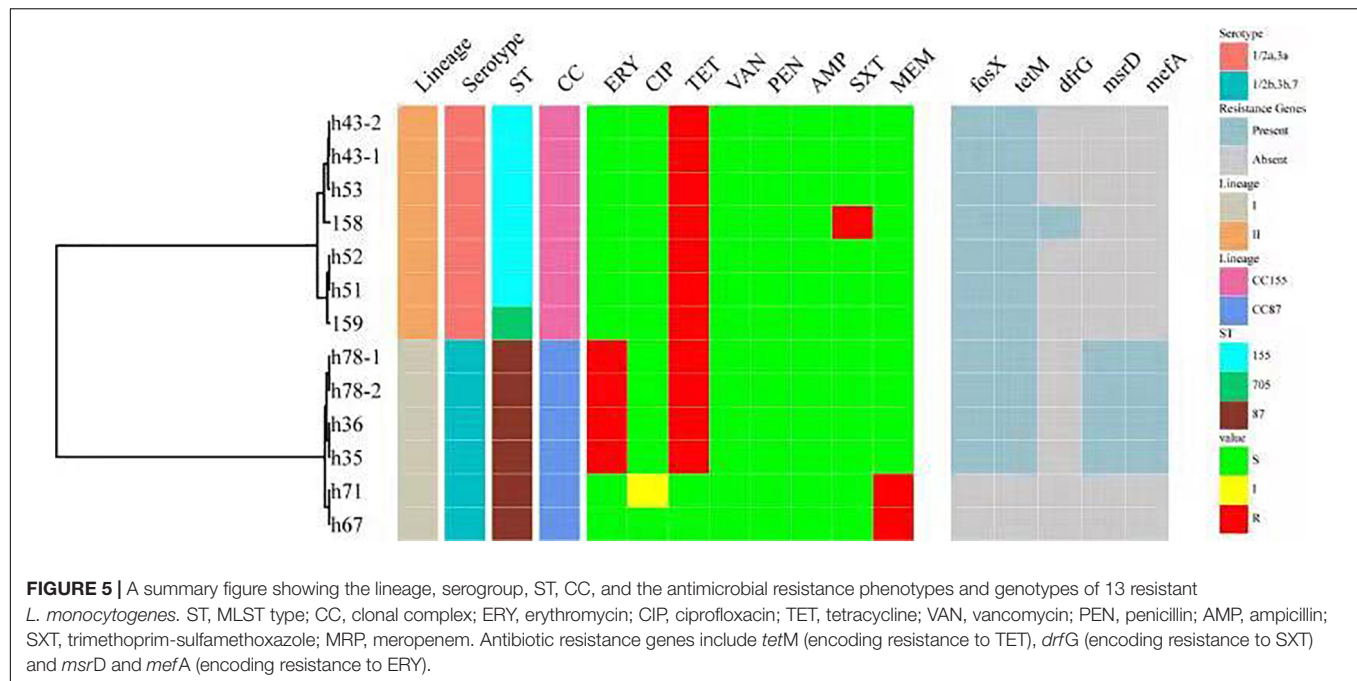
**FIGURE 4 |** Virulence profiles across the phylogeny of the 151 *L. monocytogenes* isolates. The presence/absence gene matrix represents, from left to right, genes located in the pathogenicity islands LIPI-1 (*prfA*, *plcA*, *hly*, *mpl*, *actA*, *plcB*), LIPI-3 (*lslAGHXYDP*) and LIPI-4 (LM9005581\_70009 to LM9005581\_70014), genes coding for internalins (*inlABC*, *FGK*) and other genes involved in adherence (*ami*, *fbpA*, *lap*, *lapB*), invasion (*aut*, *cwhA*, *lpeA*, *vip*, *gtcA*), stress (*clpC*, *clpE*, *clpP*), intracellular growth (*hpt*, *lplA1*, *prsA2*), immunomodulator (*IntA*), peptidase (*lspA*), immune evasion (*oatA*, *pdgA*) and bile-resistance (*bsh*).

arise the potential for common source outbreaks. CgMLST is supposed to become a universal tool for cluster detection and international communication during regional or global

listeriosis outbreaks because it improves *L. monocytogenes* typing and reduces unnecessary epidemiological investigations (Moura et al., 2016). CgMLST typing results do not require a multiple sequence alignment step, and they are easier to be interpreted by microbiologists, epidemiologists and public health professionals (Moura et al., 2016). Simplified cgMLST data can be readily exchanged between global laboratories (Halbedel et al., 2018). However, linking *L. monocytogenes* isolates to listeriosis outbreaks without epidemiological data is not feasible (Hilliard et al., 2018).

The use of cgMLST analysis helps to determine the population structure, and indicates cross-country and intercontinental transmission of *L. monocytogenes* (Moura et al., 2016). To date, only a few cross-country outbreaks have been recognized (Schmid et al., 2014; Wang et al., 2018), and most listeriosis outbreaks have gone unreported (Leclercq et al., 2014). In our study, we compared isolates with those from the United States. No closely linked isolates were found between the United States and the isolates in our study, suggesting lack of the transmission behavior of *L. monocytogenes*. The results revealed some isolates located in the same cluster with those from the United States, suggesting long-standing widespread dispersion. The results also demonstrated that ST87 and ST169 were seldom linked to human listeriosis in the United States. Consistent with our results, a study comparing ST87 isolates from various regions of the world showed that the core gene sequence-based phylogeny grouped the majority of clinical and food isolates from China into a unified clade (Yin et al., 2020).

As discussed above, WGS can be used to identify the presence of genes or pathogenicity islands associated with hypervirulence or particular modes of pathogenesis (Maury et al., 2016). In our study, LIPI-1 was present in almost all isolates, consistent with other studies (Hilliard et al., 2018). LIPI-3 plays a role in gastrointestinal colonization (Quereda et al., 2016), and is strongly associated with lineage I strains (Hilliard et al., 2018). In our study, LIPI-3 was detected in 26 lineage I strains, including CC224, CC3 and ST619 of serotype 1/2b,3b,7, and CC1 of serotype 4b,4d,4e. As shown in other studies (Hilliard et al., 2018), there was no LIPI-3 in CC2 of 4b,4d,4e strains. LIPI-4 was recently described as a gene cluster involved in neural and placental infection (Maury et al., 2016), and it appears to be strongly associated with CC4 isolates (Maury et al., 2016; Hilliard et al., 2018). In our study, there were no CC4 isolates, and this island appears to be associated with CC87 and ST619 isolates, and neural and placental infection. Among 19 pregnancy-associated patients with isolates possessing LIPI-4, 6 (31.6%) patients had abortion or fetal death, 11 (57.9%) patients were cured or infants survived, and the outcome of two cases was unknown. Among 44 pregnancy-associated patients with isolates without LIPI-4, 22 (50.0%) patients had abortion or fetal death, 21 (47.7.0%) patients were cured or infants survived, and the outcome of two cases was unknown. The outcomes of patients with isolates possessing LIPI-4 were different, suggesting that other factors contributing to virulence remain to be characterized. Clinical ST619 isolates were especially specific to China (Wang et al., 2018; Zhang et al., 2019), and harbored the most virulence genes. ST619 isolates carried many virulence genes, including



*lIsX* and *ptsA* that were also found in various food products in China (Wang et al., 2018, 2021; Chen et al., 2019a,b, 2020). However, to date, little information is available on the pathogenicity of ST619 strains, which should be focused on in future studies.

In this study, 13 (8.6%) of the 151 *L. monocytogenes* isolates were resistant to at least one of the tested antibiotics that are commonly used to treat listeriosis in animals and humans in China. Using WGS, antibiotic resistance phenotypes were established. Antibiotic resistance of *L. monocytogenes* is not as serious as that in *Salmonella*, *E. coli*, *Campylobacter* and some other organisms. Previous study showed that the frequency of acquired resistance in clinical isolates is low, such as in France since 1926 (1.27%), in Poland between 1997 and 2013 (0.29%), resistance is more commonly observed in animal and food isolates (Morvan et al., 2010; Wiczorek and Osek, 2017; Kuch et al., 2018). In a study on 2,862 *L. monocytogenes* isolates from food surveillance in China, the resistance rate for tetracycline (8.7%) was the highest, followed by erythromycin (2.2%), trimethoprim/sulfamethoxazole (0.98%) and chloramphenicol (0.8%), similar to our current study (Yan et al., 2019). In this previous study, 11 MDR isolates were identified belonging to ST9, and 13 of the other 17 isolates resistant to trimethoprim/sulfamethoxazole belonged to ST155. In our study, six of the 11 antibiotic resistance isolates belonged to ST155. Two isolates were resistant to MRP, but no genes known to encode resistance to MRP were found. More research is therefore needed.

WGS of *L. monocytogenes* isolates from cases of human listeriosis in Beijing, China, between 2014 and 2018 has provided an overview of locally circulating clinical strains of the pathogen. This work identified particular STs responsible for disease in Beijing, China. CgMLST analysis revealed that isolates from

the same patient were highly related, and indicated possible outbreaks, although retrospective follow-up failed to prove any clear epidemiological links. WGS also confirmed the presence of pathogenicity genes or islands and resistance genes.

## DATA AVAILABILITY STATEMENT

The datasets presented in this study can be found in online repositories. The names of the repository/repositories and accession number(s) can be found below: NCBI BioProject, PRJNA759341.

## AUTHOR CONTRIBUTIONS

XZ, QC, and XM conceived and designed the research study. YN and XM performed the sample collection. XZ and YL performed the experiments. XZ, PZ, and YN analyzed the data. XZ and XM wrote the manuscript. All authors read and approved the final version of the article.

## FUNDING

This work was supported by Capitals Funds for Health Improvement and Research (Grant No. CFH2020-2-3012), the National Key Research and Development Program of China (Grant No. 2017YFC1601500) and the Young Talent Project of Beijing Excellent Talents Funding (Grant No. 2015000021469G186), the Cultivation Fund of Beijing Center for Disease Prevention and Control, Beijing Research Center for Preventive Medicine (No. 2020-BJYJ-10).

## SUPPLEMENTARY MATERIAL

The Supplementary Material for this article can be found online at: <https://www.frontiersin.org/articles/10.3389/fmicb.2021.751003/full#supplementary-material>

**Supplementary Figure 1** | Minimum spanning tree (MST) of 86 *L. monocytogenes* isolates that formed 30 complexes with  $\leq 7$  different alleles

## REFERENCES

- Almeida, R. M., Barbosa, A. V., Lisboa, R. C., Santos, A., Hofer, E., Vallim, D. C., et al. (2017). Virulence genes and genetic relationship of *L. monocytogenes* isolated from human and food sources in Brazil. *Braz. J. Infect. Dis.* 21, 282–289. doi: 10.1016/j.bjid.2017.01.004
- Anand, V., Holmen, J., Neely, M., Pannaraj, P. S., and Dien Bard, J. (2016). Closing the brief case: neonatal meningitis caused by *Listeria monocytogenes* diagnosed by multiplex molecular panel. *J. Clin. Microbiol.* 54:3075. doi: 10.1128/JCM.01160-16
- Barton Behravesh, C., Jones, T. F., Vugia, D. J., Long, C., Marcus, R., Smith, K., et al. (2011). Deaths associated with bacterial pathogens transmitted commonly through food: foodborne diseases active surveillance network (FoodNet), 1996–2005. *J. Infect. Dis.* 204, 263–267. doi: 10.1093/infdis/jir263
- Bergholz, T. M., den Bakker, H. C., Katz, L. S., Silk, B. J., Jackson, K. A., Kucerova, Z., et al. (2016). Determination of evolutionary relationships of outbreak-associated *Listeria monocytogenes* strains of serotypes 1/2a and 1/2b by whole-genome sequencing. *Appl. Environ. Microbiol.* 82, 928–938. doi: 10.1128/AEM.02440-15
- Bergholz, T. M., Shah, M. K., Burall, L. S., Rakic-Martinez, M., and Datta, A. R. (2018). Genomic and phenotypic diversity of *Listeria monocytogenes* clonal complexes associated with human listeriosis. *Appl. Microbiol. Biotechnol.* 102, 3475–3485. doi: 10.1007/s00253-018-8852-5
- Centers for Disease Control and Prevention (2014). *National Enteric Disease Surveillance: Listeria Annual Summary, 2014*. Washington, DC: Centers for Disease Control and Prevention.
- Centers for Disease Control and Prevention (2015). *Data from: Multistate Outbreak of Listeriosis Linked to Blue Bell Creameries Products (Final Update)*. Washington, DC: Centers for Disease Control and Prevention.
- Chen, M., Chen, Y., Wu, Q., Zhang, J., Cheng, J., Li, F., et al. (2019a). Genetic characteristics and virulence of *Listeria monocytogenes* isolated from fresh vegetables in China. *BMC Microbiol.* 19:119. doi: 10.1186/s12866-019-1488-5
- Chen, M., Cheng, J., Zhang, J., Chen, Y., Zeng, H., Xue, L., et al. (2019b). Isolation, potential virulence, and population diversity of *Listeria monocytogenes* from meat and meat products in China. *Front. Microbiol.* 10:946. doi: 10.3389/fmicb.2019.00946
- Chen, M., Wu, Q., Zhang, J., Wu, S., and Guo, W. (2015). Prevalence, enumeration, and pheno- and genotypic characteristics of *Listeria monocytogenes* isolated from raw foods in South China. *Front. Microbiol.* 6:1026. doi: 10.3389/fmicb.2015.01026
- Chen, Y., Chen, M., Wang, J., Wu, Q., Cheng, J., Zhang, J., et al. (2020). Heterogeneity, characteristics, and public health implications of *Listeria monocytogenes* in ready-to-eat foods and pasteurized milk in China. *Front. Microbiol.* 11:642. doi: 10.3389/fmicb.2020.00642
- Chenal-Francis, V., Lopez, J., Cantinelli, T., Caro, V., Tran, C., Leclercq, A., et al. (2011). Worldwide distribution of major clones of *Listeria monocytogenes*. *Emerg. Infect. Dis.* 17, 1110–1112. doi: 10.3201/eid1706.101778
- Cotter, P. D., Draper, L. A., Lawton, E. M., Daly, K. M., Groeger, D. S., Casey, P. G., et al. (2008). Listeriolysin S, a novel peptide haemolysin associated with a subset of lineage I *Listeria monocytogenes*. *PLoS Pathog.* 4:e1000144. doi: 10.1371/journal.ppat.1000144
- de Noordhout, C. M., Devleeschauwer, B., Angulo, F. J., Verbeke, G., Haagsma, J., Kirk, M., et al. (2014). The global burden of listeriosis: a systematic review and meta-analysis. *Lancet Infect. Dis.* 14, 1073–1082. doi: 10.1016/S1473-3099(14)70780-9
- Doumith, M., Buchrieser, C., Glaser, P., Jacquet, C., and Martin, P. (2004). Differentiation of the major *Listeria monocytogenes* serovars by multiplex PCR. *J. Clin. Microbiol.* 42, 3819–3822. doi: 10.1128/JCM.42.8.3819-3822.2004
- Fan, Z., Xie, J., Li, Y., and Wang, H. (2019). Listeriosis in mainland China: a systematic review. *Int. J. Infect. Dis.* 81, 17–24. doi: 10.1016/j.ijid.2019.01.007
- Gaillard, J. L., Berche, P., Frehel, C., Gouin, E., and Cossart, P. (1991). Entry of *L. monocytogenes* into cells is mediated by internalin, a repeat protein reminiscent of surface antigens from gram-positive cocci. *Cell* 65, 1127–1141. doi: 10.1016/0092-8674(91)90009-n
- Gerner-Smidt, P., Hise, K., Kincaid, J., Hunter, S., Rolando, S., Hyttiä-Trees, E., et al. (2006). PulseNet USA: a five-year update. *Foodborne Pathog. Dis.* 3, 9–19. doi: 10.1089/fpd.2006.3.9
- Gouin, E., Mengaud, J., and Cossart, P. (1994). The virulence gene cluster of *Listeria monocytogenes* is also present in *Listeria ivanovii*, an animal pathogen, and *Listeria seeligeri*, a nonpathogenic species. *Infect. Immun.* 62, 3550–3553. doi: 10.1128/iai.62.8.3550-3553.1994
- Haase, J. K., Didelot, X., Lecuit, M., Korkeala, H., and Achtman, M. (2014). The ubiquitous nature of *Listeria monocytogenes* clones: a large-scale Multilocus Sequence Typing study. *Environ. Microbiol.* 16, 405–416. doi: 10.1111/1462-2920.12342
- Halbedel, S., Prager, R., Fuchs, S., Trost, E., Werner, G., and Flieger, A. (2018). Whole-genome sequencing of recent *Listeria monocytogenes* isolates from Germany reveals population structure and disease clusters. *J. Clin. Microbiol.* 56:e00119-18. doi: 10.1128/JCM.00119-18
- Harris, S. R., Feil, E. J., Holden, M. T., Quail, M. A., Nickerson, E. K., Chantratita, N., et al. (2010). Evolution of MRSA during hospital transmission and intercontinental spread. *Science* 327, 469–474. doi: 10.1126/science.1182395
- Hernandez-Milian, A., and Payeras-Cifre, A. (2014). What is new in listeriosis? *Biomed Res. Int.* 2014:358051. doi: 10.1155/2014/358051
- Hilliard, A., Leong, D., O'Callaghan, A., Culligan, E., Morgan, C., DeLappe, N., et al. (2018). Genomic characterization of *Listeria monocytogenes* isolates associated with clinical listeriosis and the food production environment in Ireland. *Genes* 9:171. doi: 10.3390/genes9030171
- Jackson, B. R., Salter, M., Tarr, C., Conrad, A., Harvey, E., Steinbock, L., et al. (2015). Notes from the field: listeriosis associated with stone fruit—United States, 2014. *MMWR Morb. Mortal. Wkly. Rep.* 64, 282–283.
- Jacquet, C., Doumith, M., Gordon, J. I., Martin, P. M., Cossart, P., and Lecuit, M. (2004). A molecular marker for evaluating the pathogenic potential of foodborne *Listeria monocytogenes*. *J. Infect. Dis.* 189, 2094–2100. doi: 10.1086/420853
- Jennison, A. V., Masson, J. J., Fang, N. X., Graham, R. M., Bradbury, M. I., Fegan, N., et al. (2017). Analysis of the *Listeria monocytogenes* population structure among isolates from 1931 to 2015 in Australia. *Front. Microbiol.* 8:603. doi: 10.3389/fmicb.2017.00603
- Kuch, A., Goc, A., Belkiewicz, K., Filipello, V., Ronkiewicz, P., Gołbiewska, A., et al. (2018). Molecular diversity and antimicrobial susceptibility of *Listeria monocytogenes* isolates from invasive infections in Poland (1997–2013). *Sci. Rep.* 28:14562. doi: 10.1038/s41598-018-32574-0
- Kwong, J. C., Mercouliou, K., Tomita, T., Easton, M., Li, H. Y., Bulach, D. M., et al. (2016). Prospective whole-genome sequencing enhances national surveillance of *Listeria monocytogenes*. *J. Clin. Microbiol.* 54, 333–342. doi: 10.1128/JCM.02344-15
- Kylat, R. I., Bartholomew, A., Cramer, N., and Bader, M. Y. (2016). Neonatal listeriosis: uncommon or misdiagnosed? *J. Neonatal Perinatal Med.* 9, 313–316. doi: 10.3233/NPM-16915121



- Leclercq, A., Charlier, C., and Lecuit, M. (2014). Global burden of listeriosis: the tip of the iceberg. *Lancet Infect. Dis.* 14, 1027–1028. doi: 10.1016/S1473-3099(14)70903-X
- Li, W., Bai, L., Fu, P., Han, H., Liu, J., and Guo, Y. (2018). The epidemiology of *Listeria monocytogenes* in China. *Foodborne Pathog. Dis.* 15, 459–466. doi: 10.1089/fpd.2017.2409
- Li, W., Bai, L., Ma, X., Zhang, X., Li, X., Yang, X., et al. (2019). Sentinel listeriosis surveillance in selected hospitals, China, 2013–2017. *Emerg. Infect. Dis.* 25, 2274–2277. doi: 10.3201/eid2512.180892
- Li, W., Cui, Q., Bai, L., Fu, P., Han, H., Liu, J., et al. (2021). Application of whole-genome sequencing in the national molecular tracing network for foodborne disease surveillance in China. *Foodborne Pathog. Dis.* 18, 538–546. doi: 10.1089/fpd.2020.2908
- Lomonaco, S., Verghese, B., Gerner-Smidt, P., Tarr, C., Gladney, L., Joseph, L., et al. (2013). Novel epidemic clones of *Listeria monocytogenes*, United States, 2011. *Emerg. Infect. Dis.* 19, 147–150. doi: 10.3201/eid1901.121167
- Mammina, C., Aleo, A., Romani, C., Pellissier, N., Nicoletti, P., Pecile, P., et al. (2009). Characterization of *Listeria monocytogenes* isolates from human listeriosis cases in Italy. *J. Clin. Microbiol.* 47, 2925–2930. doi: 10.1128/JCM.00102-09
- Maury, M. M., Tsai, Y.-H., Charlier, C., Touchon, M., Chenal-Francisque, V., Leclercq, A., et al. (2016). Uncovering *Listeria monocytogenes* hypervirulence by harnessing its biodiversity. *Nat. Genet.* 48, 308–313. doi: 10.1038/ng.3501
- Morvan, A., Moubareck, C., Leclercq, A., Hervé-Bazin, M., Bremont, S., Lecuit, M., et al. (2010). Antimicrobial resistance of *Listeria monocytogenes* strains isolated from humans in France. *Antimicrob. Agents Chemother.* 54, 2728–2731. doi: 10.1128/AAC.01557-09
- Moura, A., Criscuolo, A., Pouseele, H., Maury, M. M., Leclercq, A., Tarr, C., et al. (2016). Whole genome-based population biology and epidemiological surveillance of *Listeria monocytogenes*. *Nat. Microbiol.* 2:16185. doi: 10.1038/nmicrobiol.2016.185
- Mutreja, A., Kim, D. W., Thomson, N. R., Connor, T. R., Lee, J. H., Kariuki, S., et al. (2011). Evidence for several waves of global transmission in the seventh cholera pandemic. *Nature* 477, 462–465. doi: 10.1038/nature10392
- Nightingale, K. K., Ivy, R. A., Ho, A. J., Fortes, E. D., Njaa, B. L., Peters, R. M., et al. (2008). InA premature stop codons are common among *Listeria monocytogenes* isolates from foods and yield virulence-attenuated strains that confer protection against fully virulent strains. *Appl. Environ. Microbiol.* 74, 6570–6583. doi: 10.1128/AEM.00997-08
- Quereda, J. J., Dussurget, O., Nahori, M. A., Ghazlane, A., Volant, S., Dillies, M. A., et al. (2016). Bacteriocin from epidemic *Listeria* strains alters the host intestinal microbiota to favor infection. *Proc. Natl. Acad. Sci. U.S.A.* 113, 5706–5711. doi: 10.1073/pnas.1523899113
- Ragon, M., Wirth, T., Hollandt, F., Lavenir, R., Lecuit, M., Le Monnier, A., et al. (2008). A new perspective on *Listeria monocytogenes* evolution. *PLoS Pathog.* 4:e1000146. doi: 10.1371/journal.ppat.1000146
- Scallan, E., Hoekstra, R. M., Angulo, F. J., Tauxe, R. V., Widdowson, M.-A., Roy, S. L., et al. (2011). Foodborne illness acquired in the United States—major pathogens. *Emerg. Infect. Dis.* 17, 7–15. doi: 10.3201/eid1701.p11101
- Schmid, D., Allerberger, F., Huhulescu, S., Pietzka, A., Amar, C., Kleta, S., et al. (2014). Whole genome sequencing as a tool to investigate a cluster of seven cases of listeriosis in Austria and Germany, 2011–2013. *Clin. Microbiol. Infect.* 20, 431–436. doi: 10.1111/1469-0691.12638
- Stasiewicz, M. J., Oliver, H. F., Wiedmann, M., den Bakker, H. C., and Elkins, C. A. (2015). Whole-genome sequencing allows for improved identification of persistent *Listeria monocytogenes* in food-associated environments. *Appl. Environ. Microbiol.* 81, 6024–6037. doi: 10.1128/AEM.01049-15
- Wang, H., Luo, L., Zhang, Z., Deng, J., Wang, Y., Miao, Y., et al. (2018). Prevalence and molecular characteristics of *Listeria monocytogenes* in cooked products and its comparison with isolates from listeriosis cases. *Front. Med.* 12, 104–112. doi: 10.1007/s11684-017-0593-9
- Wang, Y., Ji, Q., Li, S., and Liu, M. (2021). Prevalence and genetic diversity of *Listeria monocytogenes* isolated from retail pork in Wuhan, China. *Front. Microbiol.* 12:620482. doi: 10.3389/fmicb.2021.620482
- Wieczorek, K., and Osek, J. (2017). Prevalence, genetic diversity and antimicrobial resistance of *Listeria monocytogenes* isolated from fresh and smoked fish in Poland. *Food Microbiol.* 64, 164–171. doi: 10.1016/j.fm.2016.12.022
- Wu, S., Wu, Q., Zhang, J., Chen, M., and Guo, W. (2016). Analysis of multilocus sequence typing and virulence characterization of *Listeria monocytogenes* isolates from Chinese retail ready-to-eat food. *Front. Microbiol.* 7:168. doi: 10.3389/fmicb.2016.00168
- Yan, S., Li, M., Luque-Sastre, L., Wang, W., Hu, Y., Peng, Z., et al. (2019). Susceptibility (re)-testing of a large collection of *Listeria monocytogenes* from foods in China from 2012 to 2015 and WGS characterization of resistant isolates. *J. Antimicrob. Chemother.* 74, 1786–1794. doi: 10.1093/jac/dkz126
- Yin, Y., Doijad, S., Wang, W., Lian, K., Pan, X., Koryciński, I., et al. (2020). Genetic diversity of *Listeria monocytogenes* isolates from invasive listeriosis in China. *Foodborne Pathog. Dis.* 17, 215–227. doi: 10.1089/fpd.2019.2693
- Zhang, X., Niu, Y., Liu, Y., Lu, Z., Wang, D., Cui, X., et al. (2019). Isolation and characterization of clinical *Listeria monocytogenes* in Beijing, China, 2014–2016. *Front. Microbiol.* 10:981. doi: 10.3389/fmicb.2019.00981

**Conflict of Interest:** The authors declare that the research was conducted in the absence of any commercial or financial relationships that could be construed as a potential conflict of interest.

**Publisher's Note:** All claims expressed in this article are solely those of the authors and do not necessarily represent those of their affiliated organizations, or those of the publisher, the editors and the reviewers. Any product that may be evaluated in this article, or claim that may be made by its manufacturer, is not guaranteed or endorsed by the publisher.

Copyright © 2021 Zhang, Liu, Zhang, Niu, Chen and Ma. This is an open-access article distributed under the terms of the Creative Commons Attribution License (CC BY). The use, distribution or reproduction in other forums is permitted, provided the original author(s) and the copyright owner(s) are credited and that the original publication in this journal is cited, in accordance with accepted academic practice. No use, distribution or reproduction is permitted which does not comply with these terms.





# Advances in Metagenomics and Its Application in Environmental Microorganisms

Lu Zhang<sup>1†</sup>, FengXin Chen<sup>1†</sup>, Zhan Zeng<sup>2†</sup>, Mengjiao Xu<sup>1</sup>, Fangfang Sun<sup>1</sup>, Liu Yang<sup>1</sup>, Xiaoyue Bi<sup>1</sup>, Yanjie Lin<sup>2</sup>, YuanJiao Gao<sup>1</sup>, HongXiao Hao<sup>1</sup>, Wei Yi<sup>3\*</sup>, Minghui Li<sup>1,2\*</sup> and Yao Xie<sup>1,2\*</sup>

<sup>1</sup> Department of Hepatology Division 2, Beijing Ditan Hospital, Capital Medical University, Beijing, China, <sup>2</sup> Department of Hepatology Division 2, Peking University Ditan Teaching Hospital, Beijing, China, <sup>3</sup> Department of Gynecology and Obstetrics, Beijing Ditan Hospital, Capital Medical University, Beijing, China

## OPEN ACCESS

### Edited by:

Xuejun Ma,  
Chinese Center for Disease Control  
and Prevention, China

### Reviewed by:

Xiyang Wu,  
Jinan University, China  
Ahmed Abd El Wahed,  
Leipzig University, Germany

### \*Correspondence:

Minghui Li  
wuhm2000@sina.com  
orcid.org/0000-0003-3233-5473  
Wei Yi  
yiwei1215@163.com  
orcid.org/0000-0003-4241-8205  
Yao Xie  
xieyao00120184@sina.com  
orcid.org/0000-0003-4108-7037

<sup>†</sup>These authors have contributed  
equally to this work

### Specialty section:

This article was submitted to  
Food Microbiology,  
a section of the journal  
Frontiers in Microbiology

**Received:** 29 August 2021

**Accepted:** 18 November 2021

**Published:** 17 December 2021

### Citation:

Zhang L, Chen F, Zeng Z, Xu M, Sun F,  
Yang L, Bi X, Lin Y, Gao Y, Hao H,  
Yi W, Li M and Xie Y (2021) Advances  
in Metagenomics and Its Application  
in Environmental Microorganisms.  
Front. Microbiol. 12:766364.  
doi: 10.3389/fmicb.2021.766364

Metagenomics is a new approach to study microorganisms obtained from a specific environment by functional gene screening or sequencing analysis. Metagenomics studies focus on microbial diversity, community constitute, genetic and evolutionary relationships, functional activities, and interactions and relationships with the environment. Sequencing technologies have evolved from shotgun sequencing to high-throughput, next-generation sequencing (NGS), and third-generation sequencing (TGS). NGS and TGS have shown the advantage of rapid detection of pathogenic microorganisms. With the help of new algorithms, we can better perform the taxonomic profiling and gene prediction of microbial species. Functional metagenomics is helpful to screen new bioactive substances and new functional genes from microorganisms and microbial metabolites. In this article, basic steps, classification, and applications of metagenomics are reviewed.

**Keywords:** metagenomics, shotgun sequencing, next-generation sequencing, third generation sequencing, antibiotics resistance genes, bioremediation

## INTRODUCTION

Traditionally, research on microorganisms is based on cultured organisms, which has several disadvantages (Kellenberger, 2001). In 1998, Metagenome, also known as microbial environmental genome (Handelsman et al., 1998), is defined as “the genome of the total microbiota found in nature.” Metagenome currently refers to the sum of the genomes of bacteria and fungi in environmental samples. Metagenomics is the study of a collection of genetic material (genomes) from a mixed community of organisms. In short, metagenomics is a new way to study microorganisms in a specific environment by using functional gene screening or sequencing analysis. The main areas of concern of metagenomics research are microbial diversity, population structure, genetic and evolutionary relationships, functional activity, and cooperative relationships, and relationship with the environment. Metagenomics research is developing rapidly in medicine, agriculture, environmental protection, and other fields.

This article reviews the development and application of metagenomics detection technology. The review is divided into three parts. The first part focuses on molecular biology technology from the extraction of all microbial genes, heterologous expression of gene fragments, to the screening of target genes or active products, and finally the sequencing of target genes. The second part

introduces the main classification or branch of metagenomics from the research purpose or objects. The third part is about the application of metagenomics in various fields.

## BASIC STEPS OF METAGENOMICS

Metagenomics is based on gene cloning. The basic procedure of metagenomics consists of the following steps. First, all genes in environmental microbial samples are extracted and enriched. Second, the genes are cloned into the vector, which is transformed into host bacteria to establish the metagenomic library. Finally, the metagenomic library is screened and analyzed. The extraction of metagenomic DNA and construction and screening of metagenomic library are essential.

### Extraction and Enrichment of Metagenomic DNA

The traditional approach is to culture microorganisms and then extract the DNA, but 99% of the microorganisms in the environment cannot be cultured (Torsvik et al., 1990; Handelsman et al., 1998). Extracting high concentration and large fragment environmental microbial total DNA is the first and most critical step in building a metagenomic library. There are two key points to extracting metagenomic DNA. First, to extract all the genes of all microorganisms in the sample. Second, to keep the integrity and purity of the fragment. Sample collection must follow a strict procedure to extract as much DNA as possible from environmental microorganisms and maintain large DNA fragments.

According to whether or not the cells are isolated before DNA extracting, it can be divided into direct extraction and indirect extraction. Direct extraction uses physical (such as freeze-thaw) and chemical (such as the addition of protease or SDS) to lyse microorganisms directly to release microbial DNA (Gabor et al., 2003). The total DNA in all samples can be obtained by the direct extraction method, which is suitable for extracting 1–50 kb DNA. The direct extraction method is simple and efficient, but the purity is low (Schneegurt et al., 2003; Wang et al., 2011). The indirect extraction method requires isolating the microbial cells at first and then extracting DNA using a gentle method. The DNA obtained by indirect extraction is of high purity and suitable for the extraction of 20–500 kb DNA. The indirect extraction method is cumbersome and inefficient, which may cause the loss of some microbial DNA (Gabor et al., 2003).

The sample size depends on microbial concentration. The high density of microorganisms such as stool samples may require only an anal swab sample. To study the marine microbial community, which is a low-density microorganism, large numbers of water samples are captured and concentrated through filters. Samples need to be decontaminated. For example, humic acid in soil is often tightly bound to DNA, so humic acid needs to be removed during sample preparation (Daniel, 2005). When studying microorganisms in humans or animals, the DNA contamination in samples and host must be removed.

For DNA samples with low abundance, enrichment at the cell level and gene level can be carried out after DNA fragment

extraction, but this may cause certain deviations (Probst et al., 2015). The common methods of gene enrichment are stable isotope probing (SIP) (Chen and Murrell, 2010), suppression subtractive hybridization (SSH) (Galbraith et al., 2008; Chew and Holmes, 2009), DNA chip technology, etc. (Avarre et al., 2007).

### Construct Metagenome Libraries

In the construction of a metagenome library, microbial DNA should first be cut mechanically or digested into a certain size of DNA, and then randomly recombined with an appropriate clone vector, and finally transformed into suitable host cells. The goal is to isolate some target genes or preserve the entire DNA of an organism. The strategy of building microorganism DNA library changes with the research objective: low abundance genes or high abundance genes and small segments of a single gene or large segments of gene clusters in a metabolic pathway.

The vector is selected only if it is conducive to the amplification of the target DNA fragment and is convenient for screening after the transformation and expression. The common vectors include plasmid, cosmid, fosmid, or bacterial artificial chromosome (BAC), yeast artificial chromosome (YAC), and phage. Plasmids are suitable for cloning DNA fragments below 10 kb. Cosmid and fosmid are suitable for cloning large genes or multiple gene fragments (20–40 kb). BAC and YAC can be used to clone DNA fragments of 200–450 kb. The BAC shuttle vector, which can be duplicated and expressed in a variety of hosts, can be used to expand the host range (Kakirde et al., 2011).

The host cells are generally the ones with good stability of the recombinant vector, high efficiency of transformation, and effective expression of the target gene fragment. Usually, different host strains are selected according to different research purposes. *Escherichia coli* is easy to culture and is the most common host, but it is a prokaryotic host with limitations. Some new host cells are gradually applied, such as host *Streptomyces* (Rebets et al., 2017), *pseudomonas* (Craig et al., 2010), and *mycobacterium*.

There are many barriers to the study of foreign gene expression in metagenomics. For example, the target gene may be lost in the process of library construction, and the host cell cannot recognize the unique promoter, failing the expression of heterologous gene fragments. To solve this problem, multi-host expressions can be adopted. A research group expressed DNA fragments in 6 different bacteria (Craig et al., 2010). If the target gene is in cluster form, large segments of DNA need to be inserted to obtain complete metabolic enzymes and pathways. At present, the failure of DNA cloning in large fragments may be caused by the destructive effects of physical and chemical actions during the extraction process or the limited receptive capability of host bacteria.

### Screening of Metagenome Library

Currently, there are three approaches to environmental metagenomic library screening: function-driven screening, sequence-driven screening, and substrate-induced gene expression screening (SIGEX). Other techniques include DNA stable-isotope probing (DNA-SIP) (Chen and Murrell, 2010) and fluorescence *in situ* hybridization.

There are two kinds of functional screening. One is to screen the expression of active products of exogenous genes in host cells according to special characterization (such as color and plaque) on various selective media to obtain target clones (Apolinar-Hernández et al., 2016; Popovic et al., 2017). The other is to screen the host strain and its mutants based on their complementary growth characteristics under selective conditions (Cheng et al., 2017). The function-driven screening method is fast, simple, and does not rely on any known sequence information. Most biocatalysts, such as protease (Apolinar-Hernández et al., 2016), esterase (Popovic et al., 2017), are obtained by this method. The biggest disadvantage is that it depends on the expression of functional genes in foreign hosts, so the success rate of screening is very low. Thus, selecting the right host and cloning the full length of a gene or gene cluster is required. Functional analysis is suitable for gene screening of large fragment DNA libraries.

Sequence analysis usually uses oligonucleotide primers or probes to screen target genes by molecular biological methods such as PCR and gene hybridization. Only target clones with known sequences can be screened. Sequence analysis is suitable for screening highly conserved sequence enzyme genes, such as polyketide synthase gene (Ginolhac et al., 2004) and cellulase genes (Voget et al., 2003). Sequence analysis is also suitable for gene screening of small DNA fragments. The advantage of sequence analysis is that it need not rely on host cells to express the cloned genes, but the disadvantage is that it is unable to screen the unknown genes with completely different sequences from the existing genes.

Some new methods such as microarray, stable isotope labeling, and fluorescence *in situ* hybridization can also be applied to sequence screening. The DNA microarray technology, also known as gene chip technology, is based on nucleic acid hybridization (Avarre et al., 2007). First, DNA fragments are densely and orderly arranged on the solid support such as silicon wafer to form DNA microarray. Then the labeled samples are hybridized with the DNA microarray, and the genes are analyzed according to the hybridization sites and signal strength. DNA microarray technology can be used to study key genes in metabolic pathways. The DNA microarray technology has advantages of rapid detection and preliminary screening, but its specificity and sensitivity are only 1/100–1/10,000 of PCR method, so it is unsuitable for the detection of unknown functional genes (Call, 2005; Palka-Santini et al., 2009; Mauk et al., 2015).

The principle of substrate-induced gene expression screening is that metabolism-related genes or enzyme genes are usually expressed in the presence of substrate-induced conditions (Uchiyama et al., 2005; Yun and Ryu, 2005). SIGEX has several advantages, such as no modification of the substrate is required and functions of unknown enzymes and genes can be inferred from the substrate. SIGEX is a high-throughput screening method that is suitable for industrial use. But it is highly demanding on the structure and fitness of the target gene in the host and is only suitable for substrates that can enter the cytoplasm and target gene, which itself has a promoter.

What metagenomics need now are high-throughput screening methods. In 2015, a research team attempted to apply microfluidic chips integrating sample detection and automatic analysis (Colin et al., 2015), which is known as lab-on-chip (LOC). LOC only requires a sample of nanoliters or picoliter level, but the technical requirements are high. LOC requires advanced technologies such as chip sampling technology, microfluidic technology, and focusing electrophoresis technology. LOC implements various experimental steps in the laboratory, such as sample preparation, biochemical reaction, and sample detection, on a chip of several square centimeters. LOC meets the objective of overall miniaturization, automation, integration, and portability of sample testing.

## Metagenomic Sequencing and Analysis Techniques

Rapid progress has been made in sequencing technologies, from shotgun sequencing to high-throughput, next-generation sequencing (NGS) (Mardis, 2008; van Dijk et al., 2014), and third-generation sequencing (TGS) (Branton et al., 2008).

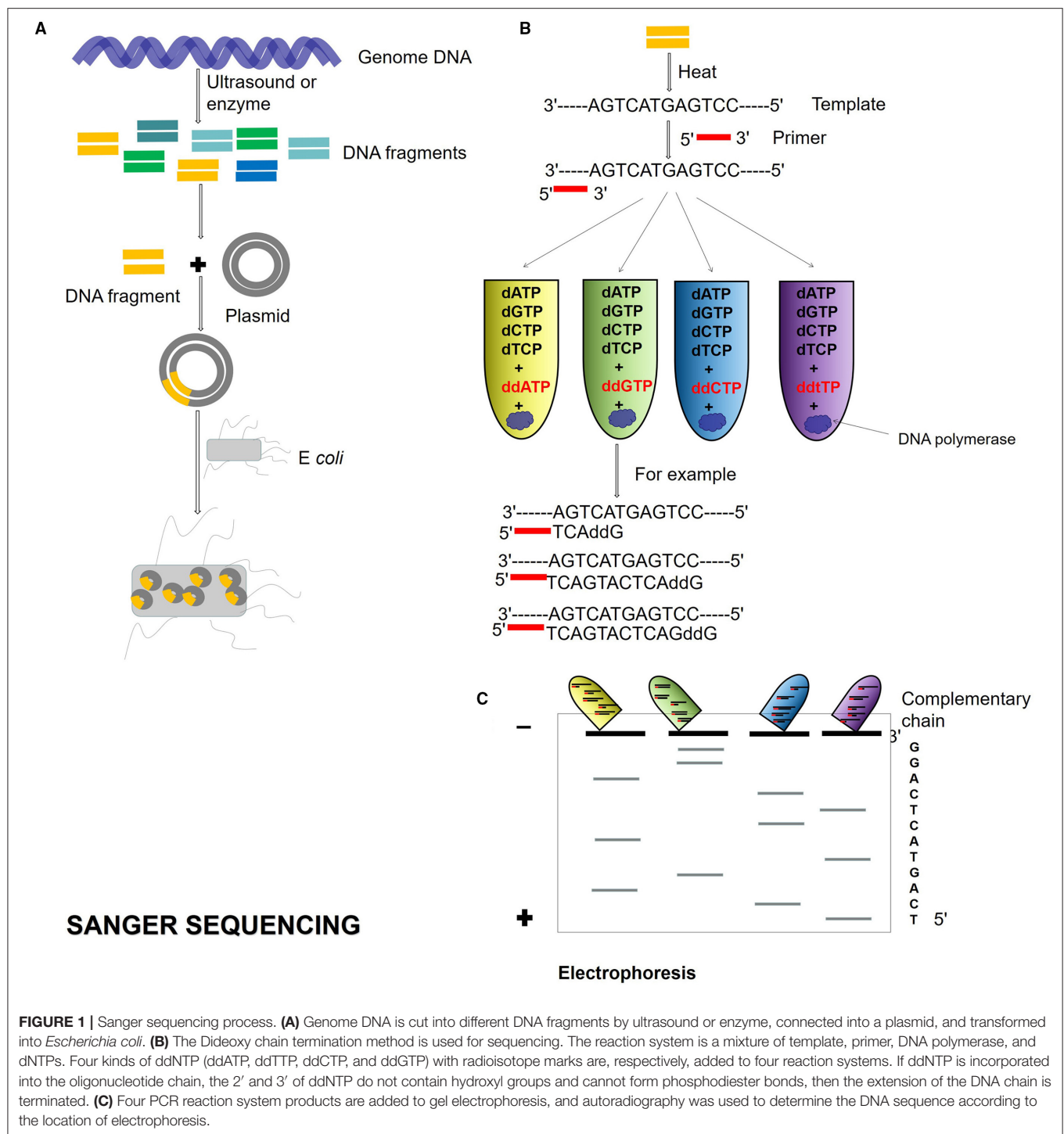
### Preparation of Metagenomic Sequencing Samples

Metagenomic DNA can be sequenced from DNA libraries obtained from target gene cloning or directly from samples. The purity and content of the DNA must be ensured before it is sequenced.

### History of DNA Sequencing Technologies and Platforms

Second-generation DNA sequencing was established on PCR techniques. The first-generation sequencing is the shotgun sequencing based on the traditional Sanger sequencing technology (Olson, 1993; Bankier, 2001; Quince et al., 2017; **Figure 1**), and the sequencing using the dideoxy chain termination method is the gold standard of sequencing. The accuracy of shotgun sequencing is higher than those of second and TGS. It has a high accuracy of long reads from 700 to 1,000 bp and can deal with repeated sequences well. The disadvantage is that only one template can be detected at a time, which is slow and time-consuming.

Next-generation sequencing uses large-scale parallel sequencing technology, which can simultaneously synthesize millions of complementary chains of sequencing templates and acquire sequence data. High-throughput and low-cost NGS is used worldwide in large-scale genome sequencing and resequencing. The NGS mainly used sequencing by synthesis (SBS) technology and sequence by ligation (SBL). Roche has developed GS FLX and GS Junior sequencing platforms with 454 sequencing technology and SBS (Marsh, 2007; Harrington et al., 2013; **Figure 2**), which can read more than 400 bp. Illumina used SBS and a 3' blocked reversible terminator for sequencing (Shendure and Ji, 2008; Ansorge, 2009; **Figure 3**). Based on this technology, the Genome Analyzer platform reads 125 bp. Illumina sequencing has become the mainstream product of NGS. Applied Biosystems, Inc. (ABI) used SBL to develop the



ABI Solid Sequencer (Mardis, 2008; Shendure and Ji, 2008; Ansorge, 2009). The advantage of sequencing by oligonucleotide ligation and detection (SOLiD) (Figure 4) is that each base can be detected two times by two-base encoding, and the detection accuracy is higher than the other NGS. The disadvantage is that only 40 bp can be read, which is only suitable for SNP mutation detection. In addition, ion torrent sequencing technology

developed by Life Technologies/Thermo Fisher Scientific adopts semiconductor chip technology (Figure 5). Four kinds of dNTPs sequential flow through the chip in turn, if one dNTP is complementary to the DNA molecule in a specific microhole of the chip, the dNTP is synthesized into the DNA strand. Subsequently, the hydrogen ions are released as the DNA strand stretches, causing the change of the pH. Finally, voltage changes



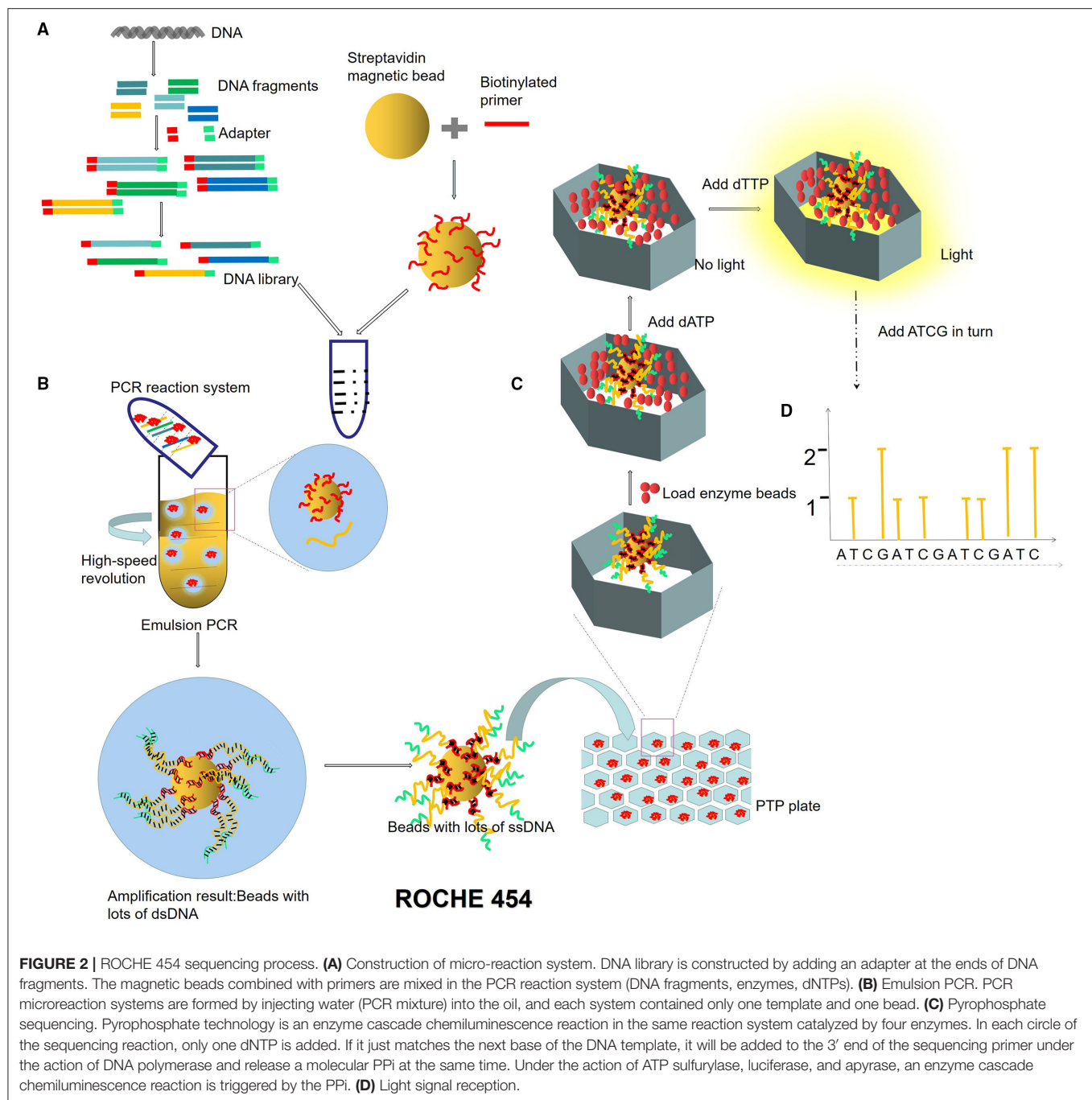
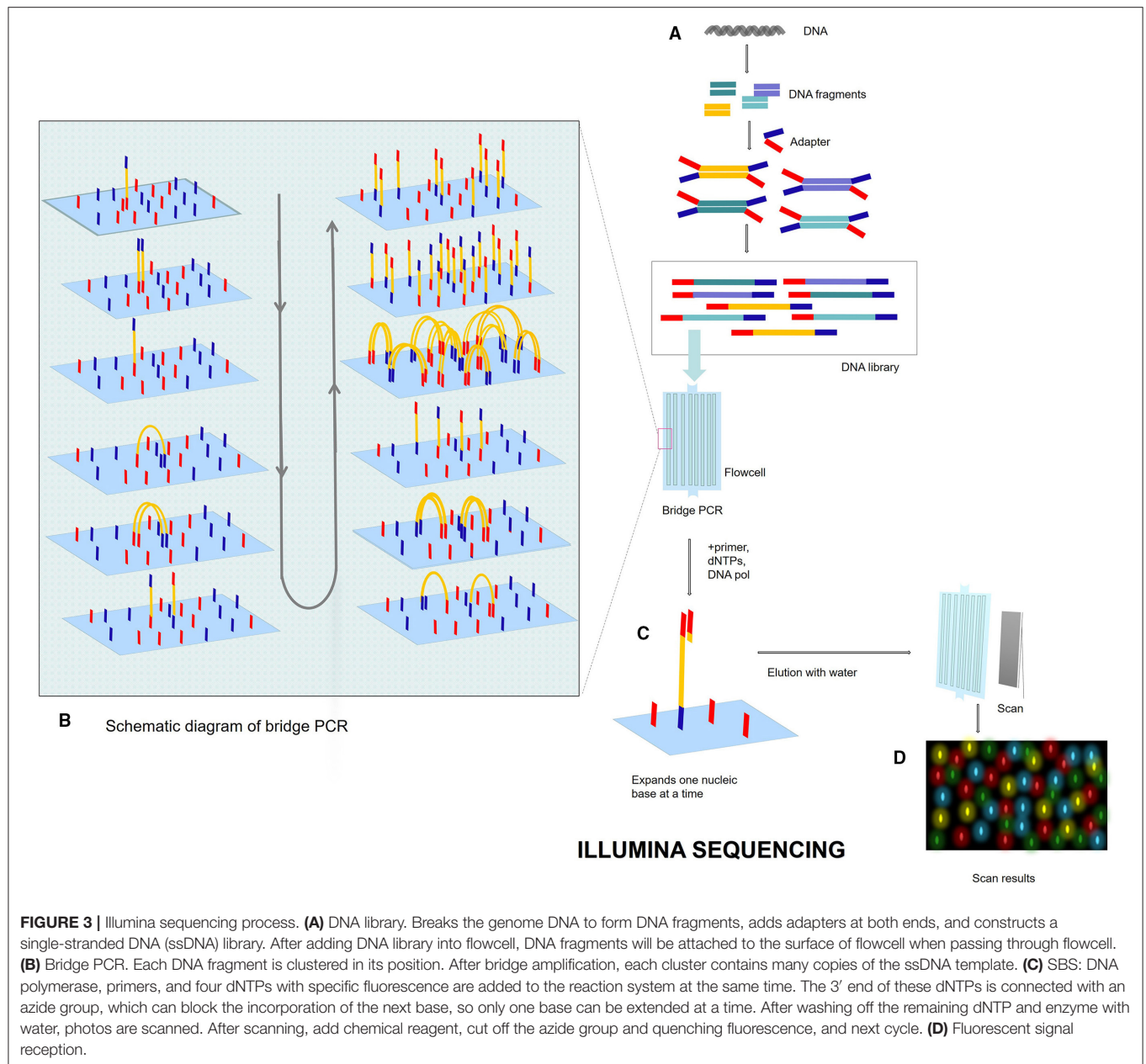


**FIGURE 2 |** ROCHE 454 sequencing process. **(A)** Construction of micro-reaction system. DNA library is constructed by adding an adapter at the ends of DNA fragments. The magnetic beads combined with primers are mixed in the PCR reaction system (DNA fragments, enzymes, dNTPs). **(B)** Emulsion PCR. PCR microreaction systems are formed by injecting water (PCR mixture) into the oil, and each system contained only one template and one bead. **(C)** Pyrophosphate sequencing. Pyrophosphate technology is an enzyme cascade chemiluminescence reaction in the same reaction system catalyzed by four enzymes. In each circle of the sequencing reaction, only one dNTP is added. If it just matches the next base of the DNA template, it will be added to the 3' end of the sequencing primer under the action of DNA polymerase and release a molecular PPI at the same time. Under the action of ATP sulfurylase, luciferase, and apyrase, an enzyme cascade chemiluminescence reaction is triggered by the PPI. **(D)** Light signal reception.

are caused. Ion Torrent has the advantages of low cost, only an electrical signal detection system, and no light/fluorescence detection system (Pennisi, 2010).

Third-generation sequencing also called *de novo* sequencing technology, is a milestone in sequencing technology, which is based on single-molecule sequencing technology (SMS) (Xu et al., 2009) and large-scale parallel sequencing technology. There are two methods for the TGS. The first is single-molecule fluorescence sequencing. The representative technology is the American Helicos SMS (True single molecular sequencing,

TSMS) and single molecular real-time sequencing (SMRT) technology from Pacific Bioscience (Xu et al., 2009; Rhoads and Au, 2015; Midha et al., 2019). SMRT Principle is SBS. DNA polymerase is anchored to the nanopore. The four fluorescent-labeled dNTPs emit different light in the base-pairing stage. The type of entering base can be determined according to the light wavelength and peak value. The phosphate group of dNTP is labeled with fluorescence in SMRT. The long reads are determined by DNA polymerase activity. SMRT requires a high-efficient optical detection system.



The second is nanopore sequencing, which is based on electrical signals and single-molecule long-read detection. The representative company is Oxford Nanopore (Branton et al., 2008; Midha et al., 2019; **Figure 6**). The principle of nanopore sequencing is to use electrophoresis technology to drive individual molecules through nanopores one by one for sequencing. The electrification properties of each ATCG base are different during nanopore sequencing, and the difference of electrical signals detected can correspond to different bases. Compared with NGS, TGS is single-molecule sequencing. TGS has no PCR amplification preference or GC preference and can be sequenced directly without PCR amplification. The TGS has a very long read length, with an average read length of 10–15 kb

and a maximum read length up to 40 kb. TGS can directly detect DNA methylation. The disadvantages of TGS are mainly shown in the following three aspects. First, sequencing errors occur randomly, with error rates of each base as high as 15%, which can be overcome and corrected by multiple sequences. Second, the cost of sequencing is high. Third, SMRT sequencing technology requires enzymes, and currently, better enzymes with much more activity and stability are needed.

When selecting different sequencing methods, there are many factors to consider, including the length of the target gene, the requirement of sequencing accuracy, the purpose of sequencing (whole genome sequencing, resequencing, or SNP), and the gene abundance of the sample. The sequencing platform should

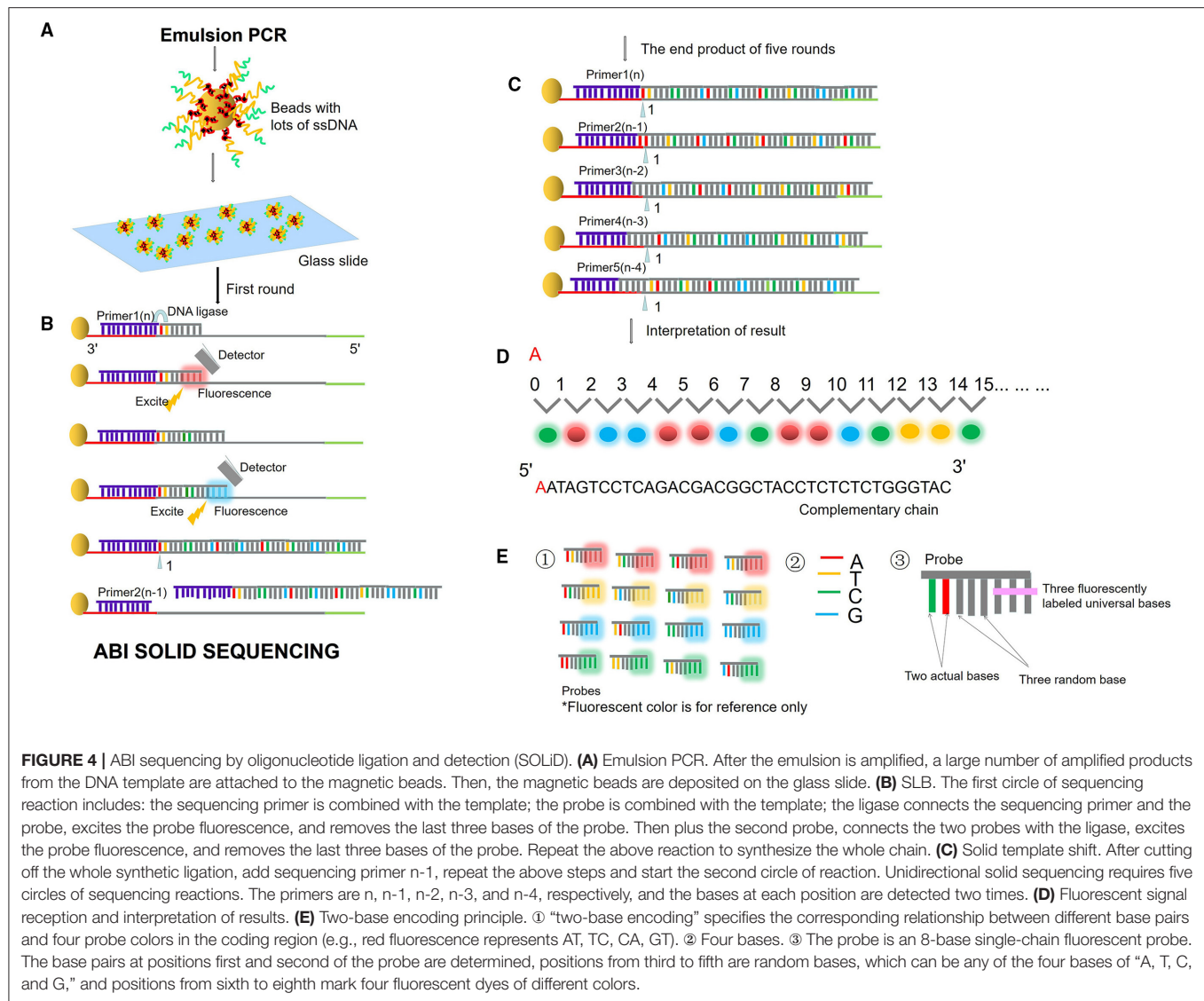


**FIGURE 4 |** ABI sequencing by oligonucleotide ligation and detection (SOLID). **(A)** Emulsion PCR. After the emulsion is amplified, a large number of amplified products from the DNA template are attached to the magnetic beads. Then, the magnetic beads are deposited on the glass slide. **(B)** SLB. The first circle of sequencing reaction includes: the sequencing primer is combined with the template; the probe is combined with the template; the ligase connects the sequencing primer and the probe, excites the probe fluorescence, and removes the last three bases of the probe. Then plus the second probe, connects the two probes with the ligase, excites the probe fluorescence, and removes the last three bases of the probe. Repeat the above reaction to synthesize the whole chain. **(C)** Solid template shift. After cutting off the whole synthetic ligation, add sequencing primer  $n-1$ , repeat the above steps and start the second circle of reaction. Unidirectional solid sequencing requires five circles of sequencing reactions. The primers are  $n$ ,  $n-1$ ,  $n-2$ ,  $n-3$ , and  $n-4$ , respectively, and the bases at each position are detected two times. **(D)** Fluorescent signal reception and interpretation of results. **(E)** Two-base encoding principle. ① "two-base encoding" specifies the corresponding relationship between different base pairs and four probe colors in the coding region (e.g., red fluorescence represents AT, TC, CA, GT). ② Four bases. ③ The probe is an 8-base single-chain fluorescent probe. The base pairs at positions first and second of the probe are determined, positions from third to fifth are random bases, which can be any of the four bases of "A, T, C, and G," and positions from sixth to eighth mark four fluorescent dyes of different colors.

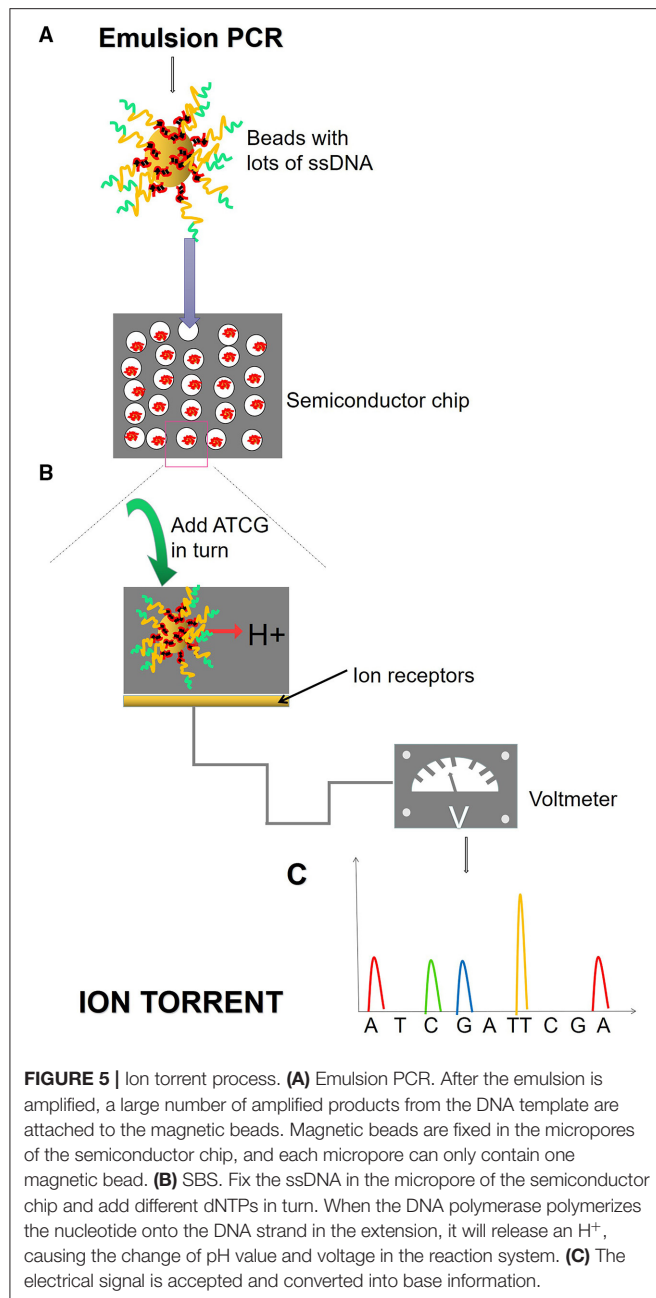
consider factors such as sequencing speed, read length, cost, error rate, methylation, and others. At present, NGS is the mainstream sequencing method, but TGS is still in the initial stage of development due to its high cost and high error rate in a single base. In practical applications, the advantages in long reads of 10–15 kb with low assembly difficulty of TGS and the characteristics of high quality in short reads of NGS can be utilized (Kumar et al., 2019; Table 1).

Different sequencing methods have their advantages and disadvantages. Shotgun sequencing is still in use today and serves as the gold standard because of its high accuracy. NGS has parallel sequencing after PCR amplification of the template and shows high throughput. At present, the market share of NGS is the highest. Illumina is currently the most widely used platform in the NGS. The Roche 454 sequencing technology has been withdrawn from the market due to its high cost. The TGS sequence directly, and the read length is longer, but the error rate is higher. Therefore, below are some suggestions

for sequencing method selection. (1) For SNP detection of genome or insertion DNA sequencing of positive clones, shotgun sequencing is recommended. (2) If whole genome sequencing is carried out, Illumina is a better choice among NGS. (3) If cost is not considered, the combination of NGS and TGS is the best choice, which has high-quality short reads of NGS to correct wrong bases generated by TGS. The future direction of sequencing is to expand the microbial reference gene database and increase the accuracy of long reads.

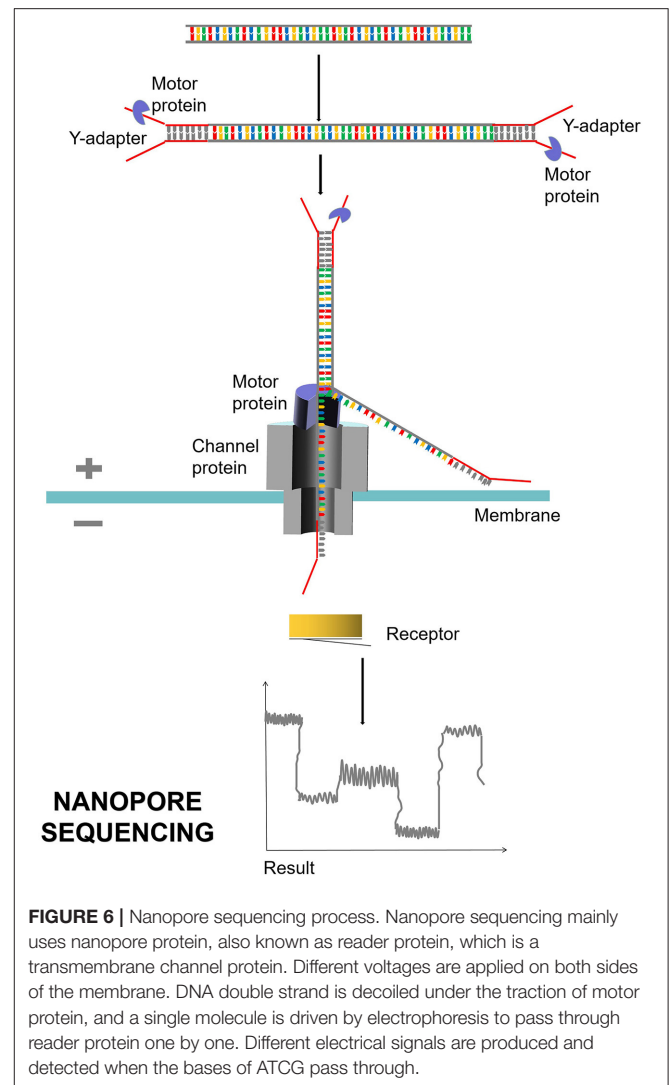
### Processing of DNA Sequencing Information Data

After a large number of reads are obtained by preliminary metagenomic DNA sequencing, the reads should be assembled into a complete genome sequence by software, and taxonomic profiling should be obtained at the same time. Then gene prediction and function annotation are carried out.



Genome sequencing mainly includes quality control (QC), sequence assembly, sequence binning, taxonomic profiling, gene prediction, and function annotation.

Quality control mainly includes two parts: de-noising and de-host sequence. It is necessary to establish a database of host sequences to be used for comparing and removing by sequence alignment (Schmieder and Edwards, 2011; Hong et al., 2014). Data analysis includes assembly-based and assembly-free metagenomic profiling. If the microbial genetic information database is complete, the post-QC data can be directly analyzed without assembly. There are currently two approaches to sequence assembly, relying on reference sequence assembly



and *de novo* assembly (Iqbal et al., 2012; Quince et al., 2017; Breitwieser et al., 2019; Olson et al., 2019; Anyansi et al., 2020). Binning refers to the sorting and clustering of metagenome sequenced segments by species. Binning operations may result in bins of unknown microbial genome sequences that cannot be cultured in the laboratory. Binning can be divided according to different types of aggregation sequence: reads binning before assembly, contig binning after assembly, and gene binning based on annotation (Alneberg et al., 2014; Cleary et al., 2015; Quince et al., 2017). Contig binning usually classifies contigs with similar composition and consistent abundance patterns into the same species. In addition, contigs binning has a better effect on contigs with higher abundance and is often applied by many software. It is possible to obtain low abundance species with reads binning, and even cluster species with abundance as low as 0.00001% (Cleary et al., 2015). Gene binning method is used in many published metagenome-wide association studies, and gene abundance is calculated (Wang and



**TABLE 1 |** Performance COMPARISON of seven sequencing instruments.

Platform	Sequencing rules	Advantages	Disadvantages	Signal received
Shotgun sequencing	Dideoxy chain termination method, capillary electrophoresis	Accuracy 99.999%, Reads 1,000 bp, High accuracy of processing repeated base, <i>De novo</i>	Low-throughput, high cost	Fluorescence
Roche 454	Pyrophosphate sequencing, SBS, Emulsion PCR	Accuracy 99%, Reads 400–600 bp, Parallel sequencing	Base insertion and deletion errors	Light
Illumina	SBS, Bridge PCR, Reversible terminator	Accuracy 99%, Reads 75–300 bp, Parallel sequencing	Base substitution error	Fluorescence
ABI solid	SBL, Emulsion PCR, Solid phase template shift, Two base encoding	Accuracy 99.94%, Reads 40 bp, Parallel sequencing, each base for sequencing twice	Prone to continuous base interpretation errors	Fluorescence
ABI/Ion torrent	Semiconductor sequencing, SBS, Emulsion PCR	Accuracy 99%, reads 200 bp, Parallel sequencing, No light/fluorescence detection system	Difficult to identify homopolymers >8 bases, Base insertion and deletion errors	Electrical signal
Pacific bioscience	SMRT, SBS	Sequencing without PCR, Detecting methylated bases, average reads 10–15 kb	Random errors (5–15%) for a base, repeated sequencing can correct random errors	Fluorescence
Oxford nanopore	Nanopore sequencing, Single-molecule sequencing, Direct detection of bases	Sequencing without PCR, No light/fluorescence detection system, Detecting methylated bases, average reads 10–15 kb, longest to 40 kb	Random errors (5–15%) for a base, Repeated sequencing can correct random errors	Electrical signal

SBS, sequencing by synthesis; SBL, sequence by ligation; ssDNA, single-stranded DNA; SMRT, single molecular real time sequencing. Solid (sequencing by oligonucleotide Ligation and Detection).

Jia, 2016). Currently, gene binning and contig binning are most widely used.

If the sequence assembly and sequence sorting are not correct, it is often impossible to identify new microorganisms. In the metagenomic sequencing report, species annotation and abundance statistics are required. The former refers to the analysis of species in the phylum, while the latter refers to the relative abundance of various microorganisms.

Metagenomic gene prediction is to use prediction tools to identify potential open reading frames (ORF) in genomic libraries and to predict the structure and function of unknown sequences of genes. Metagenomic gene prediction includes homology prediction and *de novo* prediction. Homology prediction can be obtained by alignment of homologous sequences with gene database, but the disadvantages are dependent on the existing gene database, and new genes cannot be annotated. *De novo* prediction is based on the sequence characteristics obtained by sequencing, which can predict both known and unknown genes based on different characteristics in the coding region and the non-coding region.

Function annotation is to compare a gene or protein sequence in a specific functional database, associate a gene or protein with a specific function, and help understand the relevant metabolic pathway. Through gene prediction and

functional annotation analysis, the information of metabolic pathways can be obtained. To improve the quality of sequencing analysis, Bowers RM formulated Genome Sketch Standards of Metagenome-Assembled Genome (MAG) in 2017. High-quality drafts require gene integrity >90%, contamination <5%, and inclusion of 16S, 23S, and other highly conserved genes in assembly quantity (Bowers et al., 2017).

**Commonly Used Software for Data Analysis of Sequencing Information**

Data analysis relies on continuous improvement of existing databases and analysis software. Each process such as QC, binning, assembly, gene prediction, and function annotation has its own software with its own advantages. Megan is selected for the analysis and comparison of multiple groups of metagenome data, while the software GeneMark and metagenemark are often selected for gene prediction. In 2017, researchers compared and evaluated several software regarding assembly, binning and taxonomic profiling, to help researchers to select appropriate software (Sczyrba et al., 2017). The assembly software (MEGAHIT, Minia, and Meraga) performs well, assembling significant portions of the genome over a wide range and reducing misassembly. The MaxBin2.0 genome binner has the highest good performance (70–80% integrity, >92%

purity), followed by other programs (MetaBAT, CONCOCT, and MetaWatt). The taxonomic software of PhyloPythiaS and Kraken have good results before the family level.

## CLASSIFICATION OF METAGENOMICS

Metagenomics technology does not rely on isolation and culture but directly extracts the genetic material of microorganisms from the natural environment. Then, the characteristics of microbial communities can be studied through genetic analysis. Metagenomics is classified according to research purpose and research object.

### Metagenomics Can Be Divided Into Functional Metagenomics and Sequencing Metagenomics for Research Purposes

#### Functional Metagenomics Is Mainly Used for the Discovery of New Bioactive Substances and the Screening of New Microbial Functional Genes

Metagenomics technology has found many new genes, including the biocatalyst gene (Voget et al., 2003; Uchiyama et al., 2005), polyketide synthase coding gene (Ginolhac et al., 2004), antibiotic resistance genes (ARGs) (Riesenfeld et al., 2004), and others. In 2004, researchers used functional metagenomics to find that microorganisms in the soil had aminoglycoside and tetracycline antibiotic resistance genes that were significantly different from the original gene sequences in the database (Riesenfeld et al., 2004).

Active products produced by heterologous expression of metagenomic library genes, such as antibiotics, antitumor substances, and enzymes, are screened, sequenced, and analyzed. Metagenomics has great potential for application in the discovery of new enzymes without culture. Various enzymes found in metagenomes may be derived from microbial metabolism or microbial secondary metabolites. In the last two decades, metagenomics has shortened the discovery cycle of new enzymes, such as esterase, glycosidase, and oxido-reductase. Zhang et al. (2007) screened a specific low-temperature lipase at the South Pole. A strain showing extracellular lipolytic activity toward tributyrin was isolated from the deep-sea sediment of Prydz Bay and identified as a *Psychrobacter* species. The genomic DNA library was constructed from the strain with the highest lipolytic activity and the recombinant plasmids were transformed into *E. coli*. The clones with lipase activity from 28,000 clones were identified. The insert DNA sequence of the selected clone was sequenced and an open reading frame of 954 bp coding was identified for a lipase gene by BLAST analysis. The effects of temperature on enzyme activity indicated that it was a typical cold-adapted enzyme.

There are many advantages to functional metagenomics. (1) Functional metagenomics can obtain target genes or active products through screening without culture conditions. (2) The development of new drugs was accelerated from marine and extreme environmental microbial resources. (3) Functional metagenomes help us to discover new members of existing enzyme families or enzymes that function only

under specific physicochemical conditions, which can be better used in industry. (4) Functional metagenomics combined with metabolomics helped study the C, N, and S cycle metabolism of microorganisms in the environment.

There are many challenges in functional metagenomics. (1) The living conditions of the microbial community in the environment are complex, and the genes of the microorganisms with low abundance may not be extracted. (2) There is a loss of DNA fragments in the gene cloning process. (3) The frequency of heterologous expression of foreign genes is low. (4) The existing screening methods are limited and cannot meet all the enzyme screening requirements. (5) Screening is low efficiency, and only a few positive clones can be selected from tens of thousands of clones. Therefore, we need to develop higher throughput, high sensitivity, rapid, and simple screening methods in the future. (6) Due to temperature, pH, and other limitations, only a small part of the newly discovered enzymes can be used for industrial needs. (7) Current functional metagenomic studies are geographically uneven. It is mainly concentrated in developed countries. The vast microbial resources of developing countries are underexploited.

### Sequencing Analysis of Metagenomics

To study the diversity and abundance of microbial community composition, species identification by microbial taxonomy is required. The traditional identification of microbial species composition is performed using the 16S/18S ribosomal DNA identification (16S/18S rDNA) in prokaryotic and eukaryotic cells, respectively; 16S rDNA sequencing is a commonly used molecular clock for bacterial taxonomic studies, but 16S rDNA provides limited information and may not be able to successfully identify species. Metagenomic sequencing is capable of identifying the species or the strain of a microbial community. For example, a research team used a combination of metagenome sequencing and single-cell sequencing to identify an extremely thermophilic bacterium *Candidatus kryptonia*, a new bacterium that could not be detected by 16S rDNA (Eloe-Fadrosh et al., 2016).

Metagenomic sequencing can be applied to bacteria, fungi, virus, and other microorganisms. In the absence of any available sequence information, metagenomic sequencing mainly uses *de novo* sequencing for microbial identification. Bioinformatics analysis methods were used to obtain the genomic sequence of microorganisms, such as COVID-19 (Wahba et al., 2020; Wu et al., 2020). In the presence of reference sequences, metagenome sequencing can focus on genetic variation information such as SNP, insertion/deletion of microbial significance, for example, the detection of YMDD (tyrosine—methionine—aspartic acid—aspartic acid) caused by point mutation of HBV polymerase gene region. At present, one of the hotspots of metagenomics research is disease-related human whole-exome sequencing (Wei et al., 2011).

There are many advantages to studying sequencing metagenomics. (1) Microorganisms in extreme environments are difficult to culture. Metagenomics can find such unculturable microorganisms. (2) Species, genetic, and evolutionary information of microorganisms can be obtained by studying

the diversity of the microbial community. (3) New pathogenic microbial evidence can improve the current diagnosis of medical infections. (4) In terms of emerging infectious diseases, the target of pathogenic microorganisms can be quickly identified.

The sequencing of metagenomics is facing many challenges. (1) The DNA of environmental microorganisms cannot be extracted completely. (2) Sequencing process may miss low-abundance microorganisms. (3) There is no “gold standard” for sequencing processing software. (4) Because of the imperfection of the microbial database, many sequencing data might not be analyzed, including species annotation and functional analysis. (5) A sequencing platform with long reads and high accuracy is urgently needed. (6) The determination of the abundance of microorganisms in a microbial community is influenced by many factors.

### According to the Microorganism Studied, Metagenomics Can Be Divided Into Bacterial Metagenomics, Fungal Metagenomics, and Viral Metagenomics

At present, bacterial metagenomics is the most studied one, while the development of sequence analysis metagenomics is the fastest-growing one. Fungal and viral metagenomics are mainly used in sequence analysis metagenomics. Virus metagenomics can be used for systematic analysis and identification of overly scattered and low abundance viruses from the environment, a virus can be obtained directly from the environment without isolation and culture. With the advance in metagenome sequencing, most of the new information on virus databases comes from metagenomics rather than cultures. The Bundibugyo Ebola virus was discovered in 2007 in patients having Ugandan hemorrhagic fever using viral metagenomics (Towner et al., 2008).

## APPLICATION FIELDS OF MICROORGANISM METAGENOMICS

Applications of environmental metagenomics include the study of microorganisms in oceans, soils, deep oceans, glaciers, craters, and other environments. Metagenomics also has many applications in the medical field, such as the identification of pathogenic microorganisms in the intestinal tract, bloodstream infections, lung infections, central nervous system infections, and other infections. At present, metagenomic research focuses on antibiotic-resistant bacteria (ARB) and antibiotic-resistant genes (ARGs) (Gillespie et al., 2002; Riesenfeld et al., 2004; Arango-Argoty et al., 2018; Karkman et al., 2018; Nnadozie and Odume, 2019), biocatalysts, drugs, and others.

### Environmental Object of Microorganism Metagenomics Continues to Expand

Metagenomics is used in research related to agriculture, biology, pollution control, energy, environment, atmosphere, and other fields. Microbial subjects range from land to sea and extreme environments. There are huge microorganisms in the soil, and metagenomics studies have shown that soil is a potential

cornucopia of antibiotics and antifungal agents. In 2002, the antibiotics Turbomycin A and Turbomycin B with broad-spectrum antibacterial activity were screened and named from the soil metagenomic library (Gillespie et al., 2002).

Compared with soil microorganisms, marine microorganisms have a broad prospect. Oceans, rivers, and lakes account for more than 70% of the earth's area, presenting great differences in the species, genes, and biological characteristics of microorganisms in the water. Marine microorganisms have special metabolites and metabolic regulation mechanisms. Metagenomic techniques are used to study the synthetic pathways of various marine secondary metabolites. A good example is marine actinomycetes-related metabolites (polyketone biosynthesis gene cluster), which can be used as a source of new drugs. In terms of ARGs, ARB levels in most river and lake systems are high, in particular, vancomycin-resistant *enterococcus* (VRE) and methicillin-resistant *Staphylococcus aureus* (MRSA) (Nnadozie and Odume, 2019).

The majority of extremophiles that survive in various types of extreme environments cannot be cultured artificially. In such extreme environments, it is more likely to obtain unique enzymes and abundant microbial resources. The active compounds can be screened by direct sequencing, sequence alignment with database, and functional analysis, some of which may be selected out for commercial development (Zhang et al., 2007).

### Metagenomics for Prevention and Control of Environmental Pollution

Bioremediation is a new bioengineering technology that uses the natural purification ability of environmental microorganisms. Bioremediation is expected to reduce pollutants or make them harmless by using the metabolic activities of microorganisms in the treatment system. Bioremediation needs several conditions: (1) Pollutants are organic and can be degraded by microorganisms. (2) The microorganisms possess certain metabolic activities. (3) The environment is suitable for degradation, meanwhile, for the maintenance of microbial activity. Metagenomics may help explore new functional microorganisms and genes, and construct and screen out new microbial strains with high degradation efficiency, broad applicability, and stable expression.

In the sewage treatment project, not only the organic matter in the sewage needs to be degraded but also the nitrogen and phosphorus elements in the sewage need to be removed. The wastewater treatment process deals with diverse microbial populations, such as anaerobic ammonium oxidation bacteria, phosphorus-accumulating bacteria, and electrochemically active bacteria. Metagenomic studies of water microorganisms contribute to biological nitrogen removal processes and enhanced biological phosphorus removal. Functional genes have been found in microorganisms that can degrade pesticides, plastics, polycyclic aromatic hydrocarbons, petroleum hydrocarbons, and other organic pollutants, which can play an important role in environmental bioremediation. Researchers screened a variety of new proteolytic enzymes from yard compost to degrade pesticides (Lämmle et al., 2007). In

2005, a researcher screened benzoate anaerobic degradation genes from Black Sea sediment, which contributes to the anaerobic degradation of aromatic compounds (Krüger et al., 2003). Microbial electrochemical systems (MES) use electroactive bacteria enriched in anodes to recover electrical energy directly from organic waste (Wang and Ren, 2013; Venkata Mohan et al., 2014). As an emerging sewage treatment technology, MES has been developed rapidly.

## Metagenomics Are Used in the Medical Diagnosis of Pathogenic Microorganisms

Metagenomics findings suggest that the intestinal microbiome is associated with a variety of diseases, such as non-alcoholic fatty liver disease (Aron-Wisniewsky et al., 2020), autoimmune diseases (Svoboda, 2021), and tumors (Andrews et al., 2021). Metagenomics can be used to detect drug-resistant genes for pathogens and monitor outbreaks of infectious diseases in hospitals and communities. In 2021, the Laboratory Medicine Branch of the Chinese Medical Association published an expert consensus, recommending the use of NGS on the samples of suspected infection sites in case that no evidence of etiology is obtained by routine biochemical examination or microbial culture, and empirical anti-infection therapy is ineffective. It is recommended to select sequencing metagenomics when the cause and site of infection are unknown and the pathogenic microorganisms cannot be determined by the existing detection technology. NGS can deal with a wide range of pathogenic microorganisms, including bacteria, viruses, fungi, and parasites. Samples may be collected in case of suspected central nervous system infection, respiratory tract infection, bloodstream infection, etc. Now metagenomic sequencing has been widely used in the detection of medical pathogens. Respiratory RNA viruses such as Picornaviridae, Coronaviridae, Paramyxoviridae, and Orthomyxoviridae can be diagnosed by NGS (Thorburn et al., 2015). Five organisms (*Neisseria meningitidis*, *Streptococcus agalactiae*, *Candida albicans*, *Mycobacterium fortuitum*, and *Mycobacterium abscessus*) were detected by mNGS testing in the cerebrospinal fluid (Miller et al., 2019).

Limitations of metagenomics in the medical diagnosis of pathogenic microorganisms are as follows: (1) Pathogenic microorganisms detected by metagenomics might be dead or dormant microorganisms, and their clinical significance should be carefully judged by combining with other clinical data. (2) Real-time quantitative PCR has been applied in clinical practice, and its stability and accuracy have been confirmed. While the accuracy of metagenomics on microbial abundance needs to be verified by large sample data. (3) In the case of intracellular bacterium infection, the false-negative result may occur due to an incorrect cell wall rupture method. (4) It is recommended that metagenomics should not be the first choice when immunoassay or PCR methods are available for pathogen diagnosis. (5) When interpreting whether the SNP in microbial genes is related to function, large-scale clinical trials are needed to verify the conclusion. (6) It is important to remove DNA contamination from environmental microorganisms or hosts before data analysis.

## Applications of Metagenomics in Other Aspects

Metagenomics studies the diversity, species composition, and genetic evolution of microorganisms in different environments. People have applied metagenomics to winemaking, farming, and authentication of Chinese medicine. It is found that the diversity of microbial composition and population characteristics in a wine cellar is very important to improve the flavor and quality of the wine (Stefanini and Cavalieri, 2018; Liu et al., 2021). The pharmaceutical value of Chinese medicine from different producing areas is different, which may be related to the composition of microorganisms under their unique climate and soil. The increase in crop yield is inseparable from the correlation between plant roots and soil microbial community (Sharma et al., 2018).

## OUTLOOK

At present, metagenomics is advancing rapidly in many fields. The bottlenecks of functional metagenomics lie in the failure of large fragment DNA extraction and expression of genes from metagenome libraries in heterologous hosts. High-throughput screening in metagenomic libraries is also a problem to be solved in the future. The development of NGS and TGS technology has promoted the progress of metagenomics. Although the cost of NGS sequencing is reducing and the speed of sequencing is increasing, the microbiological database is incomplete, so it is difficult to correctly assemble and bin without sequencing data for reference. For example, most viral sequences obtained by viral metagenomics have no similarity to any known sequences in the existing databases and, therefore, cannot be annotated for gene and function. In the future, with the progress of TGS sequencing technology, the accuracy rate will be greatly improved. The emergence of new computer algorithms can better process post-sequencing data.

In the future, metagenomics will be combined with metatranscriptomics, proteomics, and metabolomics. Metagenomics provides genetic information of all the environmental microorganisms. Metatranscriptomics is to study the species, functions, and expression activities of transcripts in a microbial community at the RNA level. Metaproteomics can also provide real-time information on the functional expression of environmental genes, while metabolomics studies the metabolic pathways of metabolites. The linking of these omics will lead us to study from genes to proteins and from structure to function.

## AUTHOR CONTRIBUTIONS

YX and ML contributed to the study concept and design. LZ, FC, ZZ, MX, FS, LY, XB, YL, YG, and HH collected and sorted out the literature. LY, YX, and ML drew pictures. LZ, FC, and ZZ wrote the first draft. WY, ML, and YX edited and approved the English version of the article. All authors contributed to the article and approved the submitted version.



## FUNDING

This research was supported by the Beijing Hospitals Authority Clinical Medicine Development of Special Funding Support (Nos. XMLX 201706 and XMLX 202127), the Special Public Health Project for Health Development in Capital (2021-1G-4061), the Digestive Medical Coordinated Development Center

## REFERENCES

- Alneberg, J., Bjarnason, B. S., de Bruijn, I., Schirmer, M., Quick, J., Ijaz, U. Z., et al. (2014). Binning metagenomic contigs by coverage and composition. *Nat. Methods* 11, 1144–1146. doi: 10.1038/nmeth.3103
- Andrews, M. C., Duong, C., Gopalakrishnan, V., Iebba, V., Chen, W. S., Derosa, L., et al. (2021). Gut microbiota signatures are associated with toxicity to combined CTLA-4 and PD-1 blockade. *Nat. Med.* 27, 1432–1441. doi: 10.1038/s41591-021-01406-6
- Ansorge, W. J. (2009). Next-generation DNA sequencing techniques. *New Biotechnol.* 25, 195–203. doi: 10.1016/j.nbt.2008.12.009
- Anyansi, C., Straub, T. J., Manson, A. L., Earl, A. M., and Abeel, T. (2020). Computational methods for strain-level microbial detection in colony and metagenome sequencing data. *Front. Microbiol.* 11:1925. doi: 10.3389/fmicb.2020.01925
- Apolinar-Hernández, M. M., Peña-Ramírez, Y. J., Pérez-Rueda, E., Canto-Canché, B. B., De Los Santos-Briones, C., and O'Connor-Sánchez, A. (2016). Identification and *in silico* characterization of two novel genes encoding peptidases S8 found by functional screening in a metagenomic library of Yucatán underground water. *Gene* 593, 154–161. doi: 10.1016/j.gene.2016.08.009
- Arango-Argoty, G., Garner, E., Pruden, A., Heath, L. S., Vikesland, P., and Zhang, L. (2018). DeepARG: a deep learning approach for predicting antibiotic resistance genes from metagenomic data. *Microbiome* 6:23. doi: 10.1186/s40168-018-0401-z
- Aron-Wisniewsky, J., Vigliotti, C., Witjes, J., Le, P., Holleboom, A. G., Verheij, J., et al. (2020). Gut microbiota and human NAFLD: disentangling microbial signatures from metabolic disorders. *Nat. Rev. Gastroenterol. Hepatol.* 17, 279–297. doi: 10.1038/s41575-020-0269-9
- Avarre, J. C., de Lajudie, P., and Béné, G. (2007). Hybridization of genomic DNA to microarrays: a challenge for the analysis of environmental samples. *J. Microbiol. Methods* 69, 242–248. doi: 10.1016/j.mimet.2006.11.007
- Bankier, A. T. (2001). Shotgun DNA sequencing. *Methods Mol. Biol.* 167, 89–100. doi: 10.1385/1-59259-113-2:089
- Bowers, R. M., Kyrpides, N. C., Stepanauskas, R., Harmon-Smith, M., Doud, D., Reddy, T., et al. (2017). Minimum information about a single amplified genome (MISAG) and a metagenome-assembled genome (MIMAG) of bacteria and archaea. *Nat. Biotechnol.* 35, 725–731. doi: 10.1038/nbt.3893
- Branton, D., Deamer, D. W., Marziali, A., Bayley, H., Benner, S. A., Butler, T., et al. (2008). The potential and challenges of nanopore sequencing. *Nat. Biotechnol.* 26, 1146–1153. doi: 10.1038/nbt.1495
- Breitwieser, F. P., Lu, J., and Salzberg, S. L. (2019). A review of methods and databases for metagenomic classification and assembly. *Brief. Bioinform.* 20, 1125–1136. doi: 10.1093/bib/bbx120
- Call, D. R. (2005). Challenges and opportunities for pathogen detection using DNA microarrays. *Crit. Rev. Microbiol.* 31, 91–99. doi: 10.1080/10408410590921736
- Chen, Y., and Murrell, J. C. (2010). When metagenomics meets stable-isotope probing: progress and perspectives. *Trends Microbiol.* 18, 157–163. doi: 10.1016/j.tim.2010.02.002
- Cheng, J., Romantsov, T., Engel, K., Doxey, A. C., Rose, D. R., Neufeld, J. D., et al. (2017). Functional metagenomics reveals novel  $\beta$ -galactosidases not predictable from gene sequences. *PLoS ONE* 12:e0172545. doi: 10.1371/journal.pone.0172545
- Chew, Y. V., and Holmes, A. J. (2009). Suppression subtractive hybridisation allows selective sampling of metagenomic subsets of interest. *J. Microbiol. Methods* 78, 136–143. doi: 10.1016/j.mimet.2009.05.003
- Cleary, B., Brito, I. L., Huang, K., Gevers, D., Shea, T., Young, S., et al. (2015). Detection of low-abundance bacterial strains in metagenomic datasets by eigengene partitioning. *Nat. Biotechnol.* 33, 1053–1060. doi: 10.1038/nbt.3329
- Colin, P. Y., Kintses, B., Gielen, F., Miton, C. M., Fischer, G., Mohamed, M. F., et al. (2015). Ultrahigh-throughput discovery of promiscuous enzymes by picodroplet functional metagenomics. *Nat. Commun.* 6:10008. doi: 10.1038/ncomms10008
- Craig, J. W., Chang, F. Y., Kim, J. H., Obiajulu, S. C., and Brady, S. F. (2010). Expanding small-molecule functional metagenomics through parallel screening of broad-host-range cosmid environmental DNA libraries in diverse proteobacteria. *Appl. Environ. Microbiol.* 76, 1633–1641. doi: 10.1128/AEM.02169-09
- Daniel, R. (2005). The metagenomics of soil. *Nat. Rev. Microbiol.* 3, 470–478. doi: 10.1038/nrmicro1160
- Eloe-Fadrosh, E. A., Paez-Espino, D., Jarett, J., Dunfield, P. F., Hedlund, B. P., Dekas, A. E., et al. (2016). Global metagenomic survey reveals a new bacterial candidate phylum in geothermal springs. *Nat. Commun.* 7:10476. doi: 10.1038/ncomms10476
- Gabor, E. M., de Vries, E. J., and Janssen, D. B. (2003). Efficient recovery of environmental DNA for expression cloning by indirect extraction methods. *FEMS Microbiol. Ecol.* 44, 153–163. doi: 10.1016/S0168-6496(02)00462-2
- Galbraith, E. A., Antonopoulos, D. A., and White, B. A. (2008). Application of suppressive subtractive hybridization to uncover the metagenomic diversity of environmental samples. *Methods Mol. Biol.* 410, 295–333. doi: 10.1007/978-1-59745-548-0\_16
- Gillespie, D. E., Brady, S. F., Bettermann, A. D., Cianciotto, N. P., Liles, M. R., Rondon, M. R., et al. (2002). Isolation of antibiotics turbomycin A and B from a metagenomic library of soil microbial DNA. *Appl. Environ. Microbiol.* 68, 4301–4306. doi: 10.1128/AEM.68.9.4301-4306.2002
- Ginolhac, A., Jarrin, C., Gillet, B., Robe, P., Pujic, P., Tuphile, K., et al. (2004). Phylogenetic analysis of polyketide synthase I domains from soil metagenomic libraries allows selection of promising clones. *Appl. Environ. Microbiol.* 70, 5522–5527. doi: 10.1128/AEM.70.9.5522-5527.2004
- Handelsman, J., Rondon, M. R., Brady, S. F., Clardy, J., and Goodman, R. M. (1998). Molecular biological access to the chemistry of unknown soil microbes: a new frontier for natural products. *Chem. Biol.* 5, R245–R249. doi: 10.1016/S1074-5521(98)90108-9
- Harrington, C. T., Lin, E. I., Olson, M. T., and Eshleman, J. R. (2013). Fundamentals of pyrosequencing. *Archiv. Pathol. Lab. Med.* 137, 1296–1303. doi: 10.5858/arpa.2012-0463-RA
- Hong, C., Manimaran, S., and Johnson, W. E. (2014). PathoQC: computationally efficient read preprocessing and quality control for high-throughput sequencing data sets. *Cancer Inform.* 13, 167–176. doi: 10.4137/CIN.S13890
- Iqbal, Z., Caccamo, M., Turner, I., Flicek, P., and McVean, G. (2012). De novo assembly and genotyping of variants using colored de Bruijn graphs. *Nat. Genet.* 44, 226–232. doi: 10.1038/ng.1028
- Kakirde, K. S., Wild, J., Godiska, R., Mead, D. A., Wiggins, A. G., Goodman, R. M., et al. (2011). Gram negative shuttle BAC vector for heterologous expression of metagenomic libraries. *Gene* 475, 57–62. doi: 10.1016/j.gene.2010.11.004
- Karkman, A., Do, T. T., Walsh, F., and Virta, M. (2018). Antibiotic-resistance genes in waste water. *Trends Microbiol.* 26, 220–228. doi: 10.1016/j.tim.2017.09.005
- Kellenberger, E. (2001). Exploring the unknown. The silent revolution of microbiology. *EMBO Rep.* 2, 5–7. doi: 10.1093/embo-reports/kve014

- Krüger, M., Meyerdiereks, A., Glöckner, F. O., Amann, R., Widdel, F., Kube, M., et al. (2003). A conspicuous nickel protein in microbial mats that oxidize methane anaerobically. *Nature* 426, 878–881. doi: 10.1038/nature02207
- Kumar, K. R., Cowley, M. J., and Davis, R. L. (2019). Next-generation sequencing and emerging technologies. *Semi. Thromb. Hemost.* 45, 661–673. doi: 10.1055/s-0039-1688446
- Lämmle, K., Zipper, H., Breuer, M., Hauer, B., Buta, C., Brunner, H., et al. (2007). Identification of novel enzymes with different hydrolytic activities by metagenome expression cloning. *J. Biotechnol.* 127, 575–592. doi: 10.1016/j.jbiotec.2006.07.036
- Liu, D., Legras, J. L., Zhang, P., Chen, D., and Howell, K. (2021). Diversity and dynamics of fungi during spontaneous fermentations and association with unique aroma profiles in wine. *Int. J. Food Microbiol.* 338:108983. doi: 10.1016/j.ijfoodmicro.2020.108983
- Mardis, E. R. (2008). Next-generation DNA sequencing methods. *Ann. Rev. Genomics Hum. Genet.* 9, 387–402. doi: 10.1146/annurev.genom.9.081307.164359
- Marsh, S. (2007). Pyrosequencing applications. *Methods Mol. Biol.* 373, 15–24. doi: 10.1385/1-59745-377-3:15
- Mauk, M. G., Liu, C., Sadik, M., and Bau, H. H. (2015). Microfluidic devices for nucleic acid (NA) isolation, isothermal NA amplification, and real-time detection. *Methods Mol. Biol.* 1256, 15–40. doi: 10.1007/978-1-4939-2172-0\_2
- Midha, M. K., Wu, M., and Chiu, K. P. (2019). Long-read sequencing in deciphering human genetics to a greater depth. *Hum. Genet.* 138, 1201–1215. doi: 10.1007/s00439-019-02064-y
- Miller, S., Naccache, S. N., Samayoa, E., Messacar, K., Arevalo, S., Federman, S., et al. (2019). Laboratory validation of a clinical metagenomic sequencing assay for pathogen detection in cerebrospinal fluid. *Genome Res.* 29, 831–842. doi: 10.1101/gr.238170.118
- Nnadozie, C. F., and Odume, O. N. (2019). Freshwater environments as reservoirs of antibiotic resistant bacteria and their role in the dissemination of antibiotic resistance genes. *Environ. Pollut.* 254:113067. doi: 10.1016/j.envpol.2019.113067
- Olson, M. V. (1993). The human genome project. *Proc. Natl. Acad. Sci. U.S.A.* 90, 4338–4344. doi: 10.1073/pnas.90.10.4338
- Olson, N. D., Treangen, T. J., Hill, C. M., Cepeda-Espinoza, V., Ghurye, J., Koren, S., et al. (2019). Metagenomic assembly through the lens of validation: recent advances in assessing and improving the quality of genomes assembled from metagenomes. *Brief. Bioinform.* 20, 1140–1150. doi: 10.1093/bib/bbx098
- Palka-Santini, M., Cleven, B. E., Eichinger, L., Krönke, M., and Krut, O. (2009). Large scale multiplex PCR improves pathogen detection by DNA microarrays. *BMC Microbiol.* 9:1. doi: 10.1186/1471-2180-9-1
- Pennisi, E. (2010). Genomics. Semiconductors inspire new sequencing technologies. *Science* 327:1190. doi: 10.1126/science.327.5970.1190
- Popovic, A., Hai, T., Tchigvintsev, A., Hajighasemi, M., Nocek, B., Khusnutdinova, A. N., et al. (2017). Activity screening of environmental metagenomic libraries reveals novel carboxylesterase families. *Sci. Rep.* 7:44103. doi: 10.1038/srep44103
- Probst, A. J., Weinmaier, T., DeSantis, T. Z., Santo Domingo, J. W., and Ashbolt, N. (2015). New perspectives on microbial community distortion after whole-genome amplification. *PLoS ONE* 10:e0124158. doi: 10.1371/journal.pone.0124158
- Quince, C., Walker, A. W., Simpson, J. T., Loman, N. J., and Segata, N. (2017). Shotgun metagenomics, from sampling to analysis. *Nat. Biotechnol.* 35, 833–844. doi: 10.1038/nbt.3935
- Rebets, Y., Kormanec, J., Luzhetskyy, A., Bernaerts, K., and Anné, J. (2017). Cloning and expression of metagenomic DNA in *Streptomyces lividans* and subsequent fermentation for optimized production. *Methods Mol. Biol.* 1539, 99–144. doi: 10.1007/978-1-4939-6691-2\_8
- Rhoads, A., and Au, K. F. (2015). PacBio sequencing and its applications. *Genomics Proteomics Bioinform.* 13, 278–289. doi: 10.1016/j.gpb.2015.08.002
- Riesenfeld, C. S., Goodman, R. M., and Handelsman, J. (2004). Uncultured soil bacteria are a reservoir of new antibiotic resistance genes. *Environ. Microbiol.* 6, 981–989. doi: 10.1111/j.1462-2920.2004.00664.x
- Schmieder, R., and Edwards, R. (2011). Quality control and preprocessing of metagenomic datasets. *Bioinformatics* 27, 863–864. doi: 10.1093/bioinformatics/btr026
- Schneegurt, M. A., Dore, S. Y., and Kulpa, C. F. Jr. (2003). Direct extraction of DNA from soils for studies in microbial ecology. *Curr. Issues Mol. Biol.* 5, 1–8.
- Sczyrba, A., Hofmann, P., Belmann, P., Koslicki, D., Janssen, S., Dröge, J., et al. (2017). Critical Assessment of metagenome interpretation-a benchmark of metagenomics software. *Nat. Methods* 14, 1063–1071. doi: 10.1038/nmeth.4458
- Sharma, T. R., Devanna, B. N., Kiran, K., Singh, P. K., Arora, K., Jain, P., et al. (2018). Status and prospects of next generation sequencing technologies in crop plants. *Curr. Issues Mol. Biol.* 27, 1–36. doi: 10.21775/cimb.027.001
- Shendure, J., and Ji, H. (2008). Next-generation DNA sequencing. *Nat. Biotechnol.* 26, 1135–1145. doi: 10.1038/nbt1486
- Stefanini, I., and Cavalieri, D. (2018). Metagenomic approaches to investigate the contribution of the vineyard environment to the quality of wine fermentation: potentials and difficulties. *Front. Microbiol.* 9:991. doi: 10.3389/fmicb.2018.00991
- Svoboda, E. (2021). Gut feeling yields evidence of microbial involvement in autoimmunity. *Nature* 595, S54–S55. doi: 10.1038/d41586-021-01837-8
- Thorburn, F., Bennett, S., Modha, S., Murdoch, D., Gunson, R., and Murcia, P. R. (2015). The use of next generation sequencing in the diagnosis and typing of respiratory infections. *J. Clin. Virol.* 69, 96–100. doi: 10.1016/j.jcv.2015.06.082
- Torsvik, V., Goksøyr, J., and Daae, F. L. (1990). High diversity in DNA of soil bacteria. *Appl. Environ. Microbiol.* 56, 782–787. doi: 10.1128/aem.56.3.782-787.1990
- Towner, J. S., Sealy, T. K., Khristova, M. L., Albariño, C. G., Conlan, S., Reeder, S. A., et al. (2008). Newly discovered ebola virus associated with hemorrhagic fever outbreak in Uganda. *PLoS Pathog.* 4:e1000212. doi: 10.1371/journal.ppat.1000212
- Uchiyama, T., Abe, T., Ikemura, T., and Watanabe, K. (2005). Substrate-induced gene-expression screening of environmental metagenome libraries for isolation of catabolic genes. *Nat. Biotechnol.* 23, 88–93. doi: 10.1038/nbt1048
- van Dijk, E. L., Auger, H., Jaszczyszyn, Y., and Thermes, C. (2014). Ten years of next-generation sequencing technology. *Trends Genet.* 30, 418–426. doi: 10.1016/j.tig.2014.07.001
- Venkata Mohan, S., Velvizhi, G., Vamshi Krishna, K., and Lenin Babu, M. (2014). Microbial catalyzed electrochemical systems: a bio-factory with multi-facet applications. *Bioresour. Technol.* 165, 355–364. doi: 10.1016/j.biortech.2014.03.048
- Voget, S., Leggewie, C., Uesbeck, A., Raasch, C., Jaeger, K. E., and Streitz, W. R. (2003). Prospecting for novel biocatalysts in a soil metagenome. *Appl. Environ. Microbiol.* 69, 6235–6242. doi: 10.1128/AEM.69.10.6235-6242.2003
- Wahba, L., Jain, N., Fire, A. Z., Shoura, M. J., Artilles, K. L., McCoy, M. J., et al. (2020). An extensive meta-metagenomic search identifies SARS-CoV-2-homologous sequences in pangolin lung viromes. *mSphere* 5:e00160-20. doi: 10.1128/mSphere.00160-20
- Wang, H., and Ren, Z. J. (2013). A comprehensive review of microbial electrochemical systems as a platform technology. *Biotechnol. Adv.* 31, 1796–1807. doi: 10.1016/j.biotechadv.2013.10.001
- Wang, J., and Jia, H. (2016). Metagenome-wide association studies: fine-mining the microbiome. *Nat. Rev. Microbiol.* 14, 508–522. doi: 10.1038/nrmicro.2016.83
- Wang, T. Y., Wang, L., Zhang, J. H., and Dong, W. H. (2011). A simplified universal genomic DNA extraction protocol suitable for PCR. *Genet. Mol. Res.* 10, 519–525. doi: 10.4238/vol10-1gmr1055
- Wei, X., Walia, V., Lin, J. C., Teer, J. K., Prickett, T. D., Gartner, J., et al. (2011). Exome sequencing identifies GRIN2A as frequently mutated in melanoma. *Nat. Genet.* 43, 442–446. doi: 10.1038/ng.810
- Wu, F., Zhao, S., Yu, B., Chen, Y. M., Wang, W., Song, Z. G., et al. (2020). A new coronavirus associated with human respiratory disease in China. *Nature* 579, 265–269. doi: 10.1038/s41586-020-2008-3
- Xu, M., Fujita, D., and Hanagata, N. (2009). Perspectives and challenges of emerging single-molecule DNA sequencing technologies. *Small* 5, 2638–2649. doi: 10.1002/smll.200900976
- Yun, J., and Ryu, S. (2005). Screening for novel enzymes from metagenome and SIGEX, as a way to improve it. *Microb. Cell Factor.* 4:8. doi: 10.1186/1475-2859-4-8

Zhang, J., Lin, S., and Zeng, R. (2007). Cloning, expression, and characterization of a cold-adapted lipase gene from an antarctic deep-sea psychrotrophic bacterium, *Psychrobacter* sp. 7195. *J. Microbiol. Biotechnol.* 17, 604–610.

**Conflict of Interest:** The authors declare that the research was conducted in the absence of any commercial or financial relationships that could be construed as a potential conflict of interest.

**Publisher's Note:** All claims expressed in this article are solely those of the authors and do not necessarily represent those of their affiliated organizations, or those of

the publisher, the editors and the reviewers. Any product that may be evaluated in this article, or claim that may be made by its manufacturer, is not guaranteed or endorsed by the publisher.

Copyright © 2021 Zhang, Chen, Zeng, Xu, Sun, Yang, Bi, Lin, Gao, Hao, Yi, Li and Xie. This is an open-access article distributed under the terms of the Creative Commons Attribution License (CC BY). The use, distribution or reproduction in other forums is permitted, provided the original author(s) and the copyright owner(s) are credited and that the original publication in this journal is cited, in accordance with accepted academic practice. No use, distribution or reproduction is permitted which does not comply with these terms.

# Advantages of publishing in Frontiers



## OPEN ACCESS

Articles are free to read  
for greatest visibility  
and readership



## FAST PUBLICATION

Around 90 days  
from submission  
to decision



## HIGH QUALITY PEER-REVIEW

Rigorous, collaborative,  
and constructive  
peer-review



## TRANSPARENT PEER-REVIEW

Editors and reviewers  
acknowledged by name  
on published articles

## Frontiers

Avenue du Tribunal-Fédéral 34  
1005 Lausanne | Switzerland

Visit us: [www.frontiersin.org](http://www.frontiersin.org)

Contact us: [frontiersin.org/about/contact](http://frontiersin.org/about/contact)



## REPRODUCIBILITY OF RESEARCH

Support open data  
and methods to enhance  
research reproducibility



## DIGITAL PUBLISHING

Articles designed  
for optimal readership  
across devices



## FOLLOW US

@frontiersin



## IMPACT METRICS

Advanced article metrics  
track visibility across  
digital media



## EXTENSIVE PROMOTION

Marketing  
and promotion  
of impactful research



## LOOP RESEARCH NETWORK

Our network  
increases your  
article's readership